

**Synthesis and pharmacological characterization of
argininamide-type neuropeptide Y (NPY) Y₁ and Y₂
receptor antagonists and synthesis of non-peptide
potential NPY Y₄ receptor ligands**



Dissertation

zur Erlangung des Doktorgrades der Naturwissenschaften

(Dr. rer. nat.)

an der Fakultät für Chemie und Pharmazie an der Universität Regensburg

vorgelegt von

Jonas Buschmann

aus Aachen

2020

Die vorliegende Arbeit entstand in der Zeit von April 2015 bis April 2020 unter der Leitung von Herrn Prof. Dr. Günther Bernhardt und Prof. Dr. Armin Buschauer (verstorben am 18.07.2017) am Institut für Pharmazie der Fakultät für Chemie und Pharmazie der Universität Regensburg.

Das Promotionsgesuch wurde eingereicht am: 12.06.2020

Tag der mündlichen Prüfung: 24.07.2020

Vorsitzender des Prüfungsausschusses: Prof. Dr. Dominik Horinek

Erstgutachter: Prof. Dr. Günther Bernhardt

Zweitgutachter: Prof. Dr. Bernhard Wunsch (WWU Münster)

3. Prüfer: Prof. Dr. Sigurd Elz

Publication (published prior to the submission of the thesis)

Buschmann, J.; Seiler, T.; Bernhardt, G.; Keller, M.; Wifling, D. Argininamide-type neuropeptide Y₁ receptor antagonists: the nature of *N*^ω-carbamoyl substituents determines Y₁R binding mode and affinity. *RSC Med. Chem.* **2020**, 11, 274-282.

Poster presentations

Buschmann, J.; Bauer, T.; Keller, M.; Bernhardt, G.; Buschauer, A. Synthesis and characterization of neuropeptide Y (NPY) Y₁ receptor antagonists related to UR-MK299. *8th International Summerschool "Medicinal Chemistry" 2016*, Regensburg, Germany.

Buschmann, J.; Bauer, T.; Keller, M.; Bernhardt, G.; Buschauer, A. In search for new molecular tools for the neuropeptide Y (NPY) Y₁ and Y₂ receptor based on argininamide-type ligands. *Frontiers in Medicinal Chemistry*, **2018**, Jena, Germany.

Buschmann, J.; Bauer T; Fricke, F; Müller, C; Keller, M; Bernhardt, G.; Buschauer, A. SAR of UR-MK299 derived argininamide-type neuropeptide Y (NPY) Y₁ receptor antagonists and synthesis of potential NPY Y₂ receptor radioligands. *9th International Summerschool "Medicinal Chemistry" 2018*, Regensburg, Germany.

Buschmann, J.; Bauer, T.; Keller, M.; Bernhardt, G.; Buschauer, A. Argininamide-type neuropeptide Y (NPY) Y₁ and Y₂ receptor antagonists: SAR at the Y₁R and synthesis of potential molecular tools for the Y₂R. *DPHG Annual Meeting 2018*, Hamburg, Germany.

Acknowledgements and declarations of collaborations

An dieser Stelle möchte ich mich bedanken bei:

Herrn Prof. Dr. Günther Bernhardt für seine wissenschaftlichen Ratschläge vor allem bei biologischen Testungen, die gute Betreuung, die Hilfe beim Schreiben des Manuskripts (Vgl. Chapter 2) und die konstruktive Kritik bei der Durchsicht der Arbeit.

Herrn Prof. Dr. Armin Buschauer (verstorben am 18.07.2017) für die Möglichkeit der Mitarbeit an einem interessanten und anspruchsvollen Forschungsprojekt, sowie seine wissenschaftlichen Förderungen.

Herrn Dr. David Wifling für die Übernahme der Senior-Autorenschaft, der Hilfe beim Schreiben des Manuskripts sowie der Durchführung der "Molecular-Docking" und "Molecular-Dynamics" Simulationen (Vgl. Chapter 2).

Herrn Dr. Max Keller für die wissenschaftlichen Ratschläge, die Organisation von Synthese und Lehrstuhlseminaren, die Hilfe beim Schreiben des Manuskripts (Vgl. Chapter 2) und die konstruktive Kritik bei der Durchsicht der Arbeit.

Frau Theresa Sailer (geb. Bauer) für die Synthese folgender Verbindungen **2.39**, **2.42**, **2.53-2.55** und der pharmakologischen Charakterisierung folgender Verbindungen **2.53-2.55** im Rahmen Ihrer Masterarbeit (Universität Regensburg, 2016) (Vgl. Chapter 2).

Herrn Lukas Grätz für für die Charakterisierung des Fluoreszenzliganden **4.58** (Sättigungsexperimente, Experimente zur Kinetik) (Vgl Chapter 4, Chapter 5) und die Bindungsexperimente von pNPY. Die Kultivierung der Zellen und das Einarbeiten von Frau Maria Beer-Krön in den BRET Bindungsexperimente.

Frau Carina Höring für für die Durchführung des "miniG Protein recruitment assays" und die Charakterisierung von pNPY, **4.1** und **4.75**. Ebenso für die Unterstützung bei der Kultivierung der Zellen, so dass ich die weitere Verbindungen in Ihrem Testsystem charakterisieren konnte (Vgl. Chapter 4).

Herrn Dr. Timo Littmann für die Hilfe beim Erlernen des " β -Arrestin2 recruitment assays" (Vgl. Chapter 3, Chapter 4, Chapter 5) und den Radioliganden-Bindungsexperimenten am Y₂R (Vgl. Chapter 4, Chapter 5).

Herrn Christoph Müller für seine wissenschaftlichen Ratschläge und die Synthese von Verbindung **2.4** (Vgl. Chapter 2, Chapter 5).

Frau Lisa Sauer und Dr. Stefanie Michaelis für die Hilfe bei der Durchführung der Konfokalmikroskopie-Experimente.

Frau Dr. Stefanie Dukorn für die Kultivierung verschiedener Zelllinien und die Beantwortung vieler Fragen bezüglich Radioligandenbindungsexperimenten am Y₂R.

Meinen engagierten Forschungspraktikanten Maria Deichner, Alexander Reichle, Alexander Hubmann, Simon Scheuerer und Florian Fricke und Wahlpflichtfachstudenten Sebastian Prien und Markus Scheiblecker für die Unterstützung bei zahlreichen Synthesen.

Frau Brigitte Wenzl für die Kultivierung verschiedener Zelllinien und die Durchführung zahlreicher Radioligand Bindungsstudien am Y₁R (Vgl. Chapter 2, Chapter 3, Chapter 4, Chapter 5).

Frau Elvira Schreiber für die tatkräftige Unterstützung bei der Durchführung von Fura-2 Ca²⁺ assays (Chapter 2).

Frau Susanne Bollwein für die Kultivierung verschiedener Zelllinien und die Hilfe bei der Durchführung von Radioligandenbindungsexperimenten an Y₂R und Y₅R.

Frau Maria Beer-Krön für die Kultivierung verschiedener Zelllinien und die Hilfe bei der Durchführung der BRET Bindungs-Experimente (Vgl. Chapter 4, Chapter 5).

Frau Lydia Schneider für die Unterstützung bei der Durchführung von Fura-2 Ca²⁺ assays (Chapter 2) und Radioligand-Bindungsexperimenten am Y₅R (Chapter 4).

Den Mitarbeitern der Zentralen Analytik für die Durchführung der NMR-Spektroskopie, Massenspektrometrie, Elementaranalysen und Röntgenstrukturanalyse. Insbesondere Herrn Fritz Kastner, der zahlreiche NMR Spektren aufgenommen hat.

Den Mitarbeitern Feinmechanische Werkstatt Chemie & Pharmazie für die Anfertigung der Absaugbrücke und Herrn Andreas Graf für die Bereitstellung der technischen Zeichnungen.

Herrn Peter Richthammer für die netten Gespräche und seine Hilfsbereitschaft bei der Lösung technischer Probleme jeder Art.

Allen Mitgliedern des Lehrstuhls für Ihre Kollegialität und das gute Arbeitsklima.

Mein besonderer Dank gilt Christoph Müller, Xueke She (Coco), Matthias Scholler, José-Esteban Olbreque Balboa, Adam Konieczny, Sabrina Biselli, Timo Littmann, Edith Bartole, Lukas Grätz, Jianfei-Wan, Frauke Antoni, Carina Höring, Katharina Tropmann, Lisa Schindler, Lisa Forster, Ulla Seibel und Andrea Pegoli für Persönliche Unterstützung und aufmunternde Gespräche.

Ein besonderer Dank gilt Christoph Müller, Lukas Wirth, Simon Scheuerer, Lukas Grätz für die gemeinsamen Abende an der Uni oder in Stadt mit einem kühlen Bier.

Ich möchte mich herzlichst bei Herrn Dr. Alastair Donald für die kritische Durchsicht der vorliegenden Arbeit, die vielen wertvollen Kommentare sowie die sprachlichen Hinweise bedanken. Ebenso möchte ich Herrn Dr. Michael Größ für die Hinweise und Kommentare bezüglich Kristallstrukturen (Vgl. Chapter 6) danken.

Abschließend möchte ich mich bei meinen Eltern, meiner Schwester Hannah und meinem Bruder Simon für Ihre Unterstützung über die letzten 5 Jahre bedanken. An dieser Stelle sei auch Werner und Lis gedankt. Ebenso möchte ich mich bei Arber Shima bedanken, der mir bei einigen Formatierungsproblemen geholfen hat und in den letzten 5 Jahren zu einem guten Freund geworden ist.

Contents

1. General introduction	1
1.1. Neuropeptide Y (NPY) receptors: endogenous ligands, signalling pathway and biological effects.....	2
1.2. NPY Y ₁ R and ligands	3
1.3. NPY Y ₂ R and ligands	4
1.4. NPY Y ₄ R and ligands	5
1.5. NPY Y ₅ R and ligands	7
1.6. Scope	8
1.7. References	10
2. Argininamide-type neuropeptide Y Y₁ receptor antagonists: the nature of N^ω-carbamoyl substituents determines Y₁R binding mode and affinity	21
2.1. Introduction.....	22
2.2. Results and discussion	24
2.2.1. Synthesis	24
2.2.2. Competition binding and functional studies	25
2.2.3. Correlation of p <i>K_i</i> values with van der Waals volumes of the carbamoyl residues	28
2.2.4. Induced fit docking and molecular dynamics (MD) simulations.....	29
2.3. Conclusion.....	31
2.4. Experimental section.....	32
2.4.1. General experimental conditions	32
2.4.2. Synthesis protocols and analytical data.....	33
2.4.3. Investigation of the chemical stability of 2.56 , 2.58-2.61 , 2.63 and 2.68	52
2.4.4. Pharmacological methods: radioligand competition binding assay in SK-N-MC cells and Fura-2 Ca ²⁺ assay	52
2.4.4.1. Radioligand competition binding assay in SK-N-MC cells	52
2.4.4.2. Fura-2 Ca ²⁺ assay	52
2.4.5. Screening for pan-assay interference compounds (PAINS).....	52
2.4.6. Computational chemistry	52
2.4.6.1. Receptor and ligand preparation	52
2.4.6.2. Induced-fit docking	53
2.4.6.3. Molecular dynamics (MD) simulation	53
2.4.7. Calculation of van der Waals volumes.....	53
2.4.8. Data analysis	54
2.5. References	55
3. Additional characterization of argininamide-type neuropeptide Y Y₁ receptor antagonists presented in chapter 2: β arrestin2 recruitment, Y₁R selectivity and investigation of potential irreversibly binding ligands	59
3.1. Introduction.....	60
3.2. Results and discussion	60

3.2.1. Pharmacological methods: Y ₁ R antagonism (pK _b) in a β-arrestin2 recruitment assay, NPY Y ₁ R subtype selectivity and potential irreversibly binding ligands (2.60 and 2.63)	60
3.2.1.1. Determination of pK _b values in a β-arrestin2 recruitment assay	60
3.2.1.2. NPY Y ₁ R subtype selectivity.....	62
3.2.1.3. Investigation on potential irreversibly binding ligands (2.60 and 2.63).....	63
3.3. Conclusion.....	68
3.4. Experimental section.....	69
3.4.1. General experimental conditions	69
3.4.2. Investigation of chemical stability of compounds 2.60 and 2.63 in presence of 2-mercaptoethanol.....	69
3.4.3. Pharmacological methods: cell culture, β-arrestin2 recruitment assay (Y ₁ R), saturation binding assay, radioligand binding assay for hY ₄ R and hY ₅ R	69
3.4.3.1. Cell culture.....	69
3.4.3.2. β-Arrestin2 recruitment assay (Y ₁ R).....	70
3.4.3.3. Saturation binding assay	71
3.4.3.4. Radioligand binding assay for hY ₄ R and hY ₅ R.....	71
3.4.4. Data analysis	72
3.5. References.....	73
4. Synthesis, pharmacological characterization and application of the fluorescent (S)-argininamide-type hY₂R antagonist UR-jb264 (4.58)	75
4.1. Introduction.....	76
4.2. Results and discussion	78
4.2.1. Synthesis	78
4.2.2. Investigation of the chemical stability of 4.50 , 4.51 and 4.58	83
4.2.3. Fluorescence properties	84
4.2.4. Pharmacological methods: Y ₂ R affinity (pK _i) and antagonism (pK _b) of synthesized (S)-argininamides, application of 4.58 to BRET based binding assays and confocal microscopy, NPY Y ₂ R subtype selectivity.....	86
4.2.4.1. Radioligand binding assay in HEK293T hY ₂ R + βArr2 cells	86
4.2.4.2. Determination of pK _b values in a β-arrestin2 recruitment assay	89
4.2.4.3. Determination of pK _b values in a miniG protein recruitment assay	91
4.2.4.4. Application of 4.58 to BRET based binding assays	92
4.2.4.5. Application of 4.58 to confocal microscopy	98
4.2.4.6. NPY Y ₂ R subtype selectivity.....	99
4.3. Conclusion.....	100
4.4. Experimental section.....	101
4.4.1. General experimental conditions	101
4.4.2. Synthesis protocols and analytical data.....	102
4.4.3. Investigation of the chemical stability of 4.50 , 4.51 and 4.58	129
4.4.4. Fluorescence properties	130

4.4.5. Pharmacological methods: cell culture, crystal violet assay, saturation and competition binding experiments with [³ H]propionyl-pNPY in HEK293T βArr2 + Y ₂ R cells, β-arrestin2 recruitment assay (Y ₂ R), miniG protein recruitment assay, BRET based binding assay, confocal microscopy and radioligand binding assay for hY ₁ R, hY ₄ R and hY ₅ R	130
4.4.5.1. Cell culture.....	130
4.4.5.2. Crystal violet assay.....	131
4.4.5.3. Saturation and competition binding with [³ H]propionyl-pNPY in HEK293T βArr2 + Y ₂ R cells	132
4.4.5.4. β-Arrestin2 recruitment assay (Y ₂ R).....	133
4.4.5.5. MiniG protein recruitment assay.....	134
4.4.5.6. BRET based binding assay	134
4.4.5.7. Confocal microscopy	135
4.4.5.8. Radioligand binding assay for hY ₁ R, hY ₄ R and hY ₅ R	136
4.4.6. Data analysis	136
4.5. References	138
5. In search for labelled Y₂R antagonists: synthesis and pharmacological characterization of labelling precursors and “cold” forms of potential Y₂R radioligands obtained by modification of the (S)-argininamide BIIE-0246 at the dibenzoazepinone moiety	145
5.1. Introduction.....	146
5.2. Results and discussion	147
5.2.1. Synthesis	147
5.2.2. Investigation of the chemical stability of 4.23 , 4.24 , 4.27 , 5.9 , 5.30 and 5.32	149
5.2.3. Pharmacological methods: Y ₂ R affinity (pK _i) and antagonism (pK _b) of synthesized (S)-argininamides.....	150
5.2.3.1. Determination of pK _i values in a radioligand binding assay in HEK293T hY ₂ R + βArr2 cells.....	151
5.2.3.2. Determination of pK _i values in a BRET based binding assay	152
5.2.3.3. Determination of pK _b values in a β-arrestin2 recruitment assay	153
5.2.3.4. NPY Y ₂ R subtype selectivity.....	154
5.3. Conclusion.....	155
5.4. Experimental section.....	156
5.4.1. General experimental conditions	156
5.4.2. Synthesis protocols and analytical data.....	157
5.4.3. Investigation of the chemical stability of 4.23 , 4.24 , 4.27 , 5.9 , 5.30 and 5.32	171
5.4.4. Pharmacological methods: cell culture, radioligand competition binding assay on HEK293T βArr2 + Y ₂ R cells, BRET based binding assay and β-arrestin2 recruitment assay (Y ₂ R), radioligand binding assay for hY ₁ R, hY ₄ R and hY ₅ R	171
5.4.4.1. Cell culture.....	171

5.4.4.2.	Radioligand competition binding assay in HEK293T β Arr2 + Y ₂ R cells.....	171
5.4.4.3.	BRET based binding assay	171
5.4.4.4.	β -Arrestin2 recruitment assay (Y ₂ R).....	171
5.4.4.5.	Radioligand binding assay for hY ₁ R, hY ₄ R and hY ₅ R	171
5.4.5.	Data analysis	171
5.5.	References	172
6.	Synthesis and pharmacological investigation of substituted	
	(<i>R,R</i>)-diaminocyclohexanes as potential non-peptide ligands for the hY₄R	175
6.1.	Introduction.....	176
6.2.	Results and discussion	178
6.2.1.	Annotation concerning stereochemistry.....	178
6.2.2.	Synthesis	178
6.2.3.	Pharmacological methods: investigations of test compounds in a radioligand binding assay, an aequorin Ca ²⁺ assay and a cytotoxicity assay (live/dead staining)	183
6.2.3.1.	Displacement studies of investigated compounds in a radioligand competition binding assay on CHO-hY ₄ R-G _{q15} -mtAEQ cells	184
6.2.3.2.	Modulatory effects of test compounds on the action of hPP in an aequorin Ca ²⁺ assay.....	185
6.2.3.3.	Investigation of cytotoxicity by ethidium bromide/acridine orange staining (live/dead staining)	187
6.3.	Conclusion.....	187
6.4.	Experimental section.....	189
6.4.1.	General experimental conditions	189
6.4.2.	Synthesis protocols and analytical data.....	190
6.4.3.	X-Ray crystallography of compounds (<i>R,R,S</i>)- 6.6b and (<i>R</i>)- 6.17	208
6.4.3.1.	X-Ray crystallography of compounds (<i>R,R,S</i>)- 6.6b	208
6.4.3.2.	X-Ray crystallography of (<i>R</i>)- 6.17	210
6.4.4.	Pharmacological methods: cell culture, radioligand competition binding assay in CHO-hY ₄ R-G _{q15} -mtAEQ cells, aequorin Ca ²⁺ assay, ethidium bromide/acridine orange staining (live/dead staining).....	212
6.4.4.1.	Cell culture.....	212
6.4.4.2.	Radioligand competition binding assay in CHO-hY ₄ R-G _{q15} -mtAEQ cells	212
6.4.4.3.	Aequorin Ca ²⁺ assay.....	212
6.4.4.4.	Ethidium bromide/acridine orange staining (live/dead staining).....	213
6.4.5.	Data analysis	213
6.5.	References	215
7.	Summary.....	219
8.	Appendix.....	223
8.1.	Chapter 2.....	224
8.1.1.	Supplementary figure 8.1.....	224

8.1.2.	Supplementary table 8.1	225
8.1.3.	¹ H-NMR and ¹³ C-NMR spectra of compounds 2.53-2.76	226
8.1.4.	RP-HPLC purity chromatograms (220 nm) of compounds 2.53-2.76 and 2.78	250
8.1.5.	Investigation of the chemical stability of compounds 2.58-2.61 , 2.63 and 2.68	255
8.1.5.1.	Supplementary figure 8.2	255
8.1.5.2.	Supplementary figure 8.3	256
8.2.	Chapter 4.....	257
8.2.1.	Supplementary figure 8.4.....	257
8.2.2.	¹ H-NMR and ¹³ C-NMR spectra of compounds 4.1 , 4.5 , 4.23 , 4.24 , 4.27 , 4.32 , 4.50 , 4.51 and 4.75	258
8.2.3.	RP-HPLC purity chromatograms (220 nm) of compounds 4.1 , 4.5 , 4.23 , 4.24 , 4.27 , 4.32 , 4.50 , 4.51 , 4.58 , 4.59 , 4.61 , 4.62 and 4.75	270
8.3.	Chapter 5.....	273
8.3.1.	Investigation of the chemical stability of compounds 5.9 and 5.30	273
8.3.1.1.	Supplementary figure 8.5	274
8.3.2.	¹ H-NMR and ¹³ C-NMR spectra of compounds 5.9 , 5.12 , 5.20 and 5.29-5.32	271
8.3.3.	RP-HPLC purity chromatograms (220 nm) of compounds 5.9 , 5.12 , 5.20 and 5.29-5.32	285
8.4.	Chapter 6.....	287
8.4.1.	¹ H-NMR and ¹³ C-NMR spectra of compounds (<i>R,R,S*</i>)- 6.6a , (<i>R,R,S</i>)- 6.6b , (<i>R,R,S*</i>)- 6.7a , (<i>R,R,S*</i>)- 6.6b , 6.7 , 6.9 , 6.12 , 6.13 , (<i>S*</i>)- 6.18a , (<i>S*</i>)- 6.18b , 6.34-6.44 , 6.47 and 6.48	287
8.4.2.	RP-HPLC purity chromatograms (220 nm) of compounds (<i>R,R,S*</i>)- 6.6a , (<i>R,R,S</i>)- 6.6b , (<i>R,R,S*</i>)- 6.7a , (<i>R,R,S*</i>)- 6.6b , 6.7 , 6.9 , 6.12 , 6.13 , (<i>S*</i>)- 6.18a , (<i>S*</i>)- 6.18b , 6.34-6.44 , 6.47 and 6.48	310
8.4.3.	Crystal data of compounds (<i>R,R,S</i>)- 6.6a and (<i>R</i>)- 17	314
8.4.3.1.	Crystal data of (<i>R,R,S</i>)- 6.6a	314
8.4.3.2.	Crystal data of (<i>R</i>)- 6.17	321
8.5.	Abbreviations	329
8.6.	References	333

Chapter 1

General introduction

1.1. Neuropeptide Y (NPY) receptors: endogenous ligands, signalling pathway and biological effects

The neuropeptide Y (NPY) receptors belong to the superfamily of G-protein coupled receptors (GPCRs) class A (rhodopsin-like receptors).¹ Four different subtypes (Y₁R,^{2, 3} Y₂R,⁴⁻⁶ Y₄R,⁷⁻⁹ and Y₅R^{9, 10}) are functional in human beings and distributed both in the central nervous system (CNS) and the periphery.^{11, 12} The Y₆R is not functional in humans, absent in rats and proved to be functional in mice and rabbits.¹³ These receptors are activated by a family of peptides (neuropeptide Y (NPY), peptide YY (PYY) and pancreatic polypeptide (PP)), which share (structural) similarities such as a sequence comprising 36 amino acids, a large number of tyrosine residues and an amidated C-terminus (Figure 1.1).^{14, 15} NPY and PYY show higher affinity towards Y₁R, Y₂R and Y₅R compared to the Y₄R, whereas PP binds preferentially to the Y₄R.¹⁴ Porcine neuropeptide Y (pNPY) shows nearly the same affinity and potency compared to hNPY and is preferably used (*in vitro* studies) because of its higher chemical stability.^{16, 17} The amino acid sequences of the aforementioned peptides differ in position 17, whereas in pNPY the methionine (M) residue is replaced by a leucine (L) residue.^{16, 17}

YPSKPDNPGEDAPAEDMARYYSALRHYINLITRQRY-NH ₂	hNPY
YPIKPEAPGEDASPEELNRYASLRHYLNLVTRQRY-NH ₂	hPYY
APLEPVYPGDNATPEQMAQYAADLRRYINMLTRPRY-NH ₂	hPP

Figure 1.1. Amino acid sequences (one letter code) of hNPY, hPYY and hPP.

The NPY receptor subtypes (Y₂R and Y₄R) show sensitivity to sodium cations, which leads to a discrepancy in determined affinities of agonists in sodium containing and sodium-free buffers.¹⁸⁻²⁰ The phenomenon of negative allosteric modulation of the Y₄R by sodium cations has also been reported in the literature for other GPCRs (e.g. μ OR,²¹ A_{2A}R,²² PAR1²³, D_{2L}R²⁴ and β ₁AR²⁵), with sodium cations stabilizing the inactive states of the receptors.²⁶ Therefore, affinities of ligands at NPY receptors (Y₁R, Y₂R, Y₄R and Y₅R) were determined in radioligand competition binding assays in sodium-containing (Y₁R, Y₅R) or sodium-free binding buffer (Y₂R, Y₄R) according to published procedures (*cf.* Chapter 2, 4, and 6).^{19, 27-29}

When the NPY receptors are activated by endogenous ligands (NPY, PYY or PP), the signalling is mediated by the G_i/G_o α subunit, which inhibit the adenylyl cyclase (AC). As a result, the transformation of ATP to the second messenger cAMP is prevented.^{14, 30, 31} It is reported that NPY receptors can activate the phospholipase C (PLC), which catalyzes the production of inositol-1,4,5-trisphosphate (IP₃) and leads to Ca²⁺ release from intracellular stores.³¹⁻³⁵ The extent of the Ca²⁺ response is dependent on the cell-type.³⁰

The stimulation of NPY receptors (Table 1.2) by endogenous ligands (NPY, PYY, PP) has an impact on several biological processes that are also involved in multiple diseases: energy homeostasis (obesity, obesity-associated diseases),^{12, 36-41} circadian rhythm,^{42, 43} seizures (epilepsy),^{44, 45} pain modulation,^{46, 47} inhibition of trigeminovascular pathway (migraine),^{48, 49} neurodegeneration (Huntington's and Alzheimer's disease),^{12, 50-52} blood pressure (hypertension),^{53, 54} regulation of processes involved in tumour growth (angiogenesis, cell proliferation)^{55, 56} and psychotic disorders (anxiety, schizophrenia, alcohol abuse, depression).^{12, 57-60}

Table 1.1. Overview of receptor expression (Y₁R, Y₂R, Y₄R and Y₅R) and biological effects elicited upon stimulation of the individual NPY receptor subtypes

Receptor subtypes	Receptor expression	Biological effects
Y ₁ R	brain, blood vessels, heart, kidney, gastrointestinal tract (GIT)	food intake (↑), energy homeostasis (↓), regulation of blood pressure (vasoconstriction), anxiety (↓), seizure (↑), depression (↓), pain sensitivity (↓), regulation of ethanol consumption, angiogenesis, inhibition of trigeminovascular pathway (migraine), luteinizing hormone (LH) secretion (↑), gastrointestinal motility (↑)
Y ₂ R	brain, intestine, blood vessels, liver, spleen, adipose tissue	food intake (↓), energy homeostasis (↑), regulation of blood pressure (bradycardia), anxiety (↑), enhanced memory retention, bone formation (hypothalamic regulated), seizure (↓), depression (↑), pain sensitivity (?), gastrointestinal motility (↓), angiogenesis (↑), schizophrenia-related symptoms (↑), regulation (presynaptic autoreceptor) of NPY release (↓), neurotransmitter release (e.g. noradrenaline) (↓), neuroprotection (associated in patients with Huntington's disease)
Y ₄ R	brain, skeletal muscle, thyroid gland, GIT	food intake (↓), anxiety (?), gastrointestinal motility (↑), LH secretion (↑), pancreatic secretion (↓), gall bladder contraction
Y ₅ R	brain, intestine, ovary, pancreas, skeletal muscle, spleen	food intake (↑), anxiety (?), seizure (?), angiogenesis (↑), regulation of circadian rhythm, LH secretion (↓)

Information was collected from the following publications: Shende et al.⁶¹, Gehlert,⁶² Pedrazzini et al.,⁶³ Yi et al.,¹¹ Merten et al.,⁶⁴ Li et al.,⁶⁵ Martins-Oliveira et al.,⁴⁸ Chen et al.,⁶⁶ Zukowska et al.⁶⁷ and Reichmann et al.¹²

1.2. NPY Y₁R and ligands

The Y₁R is expressed in the brain (hypothalamus, hippocampus, neocortex), in blood vessels, heart, kidney and the gastrointestinal tract.^{61, 64, 65} As the Y₁R is overexpressed in different types of cancer (e.g. breast cancer, renal cell carcinomas, ovarian cancer),⁶⁸⁻⁷⁰ therefore labelled ligands can be used as imaging agents (PET-ligands).⁶⁵ Furthermore, selective Y₁R ligands conjugated to cytotoxic agents (e.g. doxorubicine) could be of potential use in the treatment of breast cancer to reduce side effects in tumour therapy.^{65, 69, 71} Several structurally diverse and selective non-peptide Y₁R antagonists have been reported in literature (Figure 1.2).

The (*R*)-argininamide-type ligand BIBP-3226⁷² was the first selective Y₁R antagonist, which was intended to mimic the C-terminal part of NPY. A *D*-alanine scan of NPY revealed the importance of the C-terminal amidated pentapeptide for Y₁R and Y₂R binding and emphasized the importance of arginine residues 33 and 35 for Y₁R binding.⁷³ The stereoselectivity of Y₁R binding of BIBP-3226 became obvious, as the (*S*)-enantiomer of BIBP-3226 (BIBP-3435) show very low affinity against Y₁R and Y₂R ($pK_i < 5$).⁷⁴ The (*R*)-argininamide type hY₁R antagonists BIBP-3226⁷², and BIBO-3304⁷⁵ have been used in our group for the synthesis of molecular tools^{27, 76, 77} (e.g. radio- and fluorescence-labelled ligands) and PET ligands.^{78, 79} Additionally, bivalent ligands based on BIBP-3226 have been prepared as molecular tools to investigate Y₁R dimerization.⁸⁰ *N*^ω-carbamoylation of BIBP-3226 led to the high affinity

ligands UR-HU-404^{27, 81} and UR-MK299²⁷, the latter being the cold form of the valuable radioligand [³H]UR-MK299, useful for the determination of binding constants of non-labelled compounds.⁸² For X-ray diffraction analysis, the hY₁R was recently co-crystallized with the selective Y₁R antagonists BMS-193885 and UR-MK299.⁸³ From the crystal structure, it became obvious that the carbamoylguanidine group of UR-MK299 forms a hydrogen-assisted salt bridge with D287^{6.59} and the diphenylacetyl residue showed hydrophobic interactions with F282^{6.54}, F286^{6.58} and F302^{7.35, 83}

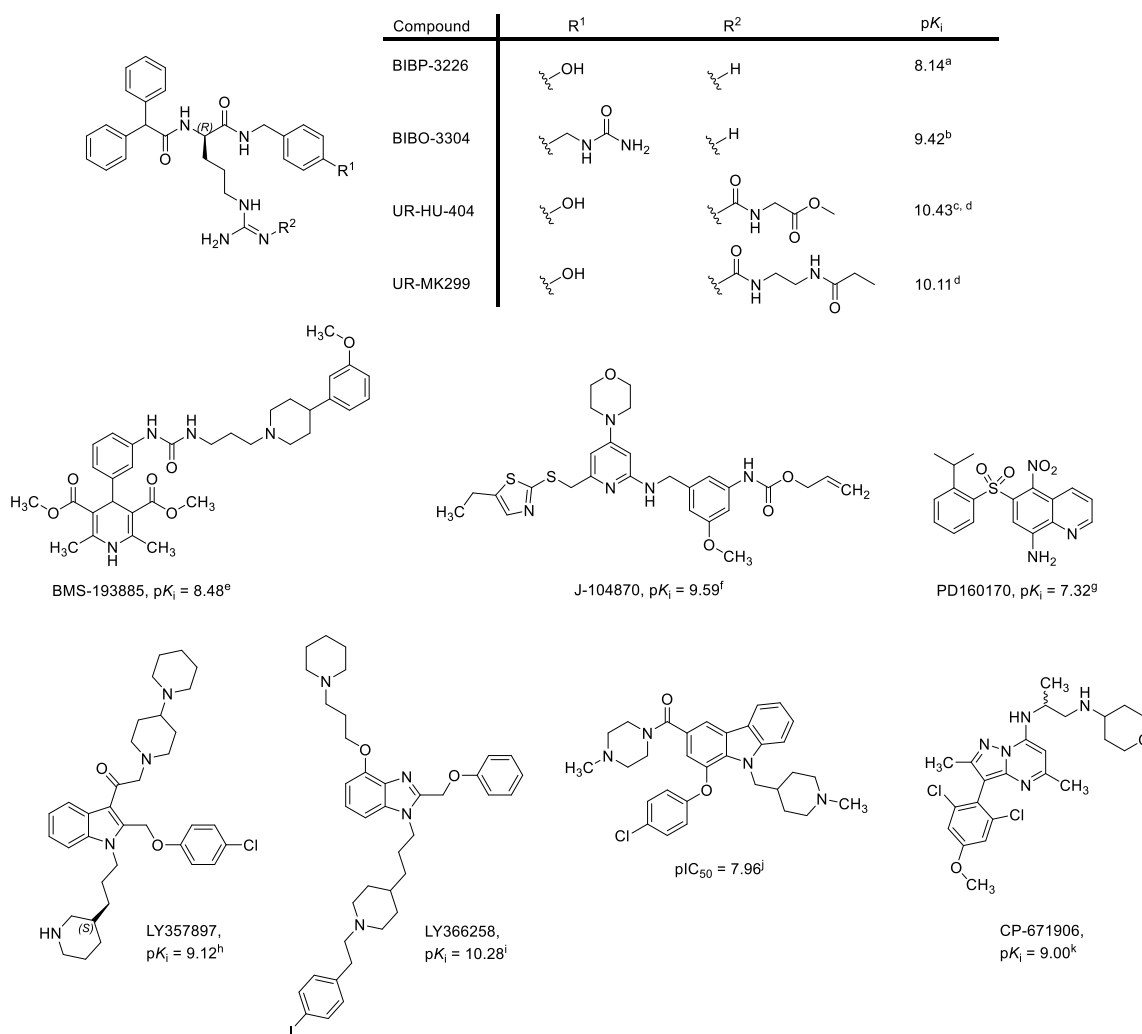


Figure 1.2. Structures of selected non-peptide NPY Y₁R antagonists. References: (a) Rudolf et al.,⁷² (b) Wieland et al.,⁷⁵ (c) Hutzler, PhD Thesis, University of Regensburg, 2001,⁸¹ (d) Keller et al.,²⁷ (e) Poindexter et al.,⁸⁴ (f) Kanatani et al.,⁸⁵ (g) Wright et al.,⁸⁶ (h) Hipskind et al.,⁸⁷ (i) Zarrinmayeh et al.,⁸⁸ (j) Leslie et al.,⁸⁹ (k) Griffith et al.⁹⁰ Reported K_i (IC₅₀) values were converted to pK_i (pIC₅₀) values.

1.3. NPY Y₂R and ligands

The Y₂R is mostly expressed in the brain (hippocampus, thalamus, hypothalamus), intestine, postrema, in blood vessels, liver, spleen and adipose tissue.^{61, 64, 65} Beside the endogenous ligands NPY and PYY, several selective Y₂R agonists (e.g. NPY(13-36), PYY(3-36))⁹¹⁻⁹³ and non-peptide antagonists have been reported (Figure 1.3). The (S)-argininamide BIIE-0246⁹⁴ was the first non-peptide Y₂R selective antagonist with a one-digit nanomolar binding constant determined by radioligand competition binding assay. A D-alanine scan of NPY (as already mentioned previously), revealed the importance of Arg³⁵ and Tyr³⁶ residues for Y₂R binding.⁷³ Furthermore, site directed mutagenesis of the Y₂R and docking

studies in a homology model of the Y₂R revealed that the dibenzoazepinone moiety of BIIE-0246 binds in a deep hydrophobic pocket (L^{4.60}, L^{5.46}, L^{6.51}) and shows interactions with TM II and VII (Y^{2.64}, F^{7.35}).⁹⁵ Additionally, this study demonstrated that BIIE-0246 and NPY share an interaction, which is not addressed by other antagonists (e.g. derivatives of CYM-9484) with the Y₂R.⁹⁵ The guanidine-acylguanidine bioisosteric approach led to a series of BIIE-0246 related Y₂R antagonists.⁹⁶⁻⁹⁸ These synthesized acylguanidines showed similar affinity and selectivity compared to the lead compound BIIE-0246.⁹⁶⁻⁹⁸ This was the starting point in our workgroup for the synthesis of radio-labelled (e.g. [³H]UR-PLN196⁹⁹), fluorescent⁹⁸ and bivalent⁹⁸ ligands. The *N*^ω-acylated (*S*)-argininamide [³H]UR-PLN196 (p*K*_d = 7.2, reported *K*_d value was converted to p*K*_d value) was the first selective non-peptide radioligand at the Y₂R.⁹⁹ Dissociation experiments revealed pseudo-irreversible binding of [³H]UR-PLN196 at the Y₂R, whilst in functional assays the cold form UR-PLN196 showed insurmountable antagonism.⁹⁹

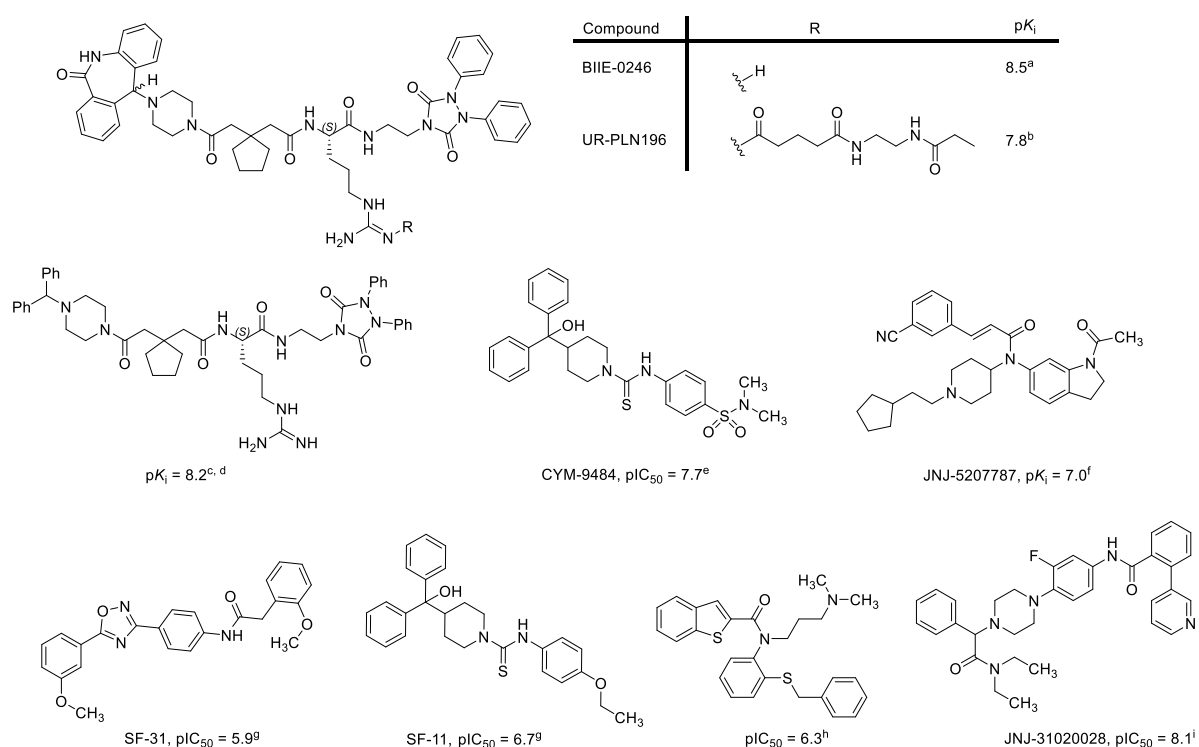


Figure 1.3. Structures of selected non-peptide NPY Y₂R antagonists. References: (a) Doods et al.,⁹⁴ (b) Pluym et al.,⁹⁹ (c) Dollinger et al.,¹⁰⁰ (d) Ziemek et al.,¹⁰¹ (e) Mittapalli et al.,¹⁰² (f) Bonaventure et al.,¹⁰³ (g) Brothers et al.,¹⁰⁴ (h) Andres et al.,¹⁰⁵ (i) Shoblock et al.¹⁰⁶ Reported *K*_i (IC₅₀) values were converted to p*K*_i (pIC₅₀) values.

1.4. NPY Y₄R and ligands

The Y₄R is distributed in the brain, skeletal muscle, the thyroid gland and the gastrointestinal tract.^{61, 64, 65} Several peptidic NPY Y₄R ligands are reported in literature (Figure 1.4). Previously Dukorn et al.¹⁸ described an analogue of [Lys⁴]hPP in which methionine residues were replaced by norleucine ([Lys⁴Nle^{17,39}]hPP) to prevent oxidation of methionine residues. [Lys⁴Nle^{17,39}]hPP was used as a precursor for fluorescence- and radio-labelling to obtain molecular tools.¹⁸

The dimeric peptide BVD-74 is a diastereomeric mixture, which shows high affinity and selectivity for the Y₄R as reported by Balasubramaniam et al.¹⁰⁷ BVD-74 contains two C-terminally amidated pentapeptides (Tyr-Arg-Leu-Arg-Tyr-NH₂) and 2,7-diaminooctanedioic acid as a linker. Kuhn et al.¹⁹ and

Liu et al.¹⁰⁸ have described the stereoselective synthesis of the (2*R*,7*R*)-diaminooctanedioic acid, which enabled the preparation of (2*R*,7*R*)-BVD-74. The described compound (2*R*,7*R*)-BVD-74 showed 5-fold higher binding affinity (with respect to K_i values) to the Y_4R than its diastereomer (2*S*,7*S*)-BVD-74 ($pK_i = 8.6$).¹⁹ Therefore, (2*R*,7*R*)-BVD-74 was used as a precursor for radio ($[^3H]$ UR-KK193) and fluorescence labelling (Figure 1.4).^{19, 108} Furthermore, Kuhn et al.¹⁹ described the synthesis of the heterodimeric radioligand $[^3H]$ UR-KK200. The linker in BVD-74 was replaced by non-chiral octanedioic acid and in one pentapeptide a *N*^ω-carbamoylated arginine was introduced to obtain a precursor for radiolabelling.¹⁹

In search for molecular tools targeting the Y_4R , a fluorescently labelled hexapeptide that showed moderate affinity was synthesized in our group.¹⁰⁹

The bivalent ligands UR-MK188 and UR-MEK288, originally synthesized to target the hY_1R , were the first described non-peptide antagonists that showed moderate affinity to the hY_4R (Figure 1.5). The replacement of the BIBP-3226 moiety in UR-MK188 by its *S*-configured optical antipode BIBP-3435 led to the selective hY_4R antagonist UR-MEK288.¹¹⁰

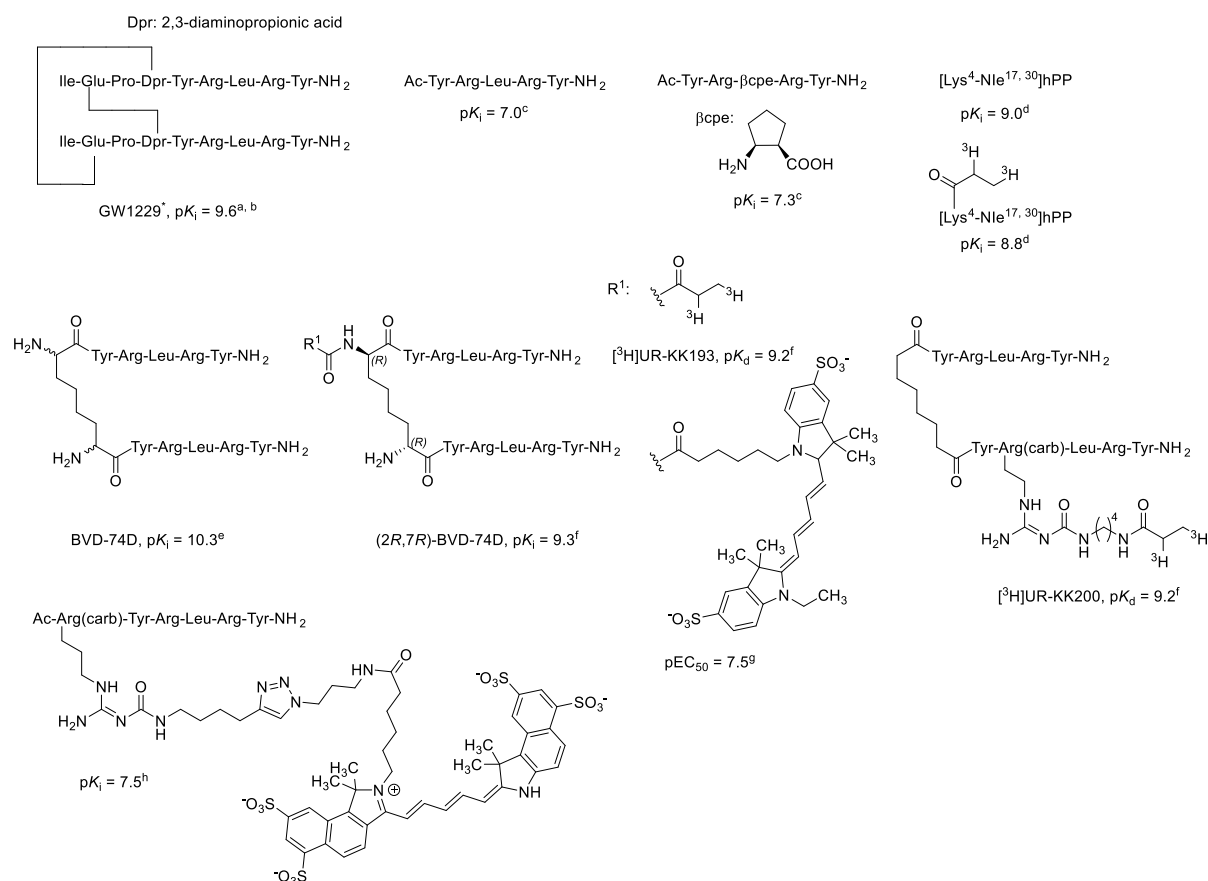


Figure 1.4. Structures of selected peptidic NPY Y_4R ligands. References: (a) Daniels et al.,¹¹¹ (b) Parker et al.,¹¹² (c) Berlicki et al.,¹¹³ (d) Dukorn et al.,¹⁸ (e) Balasubramaniam et al.,¹⁰⁷ (f) Kuhn et al.,¹⁹ (g) Liu et al.,¹⁰⁸ (h) Spinnler et al.¹⁰⁹ Reported K_i (K_d) values were converted to pK_i (pK_d) values. *note also designated GR231118 and 122U91.

Niclosamide and tBPC were reported as allosteric modulators of the hY_4R by Sliwowski et al.¹¹⁴ and Schubert et al.¹¹⁵ These ligands increased the response induced by PP in functional assays. The reported EC₅₀ values of niclosamide and tBPC were determined in an inositol phosphate (IP) accumulation assay (performed on COS7_ Y_4R -eYFP_Δ6Gα_{qi4}-myr cells) and in a Ca²⁺ assay (performed

on COS7_Y4R-eYFP_Δ6Gα_{qi4-myr} cells), respectively. In these assays, niclosamide or tBPC were added at increasing concentrations to a fixed concentration of PP that induced 20% of the maximal response (EC₂₀).^{114, 115}

Sun et al.¹¹⁶ and Ewing et al.^{117, 118} reported a series of adipic acids and (*R,R*)-diaminocyclohexanes as hY₄R ligands, termed as agonists, antagonists or modulators at the Y₄R. The pharmacological data is incomplete, as only subset of compounds were evaluated in a cAMP assay. According to the information (procedures) disclosed in the patent, these ligands should be considered as agonists.¹¹⁶⁻¹¹⁸

Kang et al.¹¹⁹ (Figure 1.5) identified a series of structurally diverse agonists via homology modelling. The potencies of these compounds as determined in a cAMP assay (prevention of forskolin stimulated transformation of ATP to cAMP in HEK293/NPY4R cells) were in the double-digit micromolar range.

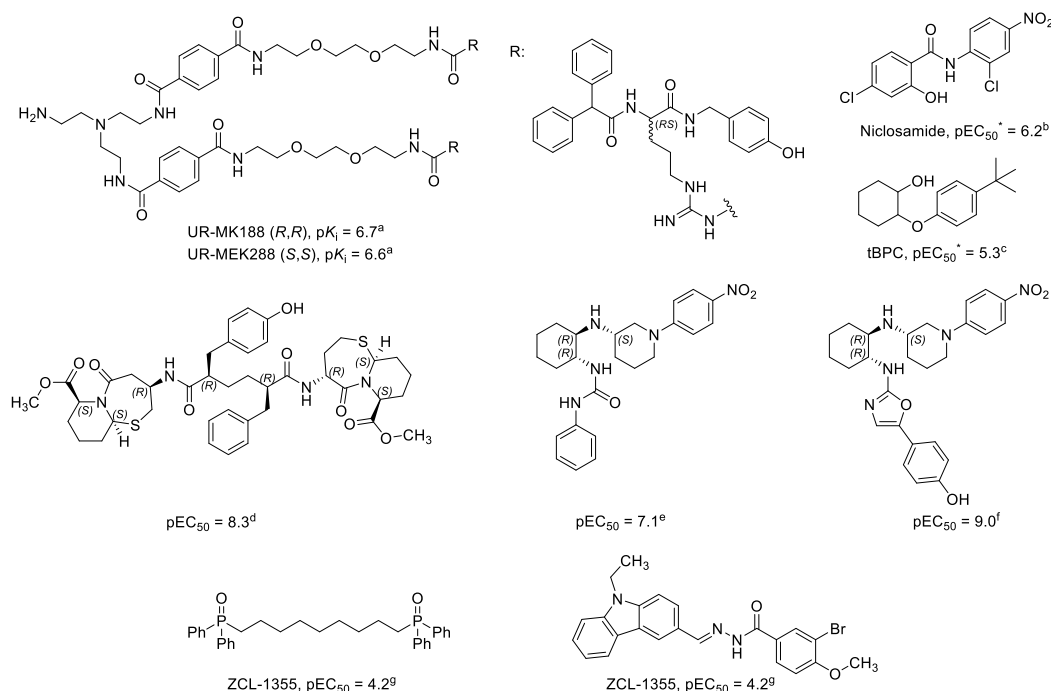


Figure 1.5. Structures of selected non-peptide hY₄R ligands (agonists, antagonists and modulators). References: (a) Keller et al.,¹¹⁰ (b) Sliwoski et al.,¹¹⁴ (c) Schubert et al.,¹¹⁵ (d) Sun et al.,¹¹⁶ (e) Ewing et al.,¹¹⁷ (f) Ewing et al.,¹¹⁸ (g) Kang et al.¹¹⁹ Reported pEC₅₀ (K_b) were converted to pEC₅₀ (K_b). *Niclosamide and tBPC increased the response induced by PP. pEC₅₀ values of modulators: Increasing concentrations of the ligands were added to a constant PP concentration (EC₂₀), that induced 20% of the maximal response.

1.5. NPY Y₅R and ligands

The Y₅R is expressed in the brain (hypothalamus, hippocampus), intestine, ovary, pancreas, skeletal muscle and spleen.^{61, 64, 65} A set of selective peptide Y₅R agonists ([D-Trp³⁴]-NPY, [cPP¹⁻⁷, NPY¹⁹⁻²³, Ala³¹, Aib³², Gln³⁴]-hPP) is described in literature^{120, 121} and several structurally distinct non-peptide Y₅R antagonist are known (Figure 1.6). Rüeeger et al.^{122, 123} (Rueeeger et al.) reported the first non-peptide antagonist CGP 71683A. It was shown that food intake in rat induced by NPY was blocked by CGP 71683A.^{123, 124} However, Della Zuana et al.¹²⁵ reported off-target effects (e.g. interactions with cholinergic-muscarinic receptors, α₂ adrenergic receptors and serotonin reuptake recognition site) of CGP 71683A, suggesting weight loss is likely not fully Y₅R mediated.^{46, 124, 125} It should be noted that the selective Y₅R antagonist MK-0577 entered clinical trials (multicentre, randomized, trial with 1661

obese patients, 52 weeks), but showed no relevant weight loss in obese patients.^{124, 126} To date, no Y₅R antagonist has entered the market for the treatment of obesity or any other medical indication.

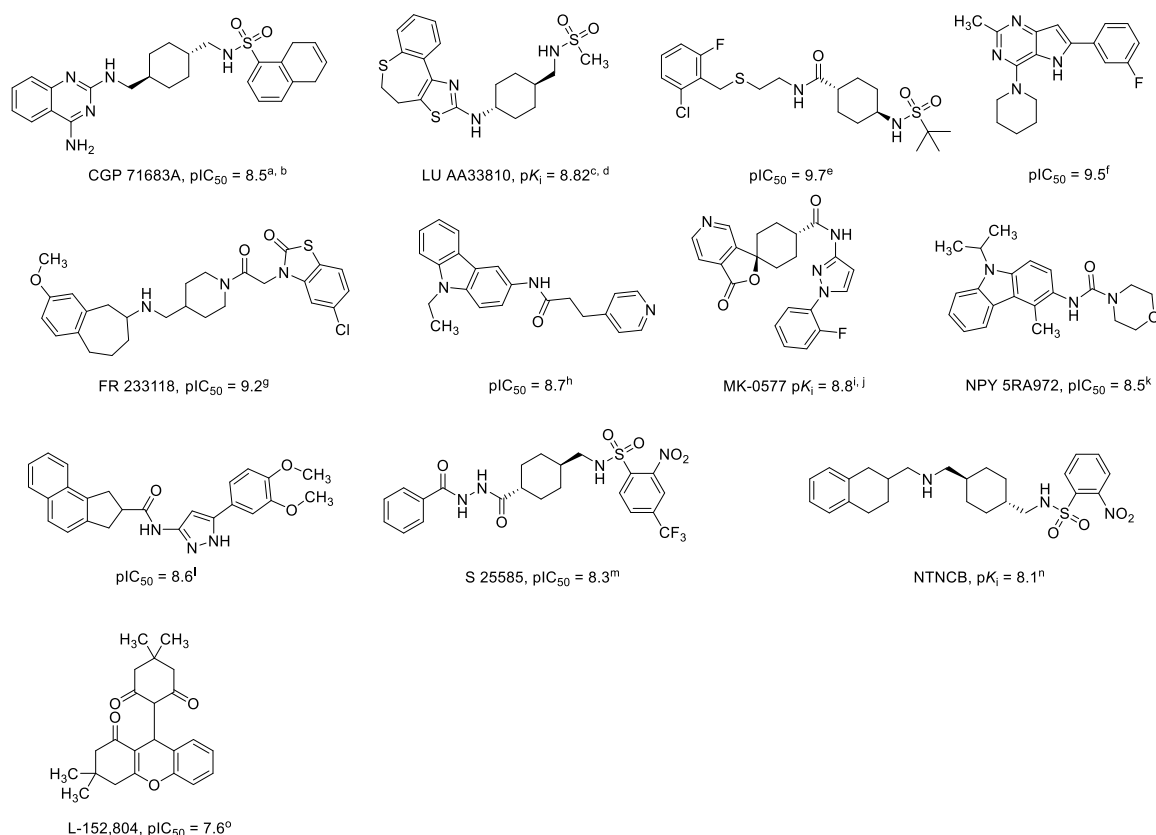


Figure 1.6. Structures of selected non-peptide NPY Y₅R antagonists. References: (a) R ueger et al.,¹²² (b) Rueeger et al.,¹²³ (c) Walker et al.,¹²⁷ (d) Packiarajan et al.,¹²⁸ (e) Kawanishi et al.,¹²⁹ (f) Norman et al.,¹³⁰ (g) Itani et al.,¹³¹ (i) Fukami et al.,¹³² (j) Fichtner et al.,¹³³ (k) Turnbull et al.,¹³⁴ (l) Sato et al.,¹³⁵ (m) Della-Zuana et al.,¹³⁶ (n) Islam et al.,¹³⁷ (o) Kanatani et al.¹³⁸ Reported K_i (IC₅₀) values were converted to pK_i (pIC₅₀) values.

1.6 Scope

Neuropeptide Y (NPY) is one of the most abundant peptides in the CNS and in the periphery, with four receptor subtypes (Y₁R, Y₂R, Y₄R and Y₅R) functional in humans.^{11, 12, 14} These NPY receptors are involved in many biological processes, such as food intake, seizures, stress response and circadian rhythm, to name but a few. Several of these biological processes are involved in diseases, such as metabolic syndrome, obesity and epilepsy.^{12, 61, 62} Furthermore, NPY receptors are overexpressed in several malignant tumours (e.g. breast cancer, renal cell carcinoma, ovarian cancer), which makes them promising targets for the diagnosis (PET-ligands) and treatment of cancers.⁶⁵ For the synthesis of PET, radio or fluorescence ligands an extensive knowledge of receptor ligand interaction is needed, which can be gained by SAR studies and analyzing crystal structures of the receptor.

The high-affinity ligand UR-MK299 was obtained by *N*^ω-carbamoylation of the (*R*)-argininamide type hY₁R antagonist BIBP-3226.²⁷ Recently, the hY₁R was co-crystallized with UR-MK299 and revealed that the carbamoylguanidine of UR-MK299 forms a hydrogen-assisted salt bridge with D287^{6,59} and the propionyl residue is buried in the subpocket between TM V and VI.⁸³ This subpocket seems to be incompletely filled by the propionyl moiety of UR-MK299.⁸³ The introduction of bulky moieties (e.g.

fluorophores) in *N*^ω-carbamoylated (*R*)-argininamides and their retained affinity does not seem to be compatible with the binding mode of UR-MK299.

One aim of this thesis was to answer the question of how the size (van der Waals volume) and structure of the carbamoyl residue of *N*^ω-carbamoylated (*R*)-argininamides structurally related to UR-MK299 affects Y₁R affinity and the binding mode. Therefore, a series of (*R*)-argininamides had to be synthesized and pharmacologically characterized in radioligand binding and functional assays. The most interesting compounds should be investigated by induced fit docking and molecular dynamics simulations to gain a deeper understanding of (*R*)-argininamide-type ligand binding at hY₁R, which is needed for the synthesis of novel PET or fluorescent ligands with retained affinity compared to UR-MK299.

The (*S*)-argininamide BIIE-0246 was the first non-peptide Y₂R antagonist.⁹⁴ BIIE-0246 was adopted as a lead structure for the synthesis of novel precursors for fluorescence- and radio-labelling, due to its high affinity towards the Y₂R. The pursuit of the guanidine-acyl guanidine approach led to the radioligand [³H]UR-PLN196⁹⁹, which was the first selective non-peptide radioligand addressing the Y₂R. In binding studies, this radioligand was displaced by pNPY in a biphasic manner, indicating that [³H]UR-PLN196 is not suitable for the determination of binding constants of peptides. To obtain more information on (*S*)-argininamide binding at the Y₂R, a different labelling strategy has to be applied. One aim of this approach was the discovery of new labelling sites in BIIE-0246 to obtain fluorescence or radiotracers. Therefore, the dipenzoazepinone moiety of BIIE-0246 should be replaced by an amino-functionalized benzhydryl moiety. Moreover, the replacement of the cyclopentyl moiety by an amine functionalized moiety could pave the way to novel labelled compounds. A new non-peptide radio- or fluorescent ligand could be useful for the determination of Y₂R binding data. Moreover, a novel amine functionalized precursor could be useful for the synthesis of PET ligands.

Ewing et al.^{117, 118} reported a series of (*R,R*)-diaminocyclohexanes, which purportedly act as agonists, antagonists or modulators at the hY₄R. Some of the reported ligands were investigated in a cAMP assay as agonists, but neither Y₄R affinities nor characterization as modulators were described in detail. Furthermore, niclosamide and tBPC were reported as first allosteric modulators at the hY₄R, augmenting the effect of the endogenous ligand.^{114, 115} Addressing the Y₄R by positive allosteric modulation instead of agonism could be a new therapeutic opportunity for the treatment of obesity. Based on the data published by Ewing et al.^{117, 118} another objective of this thesis was the synthesis of selected (*R,R*)-diaminocyclohexanes and to determine the affinities in established radioligand competition binding experiments and functional assays. Furthermore, the allosteric modulation of niclosamide and tBPC needs to be evaluated in functional assays.

1.7 References

1. Joost, P.; Methner, A. Phylogenetic analysis of 277 human G-protein-coupled receptors as a tool for the prediction of orphan receptor ligands. *Genome Biol* **2002**, *3*, research0063.1.
2. Larhammar, D.; Blomqvist, A. G.; Yee, F.; Jazin, E.; Yoo, H.; Wahlested, C. Cloning and functional expression of a human neuropeptide Y/peptide YY receptor of the Y1 type. *J Biol Chem* **1992**, *267*, 10935-10938.
3. Eva, C.; Keinänen, K.; Monyer, H.; Seeburg, P.; Sprengel, R. Molecular cloning of a novel G protein-coupled receptor that may belong to the neuropeptide receptor family. *FEBS Lett.* **1990**, *271*, 81-84.
4. Rose, P. M.; Fernandes, P.; Lynch, J. S.; Frazier, S. T.; Fisher, S. M.; Kodukula, K.; Kienzle, B.; Seethala, R. Cloning and functional expression of a cDNA encoding a human type 2 neuropeptide Y receptor. *J Biol Chem* **1995**, *270*, 22661-22664.
5. Gerald, C.; Walker, M. W.; Vaysse, P. J.; He, C.; Branchek, T. A.; Weinshank, R. L. Expression cloning and pharmacological characterization of a human hippocampal neuropeptide Y/peptide YY Y2 receptor subtype. *J Biol Chem* **1995**, *270*, 26758-26761.
6. Rimland, J. M.; Seward, E. P.; Humbert, Y.; Ratti, E.; Trist, D. G.; North, R. A. Coexpression with potassium channel subunits used to clone the Y₂ receptor for neuropeptide Y. *Mol. Pharmacol.* **1996**, *49*, 387-390.
7. Lundell, I.; Blomqvist, A. G.; Berglund, M. M.; Schober, D. A.; Johnson, D.; Statnick, M. A.; Gadski, R. A.; Gehlert, D. R.; Larhammar, D. Cloning of a human receptor of the NPY receptor family with high affinity for pancreatic polypeptide and peptide YY. *J Biol Chem* **1995**, *270*, 29123-29128.
8. Gregor, P.; Millham, M. L.; Feng, Y.; DeCarr, L. B.; McCaleb, M. L.; Cornfield, L. J. Cloning and characterization of a novel receptor to pancreatic polypeptide, a member of the neuropeptide Y receptor family. *FEBS Lett.* **1996**, *381*, 58-62.
9. Gerald, C.; Walker, M. W.; Criscione, L.; Gustafson, E. L.; Batzl-Hartmann, C.; Smith, K. E.; Vaysse, P.; Durkin, M. M.; Laz, T. M.; Linemeyer, D. L.; Schaffhauser, A. O.; Whitebread, S.; Hofbauer, K. G.; Taber, R. I.; Branchek, T. A.; Weinshank, R. L. A receptor subtype involved in neuropeptide-Y-induced food intake. *Nature* **1996**, *382*, 168-171.
10. Hu, Y.; Bloomquist, B. T.; Cornfield, L. J.; DeCarr, L. B.; Flores-Riveros, J. R.; Friedman, L.; Jiang, P.; Lewis-Higgins, L.; Sadlowski, Y.; Schaefer, J.; Velazquez, N.; McCaleb, M. L. Identification of a novel hypothalamic neuropeptide Y receptor associated with feeding behavior. *J Biol Chem* **1996**, *271*, 26315-26319.
11. Yi, M.; Li, H.; Wu, Z.; Yan, J.; Liu, Q.; Ou, C.; Chen, M. A Promising Therapeutic Target for Metabolic Diseases: Neuropeptide Y Receptors in Humans. *Cell. Physiol. Biochem.* **2018**, *45*, 88-107.
12. Reichmann, F.; Holzer, P. Neuropeptide Y: A stressful review. *Neuropeptides* **2016**, *55*, 99-109.
13. Larhammar, D.; Wraith, A.; Berglund, M. M.; Holmberg, S. K. S.; Lundell, I. Origins of the many NPY-family receptors in mammals. *Peptides* **2001**, *22*, 295-307.
14. Michel, M. C.; Beck-Sickinger, A.; Cox, H.; Doods, H. N.; Herzog, H.; Larhammar, D.; Quirion, R.; Schwartz, T.; Westfall, T. XVI. International Union of Pharmacology recommendations for

- the nomenclature of neuropeptide Y, peptide YY, and pancreatic polypeptide receptors. *Pharmacol. Rev.* **1998**, 50, 143-50.
15. Larhammar, D. Evolution of neuropeptide Y, peptide YY and pancreatic polypeptide. *Regul. Pept.* **1996**, 62, 1-11.
 16. Martel, J. C.; Fournier, A.; St-Pierre, S.; Dumont, Y.; Forest, M.; Quirion, R. Comparative structural requirements of brain neuropeptide Y binding sites and vas deferens neuropeptide Y receptors. *Mol. Pharmacol.* **1990**, 38, 494-502.
 17. Clark, J. T.; Sahu, A.; Kalra, P. S.; Balasubramaniam, A.; Kalra, S. P. Neuropeptide Y (NPY)-induced feeding behavior in female rats: comparison with human NPY ([Met¹⁷]NPY), NPY analog ([norLeu⁴]NPY) and peptide YY. *Regul. Pept.* **1987**, 17, 31-39.
 18. Dukorn, S.; Littmann, T.; Keller, M.; Kuhn, K.; Cabrele, C.; Baumeister, P.; Bernhardt, G.; Buschauer, A. Fluorescence- and Radiolabeling of [Lys⁴,Nle^{17,30}]hPP Yields Molecular Tools for the NPY Y₄ Receptor. *Bioconjug. Chem.* **2017**, 28, 1291-1304.
 19. Kuhn, K. K.; Ertl, T.; Dukorn, S.; Keller, M.; Bernhardt, G.; Reiser, O.; Buschauer, A. High Affinity Agonists of the Neuropeptide Y (NPY) Y₄ Receptor Derived from the C-Terminal Pentapeptide of Human Pancreatic Polypeptide (hPP): Synthesis, Stereochemical Discrimination, and Radiolabeling. *J. Med. Chem.* **2016**, 59, 6045-6058.
 20. Dukorn, S. Pharmacological tools for the NPY receptors: [³⁵S]GTPγS binding assays, luciferase gene reporter assays and labeled peptides PhD Thesis, University of Regensburg, 2017.
 21. Huang, W.; Manglik, A.; Venkatakrishnan, A. J.; Laeremans, T.; Feinberg, E. N.; Sanborn, A. L.; Kato, H. E.; Livingston, K. E.; Thorsen, T. S.; Kling, R. C.; Granier, S.; Gmeiner, P.; Husbands, S. M.; Traynor, J. R.; Weis, W. I.; Steyaert, J.; Dror, R. O.; Kobilka, B. K. Structural insights into μ-opioid receptor activation. *Nature* **2015**, 524, 315-321.
 22. Liu, W.; Chun, E.; Thompson, A. A.; Chubukov, P.; Xu, F.; Katritch, V.; Han, G. W.; Roth, C. B.; Heitman, L. H.; IJzerman, A. P.; Cherezov, V.; Stevens, R. C. Structural Basis for Allosteric Regulation of GPCRs by Sodium Ions. *Science* **2012**, 337, 232-236.
 23. Zhang, C.; Srinivasan, Y.; Arlow, D. H.; Fung, J. J.; Palmer, D.; Zheng, Y.; Green, H. F.; Pandey, A.; Dror, R. O.; Shaw, D. E.; Weis, W. I.; Coughlin, S. R.; Kobilka, B. K. High-resolution crystal structure of human protease-activated receptor 1. *Nature* **2012**, 492, 387-392.
 24. Neve, K. A.; Cumbay, M. G.; Thompson, K. R.; Yang, R.; Buck, D. C.; Watts, V. J.; DuRand, C. J.; Teeter, M. M. Modeling and Mutational Analysis of a Putative Sodium-Binding Pocket on the Dopamine D₂ Receptor. *Mol. Pharmacol.* **2001**, 60, 373-381.
 25. Miller-Gallacher, J. L.; Nehmé, R.; Warne, T.; Edwards, P. C.; Schertler, G. F. X.; Leslie, A. G. W.; Tate, C. G. The 2.1 Å Resolution Structure of Cyanopindolol-Bound β₁-Adrenoceptor Identifies an Intramembrane Na⁺ Ion that Stabilises the Ligand-Free Receptor. *PLOS ONE* **2014**, 9, e92727.
 26. Katritch, V.; Fenalti, G.; Abola, E. E.; Roth, B. L.; Cherezov, V.; Stevens, R. C. Allosteric sodium in class A GPCR signaling. *Trends Biochem. Sci.* **2014**, 39, 233-244.
 27. Keller, M.; Weiss, S.; Hutzler, C.; Kuhn, K. K.; Mollereau, C.; Dukorn, S.; Schindler, L.; Bernhardt, G.; König, B.; Buschauer, A. N^ω-Carbamoylation of the Argininamide Moiety: An Avenue to Insurmountable NPY Y₁ Receptor Antagonists and a Radiolabeled Selective High-

- Affinity Molecular Tool ($[^3\text{H}]\text{UR-MK299}$) with Extended Residence Time. *J. Med. Chem.* **2015**, 58, 8834-8849.
28. Moser, C.; Bernhardt, G.; Michel, J.; Schwarz, H.; Buschauer, A. Cloning and functional expression of the hNPY Y₅ receptor in human endometrial cancer (HEC-1B) cells. *Can. J. Physiol. Pharmacol.* **2000**, 78, 134-42.
 29. Ziemek, R.; Schneider, E.; Kraus, A.; Cabrele, C.; Beck-Sickinger, A. G.; Bernhardt, G.; Buschauer, A. Determination of Affinity and Activity of Ligands at the Human Neuropeptide Y Y₄ Receptor by Flow Cytometry and Aequorin Luminescence. *J. Recept. Signal Transduct. Res.* **2007**, 27, 217-233.
 30. Holliday, N. D.; Michel, M. C.; Cox, H. M. NPY Receptor Subtypes and Their Signal Transduction. In *Neuropeptide Y and Related Peptides*, Michel, M. C., Ed. Springer Berlin Heidelberg: Berlin, Heidelberg, 2004; pp 45-73.
 31. Persaud, S. J.; Bewick, G. A. Peptide YY: more than just an appetite regulator. *Diabetologia* **2014**, 57, 1762-1769.
 32. Aakerlund, L.; Gether, U.; Fuhlendorff, J.; Schwartz, T. W.; Thastrup, O. Y₁ receptors for neuropeptide Y are coupled to mobilization of intracellular calcium and inhibition of adenylate cyclase. *FEBS Lett.* **1990**, 260, 73-78.
 33. Motulsky, H. J.; Michel, M. C. Neuropeptide Y mobilizes Ca²⁺ and inhibits adenylate cyclase in human erythroleukemia cells. *American Journal of Physiology-Endocrinology and Metabolism* **1988**, 255, E880-E885.
 34. Criscione, L.; Rigollier, P.; Batzl-Hartmann, C.; Rüeger, H.; Stricker-Krongrad, A.; Wyss, P.; Brunner, L.; Whitebread, S.; Yamaguchi, Y.; Gerald, C.; Heurich, R. O.; Walker, M. W.; Chiesi, M.; Schilling, W.; Hofbauer, K. G.; Levens, N. Food intake in free-feeding and energy-deprived lean rats is mediated by the neuropeptide Y₅ receptor. *J. Clin. Invest.* **1998**, 102, 2136-2145.
 35. Grouzmann, E.; Meyer, C.; Bürki, E.; Brunner, H. Neuropeptide Y Y₂ receptor signalling mechanisms in the human glioblastoma cell line LN319. *Peptides* **2001**, 22, 379-386.
 36. Loh, K.; Herzog, H.; Shi, Y.-C. Regulation of energy homeostasis by the NPY system. *Trends Endocrinol. Metab.* **2015**, 26, 125-135.
 37. Zhang, L.; Nguyen, A. D.; Lee, I. C. J.; Yulyaningsih, E.; Riepler, S. J.; Stehrer, B.; Enriquez, R. F.; Lin, S.; Shi, Y. C.; Baldock, P. A.; Sainsbury, A.; Herzog, H. NPY modulates PYY function in the regulation of energy balance and glucose homeostasis. *Diabetes Obes Metab* **2012**, 14, 727-736.
 38. Li, J.-B.; Asakawa, A.; Terashi, M.; Cheng, K.; Chaolu, H.; Zoshiki, T.; Ushikai, M.; Sheriff, S.; Balasubramaniam, A.; Inui, A. Regulatory effects of Y₄ receptor agonist (BVD-74D) on food intake. *Peptides* **2010**, 31, 1706-1710.
 39. Qi, Y.; Fu, M.; Herzog, H. Y₂ receptor signalling in NPY neurons controls bone formation and fasting induced feeding but not spontaneous feeding. *Neuropeptides* **2016**, 55, 91-97.
 40. Olza, J.; Gil-Campos, M.; Leis, R.; Rupérez, A. I.; Tojo, R.; Cañete, R.; Gil, Á.; Aguilera, C. M. Influence of variants in the NPY gene on obesity and metabolic syndrome features in Spanish children. *Peptides* **2013**, 45, 22-27.

41. Aerts, E.; Geets, E.; Sorber, L.; Beckers, S.; Verrijken, A.; Massa, G.; Van Hoorenbeeck, K.; Verhulst, S. L.; Van Gaal, L. F.; Van Hul, W. Evaluation of a Role for *NPY* and *NPY2R* in the Pathogenesis of Obesity by Mutation and Copy Number Variation Analysis in Obese Children and Adolescents. *Ann. Hum. Genet.* **2018**, *82*, 1-10.
42. Soscia, S. J.; Harrington, M. E. Neuropeptide Y does not reset the circadian clock in *NPY Y2*^{-/-} mice. *Neurosci. Lett.* **2005**, *373*, 175-178.
43. Gribkoff, V. K.; Pieschl, R. L.; Wisialowski, T. A.; van den Pol, A. N.; Yocca, F. D. Phase Shifting of Circadian Rhythms and Depression of Neuronal Activity in the Rat Suprachiasmatic Nucleus by Neuropeptide Y: Mediation by Different Receptor Subtypes. *J. Neurosci.* **1998**, *18*, 3014-3022.
44. Colmers, W. F.; El Bahh, B. Neuropeptide Y and Epilepsy. *Epilepsy Curr* **2003**, *3*, 53-58.
45. Vezzani, A.; Sperk, G. Overexpression of NPY and Y2 receptors in epileptic brain tissue: an endogenous neuroprotective mechanism in temporal lobe epilepsy? *Neuropeptides* **2004**, *38*, 245-252.
46. Diaz-delCastillo, M.; Woldbye, D. P. D.; Heegaard, A. M. Neuropeptide Y and its Involvement in Chronic Pain. *Neuroscience* **2018**, *387*, 162-169.
47. Hua, X. Y.; Boublik, J. H.; Spicer, M. A.; Rivier, J. E.; Brown, M. R.; Yaksh, T. L. The antinociceptive effects of spinally administered neuropeptide Y in the rat: systematic studies on structure-activity relationship. *J. Pharmacol. Exp. Ther.* **1991**, *258*, 243-248.
48. Martins-Oliveira, M.; Akerman, S.; Tavares, I.; Goadsby, P. J. Neuropeptide Y inhibits the trigeminovascular pathway through *NPY Y₁* receptor: implications for migraine. *Pain* **2016**, *157*, 1666-1673.
49. Strother, L. C.; Srikiatkachorn, A.; Suprongsinchai, W. Targeted Orexin and Hypothalamic Neuropeptides for Migraine. *Neurotherapeutics* **2018**, *15*, 377-390.
50. Kloster, E.; Saft, C.; Akkad, D. A.; Epplen, J. T.; Arning, L. Association of age at onset in Huntington disease with functional promoter variations in *NPY* and *NPY2R*. *J. Mol. Med.* **2014**, *92*, 177-184.
51. Croce, N.; Gelfo, F.; Ciotti, M. T.; Federici, G.; Caltagirone, C.; Bernardini, S.; Angelucci, F. NPY modulates miR-30a-5p and BDNF in opposite direction in an in vitro model of Alzheimer disease: a possible role in neuroprotection? *Mol. Cell. Biochem.* **2013**, *376*, 189-195.
52. Duarte-Neves, J.; Pereira de Almeida, L.; Cavadas, C. Neuropeptide Y (NPY) as a therapeutic target for neurodegenerative diseases. *Neurobiol. Dis.* **2016**, *95*, 210-224.
53. Capurro, D.; Huidobro-Toro, J. P. The involvement of neuropeptide Y *Y₁* receptors in the blood pressure baroreflex: studies with BIBP 3226 and BIBO 3304. *Eur. J. Pharm.* **1999**, *376*, 251-255.
54. Abrahamsson, C. Neuropeptide Y1- and Y2-Receptor-Mediated Cardiovascular Effects in the Anesthetized Guinea Pig, Rat, and Rabbit. *J. Cardiovasc. Pharmacol.* **2000**, *36*, 451-458.
55. Tilan, J.; Kitlinska, J. Neuropeptide Y (NPY) in tumor growth and progression: Lessons learned from pediatric oncology. *Neuropeptides* **2016**, *55*, 55-66.

56. Medeiros, P. J.; Al-Khazraji, B. K.; Novielli, N. M.; Postovit, L. M.; Chambers, A. F.; Jackson, D. N. Neuropeptide Y stimulates proliferation and migration in the 4T1 breast cancer cell line. *Int. J. Cancer* **2012**, 131, 276-286.
57. Giesbrecht, C. J.; Mackay, J. P.; Silveira, H. B.; Urban, J. H.; Colmers, W. F. Countervailing Modulation of I_h by Neuropeptide Y and Corticotrophin-Releasing Factor in Basolateral Amygdala As a Possible Mechanism for Their Effects on Stress-Related Behaviors. *J. Neurosci.* **2010**, 30, 16970-16982.
58. Stadlbauer, U.; Langhans, W.; Meyer, U. Administration of the Y2 Receptor Agonist PYY₃₋₃₆ in Mice Induces Multiple Behavioral Changes Relevant to Schizophrenia. *Neuropsychopharmacol.* **2013**, 38, 2446-2455.
59. Pleil, K. E.; Rinker, J. A.; Lowery-Gionta, E. G.; Mazzone, C. M.; McCall, N. M.; Kendra, A. M.; Olson, D. P.; Lowell, B. B.; Grant, K. A.; Thiele, T. E.; Kash, T. L. NPY signaling inhibits extended amygdala CRF neurons to suppress binge alcohol drinking. *Nat. Neurosci.* **2015**, 18, 545-552.
60. Morales-Medina, J. C.; Dumont, Y.; Quirion, R. A possible role of neuropeptide Y in depression and stress. *Brain Res.* **2010**, 1314, 194-205.
61. Shende, P.; Desai, D. Physiological and Therapeutic Roles of Neuropeptide Y on Biological Functions. In *Cell Biology and Translational Medicine, Volume 7: Stem Cells and Therapy: Emerging Approaches*, Turksen, K., Ed. Springer International Publishing: Cham, 2020; pp 37-47.
62. Gehlert, D. R. Introduction to the reviews on neuropeptide Y. *Neuropeptides* **2004**, 38, 135-40.
63. Pedrazzini, T.; Pralong, F.; Grouzmann, E. Neuropeptide Y: the universal soldier. *Cell. Mol. Life Sci.* **2003**, 60, 350-77.
64. Merten, N.; Beck-Sickinger, A. G. Molecular ligand-receptor interaction of the NPY/PP peptide family. In *NPY Family of Peptides in Neurobiology, Cardiovascular and Metabolic Disorders: from Genes to Therapeutics*, Zukowska, Z.; Feuerstein, G. Z., Eds. Birkhäuser Basel: Basel, 2006; pp 35-62.
65. Li, J.; Tian, Y.; Wu, A. Neuropeptide Y receptors: a promising target for cancer imaging and therapy. *Regener. Biomater.* **2015**, 2, 215-219.
66. Chen, C. H.; Stephens, R. L., Jr.; Rogers, R. C. PYY and NPY: control of gastric motility via action on Y1 and Y2 receptors in the DVC. *Neurogastroenterol. Motil.* **1997**, 9, 109-16.
67. Zukowska, Z.; Feuerstein, G. Z. Future directions and therapeutic perspectives for NPY/PYYbased anti-inflammatory and tumor suppressor drugs. In *The NPY Family of Peptides in Immune Disorders, Inflammation, Angiogenesis and Cancer*, Zukowska, Z.; Feuerstein, G. Z., Eds. Birkhäuser Basel: Basel, 2005; pp 251-253.
68. Reubi, J. C.; Gugger, M.; Waser, B.; Schaer, J. C. Y₁-mediated effect of neuropeptide Y in cancer: breast carcinomas as targets. *Cancer Res.* **2001**, 61, 4636-41.
69. Körner, M.; Reubi, J. C. NPY receptors in human cancer: A review of current knowledge. *Peptides* **2007**, 28, 419-425.
70. Zhang, L.; Bijker, M. S.; Herzog, H. The neuropeptide Y system: Pathophysiological and therapeutic implications in obesity and cancer. *Pharmacol. Ther.* **2011**, 131, 91-113.

71. Hoppenz, P.; Els-Heindl, S.; Kellert, M.; Kuhnert, R.; Saretz, S.; Lerchen, H.-G.; Köbberling, J.; Riedl, B.; Hey-Hawkins, E.; Beck-Sickinger, A. G. A Selective Carborane-Functionalized Gastrin-Releasing Peptide Receptor Agonist as Boron Delivery Agent for Boron Neutron Capture Therapy. *J. Org. Chem.* **2020**, *85*, 1446-1457.
72. Rudolf, K.; Eberlein, W.; Engel, W.; Wieland, H. A.; Willim, K. D.; Entzeroth, M.; Wienen, W.; Beck-Sickinger, A. G.; Doods, H. N. The first highly potent and selective non-peptide neuropeptide Y Y₁ receptor antagonist: BIBP3226. *Eur. J. Pharmacol.* **1994**, *271*, R11-3.
73. Beck-Sickinger, A. G.; Wieland, H. A.; Wittneben, H.; Willim, K.-D.; Rudolf, K.; Jung, G. Complete L-Alanine Scan of Neuropeptide Y Reveals Ligands Binding to Y₁ and Y₂ Receptors with Distinguished Conformations. *Eur. J. Biochem.* **1994**, *225*, 947-958.
74. Wieland, H. A.; Willim, K. D.; Entzeroth, M.; Wienen, W.; Rudolf, K.; Eberlein, W.; Engel, W.; Doods, H. N. Subtype selectivity and antagonistic profile of the nonpeptide Y₁ receptor antagonist BIBP 3226. *J. Pharmacol. Exp. Ther.* **1995**, *275*, 143-149.
75. Wieland, H. A.; Engel, W.; Eberlein, W.; Rudolf, K.; Doods, H. N. Subtype selectivity of the novel nonpeptide neuropeptide Y₁ receptor antagonist BIBO3304 and its effect on feeding in rodents. *Br. J. Pharmacol.* **1998**, *125*, 549-555.
76. Keller, M.; Bernhardt, G.; Buschauer, A. [³H]UR-MK136: A Highly Potent and Selective Radioligand for Neuropeptide Y Y₁ Receptors. *ChemMedChem* **2011**, *6*, 1566-1571.
77. Keller, M.; Erdmann, D.; Pop, N.; Pluym, N.; Teng, S.; Bernhardt, G.; Buschauer, A. Red-fluorescent argininamide-type NPY Y₁ receptor antagonists as pharmacological tools. *Bioorg. Med. Chem.* **2011**, *19*, 2859-78.
78. Keller, M.; Maschauer, S.; Brennauer, A.; Tripal, P.; Koglin, N.; Dittrich, R.; Bernhardt, G.; Kuwert, T.; Wester, H.-J.; Buschauer, A.; Prante, O. Prototypic ¹⁸F-Labeled Argininamide-Type Neuropeptide Y Y₁R Antagonists as Tracers for PET Imaging of Mammary Carcinoma. *ACS Med. Chem. Lett.* **2017**, *8*, 304-309.
79. Maschauer, S.; Ott, J. J.; Bernhardt, G.; Kuwert, T.; Keller, M.; Prante, O. ¹⁸F-labelled triazolyl-linked argininamides targeting the neuropeptide Y Y₁R for PET imaging of mammary carcinoma. *Sci Rep* **2019**, *9*, 12990.
80. Keller, M.; Teng, S.; Bernhardt, G.; Buschauer, A. Bivalent Argininamide-Type Neuropeptide Y Y₁ Antagonists Do Not Support the Hypothesis of Receptor Dimerisation. *ChemMedChem* **2009**, *4*, 1733-1745.
81. Hutzler, C. Synthesis and pharmacological activity of new neuropeptide Y receptor ligands: from *N,N*-disubstituted alkanamides to highly potent argininamide-type Y₁ antagonists. PhD Thesis, University of Regensburg, 2001.
82. Keller, M.; Weiss, S.; Hutzler, C.; Kuhn, K. K.; Mollereau, C.; Dukorn, S.; Schindler, L.; Bernhardt, G.; König, B.; Buschauer, A. N^o-Carbamoylation of the Argininamide Moiety: An Avenue to Insurmountable NPY Y₁ Receptor Antagonists and a Radiolabeled Selective High-Affinity Molecular Tool ([³H]UR-MK299) with Extended Residence Time. *J. Med. Chem.* **2015**, *58*, 8834-49.
83. Yang, Z.; Han, S.; Keller, M.; Kaiser, A.; Bender, B. J.; Bosse, M.; Burkert, K.; Kogler, L. M.; Wifling, D.; Bernhardt, G.; Plank, N.; Littmann, T.; Schmidt, P.; Yi, C.; Li, B.; Ye, S.; Zhang, R.;

- Xu, B.; Larhammar, D.; Stevens, R. C.; Huster, D.; Meiler, J.; Zhao, Q.; Beck-Sickinger, A. G.; Buschauer, A.; Wu, B. Structural basis of ligand binding modes at the neuropeptide Y Y₁ receptor. *Nature* **2018**, 556, 520-524.
84. Poindexter, G. S.; Bruce, M. A.; LeBoulluec, K. L.; Monkovic, I.; Martin, S. W.; Parker, E. M.; Iben, L. G.; McGovern, R. T.; Ortiz, A. A.; Stanley, J. A.; Mattson, G. K.; Kozlowski, M.; Arcuri, M.; Antal-Zimanyi, I. Dihydropyridine Neuropeptide Y Y₁ Receptor Antagonists. *Bioorg. Med. Chem. Lett.* **2002**, 12, 379-382.
85. Kanatani, A.; Kanno, T.; Ishihara, A.; Hata, M.; Sakuraba, A.; Tanaka, T.; Tsuchiya, Y.; Mase, T.; Fukuroda, T.; Fukami, T.; Ihara, M. The Novel Neuropeptide Y Y₁ Receptor Antagonist J-104870: A Potent Feeding Suppressant with Oral Bioavailability. *Biochem. Biophys. Res. Commun.* **1999**, 266, 88-91.
86. Wright, J.; Bolton, G.; Creswell, M.; Downing, D.; Georgic, L.; Heffner, T.; Hodges, J.; MacKenzie, R.; Wise, L. 8-amino-6-(arylsulphonyl)-5-nitroquinolines: novel nonpeptide neuropeptide Y₁ receptor antagonists. *Bioorg. Med. Chem. Lett.* **1996**, 6, 1809-1814.
87. Hipskind, P. A.; Lobb, K. L.; Nixon, J. A.; Britton, T. C.; Bruns, R. F.; Catlow, J.; Dieckman-McGinty, D. K.; Gackenheimer, S. L.; Gitter, B. D.; Iyengar, S.; Schober, D. A.; Simmons, R. M. A.; Swanson, S.; Zarrinmayeh, H.; Zimmerman, D. M.; Gehlert, D. R. Potent and Selective 1,2,3-Trisubstituted Indole NPY Y-1 Antagonists. *J. Med. Chem.* **1997**, 40, 3712-3714.
88. Zarrinmayeh, H.; Zimmerman, D. M.; Cantrell, B. E.; Schober, D. A.; Bruns, R. E.; Gackenheimer, S. L.; Ornstein, P. L.; Hipskind, P. A.; Britton, T. C.; Gehlert, D. R. Structure-activity relationship of a series of diaminoalkyl substituted benzimidazole as neuropeptide Y Y₁ receptor antagonists. *Bioorg. Med. Chem. Lett.* **1999**, 9, 647-652.
89. Leslie, C. P.; Fabio, R. D.; Bonetti, F.; Borriello, M.; Braggio, S.; Forno, G. D.; Donati, D.; Falchi, A.; Ghirlanda, D.; Giovannini, R.; Pavone, F.; Pecunioso, A.; Pentassuglia, G.; Pizzi, D. A.; Rumboldt, G.; Stasi, L. Novel carbazole derivatives as NPY Y₁ antagonists. *Bioorg. Med. Chem. Lett.* **2007**, 17, 1043-1046.
90. Griffith, D. A.; Hargrove, D. M.; Maurer, T. S.; Blum, C. A.; De Lombaert, S.; Inthavongsay, J. K.; Klade, L. E.; Mack, C. M.; Rose, C. R.; Sanders, M. J.; Carpino, P. A. Discovery and evaluation of pyrazolo[1,5-a]pyrimidines as neuropeptide Y₁ receptor antagonists. *Bioorg. Med. Chem. Lett.* **2011**, 21, 2641-2645.
91. Cabrele, C.; Beck-Sickinger, A. G. Molecular characterization of the ligand-receptor interaction of the neuropeptide Y family. *J. Pept. Sci.* **2000**, 6, 97-122.
92. Dumont, Y.; Fournier, A.; St-Pierre, S.; Quirion, R. Characterization of neuropeptide Y binding sites in rat brain membrane preparations using [¹²⁵I][Leu³¹,Pro³⁴]peptide YY and [¹²⁵I]peptide YY₃₋₃₆ as selective Y₁ and Y₂ radioligands. *J. Pharmacol. Exp. Ther.* **1995**, 272, 673-80.
93. Balasubramaniam, A.; Joshi, R.; Su, C.; Friend, L. A.; James, J. H. Neuropeptide Y (NPY) Y₂ receptor-selective agonist inhibits food intake and promotes fat metabolism in mice: Combined anorectic effects of Y₂ and Y₄ receptor-selective agonists. *Peptides* **2007**, 28, 235-240.
94. Doods, H.; Gaida, W.; Wieland, H. A.; Dollinger, H.; Schnorrenberg, G.; Esser, F.; Engel, W.; Eberlein, W.; Rudolf, K. BIIE0246: A selective and high affinity neuropeptide Y Y₂ receptor antagonist. *Eur. J. Pharm.* **1999**, 384, R3-R5.

95. Burkert, K.; Zellmann, T.; Meier, R.; Kaiser, A.; Stichel, J.; Meiler, J.; Mittapalli, G. K.; Roberts, E.; Beck-Sickingler, A. G. A Deep Hydrophobic Binding Cavity is the Main Interaction for Different Y₂R Antagonists. *ChemMedChem* **2017**, *12*, 75-85.
96. Pluym, N.; Brennauer, A.; Keller, M.; Ziemek, R.; Pop, N.; Bernhardt, G.; Buschauer, A. Application of the Guanidine–Acylguanidine Bioisosteric Approach to Argininamide-Type NPY Y₂ Receptor Antagonists. *ChemMedChem* **2011**, *6*, 1727-1738.
97. Brennauer, A. Acylguanidines as bioisosteric groups in argininamide-type neuropeptide Y Y₁ and Y₂ receptor antagonists: synthesis, stability and pharmacological activity. PhD Thesis, University of Regensburg, 2006.
98. Pluym, N. Application of the Guanidine-Acylguanidine Bioisosteric Approach to NPY Y₂ Receptors Antagonists: Bivalent, Radiolabeled and Fluorescent Pharmacological Tools. PhD Thesis, University of Regensburg, 2011.
99. Pluym, N.; Baumeister, P.; Keller, M.; Bernhardt, G.; Buschauer, A. [³H]UR-PLN196: A Selective Nonpeptide Radioligand and Insurmountable Antagonist for the Neuropeptide Y Y₂ Receptor. *ChemMedChem* **2013**, *8*, 587-593.
100. Dollinger, H.; Esser, F.; Mihm, G.; Rudolf, K.; Schnorrenberg, G.; Gaida, W.; Doods, N. H. Neue substituierte Aminosäurederivate, Verfahren zu ihrer Herstellung und diese Verbindungen enthaltene pharmazeutische Zusammensetzungen. DE19816929A1, 1998.
101. Ziemek, R.; Brennauer, A.; Schneider, E.; Cabrele, C.; Beck-Sickingler, A. G.; Bernhardt, G.; Buschauer, A. Fluorescence- and luminescence-based methods for the determination of affinity and activity of neuropeptide Y₂ receptor ligands. *Eur. J. Pharm.* **2006**, *551*, 10-18.
102. Mittapalli, G. K.; Vellucci, D.; Yang, J.; Toussaint, M.; Brothers, S. P.; Wahlestedt, C.; Roberts, E. Synthesis and SAR of selective small molecule neuropeptide Y Y₂ receptor antagonists. *Bioorg. Med. Chem. Lett.* **2012**, *22*, 3916-3920.
103. Bonaventure, P.; Nepomuceno, D.; Mazur, C.; Lord, B.; Rudolph, D. A.; Jablonowski, J. A.; Carruthers, N. I.; Lovenberg, T. W. Characterization of *N*-(1-Acetyl-2,3-dihydro-1H-indol-6-yl)-3-(3-cyano-phenyl)-*N*-[1-(2-cyclopentyl-ethyl)-piperidin-4yl]acrylamide (JNJ-5207787), a Small Molecule Antagonist of the Neuropeptide Y Y₂ Receptor. *J. Pharmacol. Exp. Ther.* **2004**, *308*, 1130-1137.
104. Brothers, S. P.; Saldanha, S. A.; Spicer, T. P.; Cameron, M.; Mercer, B. A.; Chase, P.; McDonald, P.; Wahlestedt, C.; Hodder, P. S. Selective and Brain Penetrant Neuropeptide Y Y₂ Receptor Antagonists Discovered by Whole-Cell High Throughput Screening. *Mol. Pharmacol.* **2009**, mol.109.058677.
105. Andres, C. J.; Antal Zimanyi, I.; Deshpande, M. S.; Iben, L. G.; Grant-Young, K.; Mattson, G. K.; Zhai, W. Differentially functionalized diamines as novel ligands for the NPY₂ receptor. *Bioorg. Med. Chem. Lett.* **2003**, *13*, 2883-2885.
106. Shoblock, J. R.; Welty, N.; Nepomuceno, D.; Lord, B.; Aluisio, L.; Fraser, I.; Motley, S. T.; Sutton, S. W.; Morton, K.; Galici, R.; Atack, J. R.; Dvorak, L.; Swanson, D. M.; Carruthers, N. I.; Dvorak, C.; Lovenberg, T. W.; Bonaventure, P. In vitro and in vivo characterization of JNJ-31020028 (N-(4-{4-[2-(diethylamino)-2-oxo-1-phenylethyl]piperazin-1-yl}-3-fluorophenyl)-2-pyridin-3-

- ylbenzamide), a selective brain penetrant small molecule antagonist of the neuropeptide Y Y₂ receptor. *J. Psychopharmacol.* **2009**, 208, 265.
107. Balasubramaniam, A.; Mullins, D. E.; Lin, S.; Zhai, W.; Tao, Z.; Dhawan, V. C.; Guzzi, M.; Knittel, J. J.; Slack, K.; Herzog, H.; Parker, E. M. Neuropeptide Y (NPY) Y₄ Receptor Selective Agonists Based on NPY(32–36): Development of an Anorectic Y₄ Receptor Selective Agonist with Picomolar Affinity. *J. Med. Chem.* **2006**, 49, 2661-2665.
108. Liu, M.; Mountford, S. J.; Richardson, R. R.; Groenen, M.; Holliday, N. D.; Thompson, P. E. Optically Pure, Structural, and Fluorescent Analogues of a Dimeric Y₄ Receptor Agonist Derived by an Olefin Metathesis Approach. *J. Med. Chem.* **2016**, 59, 6059-6069.
109. Spinnler, K.; von Krüchten, L.; Konieczny, A.; Schindler, L.; Bernhardt, G.; Keller, M. An Alkyne-functionalized Arginine for Solid-Phase Synthesis Enabling “Bioorthogonal” Peptide Conjugation. *ACS Med. Chem. Lett.* **2020**, 11, 334-339.
110. Keller, M.; Kaske, M.; Holzammer, T.; Bernhardt, G.; Buschauer, A. Dimeric argininamide-type neuropeptide Y receptor antagonists: Chiral discrimination between Y₁ and Y₄ receptors. *Bioorg. Med. Chem.* **2013**, 21, 6303-6322.
111. Daniels, A. J.; Matthews, J. E.; Slepatis, R. J.; Jansen, M.; Viveros, O. H.; Tadepalli, A.; Harrington, W.; Heyer, D.; Landavazo, A.; Leban, J. J. High-affinity neuropeptide Y receptor antagonists. *Proc. Natl. Acad. Sci. USA* **1995**, 92, 9067-9071.
112. Parker, E. M.; Babij, C. K.; Balasubramaniam, A.; Burrier, R. E.; Guzzi, M.; Hamud, F.; Gitali, M.; Rudinski, M. S.; Tao, Z.; Tice, M.; Xia, L.; Mullins, D. E.; Salisbury, B. G. GR231118 (1229U91) and other analogues of the C-terminus of neuropeptide Y are potent neuropeptide Y Y₁ receptor antagonists and neuropeptide Y Y₄ receptor agonists. *Eur. J. Pharm.* **1998**, 349, 97-105.
113. Berlicki, Ł.; Kaske, M.; Gutiérrez-Abad, R.; Bernhardt, G.; Illa, O.; Ortuño, R. M.; Cabrele, C.; Buschauer, A.; Reiser, O. Replacement of Thr³² and Gln³⁴ in the C-Terminal Neuropeptide Y Fragment 25–36 by cis-Cyclobutane and cis-Cyclopentane β-Amino Acids Shifts Selectivity toward the Y₄ Receptor. *J. Med. Chem.* **2013**, 56, 8422-8431.
114. Sliwoski, G.; Schubert, M.; Stichel, J.; Weaver, D.; Beck-Sickinger, A. G.; Meiler, J. Discovery of Small-Molecule Modulators of the Human Y₄ Receptor. *PLOS ONE* **2016**, 11, e0157146.
115. Schubert, M.; Stichel, J.; Du, Y.; Tough, I. R.; Sliwoski, G.; Meiler, J.; Cox, H. M.; Weaver, C. D.; Beck-Sickinger, A. G. Identification and Characterization of the First Selective Y₄ Receptor Positive Allosteric Modulator. *J. Med. Chem.* **2017**, 60, 7605-7612.
116. Sun, C.; Ewing, W. R.; Bolton, S. A.; Gu, Z.; Huang, Y.; Murugesan, N.; Zhu, Y. Substituted adipic acid amides and uses thereof. WO 2012/125622 A1, 2012.
117. Ewing, W. R.; Zhu, Y.; Sun, C.; Huang, Y.; Sivasamban, M.; Karatholuvhu. Diaminocyclohexane compounds and uses thereof. US 2013/0184262 A1, 2013.
118. Ewing, W. R.; Zhu, Y.; Sun, C.; Huang, Y.; Sivasamban, M.; Karatholuvhu; Bolton, S. A.; Pasunoori, L.; Mandal, S. K.; Sher, P. M. Diaminocyclohexane compounds and uses thereof. US 2013/0184284 A1, 2013.

119. Kang, N.; Wang, X.-L.; Zhao, Y. Discovery of small molecule agonists targeting neuropeptide Y4 receptor using homology modeling and virtual screening. *Chem Biol Drug Des* **2019**, *94*, 2064-2072.
120. Cabrele, C.; Langer, M.; Bader, R.; Wieland, H. A.; Doods, H. N.; Zerbe, O.; Beck-Sickinger, A. G. The first selective agonist for the neuropeptide YY₅ receptor increases food intake in rats. *J Biol Chem* **2000**, *275*, 36043-8.
121. Parker, E. M.; Balasubramaniam, A.; Guzzi, M.; Mullins, D. E.; Salisbury, B. G.; Sheriff, S.; Witten, M. B.; Hwa, J. J. [D-Trp³⁴] neuropeptide Y is a potent and selective neuropeptide Y Y₅ receptor agonist with dramatic effects on food intake☆. *Peptides* **2000**, *21*, 393-399.
122. Rüeger, H.; Schmidlin, T.; Rigollier, P.; Yamaguchi, Y.; Tintelnot-Blomley, M.; Schilling, W.; Criscione, L.; Mah, R. 2-amino quinazoline derivatives as npy receptor antagonists. WO1997020823A2, 1997.
123. Rueeger, H.; Rigollier, P.; Yamaguchi, Y.; Schmidlin, T.; Schilling, W.; Criscione, L.; Whitebread, S.; Chiesi, M.; Walker, M. W.; Dhanoa, D.; Islam, I.; Zhang, J.; Gluchowski, C. Design, synthesis and SAR of a series of 2-substituted 4-amino-quinazoline neuropeptide Y Y₅ receptor antagonists. *Bioorg. Med. Chem. Lett.* **2000**, *10*, 1175-1179.
124. MacNeil, D. J. NPY Y1 and Y5 receptor selective antagonists as anti-obesity drugs. *Current topics in medicinal chemistry* **2007**, *7*, 1721-33.
125. Della Zuana, O.; Sadlo, M.; Germain, M.; Félétou, M.; Chamorro, S.; Tisserand, F.; de Montrion, C.; Boivin, J. F.; Duhault, J.; Boutin, J. A.; Levens, N. Reduced food intake in response to CGP 71683A may be due to mechanisms other than NPY Y₅ receptor blockade. *Int. J. Obes. Relat. Metab. Disord.* **2001**, *25*, 84-94.
126. Erondu, N.; Gantz, I.; Musser, B.; Suryawanshi, S.; Mallick, M.; Addy, C.; Cote, J.; Bray, G.; Fujioka, K.; Bays, H.; Hollander, P.; Sanabria-Bohórquez, S. M.; Eng, W.; Långström, B.; Hargreaves, R. J.; Burns, H. D.; Kanatani, A.; Fukami, T.; MacNeil, D. J.; Gottesdiener, K. M.; Amatruda, J. M.; Kaufman, K. D.; Heymsfield, S. B. Neuropeptide Y5 receptor antagonism does not induce clinically meaningful weight loss in overweight and obese adults. *Cell Metabolism* **2006**, *4*, 275-282.
127. Walker, M. W.; Wolinsky, T. D.; Jubian, V.; Chandrasena, G.; Zhong, H.; Huang, X.; Miller, S.; Hegde, L. G.; Marsteller, D. A.; Marzabadi, M. R.; Papp, M.; Overstreet, D. H.; Gerald, C. P. G.; Craig, D. A. The Novel Neuropeptide Y Y₅ Receptor Antagonist Lu AA33810 [N-[[trans-4-[(4,5-Dihydro[1]benzothiepine[5,4-d]thiazol-2-yl)amino]cyclohexyl]methyl]-methanesulfonamide] Exerts Anxiolytic- and Antidepressant-Like Effects in Rat Models of Stress Sensitivity. *J. Pharmacol. Exp. Ther.* **2009**, *328*, 900-911.
128. Packiarajan, M.; Marzabadi, M. R.; Desai, M.; Lu, Y.; Noble, S. A.; Wong, W. C.; Jubian, V.; Chandrasena, G.; Wolinsky, T. D.; Zhong, H.; Walker, M. W.; Wiborg, O.; Andersen, K. Discovery of Lu AA33810: A highly selective and potent NPY5 antagonist with in vivo efficacy in a model of mood disorder. *Bioorg. Med. Chem. Lett.* **2011**, *21*, 5436-5441.
129. Yasyuki Kawanishi; Hideyuki Takenaka; Kohji Hanasaki; Okada, T. NPY Y5 antagonist. US 2004/0180964 A1, 2004.

-
130. Norman, M. H.; Chen, N.; Chen, Z.; Fotsch, C.; Hale, C.; Han, N.; Hurt, R.; Jenkins, T.; Kincaid, J.; Liu, L.; Lu, Y.; Moreno, O.; Santora, V. J.; Sonnenberg, J. D.; Karbon, W. Structure–Activity Relationships of a Series of Pyrrolo[3,2-d]pyrimidine Derivatives and Related Compounds as Neuropeptide Y5 Receptor Antagonists. *J. Med. Chem.* **2000**, 43, 4288-4312.
131. Itani, H.; Ito, H.; Sakata, Y.; Hatakeyama, Y.; Oohashi, H.; Satoh, Y. Novel Potent Antagonists of Human Neuropeptide Y Y5 Receptors. Part 3: 7-Methoxy-1-hydroxy-1-substituted Tetraline Derivatives. *Bioorg. Med. Chem. Lett.* **2002**, 12, 799-802.
132. Takehiro Fukami; Akio Kanatani; Akane Ishihara; Yasuyuki Ishii; Toshiyuki Takahashi; Yuji Haga; Toshihiro Sakamoto; Ito, T. Novel Spiro Compounds. WO2001014376A1, 2001.
133. Fichtner, M.; Lee, E.; Tomlinson, E.; Scott, D.; Cornelius, P.; Patterson, T. A.; Carpino, P. A. Discovery and evaluation of spirocyclic derivatives as antagonists of the neuropeptide Y5 receptor. *Bioorg. Med. Chem. Lett.* **2012**, 22, 2738-2743.
134. Turnbull, A. V.; Ellershaw, L.; Masters, D. J.; Birtles, S.; Boyer, S.; Carroll, D.; Clarkson, P.; Loxham, S. J. G.; McAulay, P.; Teague, J. L.; Foote, K. M.; Pease, J. E.; Block, M. H. Selective Antagonism of the NPY Y5 Receptor Does Not Have a Major Effect on Feeding in Rats. *Diabetes* **2002**, 51, 2441-2449.
135. Sato, N.; Takahashi, T.; Shibata, T.; Haga, Y.; Sakuraba, A.; Hirose, M.; Sato, M.; Nonoshita, K.; Koike, Y.; Kitazawa, H.; Fujino, N.; Ishii, Y.; Ishihara, A.; Kanatani, A.; Fukami, T. Design and Synthesis of the Potent, Orally Available, Brain-Penetrable Arylpyrazole Class of Neuropeptide Y5 Receptor Antagonists. *J. Med. Chem.* **2003**, 46, 666-669.
136. Della-Zuana, O.; Revereault, L.; Beck-Sickinger, A.; Monge, A.; Caignard, D. H.; Fauchère, J. L.; Henlin, J. M.; Audinot, V.; Boutin, J. A.; Chamorro, S.; Félétou, M.; Levens, N. A potent and selective NPY Y₅ antagonist reduces food intake but not through blockade of the NPY Y₅ receptor. *Int. J. Obes.* **2004**, 28, 628-639.
137. Islam, I.; Dhanoa, D.; Finn, J.; Du, P.; Walker, M. W.; Salon, J. A.; Zhang, J.; Gluchowski, C. Discovery of potent and selective small molecule NPY Y5 receptor antagonists. *Bioorg. Med. Chem. Lett.* **2002**, 12, 1767-1769.
138. Kanatani, A.; Ishihara, A.; Iwaasa, H.; Nakamura, K.; Okamoto, O.; Hidaka, M.; Ito, J.; Fukuroda, T.; MacNeil, D. J.; Van der Ploeg, L. H. T.; Ishii, Y.; Okabe, T.; Fukami, T.; Ihara, M. L-152,804: Orally Active and Selective Neuropeptide Y Y5 Receptor Antagonist. *Biochem. Biophys. Res. Commun.* **2000**, 272, 169-173.

Chapter 2

Argininamide-type neuropeptide Y Y₁ receptor antagonists: the nature of N^ω-carbamoyl substituents determines Y₁R binding mode and affinity

Note: Prior to the submission of the thesis this chapter was published in cooperation with partners (schemes, tables, figures and text may differ from published version): Buschmann, J.; Seiler, T.; Bernhardt, G.; Keller, M.; Wifling, D. Argininamide-type neuropeptide Y Y₁ receptor antagonists: the nature of N^ω-carbamoyl substituents determines Y₁R binding mode and affinity. *RSC Med. Chem.* **2020**, 11, 274-282 DOI: 10.1039/C9MD00538B – adopted by permission of The Royal Society of Chemistry

Jonas Buschmann (2.23-2.34, 2.38, 2.41, 2.56-2.75 and 2.76) and Theresa Seiler (2.39, 2.42, 2.53-2.55) performed the synthesis, analytical characterization, competition binding, functional experiments and analyzed the data. David Wifling performed molecular docking, molecular dynamics simulations and processed the data.

The preparatory work of Theresa Sailer was performed during her Master Thesis (University of Regensburg, 2016)

Jonas Buschmann, David Wifling, Max Keller and Günther Bernhardt wrote the manuscript.

The authors thank Brigitte Wenzl, Maria Beer-Krön, Susanne Bollwein, Elvira Schreiber and Lydia Schneider for their excellent technical assistance, Christoph Müller for providing 2.4, and the Leibniz Rechenzentrum (LRZ) in Munich for providing software (Schrödinger suite) and computing resources.

2.1. Introduction

Neuropeptide Y (NPY) receptors belong to the class A of G-protein coupled receptors (GPCRs).¹ The four functionally expressed subtypes in man (Y₁R, Y₂R, Y₄R and Y₅R) are distributed in the central nervous system and in the periphery.² They are activated by the endogenous peptides neuropeptide Y (NPY), peptide YY (PYY) and pancreatic polypeptide (PP). The NPY Y₁R has been shown to be overexpressed in a number of different cancers (e.g. breast cancer).^{3, 4} Labelled Y₁R ligands have therefore been proposed as potential tumour imaging agents.⁵ The first described selective non-peptidic Y₁R antagonist BIBP-3226 (**2.1**, Table 2.1) has a binding affinity in the low nanomolar range.⁶ Carbamoylation of the guanidine moiety of **2.1** led to UR-MK299 (**2.2**, Table 2.1), a Y₁R antagonist with picomolar affinity,⁷ that was recently co-crystallized with the NPY Y₁R.³ In the crystal structure, the carbamoylguanidine group of **2.2** forms a hydrogen-assisted salt bridge with D287^{6,59}. The propionyl group of the carbamoyl residue is buried in the sub-pocket formed between TM helices V and VI, this pocket appears to be incompletely filled (Figure 2.1).³ This finding is in agreement with the high Y₁R affinity (albeit lower compared to **2.2**) of (*R*)-argininamides possessing slightly larger carbamoyl residues than found in **2.2** (e.g. compounds **2.3-2.5**, Table 2.1).^{7, 8} However, the experimentally determined binding mode of **2.2** is incompatible with the attachment of very bulky groups to the guanidine group of **2.1**; fluorophores (**2.7** and **2.8**) or alternative carbamoyl residues (**2.9**) have low Y₁R affinities (Table 2.1).

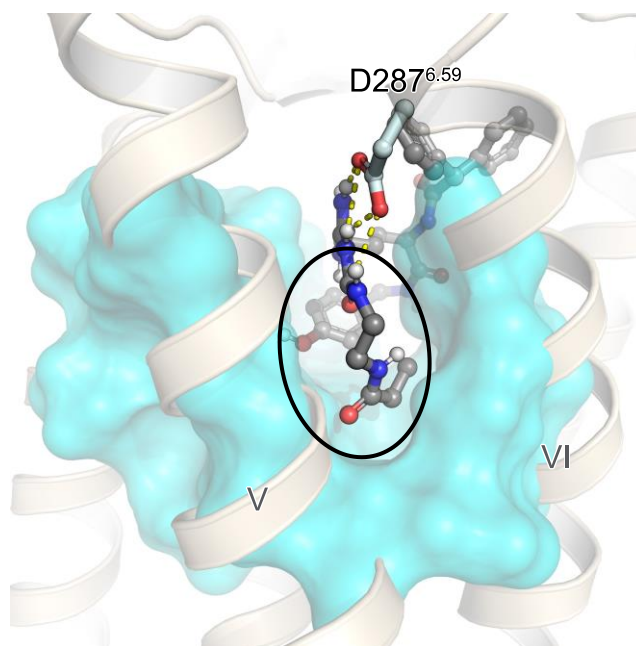


Figure 2.1. Extended view of the orthosteric binding pocket of the Y₁R occupied by **2.2** (ball and stick representation) (PDB ID: 5ZBQ³). The carbamoyl residue of **2.2** occupies a subpocket (oval area), located between TM helices V and VI. The crystal structure was post processed by addition of hydrogen atoms, minimization, etc.; see experimental section 2.4.5.2 and 2.4.5.3.

In order to address the question how the size and structure of the carbamoyl residue of *N*^ω-carbamoylated argininamides, structurally related to **2.2** and **2.3**, effects Y₁R affinity and the binding mode (as determined by competition binding and functional studies at the Y₁R) a series of *N*^ω-carbamoylated (*R*)-argininamides bearing carbamoyl residues of different sizes were synthesized

and pharmacologically characterized. The Y₁R binding mode of selected compounds was studied by induced-fit docking and molecular dynamics (MD) simulations.

Table 2.1. Structures and Y₁R affinities of reported (*R*)-argininamides **2.1-2.9**.

1-9

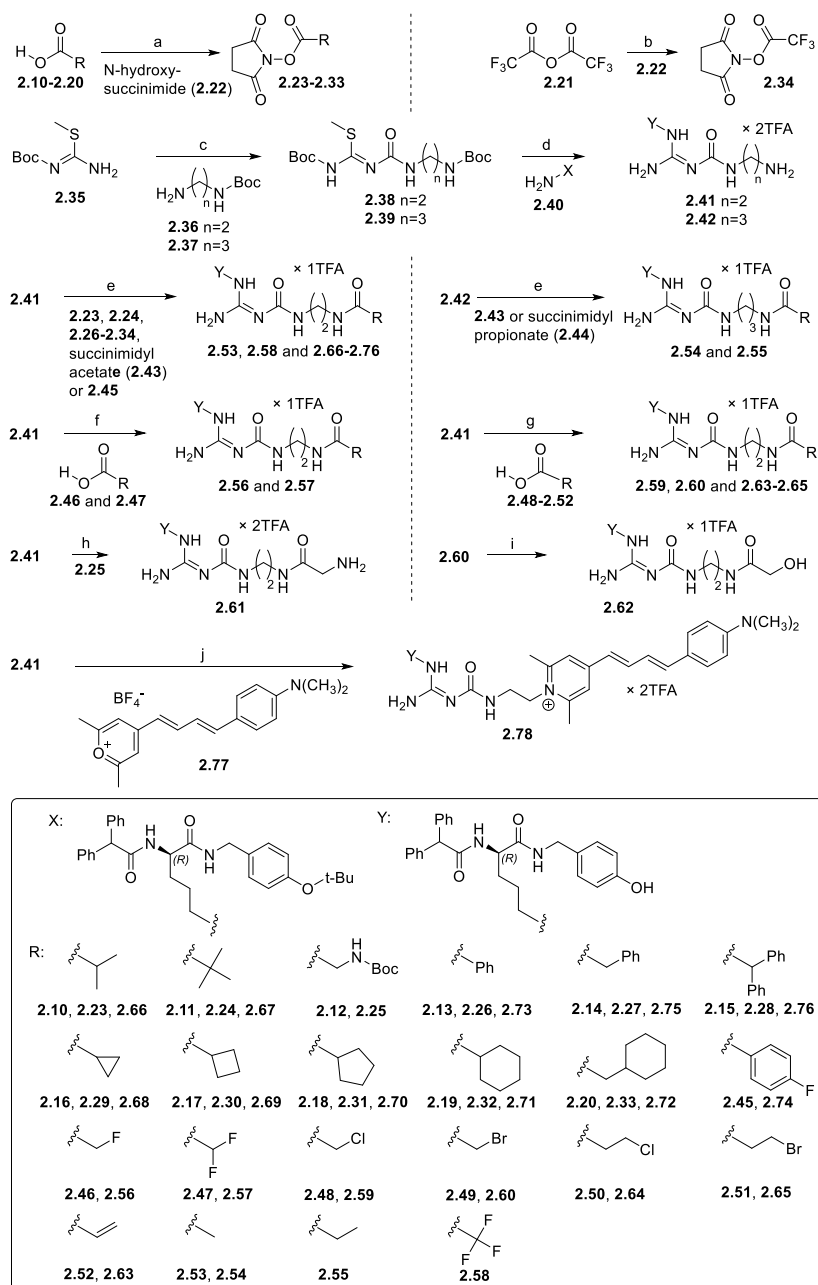
compound	Ref.	R	p <i>K_i</i>
2.1 (BIBP-3226)	a, b		9.00
2.2 (UR-MK299)	a		10.11
2.3 (UR-MK136)	a, c		8.92
2.4	a		9.25
2.5	a		8.16
2.6	a		7.39
2.7	d		6.82
2.8	a		<6.00
2.9	a		6.40

References: (a) Keller et al.,⁷ these authors determined affinities of **2.1-2.6**, **2.8** and **2.9** by use of [³H]**2.2** (*C*_{final} = 0.15 nM, *K_d* = 0.044 nM²) and SK-N-MC cells; (b) Rudolf et al.;⁶ (c) Keller et al.;⁸ (d) Keller et al.,⁹ these authors determined affinity of **2.7** by use of [³H]UR-MK114 (*K_d* = 1.2 nM, *C*_{final} = 1.5 nM) and SK-N-MC cells. Reported *K_i* values were converted to p*K_i* values.

These studies suggest that reported fluorescent (*R*)-argininamide-type Y₁R ligands (labelled via *N*^ω-carbamoyl residues), exhibiting *K_i* values (Y₁R) between 20 and 150 nM,⁹ **2.10** bind to the Y₁R in a different manner compared to **2.2**.

2.2. Results and discussion

2.2.1. Synthesis



Scheme 2.1. Synthesis of the *N*^ω-carbamoylated (*R*)-argininamides **2.53-2.76** and **78**. Reagents and conditions: (a) DCC, CH₂Cl₂, THF or DMF, 30-86%; (b) THF, 100%; (c) triphosgene, DIPEA, 50-71%; (d) (1) CH₂Cl₂, HgCl₂, DIPEA, (2) TFA/CH₂Cl₂ 1:1, 45-68%; (e) DIPEA, DMF, 21-84%; (f) DCC, DIPEA, DMF, 16-29%; (g) DCC, DMF, 9-16%; (h) (1) DIPEA, DMF, (2) CH₂Cl₂/TFA 1:1, 46%; (i) DMSO; (j) DIPEA, DMF, 22%.

The *N*^ω-carbamoylated (*R*)-argininamides **2.53-2.76** and **2.78** were prepared as follows (note: the assignment of the numbers of target compounds **2.53-2.76**, and **2.78** was guided by the size of the carbamoyl residue (Table 2.1) and not by their synthetic accessibility outlined in Scheme 2.1): the

carboxylic acids **2.10-2.20** were transformed to the respective succinimidyl esters **2.23-2.33** in the presence of DCC, and trifluoroacetic acid anhydride (**2.21**) was treated with *N*-hydroxysuccinimide (**2.22**) to obtain succinimidyl ester **2.34** (Scheme 2.1).

Treatment of *tert*-butyl (2-aminoethyl)carbamate (**2.36**) or *tert*-butyl (3-aminopropyl)carbamate (**2.37**) with triphosgene gave isocyanates as intermediates, which were converted to the isothiourea derivatives **2.38** and **2.39** by the addition of **2.35** to the reaction mixture. The amine-functionalized (*R*)-argininamides **2.41** and **2.42** were obtained by guanidinylation of amine **2.40** using **2.38** and **2.39**, respectively, and subsequent removal of the Boc and *tert*-butyl groups by treatment with TFA (Scheme 2.1).

The target compounds **2.53-2.55**, **2.58** and **2.66-2.76** were synthesized by treatment of amines **2.41** or **2.42** with the succinimidyl esters **2.23**, **2.24**, **2.26-2.34** or **2.43-2.45** (Scheme 2.1). Compounds **2.56** and **2.57** were synthesized by amide bond formation between **2.41** and the carboxylic acids **2.46** and **2.47**, respectively, using DCC as coupling reagent (Scheme 2.1). Compounds **2.59**, **2.60** and **2.63-2.65** were synthesized from **2.41** and the carboxylic acids **2.48-2.52** according to the same procedure, but without the addition of DIPEA. Compound **2.61** was obtained by acylation of **2.41** using **2.25** and subsequent deprotection (Scheme 2.1). Alcohol **2.62** was isolated as degradation product of **2.60** after 6 months of storage of a 10 mM solution of **2.60** in DMSO at -20 °C. Compound **2.78** was synthesized by coupling of **2.41** with the pyrylium dye Py-5^{10, 11} (**2.77**) according to a procedure reported previously by Keller et al.⁹ Chemical stabilities of compounds **2.56**, **2.58-2.61**, **2.63** and **2.68** were proven in aqueous solution, pH 7, at room temperature over 24 h (Experimental section 2.4.3 and Chapter 8, 8.1.5.).

2.2.2. Competition binding and functional studies

Results from Y₁R competition binding experiments, performed in intact SK-N-MC cells using [³H]**2.2** as radioligand, are summarized in Table 2.2. Elongation by two methylene groups (**2.3**) has been reported to result in an approximately 30-fold decrease in affinity.¹² The replacement of the propionyl group in **2.2** by mono- (**2.56**, **2.59**, **2.60**, **2.64** and **2.65**), di- (**2.57**) or tri- (**2.58**) halogenated acetyl or propionyl residues, as well as by amino (**2.61**) or hydroxy (**2.62**) functionalized acetyl residues did not significantly affect Y₁R affinity. Whereas the introduction of an acryl (**2.63**) or 2-methylpropionyl (**2.66**) residues followed the same trend, the more bulky 2,2-dimethylpropionyl residue in compound **2.67** led to an around 1000-fold decrease in Y₁R affinity compared to **2.2** (Table 2.2). In the series of compounds bearing aliphatic rings of increasing size (from cyclopropane to cyclohexane, **2.68-2.71**), Y₁R affinity decreased considerably (up to 5000-fold compared to **2.2**) in the case of the cyclopentyl (**2.70**) and cyclohexyl (**2.71**) groups (Tables 2.1 and 2.2; competition binding curves shown in Figure 2.2 A). The insertion of a methylene group between the aliphatic ring and the amide group in **2.71**, resulting in **2.72**, even led to a further decrease in Y₁R affinity (> 20,000-fold compared to **2.2**; Tables 2.1, 2.2 and Figure 2.2 A). Interestingly, replacement of the aliphatic rings in **2.71** and **2.72** by a phenyl moiety (**2.73** and **2.75**) resulted in an approx. 10-fold increase in Y₁R affinity (Table 2.2, Figure 2.2 C). Surprisingly, the introduction of a second benzene ring in **2.75**, leading to **2.76**, did not alter binding affinity, and, moreover, the introduction of a bulky pyridinium-type fluorescent dye (**2.78**) even resulted in a slightly higher affinity compared to **2.75/2.76** (Table 2.2, Figure 2.2 C).

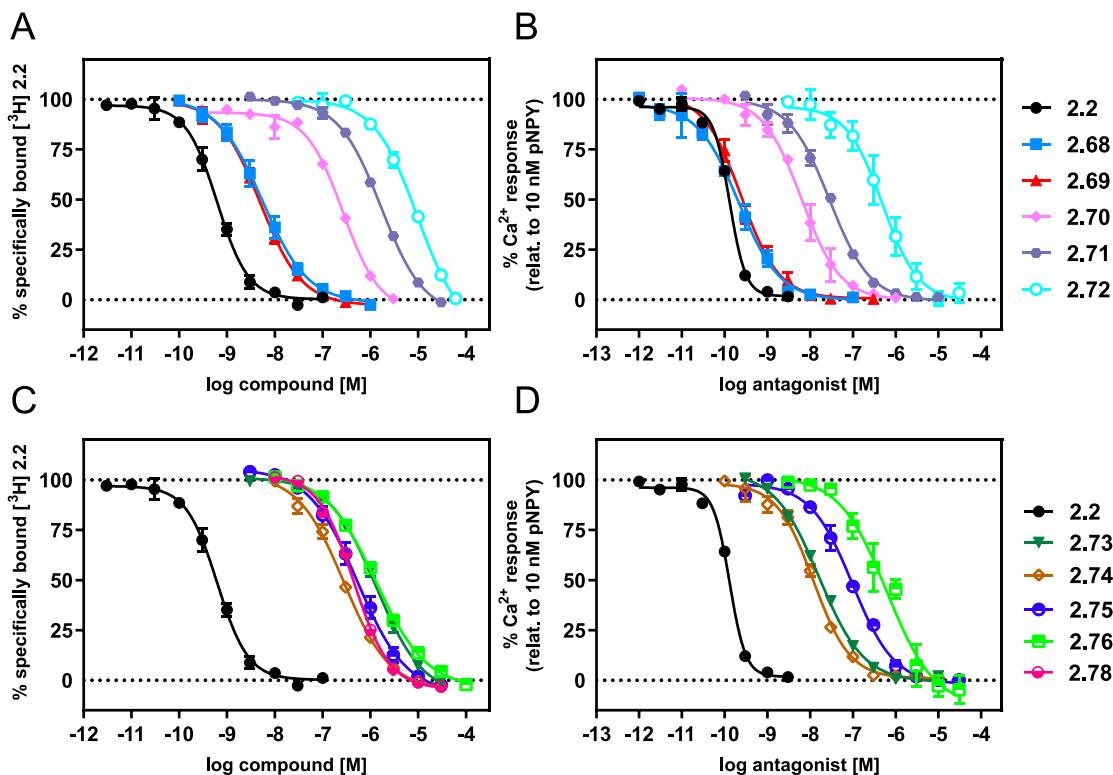
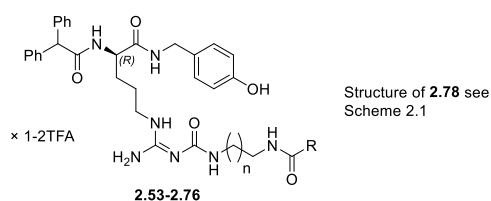


Figure 2.2. (A, C) Displacement curves of [³H]2.2 ($C_{\text{final}} = 0.15$ nM, $K_{\text{d}} = 0.044$ nM) obtained from competition binding studies with (A) 2.68-2.72, 2.73-2.76, (C) 2.78 and reference compound 2.2 in Y₁R-expressing SK-N-MC cells. (B, D) Concentration dependent inhibition curves obtained from the Fura-2 Ca²⁺ assay in intact HEL cells. The intracellular Ca²⁺ mobilization was induced by 10 nM pNPY after pre-incubation of the cells with (B) 2.68-2.72, (D) 2.73-2.76, respectively, for 15 min or the reference compound 2.2 for 20 min. (A-D) Data of compound 2.2 were taken from Keller et. al.⁷

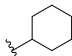
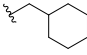
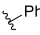
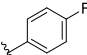
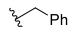
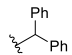
Y₁R antagonism (pK_{b} values) of 2.56-2.76, determined in a Fura-2 Ca²⁺ assay in HEL cells (inhibition of the intracellular Ca²⁺ mobilization induced by 10 nM pNPY), reflected the trends observed in the competition binding studies. However, the pK_{b} values proved to be consistently slightly higher than the pK_{i} values (Table 2; inhibition curves shown in Figure 2.2 B, 2.2 D). It is notable that, modification of the carbamoyl substituent did not affect the mode of action of the Y₁R ligands, i.e. all compounds behaved as neutral antagonists.

Table 2.2. Y_1 Receptor affinities (pK_i) and antagonism (pK_b) of the synthesized N^{β} -carbamoylated (R)-argininamides, determined by equilibrium competition binding with [3H]2.2 and in the Fura-2 Ca^{2+} assay, respectively.



Compound	n	R	$pK_i \pm SEM^a$	$pIC_{50} \pm SEM / pK_b \pm SEM^b$
2.53	1		10.23 ± 0.06	n.d.
2.54	2		10.20 ± 0.05	n.d.
2.55	2		10.13 ± 0.04	n.d.
2.56	1		10.50 ± 0.04	$10.26 \pm 0.04 / -$
2.57	1		10.17 ± 0.07	$9.96 \pm 0.12 / -$
2.58	1		10.15 ± 0.06	$9.90 \pm 0.05 / -$
2.59	1		10.28 ± 0.04	$10.10 \pm 0.04 / -$
2.60	1		9.90 ± 0.07	$10.21 \pm 0.01 / 11.08 \pm 0.01$
2.61	1		9.62 ± 0.03	$9.55 \pm 0.03 / 10.43 \pm 0.03$
2.62	1		9.84 ± 0.05	$10.04 \pm 0.10 / 10.92 \pm 0.10$
2.63	1		9.95 ± 0.07	$9.73 \pm 0.05 / 10.61 \pm 0.05$
2.64	1		9.42 ± 0.05	$9.23 \pm 0.08 / -$
2.65	1		9.16 ± 0.10	$9.39 \pm 0.10 / 10.27 \pm 0.10$
2.66	1		9.51 ± 0.09	$10.18 \pm 0.12 / 11.06 \pm 0.12$
2.67	1		7.34 ± 0.11	$7.84 \pm 0.08 / 8.71 \pm 0.08$
2.68	1		8.93 ± 0.12	$9.62 \pm 0.10 / 10.50 \pm 0.10$
2.69	1		8.96 ± 0.05	$9.62 \pm 0.09 / 10.49 \pm 0.09$
2.70	1		7.28 ± 0.07	$8.12 \pm 0.15 / 9.00 \pm 0.15$

Table 2.2 continued.

Compound	n	R	pK _i ± SEM ^a	pIC ₅₀ ± SEM / pK _b ± SEM ^b
2.71	1		6.42 ± 0.07	7.51 ± 0.01 / 8.39 ± 0.01
2.72	1		5.67 ± 0.05	6.34 ± 0.18 / 7.22 ± 0.18
2.73	1		7.25 ± 0.11	7.94 ± 0.03 / 8.82 ± 0.03
2.74	1		6.53 ± 0.07	7.79 ± 0.02 / 8.67 ± 0.02
2.75	1		6.52 ± 0.06	7.02 ± 0.04 / 7.90 ± 0.04
2.76	1		6.53 ± 0.01	6.28 ± 0.20 / 7.16 ± 0.20
2.78	1	n.a.	6.99 ± 0.04	n.d.

^aRadioligand competition binding assay with [³H]2.2 (C_{final} = 0.15 nM, K_d = 0.044 nM⁷) in intact SK-N-MC cells. Mean values ± SEM from at least three independent experiments, each performed in triplicate. ^bAntagonistic activities as determined in a Fura-2 Ca²⁺ assay in intact HEL cells.^{13, 14} Intracellular Ca²⁺ mobilization was induced by 10 nM pNPY after pre-incubation of the cells with the antagonist for 15 min.⁷ pK_b values are excluded, if the slope factor of the inhibition curve (four parameter logistic fit) was significantly different from unity (P ≤ 0.05, see Chapter 8, Table 8.1) and not close (< -1.25 or > -0.75) to unity, as a steep slope factor might be indicative of a more complex interaction not purely following the law of mass action. Mean values ± SEM from at least three independent experiments performed in singlet. n.d.: not determined. n.a.: not applicable.

2.2.3. Correlation of pK_i values with van der Waals volumes of the carbamoyl residues

For compounds 2.2-2.6 and 2.53-2.75, the experimentally determined pK_i values and the calculated van der Waals volumes of the respective carbamoyl residues showed an inverse correlation (R² = 0.84) between the size of the carbamoyl residue and the Y₁R affinity of the respective (R)-argininamide-type Y₁R antagonists (Figure 2.3). By contrast, both, 2.1, which is unsubstituted at the guanidine group, and compounds bearing large carbamoyl residues (2.7, 2.9, 2.76, 2.78), appeared to be outliers in the regression analysis (Figure 2.3). For 2.1, a much higher pK_i value would have been expected, and for 2.7, 2.9, 2.76 and 2.78 much lower values (Figure 2.3). Consequently, the attachment of small carbamoyl residues to the guanidine moiety (N^ω) of 2.1 (see compounds 2.2, 2.4, 2.53-2.66) led to a significant (up to more than one order of magnitude) increase in Y₁R affinity (Tables 2.1, 2.2 and Figure 2.3). By contrast, increasing van der Waals volumes of the carbamoyl residues (see compounds 2.3, 2.5, 2.6 and 2.67-2.75; Tables 2.1, 2.2 and Figure 2.3) affected Y₁R binding. However, exceeding a critical volume (212 Å³) of the carbamoyl substituent (in compound 2.72), Y₁R affinity did not further decrease, but even increased (compounds 2.7, 2.9, 2.76 and 2.78; Tables 2.1, 2.2 and Figure 2.3). In order to find a molecular explanation for this phenomenon, computational studies were performed.

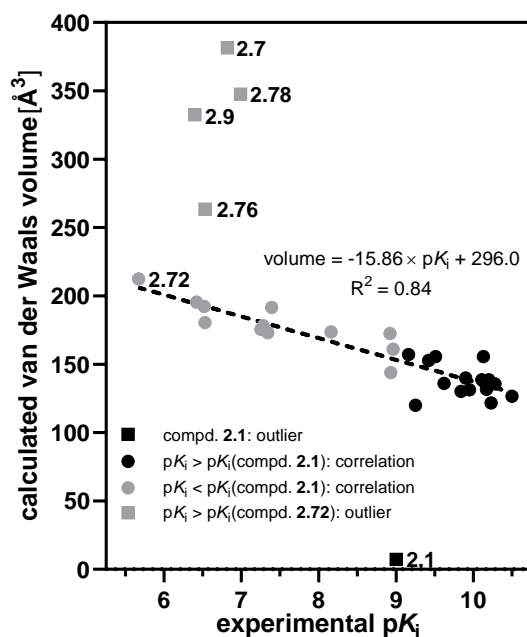


Figure 2.3. Correlation between the experimentally determined ligand (**2.2-2.6** and **2.53-2.75**) pK_i values and calculated van der Waals volumes of the respective carbamoyl residues. Two types of outliers (squares) were observed: (1) (*R*)-argininamide **2.1**, devoid of a carbamoyl substituent, supposed to bind in the same orientation as **2.2**, but unable to occupy the subpocket between TM V and VI (Figure 2.1); (2) compounds **2.7**, **2.9**, **2.76** and **2.78**, bearing bulkier carbamoyl moieties than **2.72**, considered to bind to the Y_1R in a totally different orientation compared to **2.2**.

2.2.4. Induced-fit docking and molecular dynamics (MD) simulations

To shed light on the binding modes of the most striking compounds (**2.1-2.3**, **2.68**, **2.72**, **2.76**, **2.78**) and to get insight into the molecular interactions leading to differences in Y_1R affinities, we performed MD simulations (**2.1-2.3**) and induced-fit docking (**2.68**, **2.72**, **2.76**, **2.78**) (Figure 2.4). All compounds showed the favorable hydrogen-assisted salt bridge (**2.1-2.3**, **2.68**, **2.76**, **2.78**) or hydrogen bond (**2.72**) between the carbamoylguanidine moiety and D287^{6.59} in cluster 1 of the MD simulations (**2.1-2.3**) or the lowest free energy (MM-GBSA score) binding poses of induced-fit docking (**2.68**, **2.72**, **2.76**, **2.78**) (Figure 3B, 3E-F, 3H-I, 3K-L). It is notable that when comparing the Y_1R affinity of **2.5** with its congener **2.6** (methylated at the carbamoyl nitrogen, see Table 1), it becomes obvious that the carbamoyl N-H group is involved in binding. In addition to the interaction with D287^{6.59}, the carbamoylguanidine moiety of most compounds (**2.2**, **2.3**, **2.68**, **2.76**, **2.78**) simultaneously forms a hydrogen-assisted salt bridge with D200^{ECL2} (Figure 3E-F, 3H, 3K-L). By contrast, the guanidine moiety of **2.1** was either in contact with D287^{6.59} or D200^{ECL2} in the MD simulation (*cf.* Chapter 8, Figure 8.1). Interestingly, in addition to the interaction with the carbamoylguanidine moiety of the ligands, D200^{ECL2} showed an intra-molecular salt bridge with R208^{ECL2}, which was most pronounced in the case of **2.2** (Figure 2.4 E).

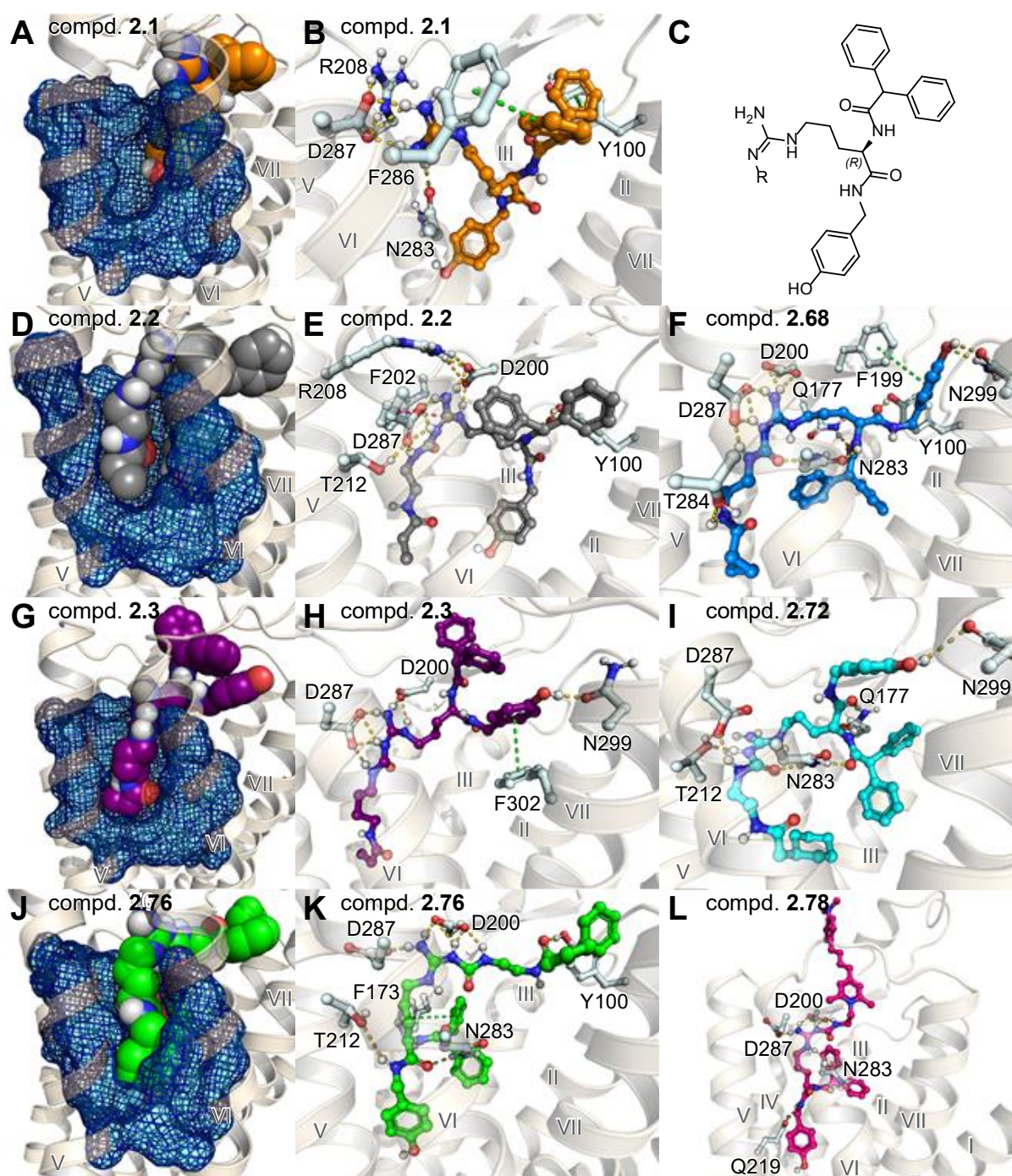


Figure 2.4. Cluster 1 binding poses of MD simulations (2 μ s) of the Y₁R (inactive state, PDB ID: 5ZBQ¹⁵) bound to (A, B, orange) **2.1**, (D, E, grey) **2.2** or (G, H, purple) **2.3**, and lowest free energy (MM-GBSA) conformations of (F, blue) **2.68**, (I, cyan) **2.72**, (J, K, green) **2.76** and (L, magenta) **2.78** obtained by induced-fit docking to the Y₁R. (C) (*R*)-Argininamide core structure. In A, D, G and J, the space within the subpocket between TM helices V and VI of the orthosteric binding pocket is highlighted with a blue surface/ mesh illustration. Amino acids involved in H-bonding or salt bridges (indicated as yellow dashed lines), π - π interactions (green dashed lines) or cation- π interactions (magenta dashed lines) with the ligands are labeled: Y100^{2,64} (π - π): in B; Y100^{2,64} (HB): in E, F, K; F173^{4,60} (π - π): in K; Q177^{ECL2} (HB): in F, I; F199^{ECL2} (π - π): in F; D200^{ECL2} (HB, SB): in E, F, H, K, L; F202^{ECL2} (CAT- π): in E; T212^{5,39} (HB): in I, K; Q219^{5,46} (HB): in L; N283^{6,55} (HB): in B, F, I, K, L; T284^{6,56} (HB): in F; F286^{6,58} (π - π): in B; D287^{6,59} (HB, SB): in B, E, F, H, K, L; D287^{6,59} (HB): in I; N299^{7,32} (HB): in F, H, I; F302^{7,35} (π - π): in H. Amino acids involved in intra-molecular H-bonding or salt bridges (indicated as yellow dashed lines) are labeled: in B, R208^{ECL2}-D287^{6,59} (HB, SB); in E, D200^{ECL2}-R208^{ECL2} (HB, SB), T212^{5,39}-D287^{6,59} (HB). HB = hydrogen bond. SB = salt bridge. CAT = cation.

Further specific (non-hydrophobic) interactions between amino acids of the Y₁R and the ligands were hydrogen bonds (Y100^{2.64} (**2.2**, **2.68**, **2.76**), Q177^{ECL2} (**2.68**, **2.72**), T212^{5.39} (**2.2**, **2.72**, **2.76**), Q219^{5.46} (**2.78**), N283^{6.55} (**2.1**, **2.68**, **2.72**, **2.76**, **2.78**), T284^{6.56} (**2.68**), N299^{7.32} (**2.3**, **2.68**, **2.72**)), π-π (Y100^{2.64} (**2.1**), F173^{4.60} (**2.76**), F199^{ECL2} (**2.68**), F286^{6.58} (**2.1**), F302^{7.35} (**2.3**)) or cation-π contacts (F202^{ECL2} (**2.2**)) (Figure 2.4).

In MD simulations, reference compound **2.1**, bearing no carbamoyl substituent at the guanidine group, showed a binding mode (Figure 2.4 A, 2.4 B) comparable to that of **2.2** (Figure 2.4 D, 2.4 E). However, in contrast to **2.2**, **2.3**, **2.68** and **2.72**, (*R*)-argininamide **2.1** did not occupy the subpocket between TM helices V and VI due to absence of the guanidine group substituent (Figure 2.4 A-B and 2.4 D-I).

2.3. Conclusion

A series of (*R*)-argininamide-type Y₁R antagonists, bearing different carbamoyl residues (small (**2.53-2.69**) vs. bulky (**2.70-2.76** and **2.78**), cyclic (**2.68-2.76** and **2.78**) vs. acyclic (**2.53-2.67**)) at the guanidine group, were synthesized. Up to a critical size, the increase in size of the carbamoyl side chain (e.g. compound **2.72**), correlated inversely with Y₁R affinity (p*K_i* values: 5.67-10.50), indicating that the van der Waals volume of considerably larger carbamoyl substituents than in reference compound **2.2** is too large to allow the occupation of the sub-pocket located between TM helix V and TM helix VI (Figure 2.5). Induced-fit docking and MD simulations suggest that, (*R*)-argininamides bearing very bulky carbamoyl residues (e.g. fluorescent ligand **2.78**) bind in an inverted mode (compared to **2.2**), accompanied by a moderate recovery of Y₁R affinity (p*K_i* of **2.78**: 6.99). The present study revealed that the subpocket of the Y₁R, perfectly occupied by the carbamoyl residue of the high affinity Y₁R antagonist **2.2**,¹⁵ cannot harbour large moieties such as fluorescent dyes. High affinity fluorescent ligands for the Y₁R derived from **2.2** will, therefore require a labelling strategy directed to positions other than the carbamoyl residue, e.g. the diphenyl acetyl moiety pointing towards the receptor surface.

2.4. Experimental section

2.4.1. General experimental conditions

The following reagents and solvents (analytical grade) were purchased from commercial suppliers and used without further purification: CH₂Cl₂, DMF (Fisher Scientific, Schwerte, Germany); DCC, TFA, HgCl₂, **2.10**, **2.11**, **2.13-2.20**, **2.22** and **2.46-2.51** (Sigma Aldrich, Taufkirchen, Germany); triphosgene and **2.21** (TCI, Eschborn, Germany); DIPEA, **2.36** (ABCR, Karlsruhe, Germany); **2.52** (Merck, Darmstadt, Germany). For pharmacological characterization, pNPY was purchased from Synpeptide (Shanghai, China).

Compounds **2.12**¹⁶, **2.35**¹⁴, **2.37**¹⁷, **2.40**¹⁸, **2.44**¹⁹, **2.45**²⁰ and **2.77**^{10, 11} were synthesized as previously described.

Column chromatography was performed using Merck Geduran 60 silica gel (0.063-0.200 mm) or Merck flash silica gel 60 (0.040-0.063 mm). For thin layer chromatography, TLC sheets ALUGRAM Xtra SIL G/UV254 from Macherey-Nagel GmbH & Co. KG (Düren, Germany) were used. Compounds were detected by irradiation with UV light (254 nm), and staining was performed with ninhydrin.

Acetonitrile (HPLC grade), used for HPLC, was purchased from Sigma-Aldrich. Millipore water was used for eluents of analytical and preparative HPLC. Compounds **2.41**, **2.42**, **2.53-2.76** and **2.78** were purified by a preparative HPLC-system from Knauer (Berlin, Germany) consisting of two pumps (K-1800) and a detector (K-2001). A Kinetex XB C18, 5 µm, 250 x 21 mm (Phenomenex, Aschaffenburg, Germany) served as RP-column at a flow rate of 18 mL/min. All injected solutions were filtered with syringe filters (0.45 µm). The mobile phase contained the solvents A (0.1% aq TFA) and B (acetonitrile). The detection wavelength was 220 nm. Acetonitrile was removed from the eluates at 40 °C under reduced pressure. The eluates, containing isolated compounds, were lyophilized using a Christ alpha 2-4 LD (Martin Christ Gefriertrocknungsanlagen, Osterode am Harz, Germany) or a Scanvac CoolSafe 100-9 (Labogene, Allerød, Denmark) lyophilization apparatus equipped with a Vacuubrand RZ rotary vane vacuum pump (Vacuubrand, Wertheim, Germany).

The purity of compounds **2.53-2.65**, **2.73** and **2.78** was determined by analytical HPLC (RP-HPLC) on a 1100 series system from Agilent Technologies (Santa Clara, CA USA) composed of a Degasser (G1379A), a Binary Pump (G1312A), a Diode Array Detector (G1315A), a thermostated Column Compartment (G1316A) and an Autosampler (G1329A). A Phenomenex Kinetex 5u XB-C18 100A, 250 x 4.6 mm was used as stationary phase. The flow rate was 1 mL/min, the detection wavelength was set to 220 nm (compound **2.78** was additionally detected at 480 nm), the oven temperature was set to 30 °C and the injection volume was 50 µL. Mixtures of solvents A (0.1% aq TFA) and B (acetonitrile) were used as mobile phase. The following gradient was applied: Method A: 0-25 min, A/B 90:10–5:95; 25-35 min, 5:95. Analytical HPLC analysis of compounds **2.66-2.72** and **2.74-2.76** was performed on a system from Merck-Hitachi composed of a Pump (L-6200A), an Interface (D600 IF), an Autosampler (AS-2000) and an UV-Detector (L-4000A). A Phenomenex Kinetex 5u XB-C18 100A, 250 x 4.6 mm (Phenomenex) was used as stationary phase. The flow rate was 0.8 mL/min, the detection wavelength was set to 200 nm, the oven temperature was set to 30 °C and the injection volume was 35 µL. A mixture of solvents A (0.05% aq TFA) and B (acetonitrile supplemented with 0.05% TFA) was used as mobile

phase. The following gradients were applied: Method B: 0-25 min, A/B 90:10–5:95; 25-35 min, 5:95 and Method C: 0-30 min, 95:5–20:80; 30-32 min, 20:80–5:95; 32-42 min, 5:95.

Deuterated solvents for NMR spectroscopy (DMSO- d_6 , $CDCl_3$) were obtained from Deutero (Kastellaun, Germany) in ampoules (1 mL). NMR spectra were recorded on a Bruker Avance 300 (1H , 300 MHz; ^{13}C , 75 MHz), a Bruker Avance III 400 (1H , 400 MHz; ^{13}C , 101 MHz) and a Bruker Avance 600 with cryogenic probe (1H , 600 MHz; ^{13}C , 150 MHz) (Bruker, Karlsruhe, Germany). Chemical shifts are given in ppm and were referenced to the solvent residual peak (DMSO- d_6 , at 2.50 ppm (1H -NMR) and at 39.52 ppm (^{13}C -NMR); $CDCl_3$, at 7.26 ppm (1H -NMR) and at 77.16 ppm (^{13}C -NMR)).²¹ The coupling constants (J) are given in Hertz (Hz). The splitting of the signals is described as follows: s = singlet, bs = broad singlet, d = doublet, t = triplet, q = quartet, m = multiplet.

Mass spectrometry (HRMS) analysis was performed either on an Agilent 6540 UHD Accurate-Mass Q-TOF LC/MS system (Agilent Technologies) using an electrospray source (ESI) or on an Agilent GC7890A GC/MS system (Agilent Technologies) using an atmospheric pressure chemical ionization (APCI) source.

Stock solutions were prepared in DMSO at concentrations of 2 mM (**2.78**) or 10 mM.

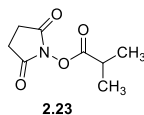
2.4.2. Synthesis protocols and analytical data

General synthesis procedures

General procedure A. The precursors **2.41** or **2.42** were dissolved in DMF, and DIPEA was added. The succinimidyl esters **2.23-2.33**, **2.43-2.45**, except **2.34**, were dissolved in DMF and added to the solution of **2.41** or **2.42**. The reaction mixture was stirred at rt for 1-2 h. 10% aq TFA (10 equiv.) was added and the product was isolated by preparative HPLC.

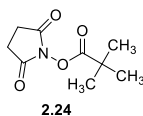
General procedure B. A freshly prepared solution of the carboxylic acids **2.48-2.52** and DCC in DMF (0.5 mL) was added dropwise to a solution of **2.41** in DMF (1 mL) and the mixture was stirred at rt for 2-3 h. The precipitate was removed by filtration and the product purified by preparative HPLC.

General procedure C. In contrast to general procedure B, DIPEA (2.5 equiv.) was added to the solution of **2.41** in DMF, along with the carboxylic acid **2.46** or **2.47**.

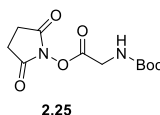


Succinimidyl 2-methylpropionate (2.23).²² A solution of DCC (0.89 g, 4.31 mmol) in CH_2Cl_2 (1 mL) and a solution of 2-methylpropionic acid (**2.10**) (369 μ L, 3.98 mmol) in CH_2Cl_2 (1 mL) were added dropwise to an ice-cold solution of **2.22** (0.46 g, 4.00 mmol) in CH_2Cl_2 (6 mL) and DMF (0.4 mL). The reaction mixture was stirred on an ice bath for 2 h and then at rt overnight. The precipitate was removed by filtration, and the solid was washed (3x) with CH_2Cl_2 . The filtrate was then washed with a saturated solution of $NaHCO_3$ (100 mL) and the organic phase was dried over Na_2SO_4 . The solvent was removed by evaporation, the residue was taken up in CH_2Cl_2 and crystallization, initiated by the addition of light petroleum, afforded **2.23** as a white solid (0.22 g, 1.19 mmol, 30%). **1H -NMR** (300 MHz, $CDCl_3$): δ (ppm) 1.32 (d, $J = 7.0$ Hz, 6H), 2.82 (s, 4H, interfering with the next signal), 2.88 (septet, $J = 7.0$ Hz, 1H).

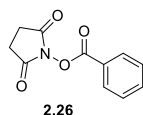
¹³C-NMR (75 MHz, CDCl₃): δ (ppm) 18.9, 25.7, 31.8, 169.4, 172.2. **HRMS** (APCI): m/z [M+H]⁺ calcd. for [C₈H₁₂NO₄]⁺ 186.0761, found 186.0765. C₈H₁₁NO₄ (185.18).



Succinimidyl 2,2-dimethylpropionate (2.24).²³ A solution of DCC (1.13 g, 5.48 mmol) in CH₂Cl₂ (1 mL) and a solution of 2,2-dimethylpropionic acid (**2.11**) (0.50 g, 4.90 mmol) in CH₂Cl₂ (1 mL) were added dropwise to an ice-cold solution of **2.22** (0.46 g, 4.00 mmol) in CH₂Cl₂ (6 mL) and DMF (0.4 mL). The reaction mixture was stirred on an ice bath for 2 h and then at rt overnight. The precipitate was removed by filtration, and the solid was washed (3x) with CH₂Cl₂. The filtrate was washed with a saturated solution of NaHCO₃ (100 mL), and the organic phase was dried over Na₂SO₄. The solvent was removed by evaporation, the residue was taken up in CH₂Cl₂ and crystallization, initiated by the addition of light petroleum, afforded **2.24** as a white solid (0.28 g, 1.41 mmol, 35%). **¹H-NMR** (400 MHz, CDCl₃): δ (ppm) 1.37 (s, 9H), 2.78-2.84 (m, 4H). **¹³C-NMR** (101 MHz, CDCl₃): δ (ppm) 25.7, 27.1, 38.5, 169.3, 173.5. **HRMS** (APCI): m/z [M+H]⁺ calcd. for [C₉H₁₄NO₄]⁺ 200.0917, found 200.0918. C₉H₁₃NO₄ (199.21).

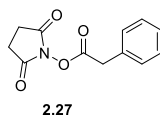


Succinimidyl N-Boc-glycinate (2.25).²⁴ DCC (0.61 g, 2.97 mmol) was dissolved in CH₂Cl₂ and added dropwise to an ice-cold solution of **2.22** (0.34 g, 2.97 mmol) and N-Boc-glycinate (**12**) (0.40 g, 2.28 mmol) in CH₂Cl₂ (10 mL). The reaction mixture was stirred on an ice bath for 2 h. The precipitate was separated by filtration, and the solid was washed (3x) with CH₂Cl₂. The filtrate was washed with a saturated solution of NaHCO₃ (2x 75 mL), and the organic phase was dried over Na₂SO₄. The solvent was removed by evaporation at reduced pressure to give **2.25** as a white solid (0.53 g, 1.95 mmol, 86%). **¹H-NMR** (400 MHz, DMSO-*d*₆): δ (ppm) 1.39 (s, 9H), 2.81 (s, 4H), 4.09 (d, *J* = 6.2 Hz, 2H), 7.48 (t, *J* = 6.1 Hz, 1H). **¹³C-NMR** (101 MHz, DMSO-*d*₆): δ (ppm) 25.4, 28.1, 39.8, 78.8, 155.6, 166.9, 170.0. **HRMS** (APCI): m/z [M+NH₄]⁺ calcd. for [C₁₁H₂₀N₃O₆]⁺ 290.1347, found 290.1350. C₁₁H₁₆N₂O₆ (272.26).

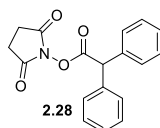


Succinimidyl benzoate (2.26).²⁵ DCC (1.10 g, 5.33 mmol) was dissolved in THF (10 mL) and added dropwise to an ice-cold solution of **2.22** (0.82 g, 3.13 mmol) and benzoic acid (**2.13**) (0.50 g, 4.09 mmol) in THF (30 mL). The reaction mixture was stirred on an ice bath for 2 h and then at rt overnight. The precipitate was removed by filtration, and the solid was washed (2x) with THF (5 mL). The filtrate was dried over Na₂SO₄ and evaporated at reduced pressure. The crude product was purified by column chromatography (eluent: CH₂Cl₂/MeOH 97:3) to give **2.26** as white solid (0.59 g, 2.69 mmol, 86%). **¹H-NMR** (300 MHz, DMSO-*d*₆): δ (ppm) 2.90 (s, 4H), 7.62-7.70 (m, 2H), 7.80-7.88 (m, 1H), 8.07-8.14

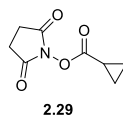
(m, 2H). $^{13}\text{C-NMR}$ (75 MHz, $\text{DMSO-}d_6$): δ (ppm) 25.4, 124.4, 129.45, 129.88, 135.5, 161.7, 170.2. **HRMS** (APCI): m/z $[\text{M}+\text{H}]^+$ calcd. for $[\text{C}_{11}\text{H}_{10}\text{NO}_4]^+$ 220.0604, found 220.0608. $\text{C}_{11}\text{H}_9\text{NO}_4$ (219.20).



Succinimidyl phenylacetate (2.27).²⁶ A solution of DCC (0.84 g, 4.07 mmol) in DMF (1 mL) and a solution of 2-phenylacetic acid (**2.14**) (0.50 g, 3.67 mmol) in DMF (1 mL) were added dropwise to an ice-cold solution of **2.22** (0.36 g 7.12 mmol) in DMF (4 mL). The reaction mixture was stirred on an ice bath for 2 h and then at rt overnight. The precipitate was removed by filtration, and the solid was washed (5x) with DMF (1 mL). The filtrate was poured into a saturated NaHCO_3 solution (75 mL), and the aqueous phase was extracted with ethyl acetate (3x 75 mL). The combined organic phases were washed (2x) with water, dried over MgSO_4 , and evaporated under reduced pressure. The crude product was purified by column chromatography (eluent: light petroleum/ethyl acetate 1:2) to give **2.27** as white solid (0.61 g, 2.62 mmol, 84%). $^1\text{H-NMR}$ (300 MHz, CDCl_3): δ (ppm) 2.81 (s, 4H), 3.94 (s, 2H), 7.28-7.41 (m, 5H). $^{13}\text{C-NMR}$ (75 MHz, CDCl_3): δ (ppm) 25.7, 37.7, 127.9, 129.0, 129.4, 131.5, 166.9, 169.1. **HRMS** (APCI): m/z $[\text{M}+\text{H}]^+$ calcd. for $[\text{C}_{12}\text{H}_{12}\text{NO}_4]^+$ 234.0761, found 234.0765. $\text{C}_{12}\text{H}_{11}\text{NO}_4$ (233.22).

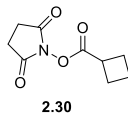


Succinimidyl diphenylacetate (2.28).¹⁸ DCC (1.08 g, 5.23 mmol) was dissolved in CH_2Cl_2 (1 mL) and added dropwise to an ice-cold solution of **2.22** (0.36 g, 3.1 mmol) and diphenyl acetic acid (**2.15**) (0.20 g, 0.94 mmol) in CH_2Cl_2 (10 mL). The reaction mixture was stirred on an ice bath for 2 h. The precipitate was removed by filtration and the solid was washed (3x) with CH_2Cl_2 . The filtrate was washed with a saturated solution of NaHCO_3 (3x 100 mL) and the organic phase was dried over Na_2SO_4 . The solvent was evaporated at reduced pressure and the crude product was purified by column chromatography (eluent light petroleum/ethyl acetate 2:1 to 1:1) to give **2.28** as a white solid (0.50 g, 1.62 mmol, 72%). $^1\text{H-NMR}$ (400 MHz, CDCl_3): δ (ppm) 2.66 (s, 4H), 5.25 (s, 1H), 7.18-7.31 (m, 10H). $^{13}\text{C-NMR}$ (101 MHz, CDCl_3): δ (ppm) 25.7, 54.1, 128.00, 128.79, 128.96, 136.8, 168.2, 169.0. **HRMS** (APCI): m/z $[\text{M}+\text{H}]^+$ calcd. for $[\text{C}_{18}\text{H}_{16}\text{NO}_4]^+$ 310.1074, found 310.1075. $\text{C}_{18}\text{H}_{15}\text{NO}_4$ (309.32).

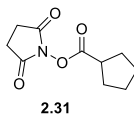


Succinimidyl cyclopropanecarboxylate (2.29).²⁷ A solution of DCC (0.93 g, 4.51 mmol) in CH_2Cl_2 (1 mL) and a solution of cyclopropane carboxylic acid (**2.16**) (324 μL , 4.07 mmol) in CH_2Cl_2 (1 mL) were added dropwise to an ice-cold solution of **2.22** (0.48 g, 4.17 mmol) in CH_2Cl_2 (6 mL) and DMF (0.4 mL). The reaction mixture was stirred on an ice bath for 2 h and then at rt overnight. The precipitate was removed by filtration, and the solid was washed (3x) with CH_2Cl_2 . The filtrate was washed with a saturated solution of NaHCO_3 (100 mL), and the organic phase was dried over Na_2SO_4 . The solvent was removed by evaporation, the residue was taken up in CH_2Cl_2 and crystallization, initiated by the

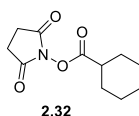
addition of light petroleum, afforded **2.29** as a white solid (0.33 g, 1.80 mmol, 43%). **¹H-NMR** (400 MHz, CDCl₃): δ (ppm) 1.05-1.24 (m, 4H), 1.81-1.94 (m, 1H), 2.80 (s, 4H). **¹³C-NMR** (101 MHz, CDCl₃): δ (ppm) 10.3, 10.6, 25.6, 169.4, 170.3. **HRMS** (APCI): m/z [M+H]⁺ calcd. for [C₈H₁₀NO₄]⁺ 184.0604, found 184.0606. C₈H₉NO₄ (183.16).



Succinimidyl cyclobutanecarboxylate (2.30).²⁸ A solution of DCC (0.81 g, 3.93 mmol) in ethyl acetate (1 mL) and a solution of cyclobutanecarboxylic acid (**2.17**) (335 μL, 3.50 mmol) in ethyl acetate (1 mL) were added dropwise to an ice-cold solution of **2.22** (0.35 g, 3.04 mmol) in ethyl acetate (6 mL) and DMF (0.4 mL). The reaction mixture was stirred on an ice bath for 2 h and then at rt overnight. The precipitate was removed by filtration, and the solid was washed (3x) with CH₂Cl₂. The filtrate was washed with a saturated solution of NaHCO₃ (100 mL), and the organic phase was dried over Na₂SO₄. The solvent was removed by evaporation, the residue was taken up in CH₂Cl₂ and crystallization, initiated by the addition of light petroleum, afforded **2.30** as a white solid (0.22 g, 1.11 mmol, 37%). **¹H-NMR** (300 MHz, CDCl₃): δ (ppm) 1.93-2.14 (m, 2H), 2.30-2.53 (m, 4H), 2.78-2.89 (m, 4H), 3.37-3.51 (m, 1H). **¹³C-NMR** (75 MHz, CDCl₃): δ (ppm) 18.9, 25.5, 25.8, 35.2, 169.5, 170.7. **HRMS** (APCI): m/z [M+H]⁺ calcd. for [C₉H₁₂NO₄]⁺ 198.0761, found 198.0764. C₉H₁₁NO₄ (197.19).

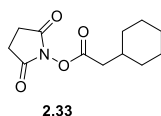


Succinimidyl cyclopentanecarboxylate (2.31). A solution of DCC (0.70 g, 3.39 mmol) in ethyl acetate (1 mL) and a solution of cyclopentanecarboxylic acid (**2.18**) (333 μL, 3.07 mmol) in ethyl acetate (1 mL) were added dropwise to an ice-cold solution of **2.22** (0.35 g, 3.04 mmol) in ethyl acetate (6 mL) and DMF (0.4 mL). The reaction mixture was stirred on an ice bath for 2 h and then at rt overnight. The precipitate was removed by filtration, and the solid was washed (3x) with CH₂Cl₂. The filtrate was washed with a saturated solution of NaHCO₃ (100 mL), and the organic phase was dried over Na₂SO₄. The solvent was removed by evaporation, the residue was taken up in CH₂Cl₂ and crystallization, initiated by the addition of light petroleum, afforded **2.31** as a white solid (0.33 g, 1.56 mmol, 51%). **¹H-NMR** (300 MHz, CDCl₃): δ (ppm) 1.58-1.79 (m, 4H), 1.89-2.09 (m, 4H), 2.78-2.88 (m, 4H), 2.97-3.11 (m, 1H). **¹³C-NMR** (75 MHz, CDCl₃): δ (ppm) 25.7, 26.0, 30.3, 40.7, 169.5, 172.0. **HRMS** (APCI): m/z [M+NH₄]⁺ calcd. for [C₁₀H₁₇N₂O₄]⁺ 229.1183, found 229.1187. C₁₀H₁₃NO₄ (211.22).

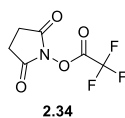


Succinimidyl cyclohexanecarboxylate (2.32).^{28, 29} A solution of DCC (0.77 g, 3.73 mmol) in ethyl acetate (1 mL) and a solution of cyclohexanecarboxylic acid (**2.19**) (0.36 g, 2.81 mmol) in ethyl acetate (1 mL) were dropped to an ice-cold solution of **2.22** (0.41 g, 3.56 mmol) in ethyl acetate (6 mL) and DMF (0.4 mL). The reaction mixture was stirred on an ice bath for 2 h and then at rt overnight. The precipitate

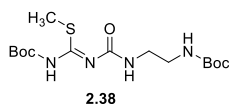
was removed by filtration and the solid was washed (3x) with CH₂Cl₂. The filtrate was washed with a saturated solution of NaHCO₃ (100 mL), and the organic phase was dried over Na₂SO₄. The solvent was removed by evaporation, the residue was taken up in CH₂Cl₂ and crystallization, initiated by the addition of light petroleum, afforded **2.32** as a white solid (0.40 g, 1.67 mmol, 59%). **¹H-NMR** (300 MHz, DMSO-*d*₆): δ (ppm) 1.19-1.62 (m, 7H), 1.64-1.75 (m, 2H), 1.86-1.96 (m, 2H), 2.80 (s, 4H). **¹³C-NMR** (75 MHz, DMSO-*d*₆): δ (ppm) 24.3, 25.0, 25.5, 28.4, 39.4, 170.3, 170.9. **HRMS** (APCI): *m/z* [M+NH₄]⁺ calcd. for [C₁₁H₁₉N₂O₄]⁺ 243.1339, found 243.1346. C₁₁H₁₉N₂O₄ (225.24).



Succinimidyl cyclohexylacetate (2.33). A solution of DCC (0.58 g, 2.81 mmol) in CH₂Cl₂ (1 mL) and a solution of cyclohexylacetic acid (**2.20**) (0.36 g, 2.53 mmol) in CH₂Cl₂ (1 mL) were added dropwise to an ice-cold solution of **2.22** (0.29 g, 2.52 mmol) in CH₂Cl₂ (6 mL) and DMF (0.4 mL). The reaction mixture was stirred on an ice bath for 2 h and then at rt overnight. The precipitate was removed by filtration, and the solid was washed (3x) with CH₂Cl₂. The filtrate was washed with a saturated solution of NaHCO₃ (100 mL), and the organic phase was dried over Na₂SO₄. The solvent was removed by evaporation, the residue was taken up in CH₂Cl₂ and crystallization, initiated by the addition of light petroleum, afforded **2.33** as a white solid (0.25 g, 1.04 mmol, 41%). **¹H-NMR** (300 MHz, CDCl₃): δ (ppm) 0.99-1.33 (m, 5H), 1.62-1.92 (m, 6H), 2.46 (d, *J* = 6.7 Hz, 2H), 2.83 (s, 4H). **¹³C-NMR** (75 MHz, CDCl₃): δ (ppm) 25.8, 26.1, 26.2, 33.0, 35.1, 38.8, 168.1, 169.5. **HRMS** (APCI): *m/z* [M+NH₄]⁺ calcd. for [C₁₂H₂₁N₂O₄]⁺ 257.1496, found 257.1506. C₁₂H₂₁N₂O₄ (239.27).

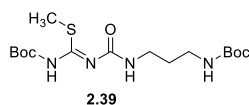


Succinimidyl trifluoroacetate (2.34).³⁰ **2.22** (0.35 g, 3.04 mmol) was dissolved in THF (6 mL), trifluoroacetic acid anhydride (**2.21**) (0.90 mL, 6.38 mmol) was added dropwise and the solution stirred at rt for 3 h. After evaporation of the solvent, toluene (3 mL) was added and evaporated (3x) to obtain **2.34** as a white solid (0.64 g, 3.04 mmol, 100%). **¹H-NMR** (300 MHz, DMSO-*d*₆): δ (ppm) 2.59 (s, 4H). C₆H₄F₃NO₄ (211.10).

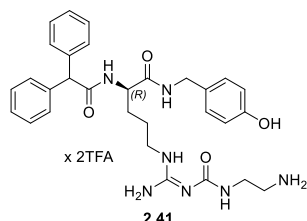


***N*-tert-Butoxycarbonyl-*N'*-[2(*tert*-butoxycarbonylamino)ethyl]aminocarbonyl-*S*-methylisothiourea (2.38).**^{7, 31} A solution of *tert*-butyl (2-aminoethyl)carbamate (**2.36**) (0.62 g, 3.87 mmol) and DIPEA (1.91 mL, 11.2 mmol) in anhydrous CH₂Cl₂ (7 mL) was added dropwise to an ice-cold solution of triphosgene (0.57 g, 1.92 mmol) in anhydrous CH₂Cl₂ (5 mL). The reaction mixture was stirred at rt for 30 min, *N*-Boc-*S*-methylisothiourea (**2.35**) (0.79 g, 4.93 mmol) was added, and after 1.5 h, the solvent was removed by evaporation at reduced pressure. The product was purified directly by column chromatography (eluent CH₂Cl₂/ethyl acetate 98:2 to 90:10) to give **2.38** as a white solid (1.03 g, 2.74 mmol, 71%). **¹H-NMR** (300 MHz, DMSO-*d*₆): δ (ppm) 1.37 (s, 9H), 1.44 (s, 9H), 2.28 (s, 3H), 2.97-

3.11 (m, 4H), 6.82 (t, $J = 5.2$ Hz, 1H), 7.72 (t, $J = 5.3$ Hz, 1H), 12.32 (br s, 1H). **¹³C-NMR** (75 MHz, DMSO-*d*₆): δ (ppm) 13.5, 27.5, 28.1, 39.5, 39.8, 77.6, 82.1, 150.1, 155.6, 161.5, 164.8. **HRMS** (ESI): m/z [M+H]⁺ calcd. for [C₁₅H₂₉N₄O₅S]⁺ 377.1853, found 377.1866. C₁₅H₂₈N₄O₅S (376.47).

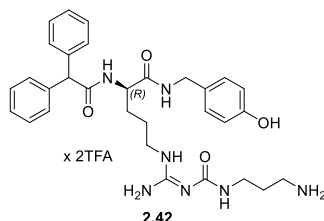


***N*-tert-Butoxycarbonyl-*N'*-[3(*tert*-butoxycarbonylamino)propyl]aminocarbonyl-*S*-methylisothiourea (2.39).**³¹ A solution of *tert*-butyl (3-aminopropyl)carbamate (**2.37**) (5.00 g, 28.7 mmol) and DIPEA (14.7 mL, 86.1 mmol) in anhydrous CH₂Cl₂ (50 mL) was added dropwise to an ice-cold solution of triphosgene (4.26 g, 14.4 mmol) in anhydrous CH₂Cl₂ (45 mL). The reaction mixture was stirred at rt for 30 min, *N*-Boc-*S*-methylisothiourea (**2.35**) (6.55 g, 34.4 mmol) was added, and after 2 h, the solvent was removed by evaporation at reduced pressure. The product was directly purified by column chromatography (eluent CH₂Cl₂/ethyl acetate 98:2 to 96:4; eluent light petroleum/ethyl acetate 87:13 to 82:18) to give **2.39** as a yellowish oil (5.56 g, 14.2 mmol, 50%). **¹H-NMR** (400 MHz, DMSO-*d*₆): δ (ppm) 1.37 (s, 9H), 1.44 (s, 9H), 1.50-1.60 (m, 2H), 2.28 (s, 3H), 2.87-2.97 (m, 2H), 2.99-3.07 (m, 2H), 6.76 (t, $J = 6.8$ Hz, 1H), 7.73 (t, $J = 5.8$ Hz, 1H), 12.39 (br s, 1H). **¹³C-NMR** (101 MHz, DMSO-*d*₆): δ (ppm) 13.6, 27.6, 28.2, 29.5, 37.1, 37.7, 77.4, 82.1, 150.2, 155.6, 161.9, 164.8. **HRMS** (ESI): m/z [M+H]⁺ calcd. for [C₁₆H₃₀N₄O₅Sn]⁺ 413.1829, found 413.1832. C₁₆H₃₀N₄O₅S (390.50).

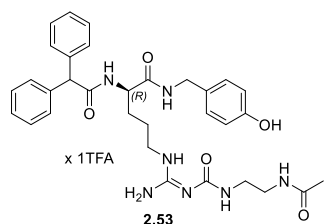


(*R*)-*N*^α-Diphenylacetyl-*N*^ω-(aminoethyl)aminocarbonyl(4-hydroxybenzyl)argininamide bis(hydrotrifluoroacetate) (2.41).⁷ (*R*)-*N*-(4-*tert*-Butoxybenzyl)-*N*^α-(2,2-diphenylacetyl)ornithinamide (**2.40**) (1.31 g, 3.49 mmol) and *N*-*tert*-butoxycarbonyl-*N'*-[2(*tert*-butoxycarbonylamino)ethyl]aminocarbonyl-*S*-methylisothiourea (**2.38**) (1.50 g, 3.08 mmol) were dissolved in CH₂Cl₂ (30 mL). HgCl₂ (1.26 g, 4.62 mmol) and DIPEA (1.31 mL, 7.70 mmol) were added and the mixture was stirred at rt for 1 h to afford the crude product, that was purified directly by column chromatography (eluent CH₂Cl₂/ethyl acetate 1:1). The purified product was dissolved in CH₂Cl₂ (7.5 mL), the reaction mixture was cooled to 0 °C and TFA (7.5 mL) was added. After 1 h, the mixture was allowed to warm to rt, then stirred overnight. The solvent was evaporated, and the crude product was purified by HPLC (gradient: 0-35 min, A/B 85:15–38:62, $t_R = 16$ min) to give **2.41** as a fluffy white solid (372.11 mg, 47 mmol, 68%). **¹H-NMR** (600 MHz, DMSO-*d*₆): δ (ppm) 1.36-1.50 (m, 2H), 1.51-1.58 (m, 1H), 1.64-1.72 (m, 1H), 2.93 (br s, 2H), 3.18-3.26 (m, 2H), 3.33-3.38 (m, 2H), 4.09-4.20 (m, 2H), 4.30-4.36 (m, 1H), 5.13 (s, 1H), 6.65-6.69 (m, 2H), 6.98-7.02 (m, 2H), 7.20-7.25 (m, 2H), 7.26-7.31 (m, 8H), 7.61 (br s, 1H), 7.89 (br s, 3H), 8.36 (t, $J = 5.7$ Hz, 1H), 8.42-8.65 (br s, 2H, interfering with the next signal), 8.49 (d, $J = 8.1$ Hz, 1H), 9.05 (br s, 1H), 9.33 (br s, 1H), 10.81 (br s, 1H). **¹³C-NMR** (151 MHz, DMSO-*d*₆): δ (ppm) 24.6, 29.4, 37.2, 38.5, 40.4, 41.6, 52.3, 55.9, 115.0, 117.0 (q, $J = 297.1$ Hz) (TFA), 126.57, 126.61, 128.17, 128.21, 128.40, 128.50, 128.52, 129.13, 140.3, 140.5, 153.7, 154.4, 156.3, 158.9 (q, $J = 31.6$ Hz) (TFA),

170.97, 171.04. **HRMS** (ESI): m/z $[M+H]^+$ calcd. for $[C_{30}H_{38}N_7O_4]^+$ 560.2980, found 560.2986. $C_{30}H_{37}N_7O_4 \times C_4H_2F_6O_4$ (559.67 + 228.05).

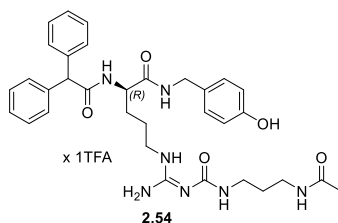


(R)-N^α-Diphenylacetyl-N^ω-(aminopropyl)aminocarbonyl(4-hydroxybenzyl)argininamide bis(hydrotrifluoroacetate) (2.42).³² (R)-N-(4-*tert*-Butoxybenzyl)-N^α-(2,2-diphenylacetyl)ornithinamide (**2.40**) (150 mg, 0.31 mmol) and *N-tert*-butoxycarbonyl-N-[3(*tert*-butoxycarbonylamino)propyl]amino-carbonyl-S-methylisothiourea (**2.39**) (132 mg, 0.34 mmol) were dissolved in CH_2Cl_2 (30 mL). $HgCl_2$ (126 mg, 0.46 mmol) and DIPEA (100 mg, 0.76 mmol) were added and the mixture was stirred at rt overnight to afford the crude product, that was purified by column chromatography (eluent CH_2Cl_2 /ethyl acetate 10:1 to 1:1). The purified product was dissolved in a mixture (10.5 mL) of CH_2Cl_2 , TFA and water (1:1:0.1). Afterwards, CH_2Cl_2 (20 mL) was added, the organic solvent was evaporated (2x) at reduced pressure, and the crude product was purified by HPLC (gradient: 0-35 min, A/B 85:15–38:62, t_R = 19 min) to obtain **2.42** as a fluffy white solid (112 mg, 0.14 mmol, 45%). **¹H-NMR** (600 MHz, $DMSO-d_6$): δ (ppm) 1.36-1.50 (m, 2H), 1.50-1.60 (m, 1H), 1.63-1.79 (m, 3H), 2.77-2.88 (m, 2H), 3.14-3.26 (m, 4H), 4.10-4.21 (m, 2H), 4.29-4.38 (m, 1H), 5.13 (s, 1H), 6.64-6.71 (m, 2H), 6.98-7.03 (m, 2H), 7.18-7.24 (m, 2H), 7.26-7.34 (m, 8H), 7.67 (br s, 1H), 7.87 (br s, 3H), 8.37 (t, J = 5.5 Hz, 1H), 8.41-8.61 (m, 3H), 9.03 (br s, 1H), 9.36 (br s, 1H), 10.78 (br s, 1H). **¹³C-NMR** (151 MHz, $DMSO-d_6$): δ (ppm) 24.6, 27.3, 29.4, 36.5, 36.7, 40.4, 41.7, 52.4, 56.0, 115.0, 117.0 (q, J = 298.4 Hz) (TFA), 126.59, 126.62, 128.18, 128.22, 128, 4, 128.52, 128.57, 129.2, 140.3, 140.5, 153.8, 154.1, 156.3, 159.2 (q, J = 32.1 Hz) (TFA), 171.04, 171.08. **HRMS** (ESI): m/z $[M+H]^+$ calcd. for $[C_{31}H_{40}N_7O_4]^+$ 574.3136, found 574.3142. $C_{31}H_{39}N_7O_4 \times C_4H_2F_6O_4$ (573.70 + 228.05).

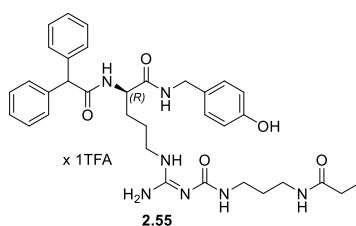


(R)-N^α-Diphenylacetyl-N^ω-(acetylaminoethyl)aminocarbonyl(4-hydroxybenzyl)argininamide hydrotrifluoroacetate (2.53). Compound **2.53** was prepared using *general procedure A*, the reactants **2.41** (34.6 mg, 43.9 μ mol), succinimidyl acetate (**2.43**) (7.3 mg, 32.5 μ mol), DIPEA (29 μ L, 166 μ mol) and the solvent DMF (300 μ L). Purification by preparative HPLC (gradient: 0-35 min, A/B 85:15–45:55, t_R = 20 min) afforded **2.53** as a fluffy white solid (22.4 mg, 31.3 μ mol, 71%). **¹H-NMR** (600 MHz, $DMSO-d_6$): δ (ppm) 1.36-1.50 (m, 2H), 1.51-1.61 (m, 1H), 1.64-1.72 (m, 1H), 1.80 (s, 3H), 3.10-3.27 (m, 6H), 4.09-4.20 (m, 2H), 4.31-4.37 (m, 1H), 5.13 (s, 1H), 6.65-6.71 (m, 2H), 6.98-7.03 (m, 2H), 7.19-7.25 (m, 2H), 7.26-7.33 (m, 8H), 7.50-7.56 (m, 1H), 7.90-8.00 (m, 1H), 8.36 (t, J = 5.8 Hz, 1H), 8.43 (br s, 2H, interfering with two surrounding signals), 8.49 (d, J = 8.1 Hz, 1H), 8.96 (br s, 1H), 9.31 (br s, 1H),

10.25 (br s, 1H). **¹³C-NMR** (151 MHz, DMSO-*d*₆): δ (ppm) 22.6, 24.6, 29.4, 38.1, 39.1, 40.3, 41.6, 52.3, 55.9, 115.0, 115.7 (TFA), 117.6 (TFA), 126.57, 126.61, 128.17, 128.21, 128.42, 128.50, 128.53, 129.1, 140.3, 140.5, 153.6, 153.9, 156.3, 158.9 (q, *J* = 33.2 Hz) (TFA), 169.6, 170.99, 171.03. **RP-HPLC** (Method A, 220 nm): 100% (*t*_R = 11.8 min, *k* = 3.5). **HRMS** (ESI): *m/z* [M+H]⁺ calcd. for [C₃₂H₄₀N₇O₅]⁺ 602.3085, found 602.3092. C₃₂H₃₉N₇O₅ × C₂HF₃O₂ (601.71 + 114.02).

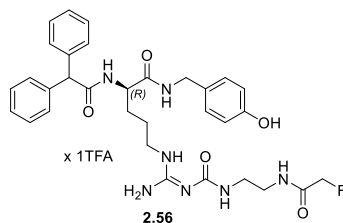


(R)-N^ω-Diphenylacetyl-N^ω-(acetylamino)propylaminocarbonyl(4-hydroxybenzyl)argininamide hydrotrifluoroacetate (2.54). Compound **2.54** was prepared using *general procedure A*, the reactants **2.42** (26.3 mg, 32.8 μmol), succinimidyl acetate (**2.43**) (5.1 mg, 32 μmol), DIPEA (22 μL, 126 μmol) and the solvent DMF (300 μL). Purification by preparative HPLC (gradient: 0-35 min, A/B 85:15–45:55, *t*_R = 20 min) afforded **2.54** as a fluffy white solid (15.7 mg, 18.6 μmol, 57%). **¹H-NMR** (600 MHz, DMSO-*d*₆): δ (ppm) 1.36-1.50 (m, 2H), 1.52-1.60 (m, 3H), 1.64-1.72 (m, 1H), 1.80 (s, 3H), 3.03-3.08 (m, 2H), 3.08-3.13 (m, 2H), 3.16-3.24 (m, 2H), 4.10-4.20 (m, 2H), 4.31-4.37 (m, 1H), 5.13 (s, 1H), 6.66-6.69 (m, 2H), 6.98-7.02 (m, 2H), 7.19-7.25 (m, 2H), 7.26-7.31 (m, 8H), 7.49 (t, *J* = 5.1 Hz, 1H), 7.88 (t, *J* = 5.4 Hz, 1H), 8.36 (t, *J* = 5.8 Hz, 1H), 8.40 (br s, 2H, interfering with two surrounding signals), 8.49 (d, *J* = 8.0 Hz, 1H), 8.94 (br s, 1H), 9.30 (br s, 1H), 10.16 (br s, 1H). **¹³C-NMR** (151 MHz, DMSO-*d*₆): δ (ppm) 22.6, 24.6, 29.2, 29.4, 36.0, 37.0, 40.3, 41.6, 52.3, 55.9, 115.0, 115.4 (TFA), 117.4 (TFA), 126.57, 126.60, 128.17, 128.20, 128.42, 128.50, 128.53, 129.1, 140.3, 140.5, 153.6, 153.7, 156.3, 158.7 (q, *J* = 34.0 Hz) (TFA), 169.3, 170.99, 171.03. **RP-HPLC** (Method A, 220 nm): 100% (*t*_R = 11.9 min, *k* = 3.6). **HRMS** (ESI): *m/z* [M+H]⁺ calcd. for [C₃₃H₄₂N₇O₅]⁺ 616.3242, found 616.3250. C₃₃H₄₁N₇O₅ × C₂HF₃O₂ (615.74 + 114.02).

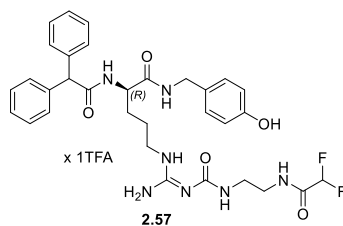


(R)-N^ω-Diphenylacetyl-N^ω-(propionylamino)propylaminocarbonyl(4-hydroxybenzyl)argininamide hydrotrifluoroacetate (2.55). Compound **2.55** was prepared using *general procedure A*, the reactants **2.42** (26.3 mg, 32.8 μmol), succinimidyl propionate (**2.44**) (6.1 mg, 35.6 μmol), DIPEA (22 μL, 126 μmol) and the solvent DMF (300 μL). Purification by preparative HPLC (gradient: 0-35 min, A/B 85:10–45:55, *t*_R = 22 min) afforded **2.55** as a fluffy white solid (17.5 mg, 23.5 μmol, 72%). **¹H-NMR** (600 MHz, DMSO-*d*₆): δ (ppm) 0.99 (t, *J* = 7.6 Hz, 3H), 1.36-1.50 (m, 2H), 1.50-1.60 (m, 3H), 1.64-1.72 (m, 1H), 2.07 (q, *J* = 7.6 Hz, 2H), 3.04-3.13 (m, 4H), 3.16-3.23 (m, 2H), 4.10-4.20 (m, 2H), 4.31-4.37 (m, 1H), 5.13 (s, 1H), 6.66-6.70 (m, 2H), 6.99-7.02 (m, 2H), 7.19-7.25 (m, 2H), 7.26-7.31 (m, 8H), 7.50 (br s, 1H), 7.80 (t, *J* = 5.5 Hz, 1H), 8.36 (t, *J* = 5.8 Hz, 1H), 8.41 (br s, 2H, interfering with two surrounding signals),

8.49 (d, $J = 8.1$ Hz, 1H), 8.95 (br s, 1H), 9.31 (br s, 1H, interfering with previous signal), 10.21 (br s, 1H). $^{13}\text{C-NMR}$ (151 MHz, $\text{DMSO-}d_6$): δ (ppm) 10.0, 24.6, 28.5, 29.28, 29.42, 35.9, 37.0, 40.3, 41.6, 52.3, 55.9, 115.0, 115.5 (TFA), 117.5 (TFA), 126.57, 126.60, 128.16, 128.20, 128.42, 128.50, 128.53, 129.1, 140.3, 140.5, 153.63, 153.71, 156.3, 158.8 (q, $J = 33.6$ Hz) (TFA), 170.99, 171.03, 170.07. **RP-HPLC** (Method A, 220 nm): 99% ($t_R = 12.4$ min, $k = 3.8$). **HRMS** (ESI): m/z $[\text{M}+\text{H}]^+$ calcd. for $[\text{C}_{34}\text{H}_{44}\text{N}_7\text{O}_5]^+$ 630.3398, found 630.3403. $\text{C}_{34}\text{H}_{43}\text{N}_7\text{O}_5 \times \text{C}_2\text{HF}_3\text{O}_2$ (629.76 + 114.02).

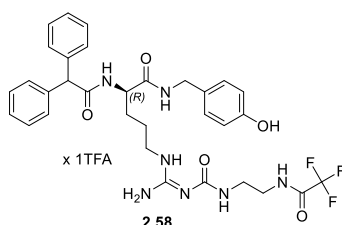


(R)-N^α-Diphenylacetyl-N^ω-(2-fluoroacetylaminoethyl)aminocarbonyl(4-hydroxybenzyl)argininamide hydrotrifluoroacetate (2.56). Compound **2.56** was prepared using *general procedure C* and the reactants **2.41** (99.71 mg, 126.6 μmol), 2-fluoroacetic acid (**2.46**) (28.99 mg, 371.5 μmol), DIPEA (55 μL , 315.7 μmol), DCC (39.44 mg, 191.2 μmol). Purification by preparative HPLC (gradient: 0-35 min, A/B 85:15–38:62, $t_R = 21$ min) afforded **2.56** as a fluffy white solid (26.6 mg, 36.3 μmol , 29%). $^1\text{H-NMR}$ (600 MHz, $\text{DMSO-}d_6$): δ (ppm) 1.36-1.49 (m, 2H), 1.50-1.58 (m, 1H), 1.64-1.71 (m, 1H), 3.17-3.26 (m, 6H), 4.09-4.18 (m, 2H), 4.30-4.35 (m, 1H), 4.78 (d, $J = 47.1$ Hz, 2H), 5.12 (s, 1H), 6.65-6.68 (m, 2H), 6.98-7.01 (m, 2H), 7.18-7.24 (m, 2H), 7.27-7.30 (m, 8H), 7.56 (br s, 1H), 8.26 (t, $J = 5.0$ Hz, 1H), 8.35 (t, $J = 5.8$ Hz, 1H), 8.44 (br s, 2H, interfering with two surrounding signals), 8.48 (d, $J = 8.1$ Hz, 1H), 8.97 (br s, 1H), 9.31 (br s, 1H), 10.36 (br s, 1H). $^{13}\text{C-NMR}$ (150 MHz, $\text{DMSO-}d_6$): δ (ppm) 24.6, 29.4, 37.8, 38.8, 40.4, 41.6, 52.3, 55.9, 80.0 (d, $J = 180.4$ Hz), 115.0, 116.0 (TFA), 118.0 (TFA), 126.58, 126.62, 128.17, 128.22, 128.43, 128.51, 128.54, 129.1, 140.3, 140.5, 153.7, 154.0, 156.3, 159.0 (q, $J = 32.2$ Hz) (TFA), 167.5 (d, $J = 18.2$ Hz), 171.01, 171.05. **RP-HPLC** (Method A, 220 nm): 98% ($t_R = 12.6$ min, $k = 3.9$). **HRMS** (ESI): m/z $[\text{M}+\text{H}]^+$ calcd. for $[\text{C}_{32}\text{H}_{39}\text{FN}_7\text{O}_5]^+$ 620.2991, found 620.2999. $\text{C}_{32}\text{H}_{38}\text{FN}_7\text{O}_5 \times \text{C}_2\text{HF}_3\text{O}_2$ (619.70 + 114.02).

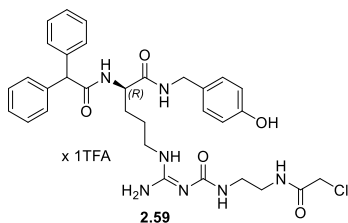


(R)-N^α-Diphenylacetyl-N^ω-(2,2-difluoroacetylaminoethyl)aminocarbonyl(4-hydroxybenzyl)argininamide hydrotrifluoroacetate (2.57). Compound **2.57** was prepared using *general procedure C* and the reactants **2.41** (66.4 mg, 84.3 μmol), 2,2-difluoroacetic acid (**2.47**) (15 μL , 238.4 μmol), DIPEA (36 μL , 206.7 μmol), DCC (26.3 mg, 127.5 μmol). Purification by preparative HPLC (gradient: 0-35 min, A/B 85:15–38:62, $t_R = 21$ min) afforded **2.57** as a fluffy white solid (10.0 mg, 13.3 μmol , 16%). $^1\text{H-NMR}$ (600 MHz, $\text{DMSO-}d_6$): δ (ppm) 1.35-1.48 (m, 2H), 1.49-1.57 (m, 1H), 1.63-1.70 (m, 1H), 3.17-3.27 (m, 6H), 4.08-4.19 (m, 2H), 4.30-4.35 (m, 1H), 5.12 (s, 1H), 6.19 (t, $J = 53.7$ Hz, 1H), 6.64-6.69 (m, 2H), 6.97-7.00 (m, 2H), 7.18-7.24 (m, 2H), 7.25-7.31 (m, 8H), 7.58 (br s, 1H), 8.35 (t, $J = 5.7$ Hz, 1H), 8.44

(br s, 2H, interfering with two surrounding signals), 8.48 (d, $J = 8.1$ Hz, 1H), 8.86 (t, $J = 5.1$ Hz, 1H), 8.94 (br s, 1H), 9.30 (br s, 1H), 10.23 (br s, 1H). **¹³C-NMR** (150 MHz, DMSO-*d*₆): δ (ppm) 24.6, 29.4, 38.2, 38.4, 40.3, 41.6, 52.3, 55.9, 108.5 (t, $J = 247.2$ Hz), 115.0, 116.1 (TFA), 118.1 (TFA), 126.56, 126.60, 128.16, 128.20, 128.41, 128.49, 128.52, 129.1, 140.3, 140.5, 153.6, 153.9, 156.3, 158.6 (q, $J = 31.4$ Hz) (TFA), 162.6 (t, $J = 25.1$ Hz), 170.97, 171.02. **RP-HPLC** (Method A, 220 nm): 98% ($t_R = 12.8$ min, $k = 4.0$). **HRMS** (ESI): m/z [M+H]⁺ calcd. for [C₃₂H₃₈F₂N₇O₅]⁺ 638.2897, found 638.2905. C₃₂H₃₇F₂N₇O₅ × C₂HF₃O₂ (637.69 + 114.02).

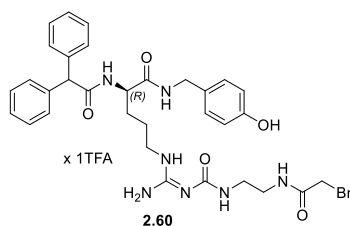


(R)-N^ω-Diphenylacetyl-N^ω-(trifluoroacetyl-aminoethyl)aminocarbonyl(4-hydroxybenzyl)argininamide hydrotrifluoroacetate (2.58). Compound **2.58** was prepared using *general procedure A*, the reactants **2.41** (30 mg, 38.1 μ mol), succinimidyl trifluoroacetate (**2.34**) (20 mg, 88.3 μ mol), DIPEA (20 μ L, 114.8 μ mol) and the solvent DMF (100 μ L). Purification by preparative HPLC (gradient: 0-30 min, A/B 85:15–38:62, $t_R = 19$) afforded **2.58** as a fluffy white solid (6.24 mg, 8.1 μ mol, 21%). **¹H-NMR** (600 MHz, DMSO-*d*₆): δ (ppm) 1.36-1.49 (m, 2H), 1.50-1.58 (m, 1H), 1.63-1.71 (m, 1H), 3.17-3.23 (m, 2H), 3.24-3.28 (m, 2H), 3.29-3.32 (m, 2H), 4.08-4.21 (m, 2H), 4.30-4.37 (m, 1H), 5.12 (s, 1H), 6.66-6.69 (m, 2H), 6.98-7.02 (m, 2H), 7.20-7.25 (m, 2H), 7.27-7.30 (m, 8H), 7.61 (t, $J = 5.5$ Hz, 1H), 8.36 (t, $J = 5.9$ Hz, 1H), 8.44 (br s, 2H, interfering with two surrounding signals), 8.48 (d, $J = 8.1$ Hz, 1H), 8.91 (br s, 1H), 9.30 (br s, 1H), 9.48 (t, $J = 5.2$ Hz, 1H), 10.17 (br s, 1H). **¹³C-NMR** (150 MHz, DMSO-*d*₆): δ (ppm) 24.6, 29.4, 36.5, 38.1, 38.9, 40.4, 41.6, 52.3, 56.0, 114.96 (TFA), 115.03, 116.9 (TFA), 117.1 (q, $J = 298.6$ Hz), 126.58, 126.61, 128.17, 128.21, 128.42, 128.51, 128.56, 129.1, 140.3, 140.5, 153.7, 154.2, 156.5, 156.8 (the last signals belong to a quartet that is not fully resolved), 158.8 (q, $J = 31.7$ Hz) (TFA), 171.04, 171.07. **RP-HPLC** (Method A, 220 nm): 98% ($t_R = 13.6$ min, $k = 4.3$). **HRMS** (ESI): m/z [M+H]⁺ calcd. for [C₃₂H₃₇F₃N₇O₅]⁺ 656.2803, found 656.2814. C₃₂H₃₆F₃N₇O₅ × C₂HF₃O₂ (655.68 + 114.02).

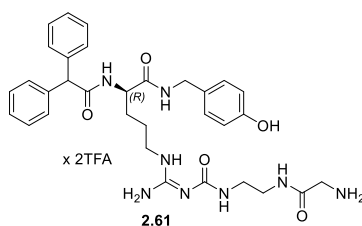


(R)-N^ω-Diphenylacetyl-N^ω-(2-chloroacetyl-aminoethyl)aminocarbonyl(4-hydroxybenzyl)argininamide hydrotrifluoroacetate (2.59). Compound **2.59** was prepared using *general procedure B* and the reactants **2.41** (106.74 mg, 135.5 μ mol), 2-chloroacetic acid (**2.48**) (37.4 mg, 395.8 μ mol), DCC (38 mg, 184.2 μ mol). Purification by preparative HPLC (gradient: 0-30 min, A/B 85:15–38:62, $t_R = 18$ min) afforded **2.59** as a fluffy white solid (16.61 mg, 22.14 μ mol, 16%). **¹H-NMR** (600 MHz, DMSO-*d*₆): δ (ppm) 1.37-1.50 (m, 2H), 1.51-1.58 (m, 1H), 1.64-1.73 (m, 1H), 3.17-3.24 (m, 6H), 4.05 (s, 2H), 4.10-

4.20 (m, 2H), 4.31-4.36 (m, 1H), 5.13 (s, 1H), 6.65-6.70 (m, 2H), 6.98-7.02 (m, 2H), 7.19-7.25 (m, 2H), 7.26-7.32 (m, 8H), 7.56 (br s, 1H), 8.31-8.35 (m, 1H), 8.36 (t, $J = 5.8$ Hz, 1H), 8.45 (br s, 2H, interfering with two surrounding signals), 8.49 (d, $J = 8.1$ Hz, 1H), 8.96 (br s, 1H), 9.31 (br s, 1H), 10.32 (br s, 1H). $^{13}\text{C-NMR}$ (150 MHz, $\text{DMSO-}d_6$): δ (ppm) 24.6, 29.4, 38.6, 38.7, 40.3, 41.6, 42.6, 52.3, 55.9, 115.01, 115.9 (TFA), 117.9 (TFA), 126.56, 126.61, 128.16, 128.21, 128.42, 128.50, 128.53, 129.13, 140.3, 140.5, 153.6, 153.9, 156.3, 158.8 (q, $J = 32.5$ Hz) (TFA), 166.3, 170.98, 171.03. **RP-HPLC** (Method A, 220 nm): 100% ($t_R = 12.8$ min, $k = 4.0$). **HRMS** (ESI): m/z $[\text{M}+\text{H}]^+$ calcd. for $[\text{C}_{32}\text{H}_{39}\text{ClN}_7\text{O}_5]^+$ 636.2696, found 636.2699. $\text{C}_{32}\text{H}_{38}\text{ClN}_7\text{O}_5 \times \text{C}_2\text{HF}_3\text{O}_2$ (636.15 + 114.02).

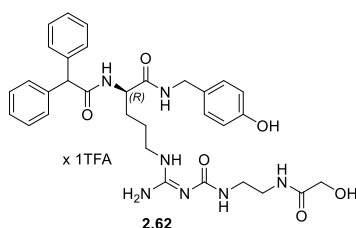


(R)-N^α-Diphenylacetyl-N^ω-(2-bromoacetylaminoethyl)aminocarbonyl(4-hydroxybenzyl)argininamide hydrotrifluoroacetate (2.60). Compound **60** was prepared using *general procedure B* and the reactants **2.41** (93.44 mg, 118.6 μmol), 2-bromoacetic acid (**2.49**) (37.5 mg, 269.9 μmol), DCC (31.1 mg, 150.7 μmol). Purification by preparative HPLC (gradient: 0-30 min, A/B 85:15–38:62, $t_R = 19$ min) afforded **2.60** as a fluffy white solid (15.40 mg, 19.4 μmol , 16%). $^1\text{H-NMR}$ (600 MHz, $\text{DMSO-}d_6$): δ (ppm) 1.37-1.50 (m, 2H), 1.51-1.58 (m, 1H), 1.64-1.73 (m, 1H), 3.17-3.24 (m, 6H), 3.85 (s, 2H), 4.10-4.20 (m, 2H), 4.31-4.36 (m, 1H), 5.13 (s, 1H), 6.65-6.70 (m, 2H), 6.98-7.02 (m, 2H), 7.19-7.25 (m, 2H), 7.26-7.32 (m, 8H), 7.56 (br s, 1H), 8.31-8.35 (m, 1H), 8.36 (t, $J = 5.8$ Hz, 1H), 8.45 (br s, 2H, interfering with two surrounding signals), 8.49 (d, $J = 8.1$ Hz, 1H), 8.97 (br s, 1H), 9.31 (br s, 1H), 10.32 (br s, 1H). $^{13}\text{C-NMR}$ (150 MHz, $\text{DMSO-}d_6$): δ (ppm) 24.6, 29.40, 29.44, 38.66, 38.73, 40.4, 41.6, 52.3, 55.9, 115.0, 126.56, 126.61, 128.16, 128.21, 128.42, 128.50, 128.52, 129.13, 140.3, 140.5, 153.6, 153.9, 156.3, 158.8 (q, $J = 32.9$ Hz), 166.5, 170.97, 171.03. **RP-HPLC** (Method A, 220 nm): 99% ($t_R = 12.9$ min, $k = 4.0$). **HRMS** (ESI): m/z $[\text{M}+\text{H}]^+$ calcd. for $[\text{C}_{32}\text{H}_{39}\text{BrN}_7\text{O}_5]^+$ 680.2191, found 680.2193. $\text{C}_{32}\text{H}_{38}\text{BrN}_7\text{O}_5 \times \text{C}_2\text{HF}_3\text{O}_2$ (680.60 + 114.02).

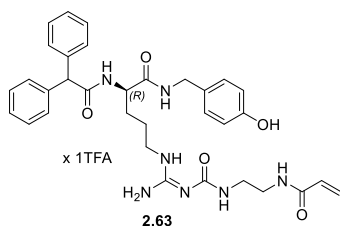


(R)-N^α-Diphenylacetyl-N^ω-(glycinylaminoethyl)aminocarbonyl(4-hydroxybenzyl)argininamide bis(hydrotrifluoroacetate) (2.61). Compound **2.61** was prepared using *general procedure A*, the reactants **2.41** (41.4 mg, 52.6 μmol), succinimidyl *N*-Boc-glycinate (**2.25**) (17.6 mg, 64.6 μmol), DIPEA (35 μL , 200.9 μmol) and the solvent DMF (1 mL). Additionally, the crude product was poured into a solution of 100 mL water (5% acetonitrile, 0.5% TFA). After lyophilization, the crude product was dissolved in a mixture (2 mL) of CH_2Cl_2 and TFA (1:1) and stirred at rt for 2 h. The solvent was evaporated, and the crude product purified by preparative HPLC (gradient: 0-30 min, A/B 85:15–40:60,

$t_R = 15$ min) which afforded **2.61** as a fluffy white solid (20.5 mg, 24.4 μ mol, 46%). **¹H-NMR** (600 MHz, DMSO-*d*₆): δ (ppm) 1.36-1.50 (m, 2H), 1.51-1.58 (m, 1H), 1.64-1.72 (m, 1H), 3.17-3.26 (m, 6H), 3.53 (s, 2H), 4.09-4.19 (m, 2H), 4.31-4.36 (m, 1H), 5.13 (s, 1H), 6.66-6.70 (m, 2H), 6.98-7.02 (m, 2H), 7.19-7.25 (m, 2H), 7.26-7.31 (m, 8H), 7.64 (br s, 1H), 8.08 (br s, 3H), 8.36 (t, $J = 5.7$ Hz, 1H), 8.42-8.56 (m, 4H), 9.02 (br s, 1H), 9.34 (br s, 1H), 10.73 (br s, 1H). **¹³C-NMR** (150 MHz, DMSO-*d*₆): δ (ppm) 24.6, 29.4, 38.3, 38.7, 40.0, 40.3, 41.6, 52.3, 55.9, 115.0, 116.1 (TFA), 118.0 (TFA), 126.58, 126.61, 128.17, 128.21, 128.41, 128.51, 128.54, 129.1, 140.3, 140.5, 153.7, 154.1, 156.3, 158.9 (q, $J = 31.7$ Hz) (TFA), 166.2, 171.01, 171.06. **RP-HPLC** (Method A, 220 nm): 96% ($t_R = 10.9$ min, $k = 3.2$). **HRMS** (ESI): m/z [M+H]⁺ calcd. for [C₃₂H₄₁N₈O₅]⁺ 617.3194, found 617.3205. C₃₂H₄₀N₈O₅ × C₄H₂F₆O₄ (616.31 + 228.04).

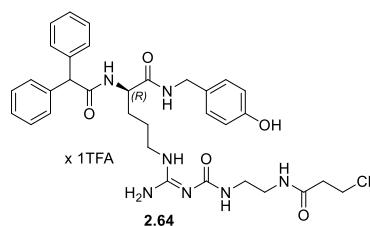


(R)-N^ω-Diphenylacetyl-N^ω-(2-hydroxyacetyl)aminocarbonyl(4-hydroxybenzyl)argininamide hydrotrifluoroacetate (2.62). Under assay conditions, **2.60** is stable for 24 h. Degradation of compound **2.60** led to a 2:1 mixture of **2.60** and **2.62** after 6 months. Purification by preparative HPLC (gradient: 0-30 min, A/B 85:15–38:62, $t_R = 15$ min) afforded **2.62** as a fluffy white solid. **¹H-NMR** (600 MHz, DMSO-*d*₆): δ (ppm) 1.35-1.49 (m, 2H), 1.50-1.58 (m, 1H), 1.64-1.72 (m, 1H), 3.17-3.25 (m, 6H), 3.81 (s, 2H), 4.09-4.20 (m, 2H), 4.31-4.36 (m, 1H), 5.12 (s, 1H), 5.50 (br s, 1H), 6.50-6.70 (m, 2H), 6.98-7.02 (m, 2H), 7.20-7.25 (m, 2H), 7.26-7.30 (m, 8H), 7.52 (br s, 1H), 7.88 (t, $J = 5.2$ Hz, 1H), 8.36 (t, $J = 5.8$ Hz, 1H), 8.40 (br s, 2H, interfering with two surrounding signals), 8.48 (d, $J = 8.1$ Hz, 1H), 8.89 (br s, 1H), 9.29 (br s, 1H), 9.89 (br s, 1H). **¹³C-NMR** (150 MHz, DMSO-*d*₆): δ (ppm) 24.6, 29.4, 37.7, 39.1, 40.3, 41.6, 52.3, 55.9, 61.4, 115.0, 126.57, 126.61, 128.16, 128.20, 128.41, 128.49, 128.50, 129.1, 140.3, 140.4, 153.5, 153.8, 156.3, 158.3 (q, $J = 31.6$ Hz) (TFA), 170.95, 171.00, 172.3. **RP-HPLC** (Method A, 220 nm): 96% ($t_R = 11.5$ min, $k = 3.5$). **HRMS** (ESI): m/z [M+H]⁺ calcd. for [C₃₂H₄₀N₇O₆]⁺ 618.3035, found 618.3038. C₃₂H₃₉N₇O₅ × C₂HF₃O₂ (617.71 + 114.02).

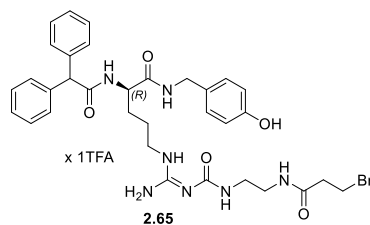


(R)-N^ω-Diphenylacetyl-N^ω-(acrylaminoethyl)aminocarbonyl(4-hydroxybenzyl)argininamide hydrotrifluoroacetate (2.63). Compound **2.63** was prepared using *general procedure B* and the reactants **2.41** (97.33 mg, 123.5 μ mol), acrylic acid (**2.52**) (20 μ L, 291.4 μ mol), DCC (25 mg, 121.2 μ mol). Purification by preparative HPLC (gradient: 0-30 min, A/B 85:15–40:60, $t_R = 18$ min) afforded **2.63** as a fluffy white solid (9.0 mg, 12.4 μ mol, 10%). **¹H-NMR** (600 MHz, DMSO-*d*₆): δ (ppm) 1.36-1.50 (m, 2H), 1.50-1.58 (m, 1H), 1.63-1.72 (m, 1H), 3.18-3.23 (m, 4H), 3.23-3.27 (m, 2H), 4.09-4.20 (m, 2H), 4.30-4.36 (m, 1H), 5.16 (s, 1H), 5.59 (dd, $^2J = 2.1$ Hz, $^3J = 10.1$ Hz, 1H), 6.08 (dd,

$^2J = 2.1$ Hz, $^3J = 17.1$ Hz, 1H), 6.20 (dd, $^2J = 10.1$ Hz, $^3J = 17.1$ Hz, 1H), 6.65-6.70 (m, 2H), 6.98-7.03 (m, 2H), 7.19-7.25 (m, 2H), 7.26-7.32 (m, 8H), 7.56 (br s, 1H), 8.23 (t, $J = 5.3$ Hz, 1H), 8.36 (t, $J = 5.8$ Hz, 1H), 8.44 (br s, 2H, interfering with two surrounding signals), 8.49 (d, $J = 8.1$ Hz, 1H), 8.96 (br s, 1H), 9.31 (br s, 1H), 10.18 (br s, 1H). $^{13}\text{C-NMR}$ (150 MHz, DMSO- d_6): δ (ppm) 24.6, 29.4, 38.1, 39.0, 40.3, 41.6, 52.3, 55.9, 115.0, 125.3, 126.56, 126.60, 128.16, 128.20, 128.41, 128.49, 128.52, 129.1, 131.6, 140.3, 140.5, 153.6, 153.9, 156.3, 158.4 (q, $J = 32.1$ Hz) (TFA), 165.0, 170.97, 171.02. **RP-HPLC** (Method A, 220 nm): 98% ($t_R = 12.4$ min, $k = 3.8$). **HRMS** (ESI): m/z $[\text{M}+\text{H}]^+$ calcd. for $[\text{C}_{33}\text{H}_{40}\text{N}_7\text{O}_5]^+$ 614.3085, found 614.3089. $\text{C}_{33}\text{H}_{39}\text{N}_7\text{O}_5 \times \text{C}_2\text{HF}_3\text{O}_2$ (613.72 + 114.02).

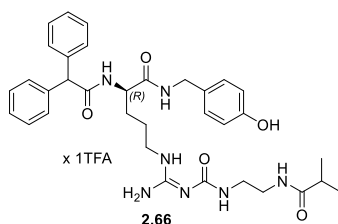


(R)- N^{α} -Diphenylacetyl- N^{ω} -(3-chloropropanoylaminoethyl)aminocarbonyl(4-hydroxybenzyl)argininamide hydrotrifluoroacetate (2.64). Compound **2.64** was prepared using *general procedure B* and the reactants **2.41** (101.15 mg, 128.4 μmol), 3-chloropropionic acid (**2.50**) (20.31 mg, 187.2 μmol), DCC (33.02 mg, 160 μmol). Purification by preparative HPLC (gradient: 0-35 min, A/B 85:15–38:62, $t_R = 21$ min) afforded **2.64** as a white solid fluffy (9.16 mg, 12.0 μmol , 9%). $^1\text{H-NMR}$ (600 MHz, DMSO- d_6): δ (ppm) 1.36-1.50 (m, 2H), 1.51-1.59 (m, 1H), 1.64-1.72 (m, 1H), 2.56 (t, $J = 6.4$ Hz, 2H), 3.14-3.23 (m, 6H), 3.77 (t, $J = 6.4$ Hz, 2H), 4.09-4.20 (m, 2H), 4.31-4.37 (m, 1H), 5.13 (s, 1H), 6.65-6.70 (m, 2H), 6.98-7.02 (m, 2H), 7.19-7.26 (m, 2H), 7.26-7.32 (m, 8H), 7.51 (br s, 1H), 8.12 (br s, 1H), 8.36 (t, $J = 5.8$ Hz, 1H), 8.44 (br s, 2H, interfering with two surrounding signals), 8.49 (d, $J = 8.1$ Hz, 1H), 8.97 (br s, 1H), 9.32 (br s, 1H), 10.34 (br s, 1H). $^{13}\text{C-NMR}$ (150 MHz, DMSO- d_6): δ (ppm) 24.6, 29.4, 38.1, 38.3, 39.1, 40.3, 40.9, 41.6, 52.3, 55.9, 115.0, 116.0 (TFA), 118.0 (TFA), 126.56, 126.60, 128.16, 128.20, 128.41, 128.49, 128.52, 129.13, 140.3, 140.5, 153.6, 153.9, 156.3, 158.7 (q, $J = 31.6$ Hz) (TFA), 169.2, 170.98, 171.03. **RP-HPLC** (Method A, 220 nm): 96% ($t_R = 12.8$ min, $k = 4.0$). **HRMS** (ESI): m/z $[\text{M}+\text{H}]^+$ calcd. for $[\text{C}_{33}\text{H}_{41}\text{ClN}_7\text{O}_5]^+$ 650.2852, found 650.2854. $\text{C}_{33}\text{H}_{40}\text{ClN}_7\text{O}_5 \times \text{C}_2\text{HF}_3\text{O}_2$ (650.18 + 114.02).

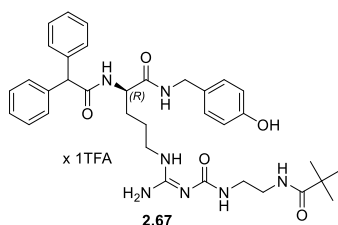


(R)- N^{α} -Diphenylacetyl- N^{ω} -(3-bromopropanoylaminoethyl)aminocarbonyl(4-hydroxybenzyl)argininamide hydrotrifluoroacetate (2.65). Compound **2.65** was prepared using *general procedure B* and the reactants **2.41** (97.3 mg, 123.5 μmol), 3-bromopropionic acid (**2.51**) (80 mg, 522.9 μmol), DCC (30 mg, 145.4 μmol). Purification by preparative HPLC (gradient: 0-35 min, A/B 85:15–38:62, $t_R = 21$ min) afforded **2.65** as a fluffy white solid (12.0 mg, 14.8 μmol , 12%). $^1\text{H-NMR}$ (600 MHz, DMSO- d_6): δ (ppm) 1.35-1.49 (m, 2H), 1.49-1.57 (m, 1H), 1.63-1.71 (m, 1H), 2.67 (t, $J = 6.5$ Hz, 2H),

3.14-3.22 (m, 6H), 3.63 (t, $J = 6.5$ Hz, 2H), 4.09-4.20 (m, 2H), 4.31-4.36 (m, 1H), 5.13 (s, 1H), 6.66-6.69 (m, 2H), 6.99-7.02 (m, 2H), 7.20-7.25 (m, 2H), 7.26-7.31 (m, 8H), 7.48-7.52 (m, 1H), 8.10-8.13 (m, 1H), 8.36 (t, $J = 5.8$ Hz, 1H), 8.42 (br s, 2H, interfering with two surrounding signals), 8.48 (d, $J = 8.48$ Hz, 1H), 8.93 (br s, 1H), 9.30 (br s, 1H), 10.14 (br s, 1H). **¹³C-NMR** (150 MHz, DMSO-*d*₆): δ (ppm) 24.6, 29.36, 29.40, 38.1, 38.5, 38.9, 40.3, 41.6, 52.3, 55.9, 115.0, 126.57, 126.60, 128.16, 128.20, 128.41, 128.49, 128.51, 129.1, 140.3, 140.5, 153.6, 153.8, 156.3, 158.6 (q, $J = 33.4$ Hz) (TFA), 169.5, 170.96, 171.02. **RP-HPLC** (Method A, 220 nm): 97% ($t_R = 13.0$ min, $k = 4.1$). **HRMS** (ESI): m/z [M+H]⁺ calcd. for [C₃₂H₄₁BrN₇O₅]⁺ 694.2347, found 694.2355. C₃₃H₄₀BrN₇O₅ × C₂HF₃O₂ (694.63 + 114.02).

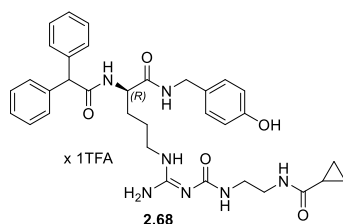


(R)-N^ω-Diphenylacetyl-N^ω-(2-methylpropionylaminoethyl)aminocarbonyl(4-hydroxybenzyl)argininamide hydrotrifluoroacetate (2.66). Compound **2.66** was prepared using *general procedure A*, the reactants **2.41** (30.98 mg, 39.3 μ mol), succinimidyl 2-methylpropionate (**2.23**) (7.76 mg, 41.9 μ mol), DIPEA (20 μ L, 114.8 μ mol) and the solvent DMF (100 μ L). Purification by preparative HPLC (gradient: 0-30 min, A/B 85:15–38:62, $t_R = 17$ min) afforded **2.66** as a fluffy white solid (24.54 mg, 33.0 μ mol, 84%). **¹H-NMR** (600 MHz, DMSO-*d*₆): δ (ppm) 0.99 (d, $J = 6.9$ Hz, 6H), 1.36-1.50 (m, 2H), 1.51-1.58 (m, 1H), 1.64-1.72 (m, 1H), 2.32 (septet, $J = 6.9$ Hz, 1H), 3.12-3.18 (m, 4H), 3.18-3.23 (m, 2H), 4.10-4.20 (m, 2H), 4.31-4.36 (m, 1H), 5.13 (s, 1H), 6.66-6.70 (m, 2H), 6.99-7.02 (m, 2H), 7.19-7.25 (m, 2H), 7.26-7.30 (m, 8H), 7.49 (br s, 1H), 7.81-7.84 (m, 1H), 8.36 (t, $J = 5.8$ Hz, 1H), 8.44 (br s, 2H, interfering with two surrounding signals), 8.49 (d, $J = 8.1$ Hz, 1H), 8.97 (br s, 1H), 9.31 (br s, 1H), 10.33 (br s, 1H). **¹³C-NMR** (151 MHz, DMSO-*d*₆): δ (ppm) 19.5, 24.6, 29.4, 34.1, 38.0, 39.1, 40.3, 41.6, 52.3, 55.9, 115.0, 115.7 (TFA), 117.7 (TFA), 126.56, 126.60, 128.16, 128.20, 128.41, 128.49, 128.52, 129.13, 140.3, 140.5, 153.6, 153.9, 156.3, 158.8 (q, $J = 33.1$ Hz) (TFA), 170.97, 171.03, 173.0. **RP-HPLC** (Method B, 220 nm): 99% ($t_R = 15.8$ min, $k = 4.5$). **HRMS** (ESI): m/z [M+H]⁺ calcd. for [C₃₄H₄₄N₇O₅]⁺ 630.3398, found 630.3410. C₃₄H₄₃N₇O₅ × C₂HF₃O₂ (629.76 + 114.02).

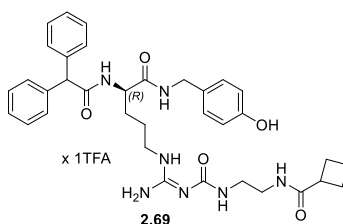


(R)-N^ω-Diphenylacetyl-N^ω-(2,2-dimethylpropionylaminoethyl)aminocarbonyl(4-hydroxybenzyl)argininamide hydrotrifluoroacetate (2.67). Compound **2.67** was prepared using *general procedure A*, the reactants **2.41** (31.06 mg, 39.4 μ mol), succinimidyl 2,2-dimethylpropionate (**2.24**) (14.09 mg, 70.7 μ mol), DIPEA (20 μ L, 114.8 μ mol) and the solvent DMF (100 μ L). Purification by preparative HPLC (gradient: 0-30 min, A/B 90:10–30:70, $t_R = 19$ min) afforded **2.67** as a fluffy white solid (26.60 mg, 35.1 μ mol, 89%). **¹H-NMR** (600 MHz, DMSO-*d*₆): δ (ppm) 1.08 (s, 9H), 1.36-1.50 (m, 2H), 1.50-1.59 (m,

1H), 1.63-1.72 (m, 1H), 3.13-3.23 (m, 6H), 4.09-4.20 (m, 2H), 4.31-4.37 (m, 1H), 5.13 (s, 1H), 6.65-6.70 (m, 2H), 6.98-7.02 (m, 2H), 7.19-7.25 (m, 2H), 7.26-7.32 (m, 8H), 7.47 (br s, 1H), 7.52-7.57 (m, 1H), 8.36 (t, $J = 5.8$ Hz, 1H), 8.43 (br s, 2H, interfering with two surrounding signals), 8.49 (d, $J = 8.0$ Hz, 1H), 8.97 (s, 1H), 9.31 (br s, 1H), 10.38 (s, 1H). $^{13}\text{C-NMR}$ (150 MHz, $\text{DMSO-}d_6$): δ (ppm) 24.6, 27.4, 29.4, 38.0, 38.5, 39.01, 40.3, 41.6, 52.3, 55.9, 115.0, 115.7 (TFA), 117.7 (TFA), 126.57, 126.60, 128.16, 128.20, 128.41, 128.50, 128.53, 129.13, 140.3, 140.5, 153.7, 154.0, 156.3, 158.9 (q, $J = 32.8$ Hz) (TFA), 170.98, 171.03, 177.9. **RP-HPLC** (Method B, 220 nm): 99% ($t_R = 17.5$ min, $k = 5.1$). **HRMS** (ESI): m/z $[\text{M}+\text{H}]^+$ calcd. for $[\text{C}_{35}\text{H}_{46}\text{N}_7\text{O}_5]^+$ 644.3555, found 644.3570. $\text{C}_{35}\text{H}_{45}\text{N}_7\text{O}_5 \times \text{C}_2\text{HF}_3\text{O}_2$ (643.79 + 114.02).

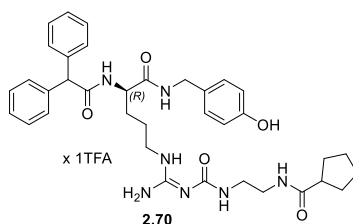


(R)-N^α-Diphenylacetyl-N^ω-(cyclopropoylaminoethyl)aminocarbonyl(4-hydroxybenzyl)argininamide hydrotrifluoroacetate (2.68). Compound **2.68** was prepared using *general procedure A*, the reactants **2.41** (30.81 mg, 39.1 μmol), succinimidyl cyclopropanecarboxylate (**2.29**) (11.13 mg, 60.8 μmol), DIPEA (20 μL , 114.8 μmol) and the solvent DMF (100 μL). Purification by preparative HPLC (gradient: 0-30 min, A/B 85:15–38:62, $t_R = 17$ min) afforded **2.68** as a fluffy white solid (19.36 mg, 26.1 μmol , 67%). $^1\text{H-NMR}$ (600 MHz, $\text{DMSO-}d_6$): δ (ppm) 0.61-0.69 (m, 4H), 1.38-1.57 (m, 4H), 1.63-1.71 (m, 1H), 3.14-3.23 (m, 6H), 4.09-4.20 (m, 2H), 4.31-4.36 (m, 1H), 5.13 (s, 1H), 6.66-6.69 (m, 2H), 6.99-7.01 (m, 2H), 7.20-7.25 (m, 2H), 7.27-7.30 (m, 8H), 7.54 (br s, 1H), 8.17 (s, 1H), 8.36 (t, $J = 5.8$ Hz, 1H), 8.44 (br s, 2H, interfering with two surrounding signals), 8.49 (d, $J = 8.1$ Hz, 1H), 8.97 (s, 1H), 9.31 (s, 1H), 10.20 (s, 1H). $^{13}\text{C-NMR}$ (151 MHz, $\text{DMSO-}d_6$): δ (ppm) 6.3, 13.6, 24.6, 29.4, 38.2, 39.3, 40.3, 41.6, 52.3, 55.9, 115.0, 116.1 (TFA), 118.1 (TFA), 126.56, 126.60, 128.16, 128.20, 128.41, 128.49, 128.52, 129.1, 140.3, 140.5, 153.6, 153.9, 156.3, 158.6 (q, $J = 32.7$ Hz) (TFA), 170.97, 171.02, 173.0. **RP-HPLC** (Method B, 220 nm): 99% ($t_R = 17.0$ min, $k = 4.9$). **HRMS** (ESI): m/z $[\text{M}+\text{H}]^+$ calcd. for $[\text{C}_{34}\text{H}_{42}\text{N}_7\text{O}_5]^+$ 628.3242, found 628.3255. $\text{C}_{34}\text{H}_{41}\text{N}_7\text{O}_5 \times \text{C}_2\text{HF}_3\text{O}_2$ (627.75 + 114.02).

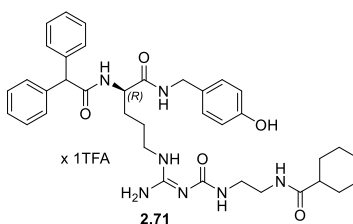


(R)-N^α-Diphenylacetyl-N^ω-(cyclobutoylaminoethyl)aminocarbonyl(4-hydroxybenzyl)argininamide hydrotrifluoroacetate (2.69). Compound **2.69** was prepared using *general procedure A*, the reactants **2.41** (30.27 mg, 38.4 μmol), succinimidyl cyclobutanecarboxylate (**2.30**) (11.46 mg, 63.1 μmol), DIPEA (20 μL , 114.8 μmol) and the solvent DMF (100 μL). Purification by preparative HPLC (gradient: 0-30 min, A/B 85:15–38:62, $t_R = 18$ min) afforded **2.69** as a fluffy white solid (20.90 mg, 27.7 μmol , 72%). $^1\text{H-NMR}$ (600 MHz, $\text{DMSO-}d_6$): δ (ppm) 1.35-1.50 (m, 2H), 1.50-1.58 (m, 1H), 1.64-1.77 (m, 2H), 1.82-1.90 (m, 1H), 1.96-2.02 (m, 2H), 2.07-2.15 (m, 2H), 2.96 (q, $J = 8.5$ Hz, 1H), 3.12-

3.17 (m, 4H), 3.18-3.23 (m, 2H), 4.10-4.20 (m, 2H), 4.31-4.36 (m, 1H), 1.53 (s, 1H), 6.66-6.69 (m, 2H), 6.99-7.02 (m, 2H), 7.20-7.25 (m, 2H), 7.27-7.30 (m, 8H), 7.51 (br s, 1H), 7.74 (br s, 1H), 8.36 (t, $J = 5.8$ Hz, 1H), 8.43 (br s, 2H, interfering with two surrounding signals), 8.49 (d, $J = 8.1$ Hz, 1H), 8.96 (br s, 1H), 9.31 (br s, 1H), 10.24 (br s, 1H). **¹³C-NMR** (151 MHz, DMSO-*d*₆): δ (ppm) 17.7, 24.7, 29.4, 36.5, 38.1, 38.7, 39.1, 40.3, 41.6, 52.3, 55.9, 115.0, 115.6 (TFA), 117.6 (TFA), 126.56, 126.60, 128.16, 128.20, 128.41, 128.49, 128.52, 129.13, 140.3, 140.5, 153.6, 153.9, 156.3, 158.7 (q, $J = 33.6$ Hz) (TFA), 170.97, 171.02, 174.3. **RP-HPLC** (Method B, 220 nm): 96% ($t_R = 16.4$ min, $k = 4.7$). **HRMS** (ESI): m/z [M+H]⁺ calcd. for [C₃₅H₄₄N₇O₅]⁺ 642.3398, found 642.3406. C₃₅H₄₃N₇O₅ × C₂HF₃O₂ (641.77 + 114.02).

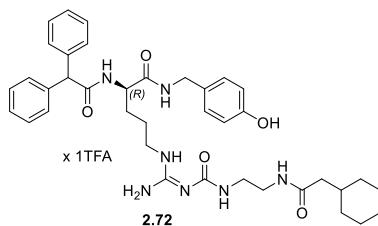


(R)-N^ω-Diphenylacetyl-N^ω-(cyclopentylaminoethyl)aminocarbonyl(4-hydroxybenzyl)argininamide hydrotrifluoroacetate (2.70). Compound **2.70** was prepared using *general procedure A*, the reactants **2.41** (30.82 mg, 39.1 μ mol), succinimidyl cyclopentanecarboxylate (**2.31**) (10.13 mg, 48.0 μ mol), DIPEA (20 μ L, 114.8 μ mol) and the solvent DMF (100 μ L). Purification by preparative HPLC (gradient: 0-30 min, A/B 85:15–38:62, $t_R = 19$ min) afforded **2.70** as a fluffy white solid (15.90 mg, 20.7 μ mol, 53%). **¹H-NMR** (600 MHz, DMSO-*d*₆): δ (ppm) 1.35-1.64 (m, 10H), 1.65-1.75 (m, 3H), 3.13 (m, 4H), 3.18-3.23 (m, 2H), 4.09-4.19 (m, 2H), 4.31 (m, 1H), 5.13 (s, 1H), 6.65-6.70 (m, 2H), 6.98-7.02 (m, 2H), 7.20-7.25 (m, 2H), 7.26-7.31 (m, 8H), 7.50 (br s, 1H), 7.86 (br s, 1H), 8.36 (t, $J = 5.8$ Hz, 1H), 8.44 (br s, 2H, interfering with two surrounding signals), 8.49 (d, $J = 8.1$ Hz, 1H), 8.96 (br s, 1H), 9.32 (br s, 1H), 10.27 (br s, 1H). **¹³C-NMR** (151 MHz, DMSO-*d*₆): δ (ppm) 24.6, 25.6, 29.4, 29.9, 38.1, 39.1, 40.3, 41.6, 44.3, 52.3, 55.9, 115.0, 115.7 (TFA), 117.6 (TFA), 126.56, 126.60, 128.15, 128.20, 128.41, 128.49, 128.52, 129.13, 140.3, 140.5, 153.6, 153.9, 156.3, 158.6 (q, $J = 33.2$ Hz) (TFA), 170.97, 171.02, 175.7. **RP-HPLC** (Method B, 220 nm): 99% ($t_R = 17.0$ min, $k = 4.9$). **HRMS** (ESI): m/z [M+H]⁺ calcd. for [C₃₆H₄₆N₇O₅]⁺ 656.3555, found 656.3571. C₃₆H₄₅N₇O₅ × C₂HF₃O₂ (655.80 + 114.02).

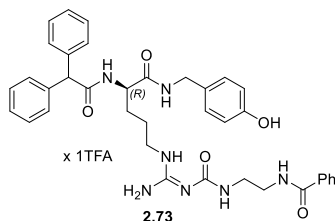


(R)-N^ω-Diphenylacetyl-N^ω-(cyclohexylaminoethyl)aminocarbonyl(4-hydroxybenzyl)argininamide hydrotrifluoroacetate (2.71). Compound **2.71** was prepared using *general procedure A*, the reactants **2.41** (29.0 mg, 36.8 μ mol), succinimidyl cyclohexanecarboxylate (**2.32**) (11.3 mg, 54.0 μ mol), DIPEA (20 μ L, 114.8 μ mol) and the solvent DMF (100 μ L). Purification by preparative HPLC (gradient: 0-30 min, A/B 85:15–38:62, $t_R = 20.0$ min) afforded **71** as a fluffy white solid (17.45 mg, 22.3 μ mol, 61%). **¹H-NMR** (600 MHz, DMSO-*d*₆): δ (ppm) 1.10-1.22 (m, 3H), 1.26-1.35 (m, 2H), 1.36-1.50 (m, 2H), 1.51-1.62 (m, 2H), 1.64-1.71 (m, 5H), 2.02-2.08 (m, 1H), 3.11-3.17 (m, 4H), 3.18-3.23 (m, 2H), 4.10-4.19 (m,

2H), 4.31-4.36 (m, 1H), 5.13 (s, 1H), 6.66-6.69 (m, 2H), 6.99-7.02 (m, 2H), 7.19-7.25 (m, 2H), 7.26-7.31 (m, 8H), 7.47 (br s, 1H), 7.75-7.80 (m, 1H), 8.36 (t, $J = 5.8$ Hz, 1H), 8.43 (br s, 2H, interfering with two surrounding signals), 8.49 (d, $J = 8.1$ Hz, 1H), 8.95 (br s, 1H), 9.31 (br s, 1H), 10.25 (br s, 1H). $^{13}\text{C-NMR}$ (150 MHz, $\text{DMSO-}d_6$): δ (ppm) 24.6, 25.3, 25.5, 29.2, 29.4, 37.9, 39.3, 40.3, 41.6, 44.1, 52.3, 55.9, 115.0, 115.6 (TFA), 117.6 (TFA), 126.57, 126.60, 128.16, 128.20, 128.41, 128.49, 128.52, 129.1, 140.3, 140.5, 153.6, 153.9, 156.3, 158.7 (q, $J = 32.4$ Hz) (TFA), 170.97, 171.02, 175.6. **RP-HPLC** (Method B, 220 nm): 99% ($t_R = 18.0$ min, $k = 5.2$). **HRMS** (ESI): m/z $[\text{M} + \text{H}]^+$ calcd. for $[\text{C}_{37}\text{H}_{48}\text{N}_7\text{O}_5]^+$ 670.3711, found 670.3722. $\text{C}_{37}\text{H}_{47}\text{N}_7\text{O}_5 \times \text{C}_2\text{HF}_3\text{O}_2$ (669.83 + 114.02).

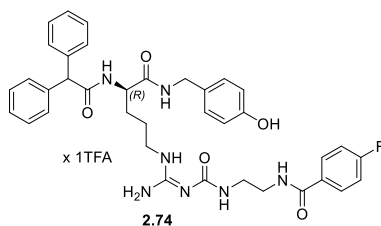


(R)-N^α-Diphenylacetyl-N^ω-(cyclohexylacetylaminoethyl)aminocarbonyl(4-hydroxybenzyl)-argininamide hydrotrifluoroacetate (2.72). Compound **2.72** was prepared using *general procedure A*, the reactants **2.41** (30.6 mg, 38.8 μmol), succinimidyl cyclohexylacetate (**2.33**) (12.7 mg, 56.9 μmol), DIPEA (20 μL , 114.8 μmol) and the solvent DMF (100 μL). Purification by preparative HPLC (gradient: 0-30 min, A/B 85:15–38:62, $t_R = 21$ min) afforded **2.72** as a fluffy white solid (15.8 mg, 19.8 μmol , 51%). $^1\text{H-NMR}$ (600 MHz, $\text{DMSO-}d_6$): δ (ppm) 0.82-0.92 (m, 2H), 1.06-1.21 (m, 3H), 1.37-1.50 (m, 2H), 1.50-1.74 (m, 8H), 1.93 (d, $J = 6.9$ Hz, 2H), 3.15 (br s, 4H), 3.18-3.22 (m, 2H), 4.09-4.20 (m, 2H), 4.31-4.36 (m, 1H), 5.13 (s, 1H), 6.65-6.70 (m, 2H), 6.97-7.03 (m, 2H), 7.19-7.25 (m, 2H), 7.26-7.31 (m, 8H), 7.48 (br s, 1H), 7.87 (br s, 1H), 8.36 (t, $J = 5.8$ Hz, 1H), 8.44 (br s, 2H, interfering with two surrounding signals), 8.49 (d, $J = 8.1$ Hz, 1H), 8.96 (br s, 1H), 9.31 (br s, 1H), 10.25 (s, 1H). $^{13}\text{C-NMR}$ (151 MHz, $\text{DMSO-}d_6$): δ (ppm) 24.6, 25.6, 25.8, 29.4, 32.5, 34.6, 37.9, 39.3, 40.3, 41.6, 43.4, 52.3, 55.9, 115.0, 126.56, 126.59, 128.15, 128.19, 128.40, 128.49, 128.52, 129.1, 140.3, 140.5, 153.6, 153.9, 156.3, 158.7 (q, $J = 34.5$ Hz) (TFA), 170.96, 171.02, 171.7. **RP-HPLC** (Method B, 220 nm): 100% ($t_R = 16.0$ min, $k = 4.6$). **HRMS** (ESI): m/z $[\text{M} + \text{H}]^+$ calcd. for $[\text{C}_{38}\text{H}_{50}\text{N}_7\text{O}_5]^+$ 684.3868, found 684.3887. $\text{C}_{38}\text{H}_{49}\text{N}_7\text{O}_5 \times \text{C}_2\text{HF}_3\text{O}_2$ (683.85 + 114.02).

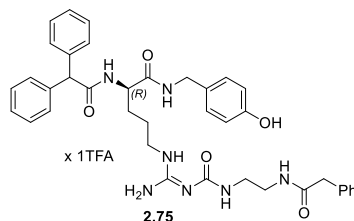


(R)-N^α-Diphenylacetyl-N^ω-(benzoylaminoethyl)aminocarbonyl(4-hydroxybenzyl)argininamide hydrotrifluoroacetate (2.73). Compound **2.73** was prepared using *general procedure A*, the reactants **2.41** (30.74 mg, 39.0 μmol), succinimidyl benzoate (**2.26**) (13 mg, 59.3 μmol), DIPEA (20 μL , 114.8 μmol) and the solvent DMF (100 μL). Purification by preparative HPLC (gradient: 0-30 min, A/B 85:15–40:60, $t_R = 21$ min) afforded **2.73** as a fluffy white solid (12.0 mg, 15.4 μmol , 39%). $^1\text{H-NMR}$ (600 MHz, $\text{DMSO-}d_6$): δ (ppm) 1.36-1.50 (m, 2H), 1.51-1.59 (m, 1H), 1.64-1.73 (m, 1H), 3.17-3.24 (m,

2H), 3.28-3.33 (m, 2H), 3.34-3.42 (m, 2H, interfering with water signal), 4.09-4.20 (m, 2H), 4.31-4.36 (m, 1H), 5.13 (s, 1H), 6.65-6.70 (m, 2H), 6.98-7.03 (m, 2H), 7.19-7.25 (m, 2H), 7.26-7.31 (m, 8H), 7.43-7.48 (m, 2H), 7.50-7.55 (m, 1H), 7.58-7.64 (m, 1H), 7.82-7.87 (m, 2H), 8.36 (t, $J = 5.7$ Hz, 1H), 8.44 (br s, 2H, interfering with two surrounding signals), 8.49 (d, $J = 8.0$ Hz, 1H), 8.56 (t, $J = 5.5$ Hz, 1H), 8.96 (br s, 1H), 9.32 (br s, 1H), 10.24 (br s, 1H). **¹³C-NMR** (150 MHz, DMSO-*d*₆): δ (ppm) 24.6, 29.4, 38.8, 39.0, 40.3, 41.6, 52.3, 55.9, 115.0, 126.56, 126.60, 127.20, 128.16, 128.20, 128.24, 128.41, 128.49, 128.52, 129.1, 131.2, 134.4, 140.3, 140.5, 153.6, 153.9, 156.3, 158.8 (q, $J = 31.5$ Hz) (TFA), 166.6, 170.98, 171.03. **RP-HPLC** (Method A, 220 nm): 99% ($t_R = 13.7$ min, $k = 4.3$). **HRMS** (ESI): m/z [M+H]⁺ calcd. for [C₃₇H₄₂N₇O₅]⁺ 664.3242, found 664.3250. C₃₇H₄₁N₇O₅ × C₂HF₃O₂ (663.78 + 114.02).

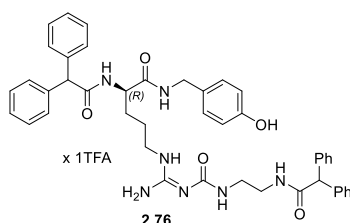


(R)-N^ω-Diphenylacetyl-N^ω-(4-fluorobenzoylaminoethyl)aminocarbonyl(4-hydroxybenzyl)argininamide hydrotrifluoroacetate (2.74). Compound **2.74** was prepared using *general procedure A*, the reactants **2.41** (30.95 mg, 39.3 μ mol), succinimidyl 4-fluorobenzoate (**2.45**) (10.21 mg, 23.4 μ mol), DIPEA (20 μ L, 114.8 μ mol) and the solvent DMF (100 μ L). Purification by preparative HPLC (gradient: 0-30 min, A/B 80:20–50:50, $t_R = 20$ min) afforded **2.74** as a fluffy white solid (13.8 mg, 17.3 μ mol, 44%). **¹H-NMR** (600 MHz, DMSO-*d*₆): δ (ppm) 1.36-1.49 (m, 2H), 1.51-1.58 (m, 1H), 1.64-1.72 (m, 1H), 3.17-3.23 (m, 2H), 3.27-3.32 (m, 2H), 3.35-3.40 (m, 2H), 4.09-4.20 (m, 2H), 4.31-4.36 (m, 1H), 5.13 (s, 1H), 6.66-6.69 (m, 2H), 6.99-7.01 (m, 2H), 7.19-7.25 (m, 2H), 7.26-7.30 (m, 10H), 7.30-7.31 (m, 1H), 7.64 (br s, 1H), 7.89-7.93 (m, 2H), 8.36 (t, $J = 5.8$ Hz, 1H), 8.44 (br s, 2H, interfering with two surrounding signals), 8.49 (d, $J = 8.1$ Hz, 1H), 8.60 (t, $J = 5.5$ Hz, 1H), 8.96 (br s, 1H), 9.31 (br s, 1H). **¹³C-NMR** (150 MHz, DMSO-*d*₆): δ (ppm) 24.6, 29.4, 38.8, 39.0, 40.3, 41.6, 52.3, 55.9, 115.0, 115.14 (d, $J = 21.7$ Hz), 126.55, 126.59, 128.14, 128.19, 128.40, 128.48, 128.51, 129.1, 129.8 (d, $J = 9.0$ Hz), 130.9 (d, $J = 3.0$ Hz), 140.3, 140.4, 153.6, 153.9, 156.3, 158.4 (q, $J = 30.7$ Hz) (TFA), 163.8 (d, $J = 248.3$ Hz), 165.5, 170.97, 171.01. **RP-HPLC** (Method C, 220 nm): 98% ($t_R = 22.9$ min, $k = 6.9$). **HRMS** (ESI): m/z [M+H]⁺ calcd. for [C₃₇H₄₁FN₇O₅]⁺ 682.3148, found 682.3157. C₃₇H₄₀FN₇O₅ × C₂HF₃O₂ (681.77 + 114.02).

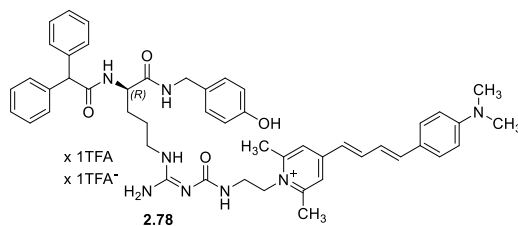


(R)-N^ω-Diphenylacetyl-N^ω-(phenylacetyl-aminoethyl)aminocarbonyl(4-hydroxybenzyl)argininamide hydrotrifluoroacetate (2.75). Compound **2.75** was prepared using *general procedure A*, the reactants **2.41** (30.18 mg, 38.3 μ mol), succinimidyl phenylacetate (**2.27**) (10.39 mg, 44.6 μ mol), DIPEA (20 μ L, 114.8 μ mol) and the solvent DMF (100 μ L). Purification by preparative HPLC (gradient: 0-30

min, A/B 85:15–38:62, $t_R = 19$ min) afforded **2.75** as a fluffy white solid (19.64 mg, 24.8 μmol , 65%). **$^1\text{H-NMR}$** (600 MHz, $\text{DMSO-}d_6$): δ (ppm) 1.36-1.51 (m, 2H), 1.51-1.59 (m, 1H), 1.64-1.73 (m, 1H), 3.14-3.24 (m, 6H), 3.40 (s, 2H), 4.09-4.20 (m, 2H), 4.30-4.38 (m, 1H), 5.13 (s, 1H), 6.66-6.69 (m, 2H), 6.98-7.02 (m, 2H), 7.19-7.31 (m, 15H), 7.53 (br s, 1H), 8.15 (br s, 1H), 8.36 (t, $J = 5.7$ Hz, 1H), 8.44 (br s, 2H, interfering with two surrounding signals), 8.49 (d, $J = 8.0$ Hz, 1H), 8.95 (br s, 1H), 9.31 (br s, 1H), 10.27 (br s, 1H). **$^{13}\text{C-NMR}$** (151 MHz, $\text{DMSO-}d_6$): δ (ppm) 24.6, 29.4, 38.2, 39.1, 40.3, 41.6, 42.4, 52.3, 55.9, 115.0, 115.8 (TFA), 117.8 (TFA), 126.3, 126.57, 126.60, 128.16, 128.20, 128.41, 128.50, 128.52, 128.99 (two carbon signals), 129.13, 136.3, 140.3, 140.5, 153.6, 153.9, 156.3, 158.7 (q, $J = 33.6$ Hz) (TFA), 170.5, 170.98, 171.03. **RP-HPLC** (Method B, 220 nm): 99% ($t_R = 17.0$ min, $k = 4.9$). **HRMS** (ESI): m/z $[\text{M}+\text{H}]^+$ calcd. for $[\text{C}_{38}\text{H}_{44}\text{N}_7\text{O}_5]^+$ 678.3398, found 678.3414. $\text{C}_{38}\text{H}_{43}\text{N}_7\text{O}_5 \times \text{C}_2\text{HF}_3\text{O}_2$ (677.81 + 114.02).



(R)-N $^{\alpha}$ -Diphenylacetyl-N $^{\omega}$ -(diphenylacetylaminoethyl)aminocarbonyl(4-hydroxybenzyl)argininamide hydrotrifluoroacetate (2.76). Compound **2.76** was prepared using *general procedure A*, the reactants **2.41** (35.81 mg, 45.5 μmol), succinimidyl diphenylacetate (**2.28**) (26 mg, 84.1 μmol), DIPEA (25 μL , 143.5 μmol) and the solvent DMF (100 μL). Purification by preparative HPLC (gradient: 0-30 min, A/B 85:15–38:62, $t_R = 16$ min) afforded **2.76** as a fluffy white solid (15 mg, 17.3 μmol , 38%). **$^1\text{H-NMR}$** (600 MHz, $\text{DMSO-}d_6$): δ (ppm) 1.37-1.48 (m, 2H), 1.50-1.58 (m, 1H), 1.64-1.73 (m, 1H), 3.14-3.24 (m, 6H), 4.07-4.20 (m, 2H), 4.29-4.37 (m, 1H), 4.90 (s, 1H), 5.12 (s, 1H), 6.65-6.68 (m, 2H), 6.98-7.01 (m, 2H), 7.18-7.24 (m, 4H), 7.26-7.29 (m, 16H), 7.49 (br s, 1H), 8.34-8.38 (m, 2H), 8.42 (br s, 2H, interfering with two surrounding signals), 8.49 (d, $J = 8.1$ Hz, 1H), 8.92 (br s, 1H), 9.30 (br s, 1H), 10.18 (br s, 1H). **$^{13}\text{C-NMR}$** (150 MHz, $\text{DMSO-}d_6$): δ (ppm) 24.6, 29.4, 38.3, 39.0, 40.4, 41.6, 52.3, 55.9, 56.6, 115.0, 116.1 (TFA), 118.1 (TFA), 126.55, 126.58 (two carbon signals), 128.14, 128.17, 128.18, 128.27, 128.34, 128.39 (2 carb.), 128.46, 128.47, 128.49, 129.11, 140.3 (2 carb.), 140.4, 153.6, 153.9, 156.3, 158.6 (q, $J = 30.5$ Hz) (TFA), 170.95, 171.01, 171.37. One aromatic carbon was not apparent. **RP-HPLC** (Method B, 220 nm): 98% ($t_R = 19.6$ min, $k = 5.8$). **HRMS** (ESI): m/z $[\text{M}+\text{H}]^+$ calcd. for $[\text{C}_{44}\text{H}_{48}\text{N}_7\text{O}_5]^+$ 754.3711, found 754.3715. $\text{C}_{44}\text{H}_{47}\text{N}_7\text{O}_5 \times \text{C}_2\text{HF}_3\text{O}_2$ (753.90 + 114.02).



(R)-N $^{\alpha}$ -Diphenylacetyl-N $^{\omega}$ -(4-((1E,3E)-4-(4-(dimethylamino)phenyl)buta-1,3-dienyl)-2,6-dimethylpyridinioethyl)aminocarbonyl(4-hydroxybenzyl)argininamide hydrotrifluoroacetate trifluoroacetate (2.78). DIPEA (2.80 μL , 16 μmol) was added to a solution of compound **2.41** (3.19 mg,

4.04 μmol) in DMF (50 μL). After 5 min, the fluorescent dye Py-5 (**2.77**) (5.74 mg, 15.6 μmol) was added, and the reaction mixture was shaken for 3 h in the dark. Purification by preparative HPLC (gradient: 0-30 min, A/B 85:15–38:62, *t_R* = 20 min) afforded **2.78** as a red solid (0.94 mg, 0.90 μmol, 22%). **RP-HPLC** (*Method A*, 220 nm): 95% (*t_R* = 14.0 min, *k* = 4.4). **HRMS** (ESI): *m/z* [M]⁺ calcd. for [C₄₉H₅₇N₈O₅]⁺ 821.4497, found 821.4509. C₄₉H₅₇N₈O₄⁺ × C₂HF₃O₂ × C₂F₃O₂⁻ (822.05 + 114.02 + 113.02).

2.4.3. Investigation of the chemical stability of **2.56**, **2.58-2.61**, **2.63** and **2.68**

To determine the chemical stability, compounds **2.56**, **2.58-2.61**, **2.63** and **2.68** (100 μM) were incubated in buffer (10 mM HEPES, 150 mM NaCl, 5 mM KCl, 2.5 mM CaCl₂·H₂O, 1.2 mM KH₂PO₄, 1.2 mM Mg₂SO₄·H₂O, 25 mM NaHCO₃, pH 7) at rt for 24 h. The solution was diluted (1:1) with 10% aq TFA and the stability was monitored at 6 time intervals (0 h, 1 h, 2 h, 4 h, 8 h and 24 h) by analytical HPLC analysis (*Method A*, 220 nm).

2.4.4. Pharmacological methods: radioligand competition binding assay in SK-N-MC cells and Fura-2 Ca²⁺ assay

2.4.4.1. Radioligand competition binding assay in SK-N-MC cells

All competition binding experiments at the Y₁R were essentially performed as described by Keller et al.⁷ using [³H]**2.2** (*C_{final}* = 0.15 nM) and SK-N-MC cells expressing the Y₁R. Three independent experiments were performed, each in triplicate.

2.4.4.2. Fura-2 Ca²⁺ assay

The Fura-2 Ca²⁺ assay at the Y₁R was essentially performed as described by Müller et al.¹³ using 10 nM pNPY for intracellular Ca²⁺ mobilization and applying a pre-incubation period of 15 min for the antagonists. Three independent experiments were performed, each in singlet.

2.4.5. Screening for pan-assay interference compounds (PAINS)

Screening of all target compounds for PAINS via the public tool <http://zinc15.docking.org/patterns/home>³³ gave no hits except for compound **2.78** (*N,N*-dimethylaniline substructure was identified as PAIN). The identity of **2.78** was proven by HRMS and the compound exhibited a purity of 95%. Moreover, there are no reports on the *N,N*-dimethylaniline scaffold to exhibit Y₁R affinity as shown for **2.78**. Therefore, interference in the radioligand competition binding assay by an impurity containing an *N,N*-dimethylaniline scaffold can be excluded.

2.4.6. Computational chemistry

2.4.6.1. Receptor and ligand preparation

The crystal structure of the inactive state Y₁R bound to the antagonist **2.2** (PDB ID: 5ZBQ¹⁵) was used as template. Minor modifications were performed using the modeling suite SYBYL-X 2.0 (Tripos Inc., St. Louis, MO USA): The ICL3 loop was reconstituted by the wild-type sequence. Non-ligand and non-receptor molecules were removed. Protein and ligand preparation (Schrödinger LLC, Portland, OR USA) including an assignment of protonation states were essentially performed as described in Pegoli et al.³⁴.³⁵ Disulfide bonds of the Y₁R were maintained between C33^{N-term} and C296^{7.29} as well as C113^{3.25} and C198^{45.50}, and a sodium ion was placed next to D86^{2.50}. Guanidine groups and the fluorophore Py-5

were singly protonated, resulting in a net charge of +1 for **2.1-2.3**, **2.68**, **2.72**, **2.76**, and +2 for the fluorescence ligand **2.78**.

2.4.6.2. Induced-fit docking

“Flexible” docking of **2.1-2.3**, **2.68**, **2.72**, **2.76** and **2.78** to the Y₁R was performed using the induced-fit docking module in Maestro (Schrödinger LLC). The ligands were docked within a box of 46 × 46 × 46 Å³ around the crystallographic binding pose of **2.2**. Redocking was performed in the extended precision mode. The resulting poses were scored using MM-GBSA (Schrödinger LLC). Amongst the most reasonable ligand binding poses, the pose corresponding to the lowest MM-GBSA value was selected as the most probable pose. For compounds **2.1-2.3**, the coordinates of this pose were used as input for subsequent MD simulations.

2.4.6.3. Molecular dynamics (MD) simulation

Simulations of the Y₁R bound to **2.1**, **2.2** or **2.3** and trajectory analysis were essentially performed as described in Pegoli et. al.³⁴ with the following modifications: The docked ligand-receptor complexes were aligned to the NTS₁R entry (PDB ID: 4BUO³⁶) in the orientations of proteins in membranes (OPM) database.³⁷ The Desmond system builder within Maestro (Schrödinger LLC) was used to insert the ligand-receptor complexes into hydrated, equilibrated palmitoylcholine (POPC) bilayers, comprising about 160 POPC molecules as well as sodium chloride at a concentration of 150 mM (net charges of the entire systems were zero). The systems contained about 78000 atoms and the box sizes were approximately 81 × 87 × 117 Å³. The coordinates were successively converted to chamber topology and coordinate files using inhouse scripts, psfgen³⁸, htmd³⁹ and chamber (AMBER 2016, University of California, San Francisco, CA USA). Ligand partial charges were further optimized using fftk⁴⁰. After minimization, the systems were heated from 0 to 100 K in the NVT ensemble during 20 ps and from 100 to 310 K in the NPT ensemble during 100 ps, applying harmonic restraints of 5 kcal · mol⁻¹ · Å⁻¹ to non-hydrogen atoms of protein and ligand. During the equilibration period (10 ns), harmonic restraints on receptor and ligand non-hydrogen atoms were reduced stepwise (0.5 kcal · mol⁻¹ · Å⁻¹ every 0.5 ns) to 2.5 kcal · mol⁻¹ · Å⁻¹ within 3 ns. While removing restraints on ligand atoms, harmonic restraints on receptor mainchain atoms were further reduced stepwise (0.5 kcal · mol⁻¹ · Å⁻¹ every 0.5 ns) to 0.5 kcal · mol⁻¹ · Å⁻¹ from 3 to 5 ns. After 5 ns, harmonic restraints on receptor mainchain atoms were removed, i.e. the residual equilibration period (5 ns) was run without restraints. The interaction cutoff was set to 9.0 Å. The final frames of the equilibration period were used as input for the simulations over 2 μs. Ligand-receptor interactions were analyzed using PLIP 1.4.2.⁴¹ Figures showing molecular structures of the Y₁R in complex with **2.1**, **2.2**, **2.3**, **2.68**, **2.72**, **2.76** or **2.78** were generated with PyMOL Molecular Graphics system, version 2.2.0 (Schrödinger LLC).

2.4.7. Calculation of van der Waals volumes

ChemAxon Marvin Calculator Plugins (Marvin 18.24.0, 2018, ChemAxon, <http://www.chemaxon.com>) were used to calculate the van der Waals volumes of the respective carbamoyl residues (containing a radical at the carbonyl group) of compounds **2.1-2.7**, **2.9**, **2.53-2.76** and **2.78**.

2.4.8. Data analysis

The retention factor k was calculated according to following equation: $k = (t_R - t_0)/t_0$ (t_R = retention time; t_0 = dead time).

Specific binding data were plotted as % (100% = bound radioligand in the absence of competitor) over log(concentration competitor) and analyzed by four-parameter logistic fits (GraphPad Prism 8.0, GraphPad, San Diego, USA) to obtain pIC₅₀ values, which were converted to pK_i values according to the Cheng-Prusoff equation⁴² (logarithmic form) (used K_d value of [³H]2.2: 0.044 nM⁷).

Relative Ca²⁺ responses were plotted as % against log(concentration antagonist) and analyzed by four-parameter logistic fits (GraphPad Prism version 8.0) to obtain pIC₅₀ values, which were converted to pK_b values according to the Cheng-Prusoff equation⁴² (logarithmic form) (used EC₅₀ value of pNPY: 1.53 nM).

2.5. References

1. Michel, M. C.; Beck-Sickinger, A.; Cox, H.; Doods, H. N.; Herzog, H.; Larhammar, D.; Quirion, R.; Schwartz, T.; Westfall, T. XVI. International Union of Pharmacology recommendations for the nomenclature of neuropeptide Y, peptide YY, and pancreatic polypeptide receptors. *Pharmacol. Rev.* **1998**, *50*, 143-50.
2. Reichmann, F.; Holzer, P. Neuropeptide Y: A stressful review. *Neuropeptides* **2016**, *55*, 99-109.
3. Zhang, L.; Bijker, M. S.; Herzog, H. The neuropeptide Y system: Pathophysiological and therapeutic implications in obesity and cancer. *Pharmacol. Ther.* **2011**, *131*, 91-113.
4. Reubi, J. C.; Gugger, M.; Waser, B.; Schaer, J. C. Y₁-mediated effect of neuropeptide Y in cancer: breast carcinomas as targets. *Cancer Res.* **2001**, *61*, 4636-41.
5. Li, J.; Tian, Y.; Wu, A. Neuropeptide Y receptors: a promising target for cancer imaging and therapy. *Regener. Biomater.* **2015**, *2*, 215-219.
6. Rudolf, K.; Eberlein, W.; Engel, W.; Wieland, H. A.; Willim, K. D.; Entzeroth, M.; Wienen, W.; Beck-Sickinger, A. G.; Doods, H. N. The first highly potent and selective non-peptide neuropeptide Y Y₁ receptor antagonist: BIBP3226. *Eur. J. Pharmacol.* **1994**, *271*, R11-3.
7. Keller, M.; Weiss, S.; Hutzler, C.; Kuhn, K. K.; Mollereau, C.; Dukorn, S.; Schindler, L.; Bernhardt, G.; Konig, B.; Buschauer, A. N^ω-Carbamoylation of the Argininamide Moiety: An Avenue to Insurmountable NPY Y₁ Receptor Antagonists and a Radiolabeled Selective High-Affinity Molecular Tool ([³H]UR-MK299) with Extended Residence Time. *J. Med. Chem.* **2015**, *58*, 8834-49.
8. Keller, M.; Bernhardt, G.; Buschauer, A. [³H]UR-MK136: A Highly Potent and Selective Radioligand for Neuropeptide Y Y₁ Receptors. *ChemMedChem* **2011**, *6*, 1566-1571.
9. Keller, M.; Erdmann, D.; Pop, N.; Pluym, N.; Teng, S.; Bernhardt, G.; Buschauer, A. Red-fluorescent argininamide-type NPY Y₁ receptor antagonists as pharmacological tools. *Bioorg. Med. Chem.* **2011**, *19*, 2859-78.
10. Höfelschweiger, B. K. The Pyrylium Dyes: A New Class of Biolabels. Synthesis, Spectroscopy, and Application as Labels and in general Protein Assay. PhD Thesis, University of Regensburg, Regensburg, 2005.
11. Wetzl, B. K.; Yarmoluk, S. M.; Craig, D. B.; Wolfbeis, O. S. Chameleon Labels for Staining and Quantifying Proteins. *Angew. Chem. Int. Ed.* **2004**, *43*, 5400-5402.
12. Keller, M.; Bernhardt, G.; Buschauer, A. [³H]UR-MK136: a highly potent and selective radioligand for neuropeptide Y Y₁ receptors. *ChemMedChem* **2011**, *6*, 1566-71.
13. Müller, M.; Knieps, S.; Geßele, K.; Dove, S.; Bernhardt, G.; Buschauer, A. Synthesis and Neuropeptide Y Y₁ Receptor Antagonistic Activity of N,N-Disubstituted ω-Guanidino- and ω-Aminoalkanoic Acid Amides. *Arch. Pharm. (Weinheim)*. **1997**, *330*, 333-342.
14. Weiss, S.; Keller, M.; Bernhardt, G.; Buschauer, A.; Konig, B. Modular synthesis of non-peptidic bivalent NPY Y₁ receptor antagonists. *Bioorg. Med. Chem.* **2008**, *16*, 9858-66.
15. Yang, Z.; Han, S.; Keller, M.; Kaiser, A.; Bender, B. J.; Bosse, M.; Burkert, K.; Kogler, L. M.; Wifling, D.; Bernhardt, G.; Plank, N.; Littmann, T.; Schmidt, P.; Yi, C.; Li, B.; Ye, S.; Zhang, R.; Xu, B.; Larhammar, D.; Stevens, R. C.; Huster, D.; Meiler, J.; Zhao, Q.; Beck-Sickinger, A. G.;

- Buschauer, A.; Wu, B. Structural basis of ligand binding modes at the neuropeptide Y Y₁ receptor. *Nature* **2018**, 556, 520-524.
16. Gavande, N.; Kim, H.-L.; Doddareddy, M. R.; Johnston, G. A. R.; Chebib, M.; Hanrahan, J. R. Design, Synthesis, and Pharmacological Evaluation of Fluorescent and Biotinylated Antagonists of ρ_1 GABAC Receptors. *ACS Med. Chem. Lett.* **2013**, 4, 402-407.
17. Montero, A.; Goya, P.; Jagerovic, N.; Callado, L. F.; Meana, J. J.; Girón, R. o.; Goicoechea, C.; Martín, M. I. Guanidinium and aminoimidazolium derivatives of N-(4-piperidyl)propanamides as potential ligands for μ opioid and I₂-imidazoline receptors: synthesis and pharmacological screening. *Bioorg. Med. Chem.* **2002**, 10, 1009-1018.
18. Keller, M.; Pop, N.; Hutzler, C.; Beck-Sickinger, A. G.; Bernhardt, G.; Buschauer, A. Guanidine–Acylguanidine Bioisosteric Approach in the Design of Radioligands: Synthesis of a Tritium-Labeled N^G-Propionylargininamide ([³H]-UR-MK114) as a Highly Potent and Selective Neuropeptide Y Y₁ Receptor Antagonist. *J. Med. Chem.* **2008**, 51, 8168-8172.
19. Wodtke, R.; Hauser, C.; Ruiz-Gómez, G.; Jäckel, E.; Bauer, D.; Lohse, M.; Wong, A.; Pufe, J.; Ludwig, F.-A.; Fischer, S.; Hauser, S.; Greif, D.; Pisabarro, M. T.; Pietzsch, J.; Pietsch, M.; Löser, R. N^ε-Acryloyllysine Piperazides as Irreversible Inhibitors of Transglutaminase 2: Synthesis, Structure–Activity Relationships, and Pharmacokinetic Profiling. *J. Med. Chem.* **2018**, 61, 4528-4560.
20. Dissoki, S.; Hagooly, A.; Elmachily, S.; Mishani, E. Labeling approaches for the GE11 peptide, an epidermal growth factor receptor biomarker. *Journal of Labelled Compounds and Radiopharmaceuticals* **2011**, 54, 693-701.
21. Gottlieb, H. E.; Kotlyar, V.; Nudelman, A. NMR Chemical Shifts of Common Laboratory Solvents as Trace Impurities. *J. Org. Chem.* **1997**, 62, 7512-7515.
22. Bastian, A. A.; Marcozzi, A.; Herrmann, A. Selective transformations of complex molecules are enabled by aptameric protective groups. *Nature Chemistry* **2012**, 4, 789.
23. Grochowski, E.; Jurczak, J. A New Method for the Preparation of N-Acyloxyphthalimides and N-Acyloxy succinimides. *Synthesis* **1977**, 1977, 277-279.
24. Laurent, S.; Botteman, F.; Elst, L. V.; Muller, R. N. Relaxivity and Transmetallation Stability of New Benzyl-Substituted Derivatives of Gadolinium DTPA Complexes. *Helv. Chim. Acta* **2004**, 87, 1077-1089.
25. Andrade, G. A.; Pistner, A. J.; Yap, G. P. A.; Lutterman, D. A.; Rosenthal, J. Photocatalytic Conversion of CO₂ to CO Using Rhenium Bipyridine Platforms Containing Ancillary Phenyl or BODIPY Moieties. *ACS Catalysis* **2013**, 3, 1685-1692.
26. Stembera, K.; Buchynskyy, A.; Vogel, S.; Knoll, D.; Osman, A. A.; Ayala, J. A.; Welzel, P. Moenomycin-Mediated Affinity Purification of Penicillin-Binding Protein 1b. *ChemBioChem* **2002**, 3, 332-340.
27. Andrews, M. D.; Bagal, S. K.; Brown, D. G.; Gibson, K. R.; Klute, W.; Morao, I.; Omoto, K.; Ryckmans, T.; Sabnis, Y.; Skerratt, S. E.; Stupp, P. A. Pyrrolo[3,2-C]Pyridine Tropomyosin-Related Kinase Inhibitors. WO2014/053968A1, 2014.
28. Wang, L.; Guillen, V. S.; Sharma, N.; Flessa, K.; Min, J.; Carlson, K. E.; Toy, W.; Braji, S.; Katzenellenbogen, B. S.; Katzenellenbogen, J. A.; Chandarlapaty, S.; Sharma, A. New Class of

- Selective Estrogen Receptor Degraders (SERDs): Expanding the Toolbox of PROTAC Degrons. *ACS Med. Chem. Lett.* **2018**, 9, 803-808.
29. Kim, M.; Han, K.-J. Convenient Synthesis of N-Hydroxysuccinimide Esters from Carboxylic Acids Using Triphosgene. *Synth. Commun.* **2009**, 39, 4467-4472.
30. Kerkovius, J. K.; Menard, F. A Practical Synthesis of 6,8-Difluoro-7-hydroxycoumarin Derivatives for Fluorescence Applications. *Synthesis* **2016**, 48, 1622-1629.
31. Pluym, N.; Baumeister, P.; Keller, M.; Bernhardt, G.; Buschauer, A. [³H]UR-PLN196: A Selective Nonpeptide Radioligand and Insurmountable Antagonist for the Neuropeptide Y Y₂ Receptor. *ChemMedChem* **2013**, 8, 587-593.
32. Kuhn, K. Molecular Tools for the NPY Y₄ Receptor Derived from the C-Terminus of hPP and from Argininamide-type Y₁R Antagonists. thesis, University of Regensburg, Regensburg, Germany, 2017.
33. Aldrich, C.; Bertozzi, C.; Georg, G. I.; Kiessling, L.; Lindsley, C.; Liotta, D.; Merz, K. M., Jr.; Schepartz, A.; Wang, S. The Ecstasy and Agony of Assay Interference Compounds. *J. Med. Chem.* **2017**, 60, 2165-2168.
34. Pegoli, A.; She, X.; Wifling, D.; Hübner, H.; Bernhardt, G.; Gmeiner, P.; Keller, M. Radiolabeled Dibenzodiazepinone-Type Antagonists Give Evidence of Dualsteric Binding at the M₂ Muscarinic Acetylcholine Receptor. *J. Med. Chem.* **2017**, 60, 3314-3334.
35. Pegoli, A.; Wifling, D.; Gruber, C. G.; She, X.; Hübner, H.; Bernhardt, G.; Gmeiner, P.; Keller, M. Conjugation of Short Peptides to Dibenzodiazepinone-Type Muscarinic Acetylcholine Receptor Ligands Determines M₂R Selectivity. *J. Med. Chem.* **2019**, 62, 5358-5369.
36. Egloff, P.; Hillenbrand, M.; Klenk, C.; Batyuk, A.; Heine, P.; Balada, S.; Schlinkmann, K. M.; Scott, D. J.; Schutz, M.; Pluckthun, A. Structure of signaling-competent neurotensin receptor 1 obtained by directed evolution in *Escherichia coli*. *Proc. Natl. Acad. Sci. U. S. A.* **2014**, 111, E655-62.
37. Lomize, M. A.; Lomize, A. L.; Pogozheva, I. D.; Mosberg, H. I. OPM: orientations of proteins in membranes database. *Bioinformatics* **2006**, 22, 623-5.
38. Humphrey, W.; Dalke, A.; Schulten, K. VMD: visual molecular dynamics. *J. Mol. Graph.* **1996**, 14, 33-8, 27-8.
39. Doerr, S.; Harvey, M. J.; Noe, F.; De Fabritiis, G. HTMD: High-Throughput Molecular Dynamics for Molecular Discovery. *J. Chem. Theory Comput.* **2016**, 12, 1845-52.
40. Mayne, C. G.; Saam, J.; Schulten, K.; Tajkhorshid, E.; Gumbart, J. C. Rapid parameterization of small molecules using the Force Field Toolkit. *J. Comput. Chem.* **2013**, 34, 2757-70.
41. Salentin, S.; Schreiber, S.; Haupt, V. J.; Adasme, M. F.; Schroeder, M. PLIP: fully automated protein-ligand interaction profiler. *Nucleic Acids Res.* **2015**, 43, W443-7.
42. Yung-Chi, C.; Prusoff, W. H. Relationship between the inhibition constant (K_i) and the concentration of inhibitor which causes 50 per cent inhibition (I₅₀) of an enzymatic reaction. *Biochem. Pharmacol.* **1973**, 22, 3099-3108.

Chapter 3

Additional characterization of argininamide-type neuropeptide Y Y₁ receptor antagonists presented in chapter 2:

β -arrestin2 recruitment, Y₁R selectivity and investigation of potential irreversibly binding ligands

Note: Thanks are due to Maria Beer-Krön, Susanne Bollwein and Brigitte Wenzl for excellent technical assistance (cultivation of cells and radioligand competition binding experiments at hY₅R and saturation binding experiments at hY₁R).

3.1. Introduction

A recently published series of (*R*)-argininamide-type neuropeptide Y Y₁ receptor antagonists (**2.53-2.76** and **2.78**), investigated in radioligand competition binding studies and Fura-2 Ca²⁺ assay, revealed that the size of the *N*^ω-carbamoyl substituent, attached at the guanidine group, considerably effects Y₁R affinity, and, as suggested by docking studies and molecular dynamics simulations, can also alter the Y₁R binding mode of the ligands (*cf.* Chapter 2).¹

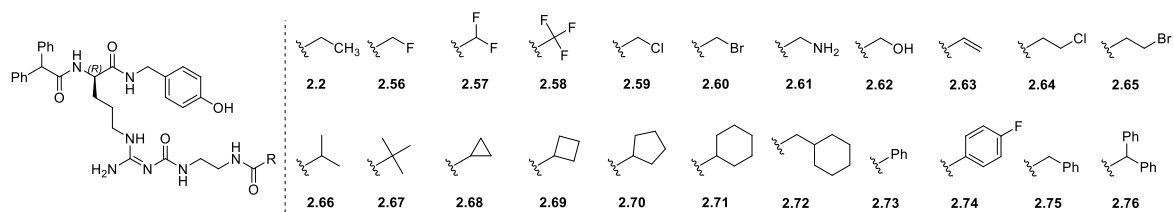


Figure 3.1. Structures of *N*^ω-carbamoylated (*R*)-argininamides hY₁R antagonists **2.2** and **2.56-2.76**.

Here, in addition to functional data obtained from a Fura-2 Ca²⁺ assay (G-protein mediated signalling) (*cf.* Chapter 2), compounds **2.1**, **2.2**, **2.56-2.59**, **2.61** and **2.65** were investigated in a β-arrestin2 recruitment assay.

Compound **2.60** proved to be unstable in DMSO during storage (6 months) at -20 °C (hydrolysis of the 2-bromoacetyl moiety). Therefore, the question arose if the bromoacetyl residue in **2.60** can serve for a covalent binding of the ligand to the hY₁R. To address this question, saturation binding experiments were performed with the Y₁R radioligand [³H]UR-MK299 ([³H]**2.2**) at SK-N-MC cells after pre-incubation of the cells with **2.60**. Compound **2.63**, bearing an acrylamide residue (Figure 3.1), was also included in these studies.

3.2. Results and discussion

3.2.1. Pharmacological methods: Y₁R antagonism (p*K*_b) in a β-arrestin2 recruitment assay, NPY Y₁R subtype selectivity and potential irreversibly binding ligands

The standard antagonists **2.1** and **2.2** as well as selected *N*^ω-carbamoylated (*R*)-argininamides (**2.56-2.59**, **2.61** and **2.65**) were investigated in the β-arrestin2 recruitment assay. Furthermore **2.56**, **2.68** and **2.72** were investigated in a radioligand competition binding assay at hY₄R and hY₅R. Potential covalent binding ligands bearing 2-bromoacetyl (**2.60**) or acrylamide (**2.63**) residues were investigated in saturation binding experiments.

3.2.1.1. Determination of p*K*_b values in a β-arrestin2 recruitment assay

The Y₁R antagonism (p*K*_b) of (*R*)-argininamides **2.1**, **2.2**, **2.56-2.59**, **2.61** and **2.65** was investigated in a β-arrestin2 recruitment assay in living HEK293T hY₁R + βArr2 cells (Figure 3.2 and Table 3.1), as described in the doctoral thesis of Felixberger.² Minor modifications were applied: β-arrestin2 recruitment was induced by 80 nM pNPY (relative to the response observed (EC₉₅) upon stimulation with pNPY) as described, and luminescence was measured as a function of time on living cells instead of measuring luminescence after cell lysis.

Antagonists **2.1**, **2.2**, **2.56-2.59**, **2.61** and **2.65** were pre-incubated with the cells for 15 min. In the case of BIBP-3226 (**2.1**), the antagonism (pK_b) observed in the β -arrestin2 recruitment assay was more than one order of magnitude lower as compared to its Y_1R affinity (pK_i), as determined in the radioligand binding assay (cf. Chapter 2, Table 2.1). Moreover, antagonism ($pK_b = 8.82$; IC_{50} value was converted to pK_b value) determined in the Fura-2 Ca^{2+} assay (inhibition of Ca^{2+} signal induced by 10 nM pNPY) described in literature³ increased compared to antagonism in the β -arrestin2 recruitment assay. The antagonism ($pK_b = 10.50$) of **2.2** in the β -arrestin2 recruitment assay was in good agreement with the affinity ($pK_i = 10.11$, K_i value was converted to pK_i value) as determined in the radioligand binding assay (cf. Chapter 2, Table 2.1) and pK_b value ($pK_b = 10.77$, the pK_b value of **2.2** was calculated from given IC_{50} value reported by Keller et al.,⁴ EC_{50} value of pNPY was taken from literature¹) which was obtained in the Fura-2 Ca^{2+} assay (**2.2** was pre-incubated for 20 min) in literature.⁴

Table 3.1. Antagonism (pK_b) of standard antagonists (**2.1** and **2.2**) and synthesized N^{ω} -carbamoylated (*R*)-argininamides **2.56-2.59**, **2.61**, **2.65**, **2.66**, **2.69** and **2.71** determined in the β -arrestin2 recruitment assay in living HEK293T hY₁R + β Arr2 cells.

Compound	$pK_b \pm SEM^a$	N	Compound	$pK_b \pm SEM^a$	N
2.1 (BIBP-3226)	7.36 ± 0.03	3	2.61	9.58 ± 0.47	2
2.2 (UR-MK299)	10.50 ± 0.08	3	2.65	9.34 ± 0.07	2
2.56	10.66 ± 0.18	3	2.66	10.10 ± 0.14	3
2.57	10.34 ± 0.08	3	2.69	10.34 ± 0.05	3
2.58	10.63 ± 0.12	3	2.71	6.83 ± 0.01	3
2.59	10.72 ± 0.17	3			

^a β -Arrestin2 recruitment assay in intact HEK293T hY₁R + β Arr2 cells. Arrestin2 recruitment was induced by 80 nM pNPY after pre-incubation of the cells with the antagonist for 15 min. Mean values \pm SEM from at least N independent experiments, each performed in triplicate.

Additionally, the potency of pNPY ($pEC_{50} = 8.05 \pm 0.01$; N = 5) was determined in a modified β -arrestin2 recruitment assay in living HEK293T hY₁R + β Arr2 cells and the potency ($pEC_{50} = 7.36$) was lower compared to that from the procedure described in the doctoral thesis of Felixberger² using the same cell line. Further investigations are needed to explain the discrepancies of pEC_{50} values of pNPY under both assay conditions. However, the obtained data determined in living HEK293T hY₁R + β Arr2 cells were in better agreement with the previously described potency of NPY ($pEC_{50} = 8.57$) as determined in a bimolecular fluorescence complementation assay.⁵

The antagonism of selected (*R*)-argininamides **2.56-2.59**, **2.61** and **2.65** obtained in the β -arrestin2 recruitment assay was in good agreement with data obtained in the radioligand competition binding experiments and Fura-2 Ca^{2+} assays. The replacement of the propionyl group in **2.2** by 2-fluoroacetyl (**2.56**), 2,2-difluoroacetyl (**2.57**), trifluoroacetyl (**2.58**), 2-chloroacetyl (**2.59**), 2-methylpropionyl (**2.66**) and cyclopropane carbonyl (**2.68**) residues did not affect the antagonism (pK_b) observed in a β -arrestin2 recruitment assay, whereas the introduction of a 2-aminoacetyl (**2.61**) moiety is less favoured.

Additionally, the introduction of a bulkier aliphatic ring (cyclohexyl) in **2.71** led to a decrease in antagonism.

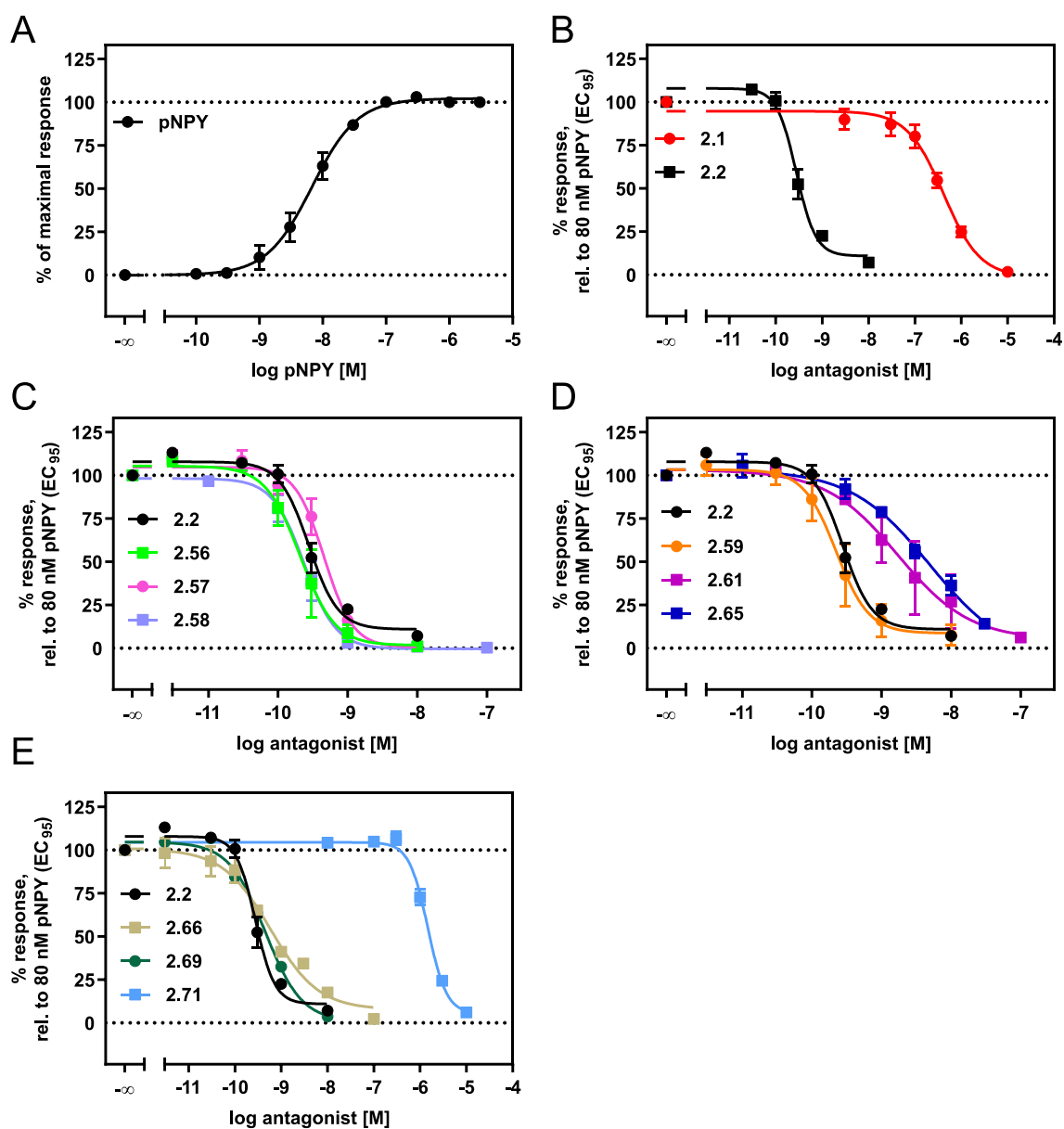


Figure 3.2. (A) β-Arrestin2 recruitment elicited by pNPY (agonist mode). (B-F) Inhibition of β-arrestin2 recruitment (induced by 80 nM pNPY) by (B) **2.1**, **2.2**, (C) **2.2**, **2.56**, **2.57**, **2.58**, (D) **2.2**, **2.59**, **2.61**, **2.65** (E) **2.2**, **2.66**, **2.69**, **2.71** (antagonist mode). All experiments were performed in living HEK293T hY₁R + βArr2 cells. Antagonists were pre-incubated with cells for 15 min. Data are presented as means ± SEM from at least two independent experiments, each performed in triplicate.

All investigated (*R*)-argininamides **2.56-2.59**, **2.61** and **2.65** showed antagonism in the β-arrestin2 recruitment assays as well as in the Fura-2 Ca²⁺ assays (cf. Chapter 2, Table 2.2 and Table 3.1). The replacement of the guanidine group in **2.1** through the bioisosteric *N*^ω-carbamoyl guanidine did not lead to a functional bias.

3.2.1.2. NPY Y₁R subtype selectivity

The hY₁R antagonists **2.58**, **2.68** and **2.72** were investigated in radioligand competition binding experiments on hY₄ and hY₅ receptors and showed no affinity towards the hY₄R and the hY₅R at

concentrations up to 10,000 nM (Table 3.2). These compounds (**2.58**, **2.68** and **2.72**) were intended to bind in the same orientation as the highly Y₁R selective compound **2.2** (*cf.* Chapter 2). The increasing volume of the carbamoyl residue did not result in hY₄R and hY₅R binding.

Table 3.2. NPY receptor subtype preference of *N*^ω-carbamoylated (*R*)-argininamides **2.56**, **2.68** and **2.72**.

compound	hY ₁ R	hY ₄ R	hY ₅ R
	p <i>K</i> _i ± SEM ^a	p <i>K</i> _i ^b	p <i>K</i> _i ^c
2.56	10.50 ± 0.04	<5.00	<5.00
2.68	8.93 ± 0.12	<5.00	<5.00
2.72	5.67 ± 0.05	<5.00	<5.00

^aRadioligand competition binding assay using [³H]**2.2** (*C*_{final} = 0.15 nM, *K*_d = 0.044 nM) in intact SK-N-MC cells.⁴ Mean values ± SEM from at least three independent experiments, each performed in triplicate. ^bRadioligand competition binding assay using [³H]UR-KK200 (*C*_{final} = 1.0 nM, *K*_d = 0.67 nM) in intact CHO-hY₄R-mtAEQ-G_{q15} cells.^{6, 7} ^cRadioligand competition binding assay using [³H]propionyl pNPY (*C*_{final} = 4.0 nM, *K*_d = 4.8 nM) in intact HEC-1B-hY₅ cells.^{4, 8} Results from at least three independent experiments, each performed in triplicate (hY₄R, hY₅R).

3.2.1.3. Investigation on potential irreversibly binding ligands (**2.60** and **2.63**)

Due to the chemical reactivity of the 2-bromoacetyl (**2.60**) and the acrylamide (**2.63**) residues with thiols, these compounds could potentially bind covalently to the hY₁R. Firstly, the (*R*)-argininamides **2.60** and **2.63** were investigated in radioligand competition binding studies and the Fura-2 Ca²⁺ assay. Their chemical stability was also investigated in 10 mM HEPES buffer (*cf.* Chapter 2). Compounds **2.60** and **2.63** proved to be stable in 10 mM HEPES buffer at rt for 24 h (no addition of 2-mercaptoethanol). In DMSO, **2.60** (10 mM) showed decomposition (ca 30%) at -20 °C over a period of 6 months (Figure 3.3). Although it is well known in the literature⁹ that α-halo-carbonyl compounds can be oxidized by DMSO in a Swern-like oxidation (Kornblum oxidation) to α-keto-aldehydes, in the present case under the applied conditions the α-hydroxyl compound **2.62** was isolated.

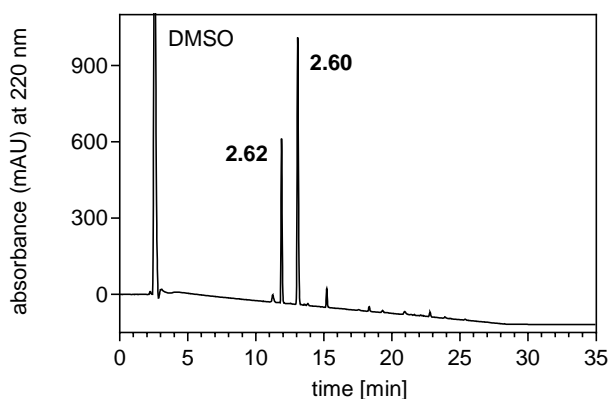
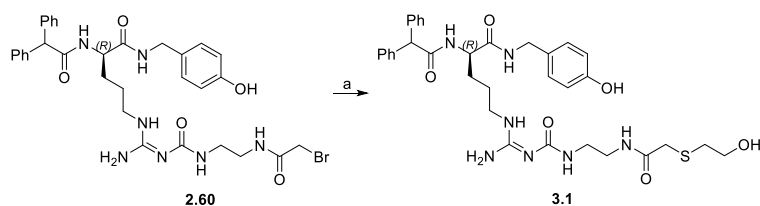


Figure 3.3. RP-HPLC (220 nm) chromatogram of **2.60** stock solution in DMSO after storage at -20 °C for a period of 6 months. Compound **2.60** showed decomposition to **2.62**.

The identity of **2.60** and **2.62** was determined by NMR and HRMS (*cf.* Chapter 2). Samples for identity confirmation were obtained by preparative HPLC separation of the DMSO stock solution.

RP-HPLC (220 nm) analysis

(*R*)-Argininamides **2.60** and **2.63** were investigated in buffer (10 mM HEPES, 150 mM NaCl, 5 mM KCl, 2.5 mM CaCl₂·H₂O, 1.2 mM KH₂PO₄, 1.2 mM Mg₂SO₄·H₂O, 25 mM NaHCO₃, pH 7) at rt for 24 h and proved to be stable (*cf.* Chapter 2). Compound **2.60** showed decomposition in DMSO stock solution (Figure 3.3). Furthermore, the chemical stability of compounds **2.60** and **2.63** was investigated in the presence of 2-mercaptoethanol (Figure 3.4).



Scheme 3.1. Formation of **3.1**. Reagents and conditions: (a) 2-mercaptoethanol ($C_{\text{final}} = 1000 \mu\text{M}$), **2.60** ($C_{\text{final}} = 100 \mu\text{M}$), 10 mM HEPES buffer, pH 7. Identity of **3.1** was determined by HRMS.

The bromoacetyl moiety of **2.60** proved to be vulnerable to nucleophilic substitution by thiols in aqueous solution at pH 7.0. Traces of water in the DMSO stock solution led to formation of **2.62** after 6 months. Compound **2.60** showed no decomposition in buffer after 24 h, when using a freshly prepared stock solution in DMSO.

(*R*)-Argininamide **2.60** was almost transformed to **3.1** after 4 h (Figure 3.4) when using a 10-fold excess of 2-mercaptoethanol over **2.60**. The reaction product was identified by RP-HPLC and HRMS, but the structure of **3.1** was not confirmed by NMR spectroscopy. It was presumed that the thiol group had a higher nucleophilicity than the alcohol of 2-mercaptoethanol.

Under similar conditions, **2.63** showed no transformation in the presence of 2-mercaptoethanol and proved to be stable up to 24 h. These experiments give hints towards the chemical stability and reactivity of compounds **2.60** and **2.63** in 10 mM HEPES buffer in the presence of 2-mercaptoethanol, but do not allow for an extrapolation to potential reactivity inside the binding pocket of the hY₁R.

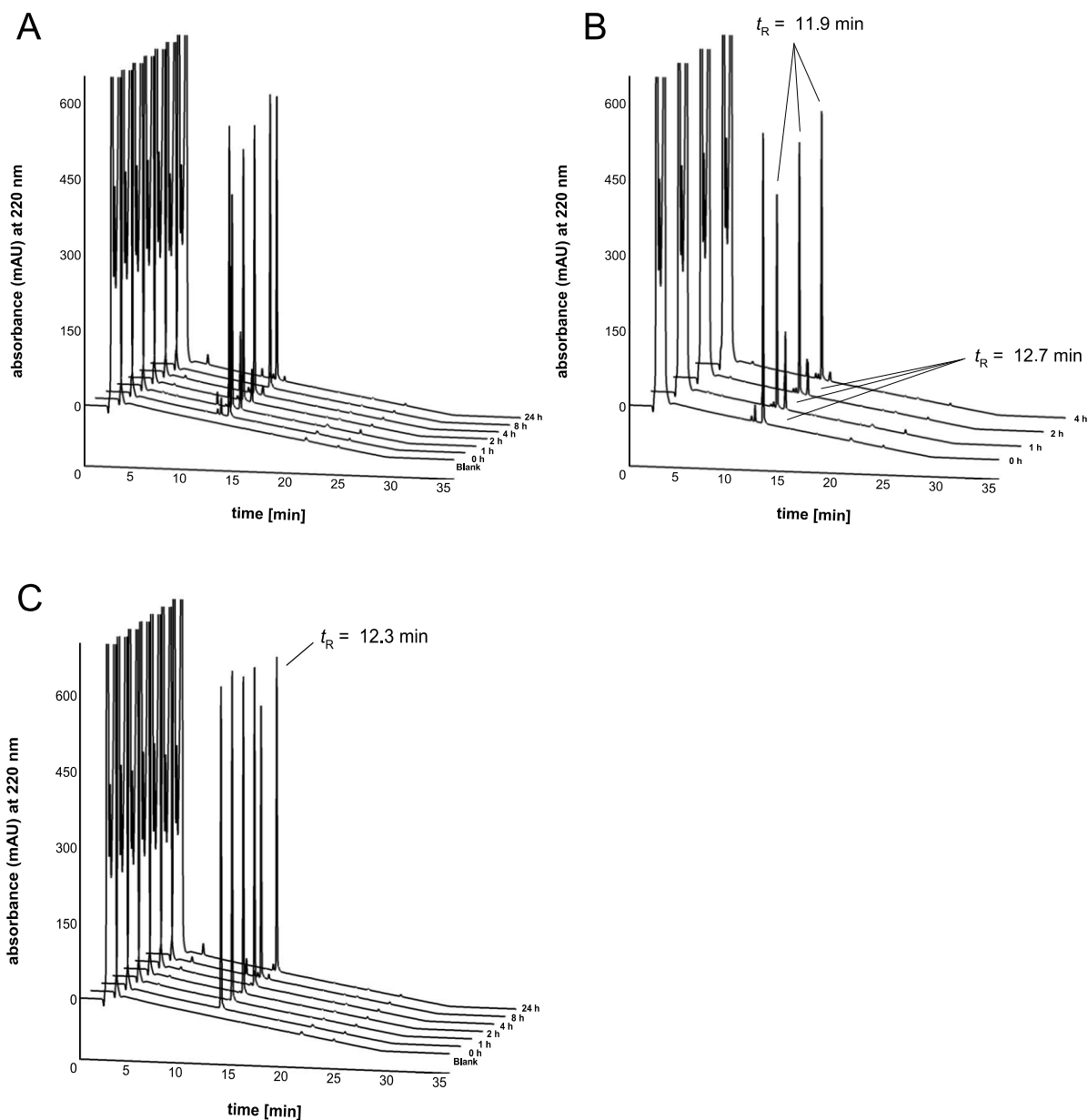


Figure 3.4. (A-C) Chromatograms of the reversed-phase HPLC (220 nm) analysis of (A-B) **2.60** and (C) **2.63** after incubation in a 10 mM HEPES buffer (pH 7) with a 10-fold excess of 2-mercaptoethanol (compared to **2.60** or **2.63**) at rt for up to 24 h. (B) Enlargement of chromatogram of the reversed-phase HPLC (220 nm) analysis of (A) **2.60**, which was transformed to **3.1** over a period of 4 h. **2.63** proved to be stable under similar conditions.

Saturation binding

Saturation binding experiments were performed in SK-N-MC cells using [3 H]**2.2**. SK-N-MC cells that were pre-incubated (rt, 2 h) with the potential covalently binding ligands **2.60** or **2.63** applied at concentrations corresponding to 10-fold the respective K_i value (Figure 3.4 and Table 3.3).

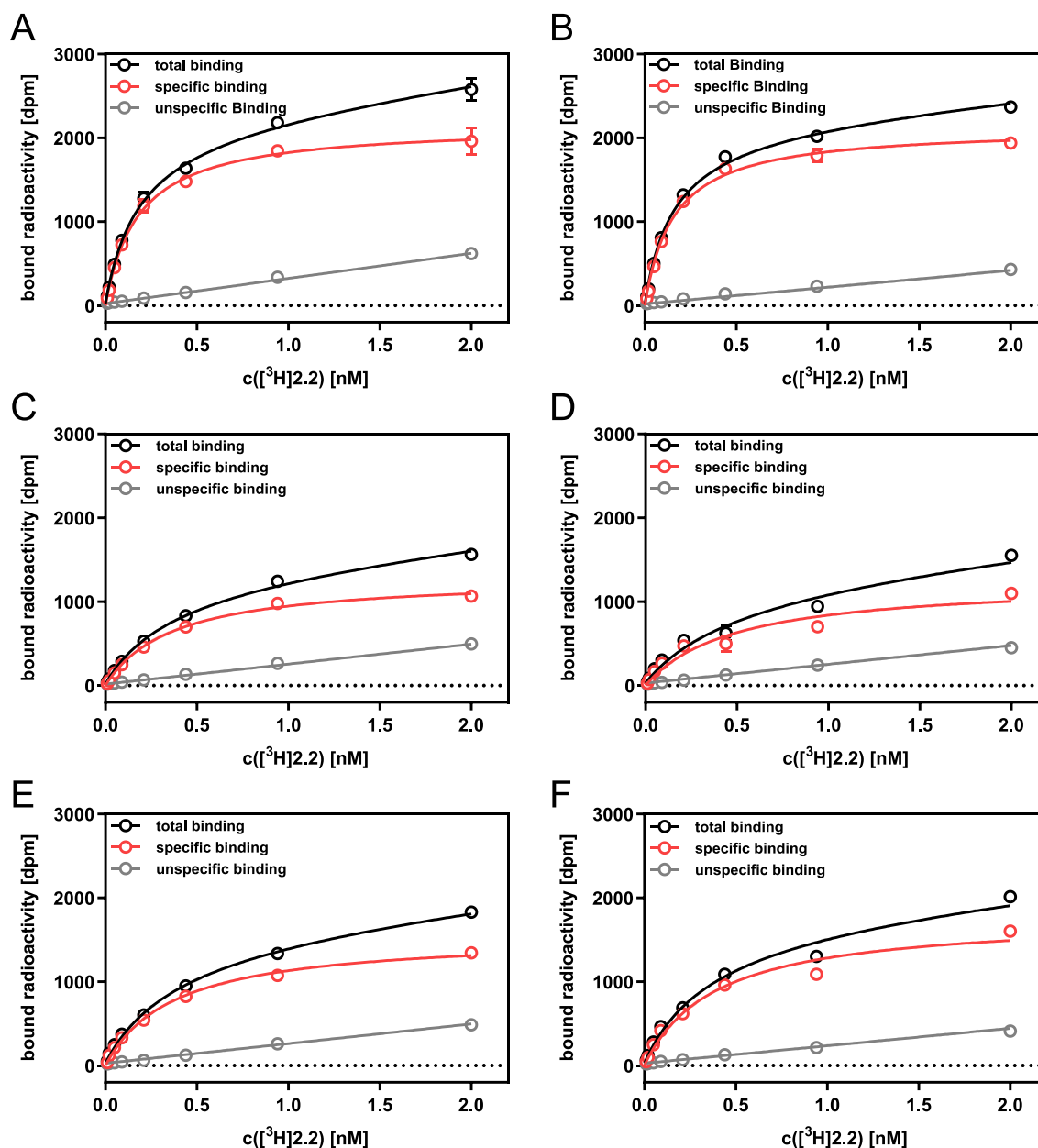


Figure 3.5. (A-F) Representative saturation isotherms (red line) of specific hY₁R binding of [³H]2.2 in intact SK-N-MC cells. Unspecific binding (grey line) was determined in the presence of a 500-fold excess of BIBO-3304. Cells were pre-incubated with (A-B) buffer (no ligand added), (C-D) 2.2 ($C_{\text{final}} = 0.77$ nM), (E) 2.60 ($C_{\text{final}} = 1.2$ nM) and (F) 2.63 ($C_{\text{final}} = 1.15$ nM) for 2 h before washing and subsequently performing the saturation binding experiments with [³H]2.2. Control experiments with (A-B) buffer and (C-D) 2.2 were performed on the same day as (E-F) experiments with potential covalently binding ligands (E) 2.60 and (F) 2.63. The experiments were performed in triplicate. Errors of specific binding were calculated according to the Gaussian law of error propagation. Error bars of total (black symbols) and nonspecific (grey symbols) binding represent the SEM.

The cells were washed twice (cells were covered with PBS buffer for 30 s) and the saturation binding experiment was performed as described in literature.⁴ The day before the experiment the cells were seeded from a single cell suspension (cells of the same passage). On the day of the saturation binding assay, cells were incubated with buffer and 2.2 ($C_{\text{final}} = 10$ -fold K_i value) as negative controls. The determined pK_d values (Table 3.3) of [³H]2.2 (control I) were slightly lower compared to equilibrium dissociation constants described in literature ($pK_d = 10.36$; K_d value was converted to pK_d value).⁴ In

contrast to the described procedure⁴ the SK-N-MC cells were incubated for 2 h with buffer before the saturation binding experiment was performed.

[³H]**2.2** (linker length: two carbons) is described as a radioligand with high residence time on the receptor (135 min) compared to [³H]**2.3** (4.8 min), differing from [³H]**2.2** in the length of the spacer.⁴ Moreover, the elongation of the spacer in [³H]**2.3** (linker length: four carbons) led to a decrease in affinity.^{4, 10} The SK-N-MC cells were incubated with the non-covalently binding ligand **2.2** (control II) to compare the results of potential covalently binding ligands **2.60** and **2.63**, because a long residence time in case of *N*^ω-carbamoylated (linker length: two carbons) ligands **2.60** and **2.60** was presumed.

Firstly, both ligands (**2.60** and **2.63**) share the ethyl spacer with **2.2**. Secondly, the bromoacetyl (**2.60**) and acrylamide (**2.63**) residues do not affect affinity compared to **2.2**, and these ligands likely share the same binding mode as **2.2** (*cf.* Chapter 2).

Table 3.3. Determination of pK_d and B_{max} values of **2.2** after incubation with buffer (control I), **2.2** (control II) and potential covalently binding ligands (**2.60** or **2.63**).

	2.60 (N = 3)		2.63 (N = 2)	
	$pK_d \pm SEM^a$	$B_{max} \pm SEM^b$ [%]	$pK_d \pm SEM^a$	$B_{max} \pm SEM^b$ [%]
control I (buffer)	9.79 ± 0.06	100	9.74 ± 0.07	100
control II (2.2)	9.39 ± 0.03	76 ± 9	9.51 ± 0.1	67 ± 14
ligand (2.60 or 2.63)	9.53 ± 0.07	74 ± 17	9.32 ± 0.01	54 ± 4

^aEquilibrium dissociation constant determined in SK-N-MC cells. Mean values ± SEM determined in N independent experiments, each performed in triplicate. ^bMaximum specific binding (one site fit, specific binding, GraphPad Prism 8). B_{max} [%] = $B_{max}(\text{control I, control II or ligand})/B_{max}(\text{control I}) \cdot 100$. Mean values ± SEM determined in N independent experiments, each performed in triplicate.

The B_{max} value corresponds to the maximum number of binding sites. It is apparent that the B_{max} value decreased compared to control I (buffer), when SK-N-MC cells were incubated with potential covalently binding ligands (**2.60** and **2.63**) (Figure 3.4 and Table 3.3). Pre-incubation with the Y₁R antagonist **2.2** (control II) led to a decrease in the B_{max} value as well, but potential covalently binding ligands (**2.60** and **2.63**) did not decrease the B_{max} value more than **2.2**. The *N*^ω-carbamoylated (*R*)-argininamide **2.2** has no structural element allowing for covalent binding to the receptor, which was also obvious in the recently resolved crystal structure.¹¹ It can be concluded from these results that compounds **2.60** and **2.63** most probably do not bind covalently to the hY₁R.

3.3. Conclusion

The investigation of **2.1**, **2.2**, **2.56-2.59**, **2.61** and **2.65** in the β-arrestin2 recruitment assay revealed no functional bias. Further investigations in the β-arrestin2 assay should focus on compounds **2.7**, **2.9**, **2.76** and **2.78**, for which a different binding mode was suggested. (*R*)-Argininamides **2.7**, **2.9** and **2.76** behaved as antagonists in the Fura-2 Ca²⁺ assay (G-protein mediated signalling). In conclusion, the inverted binding mode of these compounds (**2.7**, **2.9** and **2.76**) may lead to a functional bias.

Further investigation concerning the selectivity profile of *N*^ω-carbamoylated (*R*)-argininamides should be focussed on **2.7**, **2.9**, **2.76** and **2.78**, that do not share the binding mode of **2.2**. Moreover, the affinities of compounds **2.56**, **2.68** and **2.72** in competition radioligand binding assays were not investigated at the hY₂R, because an appropriate hY₂R binding assay was not available at that time.

Unfortunately, the question, of whether the (*R*)-argininamides **2.60** and **2.63** bind covalently could not be answered. The saturation binding experiments revealed that after incubation of the cells with ligands **2.60** and **2.63**, the B_{Max} value decreased compared to control I (buffer), which might suggest covalent binding to the receptor, however the B_{Max} value was not significantly decreased compared to incubation with **2.2** (control II). Furthermore, the RP-HPLC experiments revealed that **2.60** showed reactivity towards nucleophiles (2-mercaptoethanol) in 10 mM HEPES buffer at pH 7. To answer the question of covalent binding of these ligands (**2.60** and **2.63**), further investigations could focus on mass spectrometry. Computational studies could also be performed using the resolved crystal structure of the hY₁R.

3.4. Experimental section

3.4.1. General experimental conditions

The following reagents and solvents (analytical grade) were purchased from commercial suppliers and used without further purification: TFA (Sigma Aldrich, Taufkirchen, Germany), DMSO (Fisher Scientific, Schwerte Germany) and 2-mercaptoethanol (Merck, Darmstadt, Germany).

Acetonitrile (HPLC grade; Sigma-Aldrich) and Millipore water were used as eluents for analytical HPLC. The HPLC analysis (RP-HPLC) was performed on a 1100 series system from Agilent Technologies (Santa Clara, CA USA) composed of a Degasser (G1379A), a Binary Pump (G1312A), a Diode Array Detector (G1315A), a thermostated Column Compartment (G1316A) and an Autosampler (G1329A). A Phenomenex Kinetex 5u XB-C18 100A, 250 x 4.6 mm was used as the stationary phase. The flow rate was 1 mL/min, the detection wavelength was 220 nm, the oven temperature was set to 30 °C and the injection volume was 50 µL. Mixtures of solvents A (0.01% aq TFA) and B (acetonitrile) were used as mobile phase. The following gradient was applied: 0-25 min, A/B 90:10–5:95; 25-35 min, 5:95.

Stock solutions were prepared in DMSO at concentrations of 50 µM (**2.2**) and 10 mM (**2.56-2.59**, **2.61**, **2.65**, **2.66**, **2.69** and **2.71**).

3.4.2. Investigation of chemical stability of compounds **2.60** and **2.63** in the presence of 2-mercaptoethanol

To determine the chemical stability in presence of excess of 2-mercaptoethanol, compounds **2.60** and **2.63** (100 µM) were incubated in buffer (10 mM HEPES, 150 mM NaCl, 5 mM KCl, 2.5 mM CaCl₂·H₂O, 1.2 mM KH₂PO₄, 1.2 mM Mg₂SO₄·H₂O, 25 mM NaHCO₃, pH 7) with 2-mercaptoethanol (1000 µM) at rt for 24 h. The solution was diluted (1:1) with 10% aq TFA and the stability monitored by analytical HPLC analysis (3.4.1.) at time intervals 0 h, 1 h, 2 h, 4 h, 8 h and 24 h.

3.4.3. Pharmacological methods: cell culture, β -arrestin2 recruitment assay (Y₁R), saturation binding assay, radioligand binding assay for hY₄R and hY₅R

3.4.3.1. Cell culture

The preparation (HEK293T β Arr2 + Y₁R cells² and CHO-hY₄-G_{qi5}-mtAEQ cells⁶) and cultivation (HEK293T β Arr2 + Y₁R cells,² SK-N-MC cells,¹⁰ CHO-hY₄-G_{qi5}-mtAEQ cells⁶ and HEC-1B cells⁸) has been described elsewhere. SK-N-MC cells were obtained from the American Type Culture Collection (Rockville, USA).

HEK293T β Arr2 + Y₁R cells were cultivated in DMEM (Sigma-Aldrich, Taufkirchen, Germany) at 37 °C in a water saturated atmosphere containing 5% CO₂. DMEM was supplemented with L-glutamine (L-glutamine solution, Sigma-Aldrich; 0.584 g/mL), penicillin-streptomycin (Sigma-Aldrich; P/S, 10.000 U/mL) and 10% (v/v) FCS (Merck Biochrom, Darmstadt, Germany), zeocin (InvivoGen, San Diego, USA; 400 µg/mL) and G418 (Merck Biochrom; 600 µg/mL).

SK-N-MC cells were cultivated in EMEM (Sigma-Aldrich) at 37 °C in a water saturated atmosphere containing 5% CO₂. EMEM was supplemented with L-glutamine (L-glutamine solution, Sigma-Aldrich; 0.584 g/mL) and 5% (v/v) FCS (Merck Biochrom).

Routinely performed examinations for mycoplasma contamination using the Venor GeM Mycoplasma Detection Kit (Minerva Biolabs, Berlin, Germany) were negative for all cell types.

3.4.3.2. β-Arrestin2 recruitment assay (Y₁R)

The β-arrestin2 recruitment assays were performed as previously described in the dissertation of J. Felixberger² with modifications: luminescence was measured as a function of time on living cells instead of measuring luminescence after cell lysis.

The procedure was as follows: the day before the split-luciferase β-arrestin2 recruitment assay, the cells were detached by trypsinization and resuspended in Leibovitz's L-15 medium supplemented with 5% FCS and HEPES (10 mM). For antagonist mode, a cell density of $1.43 \cdot 10^6$ cells/mL was adjusted and 70 μL of this suspension were seeded into each well of a white flat bottom 96-well plate (Cellstar, Greiner Bio-One, Kremsmünster Österreich) (for agonist mode: $1.25 \cdot 10^6$ cells/mL; 80 μL). D-Luciferin (K⁺ salt; Pierce, Thermo Scientific, Regensburg, Germany) was suspended in HBSS (Gibco, Thermo Scientific) in a concentration of 400 mM. Further dilution of the substrate up to 10 mM in Leibovitz's L-15 medium was prepared shortly prior to the experiment. The cells were cultivated at 37 °C in a water saturated atmosphere (no additional CO₂). The dilutions of pNPY and ligands to be investigated were prepared in Leibovitz's L-15 medium containing 1% BSA.

In agonist mode, a solution of D-Luciferin ($c = 10$ mM, 10 μL) was added and the plate was incubated at 37 °C for 20 min. Baseline luminescence of the cells was recorded with an integration time of 1000 ms per well (10 entire plate repeats). Solutions of ligands to be investigated (10 μL; 10-fold concentrated compared to c_{final}) was added at increasing concentrations followed by immediate measurement of luminescence (20 entire plate repeats with an integration time of 1000 ms).

In antagonist mode, a solution of D-Luciferin ($c = 10$ mM, 10 μL) and the solutions (10 μL) of the test compounds (10-fold concentrated compared to c_{final}) at increasing concentrations were added, and the plate was incubated at 37 °C for 20 min. Baseline luminescence was recorded with an integration time of 1000 ms per well (10 entire plate reads). Then, pNPY ($c = 800$ nM, 10 μL) was added followed by immediate measurement of luminescence (20 entire plate repeats with an integration time of 1000 ms). Before measuring, the plate reader was pre-heated at 37 °C. The Luminescence was measured using a GENios Pro (Tecan, Grödig, Austria) or an Enspire (Perkin-Elmer, Rodgau, Germany) plate reader with an integration time of 1000 ms per well.

On every plate at least one triplicate of the 100% (response, corresponding to 80 nM pNPY) and the 0% control (neat buffer) were determined.

3.4.3.3. Saturation binding assay

The synthesis of [³H]**2.2** was performed as previously described.⁴ Saturation binding experiments using [³H]**2.2** at intact SK-N-MC cells were performed as previously described in literature^{4, 10} with minor modifications: prior to the saturation binding experiments the cells were incubated with solutions of **2.60**, **2.63** of ligands to be investigated as well as with controls **2.2** and buffer.

The procedure used was as follows: one or two days prior to the experiment, SK-N-MC cells were seeded in 24-well plates (product no. 83.3922, standard F, Sarstedt, Nümbrecht, Germany). On the day of the saturation binding experiments, the confluency of the cells was at least 70%, the culture medium was removed by suction, and cells were washed with ice-cold PBS buffer (1x). Prior to saturation binding experiments with [³H]**2.2** in intact SK-N-MC cells, the cells were incubated with binding buffer in a volume of 500 µL of **2.60** ($C_{\text{final}} = 1200$ pM) or **2.63** ($C_{\text{final}} = 1150$ pM) for 2 h. The binding buffer contained buffer (10 mM HEPES, 150 mM NaCl, 5 mM KCl, 2.5 mM CaCl₂·H₂O, 1.2 mM KH₂PO₄, 1.2 mM Mg₂SO₄·H₂O, 25 mM NaHCO₃, pH 7) and 1% BSA and 0.1 mg/mL of bacitracin. As control cells were additionally incubated with **2.2** ($C_{\text{final}} = 770$ pM) and binding buffer on the same day for 2 h. The solutions containing **2.2**, **2.60**, **2.63** or binding buffer control were removed, and the cells were washed twice with 500 µL of PBS buffer kept at ambient temperature (37 °C) (cells were covered with PBS buffer for 30 s for each washing step). The cells were covered with binding buffer (400 µL) per well. For determination of total binding 50 µL of buffer and solutions containing increasing concentrations (10-fold concentrated compared to final assay concentration (C_{final})) of [³H]**2.2** were added. Unspecific binding was determined in the presence of 50 µL of the competitor BIBO-3304 (500-fold excess compared to radioligand ([³H]**2.2**) concentrations and solutions containing increasing concentrations (10-fold concentrated compared to C_{final}) of [³H]**2.2** were added. After incubation at rt for 90 min the binding buffer was removed, and cells were washed twice with PBS buffer (cells were covered with 500 µL of ice-cold PBS buffer for 30 s for each washing step). Next, the cells were covered with 200 µL of lysis solution (8 M urea, 3 M acetic acid and 1% (V/m) Triton-X-100) and shaken for 30 min. This solution was then transferred into scintillation vials (6 mL) containing scintillator (Rotiscint eco plus, Roth, Karlsruhe, Germany) (3 mL). The samples were kept in the dark for at least 1 h and the radioactivity was measured using a LS 6500 β-counter (Beckmann Instruments, München, Germany).

3.4.3.4. Radioligand binding assay for hY₄R and hY₅R

All competition binding experiments at the Y₄R were performed as described by Kuhn et al.⁷ using [³H]UR-KK200 ($C_{\text{final}} = 1.0$ nM, $K_d = 0.67$ nM⁷) and CHO-hY₄R-G_{q15}-mtAEQ cells⁶ expressing the Y₄R (*cf.* Chapter 6). Three independent experiments were performed, each in triplicate.

All competition binding experiments at the Y₅R were essentially performed as described using [³H]propionyl-pNPY ($C_{\text{final}} = 4.0$ nM, $K_d = 4.8$ nM) and HEC-1B cells expressing the Y₅R.^{4, 8} At least two independent experiments were performed, each in triplicate.

3.4.4. Data analysis

All raw data obtained in the β-arrestin2 recruitment assay were processed as follows: firstly, the measured luminescence after addition of agonist (20 repeats) was corrected to an average baseline (first 10 repeats without adding agonist; ratio = luminescence after addition of agonist/baseline luminescence) for each well. Secondly, the increase in luminescence (RLU) was obtained by baseline correction with the buffer control. The plateau value of each luminescence trace was plotted as RLU against log(concentration antagonist) and analysed by four-parameter logistic fits (GraphPad Prism 8.0) to obtain pIC₅₀ values, which were converted to pK_b values according to the Cheng-Prusoff¹² equation (logarithmic form) (used EC₅₀ value of pNPY: 8.93 nM). A basal luminescence (buffer control, 0%) and response, corresponding to 80 nM pNPY (100%) were included for normalization of the data (antagonist mode). In case of pNPY (agonist mode) data were normalized to the basal value (0%) and the maximal response of pNPY at a concentration of 3,000 nM (100%).

Data for saturation binding experiments using [³H]**2.2** were processed as follows: specific binding data (dpm) were plotted against the free radioligand concentration and analysed by an equation describing hyperbolic binding (ligand binding – one-site saturation fit, GraphPad Prism 8) to obtain K_d and B_{max} values. The free radioligand concentration (nM) was calculated by subtracting the amount of specifically bound radioligand (nM) (calculated from the specifically bound radioligand in dpm, the specific activity of the radioligand, and the volume per well) from the total radioligand concentration.

3.5. References

1. Buschmann, J.; Seiler, T.; Bernhardt, G.; Keller, M.; Wifling, D. Argininamide-type neuropeptide Y Y₁ receptor antagonists: the nature of N^ω-carbamoyl substituents determines Y₁R binding mode and affinity. *RSC Med. Chem.* **2020**, *11*, 274-282.
2. Felixberger, J. Luciferase complementation for the determination of arrestin recruitment: Investigation at histamine and NPY receptors. PhD Thesis, University of Regensburg, 2014.
3. Keller, M.; Kaske, M.; Holzammer, T.; Bernhardt, G.; Buschauer, A. Dimeric argininamide-type neuropeptide Y receptor antagonists: Chiral discrimination between Y₁ and Y₄ receptors. *Bioorg. Med. Chem.* **2013**, *21*, 6303-6322.
4. Keller, M.; Weiss, S.; Hutzler, C.; Kuhn, K. K.; Mollereau, C.; Dukorn, S.; Schindler, L.; Bernhardt, G.; König, B.; Buschauer, A. N^ω-Carbamoylation of the Argininamide Moiety: An Avenue to Insurmountable NPY Y₁ Receptor Antagonists and a Radiolabeled Selective High-Affinity Molecular Tool ([³H]UR-MK299) with Extended Residence Time. *J. Med. Chem.* **2015**, *58*, 8834-8849.
5. Kilpatrick, L.; Briddon, S.; Hill, S.; Holliday, N. Quantitative analysis of neuropeptide Y receptor association with β-arrestin2 measured by bimolecular fluorescence complementation. *Br. J. Pharmacol.* **2010**, *160*, 892-906.
6. Ziemek, R.; Schneider, E.; Kraus, A.; Cabrele, C.; Beck-Sickinger, A. G.; Bernhardt, G.; Buschauer, A. Determination of Affinity and Activity of Ligands at the Human Neuropeptide Y Y₄ Receptor by Flow Cytometry and Aequorin Luminescence. *J. Recept. Signal Transduct. Res.* **2007**, *27*, 217-233.
7. Kuhn, K. K.; Ertl, T.; Dukorn, S.; Keller, M.; Bernhardt, G.; Reiser, O.; Buschauer, A. High Affinity Agonists of the Neuropeptide Y (NPY) Y₄ Receptor Derived from the C-Terminal Pentapeptide of Human Pancreatic Polypeptide (hPP): Synthesis, Stereochemical Discrimination, and Radiolabeling. *J. Med. Chem.* **2016**, *59*, 6045-6058.
8. Moser, C.; Bernhardt, G.; Michel, J.; Schwarz, H.; Buschauer, A. Cloning and functional expression of the hNPY Y₅ receptor in human endometrial cancer (HEC-1B) cells. *Can. J. Physiol. Pharmacol.* **2000**, *78*, 134-42.
9. Kornblum, N.; Jones, W. J.; Anderson, G. J. A new and selective method of oxidation. The conversion of alkyl halides and alkyl tosylates to aldehydes. *J. Am. Chem. Soc.* **1959**, *81*, 4113-4114.
10. Keller, M.; Bernhardt, G.; Buschauer, A. [³H]UR-MK136: A Highly Potent and Selective Radioligand for Neuropeptide Y Y₁ Receptors. *ChemMedChem* **2011**, *6*, 1566-1571.
11. Yang, Z.; Han, S.; Keller, M.; Kaiser, A.; Bender, B. J.; Bosse, M.; Burkert, K.; Kogler, L. M.; Wifling, D.; Bernhardt, G.; Plank, N.; Littmann, T.; Schmidt, P.; Yi, C.; Li, B.; Ye, S.; Zhang, R.; Xu, B.; Larhammar, D.; Stevens, R. C.; Huster, D.; Meiler, J.; Zhao, Q.; Beck-Sickinger, A. G.; Buschauer, A.; Wu, B. Structural basis of ligand binding modes at the neuropeptide Y Y₁ receptor. *Nature* **2018**, *556*, 520-524.
12. Yung-Chi, C.; Prusoff, W. H. Relationship between the inhibition constant (K_i) and the concentration of inhibitor which causes 50 per cent inhibition (I₅₀) of an enzymatic reaction. *Biochem. Pharmacol.* **1973**, *22*, 3099-3108.

Chapter 4

Synthesis, pharmacological characterization and application of the fluorescent (S)-argininamide-type hY₂R antagonist UR-jb264 (4.58)

Note: Experiments associated with BRET binding assays (preparation and cultivation of cells, saturation binding assay of **4.58**, association and dissociation experiments of **4.58** and competition binding experiments with pNPY) were performed by Lukas Grätz within his doctoral studies.

MiniG protein recruitment assay (preparation and cultivation of cells and functional characterization of pNPY, **4.1** and **4.75**) were done by Carina Höring as part of her doctoral studies.

Confocal microscopy was performed in the group of Prof Wegener (University of Regensburg). I gratefully acknowledge the help of Lisa Sauer and Dr. Stefanie Michaelis.

I gratefully acknowledge the support of Dr. Timo Littman for teaching and technical support in the β -arrestin2 recruitment assay.

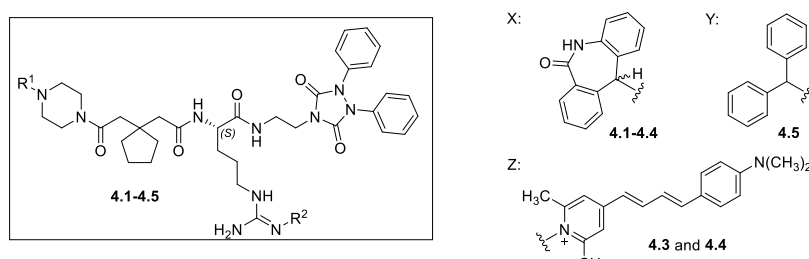
I thank (Forschungspraktikanten) Alexander Reichle, Alexander Hubmann, Simon Scheuerer and Florian Fricke for support during synthesis.

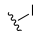
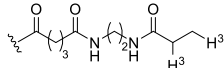
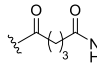
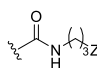
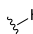
Thanks are due to Brigitte Wenzl, Maria Beer-Krön, Susanne Bollwein and Lydia Schneider for excellent technical assistance (cultivation of cells, radioligand competition binding experiments at the hY₁R and the hY₅R, and the BRET based binding assays).

4.1. Introduction

For many years fluorescent ligands have been important pharmacological tools for studying GPCRs, which are the largest target class in drug discovery.¹⁻³ Generally, fluorescently labelled receptor ligands can be applied into various luminescence-based techniques, such as Förster resonance energy transfer (FRET) microscopy, fluorescence correlation spectroscopy (FCS), scanning confocal microscopy (SCM) and fluorescence polarization (FP) to study ligand receptor interactions.^{3, 4} Moreover, the use of fluorescent ligands is advantageous regarding the legal and waste disposal requirements compared to radio labelled compounds. Essentially, a fluorescent ligand comprises of three components, which are a pharmacophore moiety, a fluorescent dye and a linker moiety.^{1, 2} The design of fluorescent ligands is driven by the goal that introduction of a fluorophore to a known pharmacophore does not change the affinity, mode of action and selectivity profile.²

Table 4.1. Structures and Y₂R affinities of reported (S)-argininamides **4.1-4.5**



Compound	Reference	R ¹	R ²	pK _i ^f /pK _d ^g
4.1 (BIIE-0246)	a	X		7.44 ^f
[³ H]4.2 ([³ H]UR-PLN196)	b	X		8.00 ^f /7.17 ^g
4.3	c	X		8.23 ^f
4.4	c	X		8.21 ^f
4.5	d, e	Y		8.17 ^f

References: (a) Dautzenberg,⁵ K_i value was determined using [¹²⁵I]PYY (C_{final} = 0.10 nM, K_d = 0.08 nM) and membranes from SMS-KAN cells. (b) Pluym et al.,⁶ the reported K_d value of [³H]4.2 was determined by saturation binding experiments in live CHO-hY₂-G_{iq5}-mtAEQ cells and the reported K_i values of 4.2 was determined in a flow cytometric binding assay using Cy5-pNPY (c = 5 nM, K_d = 5.2 nM) and CHO-hY₂-G_{iq5}-mtAEQ cells. (c) Pluym, PhD Thesis, University of Regensburg, 2011,⁷ the K_i values of 4.3 and 4.4 were determined in a flow cytometric binding assay using Cy5-pNPY (C_{final} = 5 nM) or Dy-635-pNPY (C_{final} = 10 nM) and CHO-hY₂-G_{iq5}-mtAEQ cells. (d) Dollinger et al.⁸ (e) Ziemek et al.,⁹ the reported K_i value of 4.5 was determined in a flow cytometric binding assay using Cy5-pNPY (C_{final} = 5 nM, K_d = 5.2 nM) and CHO-hY₂-G_{iq5}-mtAEQ cells. K_i (K_d) values were converted to K_i (pK_d) values.

Labelling of the endogenous ligand NPY (Neuropeptide Y) led to the fluorescent ligand Cy5-pNPY that was used in flow cytometric binding assay and flow cytometric calcium assay and showed high affinity to several NPY receptor subtypes (hY₁R, hY₂R and hY₅R).⁹ Nevertheless, fluorescently labelled peptides are prone to enzymatic degradation.^{10, 11} Work in our group aimed towards non-peptide fluorescent hY₁R ligands, using the guanidine-acylguanidine approach,^{12, 13} resulted in the synthesis of several fluorescent conjugates of (R)-argininamide BIBP-3226 (**2.1**).¹³ This labelling strategy according to the guanidine-acylguanidine bioisosteric approach was applied to the (S)-argininamide-type Y₂R

antagonist BIIE-0246 (**4.1**) and led to several radio- and fluorescently labelled molecular tools (e.g. [^3H]**4.2** and **4.3**) addressing the hY_2R .^{6, 7, 14} However, this bioisosteric replacement is limited due to the low chemical stability of acylguanidines in particular under basic conditions.¹⁵ Therefore, a different strategy (guanidine-carbamoylguanidine approach I) for the labelling of ligands was applied. M^{ω} -carbamoylation instead of acylation of argininamides led to the high affinity hY_1R antagonist **2.2**, showing no decomposition over time in phosphate buffered saline (pH 7.0) at ambient temperature.¹⁶ This strategy was proven for the synthesis of selective non-peptide (S)-argininamide-type NPY hY_2R antagonists as chemical tools (e.g. **4.4**).^{7, 17}

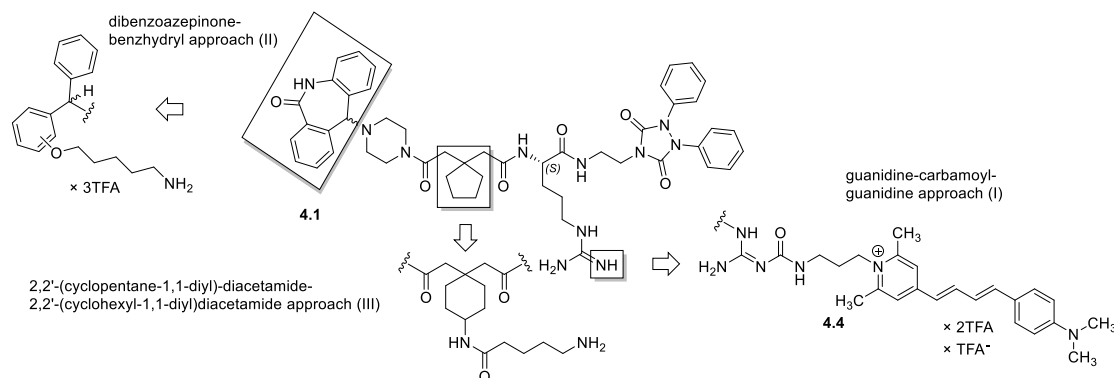


Figure 4.1. Three approaches (I-III) to molecular tools derived from BIIE-0246 (**4.1**).

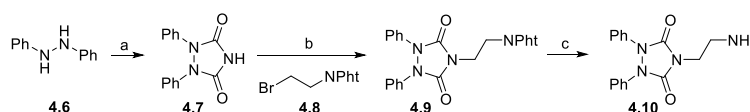
For the development of novel non-peptide fluorescently labelled Y_2R ligands as molecular tools, I decided to retain the guanidine moiety (no replacement by a carbamoylguanidine group), M^{ω} -carbamoylated (S)-argininamides showed unfavourable Y_2R binding characteristics (e.g. pNPY showed noticeably lower pK_i value determined with [^3H]**4.2** compared to affinity determined with cy5-NPY).⁶ In addition, it is suggested that the guanidine group of **4.1** shows an interaction (salt-bridge) with D^6 ,⁵⁹ whereas the dibenzoazepinone moiety of **4.1** is buried in a hydrophobic binding pocket ($\text{L}^{4.60}$, $\text{L}^{5.45}$, $\text{L}^{6.51}$) in the orthosteric binding side.¹⁸ Both of these interactions with the Y_2R (binding sites) of **4.1** were shared with the endogenous ligand NPY.¹⁸⁻²¹ The focus for the development of fluorescent ligands in this work is in search for a more favourable labelling site following approaches II and III (Figure 4.1). As already known, the dibenzoazepinone moiety (*cf.* **4.1**²²) can be replaced by a benzhydryl moiety (*cf.* **4.5**^{8, 9}). For this reason, a small library of compounds (**4.23**, **4.24**, **4.27**, **4.50** and **4.51**) was synthesized (approach II), that were modified on the benzhydryl residue, to identify a favourable labelling side of fluorescently labelled compounds. Py-1 (**4.60**) and Py-5 (**2.77**) were chosen as fluorophores, because of their fluorescence properties and their potential application in BRET (bioluminescence resonance energy transfer) based binding assays.²³⁻²⁵ Here the synthesis of the red-emitting fluorescent ligand UR-jb264 (**4.58**), the pharmacological characterization, the investigation of the chemical stability as well as its application in BRET based binding assay and in confocal microscopy are reported.

Furthermore, the 2,2'-(cyclopentane-1,1-diyl)diacetamide was replaced by a 2,2'-(cyclohexane-1,1-diyl)di-acetamide moiety, leading to compound **4.75**, which is a step towards the identification of a potential third labelling site (approach III, Figure 4.1) in argininamide-type hY_2R ligands. To address this labelling site, the first steps in the synthesis for amino functionalization of the 2,2'-(cyclohexane-1,1-diyl)diacetamide moiety were performed.

4.2. Results and discussion

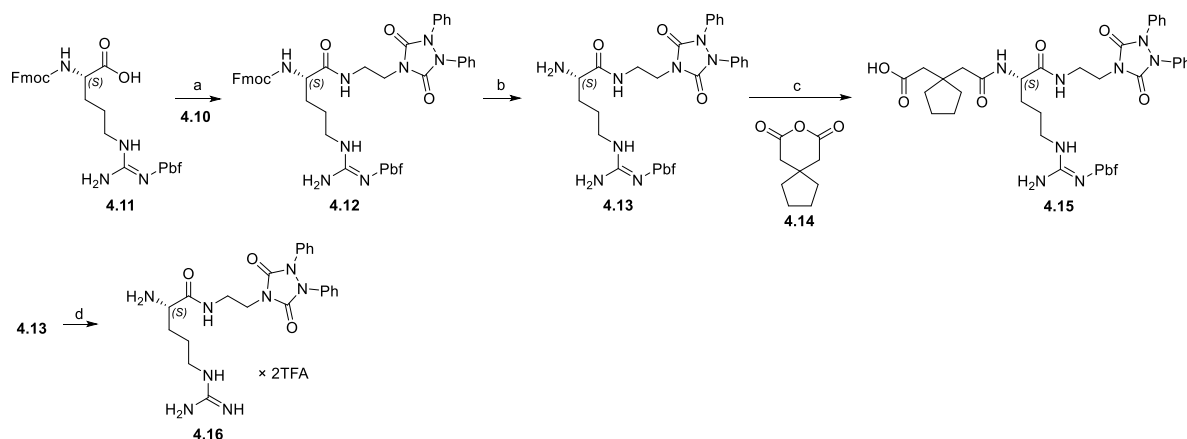
4.2.1. Synthesis

4-(2-Aminoethyl)-1,2-diphenyl-1,2,4-triazolidine-3,5-dione (**4.10**) was synthesized according to published procedures⁸ in a three-step synthesis starting from 1,2-diphenylhydrazine (**4.6**), which was treated with ethyl allophanate, giving isocyanic acid *in situ*, in p-xylene under reflux conditions to obtain 1,2-diphenyl-1,2,4-triazolidine-3,5-dione (**4.7**) (Scheme 4.1). Intermediate **4.7** was treated with sodium hydride and the phthaloyl protected ethyl linker moiety (2-(2-bromoethyl)isoindoline-1,3-dione (**4.8**)) was added. Subsequently, the phthaloyl protecting group of **4.9** was removed by hydrazine to obtain amino-functionalized 1,2-diphenyl-1,2,4-triazolidine-3,5-dione **4.10**.



Scheme 4.1. Synthesis of 4-(2-aminoethyl)-1,2-diphenyl-1,2,4-triazolidine-3,5-dione (**4.10**). Reagents and conditions: (a) ethyl allophanate, p-xylene, reflux, 40%; (b) (1) NaH, DMF, ice bath, (2) reflux, 42%; (c) hydrazine monohydrate, MeOH, THF, rt, 72%.

(S)-Arginine building blocks **4.15** and **4.16** were essentially prepared as previously described by Dollinger et al.⁸ and Brennauer.¹⁷ Fmoc-Arg(Pbf)-OH (**4.11**) was activated *in situ* in the presence of EDC·HCl and HOBT and amidated with amine **4.10** to form **4.12**. Subsequently, the Fmoc protecting group was removed by use of piperidine in DMF to obtain **4.13** in good yields (Scheme 4.2). The amino group of **4.13** was coupled with 3,3-tetramethyleneglutaric anhydride (**4.14**) to afford the carboxylic acid **4.15**. Moreover, the Pbf-protecting group of intermediate **4.13** was removed by acid (TFA/water 95:5) to obtain the (S)-argininamide **4.16** as TFA salt after purification by preparative HPLC.



Scheme 4.2. Synthesis of (S)-arginine building blocks **4.15** and **4.16**. Reagents and conditions: (a) EDC·HCl, HOBT, DMF, 93%; (b) DMF, piperidine, rt, 91%; (c) CH₂Cl₂, 99%; (d) TFA/H₂O (95:5), 70%.

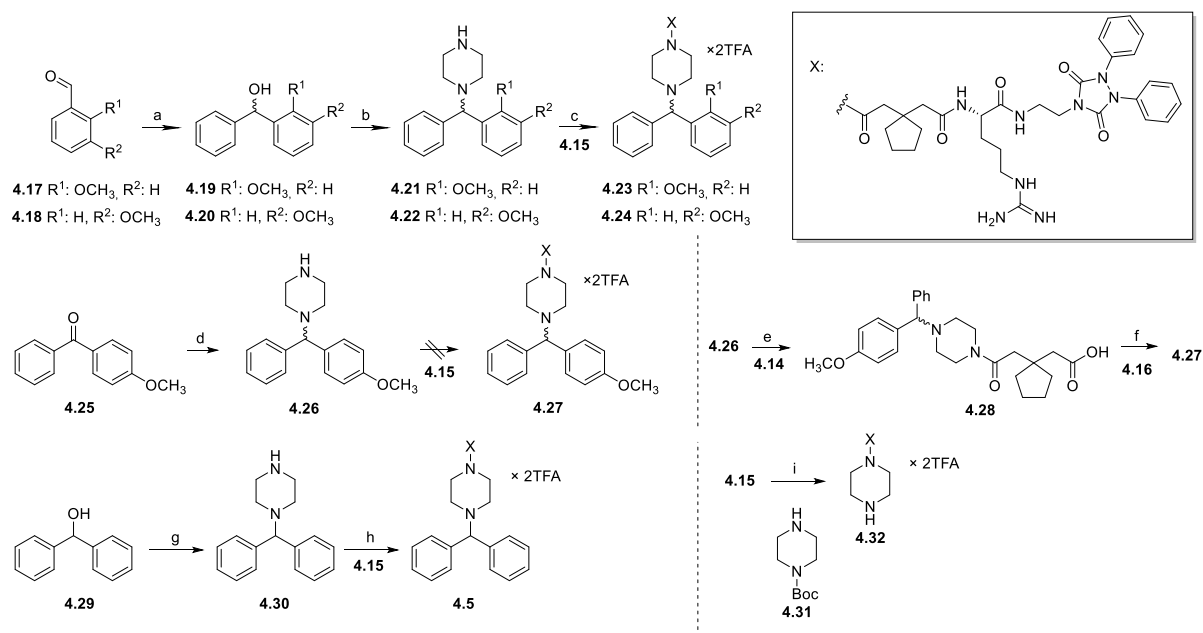
Compounds **4.23** and **4.24** were synthesized from the respective methoxy substituted benzaldehydes **4.17** or **4.18** in a three-step synthesis route (Scheme 4.3). For this purpose, **4.17** or **4.18** were converted to the 2- or 3- substituted methoxy benzhydryl alcohols (**4.19** and **4.20**) in good to excellent yields by Grignard reactions. For the synthesis of intermediates **4.21** and **4.22**, the hydroxyl groups of the benzhydryl alcohols **4.19** and **4.20** were converted into good leaving groups by treatment of **4.19** or **4.20** with sulfuryl chloride, followed by treatment with piperazine (S_N reaction) under microwave conditions. Finally, coupling of carboxylic acid **4.15** to the secondary amines **4.21** and **4.22** by the aid of coupling

reagents EDC·HCl and HOBT and subsequent treatment with aqueous TFA (Pbf deprotection) gave **4.23** and **4.24**.

1-((4-Methoxyphenyl)(phenyl)methyl)piperazine (**4.26**) was synthesized from the commercially available ketone **4.25** by a reductive amination procedure using TiCl₄ and NaBH₄ (Scheme 4.3).²⁶ (S)-Argininamide **4.27** could not be obtained by amide bond formation between **4.15** and amine **4.26**, because removal of the Pbf-protecting group under strong acidic conditions led to compound **4.32**, that was identified by HRMS and RP-HPLC (Scheme 4.3). To deal with this problem, amine **4.26** was treated with **4.14** to obtain the carboxylic acid **4.28**, that was activated with coupling reagents EDC·HCl/HOBT and coupled with the (S)-argininamide **4.16**, that Pbf group was already removed to form **4.27**.

The unsubstituted derivative **4.5** (Scheme 4.3) was synthesized from benzhydryl alcohol **4.29** using methanesulfonyl chloride for the conversion of the hydroxyl group in **4.29** to a good leaving group, followed by the treatment of the formed mesylate with piperazine (S_N reaction) to give intermediate **4.30**, which was subjected to amide bond formation with **4.15** and subsequent Pbf deprotection to afford **4.5** (Scheme 4.3).

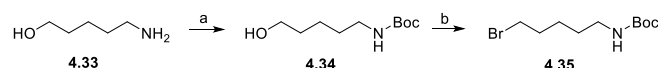
The obtained side product **4.32** was formed by amide bond formation between **4.15** and *N*-Boc-piperazine (**4.31**) and subsequent removal of Boc and Pbf protecting groups in TFA/water (95:5) (Scheme 4.3).



Scheme 4.3. Synthesis of **4.5** and related compounds **4.23**, **4.24**, **4.27** and **4.32**. Reagents and conditions: (a) (1) Mg, bromobenzene, THF, (2) H⁺/H₂O, 71-93%; (b) (1) SO₂Cl₂, CH₂Cl₂, reflux, (2) piperazine, acetonitrile, microwave device (100 °C, 30 min), 67-74%; (c) (1) EDC·HCl, HOBT, DMF, (2) TFA/H₂O 95:5, 13-18%; (d) (1) TiCl₄, piperazine, CH₂Cl₂, (2) NaBH₄, MeOH, 23%; (e) Et₃N, CH₂Cl₂, 79%; (f) EDC·HCl, HOBT, DMF, 61%; (g) (1) methanesulfonyl chloride, Et₃N, CH₂Cl₂, (2) piperazine, acetonitrile, microwave device (70 °C, 30 min), 52%; (h) (1) EDC·HCl, HOBT, DMF, (2) TFA/H₂O 95:5, 12%; (i) (1) EDC·HCl, HOBT, DMF, (2) TFA/H₂O 95:5, 37%.

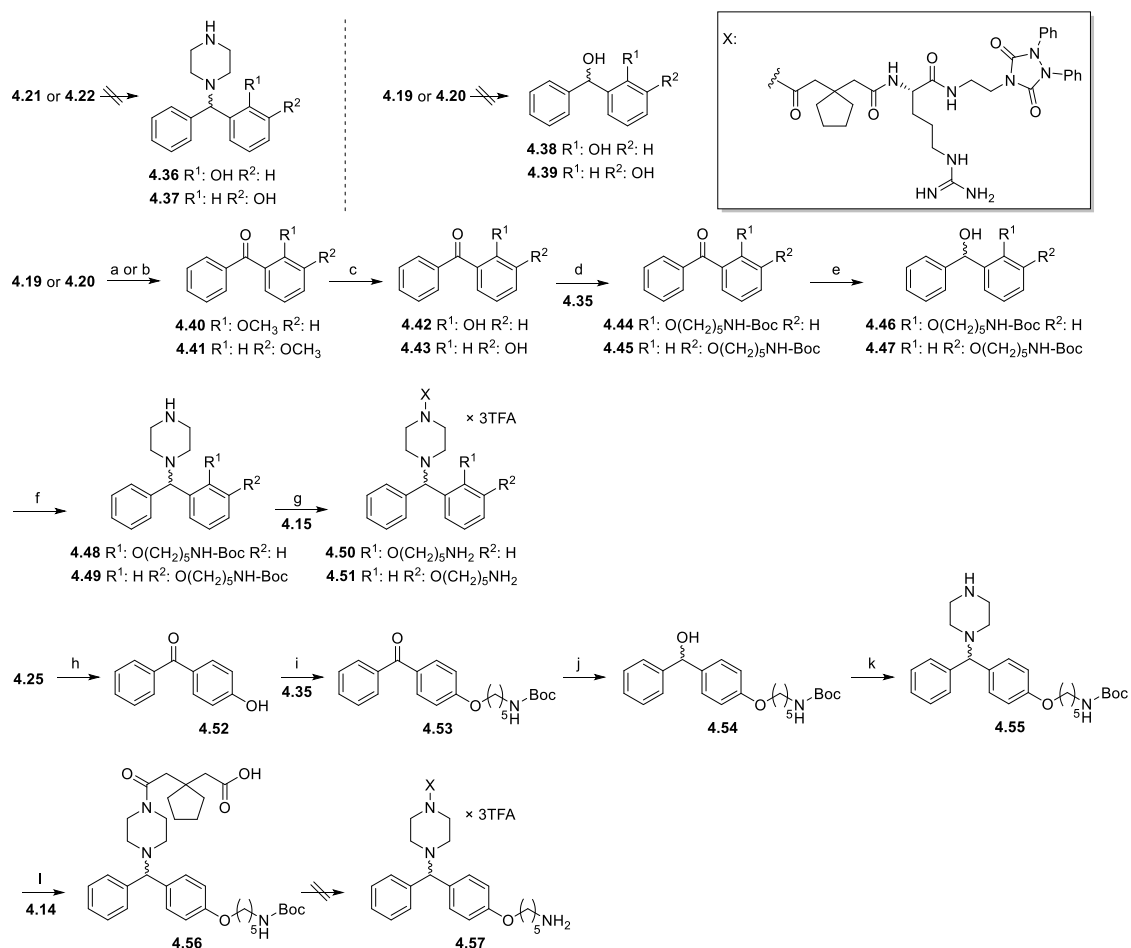
For the synthesis of fluorescently labelled compounds, the methoxy groups in **4.23** and **4.24** had to be replaced by an amino-functionalized linker (Scheme 4.4). For this purpose, 5-aminopentanol (**4.33**) was

treated with Boc₂O to give **4.34**, which was converted to bromide **4.35** using an Appel-reaction²⁷ (Scheme 4.4).



Scheme 4.4. Synthesis of *tert*-butyl (5-bromopentyl)carbamate (**4.35**). Reagents and conditions: (a) Boc₂O, Et₃N, CH₂Cl₂, 73%, (b) CBr₄, PPh₃, CH₂Cl₂, 92%.

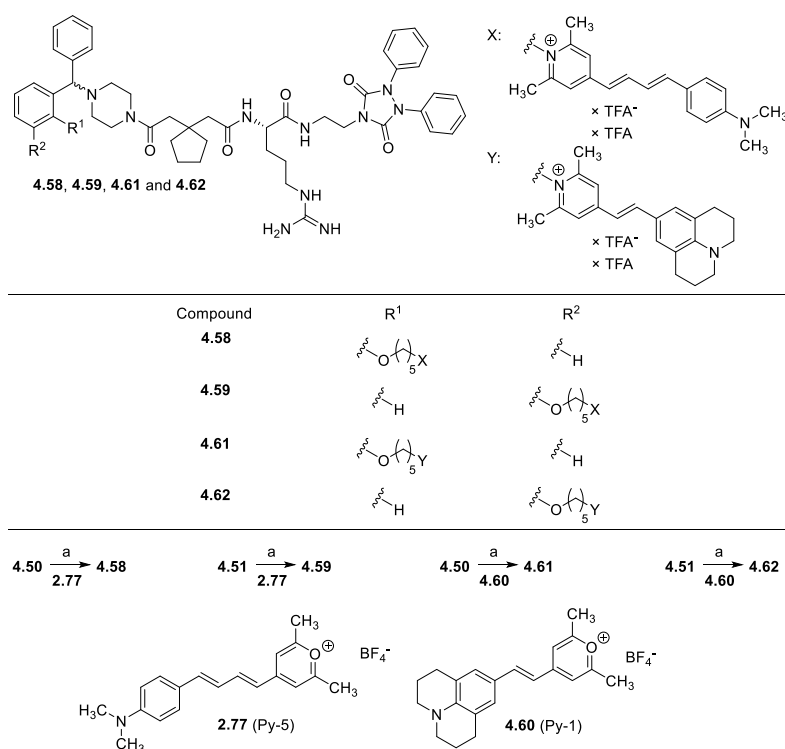
Amino-functionalized (S)-argininamides **4.50** or **4.51** were synthesized from **4.19** and **4.20**, respectively (Scheme 4.5). Initially, cleavage of the methyl ether failed, for instance, for compounds **4.19-4.22** (intended to give **4.36-4.38**). The use of standard procedures, e.g. HBr or BBr₃, led to the decomposition of starting materials. Therefore, the alcohols **4.19** and **4.20** were oxidized using PCC or pyridine-sulfur trioxide to obtain the ketones **4.40** and **4.41**, which were demethylated in refluxing aqueous HBr solution (47%) to give the free phenols **4.42** and **4.43** (S_N2 reaction). The phenols **4.42** and **4.43** were then coupled with **4.35** in DMF by use of K₂CO₃ to afford the Boc-protected amino-functionalized pentylphenylethers **4.44** and **4.45** (Williamson ether synthesis²⁸) (Scheme 4.5).



Scheme 4.5. Synthesis of amino-functionalized precursors (**4.50** and **4.51**) for fluorescence labelling. Reagents and conditions: (a) pyridine-sulfur trioxide complex, Et₃N, DMSO, 39%; (b) PCC, CH₂Cl₂, 80%; (c) aqueous HBr (47%), AcOH, reflux, 94-100%; (d) K₂CO₃, DMF, 49-52%; (e) NaBH₄, MeOH, 56%; (f) (1) methanesulfonyl chloride, Et₃N, CH₂Cl₂, (2) piperazine, acetonitrile, microwave device (70 °C, 45 min), 48-66%; (g) (1) EDC-HCl, HOBT, DMF, (2) TFA/H₂O 95:5, 16-18%; (h) aqueous HBr (48%), AcOH, reflux, 96%; (i) K₂CO₃, DMF, 70%; (j) NaBH₄, MeOH, 100%; (k) (1) methanesulfonyl chloride, Et₃N, CH₂Cl₂, (2) piperazine, acetonitrile, microwave device (70 °C, 45 min), 49%; (l) CH₂Cl₂, 70% .

Compounds **4.44** and **4.45** were reduced with NaBH₄ to obtain the corresponding alcohols **4.46** and **4.47**, which were converted to respective mesylates using methanesulfonyl chloride (Scheme 4.5). The mesylates were not isolated and directly treated with piperazine in a microwave reactor to afford amines **4.48** and **4.49**. These intermediates were coupled with **4.15** using EDC·HCl and HOBt. Removal of the Pbf-group gave **4.50** and **4.51** as precursors for fluorescence labelling.

The commercially available (4-methoxyphenyl)(phenyl)methanone (**4.25**) was treated with aqueous HBr (47%) to obtain the phenol **4.52**. Compound **4.53** was synthesized from phenol **4.52** and bromide **4.35** (Williamson ether synthesis²⁸). The reduction of 4-methoxybenzophenone (**4.53**) by use of NaBH₄ led to the corresponding benzhydryl alcohol **4.54**, which was converted to a mesylate and coupled with piperazine in a microwave device. Amide bond formation between anhydride **4.14** and amine **4.55** led to the carboxylic acid **4.56**. The synthesis of amino-functionalized (*S*)-argininamide **4.57** by amide bond formation between **4.56** and **4.16** and subsequent removal of the Boc protecting group, failed (Scheme 4.4 and 4.5). Boc deprotection under milder acidic conditions led to compound **4.32**, which was identified by HRMS and RP-HPLC. However, the synthesis of **4.57** was achieved by use of a different protecting group (instead of Boc group), that is not removed under acidic conditions. However, this synthesis strategy was not pursued, because the corresponding methyl ether **4.27** (Scheme 4.3) showed lower Y₂R affinity (4.2.4.1.) compared to compounds **4.23** and **4.24**.

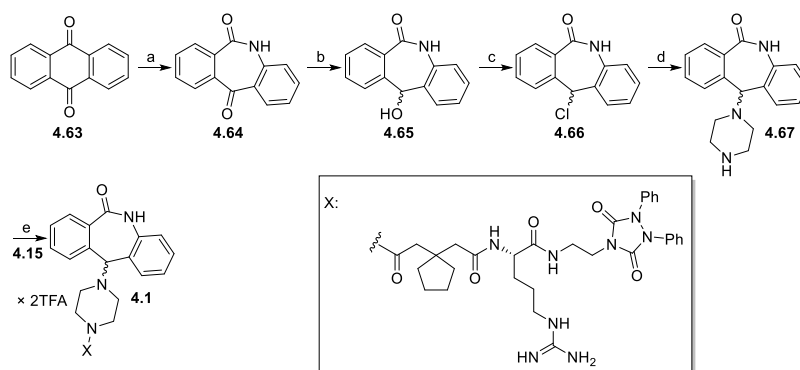


Scheme 4.6. Synthesis of fluorescently labelled compounds **4.58**, **4.59**, **4.60** and **4.61**. Reagents and conditions: (a) DIPEA, DMF, 16-45%.

The fluorescently labelled compounds **4.58**, **4.59**, **4.61** and **4.62** were synthesized according to a procedure reported¹³ for the synthesis of fluorescent Y₁R ligands with minor modifications: Treatment of amines **4.50** and **4.51** with the pyrylium dyes **2.77** (Py-5) or **4.60** (Py-1) in the presence of DIPEA (instead of Et₃N) gave the pyridinium adducts **4.58**, **4.61**, **4.59** and **4.62** (Scheme 4.6).

BIIE-0246 (**4.1**), representing the standard (S)-argininamide-type Y₂R antagonist was synthesized according to published procedures⁸ starting from anthraquinone (**4.63**) (Scheme 4.7). Compound **4.63** was transformed to amide **4.64** by a Schmidt reaction using NaN₃ and conc. H₂SO₄. Subsequently, the keto group (position 11) in **4.64** was reduced by NaBH₄ to obtain the secondary alcohol **4.65** as racemate, which was then converted to chloride **4.66** (Scheme 4.7). 11-Chloro-5,11-dihydro-6H-dibenzo[b,e]azepin-6-one was treated with piperazine to give **4.67**, which was coupled to **4.15** by amide bond formation under the conditions used for the synthesis of **4.23** and **4.24** from **4.21** or **4.22** and **4.15** (Scheme 4.3). Removal of the Pbf group with TFA yielded **4.1**.

Replacement of the cyclopentyl moiety of **4.1** by a cyclohexyl moiety led to compound **4.75** (Scheme 4.8). To prepare **4.75**, compound **4.68** was converted to 2-cyanoacetamide (**4.69**) in an ice-cold aqueous ammonia solution. The condensation (Knoevenagel-condensation²⁹) of cyclohexanone (**4.70**) and ethyl 2-cyanoacetate (**4.69**) led to compound **4.71** (Scheme 4.8).

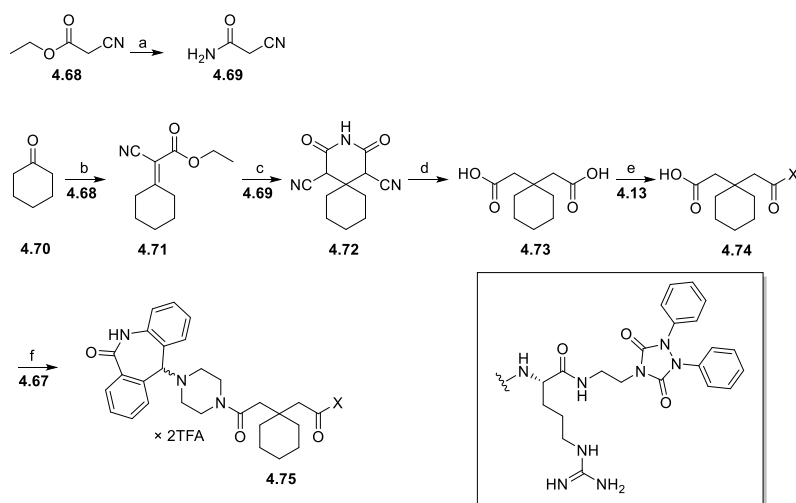


Scheme 4.7. Synthesis of **4.1** and dibenzoazepinone precursor **4.67**. Reagents and conditions: (a) (1) NaN₃, conc. H₂SO₄, CH₂Cl₂, (2) NH₃ aq, 59%; (b) NaBH₄, EtOH, 82%; (c) SOCl₂, CH₂Cl₂, reflux, 95%; (d) piperazine, dioxane, 60 °C, 77%; (e) (1) EDC·HCl, HOBT, DMF, (2) TFA/H₂O 95:5, 18%.

For the synthesis of spirocyclic compound **4.72**, 2-cyanoacetamide (**4.69**), intermediate **4.71** and a solution of sodium ethoxide were used. The spirocyclic 1,5-dicarbonitrile **4.72** was treated with concentrated sulfuric acid to obtain the dicarboxylic acid **4.73**. Compound **4.13** was coupled with the dicarboxylic acid **4.73** using EDC·HCl and HOBT to afford **4.74**. (S)-Argininamide **4.75** was synthesized by amide bond formation between amine **4.67** and carboxylic acid **4.74**.

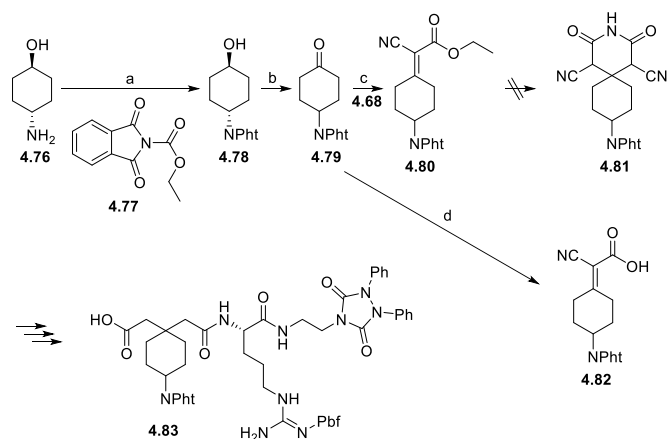
The synthetic procedure used for the preparation of **4.74** was intended to be used for the synthesis of compound **4.83** (Scheme 4.9). Unfortunately, this strategy failed. Firstly, the amino-group of *trans*-4-aminocyclohexanol (**4.76**) was protected using reagent **4.77** to give **4.78**, bearing a phthaloyl protecting group that is stable under basic and acidic conditions, for the next steps (Scheme 4.9). Oxidation of **4.78** by use of PCC (pyridinium chlorochromate, Corey-Suggs reagent) led to **4.79** in moderate yield. For the subsequent Knoevenagel-condensation of **4.68** and **4.79**, yielding **4.80** sodium methoxide was used instead of sodium ethoxide as in case for the synthesis of **4.71**, as **4.79** was found to be poorly soluble in the solution of sodium ethoxide (Scheme 4.9). The formation of the 1,5-dicarbonitrile **4.81** was not possible using the same conditions as for the preparation of **4.72** (Scheme 4.8). The variation of solvents and bases also did not pave way to **4.81** and subsequently to **4.83**. An attempt to form **4.81** in a one pot reaction by the use of ammonia as a gas dissolved in methanol, as described in literature³⁰ for a non-

amino-functionalized derivative (2,4-dioxo-9-pentyl-3-azaspiro[5.5]un-decane-1,5-dicarbonitrile), also failed to give the desired product.



Scheme 4.8. Synthesis of **4.75**. Reagents and conditions: (a) NH_3 aq, 54%; (b) AcOH , $\text{NH}_4\text{CH}_3\text{CO}_2$, toluene, reflux, 100%; (c) (1) Na , EtOH , reflux (2) HCl , H_2O , rt, 38%; (d) (1) H_2SO_4 conc., reflux, (2) H_2O , 65%; (e) $\text{EDC}\cdot\text{HCl}$, HOBT , DMF , 76%; (f) (1) $\text{EDC}\cdot\text{HCl}$, HOBT , DMF , (2) $\text{TFA}/\text{H}_2\text{O}$ 95:5, 11%.

The one pot reaction led to the formation of compound **4.82**, which was identified by HRMS as main product (Scheme 4.9). Intermediate **4.82** could not be used to prepare an amino-functionalized (*S*)-argininamide **4.83**. It will be subject of future studies to explore whether **4.82** can be used for the synthesis of fluorescently labelled hY_2R ligands.



Scheme 4.9. Synthesis of amino-functionalized dicarboxylic acid **4.81**. Reagents and conditions. (a) K_2CO_3 , H_2O , rt, 34%; (b) PCC , CH_2Cl_2 , rt, 2 h, 66%; (c) AcOH , $\text{NH}_4\text{CH}_3\text{CO}_2$, toluene, reflux (d) (1) **4.69**, MeOH , NH_3 (g) (2) H_2O , reflux, (3) conc. HCl , yield was not determined.

4.2.2. Investigation of the chemical stability of **4.50**, **4.51** and **4.58**

Decomposition of (*S*)-argininamides **4.1** and **4.5** (structures see Table 4.1) under assay-like conditions (aqueous buffer pH 7) has not been reported in the literature. The stability of the fluorescently (Py-5) labelled compound **4.58** and of its amine precursor **4.50** were investigated, as well as one amine precursor **4.51**. In contrast to the described procedure used to investigate the stability of

(R)-argininamide-type Y₁R antagonists (*cf.* 2.4.3.),³¹ compounds **4.50**, **4.51** and **4.58** were incubated in the buffer, which was used for competition binding studies with [³H]propionyl-pNPY (4.2.4.).

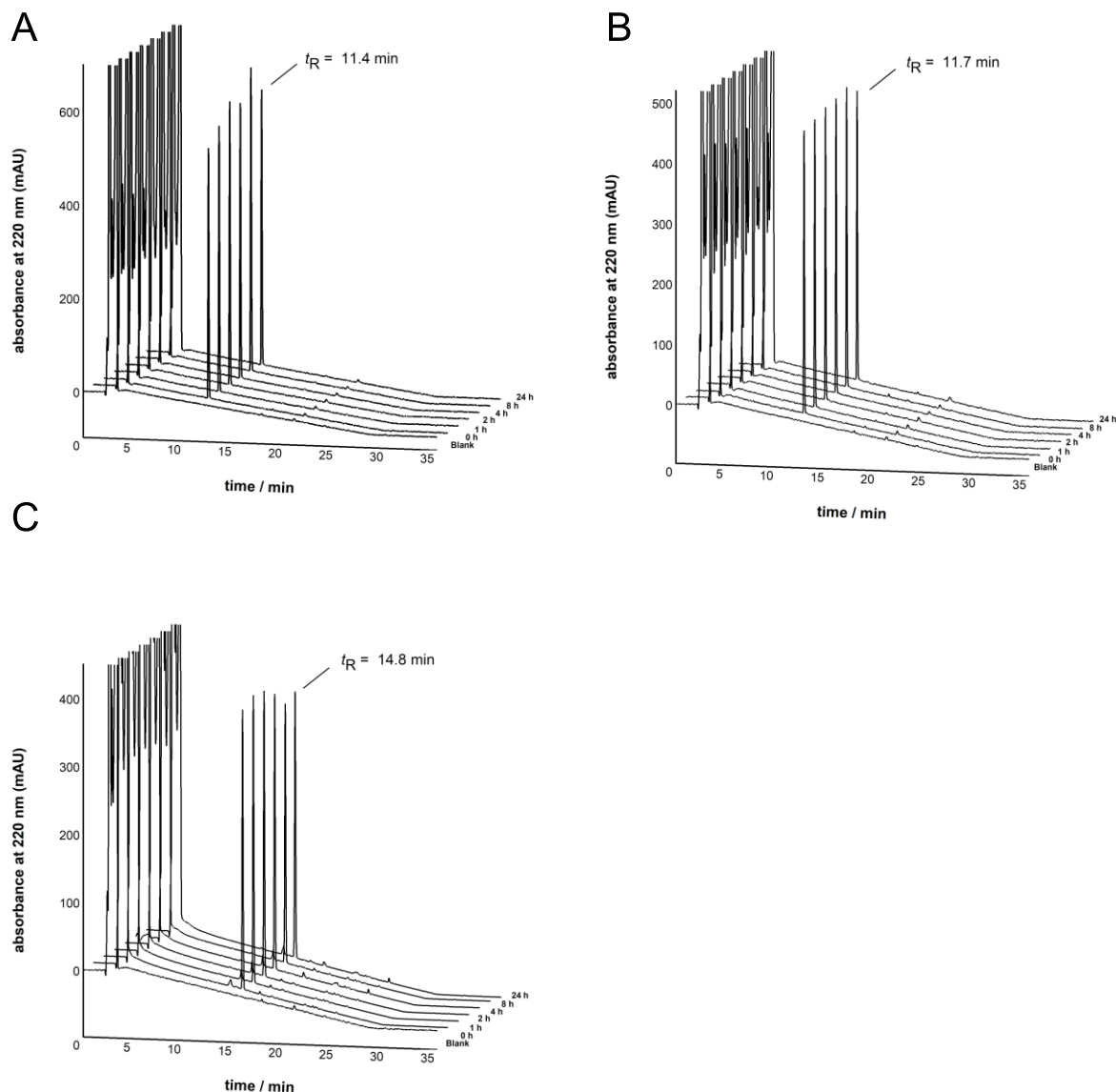


Figure 4.2. Chromatograms of the reversed-phase HPLC (220 nm) analysis of (A) **4.50**, (B) **4.51** and (C) the fluorescent ligand **4.58** after incubation in a 25 mM HEPES buffer (pH 7.0) at rt for up to 24 h. **4.50**, **4.51** and **4.58** proved to be stable.

(S)-argininamides **4.50**, **4.51** and **4.58** proved to be stable in 25 mM HEPES buffer (pH 7.0, rt) over 24 h (Figure 4.2), which qualifies them for a pharmacological characterization in functional and binding assays.

4.2.3. Fluorescence properties

The corrected excitation and emission spectra of fluorescent ligands **4.58**, **4.59**, **4.61** and **4.62** (Figure 4.3) were recorded in PBS (pH 7.4) containing 1% BSA (w/v). The concentration of the compounds was 5 μ M in each case.

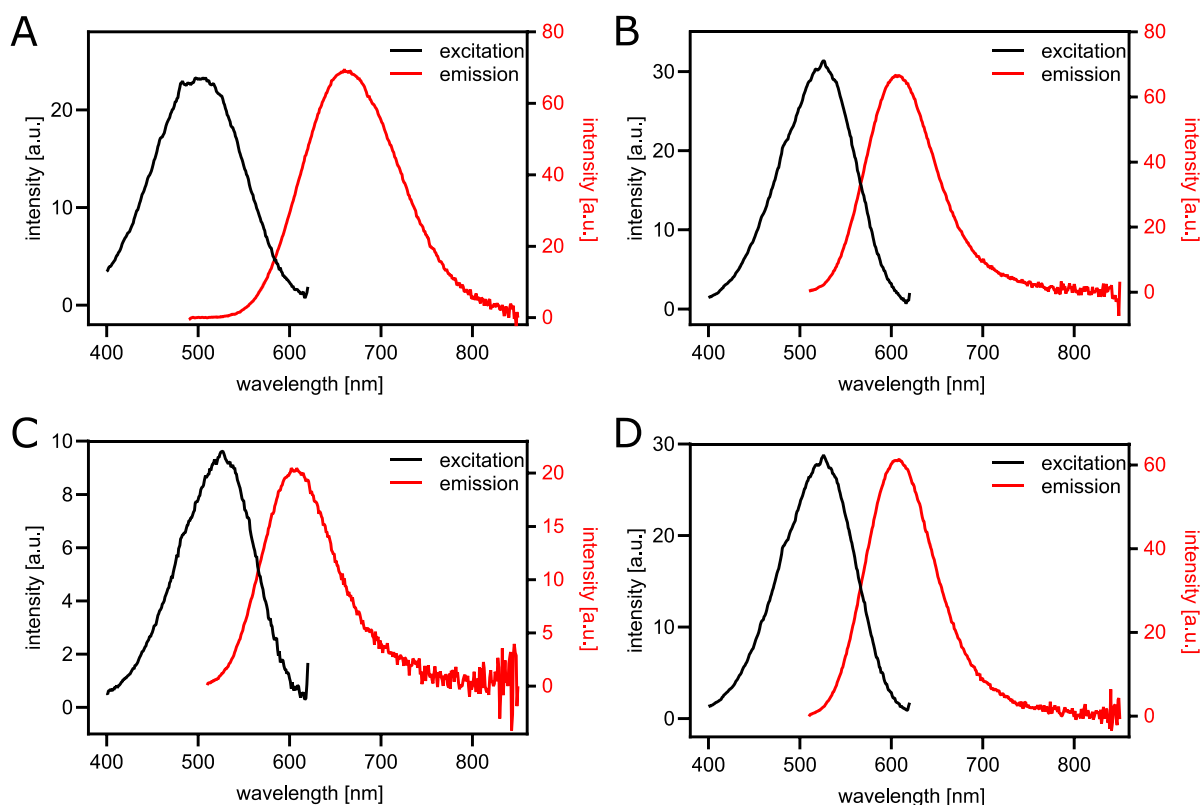


Figure 4.3. Corrected excitation and emission spectra of compounds **4.58**, **4.59**, **4.61** and **4.62** at 22 °C. The fluorescent ligands (A) **4.58**, (B) **4.59**, (C) **4.60** and (D) **4.61** were dissolved in PBS containing 1% BSA (w/v).

The Stokes shift of the Py-5 labelled fluorescent ligand **4.58** was slightly longer compared to the other Py-1 and Py-5 labelled compounds **4.59**, **4.61** and **4.62** (Table 4.2), which is advantageous for application in BRET based competition binding assays described below.

Table 4.2. Excitation and Emission maxima of compounds **4.58**, **4.59**, **4.61** and **4.62** in PBS (pH 7.4) containing 1% BSA (w/v) recorded at 22 °C.

Compound	Dye ^a	λ_{ex} [nm]	λ_{em} [nm]
4.58	2.77 (Py-5)	500	660
4.59	2.77 (Py-5)	526	605
4.61	4.60 (Py-1)	527	608
4.62	4.60 (Py-1)	526	609

^aFluorescent dyes (**2.77** or **4.60**) used for the preparation of the fluorescent ligands

4.2.4. Pharmacological methods: Y₂R affinity (pK_i) and antagonism (pK_b) of synthesized (S)-argininamides, application of 4.58 to BRET based binding assays and to confocal microscopy, NPY Y₂R subtype selectivity

In the search for a red-emitting fluorescent labelled (S)-argininamide as a molecular tool with application in BRET based binding assay and confocal microscopy, compounds **4.23**, **4.24**, **4.27**, **4.50**, **4.51**, **4.58** and **4.75** were investigated in equilibrium competition binding experiments. Moreover, compounds **4.1**, **4.5**, **4.23**, **4.24**, **4.27**, **4.32**, **4.50**, **4.51**, **4.58**, **4.59**, **4.61**, **4.62** and **4.75** were investigated in a β -arrestin2 recruitment assay. Additionally, compounds **4.1**, **4.58** and **4.75** were investigated in a miniG protein recruitment assay. UR-jb264 (**4.58**) was chosen for establishing a BRET based binding assay and for receptor localization by confocal microscopy.

4.2.4.1. Radioligand binding assay in HEK293T hY₂R + β Arr2 cells

Equilibrium competition binding experiments using [³H]propionyl-pNPY as radioligand were performed in sodium free binding buffer (25 mM HEPES, 2.5 mM CaCl₂, 1 mM MgCl₂, pH 7.4) in intact HEK293T hY₂R + β Arr2 cells. For the radioligand binding assay it is necessary to wash the living cells several times. Due to poor adherence of HEK293T cells, the 24-well (product no. 83.3922, standard F, Sarstedt, Nümbrecht, Germany) or 96-well (product no. 3610, Corning, Kaiserslautern, Germany) plates used were coated with poly-*D*-lysine or gelatin to improve cell adherence properties.

Comparison of poly-*D*-lysine and gelatin as coating materials for 24-well and 96-well plates

One day before the crystal violet assay, the HEK293T hY₂R + β Arr2 cells were seeded in coated (poly-*D*-lysine or gelatin) 24-well and 96-well plates.

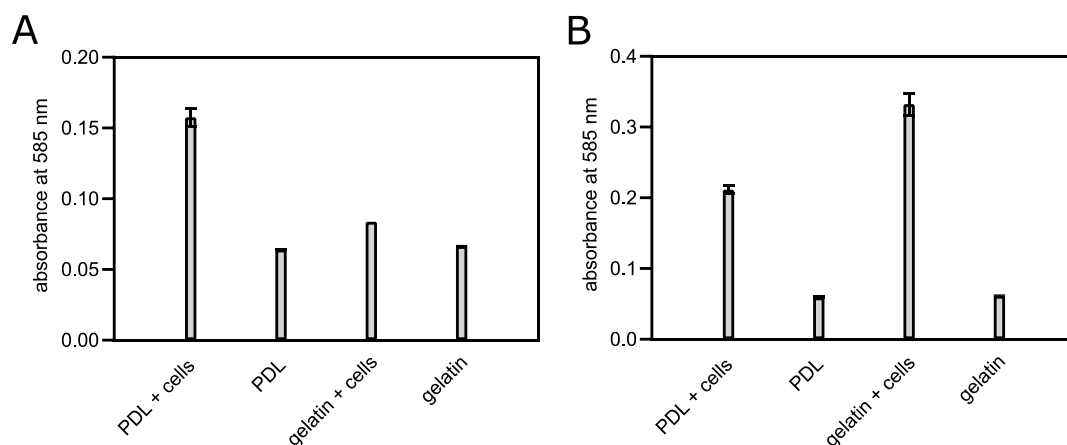


Figure 4.4. Comparison of poly-*D*-lysine (PDL) and gelatin as coating reagents in 96-well (product no. 3610, Corning, Kaiserslautern, Germany) and 24-well (product no. 83.3922, standard F, Sarstedt, Nümbrecht, Germany) plates. (A) A 96-well plate was coated with PDL (48-wells) and gelatin (48-wells), whereof 8 wells contained no cells, respectively. (B) Two 24-well plates were coated with PDL and gelatin respectively. 40 wells were coated with PDL or gelatin and 8 wells were coated with PDL or galantine and contained no cells, respectively. Data represents mean value \pm SEM from measured absorbance (mAU) at 585 nm per well.

The next day, the medium was removed and the competition binding experiment was performed as described^{9, 32} with the distinction that no radioligand was used. Instead of CHO-hY₂R-G_{qi5}-mtAEQ cells, HEK293T hY₂R + β Arr2 cells were used for the experiment. After the removal of the medium, the cells were washed with PBS and then incubated with the sodium-free binding buffer for 90 min. Afterwards

the medium was removed, and a crystal violet assay was performed to determine the amount of cells per well, in order to find a coating material, that improves the adherence of HEK293T hY₂R + β Arr2 cells to the plate material (polystyrene). In conclusion, the adherence of HEK293T hY₂R + β Arr2 cells could be improved using poly-*D*-lysine in 96-well plates and gelatin in 24-well plates.

In the following, saturation and competition binding experiments were then performed in 96-well plates. Advantages of 96-well plates are higher throughput and a more convenient coating procedure.

Determination of the pK_d value of [³H]propionyl-pNPY by saturation binding in HEK293T hY₂R + β Arr2 cells

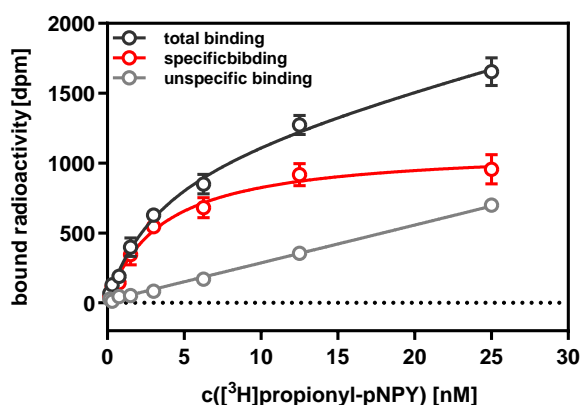


Figure 4.5. Representative saturation isotherm (red line) of specific hY₂R binding of [³H]propionyl-pNPY in intact HEK293T hY₂R + β Arr2 cells. Unspecific binding (grey line) was determined in the presence of a 200-fold excess of BIIE-0246 (4.1). The experiments were performed in triplicate. Error bars of specific binding were calculated according to the Gaussian law of error propagation. Error bars of total (black symbols), and nonspecific (grey symbols) binding represent SEM.

The radioligand [³H]propionyl-pNPY was characterized in saturation binding experiments in living HEK293T hY₂R + β Arr2 cells. The determined pK_d value of 8.53 ± 0.03 was in agreement with literature⁹ using [³H]propionyl-pNPY as radioligand in CHO-hY₂-G_{iq5}-mtAEQ-cells ($pK_d = 9.2$,⁹ K_d value was converted to pK_d value) in sodium free buffer (Figure 4.5) in the presence of 4.1. For non-specific binding the competitor (pNPY or 4.1) was pre-incubated with cells for 15 min, before the radioligand was added.

A pK_d value of [³H]propionyl-pNPY in intact HEK293T hY₂R + β Arr2 cells using sodium containing buffer could not be determined, because no saturation was observed. This problem also occurred with CHO-hY₂-G_{iq5}-mtAEQ cells as described in the thesis of S. Dukorn.³³ The effect of sodium cations on ligand binding (allosteric modulation) has also been described by Dukorn et al.³⁴ and Kuhn et al.³² for the Y₄R. Beside the NPY receptors (Y₂R and Y₄R) this phenomenon has also been shown in literature for other GPCRs (e.g. μ OR,³⁵ A_{2A}R,³⁶ and β_1 AR³⁷). An explanation for the observed discrepancies of affinities in radioligand binding studies and potencies in functional assays of agonists could be the stabilization of the inactive receptor states by sodium cations (*cf.* Chapter 1).

Determination of pK_i values in equilibrium competition binding experiments with [³H]propionyl-pNPY

The determined affinity of pNPY (Table 4.3) in a radioligand binding assay by use of [³H]propionyl-pNPY and HEK293T hY₂R + βArr2 cells was in good agreement with affinity determined by S. Dukorn in her thesis (pK_i = 8.76).⁹ The affinity of pNPY decreased slightly compared to pK_i value of 9.07 determined in a radioligand binding assay using [¹²⁵I]PYY on COS-7 cells (transiently transfected with hY₂R).³⁸

Table 4.3. Y₂R affinities (pK_i) of pNPY and BIIE-0246 (**4.1**) determined in equilibrium competition binding experiments.

Compound	pK _i ± SEM ^a	Reference data pK _i
pNPY	8.43 ± 0.35	8.76 ^b
BIIE-0246 (4.1)	8.06 ± 0.11	7.44 ^c

^aRadioligand competition binding assay with [³H]propionyl-pNPY (C_{final} = 4.0 nM, K_d = 2.97 nM) in intact HEK293T hY₂R + βArr2 cells. Mean values ± SEM from at least two independent experiments, each performed in triplicate. ^bDukorn, Phd Thesis, University of Regensburg, 2017,³³ the K_i value was determined using [³H]propionyl-pNPY (C_{final} = 1.0 nM, K_d = 1.4 nM) and CHO-hY₂-G_{iq5}-mtAEQ cells. ^cDautzenberg,⁵ K_i value was determined using [¹²⁵I]PYY (C_{final} = 0.10 nM, K_d = 0.08 nM) and membranes from SMS-KAN cells. All reported K_i values were converted to pK_i values.

BIIE-0246 (**4.1**) showed the highest Y₂ receptor affinity (pK_i) of all investigated (S)-argininamides (**4.1**, **4.23**, **4.24**, **4.27**, **4.50**, **4.51**, **4.58** and **4.75**) (Table 4.1) in the radioligand competition binding assay in HEK293T hY₂ + βArr2 cells using [³H]propionyl-pNPY as radioligand (Figure 4.2, Table 4.1).

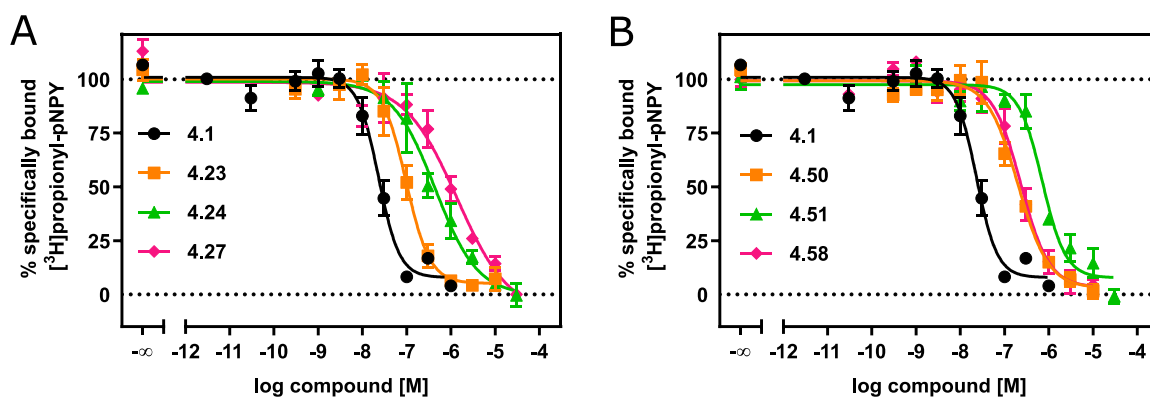


Figure 4.6. Displacement curves of [³H]propionyl-pNPY (C_{final} = 4 nM, K_d = 2.97 nM) obtained from competition binding studies with (A) **4.23**, **4.24**, **4.27**, (B) **4.50**, **4.51** and **4.58** and reference compound **4.1** in HEK293T hY₂R + βArr2 cells. Data are presented as means ± SEM from at least two independent experiments, each performed in triplicate.

The introduction of a methoxy substituted benzhydryl moiety (**4.23**, **4.24** and **4.27**), instead of the dibenzoazepinone moiety of **4.1** led to a slight decrease in affinity, whereas **4.23** showed the highest affinity within the substituted compound series. Enlargement of the substituent (amino-functionalization in **4.50** and **4.51**) led to a decrease in affinity compared to **4.23** and **4.24**. The substitution pattern of the 1-((2-methoxyphenyl)(phenyl)methyl)piperazine (**4.23**) and the 5-(2-(phenyl(piperazin-1-yl)methyl)phenoxy)pentan-1-amine (**4.50**) were favoured (Table 4.4) in comparison to **4.24** and **4.51**, respectively.

Remarkably, labelling of **4.50** with Py-5, resulting in the fluorescent ligand **4.58**, did not affect Y_2 affinity compared to **4.50**.

Replacement of the cyclopentyl moiety in **4.1** by a cyclohexyl moiety, leading to compound **4.75**, resulted in a decrease in Y_2R affinity by one order of magnitude (Table 4.4).

Table 4.4. Y_2R affinities (pK_i) of synthesized (S)-argininamids determined by equilibrium competition binding with [3H]propionyl-pNPY.

Compound	$pK_i \pm SEM^a$	N	Compound	$pK_i \pm SEM^a$	N
BIIE-0246 (4.1)	8.06 ± 0.11	2	4.50	7.06 ± 0.09	4
4.23	7.39 ± 0.13	3	4.51	6.46 ± 0.08	3
4.24	6.81 ± 0.23	3	4.58	7.03 ± 0.09	5
4.27	6.26 ± 0.03	3	4.75	7.03 ± 0.09	5

^aRadioligand competition binding assay with [3H]propionyl-pNPY ($c_{final} = 4.0$ nM, $K_d = 2.97$ nM) in intact HEK293T h Y_2R + β Arr2 cells. Mean values \pm SEM from at least N independent experiments, each performed in triplicate.

4.2.4.2. Determination of pK_b values in a β -arrestin2 recruitment assay

The β -arrestin2 recruitment assay was performed as described in the thesis of Felixberger³⁹ with minor modifications: β -arrestin2 recruitment was induced by 200 nM pNPY as described and luminescence was measured as a function of time in living HEK293T h Y_2R + β Arr2 cells instead of measuring luminescence after cell lysis. Despite the described modifications in the β -arrestin2 recruitment assay procedure, the potency ($pEC_{50} = 6.79 \pm 0.13$) of pNPY was in good agreement with the reported agonism ($pEC_{50} = 6.89$) in the thesis of Felixberger.³⁹ This functional assay was used for the characterization of standard Y_2R antagonists (BIIE-0246 (**4.1**), JNJ 31020028, CYM 9484, **4.5**) and synthesized derivatives **4.23**, **4.24**, **4.27**, **4.32**, **4.50**, **4.51**, **4.58**, **4.59**, **4.61**, **4.62** and **4.75** (Figure 4.6 and Table 4.3).

Prior to addition of the agonist pNPY, antagonists were pre-incubated with the cells for 15 min. The determined pK_b values of **4.1**, **4.23**, **4.24**, **4.27**, **4.50**, **4.51**, **4.58** and **4.75** deviate from the determined pK_i values by approximately of half an order of magnitude. An explanation for this discrepancy between pK_i and pK_b values could be the absence of sodium in the competition binding studies, but further investigation is required to answer this question, e.g. testing the set of compounds in different functional assays.

It is important to mention that the effect of sodium has been described for agonists (difference of affinity and agonism) in literature (cf 4.2.4.1.)^{34, 36}

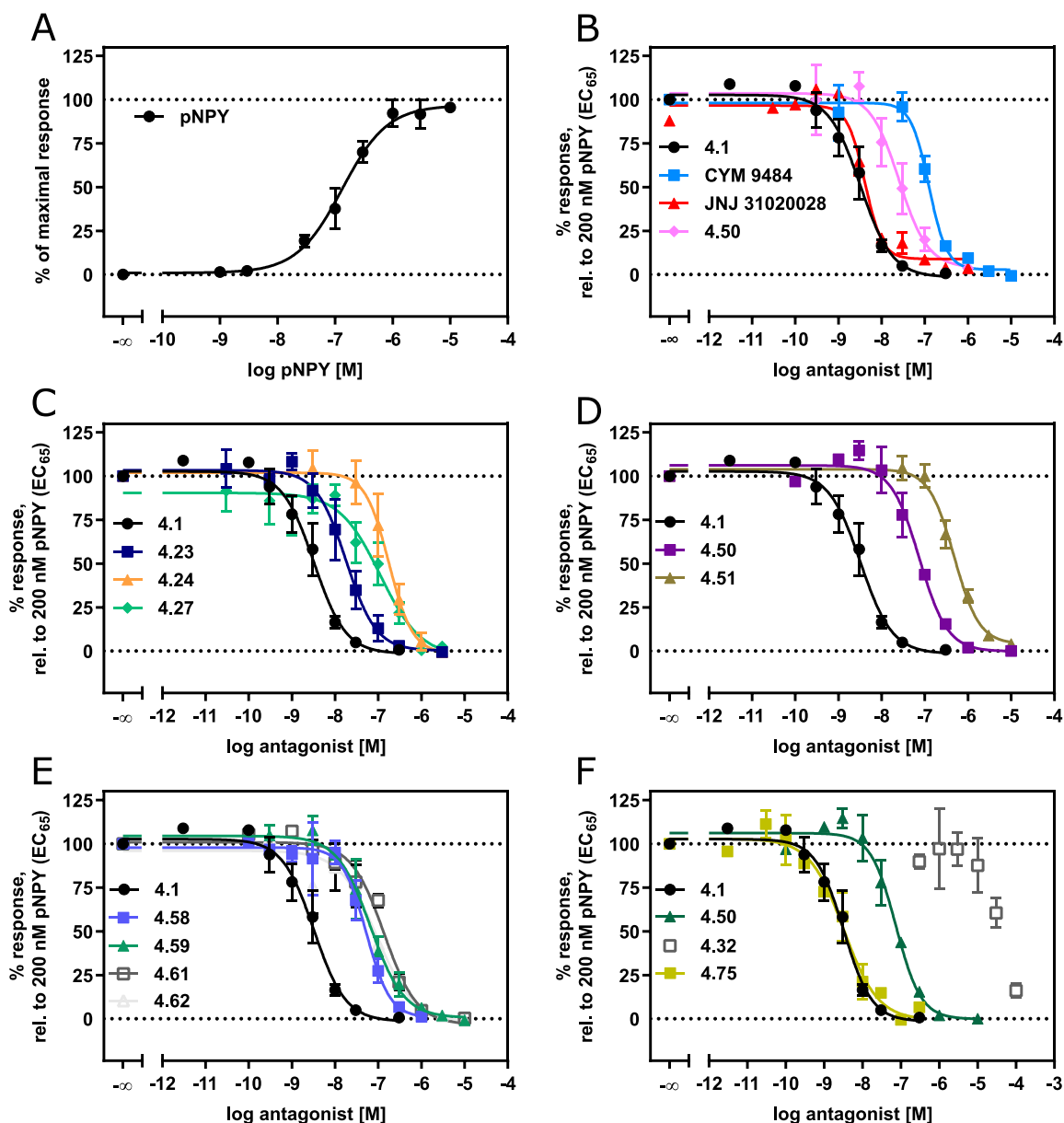


Figure 4.7. (A) β -Arrestin2 recruitment elicited by pNPY (agonist mode) and (B-F) Inhibition of β -arrestin2 recruitment (induced by 200 nM pNPY) by (B) **4.1**, **CYM 9484**, **JNJ 31020028**, **4.5**, (C) **4.1**, **4.23**, **4.24**, **4.27**, (D) **4.1**, **4.50**, **4.51**, (E) **4.1**, **4.58**, **4.59**, **4.61**, **4.62**, (F) **4.1**, **4.32**, **4.50** and **4.75** (antagonist mode). All experiments were performed in HEK293T hY₂R + β Arr2 cells. Cells were pre-incubated with the antagonists for 15 min. Data are presented as means \pm SEM from at least three independent experiments, each performed in triplicate.

The replacement of the dibenzoazepinone moiety in **4.1** by a benzhydryl moiety (**4.5**) led to a decrease in antagonism by one order of magnitude. Compound **4.32** ($pK_b < 5.00$), which bears neither a dibenzoazepinone nor a benzhydryl moiety showed no antagonism. The introduction of methoxy groups to **4.5**, resulting in compounds **4.24** (3-methoxy) and **4.27** (4-methoxy) also led to a decrease in antagonism, whereas **4.23**, representing the 1-((2-methoxyphenyl)(phenyl)methyl) derivative showed no decrease in antagonism. The introduction of 5-aminopentoxo groups in positions 2 (**4.50**) and 3 (**4.51**) led to a decrease of antagonism compared to **4.5**. Seemingly, position two in the benzhydryl moiety is favoured for further functionalisation. Fluorescently labelled ligands **4.58**, **4.59**, **4.61** and **4.62** showed comparable pK_b values, whereas **4.58** showed the highest antagonism. Interestingly the introduction of

bulkier moieties, e.g. fluorophores (Py-1 or Py-5) in position 2 (**4.58** and **4.61**) and 3 (**4.59** and **4.62**) in the benzhydryl moiety led to no decrease in antagonism compared to **4.50** and **4.51**. In consideration of the substitution pattern, the decrease in antagonistic activity was less pronounced for position 2 and 3 bearing bulky substituents such as fluorophores (**4.58** and **4.61**; **4.59** and **4.62**) is not as distinct as for the less bulky methoxy groups in position 2 and 3 (**4.23** and **4.24**).

Table 4.5. Activity (pK_b) of standard antagonists (**4.1**, JNJ 31020028, CYM 9484, **4.5**) and synthesized (S)-argininamides **4.23**, **4.24**, **4.27**, **4.32**, **4.50**, **4.51**, **4.58**, **4.59**, **4.61**, **4.62** and **4.75** determined in the β -arrestin2 recruitment assay in living HEK293T hY₂R + β Arr2 cells.

Compound	$pK_b \pm SEM^a$	Compound	$pK_b \pm SEM^a$
BIIE-0246 (4.1)	8.89 \pm 0.16	4.50	7.54 \pm 0.05
JNJ 31020028	8.51 \pm 0.16	4.51	6.74 \pm 0.09
CYM 9484	7.24 \pm 0.03	4.58	7.65 \pm 0.11
4.5	7.97 \pm 0.15	4.59	7.55 \pm 0.18
4.23	8.12 \pm 0.17	4.61	7.23 \pm 0.10
4.24	7.17 \pm 0.16	4.62	7.01 \pm 0.28
4.27	7.37 \pm 0.27	4.75	8.78 \pm 0.14
4.32	<5.00		

^a β -Arrestin2 recruitment assay in intact HEK293T hY₂R + β Arr2 cells. Arrestin2 recruitment was induced by 200 nM pNPY after pre-incubation of the cells with the antagonist for 15 min. Mean values \pm SEM from at least three independent experiments, each performed in triplicate

The replacement of the cyclopentyl moiety in **4.1** by a cyclohexyl moiety, resulting in **4.75**, had no impact on antagonism, whereas the replacement of the dibenzoazepinone moiety in **4.1** through a benzhydryl moiety (**4.5**) resulted in a decrease in antagonism by one order of magnitude.

4.2.4.3. Determination of pK_b values in a miniG protein recruitment assay

The miniG protein recruitment assay in living HEK293T NlucN-miniG_i/Y₂R-NlucC cells (established by Carina Höring as part of her doctoral studies) was used to functionally characterize selected (S)-argininamides **4.1**, **4.23**, **4.58** and **4.75** (Figure 4.8, Table 4.6). The agonist pNPY showed a potency ($pEC_{50} = 8.48 \pm 0.08$), that is in good agreement with affinity determined in radioligand binding assay (Table 4.3). For further characterization of **4.58** and its application in BRET based binding assay and by confocal microscopy, it was decided to investigate G-protein recruitment.

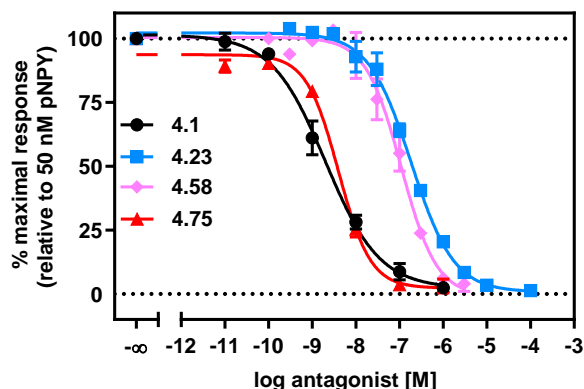


Figure 4.8. Inhibition of miniG protein recruitment (induced by 50 nM pNPY ($EC_{50} = 3.35$ nM)) by **4.1**, **4.23**, **4.58** and **4.75**. All experiments were performed in living HEK293T NlucN-miniGi/Y₂R-NlucC cells. Antagonists were pre-incubated with cells for 15 min. Data are presented as means \pm SEM from at least two independent experiments, each performed in triplicate.

The determined pK_b value of **4.58** is in good agreement with that from the β -arrestin2 recruitment assay ($pK_b = 7.65$, Table 4.5).

Table 4.6. Antagonism (pK_b) of selected (S)-argininamids (**4.1**, **4.23**, **4.58** and **4.75**) determined in the miniG protein recruitment assay at living HEK293T NlucN-miniGi/Y₂R-NlucC cells

compound	$pK_b \pm SEM^a$	N	compound	$pK_b \pm SEM^a$	N
BIIE-0246 (4.1)	9.88 ± 0.14	4	4.58	7.92 ± 0.03	3
4.23	8.06 ± 0.17	3	4.75	9.67 ± 0.22	2

^aMiniG_i recruitment was induced by 50 nM pNPY ($EC_{50} = 3.35$ nM) after pre-incubation of the cells with the antagonist for 15 min. Mean values \pm SEM from at least N independent experiments, each performed in triplicate.

4.2.4.4. Application of **4.58** to BRET based competition binding assays

The red-fluorescent (S)-argininamide-type hY₂R antagonist (**4.58**) was applied in BRET based saturation and competition binding experiments. The association and dissociation of **4.58** were studied in living HEK293T Y₂(intraNLucD197) cells. Moreover, the affinities (pK_i) of standard ligands in living HEK293T Y₂(intraNLucD197) cells (using sodium containing buffer) in 96-well plates were determined in the BRET based binding assay as an alternative to the determination of affinities (pK_i) in radiochemical assays. In principle, the fluorophore of **4.58** serves as a resonance energy acceptor and the luciferase (NanoLuc, NLuc) as a resonance energy donor.^{23, 40} The NLuc is located in the extracellular loop 2 (cloning and expression of this Y₂R construct (Y₂(intraNLucD197)) was performed by Lukas Grätz as part of his doctoral thesis). The location of the NLuc in the extracellular loop 2 is different to other published procedures for GPCR-Nluc fusion proteins, in which the luciferase is N-terminally tagged to the GPCR.⁴¹ For the determination of pK_i values in BRET based binding assays, no washing steps are required, in contrast to radioligand competition binding experiments. HEK293T Y₂(intraNLucD197) cells were also investigated in saturation binding experiments using the radioligand [³H]propionyl-pNPY in sodium-free binding buffer.

Determination of the pK_d value of **4.58** by saturation binding in HEK293T Y_2 (intraNLucD197) cells

The genetically engineered HEK293T Y_2 (intraNLucD197) cells were used to obtain the pK_d value of **4.58** in saturation binding experiments ($pK_d(\text{sat.}) = 7.75 \pm 0.03$). Unspecific binding was determined in the presence of a 100-fold excess of BIIE-0246 (**4.1**). The kinetics (association and dissociation) of **4.58** was also investigated to determine the kinetically derived K_d value ($K_d(\text{kinetic}) = 2.1 \pm 0.4$ nM). The $pK_d(\text{sat.})$ of **4.58** was in good agreement with pK_b value determined in the β -arrestin2 ($pK_b(\beta\text{Arr}2) = 7.65 \pm 0.11$) and miniG protein ($pK_b(\text{miniG}_i) = 7.92 \pm 0.03$) recruitment assays (Table 4.7), which were all performed in sodium containing buffer. The dissociation constant of **4.58** ($pK_i = 7.05 \pm 0.09$) determined using [^3H]propionyl-pNPY in competition binding experiments performed in sodium-free buffer, showed the highest discrepancy compared to the pK_d value determined in the BRET based binding assay (Figure 4.9 and Table 4.7).

Kinetics (association and dissociation) studies of **4.58** in HEK293T Y_2 (intraNLucD197) cells

Kinetic studies with **4.58** ($C_{\text{final}} = 20$ nM) in the BRET based assay revealed a relatively fast association ($k_{\text{obs}} [\text{min}^{-1}] = 0.09279 \pm 0.00996$, $k_{\text{on}} [\text{min}^{-1}] = 0.00420 \pm 0.00050$) of **4.58** to the Y_2 (intraNLucD197) receptor (Figure 4.9, B). For the determination of K_{obs} a monophasic association was assumed (fit: $B(t) = B_0 + (B_{\text{eq}} - B_0) \cdot (1 - e^{-(k_{\text{obs}} \cdot t)})$, non-linear regression, monophasic association, GraphPad Prism 8). This implies that the plateau was reached after 30 min (Figure 4.9, B, C). Therefore, the incubation time for saturation experiments was set to 35 min. By contrast, the incubation time for equilibrium competition binding experiments was set to 90 min. The incubation time for competition binding experiments was prolonged to guarantee that equilibrium conditions had been reached.

4.58 showed a slow dissociation ($K_{\text{off}} [\text{min}^{-1}] = 0.0087 \pm 0.0011$) from the Y_2 (intraNLucD197) receptor corresponding to a relatively high residence time (114 min). The dissociation was incomplete after 240 min ($B_{\text{plateau}} = 20\%$; Figure 4.9, D). Nevertheless, **4.58** could be used in competition binding experiments for the determination of equilibrium binding constants of small Y_2 R ligands. For the determination of K_{off} a monophasic decay was assumed (fit: $B(t) = (B_0 - B_{\text{plateau}}) \cdot e^{-K_{\text{off}} \cdot t} + B_{\text{plateau}}$, B_{plateau} was not constrained to zero, non-linear regression, one phase decay, GraphPad Prism 8). The kinetically derived pK_d was one order of magnitude higher compared to the pK_d value determined by saturation binding.

From the obtained kinetic data (dissociation) a pseudo irreversible binding of **4.58** might be concluded according to literature.^{6, 42} To confirm pseudo irreversible binding, the dissociation should be measured for a longer time period, but the measurable time is limited by the amount of substrate (furimazine) for the luciferase (NLuc).

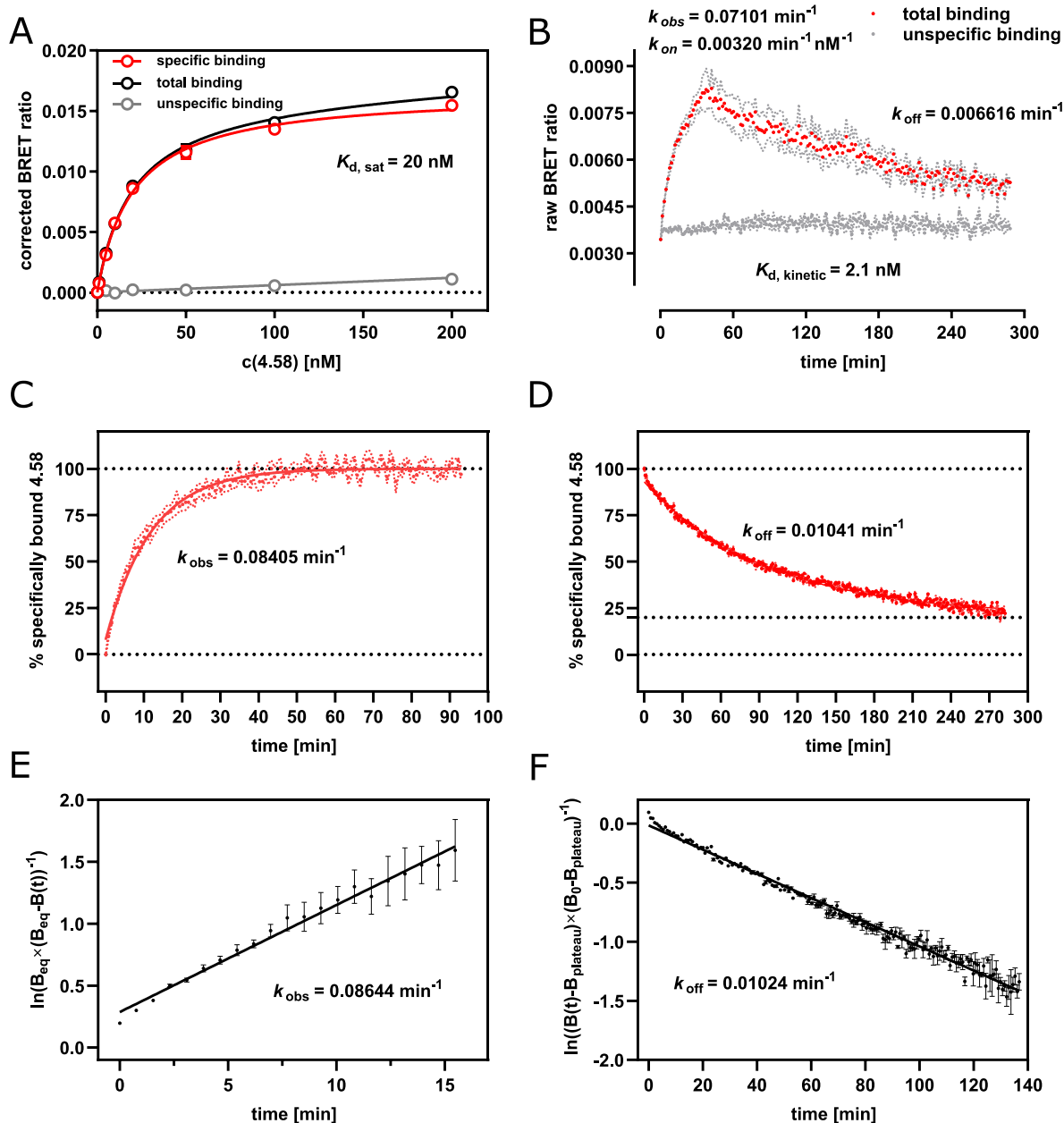


Figure 4.9. (A-F) Binding characteristics of **4.58** in BRET based binding assay in intact HEK293T Y₂(intraNLucD197) cells. (A) Representative saturation isotherm (red line) of specific hY₂R binding of **4.58**. Unspecific binding (grey line) was determined in the presence of a 100-fold excess of BIIE-0246 (**4.1**). The experiments were performed in triplicate. Error bars of specific binding were calculated according to the Gaussian law of error propagation. Error bars of total (black line), and nonspecific binding represent SEM. (B) Association of **4.58** ($c = 20 \text{ nM}$) for 32 min and dissociation for 240 min in the presence of BIIE-0246 (**4.1**) (100-fold) was performed in a single experiment. Exemplary determination of k_{obs} (0.07101 min^{-1}) and k_{off} ($0.006616 \text{ min}^{-1}$) (non-linear regression, one phase association or decay, GraphPad Prism 8). Association rate constant k_{on} ($0.00320 \text{ min}^{-1} \cdot \text{nM}^{-1}$) was derived from k_{obs} , k_{off} and ligand concentration ($k_{on} = (k_{obs} - k_{off}) \cdot [FL]^{-1}$). Raw BRET ratio as function of time. Errors of total binding (red dots) and unspecific binding (grey dots) represents SEM. Exemplary determination of kinetically derived dissociation rate constant ($K_{d, kinetic} = k_{off} \cdot k_{on}^{-1} = 2.1 \text{ nM}$). (C) Representative association for 90 min of **4.58** (% specifically bound **4.58**) and (D) dissociation for 270 min as function of time (min) for determination of k_{obs} (0.08405 min^{-1}) and k_{off} (0.01041 min^{-1}) (nonlinear regression, one phase association or dissociation; GraphPad Prism 8). Data represents SEM of a single experiment performed in triplicate. (E) Linearization of representative (C) association, $\ln(B_{eq} \times (B_{eq} - B(t))^{-1})$ versus time, slope $\cdot (-1) = k_{obs} = 0.08644 \text{ min}^{-1}$. Error bars were calculated according to the Gaussian law of error propagation. (F) Linearization of representative (D) dissociation, $\ln((B(t) - B_{plateau}) \times (B_0 - B_{plateau})^{-1})$ versus time, slope $= k_{off} = 0.01024 \text{ min}^{-1}$. Error bars of specific binding were calculated according to the Gaussian law of error propagation.

Table 4.7. Binding characteristics of **4.58**. Affinity (pK_i or pK_d) in radioligand competition binding experiments and BRET based binding assay and functional data of **4.58**. Binding kinetics (HEK293T Y₂(intraNLucD197) cells) of **4.58** in BRET based binding assay.

pK_i^a	$pK_b(\beta\text{Arr}2)^b$	$pK_b(\text{miniG}_i)^c$	$pK_{d(\text{sat})}^d$	k_{on}^e [min ⁻¹ ·nM]	k_{off}^f [min ⁻¹]	$K_d(\text{kinetic})^g$ [nM]	Residence time ^h [min]
7.05 ± 0.09	7.65 ± 0.11	7.92 ± 0.03	7.75 ± 0.03	0.00420 ± 0.00050	0.00874 ± 0.00112	2.1 ± 0.4	114

^aRadioligand competition binding assay with [³H]propionyl-pNPY ($C_{\text{final}} = 4.0$ nM, $K_d = 2.97$ nM) in intact HEK293T hY₂R + β Arr2 cells. Mean values ± SEM from at least three independent experiments, each performed in triplicate. ^b β -Arrestin2 recruitment assay in intact HEK293T hY₂R + β Arr2 cells. Arrestin2 recruitment was induced by 200 nM pNPY after pre-incubation of the cells with the antagonist for 15 min. Mean values ± SEM from at least three independent experiments, each performed in triplicate. ^cminiG Protein recruitment was induced by 50 nM pNPY after pre-incubation of the cells with the antagonist for 15 min. Mean values ± SEM from at least two independent experiments, each performed in triplicate. ^d $pK_{d(\text{sat})}$ value determined in BRET based assay by saturation binding in HEK293T Y₂(intraNLucD197) cells. Mean values ± SEM from at least three independent experiments, each performed in triplicate. ^eAssociation rate constant (k_{on}) was calculated from the observed association constant ($k_{\text{obs}} = 0.09279 \pm 0.00996$ min⁻¹). Mean values ± SEM from at least four independent experiments, each performed in triplicate, dissociation rate constant (k_{off}) and ligand concentration [FL] ($k_{\text{on}} = (k_{\text{obs}} - k_{\text{off}}) \cdot [\text{FL}]^{-1}$). $k_{\text{on}} \pm$ propagated error was calculated according to the Gaussian law of error propagation. ^fDissociation rate constant (k_{off}) derived from three independent experiments, each performed in triplicate. Mean values ± SEM from at least three independent experiments, each performed in triplicate. ^gKinetically derived dissociation rate constant ($K_d(\text{kinetic}) = k_{\text{off}} \cdot k_{\text{on}}^{-1}$) ± propagated error was calculated according to the Gaussian law of error propagation. ^hResidence time (K_{off}^{-1}).

For further investigation of the binding kinetics of **4.58** and evaluation of the association and dissociation rate constants determined in BRET based binding assays, a different method (e.g. flow cytometric based binding assay) should be used to assess binding kinetics of **4.58**. These experiments should be performed using cells expressing the native hY₂R.

Determination of pK_i values in equilibrium competition binding experiments with **4.58**

Equilibrium competition binding experiments were performed with structurally different hY₂R antagonists (BIIE-0246 (**4.1**), JNJ 31020028, CYM 9484, **4.5**; Figure 4.10). The determined affinities (pK_i) in BRET based binding assay (sodium-containing buffer) were in good agreement with the pK_b values determined in the β -arrestin2 recruitment assay (Table 4.8), whilst JNJ 31020028 showed the highest discrepancy among the investigated ligands. The pK_i values determined in intact HEK293T hY₂R + β Arr2 cells by use of the radioligand [³H]propionyl-pNPY showed a discrepancy compared to the pK_i values determined in the BRET based binding assay and the pK_b values determined in the β -arrestin2 recruitment assay. Further studies are needed to investigate potential absorption of the fluorescent ligand (**4.58**)/test compounds to the plastic material (plate surface). When comparing these data, it should be kept in mind, that a sodium-free binding buffer was used for the radioligand competition binding assay and a sodium-containing buffer for BRET based competition binding studies. As described in the thesis of S. Dukorn³³ the specific binding of the agonist [³H]propionyl-pNPY showed no saturation in sodium containing buffer in CHO-hY₂R-G_{q15}-mtAEQ cells and determined affinities in the radioligand binding assay were at least 10-fold higher compared to determined agonism of pNPY (with respect to K_i values).^{9, 33} The described discrepancy of ligand affinity (pK_i) in the presence or absence of sodium cations was also described for other GPCR's (e.g. hY₄R, adenosine receptor).^{34, 36} Although a low Y₂R

affinity of pNPY was anticipated due to the presence of sodium in the binding buffer, the determined affinity of pNPY in the BRET based binding assay was markedly lower ($pK_i < 6.00$) (Table 4.9). At the concentrations used, pNPY did not fully displace **4.58**. To shed light on the binding of pNPY in intact HEK293T Y₂(intraNLucD197) cells, saturation binding by use of [³H]propionyl-pNPY was performed (Figure 4.10). A high unspecific binding, which was determined in the presence of a 300-fold excess pNPY in intact HEK293T Y₂(intraNLucD197) cells in sodium-free binding buffer was observed. Due to high unspecific binding, the saturation binding experiment could not be evaluated. To obey the ALARA (as low as reasonable achievable) principle (*cf.* Recommendations of International Commission on Radiological Protection (ICRP): Publication 26⁴³ and 103⁴⁴) the amount of radioactivity in the assay was not increased.

The results from these studies suggested that binding of the large ligand pNPY to the Y₂(intraNLucD197) receptor is sterically hindered by the luciferase inserted in ECL2 of the receptor cells. Further investigations could focus on saturation binding experiments using a non-peptide radioligand (e.g. [³H]**4.2**). Unspecific binding may be reduced in saturation binding experiments using a small ligand with Y₂R affinity e.g. JNJ 31020028.

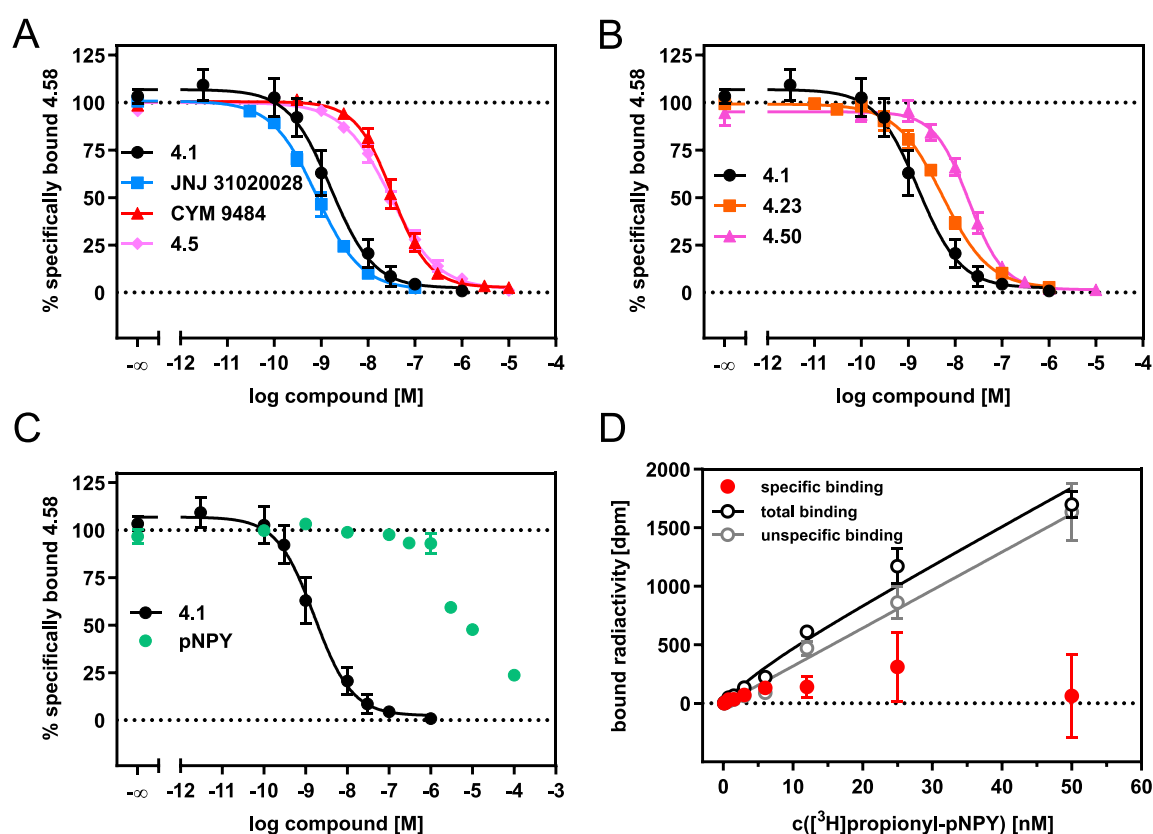


Figure 4.10. (A-C) Displacement curves of **4.58** ($C_{final} = 20$ nM, $K_d = 17.9$ nM) obtained from competition binding studies with (A) BIIE-0246 (**4.1**), JNJ 31020028, CYM 9484, **4.5**, (B) **4.1**, **4.23**, **4.50**, (C) **4.1** and pNPY in HEK293T Y₂(intraNLucD197) cells. Data are presented as means \pm SEM from at least three independent experiments, each performed in triplicate. (D) Representative saturation binding experiment of total hY₂R binding (black line) of [³H]propionyl-pNPY in HEK293T Y₂(intraNLucD197) cells. Unspecific binding (grey line) was determined in the presence of 300-fold excess of pNPY. Two independent experiments were performed in triplicate. Error bars of specific binding were calculated according to the Gaussian law of error propagation. Error bars of total (black symbols), and nonspecific binding (grey symbols) represent SEM.

It should be noted that **4.58** belongs to the class of (*S*)-argininamides (e.g. **4.1** and **4.2**), that have been reported to exhibit insurmountable Y₂R antagonism.^{6, 45} In addition, pNPY could not fully displace the radioligand **4.2** and a displacement of the radioligand in a biphasic manner was assumed.⁶ This described behaviour for pNPY was not observed in the BRET based binding assay.

Future investigations should focus on studying the binding kinetics of **4.58** in cells expressing the native hY₂R using a flow cytometric assay. Nevertheless, the affinity of small antagonists, not structurally related to **4.58**, can be determined in the BRET based binding assay.

Table 4.8. Affinities (pK_i) determined in radioligand competition binding (sodium-free buffer), BRET based (sodium-containing buffer) competition binding assays as well as agonism (pEC₅₀) of pNPY and antagonism (pK_b) in a β-arrestin2 recruitment assay of BIIE-0246 (**4.1**), JNJ 31020028, CYM 9484, **4.5**, **4.23** and **4.50**.

compound	pK _i (BRET) ± SEM ^a	pEC ₅₀ ± SEM ^b or pK _b (βArr2) ± SEM ^c	pK _i ± SEM ^d	Reference data (pK _i /pK _b)
pNPY	<6.00	6.79 ± 0.13	8.43 ± 0.35	8.76 ^e /n.a.
BIIE-0246 (4.1)	9.13 ± 0.15	8.89 ± 0.16	8.06 ± 0.11	7.44 ^f /7.82 ^g
JNJ 31020028	9.39 ± 0.14	8.51 ± 0.16	n.d.	7.53 ^e /8.04 ^h
CYM 9484	7.81 ± 0.11	7.24 ± 0.03	n.d.	7.62 ⁱ /n.a.
4.5	7.86 ± 0.10	7.97 ± 0.15	n.d.	8.18 ^j /7.65 ^k
4.23	8.60 ± 0.07	8.12 ± 0.17	7.39 ± 0.13	n.a.
4.50	8.03 ± 0.08	7.54 ± 0.05	7.06 ± 0.09	n.a.

^aBRET based binding assay with **4.58** (C_{final} = 20 nM, K_d = 17.9 nM) in intact HEK293T Y₂(intraNLucD197) cells. Mean values ± SEM from at least three independent experiments, each performed in triplicate. ^bβ-Arrestin2 recruitment of pNPY in intact HEK293T hY₂R + βArr2 cells. Mean values ± SEM from at least three independent experiments, each performed in triplicate. ^cβ-Arrestin2 recruitment assay in intact HEK293T hY₂R + βArr2 cells. Antagonism (pK_b) was determined in the presence of 200 nM pNPY after pre-incubation of the cells with the antagonist for 15 min. pK_b values are given in italics. Mean values ± SEM from at least three independent experiments, each performed in triplicate. ^dRadioligand competition binding assay with [³H]propionyl-pNPY (C_{final} = 4.0 nM, K_d = 2.97 nM) in intact HEK293T hY₂R + βArr2 cells. Mean values ± SEM from at least two independent experiments, each performed in triplicate. ^eDukorn, Phd Thesis, University of Regensburg, 2017,³³ the K_i values were determined using [³H]propionyl-pNPY (C_{final} = 1.0 nM, K_d = 1.4 nM) and CHO-hY₂-G_{q15}-mtAEQ cells. ^fDautzenberg,⁵ K_i value was determined using [¹²⁵I]PYY (C_{final} = 0.10 nM, K_d = 0.08 nM) and membranes from SMS-KAN cells. ^gPluym et al.,¹⁴ K_b value was determined in an aequorin assay in intact CHO-hY₄-G_{q15}-mtAEQ cells. Aequorin Ca²⁺ mobilization was induced by 70 nM pNPY, after pre-incubation of the cells with the antagonist for 1 h. ^hShoblock et al.,⁴⁶ the pK_b value was determined in a calcium mobilization assay in KAN-TS cells (stably expressing a chimeric G protein Gq15). Ca²⁺ was induced by 10 nM PYY (pEC₅₀ = 8.8). ⁱKuhn, Phd Thesis, University of Regensburg, 2017,⁴⁷ the reported K_i value was determined in a flow cytometric binding assay using Cy5-pNPY (C_{final} = 5 nM, K_d = 5.2 nM) and CHO-hY₂-G_{q15}-mtAEQ cells. ^jZiemek et al.,⁹ the reported K_i value was determined in a flow cytometric binding assay using Cy5-pNPY (C_{final} = 5 nM, K_d = 5.2 nM) and CHO-hY₂-G_{q15}-mtAEQ cells. ^kZiemek et al.,⁹ the reported IC₅₀ value was determined in an aequorin assay in intact CHO-hY₄-G_{q15}-mtAEQ cells. Aequorin Ca²⁺ mobilization was induced by 70 nM pNPY (EC₅₀ = 30.9), after pre-incubation of the cells with the antagonist for 1 h. The data was previously reported as IC₅₀ value and were reanalyzed to give pK_i value. Reported K_i values were converted to pK_i values. n.d. not determined. n.a. not applicable.

The Y₂R affinities of the synthesized (*S*)-argininamides **4.23** and **4.50** were in good agreement with data obtained from a β-arrestin2 recruitment assay. The affinities determined in the radioligand competition binding assay showed a discrepancy of around one order of magnitude compared to affinities

determined in a BRET binding assay. Moreover, the pK_i values determined in BRET based binding assay were in good agreement with pK_b values determined in a β-arrestin2 recruitment assay. This discrepancy was also observed for standard antagonists (Table 4.8).

Table 4.9. Affinities (pK_i) and potencies (pEC₅₀) of pNPY.

pK _i (BRET) ^a	pK _i (flow-cyto) ^b	pK _i (radioligand) ^c	pEC ₅₀ (βArr1) ^d	pEC ₅₀ (βArr2) ^e	pEC ₅₀ (Aequorin) ^f	pEC ₅₀ (miniG) ^g
< 6.00	8.92	8.43 ± 0.35	7.36	6.79	7.51	8.48 ± 0.08

^aBRET based binding assay with **4.58** (C_{final} = 20 nM, K_d = 17.9 nM) in intact HEK293T Y₂(intraNLucD197) cells. Mean values ± SEM from at least three independent experiments, each performed in triplicate. ^bK_i value reported from Schneider et al.⁴⁸ ^cRadioligand competition binding assay with [³H]propionyl-pNPY (C_{final} = 4.0 nM, K_d = 2.97 nM) in intact HEK293T hY₂R + βArr2 cells. Mean values ± SEM from at least two independent experiments, each performed in triplicate. ^{d, e}pEC₅₀ values reported by Felixberger, Phd Thesis, University of Regensburg, 2014.³⁹ ^fEC₅₀ value reported from Ziemek et al.⁹ ^gminiG Protein recruitment was induced by 50 nM pNPY after pre-incubation of the cells with the antagonist for 15 min. Mean values ± SEM from at least two independent experiments, each performed in triplicate. Reported K_i (or EC₅₀) values were converted to pK_i (or pEC₅₀) values.

4.2.4.5. Application of 4.58 to confocal microscopy

For visualization of hY₂R binding of **4.58** by confocal microscopy, a Nikon Eclipse 90i (Laser: λ_{ex} 488 nm; detector: 650 nm LP (Gain 1340)) was used. HEK293T hY₂R + βArr2 cells were seeded into cell culture dish (in 1 mL of Leibovitz's L-15 medium containing 5% FCS).

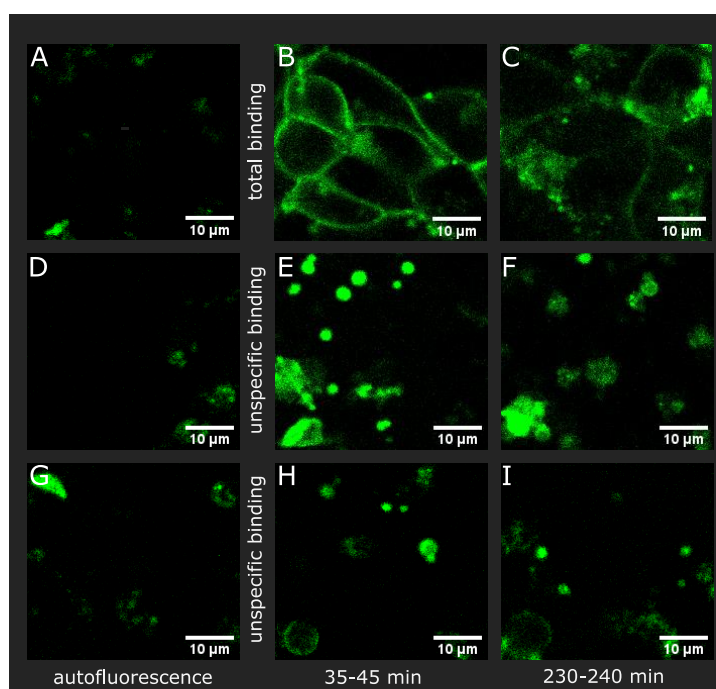


Figure 4.11. Binding of **4.58** in HEK293T hY₂R + βArr2 cells. (A, D, G) Autofluorescence and total binding of **4.58** (40 nM) after (B) 35 min and (C) 240 min. Unspecific binding was determined in the presence of a 250-fold excess of **4.1** (E, F) or pNPY (H, I) after 40 min (E), 45 min (H), 235 min (F) and 240 min (I). Cells were seeded in Leibovitz's L-15 medium containing 5% FCS. **4.1**, **4.58** and pNPY were diluted in Leibovitz's L-15 medium containing 1% BSA. Measurement details for all images: images were acquired with a Nikon eclipse 90i; water immersion objective: (Nikon NIR Apo, 60x1.0w); pinhole L; laser: λ_{ex} 488 nm; detector 650 nm LP (Gain 130).

Dilutions of **4.58** and competitors (**4.1** or pNPY) were prepared in Leibovitz's L-15 medium containing 1% BSA. Total binding of **4.58** was determined at a final concentration of 40 nM after incubation at rt for

35 min and 4 h. Unspecific binding was determined after simultaneously addition of a 12-fold concentrated solution of **4.58** ($C_{\text{final}} = 40 \text{ nM}$) and a 250-fold excess ($C_{\text{final}} = 10,000 \text{ nM}$) of **4.1** or pNPY after incubation at rt for 40-45 min and 235-240 min. There was a clear difference between total and non-specific binding using **4.1** or pNPY as competitor.

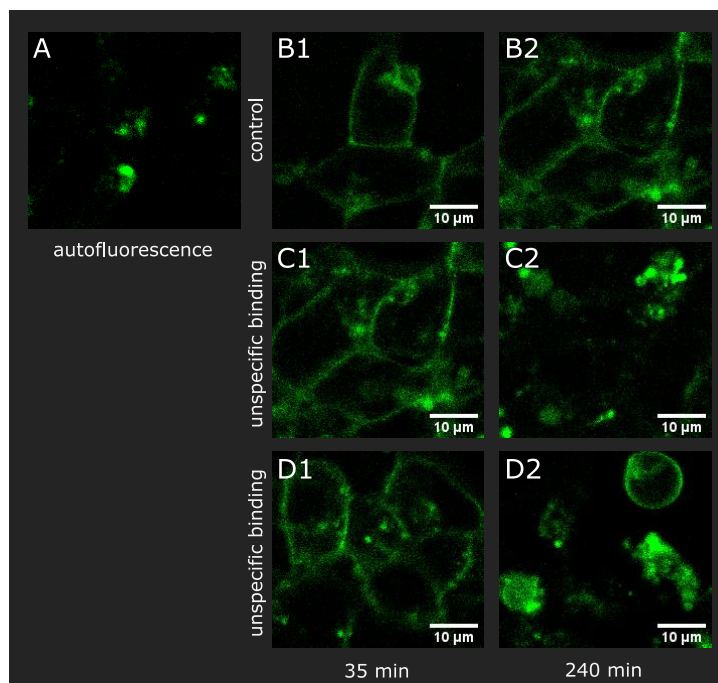


Figure 4.12. Binding of **4.58** in HEK293T hY₂R + β Arr2 cells. Autofluorescence (A) and total binding after 35 min (B1, C1, D1) and after 240 min (B2). Unspecific binding was determined in the presence of a 250-fold excess of **4.1** (C2) or pNPY (D2) after 240 min. The competitors were added after an incubation time of 35 min with the fluorescent ligand **4.58**. The cells were seeded in L-15 medium containing 5% FCS. **4.1**, **4.58** and pNPY were diluted in L-15 medium containing 1% BSA. Measurement details for all images: images were acquired with a Nikon eclipse 90i; water immersion objective: (Nikon NIR Apo, 60 \times 1.0w); pinhole L; laser: λ_{ex} 488 nm; detector 650 nm LP (Gain 130).

After incubation of the cells with **4.58** for 35 min, high fluorescence intensity at the plasma membrane was obvious (Figure 4.12; B1, C1, D1). In contrast to the procedure described above, the competitor (**4.1** or pNPY) was not added simultaneously with the fluorescent ligand **4.58**, after incubation of the cells with **4.58** for 35 min. A membrane localization of **4.58** was still visible after 240 min in the absence of competitor. When BIIE-0246 (**4.1**) was added, no membrane localization of **4.58** was observed (Figure 4.12; C2) after 240 min. Similarly, the use of pNPY as competitor resulted in no apparent membrane localization was obvious after 240 min.

In summary, the (S)-argininamide-type fluorescent Y₂R ligand **4.58** could be displaced by use of (S)-argininamide-type (**4.1**) and the peptidic ligand (pNPY) as competitors (**4.1** or pNPY) in intact HEK293T hY₂R + β Arr2 cells. There was no difference between adding **4.58** and the competitor simultaneously or addition of the competitor after pre-incubation of the cells with **4.58** for 35 min.

4.2.4.6. NPY Y₂R subtype selectivity

(S)-Argininamide **4.1** has been described as a highly selective hY₂R antagonist in literature.²² For this reason subtype selectivity was investigated for the amino precursors **4.50**, **4.51** and the fluorescent

ligand **4.58** (Table 4.10). The dibenzoazepinone-benzhydryl approach did not affect subtype selectivity in case of investigated compounds **4.50**, **4.51** and **4.58**.

Table 4.10. NPY receptor subtype binding profile of (S)-argininamides **4.50**, **4.51** and **4.58**.

Compound	hY ₁ R pK _i ^a	hY ₂ R pK _i ± SEM ^b	hY ₄ R pK _i ^c	hY ₅ R pK _i ^d
4.50	<5.52	7.54 ± 0.05	<5.00	<6.00
4.51	<5.52	6.74 ± 0.09	<5.00	<5.52
4.58	<5.00	7.65 ± 0.11	<5.00	<5.52

^aRadioligand competition binding assay using [³H]**2.2** (C_{final} = 0.15 nM, K_d = 0.044 nM) in intact SK-N-MC cells.¹⁶ ^bRadioligand competition binding assay with [³H]propionyl-pNPY (C_{final} = 4.0 nM, K_d = 2.97 nM) in intact HEK293T hY₂R + βArr2 cells. Mean values ± SEM from at least three independent experiments performed, each in triplicate. ^cRadioligand competition binding assay with [³H]UR-KK200 (C_{final} = 1.0 nM, K_d = 0.67 nM) in intact CHO-hY₄R-G_{q15}-mtAEQ.³² ^dRadioligand competition binding assay using [³H]propionyl-pNPY (C_{final} = 4.0 nM, K_d = 4.8 nM) in intact HEC-1B-hY₅ cells.^{16, 49} Results from 2-3 independent experiments, each performed in triplicate (hY₁R, hY₄R and hY₅R).

4.3. Conclusion

A small library of compounds was synthesized and pharmacologically characterized. The dibenzoazepinone moiety (**4.1**) was replaced by a methoxy substituted benzhydryl moiety (**4.23**, **4.24** and **4.27**) This small SAR study revealed that positions 2 and 3 are suitable for amino-functionalization and led to the synthesis of amino precursors **4.50** (position 2) and **4.51** (position 3). Moreover, this established labelling approach II (Figure 4.1) showed that precursors **4.50** and **4.51** can be used for fluorescence labelling and this approach did not affect subtype selectivity.

The fluorescently labelled (S)-argininamide-type selective Y₂R antagonist UR-jb264 (**4.58**) showed Y₂R binding and Y₂R antagonistic activity in the nanomolar range. The application of **4.58** in BRET based binding assays (saturation and competition binding, association and dissociation studies) as well as confocal microscopy demonstrated that **4.58** can be used as a molecular tool, e.g. to determine Y₂R affinities of non-labelled ligands. It should be stressed that the BRET based binding assay using **4.58** enables the determination of Y₂R affinities of (small) Y₂R ligands in sodium-containing buffer, which is not possible in competition binding experiments with [³H]propionyl-pNPY or Cy5-pNPY due to the low Y₂R affinity of peptidic agonists in sodium-containing buffers.

In future studies, **4.58** should also be investigated in flow cytometric Y₂R binding experiments using cells with native hY₂R, including competition with pNPY, and these data should be compared with the data obtained from the BRET based binding assays. Moreover, the amine precursors **4.50** and **4.51** can be used for the synthesis of additional fluorescent Y₂R ligands bearing fluorophores with distinct optical properties. Fluorescent labelled compounds **4.59**, **4.61** and **4.62** should be investigated in the BRET based binding assay. These ligands (**4.59**, **4.61** and **4.62**) were not investigated in a BRET based binding assay due to a lack of time, because affinities had not been determined in radioligand binding assay, but also because an appropriate hY₂R binding assay was not available at that time. Moreover, the amount of the radioligand ([³H]propionyl-pNPY) was limited.

4.4. Experimental section

4.4.1. General experimental conditions

The following reagents and solvents (analytical grade) were purchased from commercial suppliers and used without further purification: CH₂Cl₂, DMF, THF, MeOH, toluene, DMSO, ethanol, methanesulfonyl chloride (Fisher Scientific, Schwerte, Germany); EDC·HCl, HOBt, hydrazine monohydrate, piperidine, piperazine, TFA, CBr₄, acetic acid, pyridine-sulfur trioxide complex, H₂SO₄, PPh₃, **4.6**, **4.8**, **4.14**, **4.25**, **4.63**, **4.68**, **4.70** (Sigma Aldrich, Taufkirchen, Germany); ethyl allophanate, Boc₂O, PCC, **4.33**, **4.76**, **4.77** (TCI, Eschborn, Germany); DIPEA, (ABCR, Karlsruhe, Germany); p-xylene, dioxane, NaH, Mg, SOCl₂, Et₃N, NaBH₄, K₂CO₃, aqueous HBr (47%), NaN₃, NH₄CH₃CO₂, Na, **4.17**, **4.18**, **4.17**, **4.18** (Merck, Darmstadt, Germany); **4.11** (Carbolution Chemicals, St. Ingbert, Germany); conc. HCl (VWR Chemicals, Darmstadt, Germany); ammonium hydroxide (Carl Roth, Karlsruhe, Germany). For pharmacological characterization, pNPY (Synpeptide, Shanghai, China), CYM 9484 (Tocris, Bristol, United Kingdom) and JNJ 31020028 (Biomol, Hamburg, Germany) were purchased from commercial suppliers.

Compounds **2.77**^{24, 25} and **4.60**^{24, 25} were synthesized as described previously in the literature.

Column chromatography was performed using Merck Geduran 60 silica gel (0.063-0.200 mm) or Merck flash silica gel 60 (0.040-0.063 mm). For thin layer chromatography, TLC sheets ALUGRAM Xtra SIL G/UV254 from Macherey-Nagel GmbH & Co. KG (Düren, Germany) were used. Compounds were detected by irradiation with UV light (254 nm or 366 nm), and staining was performed with ninhydrin or iodine.

Acetonitrile (HPLC grade), used for HPLC, was purchased from Sigma-Aldrich. Millipore water was used for eluents for analytical and preparative HPLC. Compounds **4.23**, **4.24**, **4.27**, **4.50**, **4.51** and **4.75** were purified by a preparative HPLC-system from Knauer (Berlin, Germany) consisting of two pumps K-1800 and a detector K-2001 (HPLC A). A Kinetex XB C18, 5 µm, 250 x 21 mm (Phenomenex, Aschaffenburg, Germany) served as RP-column at a flow rate of 18 mL/min. Compounds **4.32**, **4.58**, **4.59**, **4.61** and **4.62** were purified by a preparative HPLC-system from Waters (Eschborn, Germany) consisting of a Binary Gradient Module (Waters 2545), a detector (Waters 2489 UV/visible Detector), a manual injector (Waters Prep inject) and a collector (Waters Fraction Collector III) (HPLC B). A Kinetex XB C18, 5 µm, 250 x 21 mm (Phenomenex) served as RP-column at a flow rate of 20 mL/min. All injected solutions were filtered with syringe filters (0.45 µm). The mobile phase contained the solvents A (0.1% aq TFA) and B (acetonitrile). The detection wavelength was 220 nm. The eluates, containing isolated compounds, were lyophilized using a Christ alpha 2-4 LD (Martin Christ Gefriertrocknungsanlagen, Osterode am Harz, Germany) or a Scanvac CoolSafe 100-9 (Labogene, Allerød, Denmark) lyophilization apparatus equipped with a Vacuubrand RZ rotary vane vacuum pump (Vacuubrand, Wertheim, Germany).

The purity of compounds **4.1**, **4.5**, **4.23**, **4.24**, **4.27**, **4.50**, **4.51**, **4.58**, **4.59**, **4.61**, **4.62** and **4.75** was determined by analytical HPLC (RP-HPLC) with a 1100 series system from Agilent Technologies (Santa Clara, CA USA) composed of a Degasser (G1379A), a Binary Pump (G1312A), a Diode Array Detector (G1315A), a thermostated Column Compartment (G1316A) and an Autosampler (G1329A). A Phenomenex Kinetex 5u XB-C18 100A, 250 x 4.6 mm was used as stationary phase. The flow rate was

1 mL/min, the detection wavelength was set to 220 nm, the oven temperature was set to 30 °C and the injection volume was 50 µL. Mixtures of solvents A (0.1% aq TFA) and B (acetonitrile) were used as mobile phase. The following gradient was applied: 0-25 min, A/B 90:10–5:95; 25-35 min, 5:95.

Microwave reactions were carried out on a Biotage Initiator 2.0 microwave device (Biotage, Uppsala, Sweden) using pressure stable sealed 10-20 mL vessels.

Deuterated solvents for NMR spectroscopy (DMSO-*d*₆, MeOD, CDCl₃) were obtained from Deutero (Kastellaun, Germany) in ampoules (1 mL). NMR spectra were recorded on a Bruker Avance 300 (¹H, 300 MHz; ¹³C, 75 MHz), a Bruker Avance III 400 (¹H, 400 MHz; ¹³C, 101 MHz) and a Bruker Avance 600 with cryogenic probe (¹H, 600 MHz; ¹³C, 150 MHz) (Bruker, Karlsruhe, Germany). Chemical shifts are given in ppm and were referenced to the solvent residual peak (DMSO-*d*₆, at 2.50 ppm (¹H-NMR) and at 39.52 ppm (¹³C-NMR); CDCl₃, at 7.26 ppm (¹H-NMR) and at 77.16 ppm (¹³C-NMR); CD₃OD, at 3.31 ppm (¹H-NMR) and at 49.00 ppm (¹³C-NMR)).⁵⁰ The coupling constants (*J*) are given in Hertz (Hz). The splitting of the signals is described as follows: s = singlet, bs = broad singlet, d = doublet, t = triplet, q = quartet, m = multiplet.

Mass spectrometry (HRMS) analysis was performed either on an Agilent 6540 UHD Accurate-Mass Q-TOF LC/MS system (Agilent Technologies) using an electrospray source (ESI) or on an Agilent GC7890A GC/MS system (Agilent Technologies) using an atmospheric pressure chemical ionization (APCI) source.

Elemental analysis was performed on a Vario micro cube (Elementar, Langenselbold, Germany).

Stock solutions were prepared in DMSO at concentrations of 1 mM (**4.58**, **4.59**, **4.60** and **4.61**) or 10 mM.

4.4.2. Synthesis protocols and analytical data

Annotation concerning the analytical data (NMR, HPLC) of **4.23**, **4.24**, **4.27** and **4.50**: due to the synthesis routes, these compounds were obtained as diastereomers, which are evident in the ¹H- and ¹³C-spectra (recorded in DMSO-*d*₆ or MeOH-*d*₄), but not in the RP-HPLC chromatograms.

General synthesis procedures

General procedure A for the synthesis of methoxy substituted benzhydryl alcohols **4.19** and **4.20**. A solution of bromobenzene in anhydrous THF (75 mL) was prepared (solution A). To a dry flask, containing magnesium (Mg) under an argon atmosphere THF (50 mL) was added. 5-10 mL of solution A were added dropwise to afford phenylmagnesium bromide (Grignard reagent). If it is necessary, the reaction is activated by addition of iodine or bromine. Then, the remaining solution A was added dropwise into the reaction mixture that should boiling slightly (if necessary, the reaction mixture must be cooled in an ice bath). The reaction mixture was gently heated in a water bath (30 min) until the Mg was completely consumed. After that the organometallic solution was cooled by means of an ice bath. Under stirring, a solution of 2-methoxybenzaldehyde (**4.17**) or 3-methoxybenzaldehyde (**4.18**) in dry THF (20 mL) was added dropwise into the reaction mixture. The reaction mixture was allowed to warm to rt and stirred for 2 h. Then, a mixture of water and ice (50 mL) was added and a precipitate was formed followed by careful addition of diluted HCl (conc. HCl/water 1:1) until the solid was dissolved. The product was extracted from the aqueous phase with ethyl acetate (3x 100 mL), the combined organic

layers were dried with brine and Na₂SO₄ and the solvent was evaporated. The crude product was purified by column chromatography.

General procedure B for the synthesis of 1-((2-methoxyphenyl)(phenyl)methyl)piperazine (**4.22**) and 1-((3-methoxyphenyl)(phenyl)methyl)piperazine (**4.23**). 2-Methoxy(phenyl)(phenyl)methanol (**4.19**) or 3-methoxyphenyl(phenyl)methanol (**4.20**) was dissolved in CH₂Cl₂ (15 mL). Then, sulfuryl chloride was added and the reaction mixture was refluxed for 30 min. The solvent was evaporated, and the residue was dissolved in acetonitrile (10 mL) and piperazine was added followed by heating in a microwave device (100 °C, 30 min). The solvent was evaporated, and the crude product was purified by column chromatography.

General procedure C for the synthesis of phenols **4.42**, **4.43** and **4.52** by cleavage of methyl ethers. (4-Hydroxyphenyl)(phenyl)methanone (**4.25**), (2-hydroxyphenyl)(phenyl)methanone (**4.40**) or (3-hydroxyphenyl)(phenyl)methanone (**4.41**) was dissolved in aqueous HBr (47%, 15 mL) and acetic acid was added until the starting material was completely dissolved. The reaction mixture was refluxed overnight. Then, the reaction mixture was allowed to cool to rt and was carefully poured into water (250 mL). The product was extracted from the aqueous phase with ethyl acetate (3x 150 mL), the combined organic phases were dried over Na₂SO₄. The organic solvent was evaporated, and light petroleum was added and evaporated (3x). The product was dried *in vacuo* and used without further purification.

General procedure D for the synthesis of ethers **4.44**, **4.45** and **4.53**. Compound **4.42**, **4.43** or **4.52** was dissolved in DMF (5 mL) and potassium carbonate was added, and the reaction mixture was stirred at rt for 5 min. Under stirring, *tert*-butyl (5-bromopentyl)carbamate (**4.35**) was added and the reaction mixture was stirred at rt for 24 h. Then, the reaction mixture was poured into water (200 mL) and the product was extracted from the aqueous phase with ethyl acetate (3x 100 mL). The combined organic phases were dried over Na₂SO₄ and the organic solvent was evaporated. The crude product was purified by column chromatography.

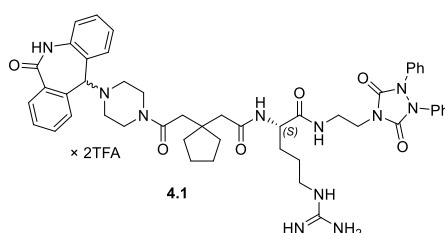
General procedure E for the synthesis of benzhydryl alcohols **4.46**, **4.47** and **4.54**. Compound **4.44**, **4.45** or **4.53** was dissolved in methanol (5-20 mL) and sodium borohydride was added portionwise. After 2-4 h the solvent was evaporated, and the crude product was purified by column chromatography.

General procedure F for the synthesis of amines **4.48**, **4.49** and **4.55**. Compound **4.46**, **4.47** or **4.55** and Et₃N were dissolved in CH₂Cl₂ (6-10 mL) and the reaction mixture was stirred in an ice bath. Under stirring, methanesulfonyl chloride was slowly added to the mixture and the reaction mixture was stirred for 3-5 hours. Then, NaOH (1 N) was added to the reaction mixture and the product was extracted from the aqueous phase with CH₂Cl₂ (3x). The combined organic phases were dried over Na₂SO₄ and the organic solvent was evaporated. Then, the residue was dissolved in acetonitrile (10 mL) and piperazine was added and the reaction mixture was heated in a microwave device (70 °C, 45 min). The solvent was evaporated, and the crude product was purified by column chromatography.

General procedure G for amide bond formation of compounds **4.1**, **4.5**, **4.23**, **4.24**, **4.32**, **4.50**, **4.51** and **4.75**. The carboxylic acid was dissolved in DMF (100 µL). EDC·HCl and HOBt were added and the reaction mixture was stirred for 5 min. Then, the reaction mixture is poured into a solution of the

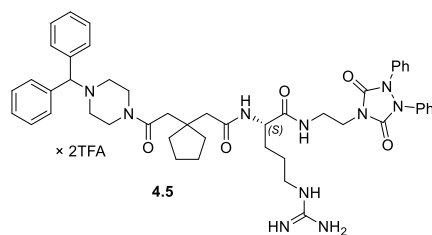
secondary or primary amine in DMF (100 μ L) and stirred at rt overnight. The reaction mixture was poured into an aqueous solution (5% acetonitrile, 0.1% TFA; 100 mL). After lyophilization, the crude product was dissolved in a mixture of TFA and water (95:5; 5 mL) and stirred at rt overnight. Then, the reaction mixture is carefully poured into an aqueous solution (5% acetonitrile, 0.1% TFA; 100 mL). After lyophilization, the crude product was purified by preparative HPLC.

General procedure H for the synthesis of fluorescent ligands **4.58**, **4.59**, **4.61** and **4.62**. Amino precursor **4.50** or **4.51** was dissolved in DMF (50-100 μ L) in a propylene micro tube (1.5 mL, Nümbrecht, Sarstedt) and DIPEA was added. The fluorescent dye (**2.77** or **4.60**) was added as a solid and the reaction mixture was shaken in the dark at rt for 3-5 h. The crude product was purified by preparative HPLC.

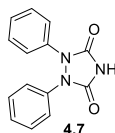


(2S)-N^c-[2-(1-{2-Oxo-2-[4(6-oxo-6,11-dihydro-5H-dibenzo[b,e]azepin-11-yl)piperazin-1-yl]ethyl}-cyclopentyl)acetyl]-[2-(3,5-dioxo-1,2-diphenyl-1,2,4-triazolidin-4-yl)ethyl]argininamide

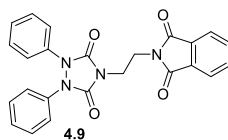
bis(hydrotrifluoroacetate) (4.1).⁸ Compound **4.1** was prepared using *general procedure G* and the reactants (S)-2-(1-(2-((1-((2-(3,5-Dioxo-1,2-diphenyl-1,2,4-triazolidin-4-yl)ethyl)amino)-1-oxo-5-(2-((2,2,4,6,7-pentamethyl-2,3-dihydrobenzofuran-5-yl)sulfonyl)guanidino)pentan-2-yl)amino)-2-oxoethyl)cyclopentyl)acetic acid (**4.15**) (180 mg, 206 μ mol), EDC·HCl (50 mg, 261 μ mol), HOBt (30 mg, 222 μ mol) and 11-(piperazin-1-yl)-5,11-dihydro-6H-dibenzo[b,e]azepin-6-one (**4.67**) (50 mg, 170 μ mol). Purification by preparative HPLC A (gradient: 0-30 min, A/B 84:16–38:62, t_R = 18 min) gave **4.1** as a fluffy white solid (35 mg, 31 μ mol, 18%). **¹H-NMR** (600 MHz, DMSO-*d*₆): δ (ppm) 1.30-1.69 (m, 13H), 2.00-2.14 (m, 3H), 2.18-2.24 (m, 1H), 2.27-2.33 (m, 1H), 2.38-2.45 (m, 1H), 2.47-2.49 (m, 1H, interfering with solvent residual peak), 2.94-3.05 (m, 2H), 3.18-3.44 (m, 6H), 3.59 (t, J = 6.1 Hz, 2H), 4.11-4.18 (m, 1H), 4.29 (br s, 1H), 6.77-7.44 (m, 21H), 7.46-7.54 (m, 1H), 7.62 (t, J = 5.6 Hz, 1H), 7.74 (d, J = 7.3 Hz, 1H), 7.97 (d, J = 8.0 Hz, 1H), 8.23 (t, J = 5.8 Hz, 1H), 10.35 (s, 1H). **¹³C-NMR** (150 MHz, DMSO-*d*₆): δ (ppm), 23.31, 23.27, 25.1, 28.8, 36.2, 37.3, 37.33, 37.36, 38.4, 39.6 (overlaid by solvent residual peak), 40.4, 40.7, 42.9, 44.06, 44.07, 45.4, 50.8, 51.3, 51.9, 73.7, 116.2 (q, J = 294.0 Hz) (TFA), 121.4, 122.6, 123.8, 126.7 (two carbon signals), 127.8, 128.1, 128.5, 129.0 (2 carb.), 130.0, 130.6, 131.5, 131.6, 136.2, 136.6, 152.6, 156.8, 158.5 (q, J = 34.5 Hz) (TFA), 168.0, 170.0, 171.3, 172.0. **RP-HPLC** (220 nm): 98% (t_R = 15.5 min, k = 5.0). **HRMS** (ESI): m/z [M+H]⁺ calcd. for [C₄₉H₅₈N₁₁O₆]⁺ 896.4566, found 896.4582. C₄₉H₅₇N₁₁O₆ × C₄H₂F₆O₄ (896.07 + 228.04).



(2S)-N^r-(2-{1-[2-(4-Benzhydrylpiperazin-1-yl)-2-oxoethyl]cyclopentyl}acetyl)[2-(3,5-dioxo-1,2-diphenyl-1,2,4-triazolidin-4-yl)ethyl]argininamide bis(hydrotrifluoroacetate) (4.5).⁸ Compound **4.5** was prepared using *general procedure G* and the reactants (S)-2-(1-(2-((1-((2-(3,5-dioxo-1,2-diphenyl-1,2,4-triazolidin-4-yl)ethyl)amino)-1-oxo-5-(2-((2,2,4,6,7-pentamethyl-2,3-dihydrobenzofuran-5-yl)sulfonyl)guanidino)-pentan-2-yl)amino)-2-oxoethyl)cyclopentyl)acetic acid (**4.15**) (123 mg, 141 μmol), EDC·HCl (33 mg, 172 μmol), HOBT (21 mg, 155 μmol), and 1-benzhydrylpiperazine (**4.30**) (41 mg, 162 μmol). Purification by preparative HPLC B (gradient: 0-30 min, A/B 65:35–47:53, *t_R* = 8 min) gave **4.5** as a fluffy white solid (18 mg, 16.6 μmol, 12%). **¹H-NMR** (600 MHz, DMSO-*d*₆): δ (ppm) 1.33-1.67 (m, 13H), 2.20-2.25 (m, 1H), 2.31-2.37 (m, 1H), 2.43-2.48 (m, 1H, interfering with solvent residual peak), 2.54-2.60 (m, 1H, interfering with solvent residual peak), 2.63-3.26 (m, 5H), 3.27-3.35 (m, 1H), 3.36-3.41 (m, 1H), 3.43-3.68 (m, 6H, interfering with the water signal), 4.11-4.19 (m, 1H), 5.49 (br s, 1H), 6.49-7.74 (m, 26H), 7.97 (d, *J* = 7.4 Hz, 1H), 8.22 (t, *J* = 5.7 Hz, 1H). **¹³C-NMR** (600 MHz, DMSO-*d*₆): δ (ppm) 23.3, 25.1, 28.8, 36.2, 37.3, 37.4, 38.5, 39.6 (overlaid by solvent residual peak), 40.4, 42.7, 44.0, 51.2, 51.6, 51.9, 114.5, 116.0 (TFA), 118.0 (TFA), 118.2, 122.6, 126.7, 127.7, 129.0, 136.5, 152.6, 156.8, 158.2 (TFA), 158.4 (TFA), 170.1, 171.3, 172.0. One carbon signal was not apparent (Ph₂CH-). **RP-HPLC** (220 nm): 99% (*t_R* = 14.0 min, *k* = 4.5). **HRMS** (ESI): *m/z* [M+H]⁺ calcd. for [C₄₈H₅₉N₁₀O₅]⁺ 855.4664, found 855.4673. C₄₈H₅₈N₁₀O₅ × C₄H₂F₆O₄ (855.06 + 228.04).

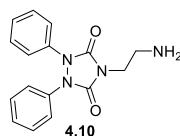


1,2-Diphenyl-1,2,4-triazolidine-3,5-dione (4.7).⁸ 1,2-Diphenylhydrazine (**4.6**) (2.02 g, 11 mmol) and ethyl allophanate (1.45 g, 11 mmol) were dissolved in *p*-xylene (35 mL) and the mixture was refluxed overnight. The reaction mixture was allowed to cool to rt and light petroleum (30 mL) was added. The solid was separated by filtration, washed two times with light petroleum (2x 30 mL) and dissolved in acetone. Insoluble components were filtered off and water was added (200 mL) leading to the formation of a precipitate, which was separated by filtration, washed with water (2x) and dried *in vacuo*. Compound **4.7** was obtained as a pale white solid (1.12 g, 4.4 mmol, 40%). **Anal. calcd.** for C₁₄H₁₁N₃O₂: C 66.40, H 4.38, N 16.59, found: C 66.23, H 4.56, N 16.76. **¹H-NMR** (300 MHz, DMSO-*d*₆): δ (ppm) 7.17-7.26 (m, 2H), 7.33-7.40 (m, 8H), 12.08 (br s, 1H). **¹³C-NMR** (75 MHz, DMSO-*d*₆): δ (ppm) 122.4, 126.5, 129.1, 136.7, 153.1. **HRMS** (ESI): *m/z* [M+H]⁺ calcd. for [C₁₄H₁₂N₃O₂]⁺ 254.0924, found 254.0927. C₁₄H₁₁N₃O₂ (253.26).

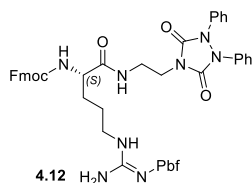


4-(2-Phthalimidoethyl)-1,2-diphenyl-1,2,4-triazolidine-3,5-dione (4.9).⁸ 1,2-Diphenyl-1,2,4-triazolidine-3,5-dione (**4.7**) (4.03 g, 15.9 mmol) was dissolved in DMF (100 mL) and the mixture was cooled in an ice bath. Under stirring, sodium hydride (0.71 g, 17.8 mmol, 60%, dispersion in mineral oil) was added portionwise. Then, 2-(2-bromoethyl)isoindoline-1,3-dione (**4.8**) (4.57 g, 18.0 mmol) was added to the reaction mixture. After the reaction mixture was refluxed for 5 h, the organic solvent was evaporated *in vacuo* (80 °C) and a saturated solution of K₂CO₃ (300 mL) was added. The precipitated solid was separated by filtration and dried *in vacuo*. Compound **4.9** was obtained after recrystallization from 2-propanol as a white crystalline solid (2.83 g, 6.64 mmol, 42%). **¹H-NMR** (400 MHz, DMSO-*d*₆): δ (ppm) 3.79-3.86 (m, 2H), 3.87-3.94 (m, 2H), 7.19-7.27 (m, 2H), 7.28-7.42 (m, 8H), 7.74-7.86 (m, 4H). **¹³C-NMR** (101 MHz, DMSO-*d*₆): δ (ppm) 35.6, 38.6, 123.06, 123.11, 127.0, 129.1, 131.4, 134.5, 136.2, 152.5, 168.0. **HRMS** (ESI): *m/z* [M+H]⁺ calcd. for [C₂₄H₁₉N₄O₄]⁺ 427.1401, found 427.1399. C₂₄H₁₈N₄O₄ (426.43).

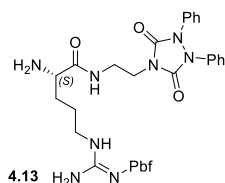
Warning: The hazards associated with the thermal decomposition of sodium hydride in *N,N*-dimethylformamide is well documented in the literature,⁵¹ therefore an upscaling of the described procedure is not recommended.



4-(2-Aminoethyl)-1,2-diphenyl-1,2,4-triazolidine-3,5-dione (4.10).^{8, 14} 4-(2-Phthalimidoethyl)-1,2-diphenyl-1,2,4-triazolidine-3,5-dione (**4.9**) (2.53 g, 5.93 mmol) was dissolved in a mixture of methanol (30 mL) and THF (60 mL). Under stirring, hydrazine hydrate 50-60% (4.90 g) was added and the reaction mixture was stirred at rt for 24 h. The solvent was evaporated and 1 N HCl (100 mL) was added and the reaction mixture was stirred at rt for 2.5 hours. The pH of the mixture was adjusted to 10 with 1N NaOH (pH 10). After the product was extracted from the aqueous phase with CH₂Cl₂ (3x 150 mL), the combined organic phases were dried over Na₂SO₄ and the organic solvent was evaporated. Then, the residue was dissolved in ethanol (125 mL) and 1 N HCl in diethyl ether (20 mL) was added. The solid was separated by filtration and washed with light petroleum. The obtained hydrochloride was dried *in vacuo* and dissolved in a mixture of ammonium hydroxide (50 mL) and water (100 mL). The product was extracted from the aqueous phase with CH₂Cl₂ (3x 100 mL). The combined organic phases were dried over Na₂SO₄ and the organic solvent was evaporated. The solid was dried *in vacuo* to give **4.10** as a yellowish solid (1.27 g, 4.27 mmol, 72%). **¹H-NMR** (400 MHz, DMSO-*d*₆): δ (ppm) 2.36 (br s, 2H, interfering with solvent residual peak), 2.81 (t, *J* = 6.3 Hz, 2H), 3.56 (t, *J* = 6.3 Hz, 2H), 7.17-7.29 (m, 2H), 7.32-7.49 (m, 8H). **¹³C-NMR** (101 MHz, DMSO-*d*₆): δ (ppm) 39.5 (overlaid from solvent residual peak), 42.9, 122.5, 126.6, 129.0, 136.6, 152.9. **HRMS** (ESI): *m/z* [M+Na]⁺ calcd. for [C₁₆H₁₆N₄O₂Na]⁺ 319.1165, found 319.1163. C₁₆H₁₆N₄O₂ (296.33).

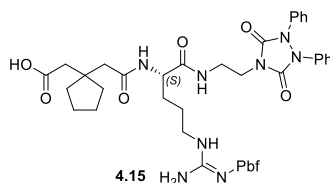


(S)- N^F [(9H-Fluoren-9-yl)methyloxycarbonyl]- N^W -2,3-dihydro-2,2,4,6,7-pentamethylbenzofuran-5-sulfonyl-[2-(3,5-dioxo-1,2-diphenyl-1,2,4-triazolidin-4-yl)ethyl]argininamide (4.12).^{14, 17} Fmoc-Arg(Pbf)-OH (**4.11**) (13.20 g, 20.3 mmol) was dissolved in DMF (180 mL), 1-ethyl-3-(3-dimethylamino-propyl)carbodiimide hydrochloride (4.63 g, 24.2 mmol) and HOBt (3.26 g, 24.1 mmol) were added to the mixture. The reaction mixture was stirred for 5 min before the addition of 4-(2-aminoethyl)-1,2-diphenyl-1,2,4-triazolidine-3,5-dione (**4.10**) (6.00 g, 20.2 mmol). After 1 day the reaction mixture was poured in ethyl acetate (750 mL) and washed three times with water (3x 1000 mL). The organic phase was dried over Na_2SO_4 and the organic solvent was evaporated. The crude product was purified by column chromatography (eluent: $\text{CH}_2\text{Cl}_2/\text{MeOH}$ 90:10) to give **4.12** as a pale white solid (17.45 g, 18.8 mmol, 93%). **$^1\text{H-NMR}$** (400 MHz, $\text{DMSO-}d_6$): δ (ppm) 1.19-1.69 (m, 11H), 1.99 (s, 3H), 2.44 (s, 3H), 2.90-3.00 (m, 4H), 3.28-3.52 (m, 4H), 3.58-3.69 (m, 2H), 3.84-3.94 (m, 1H), 4.16-4.34 (m, 3H), 6.41 (br s, 1H), 6.56-7.07 (m, 2H), 7.15-7.26 (m, 2H), 7.28-7.47 (m, 13H), 7.66-7.77 (m, 2H), 7.88 (d, $J = 7.87$ Hz, 2H), 8.18 (t, $J = 5.8$ Hz, 1H). **$^{13}\text{C-NMR}$** (101 MHz, $\text{DMSO-}d_6$): δ (ppm) 12.3, 17.6, 19.0, 25.7, 29.1, 36.1, 40.17, 40.28 (overlaid by solvent residual peak), 40.6, 42.5, 46.7, 54.4, 65.7, 86.3, 116.3, 120.1, 122.6, 124.3, 125.3, 126.6, 127.1, 127.6, 129.0, 131.5, 136.6, 137.3, 140.7, 143.7, 143.9, 152.6, 155.9, 156.1, 157.5, 172.2. **HRMS** (ESI): m/z $[\text{M}+\text{H}]^+$ calcd. for $[\text{C}_{50}\text{H}_{55}\text{N}_8\text{O}_8\text{S}]^+$ 927.3858, found 927.3891. $\text{C}_{50}\text{H}_{54}\text{N}_8\text{O}_8\text{S}$ (927.09).

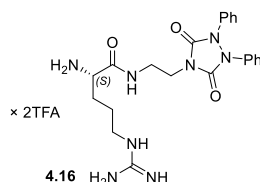


(S)- N^W -2,3-Dihydro-2,2,4,6,7-pentamethylbenzofuran-5-sulfonyl-[2-(3,5-dioxo-1,2-diphenyl-1,2,4-triazolidin-4-yl)ethyl]argininamide (4.13).¹⁷ (S)- N^F [(9H-Fluoren-9-yl)methyloxycarbonyl]- N^W -2,3-dihydro-2,2,4,6,7-pentamethylbenzofuran-5-sulfonyl-[2-(3,5-dioxo-1,2-diphenyl-1,2,4-triazolidin-4-yl)ethyl]argininamide (**4.12**) (12.03 g, 13.0 mmol) was dissolved in DMF (32 mL) and piperidine (8 mL, 81.0 mmol) was added and the reaction mixture was stirred at rt overnight. The reaction mixture was poured into water (1.5 L) and the product was extracted from the aqueous phase with ethyl acetate (3x 400 mL). The combined organic phases were dried over Na_2SO_4 and the organic solvent was evaporated. The crude product was purified by column chromatography (eluent: $\text{CH}_2\text{Cl}_2/\text{MeOH}/\text{NH}_3$ aq 90:9:1) to give **4.13** as a white solid (8.31 g, 11.8 mmol, 91%). **$^1\text{H-NMR}$** (400 MHz, $\text{DMSO-}d_6$): δ (ppm) 1.16-1.25 (m, 1H), 1.29-1.53 (m, 10H), 1.69 (br s, 1H), 1.99 (s, 3H), 2.43 (br s, 3H), 2.48 (br s, 1H, interfering with solvent residual peak), 2.92-3.01 (m, 5H), 3.30-3.47 (m, 3H), 3.62 (t, $J = 5.6$ Hz, 2H), 6.40 (br s, 1H), 6.64 (br s, 1H), 7.15-7.26 (m, 2H), 7.32-7.41 (m, 9H), 7.95 (s, 1H); 8.13 (t, $J = 6.0$ Hz, 1H). **$^{13}\text{C-NMR}$** (101 MHz, $\text{DMSO-}d_6$): δ (ppm) 12.3, 17.6, 19.0, 28.3, 31.9, 36.2, 40.2 (overlaid by solvent residual peak), 40.3 (overlaid by solvent residual peak) 42.5, 54.6, 86.3, 116.2, 122.6, 124.3, 126.6,

129.0, 131.4, 134.3, 136.6, 137.3, 152.8, 156.1, 157.4, 175.7. **HRMS** (ESI): *m/z* [M+Na]⁺ calcd. for [C₃₅H₄₄N₈O₆SNa]⁺ 727.2997, found 727.3003. C₃₅H₄₄N₈O₆S (704.85).

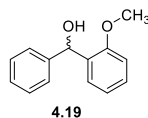


(S)-2-(1-(2-((1-((2-(3,5-Dioxo-1,2-diphenyl-1,2,4-triazolidin-4-yl)ethyl)amino)-1-oxo-5-(2-((2,2,4,6,7-pentamethyl-2,3-dihydrobenzofuran-5-yl)sulfonyl)guanidino)pentan-2-yl)amino)-2-oxoethyl)cyclopentyl)acetic acid (4.15).¹⁷ (S)-N^ω-2,3-Dihydro-2,2,4,6,7-pentamethylbenzofuran-5-sulfonyl-[2-(3,5-dioxo-1,2-diphenyl-1,2,4-triazolidin-4-yl)ethyl]argininamide (**4.13**) (4.55 g, 6.46 mmol) was dissolved in CH₂Cl₂ (90 mL) and cooled with an ice bath. Under stirring, 3,3-tetramethyleneglutaric anhydride (**4.14**) (1.10 g, 6.54 mmol) in CH₂Cl₂ (90 mL) was slowly added dropwise and the mixture was stirred in an ice bath. After 2 h, the reaction mixture was allowed to warm to rt and stirred overnight. The solvent was evaporated, and the crude product was purified by column chromatography (eluent: CH₂Cl₂/MeOH 1:0 to 9:1) to give **4.15** as a white crystalline solid (5.56 g, 6.37 mmol, 99%). **¹H-NMR** (400 MHz, DMSO-*d*₆): δ (ppm) 1.31-1.60 (m, 18H), 2.00 (s, 3H), 2.24-2.36 (m, 3H), 2.40-2.52 (m, 7H, interfering with solvent residual peak), 2.91-2.98 (m, 4H), 3.30-3.37 (m, 2H), 3.39-3.46 (m, 1H), 3.54-3.72 (m, 2H), 4.09-4.21 (m, 1H), 6.40 (s, 1H), 6.62 (s, 1H), 7.13-7.25 (m, 2H), 7.29-7.45 (m, 8H), 7.90-7.96 (m, 1H), 8.15 (t, *J* = 5.9 Hz, 1H), 12.11 (br s, 1H). **¹³C-NMR** (101 MHz, DMSO-*d*₆): δ (ppm) 17.6, 19.0, 23.6, 28.3, 29.1, 31.9, 36.2, 37.1, 37.2, 39.5 (overlaid by solvent residual peak), 39.8 (overlaid by solvent residual peak), 42.4, 42.5, 43.1, 52.1, 54.6, 86.3, 116.3, 122.6, 124.3, 126.6, 129.0, 131.5, 134.2, 136.6, 137.3, 152.6, 156.1, 157.5, 171.2, 172.0, 173.5. **HRMS** (ESI): *m/z* [M+H]⁺ calcd. for [C₄₄H₅₇N₈O₉S]⁺ 873.3964, found 873.3979. C₄₄H₅₆N₈O₉S (873.04).

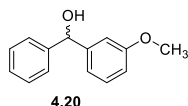


(S)-[2-(3,5-Dioxo-1,2-diphenyl-1,2,4-triazolidin-4-yl)ethyl]argininamid bis(hydrotrifluoroacetate) (4.16).⁸ (S)-N^ω-2,3-Dihydro-2,2,4,6,7-pentamethylbenzofuran-5-sulfonyl-[2-(3,5-dioxo-1,2-diphenyl-1,2,4-triazolidin-4-yl)ethyl]argininamide (**4.13**) (310 mg, 0.440 mmol) was dissolved in a mixture of TFA and water (95:5, 4 mL) and stirred at rt for 24 h. The crude product was poured into a solution of 100 mL water. After lyophilisation, the crude product was purified by preparative HPLC (gradient: 0-30 min, A/B 76:24–28:72, *t_R* = 8 min), which afforded **4.16** as a fluffy white solid (210 mg, 0.309 mmol, 70%). **¹H-NMR** (400 MHz, DMSO-*d*₆): δ (ppm) 1.41-1.56 (m, 2H), 1.60-1.76 (m, 2H), 2.94-3.04 (m, 2H), 3.27-3.40 (m, 1H), 3.56-3.74 (m, 4H), 3.93 (br s, 2H, interfering with surrounded peaks), 7.27-7.40 (br s, 2H, interfering with next two peaks), 7.20-7.27 (m, 2H), 7.37-7.40 (m, 8H), 7.92 (t, *J* = 5.5 Hz, 1H), 8.23 (br s, 3H), 8.83 (t, *J* = 5.8 Hz, 1H). **¹³C-NMR** (101 MHz, DMSO-*d*₆): δ (ppm) 23.9, 28.1, 36.3, 39.8 (overlaid by solvent residual peak), 40.5 (overlaid by solvent residual peak). 51.9, 115.5 (TFA), 118.5 (TFA),

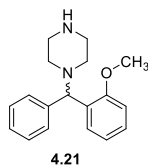
122.7, 126.8, 129.1, 136.5, 152.6, 157.0, 158.9 (q, $J = 32.1$ Hz) (TFA), 168.9. **HRMS** (ESI): m/z $[M+H]^+$ calcd. for $[C_{22}H_{29}N_8O_3]^+$ 453.2357, found 453.2358. $C_{22}H_{28}N_8O_3 \times C_4H_2F_6O_4$ (452.52 + 228.04).



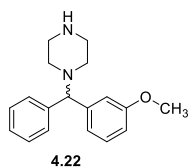
(2-Methoxyphenyl)(phenyl)methanol (4.19).^{52, 53} Compound **4.19** was prepared using *general procedure A* and the reactants Mg (1.09 g, 44.8 mmol), bromobenzene (4.6 mL, 43.9 mmol) and 2-methoxybenzaldehyde (**4.17**) (4.90 g, 36.0 mmol). The crude product was purified by column chromatography (eluent: light petroleum/ethyl acetate 90:10) to give **4.19** as a yellow liquid (7.02 g, 32.8 mmol, 91%). **Anal. calcd.** for $C_{14}H_{14}O_2 \cdot 0.1 H_2O$: C 77.83, H 6.62, found: C 77.82, H 6.51. **1H -NMR** (400 MHz, $DMSO-d_6$): δ (ppm) 3.75 (s, 3H), 5.66 (br s, 1H), 5.99 (s, 1H), 6.89-6.99 (m, 2H), 7.13-7.28 (m, 4H), 7.30-7.35 (m, 2H), 7.44-7.52 (m, 1H). **^{13}C -NMR** (101 MHz, $DMSO-d_6$): δ (ppm) 55.4, 67.8, 110.7, 120.3, 126.47, 126.48, 126.5, 127.84, 127.85, 133.7, 145.4, 155.5. **HRMS** (EIC): m/z $[M]^+$ calcd. for $[C_{14}H_{14}O_2]^+$ 214.0988, found 214.0990. $C_{14}H_{14}O_2$ (214.26).



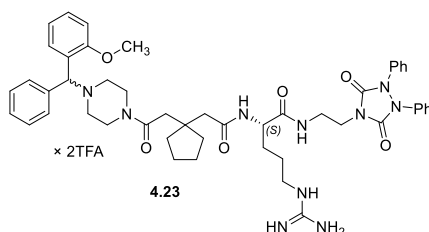
(3-Methoxyphenyl)(phenyl)methanol (4.20).⁵⁴ Compound **4.20** was prepared using *general procedure A* and the reactants Mg (0.96 g, 39.5 mmol), bromobenzene (4.0 mL, 38.2 mmol) and 3-methoxybenzaldehyde (**4.18**) (3.7 mL, 30.4 mmol). The crude product was purified by column chromatography (eluent: light petroleum to CH_2Cl_2) to give **4.20** as an orange oil (4.71 g, 22.0 mmol, 73%). **Anal. calcd.** for $C_{14}H_{14}O_2$: C 78.48, H 6.59, found: C 78.08, H 6.45. **1H -NMR** (300 MHz, $DMSO-d_6$): δ (ppm) 3.72 (s, 3H), 5.68 (d, $J = 3.5$ Hz, 1H), 5.90 (d, $J = 3.9$ Hz, 1H), 6.74-6.80 (m, 1H), 6.91-7.01 (m, 2H), 7.16-7.24 (m, 2H), 7.26-7.33 (m, 2H), 7.36-7.42 (m, 2H). **^{13}C -NMR** (75 MHz, $DMSO-d_6$): δ (ppm) 55.0, 74.2, 111.87, 111.91, 118.5, 126.2, 126.7, 128.1, 129.2, 145.6, 147.4, 159.2. **HRMS** (EIC): m/z $[M]^+$ calcd. for $[C_{14}H_{14}O_2]^+$ 214.0988, found 214.0983. $C_{14}H_{14}O_2$ (214.26).



1-((2-Methoxyphenyl)(phenyl)methyl)piperazine (4.21).⁵⁵ Compound **4.21** was prepared using *general procedure B* and the reactants (2-methoxyphenyl)(phenyl)methanol (**4.19**) (0.53 g, 2.47 mmol), sulfonyl chloride (0.7 mL, 9.65 mmol) and piperazine (0.92 g, 10.7 mmol). The crude product was purified by column chromatography (eluent: $CH_2Cl_2/MeOH/NH_3$ aq 90:9:1) to give **4.21** as a yellow oil (0.47 g, 1.66 mmol, 67%). **1H -NMR** (300 MHz, $DMSO-d_6$): δ (ppm) 2.05-2.35 (m, 4H), 2.58-2.85 (m, 5H), 3.75 (s, 3H), 4.67 (s, 1H), 6.87-6.98 (m, 2H), 7.09-7.18 (m, 2H), 7.20-7.30 (m, 2H), 7.33-7.40 (m, 2H), 7.53-7.59 (m, 1H). **^{13}C -NMR** (101 MHz, $DMSO-d_6$): δ (ppm) 45.7, 52.9, 55.5, 66.8, 111.2, 120.6, 126.5, 127.4, 127.5, 127.9, 128.2, 130.5, 142.6, 156.7. **HRMS** (ESI): m/z $[M+H]^+$ calcd. for $[C_{18}H_{23}N_2O]^+$ 283.1805, found 283.1814. $C_{18}H_{22}N_2O$ (282.39).

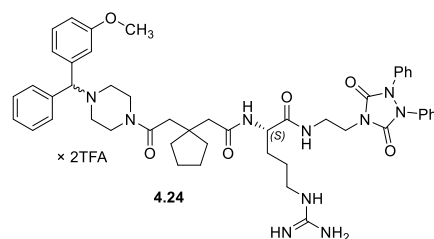


1-((3-Methoxyphenyl)(phenyl)methyl)piperazine (4.22). Compound **4.22** was prepared using *general procedure B* and the reactants (3-methoxyphenyl)(phenyl)methanol (**4.20**) (0.52 g, 2.43 mmol), sulfuric chloride (0.7 mL, 9.65 mmol) and piperazine (0.80 g, 9.29 mmol). The crude product was purified by column chromatography (eluent: CH₂Cl₂/MeOH/NH₃ aq 90:9:1) to give **4.22** as a yellow oil (0.51 g, 1.81 mmol, 74%). ¹H-NMR (300 MHz, DMSO-*d*₆): δ (ppm) 2.17-2.32 (m, 4H), 2.71-2.81 (m, 4H), 3.56 (br s, 1H), 3.70 (s, 3H), 4.21 (s, 1H), 6.70-6.77 (m, 1H), 6.90-7.02 (m, 2H), 7.14-7.22 (m, 2H), 7.25-7.32 (m, 2H), 7.38-7.47 (m, 2H). ¹³C-NMR (75 MHz, DMSO-*d*₆): δ (ppm) 45.3, 52.2, 54.9, 75.4, 111.8, 113.4, 119.8, 126.8, 127.7, 128.5, 129.6, 142.6, 144.5, 159.3. HRMS (ESI): m/z [M+H]⁺ calcd. for [C₁₈H₂₃N₂O]⁺ 283.1805, found 283.1813. C₁₈H₂₂N₂O (282.39).

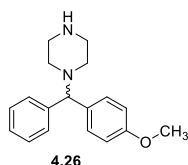


(2S)-N²-(2-{1-[2-(4-((2-Methoxyphenyl)(phenyl)methyl)piperazin-1-yl]-2-oxoethyl]cyclopentyl}-acetyl)[2-(3,5-dioxo-1,2-diphenyl-1,2,4-triazolidin-4-yl)ethyl]argininamide bis(hydrotrifluoroacetate) (4.23). Compound **4.23** was prepared using *general procedure G* and the reactants (S)-2-(1-(2-((1-((2-(3,5-dioxo-1,2-diphenyl-1,2,4-triazolidin-4-yl)ethyl)amino)-1-oxo-5-(2-((2,2,4,6,7-pentamethyl-2,3-dihydrobenzofuran-5-yl)sulfonyl)guanidino)pentan-2-yl)amino)-2-oxoethyl)cyclopentyl)acetic acid (**4.15**) (109 mg, 118 μmol), EDC·HCl (36 mg, 188 μmol), HOBt (17 mg, 126 μmol) and 1-((2-methoxyphenyl)(phenyl)methyl)piperazine (**4.21**) (39 mg, 138 μmol). Purification by preparative HPLC A (gradient: 0-30 min, A/B 85:15–38:62, t_R = 19 min) afforded **4.23** as a fluffy white solid (23 mg, 21 μmol, 18%). Ratio of diastereomers evident in NMR spectra recorded in MeOH-*d*₄: 1:1. ¹H-NMR (600 MHz, MeOH-*d*₄): δ (ppm) 1.47-1.82 (m, 13H), 2.26-2.31 (m, 1H), 2.50-2.58 (m, 2H), 2.58-2.64 (m, 1H), 2.97-3.27 (m, 6H), 3.41-3.47 (m, 1H), 3.53-3.60 (m, 1H), 3.61-4.21 (m, 8H), 4.22-4.27 (m, 1H), 5.69 (s, 0.5H), 5.70 (s, 0.5H), 7.05-7.09 (m, 1H), 7.12-7.15 (m, 1H), 7.19-7.24 (m, 2H), 7.30-7.36 (m, 4H), 7.37-7.47 (m, 8H), 7.57-7.62 (m, 1H), 7.62-7.66 (m, 2H). ¹H-NMR (600 MHz, DMSO-*d*₆) 1.32-1.67 (m, 13H), 2.16-2.27 (m, 1H), 2.30-2.40 (m, 1H), 2.41-2.48 (m, 2H, interfering with solvent residual peak), 2.54-2.67 (m, 2H), 2.67-3.25 (m, 6H), 3.27-3.32 (m, 1H), 3.35-3.39 (m, 1H), 3.54-3.65 (m, 3H), 3.83 (s, 3H), 4.11-4.15 (m, 1H), 5.75 (br s, 1H), 6.89-7.14 (m, 4H), 7.19-7.26 (m, 3H), 7.27-7.50 (m, 14H), 7.50-7.62 (m, 2H), 7.63-7.77 (m, 2H), 7.93 (d, J = 7.9 Hz, 1H), 8.20 (t, J = 5.7 Hz, 1H). ¹³C-NMR (150 MHz, MeOH-*d*₄): 24.58, 24.62 (two carbon signals), 26.32, 26.34, 30.07, 30.12, 38.21, 38.24, 39.1, 39.2, 39.3, 39.46, 39.49, 40.0, 41.18, 41.23, 41.9, 43.8, 44.31, 44.34, 45.59, 45.63, 52.50, 52.77, 52.86, 52.94, 54.0, 54.1, 56.35, 56.37, 72.3, 72.4, 113.3, 117.1 (TFA), 119.0 (TFA), 122.81, 122.83, 123.52, 123.56, 124.30, 124.32, 128.2 (2 carb.), 129.6, 129.7, 129.99, 130.04, 130.2, 130.64, 130.66, 130.74, 132.27, 132.28, 135.50, 135.53, 137.67, 137.69, 154.5, 157.76, 157.78, 158.6, 162.4 (TFA), 162.6 (TFA),

172.93, 172.95, 174.68, 174.73, 174.74. **RP-HPLC** (220 nm): 100% ($t_R = 13.8$ min, $k = 4.4$). **HRMS** (ESI): m/z $[M+H]^+$ calcd. for $[C_{49}H_{61}N_{10}O_6]^+$ 885.4770, found 885.4773. $C_{49}H_{60}N_{10}O_6 \times C_4H_2F_6O_4$ (885.08 + 228.04).

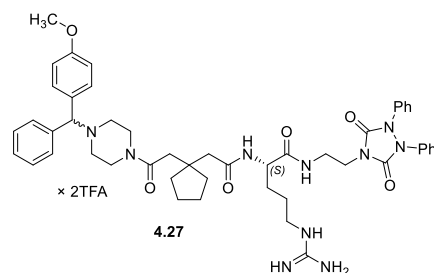


(2S)-N²-(2-{1-[2-(4-((3-Methoxyphenyl)(phenyl)methyl)piperazin-1-yl]-2-oxoethyl]cyclopentyl}-acetyl)[2-(3,5-dioxo-1,2-diphenyl-1,2,4-triazolidin-4-yl)ethyl]argininamide bis(hydrotrifluoroacetate) (4.24). Compound **4.24** was prepared using *general procedure G* and the reactants (S)-2-(1-(2-((1-((2-(3,5-dioxo-1,2-diphenyl-1,2,4-triazolidin-4-yl)ethyl)amino)-1-oxo-5-(2-((2,2,4,6,7-pentamethyl-2,3-dihydrobenzofuran-5-yl)sulfonyl)guanidino)pentan-2-yl)amino)-2-oxoethyl)cyclopentyl)-acetic acid (**4.15**) (104 mg, 112 μ mol), EDC·HCl (24 mg, 125 μ mol), HOBt (28 mg, 207 μ mol) and 1-((3-methoxyphenyl)(phenyl)methyl)piperazine (**4.22**) (34 mg, 120 μ mol). Purification by preparative HPLC A (gradient: 0-30 min, A/B 66:34–47:53, $t_R = 16$ min) afforded **4.23** as a fluffy white solid (16 mg, 14 μ mol, 13%). **¹H-NMR** (600 MHz, MeOH- d_4): δ (ppm) 1.42-1.81 (m, 13H), 2.25-2.31 (m, 1H), 2.50-2.64 (m, 3H), 2.93-3.11 (m, 4H), 3.12-3.23 (m, 2H), 3.41-3.47 (m, 1H), 3.54-3.61 (m, 1H), 3.67-3.98 (m, 8H), 4.22-4.27 (m, 1H), 5.29 (s, 1H), 6.95-7.01 (m, 1H), 7.18-7.25 (m, 4H), 7.32-7.44 (m, 10H), 7.45-7.50 (m, 2H), 7.60-7.70 (m, 2H). **¹H-NMR** (600 MHz, DMSO- d_6) 1.32-1.69 (m, 13H), 2.19-2.28 (m, 1H), 2.31-2.40 (m, 1H), 2.44-2.49 (m, 2H, interfering with solvent residual peak), 2.54-2.65 (m, 2H), 2.68-3.22 (m, 5H), 3.27-3.33 (m, 1H), 3.35-3.43 (m, 1H), 3.44-3.72 (m, 4H), 3.75 (m, 3H), 4.11-4.17 (m, 1H), 5.51 (br s, 1H), 6.78-7.27 (m, 7H), 7.28-7.50 (m, 14H), 7.50-7.74 (m, 4H), 7.95 (d, $J = 8.0$ Hz, 1H), 8.21 (t, $J = 5.6$ Hz, 1H). **¹³C-NMR** (150 MHz, MeOH- d_4) 24.60, 24.63, 25.2, 26.3, 26.6, 27.0, 30.1, 38.2, 38.6 (two carbon signals), 39.26, 39.28, 39.4, 39.5, 39.90, 39.92, 40.5, 40.9, 41.2, 41.9, 42.0, 44.1, 44.4, 45.4, 45.6, 52.9, 53.1, 54.0, 54.2, 55.9, 76.8, 114.93, 114.97, 115.81, 115.85, 117.0 (TFA), 118.9 (TFA), 151.15, 121.18, 124.34, 124.35, 124.5, 128.1, 128.3, 129.3 (2 carb.), 130.1, 130.2, 130.7, 130.8, 132.0 (2 carb.), 136.1, 137.6, 137.7, 154.5, 158.6, 162.1, 162.3 (TFA), 162.5 (TFA), 172.4, 172.9, 174.1, 174.69, 174.72. **RP-HPLC** (220 nm): 100% ($t_R = 14.2$ min, $k = 4.5$). **HRMS** (ESI): m/z $[M+H]^+$ calcd. for $[C_{49}H_{61}N_{10}O_6]^+$ 885.4770, found 885.4779. $C_{49}H_{60}N_{10}O_6 \times C_4H_2F_6O_4$ (885.08 + 228.04).



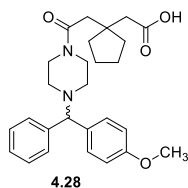
1-((4-Methoxyphenyl)(phenyl)methyl)piperazine (4.26). 4-Methoxybenzophenone (**4.25**) (1.02 g, 4.81 mmol) was dissolved in CH_2Cl_2 (30 mL) and the mixture was cooled in an ice bath. Under stirring, titanium tetrachloride (0.60 mL, 5.47 mmol) in CH_2Cl_2 (6 mL) was dropped into the mixture. Then, piperazine (1.63 g, 18.9 mmol) was added to the reaction mixture, which was allowed to warm to rt and stirred for 3 h. Sodium cyanoborohydride (0.36 g, 5.73 mmol) in methanol (10 mL) was dropped slowly

to the reaction mixture, which was stirred at rt overnight. After addition of 1 N NaOH (50 mL) the reaction mixture was stirred for 3 h and the precipitated solid was separated by filtration. The compound was extracted from the aqueous phase with ethyl acetate (3x 100 mL) and the combined organic phases were dried over Na₂SO₄ and the solvent was evaporated. The crude product was purified by column chromatography (eluent: CH₂Cl₂/MeOH/NH₃ aq 90:9:1) to give **4.26** as a yellow oil (0.31 g, 1.10 mmol, 23%). **¹H-NMR** (400 MHz, DMSO-*d*₆): δ (ppm) 2.15-2.31 (m, 4H), 2.66-2.78 (m, 4H), 3.22 (br s, 1H), 3.69 (s, 3H), 4.18 (s, 1H), 6.81-7.19 (m, 2H), 7.12-7.19 (m, 1H), 7.23-7.33 (m, 4H), 7.35-7.42 (m, 2H). **¹³C-NMR** (101 MHz, DMSO-*d*₆): δ (ppm) 45.5, 52.6, 54.9, 75.0, 113.8, 126.6, 127.5, 128.4, 128.7, 134.7, 143.2, 158.0. **HRMS** (ESI): *m/z* [M+H]⁺ calcd. for [C₁₈H₂₃N₂O]⁺ 283.1805, found 283.1807. C₁₈H₂₂N₂O (282.39).

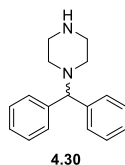


(2S)-N¹-(2-{1-[2-(4-((4-Methoxyphenyl)(phenyl)methyl)piperazin-1-yl)-2-oxoethyl]cyclopentyl}-acetyl)[2-(3,5-dioxo-1,2-diphenyl-1,2,4-triazolidin-4-yl)ethyl]argininamide bis(hydrotrifluoroacetate) (4.27**).** 2-(1-(2-(4-((4-Methoxyphenyl)(phenyl)methyl)piperazin-1-yl)-2-oxoethyl)cyclopentyl)-acetic acid (**4.28**) (29.4 mg, 64.4 μmol), EDC·HCl (20.0 mg, 104 μmol) and HOBT (10.8 mg, 79.9 μmol) were dissolved in DMF (1 mL) and the reaction mixture was stirred at rt for 5 min. Under stirring, (S)-[2-(3,5-dioxo-1,2-diphenyl-1,2,4-triazolidin-4-yl)ethyl]argininamid bis(hydrofluoroacetate) (**4.16**) (45.5 mg, 66.9 μmol) and DIPEA (22 μL, 126 μmol) in DMF (1 mL) were added into the reaction mixture, which was stirred at rt overnight. Then, the reaction mixture was poured into an aqueous solution (5% acetonitrile, 0.1% TFA) before purification by preparative HPLC A (gradient: 0-30 min, A/B 76:24–47:53, *t_R* = 13 min) afforded **4.27** as a fluffy white solid (43 mg, 39 μmol, 61%). **¹H-NMR** (600 MHz, MeOH-*d*₄): δ (ppm) 1.46-1.83 (m, 13H), 2.27-2.33 (m, 1H), 2.50-2.56 (m, 2H), 2.57-2.66 (m, 1H), 2.83-2.91 (m, 1H), 2.96-3.12 (m, 4H), 3.14-3.25 (m, 2H), 3.41-3.47 (m, 1H), 3.52-3.60 (m, 1H), 3.72-3.83 (m, 6H), 3.87-3.97 (m, 1H), 4.23-4.27 (m, 1H), 5.32 (s, 1H, two singlets falling together, because two diastereomers were evident in the spectra), 6.98-7.02 (m, 2H), 7.19-7.24 (m, 2H), 7.30-7.36 (m, 4H), 7.37-7.43 (m, 5H), 7.45-7.50 (m, 2H), 7.55-7.60 (m, 2H), 7.64-7.68 (m, 2H). **¹H-NMR** (600 MHz, DMSO-*d*₆) 1.34-1.69 (m, 13H), 2.16-2.28 (m, 1H), 2.31-2.43 (m, 1H), 2.44-2.49 (m, 2H, interfering with solvent residual peak), 2.53-2.62 (m, 2H, interfering with solvent residual peak), 2.76-3.18 (m, 5H), 3.28-3.33 (m, 1H), 3.35-3.41 (m, 1H), 3.43-3.63 (m, 4H), 3.73 (s, 3H), 4.11-4.17 (m, 1H), 5.49 (br s, 1H), 6.84-7.68 (m, 25H), 7.94 (d, *J* = 7.5 Hz, 1H), 8.16-8.25 (m, 1H). **¹³C-NMR** (150 MHz, MeOH-*d*₄) 24.57, 24.61, 24.7, 26.3 (two carbon signals), 30.1 (2 carb.), 36.9, 38.2, 39.2, 39.27 (2 carb.), 39.31, 39.43, 39.9 (2 carb.), 41.2, 41.8, 43.9, 44.3, 45.6, 52.66, 52.69, 52.9 (2 carb.), 54.0 (2 carb.), 55.9, 76.5 (2 carb.), 111.5, 116.1, 117.1 (TFA), 119.0 (TFA), 124.1, 124.3 (2 carb.), 127.30, 127.33, 128.3, 129.13, 129.14, 130.2, 130.5, 130.8 (2 carb.), 130.99, 131.01, 136.1 (2 carb.), 137.64, 137.66, 154.45, 154.47, 158.59, 158.64, 162.0, 162.4 (TFA), 162.7 (TFA), 162.9 (TFA), 172.9, 174.70, 174.71. **RP-HPLC** (220 nm): 96%

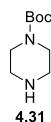
($t_R = 14.1$ min, $k = 4.5$). **HRMS** (ESI): m/z $[M+H]^+$ calcd. for $[C_{49}H_{61}N_{10}O_6]^+$ 885.4770, found 885.4776. $C_{49}H_{60}N_{10}O_6 \times C_4H_2F_6O_4$ (885.08 + 228.04).



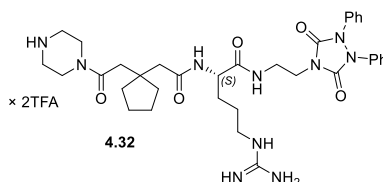
2-(1-(2-(4-((4-Methoxyphenyl)(phenyl)methyl)piperazin-1-yl)-2-oxoethyl)cyclopentyl)acetic acid (4.28). 1-((4-Methoxyphenyl)(phenyl)methyl)piperazine (**4.26**) (0.55 g, 1.95 mmol) was dissolved in CH_2Cl_2 (7 mL) and the mixture was cooled with an ice bath. Under stirring, 3,3-tetramethyleneglutaric anhydride (**4.14**) (0.36 g, 2.14 mmol) in CH_2Cl_2 (4 mL) was added dropwise to the mixture over a time period of 5 min. The reaction mixture was allowed to warm to rt and stirred overnight at rt. The solvent was evaporated, and the crude product purified by column chromatography (eluent: $CH_2Cl_2/MeOH$ 90:10) to obtain **4.28** as a yellowish solid (0.70 g, 1.55 mmol, 79%). **1H -NMR** (400 MHz, $DMSO-d_6$): δ (ppm) 1.49-1.59 (m, 8H), 2.20-2.28 (m, 4H), 2.43 (s, 2H), 2.48 (s, 2H, interfering with solvent residual peak), 3.43-3.50 (m, 4H), 3.69 (s, 3H), 4.24 (s, 1H), 6.83-7.21 (m, 2H), 7.15-7.21 (m, 1H), 7.25-7.34 (m, 4H), 7.38-7.43 (m, 2H), 11.99 (br s, 1H). **^{13}C -NMR** (101 MHz, $DMSO-d_6$): δ (ppm) 24.0, 37.9, 41.4, 42.2, 43.5, 45.9, 51.8, 52.3, 55.5, 74.6, 114.4, 127.2, 127.9, 129.0, 129.1, 134.9, 143.4, 158.6, 170.0, 174.0. **HRMS** (ESI): m/z $[M+Na]^+$ calcd. for $[C_{27}H_{34}N_2O_4Na]^+$ 473.2411, found 473.2409. $C_{27}H_{34}N_2O_4$ (450.58).



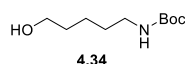
1-Benzhydrylpiperazine (4.30).⁵⁶ Diphenylmethanol **4.29** (0.42 g, 2.28 mmol), Et_3N (0.90 mL, 6.48 mmol) were dissolved in CH_2Cl_2 (10 mL) and the mixture was stirred in an ice bath. Under stirring, methanesulfonyl chloride (250 μ L, 3.23 mmol) was added into the reaction mixture. After stirring for 3 h the reaction mixture was poured into $NaOH$ (1 N, 20 mL). The product was extracted from the aqueous phase with CH_2Cl_2 (3x 20 mL). Then, the combined organic phases were dried over Na_2SO_4 , the organic solvent was evaporated, and the residue was dissolved in acetonitrile (10 mL). Piperazine (0.76 g, 8.82 mmol) was added to the reaction mixture. The reaction was stirred microwave assisted for 30 min at 70 $^{\circ}C$. The solvent was evaporated, and the crude product was purified by column chromatography (eluent: $CH_2Cl_2/MeOH/NH_3$ aq 90:9:1) to give **4.30** as an oil (0.30 g, 1.19 mmol, 52%). **1H -NMR** (400 MHz, $DMSO-d_6$): δ (ppm) 2.12-2.33 (m, 4H), 2.41 (br s, 1H), 2.64-2.80 (m, 4H), 4.24 (s, 1H), 7.13-7.20 (m, 2H), 7.24-7.32 (m, 4H), 7.36-7.44 (m, 4H). **^{13}C -NMR** (101 MHz, $DMSO-d_6$): δ (ppm) 45.5, 52.6, 75.7, 126.7, 127.6, 128.4, 142.8. **HRMS** (ESI): m/z $[M+H]^+$ calcd. for $[C_{17}H_{21}N_2]^+$ 253.1699, found 253.1717. $C_{17}H_{20}N_2$ (252.36).



tert-Butyl piperazine-1-carboxylate (4.31).⁵⁷ Piperazine (4.42 g, 51.3 mmol) was dissolved in CH₂Cl₂ (100 mL) and Boc₂O (3.20 g, 14.7 mmol) in CH₂Cl₂ (50 mL) was added dropwise to the solution. The reaction mixture was stirred at rt overnight and the solvent was evaporated. The residue was dissolved in water (200 mL) and the precipitate was separated by filtration. Then, the compound was extracted from the aqueous phase with CH₂Cl₂ (3x 150 mL), the combined organic phases were dried over Na₂SO₄. The organic solvent was evaporated to obtain **4.31** as an amorphous white solid (3.82 g, 20.5 mmol, 40%). ¹H-NMR (400 MHz, DMSO-*d*₆): δ (ppm) 1.38 (s, 9H), 2.53-2.82 (m, 4H), 3.10-3.16 (br s, 1H), 3.17-3.26 (m, 4H). ¹³C-NMR (101 MHz, DMSO-*d*₆): δ (ppm) 28.1, 45.4, 50.8, 78.5, 153.9. HRMS (ESI): m/z [M+H]⁺ calcd. for [C₉H₁₉N₂O₂]⁺ 187.1441, found 187.1439. C₉H₁₈N₂O₂ (186.26).

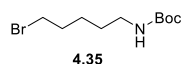


(2S)-N-(2-{1-[2-(Piperazin-1-yl)-2-oxoethyl]cyclopentyl}acetyl)[2-(3,5-dioxo-1,2-diphenyl-1,2,4-triazolidin-4-yl)ethyl]argininamide bis(hydrotrifluoroacetate) (4.32). Compound **4.32** was prepared using *general procedure G* and the reactants (S)-2-(1-(2-(((1-((2-(3,5-dioxo-1,2-diphenyl-1,2,4-triazolidin-4-yl)ethyl)amino)-1-oxo-5-(2-((2,2,4,6,7-pentamethyl-2,3-dihydrobenzofuran-5-yl)sulfonyl)-guanidino)pentan-2-yl)amino)-2-oxoethyl)cyclopentyl)acetic acid (**4.15**) (54.2 mg, 58.5 μmol), EDC-HCl (14.7 mg, 76.7 μmol), HOBt (14.7 mg, 108.8 μmol) and *tert*-butyl piperazine-1-carboxylate (**4.31**) (10.9 mg, 58.5 μmol). Purification by preparative HPLC B (gradient: 0-30 min, A/B 81:19–38:62, *t_R* = 12 min) afforded **4.32** as a fluffy white solid (19.9 mg, 21.7 μmol, 37%). ¹H-NMR (600 MHz, DMSO-*d*₆): δ (ppm) 1.35-1.68 (m, 12H), 2.25 (d, *J* = 13.7 Hz, 1H), 2.37 (d, *J* = 13.7 Hz, 1H), 2.47-2.49 (m, 1H, interfering with solvent residual peak), 2.62 (d, *J* = 15.5 Hz, 1H), 2.95-3.14 (m, 6H), 3.29-3.36 (m, 1H), 3.39-3.41 (m, 1H, overlaid by the water signal), 3.57-3.63 (m, 3H), 3.65-3.73 (m, 3H), 4.13-4.18 (m, 1H), 6.96-7.54 (m, 14H), 7.77 (t, *J* = 5.5 Hz, 1H), 7.89 (d, *J* = 8.0 Hz, 1H), 8.21 (t, *J* = 6.1 Hz, 1H), 9.08 (br s, 2H). ¹³C-NMR (150 MHz, DMSO-*d*₆): δ (ppm) 23.36, 23.41, 25.1, 28.9, 36.2, 37.3, 37.6, 37.8, 38.8, 39.6 (overlaid by solvent residual peak), 40.4, 42.4, 42.5, 42.7, 42.9, 43.8, 52.0, 117.1 (q, *J* = 298 Hz) (TFA), 122.7, 126.7, 129.1, 136.6, 152.6, 156.8, 158.7 (q, *J* = 31.6 Hz) (TFA), 170.4, 171.4, 172.0. RP-HPLC (220 nm): 97.9% (*t_R* = 10.4 min, *k* = 3.1). HRMS (ESI): m/z [M+H]⁺ calcd. for [C₃₅H₄₉N₁₀O₅]⁺ 689.3882, found 689.3885. C₃₅H₄₈N₁₀O₅ × C₄H₂F₆O₄ (688.83 + 228.04).

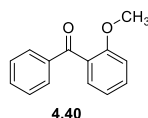


tert-Butyl (5-hydroxypentyl)carbamate (4.34).⁵⁸ 5-Aminopentanol (**4.33**) (5.02 g, 48.7 mmol) and, Et₃N (8.5 mL, 61.3 mmol) were dissolved in CH₂Cl₂ (200 mL). The mixture was stirred in an ice bath. Under stirring, Boc₂O (13.05 g, 59.8 mmol) in CH₂Cl₂ (50 mL) was added dropwise into the mixture. After 1 h the reaction mixture was allowed to warm to rt and stirred overnight. The organic phase was

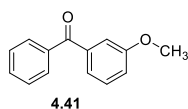
washed twice with a saturated solution of NaHCO_3 (2x 200 mL), water (1x 200 mL) and brine (1x 200 mL). The organic phase was dried over Na_2SO_4 and the organic solvent was evaporated. The crude product was purified by column chromatography (eluent: light petroleum/ethyl acetate 2:1) to give **4.34** as a colourless oil (7.26 g, 35.7 mmol, 73%). **Anal. calcd.** for $\text{C}_{10}\text{H}_{21}\text{NO}_3 \cdot 0.2 \text{H}_2\text{O}$: C 58.06, H 10.43, N 6.77, found: C 58.24, H 9.96, N 6.59 **$^1\text{H-NMR}$** (400 MHz, $\text{DMSO-}d_6$): δ (ppm) 1.68-1.29 (m, 2H), 1.29-1.45 (m, 13H), 2.88 (d, $J = 6.8 \text{ Hz}$, 2H), 3.35-3.39 (m, 2H, interfering with water signal), 4.33 (t, $J = 5.0 \text{ Hz}$, 1H), 6.73 (t, $J = 5.0 \text{ Hz}$, 1H). **$^{13}\text{C-NMR}$** (101 MHz, $\text{DMSO-}d_6$): δ (ppm) 22.8, 28.3, 29.4, 32.2, 39.9 (overlaid by solvent residual peak) 60.7, 77.3, 155.6. **HRMS** (ESI): m/z $[\text{M}+\text{Na}]^+$ calcd. for $[\text{C}_{10}\text{H}_{21}\text{NO}_3\text{Na}]^+$ 226.1414, found 226.1412. $\text{C}_{10}\text{H}_{21}\text{NO}_3$ (203.28).



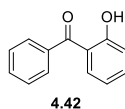
tert-Butyl (5-bromopentyl)carbamate (4.35).⁵⁹ *tert*-Butyl (5-hydroxypentyl)carbamate (**4.34**) (1.00 g, 4.92 mmol) and, PPh_3 (1.93 g, 7.36 mmol) were dissolved in THF (15 mL) and the mixture was stirred in an ice bath. Under stirring, carbon tetrabromide (2.56 g, 7.72 mmol) in THF (15 mL) was added dropwise to the reaction mixture. After 4 h additional PPh_3 (1.93 g, 7.36 mmol) and carbon tetrabromide (2.47 g, 7.45 mmol) were added and the reaction mixture was stirred at rt over night. The solvent was evaporated, and the crude product was purified by column chromatography (eluent: light petroleum/ethyl acetate 2:1) to give **4.34** as a light brown oil (1.21 g, 4.55 mmol, 92%). **$^1\text{H NMR}$** (400 MHz, $\text{DMSO-}d_6$): δ (ppm) 1.32-1.43 (m, 13H), 1.74-1.86 (m, 2H), 2.86-2.94 (m, 2H), 3.50 (t, $J = 6.7 \text{ Hz}$, 2H), 6.70-6.80 (m, 1H). **$^{13}\text{C NMR}$** (101 MHz, $\text{DMSO-}d_6$): δ (ppm) 24.8, 28.2, 28.6, 31.9, 35.0, 39.9 (overlaid by solvent residual peak), 77.3, 155.6. **HRMS** (ESI): m/z $[\text{M}+\text{H}]^+$ calcd. for $[\text{C}_{10}\text{H}_{21}\text{BrNO}_2]^+$ 266.0750, found 266.0747. $\text{C}_{10}\text{H}_{20}\text{BrNO}_2$ (266.18).



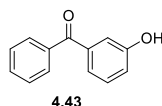
(2-Methoxyphenyl)(phenyl)methanone (4.40). (2-Methoxyphenyl)(phenyl)methanol (**4.19**) (0.99 g, 4.62 mmol) and Et_3N (3.25 mL, 23.3 mmol) were dissolved in DMSO (20 mL). Under stirring, pyridine-sulfur trioxide complex (3.79 g, 23.8 mmol) in DMSO (40 mL) was added dropwise into the mixture. Then, the reaction mixture was poured in water (800 mL). The product was extracted from the aqueous phase with ethyl acetate (3x 200 mL), the combined organic phases were dried over Na_2SO_4 and the organic solvent was evaporated. The crude product was purified by column chromatography (eluent: light petroleum/ethyl acetate 90:10) to give **4.40** as an oil (0.38 g, 1.79 mmol, 39%). **Anal. calcd.** for $\text{C}_{14}\text{H}_{12}\text{O}_2 \cdot \text{H}_2\text{O}$: C 78.56, H 5.74, found: C 78.47, H 5.94. **$^1\text{H-NMR}$** (300 MHz, $\text{DMSO-}d_6$): δ (ppm) 3.66 (s, 3H), 7.05-7.11 (m, 1H), 7.15-7.21 (m, 1H), 7.29-7.35 (m, 1H), 7.46-7.55 (m, 3H), 7.59-7.67 (m, 1H), 7.67-7.73 (m, 2H). **$^{13}\text{C-NMR}$** (75 MHz, $\text{DMSO-}d_6$): δ (ppm) 55.5, 112.0, 120.6, 128.4, 128.6, 128.7, 129.2, 132.0, 133.2, 137.1, 156.6, 195.7. **HRMS** (EIC): m/z $[\text{M}]^+$ calcd. for $[\text{C}_{14}\text{H}_{12}\text{O}_2]^+$ 212.0832, found 212.0831. $\text{C}_{14}\text{H}_{12}\text{O}_2$ (212.25).



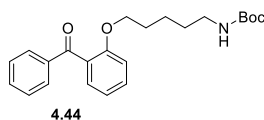
(3-Methoxyphenyl)(phenyl)methanone (4.41). PCC (2.07 g, 9.60 mmol) was suspended in CH₂Cl₂ (75 mL) and (2-methoxyphenyl)(phenyl)methanol (**4.20**) (0.99 g, 9.33 mmol) in CH₂Cl₂ (20 mL) was added dropwise to the reaction mixture. The reaction mixture was monitored by TLC and after 2 h PCC (0.86 g, 3.99 mmol) was added. After completion, the reaction mixture was filtered through a pad of silica gel. The filtrate was evaporated, and the crude product was purified by column chromatography (eluent: light petroleum/ethyl acetate 90:10) to give **4.41** as an oil (1.58 g, 7.44 mmol, 80%). **¹H-NMR** (300 MHz, DMSO-*d*₆): δ (ppm) 3.81 (s, 3H), 7.21-7.29 (m, 3H), 7.43-7.50 (m, 1H), 7.51-7.59 (m, 2H), 7.63-7.78 (m, 3H). **¹³C-NMR** (75 MHz, DMSO-*d*₆): δ (ppm) 55.5, 114.3, 118.8, 122.4, 128.8, 129.8, 129.9, 133.0, 137.1, 138.5, 159.4, 195.8. **HRMS** (EIC): *m/z* [M]⁺ calcd. for [C₁₄H₁₃O₂]⁺ 212.0832, found 212.0830. C₁₄H₁₂O₂ (212.25).



(2-Hydroxyphenyl)(phenyl)methanone (4.42). Compound **4.42** was prepared using *general procedure C* and the reactant (2-methoxyphenyl)(phenyl)methanone (**4.40**) (0.89 g, 4.19 mmol). **4.42** was obtained as an oil (0.83 g, 4.19 mmol, 100%). **Anal. calcd.** for C₁₃H₁₀O₂·H₂O: C 78.06, H 5.14, found: C 78.15, H 5.17. **¹H-NMR** (300 MHz, DMSO-*d*₆): δ (ppm) 6.90-7.04 (m, 2H), 7.32-7.40 (m, 1H), 7.41-7.57 (m, 3H), 7.60-7.68 (m, 1H), 7.68-7.75 (m, 2H), 10.49 (s, 1H). **¹³C-NMR** (75 MHz, DMSO-*d*₆): δ (ppm) 116.8, 119.1, 124.3, 128.5, 129.2, 130.6, 132.8, 133.5, 137.4, 157.3, 197.8. **HRMS** (EIC): *m/z* [M+H]⁺ calcd. for [C₁₃H₁₁O₂]⁺ 199.0754, found 199.0762. C₁₃H₁₀O₂ (198.22).

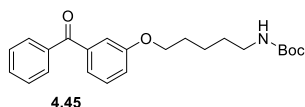


(3-Hydroxyphenyl)(phenyl)methanone (4.43). Compound **4.43** was prepared using *general procedure C* and the reactant (3-methoxyphenyl)(phenyl)methanone (**4.41**) (0.76 g, 3.58 mmol). **4.43** was obtained as a grey solid (0.67 g, 3.38 mmol, 94%). **Anal. calcd.** for C₁₃H₁₀O₂·0.1 H₂O: C 78.06, H 5.14, found: C 78.10, H 5.23. **¹H-NMR** (300 MHz, DMSO-*d*₆): δ (ppm) 7.03-7.10 (m, 1H), 7.11-7.18 (m, 2H), 7.31-7.42 (m, 1H), 7.50-7.62 (m, 2H), 7.63-7.78 (m, 3H), 9.86 (s, 1H). **¹³C-NMR** (75 MHz, DMSO-*d*₆): δ (ppm) 116.0, 119.9, 120.6, 128.5, 129.5, 129.7, 132.6, 137.3, 138.3, 157.4, 195.8. **HRMS** (EIC): *m/z* [M]⁺ calcd. for [C₁₃H₁₀O₂]⁺ 198.0675, found 198.0676. C₁₃H₁₀O₂ (198.22).

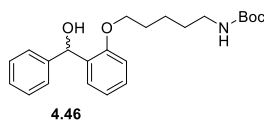


tert-Butyl (5-(2-benzoylphenoxy)pentyl)carbamate (4.44). Compound **4.44** was prepared using *general procedure D* and the reactants (2-hydroxyphenyl)(phenyl)methanone (**4.42**) (0.15 g, 0.76 mmol), K₂CO₃ (0.37 g, 2.68 mmol) and *tert*-butyl (5-bromopentyl)(methyl)carbamate (**4.35**) (0.75 g, 2.67 mmol). The crude product was purified by column chromatography (eluent: light petroleum/ethyl

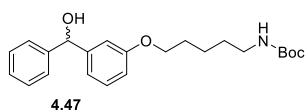
acetate 9:1 to 8:2) to give **4.44** as an orange oil (0.44 g, 1.11 mmol, 49%). **Anal. calcd.** for $C_{23}H_{29}NO_4$: C 72.04, H 7.62, N 3.65, found: C 72.08, H 7.62, N 3.20. **1H -NMR** (400 MHz, $DMSO-d_6$): δ (ppm) 0.80-0.93 (m, 2H), 1.08-1.20 (m, 2H), 1.25-1.33 (m, 2H), 1.36 (s, 9H), 2.67-2.78 (m, 2H), 3.86 (t, $J = 6.1$ Hz, 2H), 6.68 (t, $J = 5.4$ Hz, 1H), 7.02-7.17 (m, 2H), 7.32-7.38 (m, 1H), 7.44-7.56 (m, 3H), 7.58-7.69 (m, 3H). **^{13}C -NMR** (101 MHz, $DMSO-d_6$): δ (ppm) 22.4, 28.1, 28.3, 29.0, 39.6 (overlaid by solvent residual peak), 67.6, 77.3, 112.7, 120.6, 128.51, 128.53, 128.9, 129.0, 132.3, 133.0, 137.8, 155.5, 156.3, 196.2. **HRMS** (ESI): m/z $[M+H]^+$ calcd. for $[C_{23}H_{30}NO_4]^+$ 384.2169, found 384.2174. $C_{23}H_{29}NO_4$ (383.49).



tert-Butyl (5-(3-benzoylphenoxy)pentyl)carbamate (4.45). Compound **4.45** was prepared using *general procedure D* and the reactants (3-hydroxyphenyl)(phenyl)methanone (**4.43**) (0.49 g, 2.47 mmol), K_2CO_3 (0.70 g, 5.06 mmol) and *tert*-butyl (5-bromopentyl)carbamate **4.35** (0.69 g, 18.1 mmol). The crude product was purified by column chromatography (eluent: light petroleum/ethyl acetate 8:2) to give **4.45** as a yellow oil (0.45 g, 1.17 mmol, 47%). **1H -NMR** (400 MHz, $DMSO-d_6$): δ (ppm) 1.36 (s, 9H), 1.37-1.48 (m, 4H), 1.66-1.77 (m, 2H), 2.88-2.96 (m, 2H), 3.97-4.03 (m, 2H), 6.78 (t, $J = 5.5$ Hz, 1H), 7.19-7.28 (m, 3H), 7.42-7.49 (m, 1H), 7.52-7.60 (m, 2H), 7.64-7.70 (m, 1H), 7.71-7.77 (m, 2H). **^{13}C -NMR** (101 MHz, $DMSO-d_6$): δ (ppm) 22.8, 28.3 (two carbon signals), 29.2, 40.1 (overlaid by solvent residual peak), 67.6, 77.3, 114.7, 119.0, 122.0, 128.5, 129.6, 129.7, 132.7, 137.0, 138.4, 155.6, 158.6, 195.5. **HRMS** (ESI): m/z $[M+Na]^+$ calcd. for $[C_{23}H_{29}NO_4Na]^+$ 406.1989, found 406.1993. $C_{23}H_{29}NO_4$ (383.49).

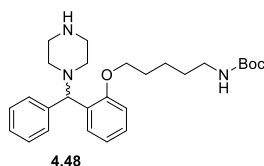


tert-Butyl (5-(2-(hydroxy(phenyl)methyl)phenoxy)pentyl)carbamate (4.46). Compound **4.46** was prepared using *general procedure E* and the reactants *tert*-butyl (5-(2-benzoylphenoxy)pentyl)carbamate (**4.44**) (0.45 g, 1.17 mmol) and $NaBH_4$ (0.095 g, 2.51 mmol). The crude product was purified by column chromatography (eluent: light petroleum/ethyl acetate 7:3) to give **4.46** as a yellow oil (0.25 g, 0.65 mmol, 56%). **1H -NMR** (400 MHz, $DMSO-d_6$): δ (ppm) 1.30-1.46 (m, 13H), 1.63-1.73 (m, 2H), 2.87-2.96 (m, 2H), 3.90 (t, $J = 6.1$ Hz, 2H), 5.61 (d, $J = 4.3$ Hz, 1H), 5.96 (d, $J = 4.3$ Hz, 1H), 6.78 (t, $J = 5.4$ Hz, 1H), 6.87-6.97 (m, 2H), 7.12-7.20 (m, 2H), 7.22-7.28 (m, 2H), 7.30-7.35 (m, 2H), 7.50-7.55 (m, 1H). **^{13}C -NMR** (101 MHz, $DMSO-d_6$): δ (ppm) 23.0, 28.3, 28.5, 29.2, 39.9 (overlaid by solvent residual peak), 67.4, 68.2, 77.4, 111.3, 120.1, 126.3, 126.47, 126.50, 127.75, 127.79, 133.7, 145.4, 154.8, 155.6. **HRMS** (ESI): m/z $[M+Na]^+$ calcd. for $[C_{23}H_{31}NO_4Na]^+$ 408.2145, found 408.2151. $C_{23}H_{31}NO_4$ (385.50).

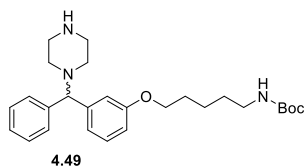


tert-Butyl (5-(3-(hydroxy(phenyl)methyl)phenoxy)pentyl)carbamate (4.47). Compound **4.47** was prepared using *general procedure E* and the reactants (*tert*-butyl (5-(3-benzoylphenoxy)pentyl)-

carbamate (**4.45**) (0.45 g, 1.17 mmol and NaBH₄ (95 mg, 2.51 mmol). The crude product was purified by column chromatography (eluent: light petroleum/ethyl acetate 7:3) to give **4.47** as a yellow oil (0.25 g, 0.65 mmol, 56%). **Anal. calcd.** for C₂₃H₃₁NO₄: C 71.66, H 8.11, N 3.63, found: C 71.59, H 7.86, N 3.41. **¹H-NMR** (300 MHz, DMSO-*d*₆): δ (ppm) 1.31-1.36 (m, 1H), 1.37 (s, 9H, interfering with surrounded signals), 1.38-1.49 (m, 3H), 1.60-1.74 (m, 2H), 2.86-2.99 (m, 2H), 3.89 (t, *J* = 6.4 Hz, 2H), 5.64 (d, *J* = 4.1 Hz, 1H), 5.86 (d, *J* = 4.1 Hz, 1H), 6.70-6.77 (m, 1H), 6.80 (t, *J* = 5.5 Hz, 1H), 6.88-6.95 (m, 2H), 7.14-7.24 (m, 2H), 7.25-7.33 (m, 2H), 7.34-7.41 (m, 2H). **¹³C-NMR** (75 MHz, DMSO-*d*₆): δ (ppm) 22.9, 28.3, 28.4, 29.3, 67.2, 74.1, 77.3, 112.35, 112.37, 118.4, 126.4, 126.7, 128.0, 129.1, 145.7, 147.4, 155.6, 158.5. One aliphatic carbon signal was not apparent (overlaid by solvent residual peak). **HRMS** (ESI): *m/z* [M+Na]⁺ calcd. for [C₂₃H₃₁NO₄Na]⁺ 408.2145, found 408.2146. C₂₃H₃₁NO₄ (385.50).

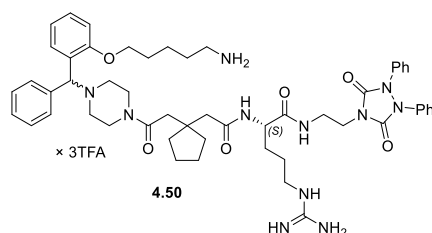


tert-Butyl (5-(2-(phenyl(piperazin-1-yl)methyl)phenoxy)pentyl)carbamate (4.48). Compound **4.48** was prepared using *general procedure F* and the reactants *tert*-butyl (5-(2-(hydroxy(phenyl)methyl)-phenoxy)pentyl)carbamate (**4.46**) (180 mg, 0.467 mmol), Et₃N (150 μL, 1.08 mmol), methanesulfonyl chloride (100 μL, 1.29 mmol) and piperazine (165 mg, 1.92 mmol). The crude product was purified by column chromatography (eluent: CH₂Cl₂/MeOH/NH₃ aq 90:9:1) to give **4.48** as a yellow oil (140 mg, 0.31 mmol, 66%). **¹H-NMR** (400 MHz, DMSO-*d*₆): δ (ppm) 1.34-1.48 (m, 13H), 1.68-1.79 (m, 2H), 2.11-2.34 (m, 4H), 2.61-2.83 (m, 4H), 2.92-2.99 (m, 2H), 3.82-3.95 (m, 2H), 4.67 (s, 1H), 6.76-6.85 (m, 1H), 6.86-6.98 (m, 2H), 7.08-7.19 (m, 2H), 7.22-7.29 (m, 2H), 7.30-7.39 (m, 2H), 7.49-7.61 (m, 1H). One exchangeable proton signal (NH-piperazine) was not apparent. **¹³C-NMR** (101 MHz, DMSO-*d*₆): δ (ppm) 23.1, 28.3, 28.5, 29.2, 40.38 (overlaid by solvent residual peak), 45.0, 46.1, 52.7, 67.5, 77.3, 111.9, 120.4, 126.6, 127.4, 127.5, 128.0, 128.2, 130.4, 142.4, 155.6, 165.1. **HRMS** (ESI): *m/z* [M+Na]⁺ calcd. for [C₂₇H₃₉N₃O₃Na]⁺ 476.2884, found 476.2900. C₂₇H₃₉N₃O₃ (453.63).

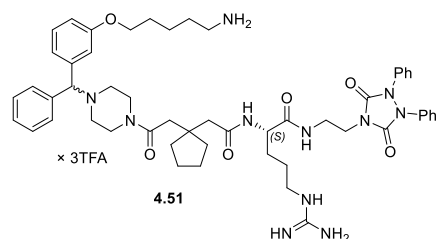


tert-Butyl (5-(3-(phenyl(piperazin-1-yl)methyl)phenoxy)pentyl)carbamate (4.49). Compound **4.49** was prepared using *general procedure F* and the reactants *tert*-butyl (5-(3-(hydroxy(phenyl)methyl)-phenoxy)pentyl)carbamate (**4.47**) (170 mg, 0.441 mmol), Et₃N (150 μL, 1.08 mmol), methanesulfonyl chloride (50 μL, 0.646 mmol) and piperazine (167 mg, 1.94 mmol). The crude product was purified by column chromatography (eluent: CH₂Cl₂/MeOH/NH₃ aq 90:9:1) to give **4.49** as a yellow oil (96 mg, 0.212 mmol, 48%). **¹H-NMR** (400 MHz, DMSO-*d*₆): δ (ppm) 1.33-1.44 (m, 13H), 1.62-1.71 (m, 2H), 2.18-2.35 (m, 4H), 2.41 (br s, 1H), 2.74-2.98 (m, 6H), 3.84-3.92 (m, 2H), 4.23 (s, 1H), 6.68-6.75 (m, 1H), 6.75-6.81 (m, 1H), 6.91-7.00 (m, 2H), 7.13-7.21 (m, 2H), 7.24-7.32 (m, 2H), 7.35-7.45 (m, 2H). **¹³C-NMR** (101 MHz, DMSO-*d*₆): δ (ppm) 22.9, 28.3, 28.4, 29.3, 44.9, 51.5, 67.2, 75.2, 77.3, 112.3, 113.8, 119.7, 126.9, 127.6, 128.5, 129.6, 142.5, 144.2, 155.6, 158.7. One aliphatic carbon signal was not apparent

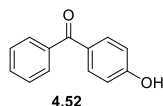
(overlaid by solvent residual peak). **HRMS** (ESI): m/z $[M+Na]^+$ calcd. for $[C_{27}H_{39}N_3O_3Na]^+$ 476.2884, found 476.2879. $C_{27}H_{39}N_3O_3$ (453.63).



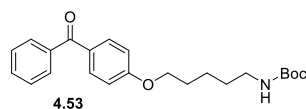
(2S)-N²-(2-{1-[2-(4-((2-(5-Aminopentyl)oxy)phenyl)(phenyl)methyl)piperazin-1-yl]-2-oxoethyl]-cyclopentyl}acetyl)[2-(3,5-dioxo-1,2-diphenyl-1,2,4-triazolidin-4-yl)ethyl]argininamide tris(hydrotrifluoroacetate) (4.50). Compound **4.50** was prepared using *general procedure G* and the reactants (S)-2-(1-(2-((1-((2-(3,5-dioxo-1,2-diphenyl-1,2,4-triazolidin-4-yl)ethyl)amino)-1-oxo-5-(2-((2,2,4,6,7-pentamethyl-2,3-dihydrobenzofuran-5-yl)sulfonyl)guanidino)pentan-2-yl)amino)-2-oxoethyl)cyclopentyl)acetic acid (**4.15**) (70 mg, 76 μ mol), EDC·HCl (20 mg, 104 μ mol), HOBT (10 mg, 74 μ mol) and *tert*-butyl (5-(2-(phenyl(piperazin-1-yl)methyl)phenoxy)pentyl)carbamate (**4.48**) (30 mg, 66 μ mol). Purification by preparative HPLC A (gradient: 0-30 min, A/B 84:16–38:62, t_R = 14 min) gave **4.50** as a fluffy white solid (16 mg, 12 μ mol, 18%). Ratio of diastereomers evident in NMR spectra recorded in MeOH- d_4 : 1:1. **¹H-NMR** (600 MHz, MeOH- d_4): δ (ppm) 1.45-1.81 (m, 17H), 1.83-1.94 (m, 2H), 2.27-2.33 (m, 1H), 2.48-2.58 (m, 2H), 2.59-2.67 (m, 1H), 2.88-3.10 (m, 5H), 3.11-3.28 (m, 2H), 3.34-3.41 (m, 1H), 3.42-3.48 (m, 1H), 3.50-3.57 (m, 1H), 3.71-4.03 (m, 5H), 4.03-4.16 (m, 1H), 4.11-4.16 (m, 1H), 4.21-4.26 (m, 1H), 5.74 (s, 0.5H), 5.75 (s, 0.5H), 7.06-7.13 (m, 2H), 7.19-7.24 (m, 2H), 7.31-7.36 (m, 4H), 7.36-7.48 (m, 8H), 7.59-7.64 (m, 2H), 7.75-7.80 (m, 1H). **¹H-NMR** (600 MHz, DMSO- d_6): 1.33-1.65 (m, 17H), 1.70-1.79 (m, 2H), 2.18-2.25 (m, 1H), 2.28-2.37 (m, 1H), 2.38-2.47 (m, 1H), 2.53-2.61 (m, 1H), 2.75-2.83 (m, 2H), 2.94-3.02 (m, 2H), 3.26-3.32 (m, 1H), 3.34-3.39 (m, 1H), 3.49-3.79 (m, 5H), 3.88-4.18 (m, 7H), 5.59 (br s, 1H), 6.83-7.54 (m, 23H), 7.62-7.78 (m, 2H), 7.82 (s, 3H), 7.96 (d, J = 7.8 Hz, 1H), 8.21 (t, J = 5.5 Hz, 1H). **¹³C-NMR** (150 MHz, MeOH- d_4): δ (ppm) 23.9, 24.0, 24.57, 24.63 (two carbon signals), 26.31, 26.32, 28.23, 28.25, 29.54, 29.56, 30.01, 30.05, 38.25, 38.28, 39.2, 39.3, 39.36, 39.38, 39.4, 39.9, 40.0, 40.6, 40.7, 41.15, 41.19, 41.8, 44.0, 44.29, 44.31, 45.59, 45.63, 52.7, 52.8, 53.0 (2 carb.), 54.07, 54.11, 69.12, 69.13, 70.3, 70.4, 69.12, 69.14, 70.29, 70.43, 113.8, 118.1 (q, J = 293 Hz) (TFA), 122.4 (2 carb.), 123.8, 124.22, 124.24, 128.20, 128.22, 128.53, 128.58, 130.0, 130.1, 130.2, 130.5 (2 carb.), 160.6 (2 carb.), 131.86, 131.89, 135.4, 137.65, 137.67, 154.5, 157.27, 157.31, 158.61, 158.66, 162.7 (q, J = 35.0 Hz) (TFA), 172.91, 172.92, 174.7 (2 carb.), 174.8. **RP-HPLC** (220 nm): 97% (t_R = 11.4 min, k = 3.4). **HRMS** (ESI): m/z $[M+H]^+$ calcd. for $[C_{53}H_{70}N_{11}O_6]^+$ 956.5505, found 956.5507. $C_{53}H_{69}N_{11}O_6 \times C_6H_3F_9O_6$ (956.21 + 342.07).



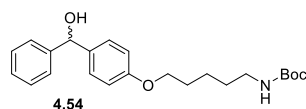
(2S)-N²-(2-{1-[2-(4-((3-((5-Aminopentyl)oxy)phenyl)(phenyl)methyl)piperazin-1-yl]-2-oxoethyl]-cyclopentyl}acetyl)[2-(3,5-dioxo-1,2-diphenyl-1,2,4-triazolidin-4-yl)ethyl]argininamide tris(hydrotrifluoroacetate) (4.51**).** Compound **4.51** was prepared using *general procedure G* and the reactants (S)-2-(1-(2-((1-((2-(3,5-dioxo-1,2-diphenyl-1,2,4-triazolidin-4-yl)ethyl)amino)-1-oxo-5-(2-((2,2,4,6,7-pentamethyl-2,3-dihydrobenzofuran-5-yl)sulfonyl)guanidino)pentan-2-yl)amino)-2-oxoethyl)cyclopentyl)acetic acid (**4.15**) (71 g, 77 μmol), EDC·HCl (24 mg, 125 μmol), HOBT (18 mg, 133.2 μmol) and *tert*-butyl (5-(3-(phenyl(piperazin-1-yl)methyl)phenoxy)pentyl)carbamate (**4.49**) (34 mg, 75 μmol). Purification by preparative HPLC A (gradient: 0-35 min, A/B 66:34–47:53, *t_R* = 8 min) gave **4.51** as a fluffy white solid (16 mg, 12 μmol, 16%). **¹H-NMR** (600 MHz, MeOH-*d*₄): δ (ppm) 1.45-1.88 (m, 19H), 2.26-2.31 (m, 1H), 2.49-2.56 (m, 2H), 2.58-2.63 (m, 1H), 2.91-3.12 (m, 6H), 3.13-3.25 (m, 2H), 3.42-3.49 (m, 1H), 3.53-3.61 (m, 1H), 3.72-4.14 (m, 7H), 4.23-4.26 (m, 1H), 5.28 (s, 1H), 6.94-6.98 (m, 1H), 7.16-7.24 (m, 3H), 7.28-7.30 (m, 1H), 7.31-7.43 (m, 10H), 7.45-7.49 (m, 2H), 7.66-7.70 (m, 2H). **¹H-NMR** (600 MHz, DMSO-*d*₆): δ (ppm) 1.32-1.67 (m, 17H), 1.68-1.75 (m, 2H), 2.20-2.26 (m, 1H), 2.33-2.39 (m, 1H), 2.43-2.48 (m, 1H), 2.55-2.64 (m, 1H), 2.64-2.94 (m, 5H), 2.94-3.06 (m, 3H), 3.26-3.36 (m, 1H), 3.34-3.41 (m, 1H), 3.42-3.88 (m, 5H), 3.89-3.99 (m, 2H), 4.09-4.18 (m, 1H), 4.86 (br s, 1H), 6.78-7.44 (m, 22H), 7.56 (br s, 2H), 7.67-7.72 (m, 1H), 7.78 (br s, 3H), 7.93-7.98 (m, 1H), 8.21 (t, *J* = 5.9 Hz, 1H). **¹³C-NMR** (150 MHz, MeOH-*d*₄): δ (ppm) 24.1 (two carbon signals), 24.58 (2 carb.), 24.62, 26.3, 28.3, 29.7 (2 carb.), 30.1, 38.2, 39.2, 39.4 (2 carb.), 39.9, 40.6, 41.2 (2 carb.), 41.9, 44.1 (2 carb.), 44.3 (2 carb.), 45.64, 45.65, 52.8, 53.1, 54.0, 68.8, 76.9, 114.82, 114.85, 116.57, 116.60, 117.1 (TFA), 119.0 (TFA), 121.46, 121.50, 124.3, 128.3, 129.3 (2 carb.), 130.2, 130.6, 130.7, 131.9, 136.2, 137.7, 154.5, 158.6, 158.7, 161.4, 162.5 (TFA), 162.7 (TFA), 172.9, 174.7. **RP-HPLC** (220 nm): 100% (*t_R* = 11.8 min, *k* = 3.6). **HRMS** (ESI): *m/z* [M+H]⁺ calcd. for [C₅₃H₇₀N₁₁O₆]⁺ 956.5505, found 956.5514. C₅₃H₆₉N₁₁O₆ × C₆H₃F₉O₆ (956.21 + 342.07).



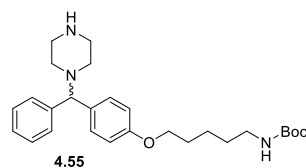
(4-Hydroxyphenyl)(phenyl)methanone (4.52**).** Compound **4.52** was prepared using *general procedure C* and the reactant (4-methoxyphenyl)(phenyl)methanone (**4.25**) (2.04 g, 9.61 mmol). **4.52** was obtained as a rose solid (183 g, 9.23 mmol, 96%). **¹H-NMR** (300 MHz, DMSO-*d*₆): δ (ppm) 6.86-6.95 (m, 2H), 7.48-7.57 (m, 2H), 7.58-7.72 (m, 5H), 10.45 (s, 1H). **¹³C-NMR** (75 MHz, DMSO-*d*₆): δ (ppm) 115.3, 127.9, 128.4, 129.2, 131.8, 132.5, 138.1, 162.0, 194.3. **HRMS** (EIC): *m/z* [M]⁺ calcd. for [C₁₃H₁₀O₂]⁺ 198.0675, found 198.0678. C₁₃H₁₀O₂ (198.22).



tert-Butyl (5-(4-benzoylphenoxy)pentyl)carbamate (4.53). Compound **4.53** was prepared using *general procedure D* and the reactants (4-hydroxyphenyl)(phenyl)methanone (**4.52**) (0.16 g, 0.81 mmol), K_2CO_3 (0.24 g, 1.74 mmol) and *tert*-butyl (5-bromopentyl)carbamate (**4.35**) (0.45 g, 1.70 mmol). The crude product was purified by column chromatography (eluent: light petroleum/ethyl acetate 2:1) to give **4.53** as a yellow oil (0.22 g, 0.57 mmol, 70%). **Anal. calcd.** for $C_{23}H_{29}NO_4$: C 72.04, H 7.62, N 3.65, found: C 71.75, H 7.23, N 3.43. **1H -NMR** (300 MHz, $DMSO-d_6$): δ (ppm) 1.37 (s, 9H), 1.38-1.48 (m, 4H), 1.66-1.79 (m, 2H), 2.87-2.99 (m, 2H), 4.05 (t, $J = 6.4$ Hz, 2H), 6.81 (t, $J = 5.5$ Hz, 1H), 7.02-7.13 (m, 2H), 7.49-7.59 (m, 2H), 7.61-7.77 (m, 5H). **^{13}C -NMR** (75 MHz, $DMSO-d_6$): δ (ppm) 22.8, 28.2, 28.3, 29.2, 39.7 (overlaid by solvent residual peak), 67.9, 77.3, 114.3, 128.4, 129.19, 129.24, 132.1, 132.2, 137.8, 155.6, 162.5, 194.4. **HRMS** (ESI): m/z $[M+H]^+$ calcd. for $[C_{23}H_{30}NO_4]^+$ 384.2169, found 384.2169. $C_{23}H_{29}NO_4$ (383.49).

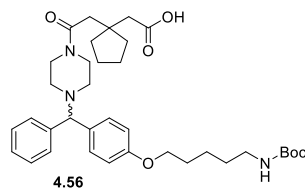


tert-Butyl (5-(4-(hydroxy(phenyl)methyl)phenoxy)pentyl)carbamate (4.54). Compound **4.54** was prepared using *general procedure E* and the reactants *tert*-butyl (5-(3-benzoylphenoxy)pentyl)carbamate (**4.53**) (100 mg, 0.26 mmol) and $NaBH_4$ (25 mg, 0.66 mmol). The crude product was purified by column chromatography (eluent: light petroleum/ethyl acetate 7:3) to give **4.54** as a yellow oil (100 mg, 0.26 mmol, 100%). **1H -NMR** (300 MHz, $DMSO-d_6$): δ (ppm) 1.01-1.46 (m, 13H), 1.61-1.73 (m, 2H), 2.86-2.96 (m, 2H), 3.89 (t, $J = 6.4$ Hz, 2H), 5.63 (s, 1H), 5.76 (s, 1H), 6.77-6.87 (m, 3H), 7.16-7.37 (m, 7H). **^{13}C -NMR** (75 MHz, $DMSO-d_6$): δ (ppm) 22.9, 28.3, 28.4, 29.2, 40.1 (overlaid by solvent residual peak), 67.3, 73.8, 77.3, 113.9, 126.1, 126.6, 127.4, 128.0, 137.7, 146.0, 155.6, 157.5. **HRMS** (ESI): m/z $[M+Na]^+$ calcd. for $[C_{32}H_{31}NO_4Na]^+$ 408.2145, found 408.2153. $C_{23}H_{31}NO_4$ (385.50).

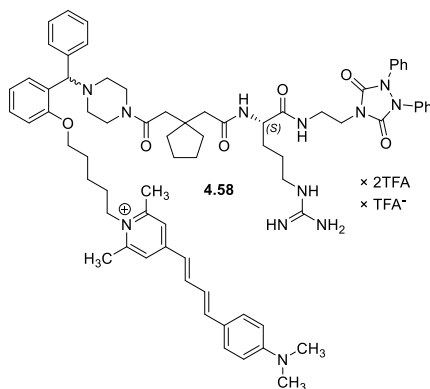


tert-Butyl (5-(4-(phenyl(piperazin-1-yl)methyl)phenoxy)pentyl)carbamate (4.55). Compound **4.55** was prepared using *general procedure F* and the reactants *tert*-butyl (5-(4-(hydroxy(phenyl)methyl)phenoxy)pentyl)carbamate (**4.54**) (100 mg, 0.259 mmol), Et_3N (100 μ L, 0.720 mmol), methanesulfonyl chloride (20 μ L, 0.258 mmol) and piperazine (160 mg, 1.86 mmol). The crude product was purified by column chromatography (eluent: $CH_2Cl_2/MeOH/NH_3$ aq. 90:9:1) to give **4.55** as a yellow oil (57 mg, 0.126 mmol, 49%). **1H -NMR** (300 MHz, $DMSO-d_6$): δ (ppm) 1.29-1.44 (m, 13H), 1.58-1.73 (m, 2H), 2.14-2.35 (m, 4H), 2.63-2.79 (m, 4H), 2.85-2.97 (m, 2H), 3.87 (t, $J = 6.3$ Hz, 2H), 4.16 (s, 1H), 6.77-6.83 (m, 3H), 7.11-7.19 (m, 1H), 7.21-7.33 (m, 4H), 7.34-7.44 (m, 2H). Exchangeable proton signal (NH -piperazine) was not apparent. **^{13}C -NMR** (75 MHz, $DMSO-d_6$): δ (ppm) 22.9, 28.3, 28.4, 29.2, 45.6, 52.7, 67.2, 75.0, 77.3, 114.3, 126.6, 127.5, 128.4, 128.7, 134.6, 143.3, 155.6, 157.5. One aliphatic carbon

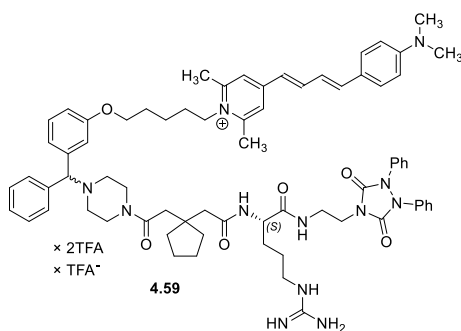
signal was not apparent (overlaid by solvent residual peak). **HRMS** (ESI): m/z $[M+H]^+$ calcd. for $[C_{27}H_{40}N_3O_3]^+$ 454.3064, found 454.3064. $C_{27}H_{39}N_3O_3$ (453.63).



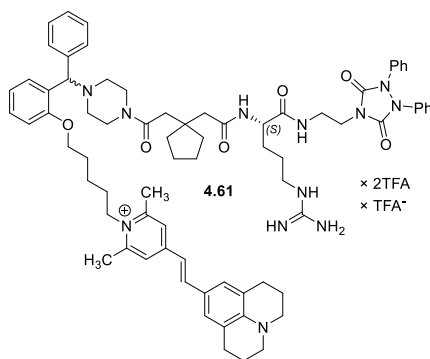
2-(1-(2-(4-((4-((5-((*tert*-Butoxycarbonyl)amino)pentyl)oxy)phenyl)(phenyl)methyl)piperazin-1-yl)-2-oxoethyl)cyclopentyl)acetic acid (4.56**).** *tert*-Butyl (5-(4-(phenyl(piperazin-1-yl)methyl)phenoxy)pentyl)carbamate (**4.55**) (23 mg, 50.7 μ mol) was dissolved in CH_2Cl_2 (5 mL) and the mixture was stirred in an ice bath. Under stirring, 3,3-tetramethylene-glutaric anhydride (**4.14**) (8.53 mg, 50.7 μ mol) in CH_2Cl_2 (1 mL) was added dropwise to the mixture over a time period of 5 min. The reaction mixture was allowed to warm to rt and stirred overnight at rt. The solvent was evaporated, and the crude product was purified by column chromatography (eluent: $CH_2Cl_2/MeOH$ 90:10) to give **4.56** as an oil (30.4 mg, 48.8 μ mol, 96%). **¹H-NMR** (400 MHz, $DMSO-d_6$): δ (ppm) 1.29-1.40 (m, 12H), 1.42-1.48 (m, 3H), 1.49-1.58 (m, 8H), 2.18-2.29 (m, 4H), 2.42 (s, 2H), 2.48 (s, 2H, interfering with solvent residual peak), 2.86-2.95 (m, 2H), 3.40-3.53 (m, 4H), 3.88 (t, $J = 6.2$ Hz, 2H), 4.23 (s, 1H), 6.74-6.80 (m, 1H), 6.81-6.87 (m, 2H), 7.14-7.22 (m, 1H), 7.25-7.33 (m, 4H), 7.38-7.44 (m, 2H), 11.98 (br s, 1H). **¹³C-NMR** (101 MHz, $DMSO-d_6$): δ (ppm) 22.8, 23.6, 28.4, 29.2, 36.8, 37.5, 36.8, 37.5, 39.7 (overlaid by solvent residual peak), 40.9, 43.0, 45.4, 67.2, 74.1, 77.3, 114.4, 126.7, 127.4, 128.5, 128.7, 134.2, 143.0, 155.6, 157.6, 167.6, 169.6. **HRMS** (ESI): m/z $[M+Na]^+$ calcd. for $[C_{36}H_{51}N_3O_6Na]^+$ 644.3670, found 644.3669. $C_{36}H_{51}N_3O_6$ (621.82).



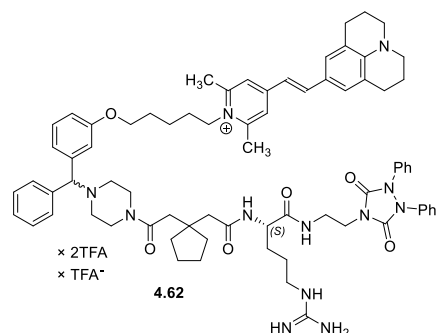
(2S)-N⁺-(2-{1-[2-(4-((3-((5-(4-((1*E*,3*E*)-4-(4-(Dimethylamino)phenyl)buta-1,3-dien-1-yl)-2,6-dimethylpyridinio)pentyl)oxy)phenyl)(phenyl)methyl)piperazin-1-yl)-2-oxoethyl]cyclopentyl}acetyl)[2-(3,5-dioxo-1,2-diphenyl-1,2,4-triazolidin-4-yl)ethyl]argininamide bis(hydrotrifluoroacetate) trifluoroacetate (4.58**).** Compound **4.58** was prepared using *general procedure H* and the reactants **4.50** (4.21 mg, 3.24 μ mol), DIPEA (2.1 μ L, 12.3 μ mol) and **2.77** (3.77 mg, 10.3 μ mol). Purification by preparative HPLC B (gradient: 0-30 min, A/B 76:24–38:62, $t_R = 20$ min) afforded **4.58** as a fluffy red solid (0.954 mg, 0.611 μ mol, 19%). **RP-HPLC** (Method A, 220 nm): 95% ($t_R = 14.6$ min, $k = 4.7$). **HRMS** (ESI): m/z $[M]^+$ calcd. for $[C_{72}H_{89}N_{12}O_6]^+$ 1217.7023, found 1217.7021. $C_{72}H_{89}N_{12}O_6^+ \times C_4H_2F_6O_2 \times C_2F_3O_2^-$ (1218.58 + 228.04 + 112.02).



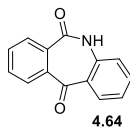
(2S)-N²-(2-{1-[2-(4-((3-((5-(4-((1E,3E)-4-(4-(Dimethylamino)phenyl)buta-1,3-dien-1-yl)-2,6-dimethylpyridinio)pentyl)oxy)phenyl)(phenyl)methyl)piperazin-1-yl]-2-oxoethyl}cyclopentyl)acetyl)[2-(3,5-dioxo-1,2-diphenyl-1,2,4-triazolidin-4-yl)ethyl]argininamide bis(hydrotrifluoroacetate) trifluoroacetate (4.59). Compound **4.59** was prepared using *general procedure H* and the reactants **4.51** (4.06 mg, 3.12 μmol), DIPEA (2.2 μL, 12.9 μmol) and **2.77** (4.50 mg, 12.3 μmol). Purification by preparative HPLC B (gradient: 0-35 min, A/B 85:15–38:62, $t_R = 23$ min) afforded **4.59** as a fluffy red solid (2.192 mg, 1.40 μmol, 45%). **RP-HPLC** (Method A, 220 nm): 95% ($t_R = 15.3$ min, $k = 5.0$). **HRMS** (ESI): m/z [M]⁺ calcd. for [C₇₂H₈₉N₁₂O₆]⁺ 1217.7023, found 1217.7027. C₇₂H₈₉N₁₂O₆⁺ × C₄H₂F₆O₂ × C₂F₃O₂⁻ (1218.58 + 228.04 + 112.02).



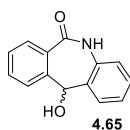
(2S)-N²-(2-{1-[2-(4-((2-((5-(2,6-Dimethyl-4-(1E)-(2-(2,3,6,7-tetrahydro-1H,5H-pyrido[3,2,1-ij]quinolin-9-yl)vinyl)pyridinio)pentyl)oxy)phenyl)(phenyl)methyl)piperazin-1-yl]-2-oxoethyl}cyclopentyl)acetyl)[2-(3,5-dioxo-1,2-diphenyl-1,2,4-triazolidin-4-yl)ethyl]argininamide bis(hydrotrifluoroacetate) trifluoroacetate (4.61). Compound **4.61** was prepared using *general procedure H* and the reactants **4.50** (4.01 mg, 3.09 μmol), DIPEA (2.2 μL, 12.9 μmol) and **4.60** (3.01 mg, 7.65 μmol). Purification by preparative HPLC B (gradient: 0-35 min, A/B 85:15–38:62, $t_R = 27$ min) afforded **4.61** as a fluffy red solid (2.19 mg, 1.38 μmol, 45%). **RP-HPLC** (Method A, 220 nm): 92% ($t_R = 15.8$ min, $k = 5.2$). **HRMS** (ESI): m/z [M]⁺ calcd. for [C₇₄H₉₁N₁₂O₆]⁺ 1243.7179, found 1243.7187. C₇₄H₉₁N₁₂O₆⁺ × C₄H₂F₆O₂ × C₂F₃O₂⁻ (1244.62 + 228.04 + 112.02).



(2S)-N^F-(2-{1-[2-(4-((3-((5-(2,6-Dimethyl-4-(1*E*)-(2-(2,3,6,7-tetrahydro-1*H*,5*H*-pyrido[3,2,1-*ij*]quinolin-9-yl)vinyl)pyridinio)pentyl)oxy)phenyl)(phenyl)methyl)piperazin-1-yl)-2-oxoethyl]cyclopentyl} acetyl)[2-(3,5-dioxo-1,2-diphenyl-1,2,4-triazolidin-4-yl)ethyl]argininamide bis(hydrotrifluoroacetate) trifluoroacetate (**4.62**). Compound **4.62** was prepared using *general procedure H* and the reactants **4.51** (4.30 mg, 3.31 μmol), DIPEA (2.4 μL, 14.1 μmol) and **4.60** (2.70 mg, 6.87 μmol). Purification by preparative HPLC B (gradient: 0-35 min, A/B 85:15-38:62, *t_R* = 28 min) afforded **4.62** as a fluffy red solid (0.817 mg, 0.515 μmol, 16%). **RP-HPLC** (Method A, 220 nm): 91% (*t_R* = 16.8 min, *k* = 5.5). **HRMS** (ESI): *m/z* [M]⁺ calcd. for [C₇₄H₉₁N₁₂O₆]⁺ 1243.7179, found 1243.7179. C₇₄H₉₁N₁₂O₆⁺ × C₄H₂F₆O₂ × C₂F₃O₂⁻ (1244.62 + 228.04 + 112.02).

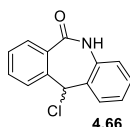


5*H*-Dibenzo[b,e]azepine-6,11-dione (4.64).¹⁴ Anthraquinone (**4.63**) (25.2 g, 121 mmol) and sodium azide (9.70 g, 149 mmol) were suspended in chloroform (250 mL) and cooled in an ice bath. Under stirring, conc. H₂SO₄ (72 mL) was added dropwise to the suspension. The reaction mixture was refluxed overnight. Then, the reaction mixture was allowed to cool to rt and added carefully to a potassium carbonate solution (900 mL, 10%). Consecutively, the aqueous solution was basified with ammonium hydroxide and a solid precipitated. The precipitate was separated by decantation and methanol (320 mL) was added. Then, the solid was separated by filtration and washed with Et₂O. The crude product was purified by recrystallization from hot acetic acid. The solid was dried *in vacuo* (60 °C) to obtain **4.64** as a white solid (16.0 g, 71.6 mmol, 59%). **Anal. calcd.** for C₁₄H₉NO₂·0.2 H₂O: C 74.13, H 4.18, N 6.18, found: C 74.58, H 4.13, N 6.11. **¹H-NMR** (300 MHz, DMSO-*d*₆): δ (ppm) 7.17-7.26 (m, 1H), 7.31-7.37 (m, 1H), 7.54-7.63 (m, 1H), 7.68-7.75 (m, 1H), 7.77-7.86 (m, 3H), 8.13-8.21 (m, 1H), 11.13 (br s, 1H). **¹³C-NMR** (75 MHz, DMSO-*d*₆): δ (ppm) 120.4, 123.8, 128.2, 129.3, 129.6, 130.2, 131.2, 132.96, 133.13, 133.8, 136.7, 138.2, 165.5, 192.5. **HRMS** (ESI): *m/z* [M+H]⁺ calcd. for [C₁₄H₁₀NO₂]⁺ 224.0706; found 224.0709. C₁₄H₉NO₂ (223.23).

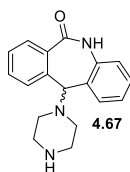


11-Hydroxy-5,11-dihydro-6*H*-dibenzo[b,e]azepin-6-one (4.65).^{14, 60} **5*H*-dibenzo[b,e]azepine-6,11-dione (4.64)** (9.51 g, 42.6 mmol) was suspended in ethanol (500 mL). Under stirring, sodium borohydride (4.12 g, 108.9 mmol) was added portionwise to the suspension and the reaction mixture was refluxed

for 3 h. The volume of the organic solvent was reduced by evaporation to 150 mL and then poured into a saturated solution of ammonium chloride (400 mL). The aqueous solution was neutralized with conc. HCl. The precipitated solid was collected by filtration, washed with water (1x 100 mL), methanol (1x 100 mL) and light petroleum (100 mL). The solid was dried *in vacuo* to give **4.65** as a white solid (7.90 g, 35.1 mmol, 82%). **Anal. calcd.** for C₁₄H₁₁NO₂: C 74.65, H 4.92, N 6.22, found: C 74.37, H 5.03, N 6.08. **¹H-NMR** (300 MHz, DMSO-*d*₆): δ (ppm) 5.67 (s, 1H), 6.39 (br s, 1H), 7.04-7.26 (m, 3H), 7.28-7.42 (m, 1H), 7.45-7.83 (m, 4H), 10.53 (s, 1H). **¹³C-NMR** (75 MHz, DMSO-*d*₆): δ (ppm) 67.2, 120.8 (two carbon signals), 121.4, 122.7, 124.2, 127.1 (3 carb.), 129.5, 131.7, 134.3, 145.3, 167.9. **HRMS** (ESI): m/z [M+H]⁺ calcd. for [C₁₄H₁₂NO₂]⁺ 226.0863, found 226.0865. C₁₄H₁₁NO₂ (225.08).

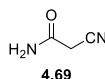


11-Chloro-5,11-dihydro-6H-dibenzo[b,e]azepin-6-one (4.66).^{14, 60} 11-Hydroxy-5,11-dihydro-6H-dibenzo[b,e]azepin-6-one (**4.65**) (7.01 g, 31.1 mmol) was suspended in chloroform (175 mL). Under stirring, thionyl chloride (10.0 mL, 137.8 mmol) was slowly added dropwise into the mixture. The reaction mixture was refluxed for 1.5 h. Then, the reaction mixture was allowed to cool to rt and the volume of the organic solvent was reduced and light petroleum (250 mL) was added. The precipitated solid was collected by filtration, washed with light petroleum (3x 100 mL) and dried *in vacuo* to give **4.66** as a white solid (7.16 g, 29.4 mmol, 95%). **Anal. calcd.** for C₁₄H₁₀ClNO: C 69.00, H 4.14, N 5.75, found: C 68.89, H 4.21, N 5.53. **¹H-NMR** (300 MHz, DMSO-*d*₆): δ (ppm) 6.58 (s, 1H), 7.08-7.17 (m, 1H), 7.19-7.26 (m, 1H), 7.31-7.41 (m, 1H), 7.45-7.63 (m, 4H), 7.85-7.93 (m, 1H), 10.86 (br s, 1H). **¹³C-NMR** (75 MHz, DMSO-*d*₆): δ (ppm) 63.2, 121.7, 124.1, 126.5, 128.5, 129.4, 129.96, 129.98, 131.4, 131.5, 132.3, 136.7, 140.3, 167.1. C₁₄H₁₀ClNO (243.69).

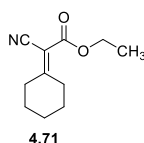


11-(Piperazin-1-yl)-5,11-dihydro-6H-dibenzo[b,e]azepin-6-one (4.67).^{14, 61} 11-Chloro-5,11-dihydro-6H-dibenzo[b,e]azepin-6-one (**4.66**) (6.50 g, 26.6 mmol) was dissolved in dioxane (130 mL). Under stirring, piperazine (11.48 g, 133 mmol) in dioxane (250 mL) was added dropwise into the reaction mixture, which was heated at 60 °C while stirring for 2 h. Then, the reaction mixture was allowed to cool to rt, the solvent was evaporated, and the residue was dissolved in water (200 mL). The compound was extracted from the aqueous phase with CH₂Cl₂ (3x 200 mL). The combined organic phases were dried over Na₂SO₄ and the organic solvent was evaporated. The product was purified by column chromatography (eluent: CH₂Cl₂/MeOH/NH₃ aq 90:9:1) to give **4.67** as a pale yellow crystalline solid (6.03 g, 20.5 mmol, 77%). **¹H-NMR** (400 MHz, DMSO-*d*₆): δ (ppm) 1.97-2.04 (m, 4H), 2.51-2.61 (m, 4H, interfering with solvent residual peak), 4.16 (s, 1H), 7.00-7.08 (m, 2H), 7.17-7.24 (m, 1H), 7.29-7.40 (m, 3H), 7.42-7.48 (m, 1H), 7.67-7.73 (m, 1H), 10.33 (br s, 1H). One exchangeable proton signal (NH-piperazine) was not apparent. **¹³C-NMR** (101 MHz, DMSO-*d*₆): δ (ppm) 45.2, 51.9, 74.7, 121.2, 123.6,

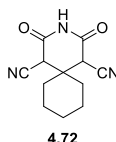
127.69, 127.75, 128.2, 129.9, 130.4, 131.2, 131.4, 131.7, 136.2, 142.5, 168.2. **HRMS** (ESI): *m/z* [M+H]⁺ calcd. for [C₁₈H₁₉N₃ONa]⁺ 316.1420, found 316.1418. C₁₈H₁₉N₃O (293.37).



2-Cyanoacetamide (4.69).⁶² Under stirring, ethyl cyanoacetate (**4.68**) (10.7 mL, 101 mmol) was added dropwise into an ice bath cooled solution of ammonium hydroxide (100 mL) and stirred for 2 h. The precipitated solid was separated by filtration and the obtained solid was washed with ice-cold ethanol (3x 10 mL). The solid was dried *in vacuo* and compound **4.69** was obtained as a white solid (4.58 g, 54.5 mmol, 54%). **¹H-NMR** (300 MHz, DMSO-*d*₆): δ (ppm) 3.58 (s, 2H), 7.33 (br s, 1H), 7.64 (br s, 1H). **¹³C-NMR** (75 MHz, DMSO-*d*₆): δ (ppm) 25.4, 116.4, 164.2. **HRMS** (ESI): *m/z* [M+H]⁺ calcd. for [C₃H₅N₂O]⁺ 85.0396, found 85.0400. C₃H₄N₂O (84.08).

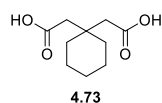


Ethyl 2-cyano-2-cyclohexylideneacetate (4.71).⁶³ Cyclohexanone (**4.70**) (5.5 mL, 53.2 mmol), ethyl cyanoacetate (**4.68**) (7.0 mL, 65.6 mmol), acetic acid (0.6 mL, 9.52 mmol) and NH₄CH₃COO (0.47 g, 6.10 mmol) were dissolved in toluene (100 mL) and heated under reflux (Dean-Stark apparatus) for 7 h. The organic solvent was washed with water (2x 100 mL) and with a saturated NaHCO₃ solution (100 mL). The organic solvent was dried over Na₂SO₄, evaporated and dried *in vacuo* to give **4.71** as a yellowish liquid (10.28 g, 53.2 mmol, 100%). **¹H-NMR** (400 MHz, DMSO-*d*₆): δ (ppm) 1.25 (t, *J* = 7.1 Hz, 3H), 1.56-1.69 (m, 4H), 1.69-1.77 (m, 2H), 2.57-2.66 (m, 2H), 2.89-2.97 (m, 2H), 4.22 (q, *J* = 7.1 Hz, 2H). **¹³C-NMR** (101 MHz, DMSO-*d*₆): δ (ppm) 13.8, 24.9, 27.8, 28.1, 30.9, 36.2, 61.4, 161.4, 180.2. **HRMS** (EIC): *m/z* [M]⁺ calcd. for [C₁₁H₁₅NO₂]⁺ 193.1097, found 193.1102. C₁₁H₁₅NO₂ (193.25).

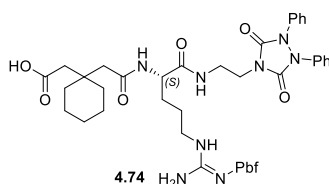


2,4-Dioxo-3-azaspiro[5.5]undecane-1,5-dicarbonitrile (4.72).⁶⁴ A solution of sodium ethoxide was freshly prepared. Sodium (0.46 g, 20 mmol) was added to a three-neck flask and ethanol (50 mL) was added dropwise carefully. After the reaction between sodium and ethanol was completed, 2-cyanoacetamide (**4.69**) (0.48 g, 5.71 mmol) was added to the solution. The reaction mixture was heated under reflux for 30 min. Under stirring, ethyl 2-cyano-2-cyclohexylideneacetate (**4.71**) (1.00 g, 5.17 mmol) was added and the reaction mixture was stirred and heated under reflux for 4 h. Then, the reaction mixture was allowed to cool to rt, the solvent was evaporated, and the residue was dissolved in diluted hydrochloric acid (HCl conc./water 1:5). The precipitated solid was collected by filtration and dried *in vacuo*. Compound **4.72** was obtained after recrystallization from chloroform as a white solid (0.450 g, 1.95 mmol, 38%). **¹H-NMR** (400 MHz, DMSO-*d*₆): δ (ppm) 1.35-1.44 (m, 2H), 1.49-1.60 (m, 6H), 1.66-1.71 (m, 2H), 4.88 (s, 2H), 12.18 (br s, 1H). **¹³C-NMR** (101 MHz, DMSO-*d*₆): δ (ppm) 19.8,

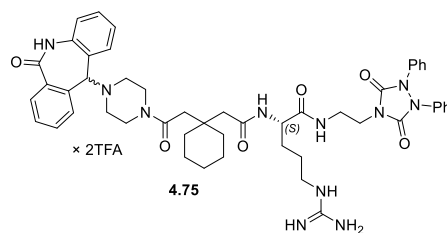
24.5, 31.5, 38.0, 45.4, 114.5, 164.1. **HRMS** (ESI): m/z $[2M+Na]^+$ calcd. for $[C_{24}H_{26}N_6O_4Na]^+$ 485.1908, found 485.1930. $C_{12}H_{13}N_3O_2$ (231.26).



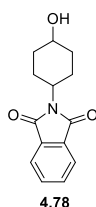
2,2'-(Cyclohexane-1,1-diyl)diacetic acid (4.73).^{30, 65} 2,4-Dioxo-3-azaspiro[5.5]undecane-1,5-dicarbonitrile (**4.72**) (450 mg, 1.95 mmol) was refluxed in a mixture of water and conc. H_2SO_4 (1:3; 12 mL). After cooling to rt, the mixture was poured into H_2O (80 mL) and stirred at rt overnight. The solid was collected by filtration. The solid was dissolved in 1 M NaOH (100 mL) and the aqueous phase was washed with ethyl acetate. Then, the aqueous phase was acidified with dilute HCl and the compound was extracted with CH_2Cl_2 . The organic phase was dried over Na_2SO_4 and the organic solvent was evaporated to give **4.73** as a white solid (0.252 g, 1.26 mmol, 65%). **1H -NMR** (300 MHz, $DMSO-d_6$): δ (ppm) 1.30-1.49 (m, 10H), 2.40 (s, 4H), 11.97 (br s, 2H). **^{13}C -NMR** (75 MHz, $DMSO-d_6$): δ (ppm) 21.1, 25.6, 34.3, 35.0, 40.7, 173.1. **HRMS** (ESI): m/z $[M+Na]^+$ calcd. for $[C_{10}H_{16}O_4Na]^+$ 223.0941, found, 223.0947. $C_{10}H_{16}O_4$ (200.23).



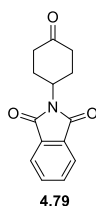
(S)-2-(1-(2-((1-((2-(3,5-Dioxo-1,2-diphenyl-1,2,4-triazolidin-4-yl)ethyl)amino)-1-oxo-5-(2-((2,2,4,6,7-pentamethyl-2,3-dihydrobenzofuran-5-yl)sulfonyl)guanidino)pentan-2-yl)amino)-2-oxoethyl)-cyclohexyl)acetic acid (4.74). 2,2'-(cyclohexane-1,1-diyl)diacetic acid (**4.73**) (45 mg, 0.225 mmol) was dissolved in CH_2Cl_2 (10 mL). Under stirring, EDC·HCl (43.13 mg, 0.225 mmol) was added and the mixture was stirred until the solution was clear. Then, HOBT (30.4 mg, 0.225 mmol) was added and the mixture was stirred until the solution was clear. (S)- N^{ω} -2,3-Dihydro-2,2,4,6,7-pentamethylbenzofuran-5-sulfonyl[2-(3,5-dioxo-1,2-diphenyl-1,2,4-triazolidin-4-yl)ethyl]argininamide (**4.13**) (0.148 g, 0.210 mmol) in CH_2Cl_2 (5 mL) was dropped slowly into the reaction mixture and stirred overnight at rt. The solvent was evaporated, and the crude product was purified by column chromatography (eluent: $CH_2Cl_2/MeOH$ 95:5) to give **4.74** as a white solid (0.141 g, 0.159 mmol, 76%). **1H -NMR** (300 MHz, $DMSO-d_6$): δ (ppm) 1.28-1.46 (m, 18H), 1.49-1.61 (m, 1H), 1.96-2.00 (m, 2H), 2.28-2.35 (m, 3H), 2.39-2.42 (m, 2H), 2.44-2.48 (m, 3H), 2.88-2.95 (m, 3H), 3.22-3.49 (m, 5H), 3.56-3.62 (m, 2H), 4.09-4.20 (m, 1H), 6.39 (br s, 1H), 6.61 (br s, 1H), 7.15-7.25 (m, 2H), 7.33-7.43 (m, 8H), 7.48-7.55 (m, 1H), 7.65-7.73 (m, 1H), 7.91-7.99 (m, 2H), 8.15 (t, $J = 5.9$ Hz, 1H), 12.87 (br s, 1H). **^{13}C -NMR** (101 MHz, $DMSO-d_6$): δ (ppm) 12.3, 17.6, 19.0, 21.0, 25.6, 28.3, 34.3, 35.1, 40.1 (overlaid by residual solvent peak), 40.6 (overlaid by solvent residual peak), 41.7, 42.5, 52.1, 86.3, 109.7, 116.3, 119.1, 122.6, 124.3, 124.4, 126.6, 127.2, 127.8, 129.0, 131.5, 136.6, 137.3, 152.6, 157.5, 171.0, 171.9, 173.1, 173.4. **HRMS** (ESI): m/z $[M+H]^+$ calcd. for $[C_{45}H_{59}N_8O_9S]^+$ 887.4120, found 887.4135. $C_{45}H_{58}N_8O_9S$ (887.07).



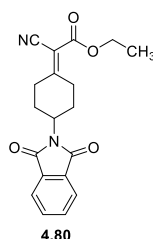
(2S)-N²-[2-(1-{2-Oxo-2-[4(6-oxo-6,11-dihydro-5H-dibenzo[b,e]azepin-11-yl)piperazin-1-yl]ethyl}-cyclohexyl)acetyl]-2-(3,5-dioxo-1,2-diphenyl-1,2,4-triazolidin-4-yl)ethyl]argininamide bis(hydrotrifluoroacetate) (4.75**).** Compound **4.75** was prepared using *general procedure G* and the reactants (S)-2-(1-(2-((1-(2-(3,5-dioxo-1,2-diphenyl-1,2,4-triazolidin-4-yl)ethyl)amino)-1-oxo-5-(2((2,2,4,6,7-pentamethyl-2,3-dihydrobenzofuran-5-yl)sulfonyl)guanidino)pentan-2-yl)amino)-2-oxoethyl)cyclohexyl)acetic acid (**4.74**) (76 mg, 85.7 μmol), EDC·HCl (20 mg, 104 μmol), HOBT (19 mg, 141 μmol) and 11-(piperazin-1-yl)-5,11-dihydro-6H-dibenzo[b,e]azepin-6-one (**4.67**) (38 mg, 129.5 μmol). Purification by preparative HPLC A (gradient: 0-30 min, A/B 85:15–19:81, *t_R* = 21 min) afforded **4.75** as a fluffy white solid (11 mg, 9.66 μmol, 11%). **¹H-NMR** (600 MHz, DMSO-*d*₆): δ (ppm) 1.08-1.68 (m, 15H), 1.84-2.19 (m, 4H), 2.25-2.46 (m, 4H), 2.92-3.04 (m, 2H), 3.21-3.42 (m, 5H), 3.59 (t, *J* = 6.0 Hz, 2H), 4.12-4.19 (m, 1H), 4.27 (br s, 1H), 6.55-7.47 (m, 21H), 7.47-7.52 (m, 1H), 7.55 (t, *J* = 5.3 Hz, 1H), 7.73 (d, *J* = 7.1 Hz, 1H), 8.13 (d, *J* = 7.5 Hz, 1H), 8.23 (t, *J* = 5.7 Hz, 1H), 10.34 (s, 1H). **¹³C-NMR** (150 MHz, DMSO-*d*₆): δ (ppm) 21.11, 21.14, 25.1, 25.6, 28.9, 35.27, 35.32, 35.7, 36.2, 36.23, 36.24, 39.6 (overlaid by solvent residual peak); 40.4, 45.8, 50.8, 51.3, 51.8, 73.6, 115.3 (TFA), 117.2 (TFA), 121.4, 122.6, 123.8, 126.6 (2 carb.), 127.8, 128.1, 128.5, 129.0 (2 carb.), 130.0, 130.5, 131.4, 131.6, 136.2, 136.6, 152.6, 156.7, 158.3 (q, *J* = 34.4 Hz) (TFA), 168.1, 169.8, 171.0, 172.0. **RP-HPLC** (220 nm): 99% (*t_R* = 13.8 min, *k* = 4.4). **HRMS** (ESI): *m/z* [M+H]⁺ calcd. for [C₅₀H₆₀N₁₁O₆]⁺ 910.4723, found 910.4721. C₅₀H₅₉N₁₁O₆ × C₄H₂F₆O₄ (910.09 + 228.04).



2-(trans-4-Hydroxycyclohexyl)isoindoline-1,3-dione (4.78**).**⁶⁶ *trans*-4-Aminocyclohexan-1-ol (**4.76**) (10.0 g, 86.8 mmol) was dissolved in H₂O (300 mL) and K₂CO₃ (36.16 g, 0.26 mol) was added and the reaction mixture was cooled in an ice bath. Under stirring, ethyl 1,3-dioxoisindoline-2-carboxylate (**4.77**) (25.0 g, 45.3 mmol) in H₂O (250 mL) was slowly added dropwise into the reaction mixture and stirred for 20 min. Then, the reaction mixture was allowed to warm to rt and stirred for 3.5 h. The precipitated solid was collected by filtration, washed with water and dried *in vacuo*. The crude product was purified by column chromatography (eluent: light petroleum/ethyl acetate 1:1 to 1:5) to give **4.78** as a white solid (11.1 g, 45.3 mmol, 52%). **¹H-NMR** (300 MHz, DMSO-*d*₆): δ (ppm) 1.17-1.35 (m, 2H), 1.60-1.73 (m, 2H), 1.85-1.96 (m, 2H), 2.04-2.23 (m, 2H), 3.38-3.53 (m, 1H), 3.87-4.04 (m, 1H), 4.65 (br s, 1H), 7.80-7.84 (m, 4H). **¹³C-NMR** (75 MHz, DMSO-*d*₆): δ (ppm) 27.3, 34.6, 49.5, 68.1, 122.9, 131.4, 134.3, 167.8. **HRMS** (ESI): *m/z* [M+H]⁺ calcd. for [C₁₄H₁₆NO₃]⁺ 246.1125, found 246.1125. C₁₄H₁₅NO₃ (245.28).



2-(4-Oxocyclohexyl)isoindoline-1,3-dione (4.79).⁶⁷ PCC (14.7 g, 68.2 mmol) was suspended in CH_2Cl_2 (300 mL) and 2-(*trans*-4-hydroxycyclohexyl)isoindoline-1,3-dione (**4.78**) (7.53 g, 30.58 mmol) in CH_2Cl_2 (100 mL) was added dropwise to the suspension. The reaction mixture was stirred at rt for 9 h. The solid was removed by filtration (Büchner funnel) and the filtrate was evaporated. The crude product was purified by column chromatography (eluent: light petroleum/ethyl acetate 1:1) to give **4.79** as a white solid (5.35 g, 22.0 mmol, 72%). **¹H-NMR** (300 MHz, $\text{DMSO}-d_6$): δ (ppm) 1.97-2.10 (m, 2H), 2.21-2.33 (m, 2H), 2.37-2.50 (m, 2H, interfering with solvent residual peak), 2.57-2.71 (m, 2H), 4.53-4.66 (m, 1H), 7.80-7.85 (m, 4H). **¹³C-NMR** (75 MHz, $\text{DMSO}-d_6$): δ (ppm) 28.2, 39.2 (overlaid by the solvent residual peak), 47.5, 123.0, 131.5, 134.4, 167.7, 209.2. **HRMS** (ESI): m/z $[\text{M}+\text{H}]^+$ calcd. for $[\text{C}_{14}\text{H}_{14}\text{NO}_3]^+$ 244.0968, found 244.0968. $\text{C}_{14}\text{H}_{13}\text{NO}_3$ (243.26).



Ethyl 2-cyano-2-(4-(1,3-dioxoisoindolin-2-yl)cyclohexylidene)acetate (4.80). Ethyl cyanoacetate (**4.68**) (2.11 mL, 19.73 mmol), 2-(4-oxocyclohexyl)-isoindoline-1,3-dione (**4.79**) (4.8 g, 19.73 mmol), $\text{NH}_4\text{CH}_3\text{COO}$ (152 mg, 1.97 mmol) and acetic acid (0.23 mL, 3.65 mmol) were dissolved in toluene (150 mL) and the reaction mixture was refluxed for 4 h. The reaction mixture was allowed to cool to rt and the organic phase was washed with brine (3x), dried with Na_2SO_4 and the solvent was removed under reduced pressure. The product was purified by column chromatography (eluent: light petroleum/ethyl acetate 1:2) to give **4.80** as a white solid (4.14 g, 12.2 mmol, 62%). **¹H-NMR** (300 MHz, $\text{DMSO}-d_6$): δ (ppm) 1.26 (t, $J = 7.1$ Hz, 3H), 1.94-2.47 (m, 5H), 2.62-2.78 (m, 1H), 2.87-3.00 (m, 1H), 3.80-3.92 (m, 1H), 4.24 (q, $J = 7.1$ Hz, 2H), 4.37-4.51 (m, 1H), 7.79-7.91 (m, 4H). **¹³C-NMR** (75 MHz, $\text{DMSO}-d_6$): δ (ppm) 13.9, 29.06, 29.28, 29.4, 34.5, 47.7, 61.7, 102.2, 115.3, 123.0, 131.5, 134.4, 161.3, 167.7, 177.3. **HRMS** (ESI): m/z $[\text{M}+\text{H}]^+$ calcd. for $[\text{C}_{19}\text{H}_{19}\text{N}_2\text{O}_4]^+$ 339.1339, found 339.1341. $\text{C}_{19}\text{H}_{18}\text{N}_2\text{O}_4$ (338.36).

4.4.3. Investigation of the chemical stability of compounds 4.50, 4.51 and 4.58

To determine the chemical stability, compounds **4.50**, **4.51** and **4.58** (100 μM) were incubated in buffer (25 mM HEPES, 2.5 mM CaCl_2 , 1 mM MgCl_2 , pH 7.4) at rt for 24 h. After incubation, the solution was diluted (1:1) with 10% aq TFA and the stability monitored at 6 time intervals (0 h, 1 h, 2 h, 4 h, 8 h and 24 h) by analytical HPLC (220 nm) analysis (4.4.1.; see described method for purity control by analytical HPLC).

4.4.4. Fluorescence properties

All emission and excitation spectra of compounds **4.58**, **4.59**, **4.60** and **4.61** were recorded on a Cary Eclipse spectrofluorimeter (Varian, Mulgrave, Victoria, Australia) in acryl cuvettes (10 x 10 mm, Sarstedt, Nümbrecht, Germany) at 22 °C. The photomultiplier voltage was set to 400 V throughout, the excitation spectra were recorded with an excitation slit of 5 nm and an emission slit of 10 nm. The emission spectra were recorded with an emission slit of 5 nm and an excitation slit of 10 nm. Following filter settings were used: “auto” (excitation filter) and “open” (emission filter). The emission starting point was set to 10 nm above the excitation wavelength. From every recorded emission spectrum, the corresponding reference spectrum was subtracted to obtain the net spectrum, that was multiplied with the corresponding lamp correction spectra, resulting in the corrected emission spectra.

The stock solution of the fluorescent ligands **4.58**, **4.59**, **4.60** and **4.61** (1 mM) were prepared in DMSO and the sample solutions (5 µM) were prepared in PBS (pH 7) containing 1% (w/v) BSA (filtered before use with a syringe filter 0.22 µm). Sample solutions for reference spectra were prepared using PBS (pH 7) containing 1% (w/v) BSA and the same amount of DMSO was added compared to solutions of fluorescent ligands (in the absence of fluorescent ligand). All solutions were freshly prepared, and they were stored in the dark.

4.4.5. Pharmacological methods: cell culture, crystal violet assay, saturation and competition binding experiments with [³H]propionyl-pNPY in HEK293T βArr2 + Y₂R cells, β-arrestin2 recruitment assay, miniG protein recruitment assay, BRET based binding assay, confocal microscopy and radioligand binding assay for hY₁R, hY₄R and hY₅R

4.4.5.1. Cell culture

The preparation (HEK293T βArr2 + Y₂R cells³⁹ and CHO-hY₄-G_{qi5}-mtAEQ cells⁶⁸) and cultivation (HEK293T βArr2 + Y₂R cells,³⁹ SK-N-MC cells,⁶⁹ CHO-hY₄-G_{qi5}-mtAEQ cells⁶⁸ and HEC-1B cells⁴⁹) was described elsewhere. SK-N-MC cells were obtained from the American Type Culture Collection (Rockville, USA).

The preparation and cultivation of HEK293T NlucN-miniG_i/Y₂R-NlucC cells, expressing the NlucN-miniG_i fusion and Y₂R-NlucC constructs were performed by Carina Höring as part of her doctoral thesis.

The preparation and cultivation of HEK293T Y₂(intraNlucD197) cells, stably expressing the Y₂(intraNlucD197) receptor construct were performed by Lukas Grätz as part of his doctoral thesis.

Cells (HEK293T βArr2 + Y₂R cells, HEK293T NlucN-miniG_i/Y₂R-NlucC cells, HEK293T Y₂(intraNlucD197) cells) were cultivated in DMEM (Sigma-Aldrich, Taufkirchen, Germany) at 37 °C in a water saturated atmosphere containing 5% CO₂. DMEM was supplemented with L-glutamine (L-glutamine solution, Sigma-Aldrich; 0.584 g/mL), penicillin-streptomycin (Sigma-Aldrich; P/S, 10.000 U/mL) and FCS (Merck Biochrom, Darmstadt, Germany; 10% (v/v)). The culture medium of HEK293T βArr2 + Y₂R cells additionally contained zeocin (InvivoGen, San Diego, USA; 400 µg/mL) and G418 (Merck Biochrom; 600 µg/mL). The culture medium of HEK293T NlucN-miniG_i/Y₂R-NlucC cells additionally contained G418 (Merck Biochrom; 600 µg/mL) and puromycin (InvivoGen, San Diego, USA;

1 µg/mL). The culture medium of HEK293T Y₂(intraNLucD197) cells additionally contained G418 (Merck Biochrom; 600 µg/mL).

Routinely performed examinations for mycoplasma contamination using the Venor GeM Mycoplasma Detection Kit (Minerva Biolabs, Berlin, Germany) were negative for all cell types.

4.4.5.2. Crystal violet assay

The 24-well plates were purchased from Sarstedt (product no. 83.3922, standard F, Nümbrecht, Germany) and 96-well plates were purchased from Corning (product no. 3610, Kaiserslautern, Germany). The coating procedures with poly-*D*-lysine or cross-linked gelatin were performed under sterile conditions.

Coating-procedure of 24-well (96-well) plates with poly-*D*-lysine

Poly-*D*-lysine (γ-irradiated) was purchased from Sigma-Aldrich as lyophilizate, which was dissolved in sterile water (1 mg/mL) and every well of 24 well plate (96 well) was filled with 300 µL (100 µL) of that solution. After 15 min the solution was removed by suction, and every well was washed with 500 µL (200 µL) of sterile water.

Coating-procedure of 24-well (96-well) plates with cross-linked gelatin

The coating was performed as described in literature⁷⁰ with modifications: every well of a 24-well (96-well) plate was filled with 250 µL (100 µL) of 0.5% gelatin solution and the plates were incubated at rt for 2 h. The gelatin solution was removed and 250 µL (100 µL) of 2.5% glutardialdehyde solution were added and incubated at rt for 10 min and then removed. Every well was washed with 1 mL (300 µL) of sterile water (3x). The wells were filled with 1 mL (300 µL) of sterile water and the plates were incubated at rt overnight. The next day the water was removed, and the plate dried at rt.

One day before a crystal violet assay, the HEK293T βArr2 + Y₂R cells were detached by trypsinization and resuspended in Ham's F12 medium (Sigma-Aldrich) containing 10% FCS. A density of 1.7·10⁵ cells/mL was adjusted and 500 µL (200 µL) of this suspension was seeded into each well of a coated 24-well (Corning) (96-well; Sarstedt) plate. The cells were cultivated at 37 °C in a water saturated atmosphere containing 5% CO₂. Before starting the experiment, the confluency of the cells was >90%. The culture medium was removed by dumping and cells were washed once with 500 µL (100 µL) of buffer (25 mM HEPES, 2.5 mM CaCl₂, 1 mM MgCl₂, pH 7.4) per well. The buffer was exchanged by 500 µL (100 µL) of binding buffer (buffer containing 1% BSA and 0.1 mg/mL of bacitracin) and the plates were incubated for 90 min at rt.

After the incubation in binding buffer followed by washing procedures (500 µL (100 µL) of PBS buffer for two times), the crystal violet assay was essentially performed in 96-well and 24-well plates as described in literature⁷¹ with minor modifications: the cells in 96-well plate (24-well) were fixed with 100 µL (500 µL) of 2% glutardialdehyde at rt for 25 min. Then, the 2% glutardialdehyde solution were removed and 100 µL (500 µL) of a 0.02% aqueous crystal violet solution were added per well. After 20 min the excess of crystal violet was removed by immersing the plates in a water bath for three times. Then every well was filled with water and incubated for 20 min. The water was removed and the cell-associated crystal violet was dissolved in 180 µL (1000 µL) of ethanol 70% (v/v) and shaken at rt for

1.5 h. The absorbance was measured on an Enspire (Perkin-Elmer, Rodgau, Germany) plate reader at 585 nm.

4.4.5.3. Saturation and competition binding with [³H]propionyl-pNPY in HEK293T βArr2 + Y₂R cells

The synthesis of [³H]propionyl-pNPY was described previously.¹⁶ The radioligand competition and saturation binding experiments were performed as described in literature^{9, 32} for CHO-hY₂R-G_{q15}-mtAEQ cells⁹ with modifications: instead of CHO-hY₂R-G_{q15}-mtAEQ cells, HEK293T βArr2 + Y₂R cells³⁹, were used. Additionally, the cells were seeded in 96-well plates (Corning, Kaiserslautern, Germany) coated (4.4.5.2.) with poly-*D*-lysine hydrobromide (Sigma-Aldrich) solution (1 mg/mL), instead of uncoated 96-well plates (Corning). One day before the competition or saturation binding experiments, the cells were detached by trypsinization and resuspended in Ham's F12 medium (Sigma-Aldrich) containing 10% FCS. A density of $1.7 \cdot 10^5$ cells/mL was adjusted and 200 μL of this suspension was seeded into each well of a coated 96-well plates (Corning). The cells were cultivated at 37 °C in a water saturated atmosphere containing 5% CO₂. Before starting the experiment (competition or saturation binding), the confluency of the cells was >90%. The culture medium was removed by dumping and cells were washed once with 100 μL of buffer (25 mM HEPES, 2.5 mM CaCl₂, 1 mM MgCl₂, pH 7.4) per well. The buffer was exchanged by 80 μL of binding buffer (composed of buffer containing 1% BSA and 0.1 mg/mL of bacitracin). All feed solutions for competition and saturation binding experiments of test compounds and the radioligand were prepared in binding buffer.

For saturation binding experiments total binding was determined by addition of 10 μL buffer and solutions (10 μL) containing increasing concentrations (10-fold concentrated compared to C_{final}) of [³H]propionyl-pNPY. The unspecific binding was determined in the presence of the competitor **4.1** (200-fold excess compared to radioligand ([³H]propionyl-pNPY) concentrations. For determination of unspecific binding 10 μL of competitor and solutions containing increasing concentrations (10-fold concentrated compared to C_{final}) of [³H]propionyl-pNPY were added.

For competition binding experiments, increasing concentrations (10-fold concentrated compared to C_{final}) of test compounds (10 μL) were added. After 15 min, the radioligand solution (10-fold concentrated compared to $C_{final} = 4$ nM) was added in every well. Non-specific binding was determined in the presence of 200-fold excess of pNPY and total binding in binding buffer (at least one triplicate of non-specific and total binding was determined on every plate).

After 90 min of incubation (competition and saturation binding experiments) the buffer was removed by suction with a suction assistance device (Figure 4.13) and then the cells were washed three times with PBS, which was allowed to warm to rt. The cells were covered with 35 μL of lysis solution (8 M urea, 3 M acetic acid and 1% (V/m) Triton-X-100) and shaken for 30 min. Then, 200 μL of liquid scintillator (Optiphase Supermix) was added and the plates were shaken in the dark for at least 3 h, before measuring radioactivity (dpm) with a MicroBeta2 plate counter (Perkin-Elmer, Rodgau, Germany).

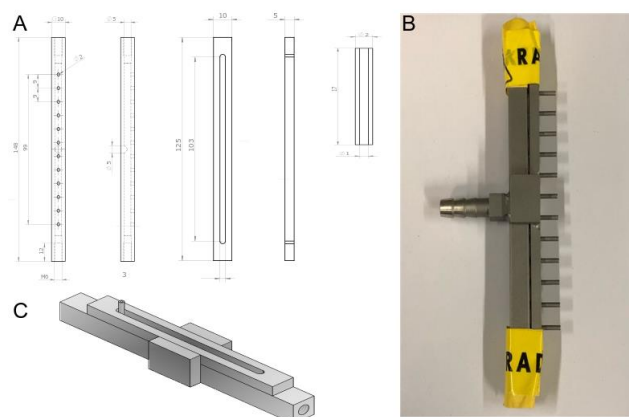


Figure 4.13. Suction assistance device for saturation binding of [^3H]propionyl-pNPY and radioligand competition binding assay on HEK293T $\beta\text{Arr}2 + \text{Y}_2\text{R}$ cells. Engineering drawing (A), photo (B) and stereoscopic view of suction assistance device. Engineering drawing (A) and stereoscopic view were thankfully provided by Andreas Graf (Feinmechanische Werkstatt Chemie & Pharmazie, Universität Regensburg).

4.4.5.4. β -Arrestin2 recruitment assay (Y_2R)

The β -arrestin2 recruitment assays were performed as described previously in the dissertation of J. Felixberger³⁹ with modifications: luminescence was measured as a function of time on living cells instead of measuring luminescence after cell lysis.

The procedure was as follows: the day before the split-luciferase β -arrestin2 recruitment assay, the cells were detached by trypsinization and resuspended in Leibovitz's L-15 medium supplemented with 5% FCS and HEPES (10 mM). For antagonist mode, a cell density of $1.43 \cdot 10^6$ cells/mL was adjusted and 70 μL of this suspension were seeded into each well of a white flat bottom 96-well plate (Cellstar, Greiner Bio-One, Kremsmünster Österreich) (for agonist mode: $1.25 \cdot 10^6$ cells/mL; 80 μL). *D*-Luciferin (K^+ salt; Pierce, Thermo Scientific, Regensburg, Germany) was suspended in HBSS (Gibco, Thermo Scientific) in a concentration of 400 mM. Further dilution of the substrate up to 10 mM in Leibovitz's L-15 medium was prepared shortly prior to the experiment. The cells were cultivated at 37 °C in a water saturated atmosphere (no additional CO_2). The dilutions of pNPY and ligands to be investigated were prepared in Leibovitz's L-15 medium containing 1% BSA.

In agonist mode, a solution of *D*-Luciferin ($c = 10$ mM, 10 μL) was added and the plate was incubated at 37 °C for 20 min. Baseline luminescence of the cells was recorded with an integration time of 1000 ms per well (10 entire plate repeats). Solutions of ligands to be investigated (10 μL ; 10-fold concentrated compared to c_{final}) were added at increasing concentrations followed by immediate measurement of luminescence (20 entire plate repeats with an integration time of 1000 ms).

In antagonist mode, a solution of *D*-Luciferin ($c = 10$ mM, 10 μL) and the solutions (10 μL) of the test compounds (10-fold concentrated compared to c_{final}) at increasing concentrations were added, and the plate was incubated at 37 °C for 20 min. Baseline luminescence was recorded with an integration time of 1000 ms per well (10 entire plate reads). Then, pNPY ($c = 2000$ nM, 10 μL) was added followed by immediate measurement of luminescence (20 entire plate repeats with an integration time of 1000 ms). Before measuring, the plate reader was pre-heated at 37 °C. The Luminescence was measured using

a GENios Pro (Tecan, Grödig, Austria) or an Enspire (Perkin-Elmer, Rodgau, Germany) plate reader with an integration time of 1000 ms per well.

On every plate at least one triplicate of the 100% (response, corresponding to 200 nM pNPY) and the 0% control (neat buffer) were determined.

4.4.5.5. MiniG protein recruitment assay (*ongoing doctoral thesis Carina Höring*)

The day before a split-luciferase (miniG protein recruitment) assay, the cells were detached by trypsinization and resuspended in Leibovitz's L-15 medium containing 5% FCS and 10 mM HEPES. A density of $1.43 \cdot 10^6$ cells/mL was adjusted for the antagonist mode and 70 μ L of this suspension were seeded into each well of a white flat bottom 96-well plate (Cellstar, Greiner Bio-one, Kremsmünster Österreich) (Agonist mode: $1.25 \cdot 10^6$ cells/mL; 80 μ L). The cells were cultivated at 37 °C in a water saturated atmosphere (no additional CO₂). The dilutions of pNPY and investigated ligands were prepared in Leibovitz's L-15 medium containing 1% BSA. A solution of the luciferase substrate furimazine (Promega, Madison, WI, USA; Cat.-No.: N2012; 10 μ L), which was diluted according to the manufacturer's protocol beforehand, were added and the baseline luminescence of the cells was recorded with an integration time of 0.1 s per well for 30 entire plate reads using an Enspire (Perkin-Elmer, Rodgau, Germany) plate reader. The solutions of the investigated ligand at increasing concentrations (10 μ L) in the antagonist mode were added, and a second luminescence baseline was recorded with an integration time of 0.1 s for 30 entire plate repeats. Then, pNPY ($C_{\text{final}} = 50$ nM, 10 μ L) in the antagonist mode was added. Subsequently, the luminescence was recorded with an integration time of 0.1 s for 90 entire plate repeats.

The plate reader was pre-heated at 37 °C, before measuring. On every plate at least one triplicate of the 100% (response, corresponding to 50 nM pNPY) and the 0% control (neat buffer) were determined.

4.4.5.6. BRET based binding assay (*ongoing doctoral thesis of Lukas Grätz*)

The day before a BRET based equilibrium binding assay, the cells were detached by trypsinization and resuspended in Leibovitz's L-15 medium with 5% FCS and 10 mM HEPES (assay medium). A density of $1.43 \cdot 10^6$ cells/mL (saturation and competition binding) or $1.25 \cdot 10^6$ cells/mL (kinetic experiments) was adjusted and 70 μ L (saturation and competition binding) or 80 μ L (kinetic experiments) of these suspensions were seeded into each well of 96-well plates (Brand GmbH & Co. KG, Wertheim, Germany). Then, the cells were incubated at 37 °C in a water saturated atmosphere (no additional CO₂) overnight to guarantee confluency (>90%) of the cells.

For saturation binding experiments, increasing concentrations (10-fold concentrated compared to c_{final}) of the fluorescent ligand (**4.85**) and competitor **4.1** (100-fold excess compared to **4.85** for unspecific binding) were prepared in buffer (Leibovitz's L-15 medium containing 2% BSA and 10 mM HEPES). Total binding was determined by adding 10 μ L of **4.58** solution and 10 μ L of buffer to the cells. For unspecific binding 10 μ L of **4.58** solution and 10 μ L of the competitor **4.1** were added to the cells. Then, the plate was incubated at 27 °C for 30 min. A solution of the luciferase substrate furimazine (Promega, Madison, WI, USA; Cat.-No.: N2012; 10 μ L), which was diluted according to the manufacturer's protocol beforehand, was added. The measurement was started after an equilibration of 5 min.

Competition equilibrium binding experiments were performed as described above using the solutions of the investigated ligand in buffer at increasing concentrations (10 μ L) and a solution of 10-fold concentrated fluorescent ligand compared to C_{final} (**4.58**; $C_{\text{final}} = 20$ nM) in buffer were added. The plate was incubated at 27 °C for 90 min, before the substrate furimazine (Promega; 10 μ L) was added.

For kinetic measurements 10 μ L of Leibovitz's L-15 medium (for total binding) or **4.1** (100-fold excess compared to **4.58** for unspecific binding) were added to the cells. Then, the substrate (furimazine) was added and the plate was equilibrated for 5 min inside the reader. The association was started after addition of 50 μ L of a 3-fold concentrated solution compared to C_{final} of the fluorescent ligand **4.58** ($C_{\text{final}} = 20$ nM) to the cells and the measurement was performed for 35-90 min. For dissociation experiments the cells were pre-incubated (35-90 min) with **4.58** as described above for association experiments. The dissociation started after addition of 50 μ L of a 4-fold concentrated solution compared to C_{final} of **4.1** (100-fold excess compared to **4.58**) to the cells and the measurement was performed for 220-280 min.

All measurements were performed with a TECAN InfiniteLumi (Tecan) plate reader at 27 °C using a Blue2 NB (460 nm \pm 35 nm) and the Red NB (>610 nm, longpass) filter combination or an GENios Pro (Tecan, Grödigg, Austria) plate reader at 27 °C using the following custom made filter combination from Chroma (Chroma Technology Corp, Vermont, USA): Chroma AT460/50 (460 nm \pm 25 nm) and the Chroma AT610lp (>610 nm, longpass) filter. An integration time of 100 ms was used for both plate readers. The integration time was increased to 500 ms, in order to reduce noise for all kinetic measurements.

4.4.5.7. Confocal microscopy

The cell culture dish was coated with poly-*D*-lysine (Sigma-Aldrich) prior to seeding of cells. For this purpose, the poly-*D*-lysine solution (1 mg/mL, 1 mL) was added, incubated at rt for 1 h and then washed with sterile water twice (2x 1 mL).

The day before confocal microscopy studies, the HEK293T β Arr2 + Y₂R cells were detached by trypsinization and resuspended in Leibovitz's L-15 medium with 5% FCS and 10 mM HEPES. A density of $0.5 \cdot 10^6$ cells/mL was adjusted and 1 mL of this suspension was seeded in a cell culture dish (35 x 10 mm; Cellstar, Greiner Bio-one, Kremsmünster Österreich) The cells were then incubated at 37 °C in a water saturated atmosphere (no additional CO₂) overnight to reach full adherence of the cells.

The fluorescent ligand **4.58** ($C_{\text{final}} = 40$ nM; 100 μ L of 11-fold concentrated compared to C_{final}) was added into the cell dish. The image for total binding was acquired after 30 min. Then, the competitor **4.1** ($C_{\text{final}} = 10,000$ nM; 100 μ L; 12-fold concentrated compared to C_{final}) or pNPY ($C_{\text{final}} = 10,000$ nM; 100 μ L; 12-fold concentrated compared to C_{final}) was added (into the same culture dish used for total binding) and the image was acquired after incubation of 4 h (unspecific binding). Unspecific binding was also determined by adding the fluorescent ligand **4.58** ($C_{\text{final}} = 40$ nM, 100 μ L) and the competitor **4.1** ($C_{\text{final}} = 10,000$ nM, 100 μ L) or pNPY ($C_{\text{final}} = 10,000$ nM, 100 μ L) at the same time into the culture dish. Then, total binding was performed by adding **4.58** ($C_{\text{final}} = 40$ nM, 100 μ L) and 100 μ L Leibovitz's L-15 medium containing 1% BSA instead of the competitor. All feed solutions of **4.1**, **4.58** and pNPY were prepared in Leibovitz's L-15 medium containing 1% BSA.

Images were acquired with a Nikon eclipse 90i (Nikon Instruments Europe, Amstelveen, Netherlands) and a water immersion objective (Nikon NIR Apo, 60×1.0w) was used. The following settings were used: Laser λ_{ex} 488 nm; Filter 650 LP; Pinhole L (102.6 μm); Gain 130.

4.4.5.8. Radioligand binding assay for hY₁R, hY₄R and hY₅R

All competition binding experiments at the Y₁R were essentially performed as described by Keller et al.¹⁶ using [³H]2.2 ($C_{\text{final}} = 0.15 \text{ nM}$, $K_{\text{d}} = 0.044 \text{ nM}$) and SK-N-MC cells expressing the Y₁R. At least two independent experiments were performed, each in triplicate.

All competition binding experiments at the Y₄R were essentially performed as described by Kuhn et al.³² using [³H]UR-KK200 ($C_{\text{final}} = 1.0 \text{ nM}$, $K_{\text{d}} = 0.67 \text{ nM}$) and CHO-hY₄R-G_{qi5}-mtAEQ cells expressing the Y₄R (cf. Chapter 6). Three independent experiments were performed, each in triplicate.

All competition binding experiments at the Y₅R were essentially performed as described using [³H]propionyl-pNPY ($C_{\text{final}} = 4.0 \text{ nM}$, $K_{\text{d}} = 4.8 \text{ nM}$) and HEC-1B cells expressing the Y₅R.^{16, 49} At least two independent experiments were performed, each in triplicate.

4.4.6. Data analysis

The retention factor k was calculated according to the equation: $k = (t_{\text{R}} - t_0)/t_0$ (t_{R} = retention time; t_0 = dead time).

Specific binding data (dpm) from radioligand saturation binding experiments were plotted against the free radioligand concentration and analyzed by an equation describing hyperbolic binding (ligand binding – one-site saturation fit, GraphPad Prism 8) to obtain K_{d} and B_{max} values. The free radioligand concentration (nM) was calculated by subtracting the amount of specifically bound radioligand (nM) (calculated from the specifically bound radioligand in dpm, the specific activity, and the volume per well) from the total radioligand concentration.

Specific binding data from radioligand competition binding experiments with [³H]propionyl-pNPY ($C_{\text{final}} = 4 \text{ nM}$) were plotted as % (100% = bound radioligand in the absence of competitor) over log(concentration competitor) and analyzed by four-parameter logistic fits (GraphPad Prism 8.0, GraphPad, San Diego, CA USA) to obtain pIC₅₀ values, which were converted to pK_i values according to the Cheng-Prusoff⁷² equation (logarithmic form) (used K_{d} value of [³H]propionyl-pNPY: 2.97 nM).

All raw data obtained in the β -arrestin2 recruitment assay were processed as follows: firstly, the measured luminescence after addition of agonist (20 repeats) was corrected to an average baseline (first 10 repeats without adding agonist; ratio = luminescence after addition of agonist/baseline luminescence) for each well. Secondly, the relative increase in luminescence (RLU) was obtained by baseline correction with the buffer control. The plateau value of each luminescence trace was plotted as RLU against log(concentration antagonist) and analyzed by four-parameter logistic fits (GraphPad Prism 8.0) to obtain pIC₅₀ values, which were converted to pK_b values according to the Cheng-Prusoff⁷² equation (logarithmic form) (used EC₅₀ value of pNPY: 168 nM). A basal luminescence (buffer control, 0%) and response, corresponding to 200 nM pNPY (100%) were included for normalization of the data (antagonist mode). In case of pNPY (agonist mode) data were normalized to the basal value (0%) and the maximal response of pNPY at a concentration of 10,000 nM (100%).

All raw data obtained in the miniG protein recruitment assay were processed as follows: firstly, the measured luminescence after addition of agonist (90 repeats) was corrected with respect to the luminescence (RLU) of the last measured value (30th repeat) of the baseline (30 repeats; ratio = luminescence after addition of agonist/baseline). Secondly, the relative increase in luminescence (RLU) was obtained by baseline correction with the buffer value. The area under the curve (AUC) of each luminescence trace was plotted as AUC against log(concentration antagonist) and analyzed by four-parameter logistic fits (GraphPad Prism version 8.0) to obtain pIC₅₀ values, which were converted to pK_b values according to the Cheng-Prusoff⁷² equation (logarithmic form) (used EC₅₀ value of pNPY: 3.35 nM). A basal luminescence (buffer control, 0%) and response, corresponding to 50 nM pNPY (100%) were included for subsequent normalization of the data (antagonist mode).

All raw data obtained in the BRET based binding assay were processed as follows: the ratios of the acceptor emission (460 nm) and the donor luminescence (610 nm) was formed (BRET ratio). The “corrected BRET ratio” in saturation binding experiments was obtained by subtracting the buffer control from every value (baseline-correction). Specific binding data from saturation binding experiments were plotted against the free fluorescent ligand concentration and analyzed by an equation describing hyperbolic binding (one site – specific binding, GraphPad Prism 8) to obtain K_d values. Unspecific binding was fitted by linear regression (GraphPad Prism 8).

The data from competition binding experiments were normalized to buffer control (0%) and a 100%-control only containing fluorescent ligand without competitor. Specific binding data from BRET based competition binding experiments with **4.58** (C_{final} = 20 nM) were plotted as % (100% = bound fluorescent ligand in the absence of competitor) over log(concentration competitor) and analyzed by four-parameter logistic fits (GraphPad Prism 8.0, GraphPad, San Diego, CA USA) to obtain pIC₅₀ values, which were converted to pK_i values according to the Cheng-Prusoff⁷² equation (logarithmic form) (used K_d value of **4.58**: 17.9 nM).

The “corrected BRET ratios” in kinetic experiments was obtained by subtracting unspecific binding from total binding. Specific binding data from fluorescent ligand association experiments were analyzed by a two-parameter equation describing an exponential rise to a maximum (one phase – association, GraphPad Prism 8) to obtain the observed association rate constant (k_{obs}), and the resulting plateau value (maximum of specifically bound fluorescent ligand) was used to calculate specifically bound fluorescent ligand (B) in %. Data from fluorescent ligand dissociation experiments in BRET based assays (% specifically bound fluorescent ligand (B) plotted over time) were analyzed by a two-parameter equation describing a monophasic exponential decline (one phase – decay, GraphPad Prism 8) to obtain dissociation rate constants (k_{off}). The association rate constant (k_{on}) was calculated from k_{obs} , k_{off} , and the fluorescent ligand concentration ([FL]) according to the following correlation: $k_{\text{on}} = (k_{\text{obs}} - k_{\text{off}}) \cdot [\text{FL}]^{-1}$. The kinetically determined dissociation rate constant ($K_{\text{i (kinetic)}}$) was determined from dissociation (k_{off}) and association (k_{on}) rate constants ($K_{\text{d}} = k_{\text{off}} \cdot k_{\text{on}}^{-1}$). Propagated errors were calculated according to the Gaussian law of errors.

4.5. References

1. Iliopoulos-Tsoutsouvas, C.; Kulkarni, R. N.; Makriyannis, A.; Nikas, S. P. Fluorescent probes for G-protein-coupled receptor drug discovery. *Expert Opin. Drug* **2018**, *13*, 933-947.
2. Vernall, A. J.; Hill, S. J.; Kellam, B. The evolving small-molecule fluorescent-conjugate toolbox for Class A GPCRs. *Br. J. Pharmacol.* **2014**, *171*, 1073-1084.
3. Kamil, K.; Katarzyna, K.-K. Fluorescent GPCR Ligands as New Tools in Pharmacology. *Curr. Med. Chem.* **2008**, *15*, 2132-2143.
4. Kamil, J. K.; Katarzyna, K.-K. Fluorescent GPCR Ligands as New Tools in Pharmacology-Update, Years 2008- Early 2014. *Curr. Med. Chem.* **2014**, *21*, 3962-3975.
5. Dautzenberg, F. M. Stimulation of neuropeptide Y-mediated calcium responses in human SMS-KAN neuroblastoma cells endogenously expressing Y₂ receptors by co-expression of chimeric G proteins. *Biochem. Pharmacol.* **2005**, *69*, 1493-1499.
6. Pluym, N.; Baumeister, P.; Keller, M.; Bernhardt, G.; Buschauer, A. [³H]UR-PLN196: A Selective Nonpeptide Radioligand and Insurmountable Antagonist for the Neuropeptide Y Y₂ Receptor. *ChemMedChem* **2013**, *8*, 587-593.
7. Pluym, N. Application of the Guanidine-Acylguanidine Bioisosteric Approach to NPY Y₂ Receptors Antagonists: Bivalent, Radiolabeled and Fluorescent Pharmacological Tools. PhD Thesis, University of Regensburg, 2011.
8. Dollinger, H.; Esser, F.; Mihm, G.; Rudolf, K.; Schnorrenberg, G.; Gaida, W.; Doods, N. H. Neue substituierte Aminosäurederivate, Verfahren zu ihrer Herstellung und diese Verbindungen enthaltene pharmazeutische Zusammensetzungen. DE19816929A1, 1998.
9. Ziemek, R.; Brennauer, A.; Schneider, E.; Cabrele, C.; Beck-Sickinger, A. G.; Bernhardt, G.; Buschauer, A. Fluorescence- and luminescence-based methods for the determination of affinity and activity of neuropeptide Y₂ receptor ligands. *Eur. J. Pharm.* **2006**, *551*, 10-18.
10. Cholewinski, M.; Lückel, B.; Horn, H. Degradation pathways, analytical characterization and formulation strategies of a peptide and a protein calcitonine and human growth hormone in comparison. *Pharm. Acta Helv.* **1996**, *71*, 405-419.
11. Manning, M. C.; Chou, D. K.; Murphy, B. M.; Payne, R. W.; Katayama, D. S. Stability of Protein Pharmaceuticals: An Update. *Pharm. Res.* **2010**, *27*, 544-575.
12. Weiss, S.; Keller, M.; Bernhardt, G.; Buschauer, A.; König, B. N^G-Acyl-argininamides as NPY Y₁ receptor antagonists: Influence of structurally diverse acyl substituents on stability and affinity. *Bioorg. Med. Chem.* **2010**, *18*, 6292-6304.
13. Keller, M.; Erdmann, D.; Pop, N.; Pluym, N.; Teng, S.; Bernhardt, G.; Buschauer, A. Red-fluorescent argininamide-type NPY Y₁ receptor antagonists as pharmacological tools. *Bioorg. Med. Chem.* **2011**, *19*, 2859-78.
14. Pluym, N.; Brennauer, A.; Keller, M.; Ziemek, R.; Pop, N.; Bernhardt, G.; Buschauer, A. Application of the Guanidine-Acylguanidine Bioisosteric Approach to Argininamide-Type NPY Y₂ Receptor Antagonists. *ChemMedChem* **2011**, *6*, 1727-1738.
15. Brennauer, A.; Keller, M.; Freund, M.; Bernhardt, G.; Buschauer, A. Decomposition of 1-(ω-aminoalkanoyl)guanidines under alkaline conditions. *Tetrahedron Lett.* **2007**, *48*, 6996-6999.

16. Keller, M.; Weiss, S.; Hutzler, C.; Kuhn, K. K.; Mollereau, C.; Dukorn, S.; Schindler, L.; Bernhardt, G.; König, B.; Buschauer, A. N^ω-Carbamoylation of the Argininamide Moiety: An Avenue to Insurmountable NPY Y₁ Receptor Antagonists and a Radiolabeled Selective High-Affinity Molecular Tool ([³H]UR-MK299) with Extended Residence Time. *J. Med. Chem.* **2015**, *58*, 8834-8849.
17. Brennauer, A. Acylguanidines as bioisosteric groups in argininamide-type neuropeptide Y Y₁ and Y₂ receptor antagonists: synthesis, stability and pharmacological activity. PhD Thesis, University of Regensburg, 2006.
18. Burkert, K.; Zellmann, T.; Meier, R.; Kaiser, A.; Stichel, J.; Meiler, J.; Mittapalli, G. K.; Roberts, E.; Beck-Sickinger, A. G. A Deep Hydrophobic Binding Cavity is the Main Interaction for Different Y₂R Antagonists. *ChemMedChem* **2017**, *12*, 75-85.
19. Merten, N.; Lindner, D.; Rabe, N.; Römpler, H.; Mörl, K.; Schöneberg, T.; Beck-Sickinger, A. G. Receptor subtype-specific docking of Asp6.59 with C-terminal arginine residues in Y receptor ligands. *J Biol Chem* **2007**, *282*, 7543-7551.
20. Berglund, M. M.; Fredriksson, R.; Salaneck, E.; Larhammar, D. Reciprocal mutations of neuropeptide Y receptor Y₂ in human and chicken identify amino acids important for antagonist binding. *FEBS Lett.* **2002**, *518*, 5-9.
21. Kaiser, A.; Müller, P.; Zellmann, T.; Scheidt, H. A.; Thomas, L.; Bosse, M.; Meier, R.; Meiler, J.; Huster, D.; Beck-Sickinger, A. G.; Schmidt, P. Die Entfaltung der C-terminalen α -Helix des Neuropeptids Y ist entscheidend für die Bindung und Aktivierung des Y₂-Rezeptors. *Angew. Chem.* **2015**, *127*, 7554-7558.
22. Doods, H.; Gaida, W.; Wieland, H. A.; Dollinger, H.; Schnorrenberg, G.; Esser, F.; Engel, W.; Eberlein, W.; Rudolf, K. BIIE0246: A selective and high affinity neuropeptide Y Y₂ receptor antagonist. *Eur. J. Pharm.* **1999**, *384*, R3-R5.
23. England, C. G.; Ehlerding, E. B.; Cai, W. NanoLuc: A Small Luciferase Is Brightening Up the Field of Bioluminescence. *Bioconjug. Chem.* **2016**, *27*, 1175-1187.
24. Höfelschweiger, B. K. The Pyrylium Dyes: A New Class of Biolabels. Synthesis, Spectroscopy, and Application as Labels and in general Protein Assay. PhD Thesis, University of Regensburg, Regensburg, 2005.
25. Wetzl, B. K.; Yarmoluk, S. M.; Craig, D. B.; Wolfbeis, O. S. Chameleon Labels for Staining and Quantifying Proteins. *Angew. Chem. Int. Ed.* **2004**, *43*, 5400-5402.
26. Carlson, R.; Larsson, U.; Hansson, L.; Nielsen, H. M.; Piedade, F. M.; Kady, M. M.; Christensen, S. B. Efficient Synthesis of Imines by a Modified Titanium Tetrachloride Procedure. *Acta Chem. Scand.* **1992**, *46*, 1211-1214.
27. Appel, R. Tertiary Phosphane/Tetrachloromethane, a Versatile Reagent for Chlorination, Dehydration, and P-N Linkage. *Angew. Chem., Int. Ed. Engl.* **1975**, *14*, 801-811.
28. Williamson, A. XLV. Theory of ætherification. *The London, Edinburgh, and Dublin Philosophical Magazine and Journal of Science* **1850**, *37*, 350-356.
29. Knoevenagel, E. Condensation von Malonsäure mit aromatischen Aldehyden durch Ammoniak und Amine. *Ber. Dtsch. Chem. Ges.* **1898**, *31*, 2596-2619.

30. Schmidt, W.; Vögtle, F.; Poetsch, E. Spiro units as building blocks in thermotropic liquid crystals: Synthesis and physical properties of terminally substituted spiro[5.5]undecanes. *Liebigs Ann.* **1995**, 1995, 1319-1326.
31. Buschmann, J.; Seiler, T.; Bernhardt, G.; Keller, M.; Wifling, D. Argininamide-type neuropeptide Y Y₁ receptor antagonists: the nature of N^ω-carbamoyl substituents determines Y₁R binding mode and affinity. *RSC Med. Chem.* **2020**, 11, 274-282.
32. Kuhn, K. K.; Ertl, T.; Dukorn, S.; Keller, M.; Bernhardt, G.; Reiser, O.; Buschauer, A. High Affinity Agonists of the Neuropeptide Y (NPY) Y₄ Receptor Derived from the C-Terminal Pentapeptide of Human Pancreatic Polypeptide (hPP): Synthesis, Stereochemical Discrimination, and Radiolabeling. *J. Med. Chem.* **2016**, 59, 6045-6058.
33. Dukorn, S. Pharmacological tools for the NPY receptors: [³⁵S]GTPγS binding assays, luciferase gene reporter assays and labeled peptides PhD Thesis, University of Regensburg, 2017.
34. Dukorn, S.; Littmann, T.; Keller, M.; Kuhn, K.; Cabrele, C.; Baumeister, P.; Bernhardt, G.; Buschauer, A. Fluorescence- and Radiolabeling of [Lys⁴,Nie^{17,30}]hPP Yields Molecular Tools for the NPY Y₄ Receptor. *Bioconjug. Chem.* **2017**, 28, 1291-1304.
35. Huang, W.; Manglik, A.; Venkatakrisnan, A. J.; Laeremans, T.; Feinberg, E. N.; Sanborn, A. L.; Kato, H. E.; Livingston, K. E.; Thorsen, T. S.; Kling, R. C.; Granier, S.; Gmeiner, P.; Husbands, S. M.; Traynor, J. R.; Weis, W. I.; Steyaert, J.; Dror, R. O.; Kobilka, B. K. Structural insights into μ-opioid receptor activation. *Nature* **2015**, 524, 315-321.
36. Liu, W.; Chun, E.; Thompson, A. A.; Chubukov, P.; Xu, F.; Katritch, V.; Han, G. W.; Roth, C. B.; Heitman, L. H.; IJzerman, A. P.; Cherezov, V.; Stevens, R. C. Structural Basis for Allosteric Regulation of GPCRs by Sodium Ions. *Science* **2012**, 337, 232-236.
37. Miller-Gallacher, J. L.; Nehmé, R.; Warne, T.; Edwards, P. C.; Schertler, G. F. X.; Leslie, A. G. W.; Tate, C. G. The 2.1 Å Resolution Structure of Cyanopindolol-Bound β₁-Adrenoceptor Identifies an Intramembrane Na⁺ Ion that Stabilises the Ligand-Free Receptor. *PLOS ONE* **2014**, 9, e92727.
38. Gerald, C.; Walker, M. W.; Vaysse, P. J.; He, C.; Branchek, T. A.; Weinshank, R. L. Expression cloning and pharmacological characterization of a human hippocampal neuropeptide Y/peptide YY Y₂ receptor subtype. *J Biol Chem* **1995**, 270, 26758-61.
39. Felixberger, J. Luciferase complementation for the determination of arrestin recruitment: Investigation at histamine and NPY receptors. PhD Thesis, University of Regensburg, 2014.
40. Lohse, M. J.; Nuber, S.; Hoffmann, C. Fluorescence/Bioluminescence Resonance Energy Transfer Techniques to Study G-Protein-Coupled Receptor Activation and Signaling. *Pharmacol. Rev.* **2012**, 64, 299-336.
41. Stoddart, L. A.; Kilpatrick, L. E.; Hill, S. J. NanoBRET Approaches to Study Ligand Binding to GPCRs and RTKs. *Trends Pharmacol. Sci.* **2018**, 39, 136-147.
42. Mullins, D.; Adham, N.; Hesk, D.; Wu, Y.; Kelly, J.; Huang, Y.; Guzzi, M.; Zhang, X.; McCombie, S.; Stamford, A.; Parker, E. Identification and characterization of pseudoirreversible nonpeptide antagonists of the neuropeptide Y Y₅ receptor and development of a novel Y₅-selective radioligand. *Eur. J. Pharm.* **2008**, 601, 1-7.
43. ICRP. 1977. Recommendations of the ICRP. ICRP Publication 26. Ann. ICRP 1 (3).

44. ICRP. 2007. The 2007 Recommendations of the International Commission on Radiological Protection. ICRP Publication 103. Ann. ICRP 37 (2-4).
45. Dautzenberg, F. M.; Neysari, S. Irreversible Binding Kinetics of Neuropeptide Y Ligands to Y₂ but Not to Y₁ and Y₅ Receptors. *Pharmacology* **2005**, *75*, 21-29.
46. Shoblock, J. R.; Welty, N.; Nepomuceno, D.; Lord, B.; Aluisio, L.; Fraser, I.; Motley, S. T.; Sutton, S. W.; Morton, K.; Galici, R.; Atack, J. R.; Dvorak, L.; Swanson, D. M.; Carruthers, N. I.; Dvorak, C.; Lovenberg, T. W.; Bonaventure, P. In vitro and in vivo characterization of JNJ-31020028 (N-(4-{4-[2-(diethylamino)-2-oxo-1-phenylethyl]piperazin-1-yl}-3-fluorophenyl)-2-pyridin-3-yl)benzamide), a selective brain penetrant small molecule antagonist of the neuropeptide Y Y₂ receptor. *J. Psychopharmacol.* **2009**, *208*, 265.
47. Kuhn, K. Molecular Tools for the NPY Y₄ Receptor Derived from the C-terminus of hPP and from Arginineamide-type Y₁R Antagonists. PhD Thesis, University of Regensburg, 2017.
48. Schneider, E.; Mayer, M.; Ziemek, R.; Li, L.; Hutzler, C.; Bernhardt, G.; Buschauer, A. A Simple and Powerful Flow Cytometric Method for the Simultaneous Determination of Multiple Parameters at G Protein-Coupled Receptor Subtypes. *ChemBioChem* **2006**, *7*, 1400-1409.
49. Moser, C.; Bernhardt, G.; Michel, J.; Schwarz, H.; Buschauer, A. Cloning and functional expression of the hNPY Y₅ receptor in human endometrial cancer (HEC-1B) cells. *Can. J. Physiol. Pharmacol.* **2000**, *78*, 134-42.
50. Fulmer, G. R.; Miller, A. J. M.; Sherden, N. H.; Gottlieb, H. E.; Nudelman, A.; Stoltz, B. M.; Bercaw, J. E.; Goldberg, K. I. NMR Chemical Shifts of Trace Impurities: Common Laboratory Solvents, Organics, and Gases in Deuterated Solvents Relevant to the Organometallic Chemist. *Organometallics* **2010**, *29*, 2176-2179.
51. Yang, Q.; Sheng, M.; Henkelis, J. J.; Tu, S.; Wiensch, E.; Zhang, H.; Zhang, Y.; Tucker, C.; Ejeh, D. E. Explosion Hazards of Sodium Hydride in Dimethyl Sulfoxide, N,N-Dimethylformamide, and N,N-Dimethylacetamide. *Org. Process Res. Dev.* **2019**, *23*, 2210-2217.
52. Ip, H.-W.; Ng, C.-F.; Chow, H.-F.; Kuck, D. Three-Fold Scholl-Type Cycloheptatriene Ring Formation around a Tribenzotriquinacene Core: Toward Warped Graphenes. *J. Am. Chem. Soc.* **2016**, *138*, 13778-13781.
53. Fan, J.; Wan, C.; Wang, Q.; Gao, L.; Zheng, X.; Wang, Z. Palladium catalyzed isomerization of alkenes: a pronounced influence of an o-phenol hydroxyl group. *Org. Biomol. Chem.* **2009**, *7*, 3168-3172.
54. Presset, M.; Paul, J.; Cherif, G. N.; Ratnam, N.; Laloi, N.; Léonel, E.; Gosmini, C.; Le Gall, E. Col-Catalyzed Barbier Reactions of Aromatic Halides with Aromatic Aldehydes and Imines. *Chem. Eur. J.* **2019**, *25*, 4491-4495.
55. Sasse, B. C.; Mach, U. R.; Leppanen, J.; Calmels, T.; Stark, H. Hybrid approach for the design of highly affine and selective dopamine D₃ receptor ligands using privileged scaffolds of biogenic amine GPCR ligands. *Bioorg. Med. Chem.* **2007**, *15*, 7258-7273.
56. Perlmutter, J. I.; Forbes, L. T.; Krysan, D. J.; Ebsworth-Mojica, K.; Colquhoun, J. M.; Wang, J. L.; Dunman, P. M.; Flaherty, D. P. Repurposing the Antihistamine Terfenadine for Antimicrobial Activity against *Staphylococcus aureus*. *J. Med. Chem.* **2014**, *57*, 8540-8562.

57. Gobbo, P.; Gunawardene, P.; Luo, W.; Workentin, M. S. Synthesis of a Toolbox of Clickable Rhodamine B Derivatives. *Synlett* **2015**, 26, 1169-1174.
58. Flack, T.; Romain, C.; White, A. J. P.; Haycock, P. R.; Barnard, A. Design, Synthesis, and Conformational Analysis of Oligobenzanilides as Multifacial α -Helix Mimetics. *Org. Lett.* **2019**, 21, 4433-4438.
59. Porter, N. J.; Shen, S.; Barinka, C.; Kozikowski, A. P.; Christianson, D. W. Molecular Basis for the Selective Inhibition of Histone Deacetylase 6 by a Mercaptoacetamide Inhibitor. *ACS Med. Chem. Lett.* **2018**, 9, 1301-1305.
60. Dhainaut, A.; Regnier, G.; Atassi, G.; Pierre, A.; Leonce, S.; Kraus-Berthier, L.; Prost, J. F. New triazine derivatives as potent modulators of multidrug resistance. *J. Med. Chem.* **1992**, 35, 2481-2496.
61. Waring, W. S.; Whittle, B. A. Basic dihydromorphanthridinones with anticonvulsant activity. *J. Pharm. Pharmacol.* **1969**, 21, 520-530.
62. Ma, L.; Yuan, L.; Xu, C.; Li, G.; Tao, M.; Zhang, W. An Efficient Synthesis of 2-Aminothiophenes via the Gewald Reaction Catalyzed by an N-Methylpiperazine-Functionalized Polyacrylonitrile Fiber. *Synthesis* **2013**, 45, 45-52.
63. Yestrepesky, B. D.; Xu, Y.; Breen, M. E.; Li, X.; Rajeswaran, W. G.; Ryu, J. G.; Sorenson, R. J.; Tsume, Y.; Wilson, M. W.; Zhang, W.; Sun, D.; Sun, H.; Larsen, S. D. Novel inhibitors of bacterial virulence: Development of 5,6-dihydrobenzo[h]quinazolin-4(3H)-ones for the inhibition of group A streptococcal streptokinase expression. *Bioorg. Med. Chem.* **2013**, 21, 1880-1897.
64. El Batran, S. A.; Osman, A. E. N.; Ismail, M. M.; El Sayed, A. M. Synthesis and evaluation of 2,6-piperidinedione derivatives as potentially novel compounds with analgesic and other CNS activities. *Inflammopharmacology* **2006**, 14, 62-71.
65. Cao, G.; Wu, W. Preparation method of 1,1-cyclohexanediacetic acid CN20091095241, 2009.
66. Wu, J.; He, L.; Noble, A.; Aggarwal, V. K. Photoinduced Deaminative Borylation of Alkylamines. *J. Am. Chem. Soc.* **2018**, 140, 10700-10704.
67. Müller, S.; Webber, M. J.; List, B. The Catalytic Asymmetric Fischer Indolization. *J. Am. Chem. Soc.* **2011**, 133, 18534-18537.
68. Ziemek, R.; Schneider, E.; Kraus, A.; Cabrele, C.; Beck-Sickinger, A. G.; Bernhardt, G.; Buschauer, A. Determination of Affinity and Activity of Ligands at the Human Neuropeptide Y Y₄ Receptor by Flow Cytometry and Aequorin Luminescence. *J. Recept. Signal Transduct. Res.* **2007**, 27, 217-233.
69. Keller, M.; Bernhardt, G.; Buschauer, A. [³H]UR-MK136: A Highly Potent and Selective Radioligand for Neuropeptide Y Y₁ Receptors. *ChemMedChem* **2011**, 6, 1566-1571.
70. Ai, H.; Mills, D. K.; Jonathan, A. S.; Jones, S. A. Gelatin-glutaraldehyde cross-linking on silicone rubber to increase endothelial cell adhesion and growth. *In Vitro Cell. Dev. Biol. Anim.* **2002**, 38, 487-92.
71. Bernhardt, G.; Reile, H.; Birnböck, H.; Spruß, T.; Schönenberger, H. Standardized kinetic microassay to quantify differential chemosensitivity on the basis of proliferative activity. *J. Cancer Res. Clin. Oncol.* **1992**, 118, 35-43.

72. Yung-Chi, C.; Prusoff, W. H. Relationship between the inhibition constant (K_i) and the concentration of inhibitor which causes 50 per cent inhibition (I_{50}) of an enzymatic reaction. *Biochem. Pharmacol.* **1973**, 22, 3099-3108.

Chapter 5

In search of labelled Y₂R antagonists: Synthesis and pharmacological characterization of labelling precursors and “cold” forms of potential Y₂R radioligands obtained by modification of the (S)-argininamide BIIE-0246 at the dibenzoazepinone moiety

Note: I gratefully acknowledge the help of Dr. Timo Littman for teaching the β -arrestin2 recruitment assay.

The preparation and cultivation of cells for the BRET based binding assay is part of the ongoing doctoral thesis of Lukas Grätz (*cf.* Chapter 4)

I gratefully acknowledge the support of my research students (Forschungspraktikanten) Alexander Reichle, Alexander Hubmann, Simon Scheuerer and Florian Fricke during synthesis.

Thanks are due to Brigitte Wenzl, Maria Beer-Krön, Susanne Bollwein and Lydia Schneider for excellent technical assistance (cultivation of cells, radioligand competition binding experiments at hY₁R and hY₅R, and BRET based competition binding assays).

5.1. Introduction

Over the last decade, several radioligands (Table 5.1) and their “cold” forms derived from the (S)-argininamide-type Y₂R antagonist **4.1**¹ by bioisosteric replacement of the guanidine group by an acylguanidine (**4.2**² and **5.1**²) or carbamoylguanidine (**5.2**^{3, 4}) moiety have been prepared in our group. It is notable that in contrast to the carbamoylguanidine approach, the use of acylguanidines is unfavourable due to the limited chemical stability of acylguanidines at neutral pH and, in particular, under basic conditions.⁵

Table 5.1. Structures and Y₂R affinities of BIIE-0246 (**4.1**), the structurally related radioligands [³H]**4.2**, [³H]**5.1** and [³H]**5.2** and the potential radioligands (“cold” forms) **4.23**, **4.24** and **4.27**.

Compound	Ref.	R ¹	R ²	pK _d	pK _i
4.1 (BIIE-0246)	a	A		n.a.	7.44
[³ H] 4.2 ([³ H]UR-PLN196)	b	A		7.17	8.00
4.23 (UR-jb206)	B	B		n.a.	7.39
4.24 (UR-jb209)	C	C		n.a.	6.81
4.27 (UR-jb208)	D	D		n.a.	6.26
[³ H] 5.1 ([³ H]UR-PLN208)	b, c	A		7.72	8.28
[³ H] 5.2 ([³ H]UR-PLN187)	c, d	A		n.a.	7.19

The binding affinities (pK_i) of **4.23**, **4.24** and **4.27** were determined in a radioligand competition binding assay using [³H]propionyl-pNPY (C_{final} = 4 nM, K_d = 2.97 nM) and HEK293T hY₂R + βArr2 cells (cf. Chapter 4). References: (a) Dautzenberg,⁶ K_i value was determined using [¹²⁵I]PYY (C_{final} = 0.10 nM, K_d = 0.08 nM) and membranes from SMS-KAN cells. (b) Pluym et al.,² the reported K_d value of [³H]**4.2** was determined by saturation binding experiments in living CHO-hY₂-G_{iq5}-mtAEQ cells and the reported K_i values of **4.2** and **5.1** were determined in a flow cytometric binding assay using Cy5-pNPY (c = 5 nM, K_d = 5.4 nM) and CHO-hY₂-G_{iq5}-mtAEQ cells. (c) Baumeister, PhD Thesis, University of Regensburg, 2014,⁴ the reported K_d value of [³H]**5.1** was determined by saturation binding experiments in living CHO-hY₂-G_{iq5}-mtAEQ cells. (d) Pluym, PhD Thesis, University of Regensburg, 2011,³ the reported K_i value of **5.2** was determined in a flow cytometric binding assay using Cy5-pNPY (c = 5 nM, K_d = 5.4 nM) and CHO-hY₂-G_{iq5}-mtAEQ cells. Reported K_i (K_d) values were converted to pK_i (pK_d) values. n.a. not applicable.

Notably, competition binding studies with pNPY and the radioligands [³H]**4.2** and [³H]**5.1** yielded considerably lower pK_i values for pNPY compared to competition binding assays using [³H]propionyl-pNPY or Cy5-pNPY as labelled ligand.^{2, 4} In view of a more favourable hY₂R radioligand, the synthesized and pharmacologically characterized compound **4.23** (synthesis see Chapter 4) represents the “cold” form of a radioligand potentially exhibiting more favourable binding characteristics at the Y₂R. To enable tritium-labelling in the last synthesis step using commercially available [³H]methyl iodide or [³H]methyl nosylate (to give [³H]UR-jb206 ([³H]**4.23**)), a precursor is required that contains a phenolic hydroxy group instead of the methoxy group found in **4.23**.

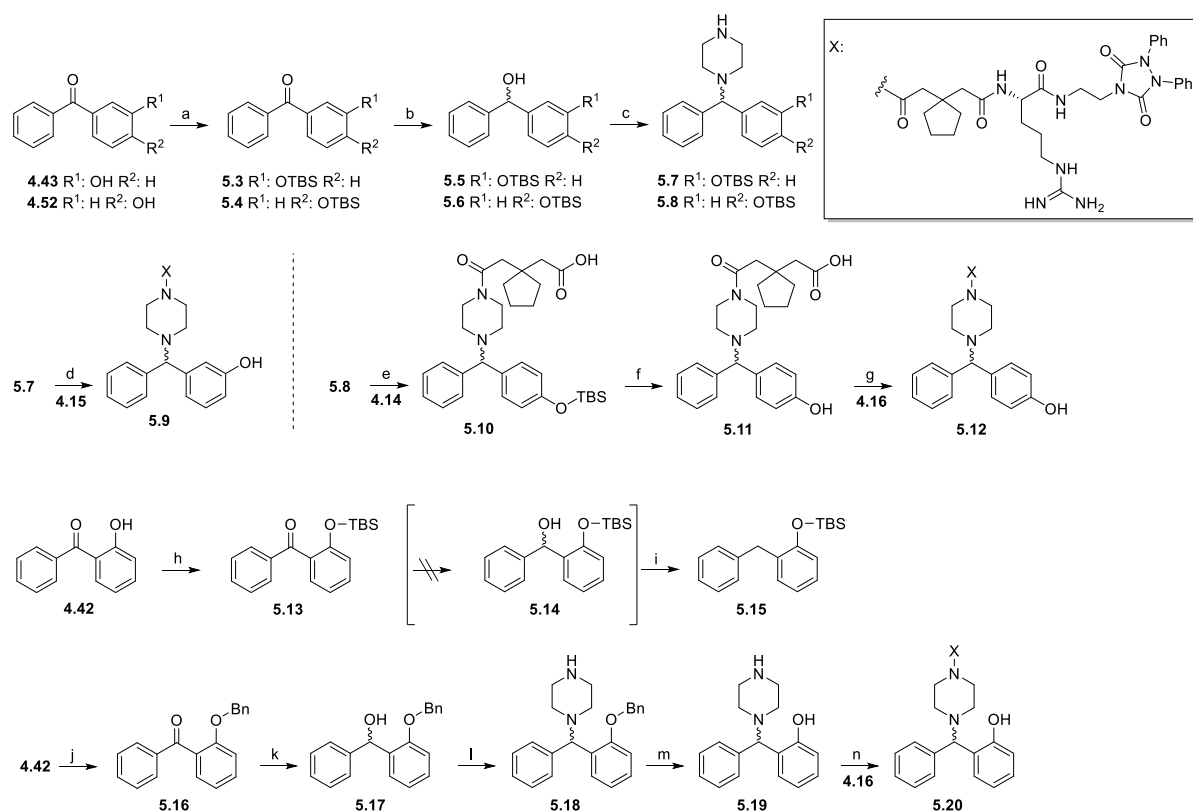
The dibenzoazepinone-benzhydryl approach i.e. bioisosteric replacement of the dibenzoazepinone scaffold in **4.1** by a benzhydryl moiety (cf. Chapter 4), resulted in several compounds that represent “cold” forms of potential radioligands (**4.23**, **4.24** and **4.27**) and an amino-functionalized precursor (**4.50**), which can be used for the synthesis of “cold” forms of potential radiotracers. In this chapter, the synthesis

of the phenolic precursors of **4.23**, **4.24** and **4.27** and their pharmacological characterization in radioligand competition binding studies and β -arrestin2 recruitment assays is described. Moreover, the amino precursor **4.50** (synthesis described in Chapter 4) was converted to potential radioligands (“cold” forms) by methylation, propionylation and 2-fluoroacetylation. These derivatives were also pharmacologically characterized. Additionally, the chemical stability was investigated in 25 mM HEPES buffer (pH 7) for selected compounds.

5.2. Results and discussion

5.2.1. Synthesis

The synthesis of compounds **4.15**, **4.16**, **4.34**, **4.42**, **4.43**, **4.50** and **4.52** was previously described in chapter 4 (*cf.* 4.2.1.). Compounds **5.9**, **5.12** and **5.20** were synthesized from the respective hydroxy substituted benzophenones **4.42**, **4.43** and **4.52** (Scheme 5.1).



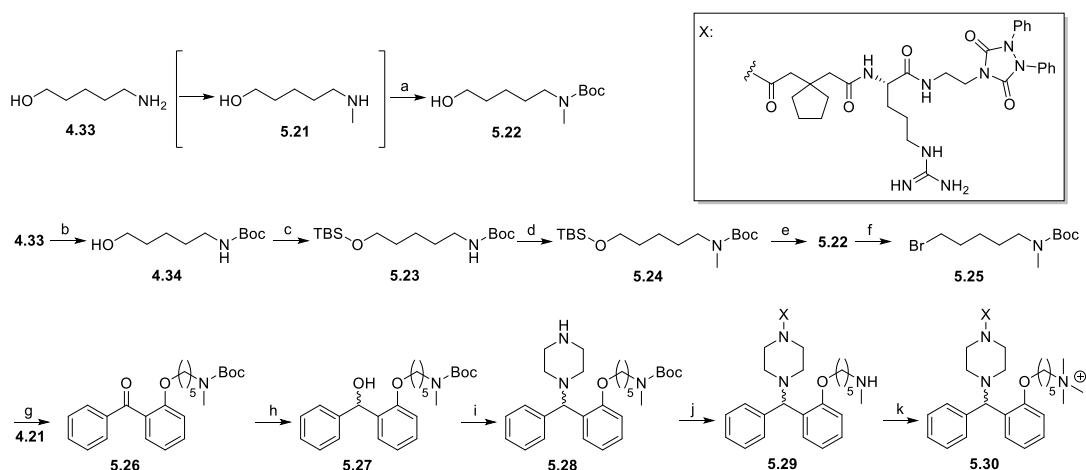
Scheme 5.1. Synthesis of the phenolic precursors **5.9**, **5.12** and **5.20**. Reagents and conditions. (a) *tert*-butyldimethylsilyl chloride, Et₃N, CH₂Cl₂, 53-62%; (b) NaBH₄, MeOH, 89-93%; (c) (1) methanesulfonyl chloride, Et₃N, CH₂Cl₂, (2) piperazine, acetonitrile, microwave device (70 °C, 30 min), 62%; (d) (1) EDC·HCl, HOBT, DMF, (2) TFA/H₂O 95:5, 16%; (e) CH₂Cl₂, 63%; (f) TBAF, THF, 100%; (g) (1) EDC·HCl, HOBT, DMF, (2) TFA/H₂O 95:5, 24%; (h) *tert*-butyldimethylsilyl chloride, Et₃N, CH₂Cl₂, 85%; (i) H₂, Pd/C, MeOH, 79%; (j) benzyl bromide, K₂CO₃, acetonitrile, microwave device (80 °C, 1 h), 70%; (k) NaBH₄, MeOH, 95%; (l) (1) methanesulfonyl chloride, Et₃N, CH₂Cl₂, (2) piperazine, acetonitrile, microwave device (70 °C, 30 min), 53%; (m) H₂ (10 bar), Pd/C, MeOH, 44%; (n) (1) EDC·HCl, HOBT, DMF, (2) TFA/H₂O 95:5, 8%.

Firstly, the phenolic hydroxy groups of **4.42**, **4.43** and **4.52** were protected using *tert*-butylmethylsilyl chloride to give silyl ethers **5.3**, **5.4** and **5.13** in moderate to good yields. Secondly, (3-((*tert*-butyldimethylsilyl)oxy)phenyl)(phenyl)methanone (**5.3**) and (4-((*tert*-butyldimethylsilyl)oxy)phenyl)-(phenyl)methanone (**5.4**) were converted to the respective alcohols (**5.5** and **5.6**) in excellent yields,

using sodium borohydride in methanol. The benzhydryl alcohols **5.5** and **5.6** were converted to the respective mesylates by use of methanesulfonyl chloride in dichloromethane and then treated with piperazine in acetonitrile (microwave device) to form amines **5.7** and **5.8**.

Compound **5.9** was obtained by amide bond formation between **5.7** and the carboxylic acid **4.14** in DMF at rt using EDC·HCl and HOBT as coupling reagents (Scheme 5.1), followed by treatment with aqueous TFA (95:5) to cleave the Pbf and TBS protecting groups. Amine **5.8** was treated with 3,3-tetramethylglutaric anhydride **4.14** to form the carboxylic acid **5.10**. The TBS protecting group of **5.10** was removed in a solution of TBAF in THF to give the phenol **5.11** in moderate yield. Consecutively, the carboxylic acid **5.11**, activated using EDC·HCl and HOBT was coupled to (S)-arginine derivative **4.16** to give **5.12**.

The reduction of (2-((*tert*-butyldimethylsilyloxy)phenyl)(phenyl)methanone **5.13**, intended to give **5.14**, failed using sodium borohydride. Furthermore, the compound **5.15** instead of **5.14** was obtained using palladium on activated charcoal and hydrogen (Scheme 5.1). Compound **5.15** was identified by ¹H-/¹³C-NMR and HRMS. Therefore, the phenolic hydroxy group in **4.42** was benzyl protected using benzyl bromide and K₂CO₃ in DMF (microwave device). The product, benzyl ether **5.16**, was reduced to alcohol **5.17** in excellent yields using methanol as solvent and sodium borohydride as reducing agent. Piperazine **5.18** was synthesized as previously described for compounds **5.7** and **5.8**, starting from benzhydryl alcohol **5.17**. Compound **5.19** was obtained by removal of the benzyl protecting group of **5.18** using palladium on activated charcoal and hydrogen in methanol. Amide bond formation between **4.16** and **5.19**, and subsequent Pbf removal was performed as described for **4.9** and **4.12**. These conditions gave **5.20** in low yield (Scheme 5.1).



Scheme 5.2. Synthesis of *N*-methylated compounds **5.29** and **5.30**. Reagents and conditions. (a) (1) benzaldehyde toluene, reflux (2) MeI, reflux, (3) H⁺/H₂O, reflux, (4) NaOH, Boc₂O, yield was not determined; (b) Boc₂O, Et₃N, CH₂Cl₂, 73%; (c) *tert*-butyldimethylsilyl chloride, Et₃N, CH₂Cl₂, 95%; (d) (1) NaH; THF, 0 °C, 15 min (2) MeI, THF, rt, 24 h, 52%; (e) TBAF, THF, 50%; (f) CBr₄, PPh₃, THF, 98%; (g) K₂CO₃, DMF, 52%; (h) NaBH₄, MeOH, 100%; (i) (1) methanesulfonyl chloride, Et₃N, CH₂Cl₂, (2) piperazine, acetonitrile, microwave device (70 °C, 30 min), 80%; (j) (1) EDC·HCl, HOBT, DMF, (2) TFA/H₂O 95:5, 20%; (k) methyl 4-nitrobenzenesulfonate, K₂CO₃, DMF, 59%.

For selective mono methylation of the primary amine **4.33**, two strategies were applied (Scheme 5.2). Firstly, to avoid overalkylation, 5-aminopentanol (**4.33**) and benzaldehyde were heated using a Dean-Stark apparatus to form an imine *in situ*, followed by the addition of methyl iodide. Consecutively, the

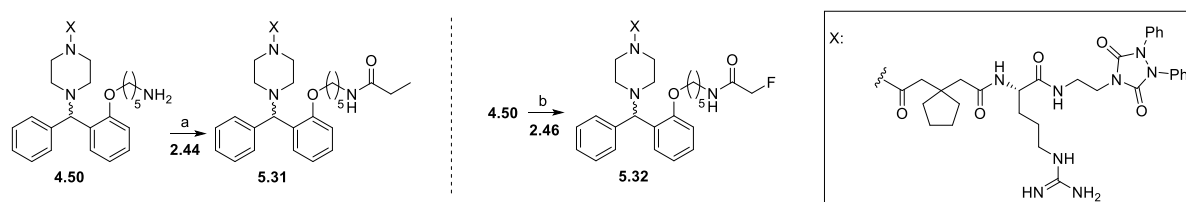
reaction mixture was acidified with aqueous HCl for hydrolysis of the imine. The aqueous phase was washed with diethyl ether twice, in order to remove benzaldehyde to obtain **5.21**.

Compound **5.21** could not be extracted from the aqueous phase. Therefore, the reaction mixture was basified with NaOH (1 N) and Boc_2O was added to obtain **5.22**. Unfortunately, purification of **5.22** by column chromatography failed.

Due to purification problems, a second synthesis route was applied to obtain **5.22** in a four-step synthesis route starting from **4.33**. For this purpose, *tert*-butyl (5-hydroxypentyl)carbamate (**4.34**) was treated with *tert*-butyldimethylsilyl chloride to give the silyl ether **5.23** in excellent yield. Mono-alkylation of **5.23** was performed using sodium hydride and methyl iodide to give **5.24** (Scheme 5.2). *tert*-Butyl (5-hydroxypentyl)(methyl)carbamate (**5.22**) was afforded by cleavage of the TBS group using TBAF. Alcohol **5.22** was then converted to the bromide (Appel reaction⁷). Compound **5.26** was synthesized in a Williamson ether synthesis from the intermediates **4.21** and **5.25**. The ketone **5.26** was converted to alcohol **5.27** in excellent yields using NaBH_4 in methanol.

Furthermore, the synthesis of amine **5.28** was performed as already described for **5.7** and **5.8** in a two-step synthesis. The alcohol **5.27** was converted to the mesylate and subsequently coupled with piperazine. Compound **5.29** was synthesized by amide bond formation as described for **5.9** and **5.20** using coupling reagents (EDC·HCl and HOBT) and subsequent removal of the Pbf group.

Overalkylation of **5.29** using methyl 4-nitrobenzenesulfonate lead to **5.30** (Scheme 5.2).



Scheme 5.3. Synthesis of potential “cold” forms of radiotracers **5.31** and **5.32**. Reagents and conditions. (a) Et_3N , DMF, 92%; (b) DCC, Et_3N , 42%.

Propionamide **5.31** and 2-fluoroacetamide **5.32** were synthesized from amine **4.50** by amide bond formation using succinimidyl propionate (**2.44**) and 2-fluoroacetic acid (**2.46**) activated by DCC, respectively (Scheme 5.3). Compound **5.32** represents the “cold” form of a potential Y_2R PET ligand.

5.2.2. Investigation of the chemical stability of **4.23**, **4.24**, **4.27**, **5.30** and **5.32**

The stability of selected (*S*)-argininamides (**4.23**, **4.24**, **4.27**, **5.30** and **5.32**) was investigated in the buffer (25 mM HEPES, 2.5 mM CaCl_2 , 1 mM MgCl_2 , pH 7) used for [^3H]propionyl-pNPY displacement studies at the Y_2R (cf. 4.2.4.1. and 5.2.3.1.). Compounds **4.23**, **4.24**, **4.27**, **5.9**, **5.30** and **5.32** were obtained as diastereomers due to the applied synthesis route. The diastereomers were not apparent in the chromatograms of the reversed-phase HPLC (220 nm) analysis. (*S*)-Argininamide-type Y_2R antagonists **4.23**, **4.24**, **4.27**, **5.9**, **5.30** and **5.32** (100 μM) were incubated at rt for 24 h. Prior to analytical RP-HPLC (220 nm) analysis the solution was diluted (1:1) with 10% aq. TFA. Analyses were performed after 0 h, 1 h, 2 h, 4 h, 8 h and 24 h. The procedure was described in the literature⁸ (cf. 2.4.3.) and slightly modified as described in chapter 4 (cf. 4.4.2.).

All investigated compounds proved to be stable (chromatograms of **4.23**, **4.24**, **4.27**, **5.9** and **5.32** see Figure 5.1 and *cf.* Figure 8.5 (8.4.1.1.) for **5.9** and **5.30**) at pH 7. Future studies should investigate plasma stability to explore possible enzymatic degradation of the compounds.

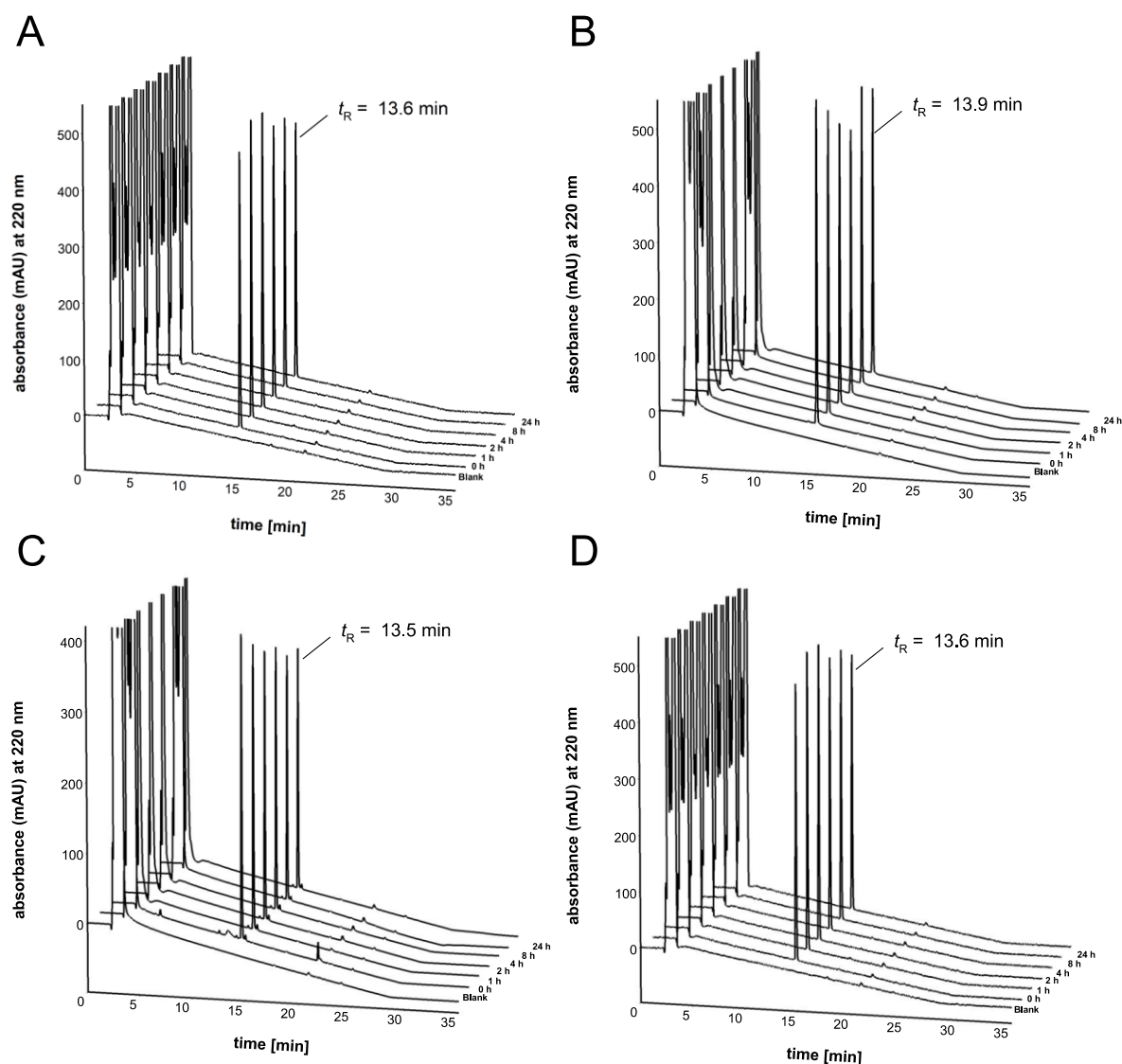


Figure 5.1. Chromatograms of the reversed-phase HPLC (220 nm) analysis of phenol ethers (A) **4.23**, (B) **4.24**, (C) **4.27** and the propionylated compound (D) **5.32** after incubation in a 25 mM HEPES buffer (pH 7.0) at rt for up to 24 h. **4.23**, **4.24**, **4.27** and **5.32** proved to be stable.

5.2.3. Pharmacological methods: Y₂R affinity (pK_i) and antagonism (pK_b) of synthesized (S)-argininamides

(S)-Argininamides **5.9**, **5.12**, **5.20**, **5.29** and **5.31** were investigated in a competition radioligand binding assay to determine their Y₂R affinities (5.2.3.1.). Furthermore, Y₂R affinities (pK_i) of compounds **4.24**, **5.29** and **5.30-5.31** were determined in a BRET based binding assay (5.2.3.2.), Y₂R antagonism (pK_b) of **5.9**, **5.12**, **5.20** and **5.29-5.31** was studied in a β-arrestin2 recruitment assay (5.2.3.3.).

5.2.3.1. Determination of pK_i values in a radioligand binding assay in HEK293T hY₂R + β Arr2 cells

The radioligand competition binding assay was performed according to the literature⁹ with minor modifications (*cf.* 4.2.4.1.) in living HEK293T hY₂R + β Arr2 cells¹⁰ using [³H]propionyl-pNPY ($C_{\text{final}} = 4 \text{ nM}$, $K_d = 2.97 \text{ nM}$) in sodium-free binding buffer (competition binding curves shown in Figure 5.2, pK_i values summarized in Table 5.2).

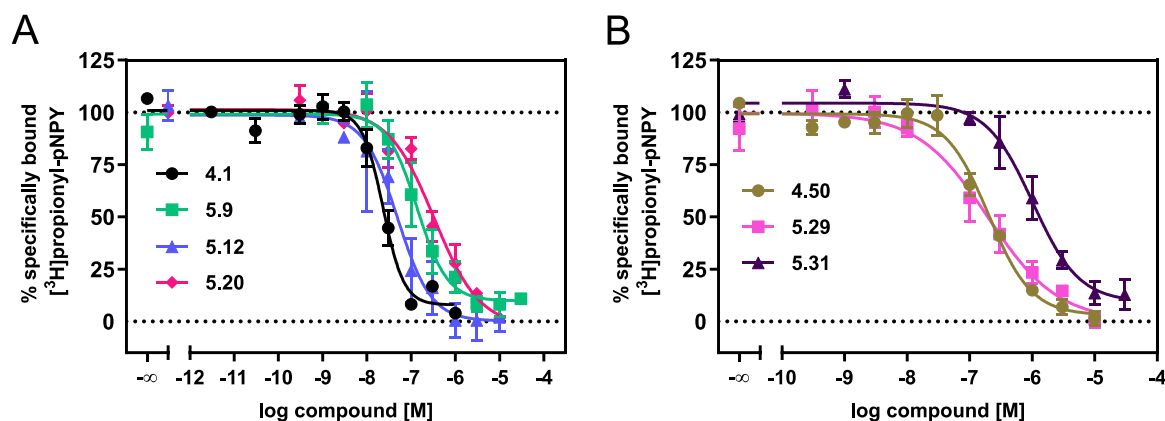


Figure 5.2. Displacement curves of [³H]propionyl-pNPY ($C_{\text{final}} = 4 \text{ nM}$, $K_d = 2.97 \text{ nM}$) obtained from competition binding studies with (A) **4.1**, **5.9**, **5.12**, **5.20**, (B) **4.50**, **5.29** and **5.31** in HEK293T hY₂R + β Arr2 cells. Data are presented as means \pm SEM from at least two independent experiments, each performed in triplicate.

The affinity (pK_i) of 2-methoxysubstituted compound **4.23** was slightly lower compared to that of the phenolic precursor **5.20** (Table 5.2). In addition, Y₂R affinities of the phenolic precursors of 3-hydroxy (**5.9**) and 4-hydroxy (**5.20**) substituted derivatives were higher (around one order of magnitude compared to the respective 3- or 4-methoxy substituted compounds).

Table 5.2. Y₂R affinities (pK_i) of synthesized (S)-argininamids determined in equilibrium competition binding with [³H]propionyl-pNPY.

Compound	$pK_i \pm \text{SEM}^a$	N	Compound	$pK_i \pm \text{SEM}^a$	N
4.1	8.06 ± 0.11	2	5.9	7.20 ± 0.20	2
4.23	7.39 ± 0.13	3	5.12	7.77 ± 0.10	2
4.24	6.81 ± 0.23	3	5.20	6.73 ± 0.15	3
4.27	6.26 ± 0.03	3	5.29	7.12 ± 0.31	2
4.50	7.06 ± 0.09	4	5.31	6.34 ± 0.08	3

^aRadioligand competition binding assay with [³H]propionyl-pNPY ($C_{\text{final}} = 4.0 \text{ nM}$, $K_d = 2.97 \text{ nM}$) in intact HEK293T hY₂R + β Arr2 cells. Mean values \pm SEM from at least N independent experiments, each performed in triplicate.

As previously described in chapter 4 (*cf.* 4.2.4.1.) and as mentioned above, the introduction of methoxy groups at the benzhydryl moiety led to a slight decrease in affinity. Among these methoxy substituted compounds (**4.23**, **4.24** and **4.27**), the 2-methoxy substituted derivative (**4.23**) showed the highest affinity. This trend was not observed in case of the hydroxy substituted derivatives **5.9**, **5.12** and **5.20**.

The 3-hydroxy substituted compound (**5.9**) showed the highest affinity and the 2-hydroxy substituted derivative (**5.20**) exhibited the lowest Y₂R affinity among the phenolic precursors. The introduction of one methyl group at the primary amino group of compound **4.50**, resulting in **5.29**, did not affect Y₂R affinity. The propionylated derivative of amine precursor **4.50** (compound **5.31**) showed lower Y₂R affinity compared to **4.50**. Interestingly, compound **4.58**, bearing a bulky fluorescent dye instead of the small propionyl moiety in **5.31**, displayed higher Y₂R affinity than **5.31** (pK_i values (hY₂R): 7.03 vs. 6.32).

5.2.3.2. Determination of pK_i values in a BRET based binding assay

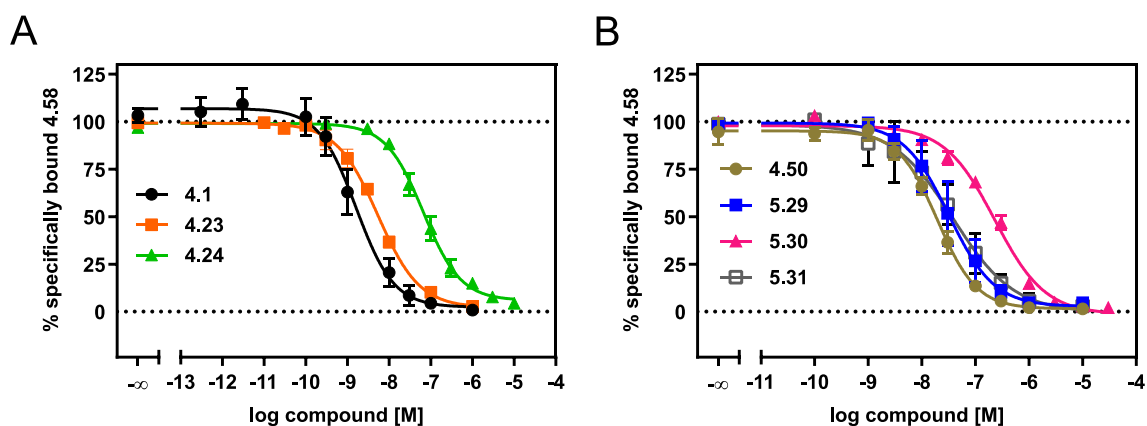


Figure 5.3. Displacement curves of **4.58** ($C_{\text{final}} = 20 \text{ nM}$, $K_{\text{d}} = 17.9 \text{ nM}$) obtained from competition binding studies with (A) **4.1**, **4.23**, **4.24**, (B) **4.50**, and **5.30-5.32** at HEK293T Y₂(intraNLucD197) cells. Data are presented as means \pm SEM from at least three independent experiments, each performed in triplicate.

The BRET based competition binding assay was performed in living HEK293T Y₂(intraNLucD197) cells with **4.58** ($C_{\text{final}} = 20 \text{ nM}$, $K_{\text{d}} = 17.9 \text{ nM}$) (*cf.* chapter 4) in sodium containing buffer (Figure 5.3 and Table 5.3). Compound **4.23** (2-methoxy substituted) showed the highest Y₂R affinity among the investigated (S)-argininamides (**4.24**, **5.29-5.31**), consistent with the results obtained from the radioligand competition binding experiments. Furthermore, Y₂R binding of **4.23** was higher compared tot hat of **4.24** (3-methoxy substituted).

Table 5.3. Affinities (pK_i) of selected (S)-argininamides **4.1**, **4.23**, **4.24**, **4.50** and **5.30-5.32** determined in a BRET based competition binding assay

Compound	pK _i ^a	Compound	pK _i ^a
4.1	9.13 \pm 0.15	5.30	7.83 \pm 0.26
4.23	8.60 \pm 0.07	5.31	7.16 \pm 0.07
4.24	7.43 \pm 0.10	5.32	7.78 \pm 0.16
4.50	8.03 \pm 0.08		

^aBRET based competition binding assay with **4.58** ($C_{\text{final}} = 20 \text{ nM}$, $K_{\text{d}} = 17.9 \text{ nM}$) in intact HEK293T Y₂(intraNLucD197) cells. Mean values \pm SEM from at least three independent experiments performed, each in triplicate.

The decrease in affinity (pK_i) from the dibenzoazepinone (**4.1**) to 2-methoxy (**4.23**) and 3-methoxy (**4.24**) benzhydryl derivatives demonstrated the same trend compared to pK_i values determined in a radioligand competition binding experiments using a sodium-free buffer (Table 5.2 and Table 5.3). Y_2R affinities of the (5-(trimethylaminio)pentyl)oxy (*N*-,overalkylated“) derivative **5.30**, the propionylated (**5.31**) and the 2-fluoroacetylated (**5.32**) congeners were slightly lower compared to the amine precursor **4.50**.

5.2.3.3. Determination of pK_b values in a β -arrestin2 recruitment assay

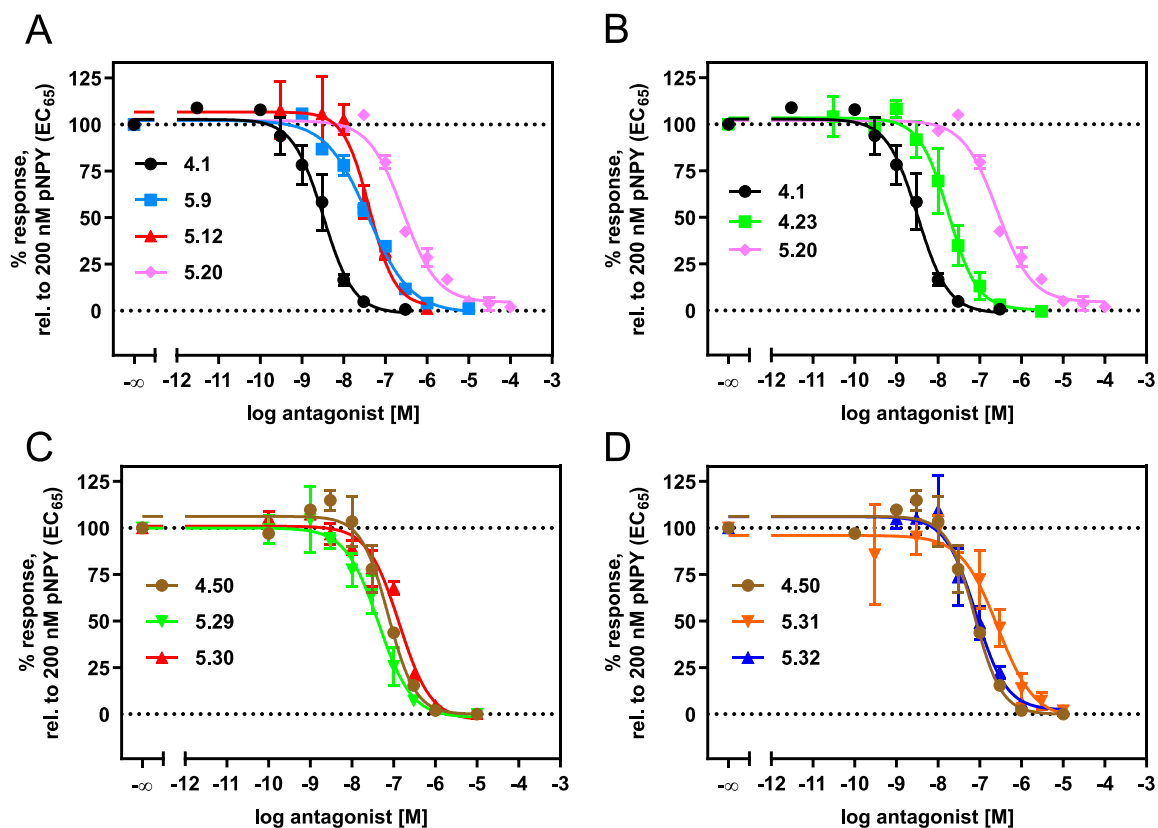


Figure 5.4. (A-D) Inhibition of β -arrestin2 recruitment (induced by 200 nM pNPY) by (A) **4.1**, **5.9**, **5.12**, **5.20**, (B) **4.1**, **4.23**, **5.20**, (C) **4.50**, **5.31**, **5.32** (D) **4.50** and **5.29-5.30**. All experiments were performed in HEK293T h Y_2R + β Arr2 cells. Cells were pre-incubated with the antagonists for 15 min. Data are presented as means \pm SEM from at least three independent experiments, each performed in triplicate.

Y_2R antagonism (pK_b) of (*S*)-argininamides **5.9**, **5.20** and **5.29-5.31** was investigated in a β -arrestin2 recruitment assay in living HEK293T h Y_2R + β Arr2 cells (Figure 5.4 and Table 5.4). The applied β -arrestin2 recruitment assay was previously described in the thesis of Felixberger¹⁰ with minor modifications (*cf.* 4.2.4.2.): β -arrestin2 recruitment was induced by 200 nM pNPY as described and luminescence was measured as a function of time in live cells rather than measurement of luminescence after cell lysis.

Furthermore, the Y_2R antagonism (Figure 5.4) of the 2-hydroxy substituted compound **5.20** ($pK_b = 7.14$) was slightly less pronounced compared to **5.9** ($pK_b = 7.73$) and **5.12** ($pK_b = 7.71$). Methylation of **5.20** (yielding **4.23**), resulted in a decrease in antagonism by one order of magnitude, whilst methylation of **5.9** and **5.12** (yielding **4.24** and **4.27**) led to a slight decrease in Y_2R antagonism.

The methylated compounds **5.29** and **5.30** showed Y₂R antagonism comparable to that of the amino precursor **4.50**. Furthermore, propionylation of **4.50** (**4.31**) led to a decrease in antagonism, whereas the introduction of a 2-fluoroacetyl moiety (**5.32**) showed neither a decrease nor an increase in Y₂R antagonism.

Table 5.4. Antagonism (pK₀) of (S)-argininamides **4.1**, **4.23**, **4.24**, **4.27**, **4.50**, **5.9**, **5.12**, **5.20** and **5.29-5.31** in the β-arrestin2 recruitment assay

Compound	pK ₀ ± SEM ^a	Compound	pK ₀ ± SEM ^a
4.1	8.89 ± 0.16	5.12	7.71 ± 0.03
4.23	8.12 ± 0.17	5.20	7.14 ± 0.27
4.24	7.17 ± 0.16	5.29	7.74 ± 0.17
4.27	7.37 ± 0.27	5.30	7.23 ± 0.18
4.50	7.54 ± 0.05	5.31	6.73 ± 0.11
5.9	7.73 ± 0.04	5.32	7.66 ± 0.19

^aβ-Arrestin2 recruitment assay in intact HEK293T hY₂R + βArr2 cells. Arrestin2 recruitment was induced by 200 nM pNPY after pre-incubation of the cells with the antagonist for 15 min. Mean values ± SEM from at least three independent experiments, each performed in triplicate.

The trends obtained from the β-arrestin2 recruitment assay data were in good agreement with data from the competition radioligand and BRET based binding assay (Table 5.2, Table 5.3, and Table 5.4).

5.2.3.4. NPY Y₂R subtype selectivity

NPY receptor subtype selectivity data were determined for (S)-argininamides **4.23** and **4.24** (Table 5.5). The substitution pattern of **4.23** and **4.24** did not affect subtype selectivity compared to the parent compound **4.1**.

Table 5.5. NPY receptor subtype binding profile of (S)-argininamides **4.23** and **4.24**.

Compound	hY ₁ R	hY ₂ R	hY ₄ R	hY ₅ R
	pK _i ^a	pK _i ± SEM ^b	pK _i ^c	pK _i ^d
4.23	<5.52	7.39 ± 0.13	<5.00	<5.00
4.24	<5.52	6.81 ± 0.23	<5.00	<5.00

^aRadioligand competition binding assay using [³H]**2.2** (C_{final} = 0.15 nM, K_d = 0.044 nM) in intact SK-N-MC cells.¹¹ ^bRadioligand competition binding assay using [³H]propionyl-pNPY (C_{final} = 4.0 nM, K_d = 2.97 nM) in intact HEK293T hY₂R + βArr2 cells (cf. 4.2.4.1.). Mean values ± SEM from at least three independent experiments, each performed in triplicate. ^cRadioligand competition binding assay using [³H]UR-KK200 (C_{final} = 1.0 nM, K_d = 0.67 nM) in intact CHO-hY₄R-G_{q15}-mtAEQ cells.^{12, 13} ^dRadioligand competition binding assay using [³H]propionyl-pNPY (C_{final} = 4.0 nM, K_d = 4.8 nM) in intact HEC-1B-hY₅ cells.^{11, 14} Results from at least 2-3 independent experiments, each performed in triplicate (hY₁R, hY₄R and hY₅R).

5.3. Conclusion

In this chapter the synthesis of phenolic precursors (**5.9**, **5.12** and **5.20**) derived from the argininamide-type Y₂R antagonist BIIE-0246 (**4.1**) is described. Methylation of **5.9**, **5.12** and **5.20** at the phenolic hydroxy group gave the “cold” forms of potential radioligands (**4.23**, **4.24** and **4.27**; *cf.* Chapter 4). Compound **4.23**, which showed the highest Y₂R affinity, was characterized in a number of cell based assays, namely a radioligand binding assay ($pK_i = 7.39$), a BRET based binding assay ($pK_i = 8.60$), a β -arrestin2 recruitment assay ($pK_b = 8.12$) and a miniG protein recruitment assay ($pK_i = 8.06$) (*cf.* Chapter 4) as well as in Y₁R, Y₄R and Y₅R binding assays to study subtype selectivity (Table 5.4). With a pK_i value of 7.39 (radioligand binding assay) the Y₂R affinity of compound **4.23** is comparable to that of reported argininamide-type Y₂R radioligands, which showed unfavourable physicochemical properties, limited chemical stability and unfavourable binding characteristics.^{2, 5} Therefore, the tritiated form of **4.23** would potentially represent a more favourable radiotracer compared to the reported radioligands.

Additionally, the derivatization of amine precursor **4.50** led to compounds **5.29-5.32**, which were pharmacologically characterized a potential “cold” forms of radioligands. The most promising candidate for radio labelling was the novel mono methylated compound **5.29**, so far not described in literature, which was obtained in moderate yield (20%) by an established synthesis route of monoalkylation of **4.50**. Unfortunately, the established synthesis route is unsuitable for the synthesis of radioligands, because the labelling step should be ideally performed in the last synthesis step. Methylation of **4.50** using e.g. methyl iodide or methyl nosylate would likely result in a mixture of mono (**5.29**), di and tri (**5.30**) methylated compounds, because for the synthesis of the radioligand requires an excess of precursor **4.50** compared to the labelling (methylation) reagent would be used. Pursuing this strategy would lead to issues with the separation of mono (**5.29**), di and tri (**5.30**) methylated compounds by HPLC.

5.4. Experimental section

5.4.1. General experimental conditions (cf. 4.4.1.)

The following reagents and solvents (analytical grade) were purchased from commercial suppliers and used without further purification: CH₂Cl₂, DMF, THF, MeOH, DMSO, methanesulfonyl chloride (Fisher Scientific, Schwerte, Germany); EDC·HCl, HOBt, piperazine TFA, CBr₄, PPh₃, **4.14**, 10% palladium on activated charcoal (Pd/C), TBAF (1.1 M) in solution, methyl 4-nitrobenzenesulfonate (Sigma Aldrich, Taufkirchen, Germany); Boc₂O, benzyl bromide, *tert*-butyldimethylsilyl chloride (TCI, Eschborn, Germany); DIPEA, (ABCR, Karlsruhe, Germany); NaH, Et₃N, NaBH₄, K₂CO₃, methyl iodide (Merck, Darmstadt, Germany); conc. HCl (VWR Chemicals, Darmstadt, Germany); ammonium hydroxide (Carl Roth, Karlsruhe, Germany). For pharmacological characterization, pNPY was purchased from Synpeptide (Shanghai, China).

The synthesis of compounds **4.15**, **4.16**, **4.34**, **4.42**, **4.43**, **4.50** and **4.52** was described in chapter 4 (cf. 4.4.2.). Compound **2.44**¹⁵ was synthesized according to the literature procedure.

Column chromatography was performed using Merck Geduran 60 silica gel (0.063-0.200 mm) or Merck flash silica gel 60 (0.040-0.063 mm). For thin layer chromatography, TLC sheets ALUGRAM Xtra SIL G/UV254 from Macherey-Nagel GmbH & Co. KG (Düren, Germany) were used. Compounds were detected by irradiation with UV light (254 nm or 366 nm), and staining was performed with ninhydrin.

Acetonitrile (HPLC grade), used for HPLC, was purchased from Sigma-Aldrich. Millipore water was used for eluents for analytical and preparative HPLC. Compounds **5.9**, **5.12**, **5.20** and **5.29-5.31** were purified by a preparative HPLC-system B from Waters (Eschborn, Germany) consisting of a Binary Gradient Module (Waters 2545), a detector (Waters 2489 UV/visible Detector), a manual injector (Waters Prep inject) and a collector (Waters Fraction Collector III). A Kinetex XB C18, 5 µm, 250 x 21 mm (Phenomenex) served as RP-column at a flow rate of 20 mL/min. All injected solutions were filtered with syringe filters (0.45 µm). The mobile phase contained the solvents A (0.1% aq TFA) and B (acetonitrile). The detection wavelength was 220 nm. The eluates, containing isolated compounds, were lyophilized using a Christ alpha 2-4 LD (Martin Christ Gefriertrocknungsanlagen, Osterode am Harz, Germany) or a Scanvac CoolSafe 100-9 (Labogene, Allerød, Denmark) lyophilization apparatus equipped with a Vacuubrand RZ rotary vane vacuum pump (Vacuubrand, Wertheim, Germany).

The purity of compounds **5.9**, **5.12**, **5.20** and **5.29-5.31** was determined by analytical HPLC (RP-HPLC) with a 1100 series system from Agilent Technologies (Santa Clara, CA USA) composed of a Degasser (G1379A), a Binary Pump (G1312A), a Diode Array Detector (G1315A), a thermostated Column Compartment (G1316A) and an Autosampler (G1329A). A Phenomenex Kinetex 5u XB-C18 100A, 250 x 4.6 mm was used as stationary phase. The flow rate was 1 mL/min, the detection wavelength was set to 220 nm, the oven temperature was set to 30 °C and the injection volume was 50 µL. Mixtures of solvents A (0.1% aq TFA) and B (acetonitrile) were used as mobile phase. The following gradient was applied: 0-25 min, A/B 90:10–5:95; 25-35 min, 5:95.

Microwave reactions were carried out on a Biotage Initiator 2.0 microwave device (Biotage, Uppsala, Sweden) using pressure stable sealed 10-20 mL vessels.

Deuterated solvents for NMR spectroscopy (DMSO- d_6 , MeOD) were obtained from Deutero (Kastellaun, Germany) in ampoules (1 mL). NMR spectra were recorded on a Bruker Avance 300 (^1H , 300 MHz; ^{13}C , 75 MHz), a Bruker Avance III 400 (^1H , 400 MHz; ^{13}C , 101 MHz) and a Bruker Avance 600 with cryogenic probe (^1H , 600 MHz; ^{13}C , 150 MHz) (Bruker, Karlsruhe, Germany). Chemical shifts are given in ppm and were referenced to the solvent residual peak (DMSO- d_6 , at 2.50 ppm (^1H -NMR) and at 39.52 ppm (^{13}C -NMR); CD $_3$ OD, at 3.31 ppm (^1H -NMR) and at 49.00 ppm (^{13}C -NMR)).¹⁶ The coupling constants (J) are given in Hertz (Hz). The splitting of the signals is described as follows: s = singlet, bs = broad singlet, d = doublet, t = triplet, q = quartet, m = multiplet.

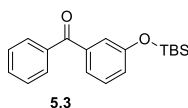
Mass spectrometry (HRMS) analysis was performed either on an Agilent 6540 UHD Accurate-Mass Q-TOF LC/MS system (Agilent Technologies) using an electrospray source (ESI) or on an Agilent GC7890A GC/MS system (Agilent Technologies) using an atmospheric pressure chemical ionization (APCI) source.

5.4.2. Synthesis protocols and analytical data

Annotation concerning the analytical data (NMR, HPLC) of **5.9**, **5.12**, **5.20** and **5.29-5.32**: due to the synthesis routes, these compounds were obtained as diastereomers, which are evident in the ^1H - and ^{13}C -spectra (recorded in DMSO- d_6 or MeOH- d_4), but not in the RP-HPLC chromatograms.

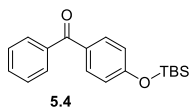
General synthesis procedure

General procedure A (cf. 4.4.2. general procedure G) Compounds **5.9**, **5.12**, **5.20** and **5.29** were prepared by amide bond formation according to a reported procedures.^{17, 18} The respective carboxylic acid was dissolved in DMF (100 μL). EDC·HCl and HOBt were added, and the reaction mixture was stirred for 5 min. Then, the mixture was poured into a solution of the secondary or primary amine in DMF (100 μL) and was stirred at rt overnight. The reaction mixture was poured into an aqueous solution (5% acetonitrile, 0.1% TFA; 100 mL). After lyophilization, the crude product was dissolved in a mixture of TFA and water (95:5; 5 mL) and stirred at rt overnight. Then, the reaction mixture was poured into an aqueous solution (5% acetonitrile, 0.1% TFA; 100 mL). After lyophilization, the crude product was purified by preparative HPLC.

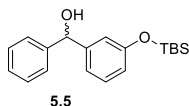


(3-((tert-Butyldimethylsilyl)oxy)phenyl)(phenyl)methanone (5.3). (3-Hydroxyphenyl)(phenyl)methanone (**4.43**) (310 mg, 1.56 mmol) was dissolved in CH $_2$ Cl $_2$ (10 mL), Et $_3$ N (0.45 mL, 3.25 mmol) was added and the mixture was cooled in an ice-bath. Under stirring, *tert*-butyldimethylsilyl chloride (430 mg, 2.85 mmol) in CH $_2$ Cl $_2$ (10 mL) was dropped slowly into the mixture over a time-period of 1 h. The reaction mixture was allowed to warm to rt and stirred overnight. The organic solvent was evaporated, and the crude product was purified by column chromatography (eluent: light petroleum/ethyl acetate 10:1) to give **5.3** as an oil (300 mg, 0.960 mmol, 62%). ^1H -NMR (400 MHz, DMSO- d_6): δ (ppm) 0.19 (s, 6H), 0.94 (s, 9H), 7.11-7.19 (m, 2H), 7.27-7.36 (m, 1H), 7.41-7.47 (m, 1H), 7.52-7.58 (m, 2H), 7.64-7.77 (m, 3H). ^{13}C -NMR (101 MHz, DMSO- d_6): δ (ppm) -4.6, 17.9, 25.5, 120.4, 122.9, 124.2, 128.5, 129.5,

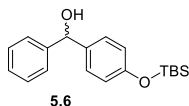
129.9, 132.7, 136.9, 138.5, 155.0, 195.3. **HRMS** (APCI): *m/z* [M]⁺ calcd. for [C₁₉H₂₄O₂Si]⁺ 312.1540, found 312.1542. C₁₉H₂₄O₂Si (312.48).



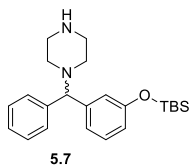
(4-((*tert*-Butyldimethylsilyl)oxy)phenyl)(phenyl)methanone (5.4).¹⁹ (4-Hydroxyphenyl)(phenyl)methanone (**4.52**) (500 mg, 2.52 mmol) was dissolved in CH₂Cl₂ (15 mL), Et₃N (0.70 mL, 5.05 mmol) was added and the mixture was cooled in an ice bath. Under stirring, *tert*-butyldimethylsilyl chloride (910 mg, 6.04 mmol) in CH₂Cl₂ (10 mL) was dropped slowly into the mixture over a time period of 1 h. The reaction mixture was allowed to warm to rt and was stirred overnight. The organic solvent was evaporated, and the crude product was purified by column chromatography (light petroleum/ethyl acetate 10:1) to give **5.4** as an oil (420 mg, 1.34 mmol, 53%). **¹H-NMR** (400 MHz, DMSO-*d*₆): δ (ppm) 0.24 (s, 6H), 0.95 (s, 9H), 6.97-7.02 (m, 2H), 7.51-7.57 (m, 2H), 7.61-7.73 (m, 5H). **¹³C-NMR** (101 MHz, DMSO-*d*₆): δ (ppm) -4.6, 17.9, 25.4, 119.7, 128.4, 129.2, 130.2, 132.1, 132.2, 137.6, 159.3, 194.4. **HRMS** (APCI): *m/z* [M]⁺ calcd. for [C₁₉H₂₄O₂Si]⁺ 312.1540, found 312.1539. C₁₉H₂₄O₂Si (312.48).



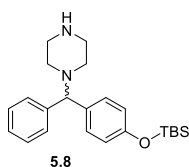
(3-((*tert*-Butyldimethylsilyl)oxy)phenyl)(phenyl)methanol (5.5). (3-((*tert*-Butyldimethylsilyl)oxy)phenyl)(phenyl)methanone (**5.3**) (290 mg, 0.928 mmol) was dissolved in methanol (5 mL) and sodium borohydride (100 mg, 2.64 mmol) was added portionwise into the mixture and stirred at rt for 3 h. The solvent was evaporated, and the crude product was purified by column chromatography (eluent: light petroleum/ethyl acetate 90:10) to give **5.5** as an oil (260 mg, 0.827 mmol, 89%). **¹H-NMR** (400 MHz, DMSO-*d*₆): δ (ppm) 0.15 (s, 6H), 0.93 (s, 9H), 5.65 (d, *J* = 4.1 Hz, 1H), 5.86 (d, *J* = 4.1 Hz, 1H), 6.64-6.69 (m, 1H), 6.84-6.88 (m, 1H), 6.93-6.99 (m, 1H), 7.14-7.23 (m, 2H), 7.26-7.33 (m, 2H), 7.34-7.39 (m, 2H). **¹³C-NMR** (101 MHz, DMSO-*d*₆): δ (ppm) -4.5, 17.9, 25.6, 73.9, 117.6, 118.0, 119.4, 126.2, 126.7, 128.0, 129.1, 145.6, 147.5, 154.9. **HRMS** (APCI): *m/z* [M]⁺ calcd. for [C₁₉H₂₆O₂Si]⁺ 314.1697, found 314.1700. C₁₉H₂₆O₂Si (314.50).



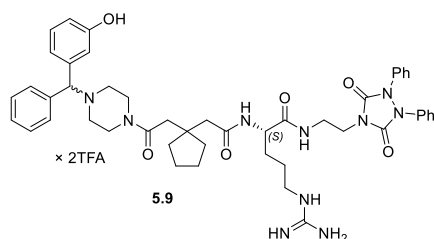
(4-((*tert*-Butyldimethylsilyl)oxy)phenyl)(phenyl)methanol (5.6).²⁰ (4-((*tert*-Butyldimethylsilyl)oxy)phenyl)(phenyl)methanone (**5.4**) (330 mg, 1.06 mmol) was dissolved in methanol (5 mL) and sodium borohydride (110 mg, 2.91 mmol) was added portionwise into the reaction mixture and stirred at rt for 3 h. The organic solvent was evaporated, and the crude product was purified by column chromatography (eluent: light petroleum/ethyl acetate 90:10) to give **5.6** as an oil (310 mg, 0.986 mmol, 93%). **¹H-NMR** (400 MHz, DMSO-*d*₆): δ (ppm) 0.16 (s, 6H), 0.94 (s, 9H), 5.64 (d, *J* = 3.6 Hz, 1H), 5.76-5.83 (m, 1H), 6.72-6.84 (m, 2H), 7.16-7.42 (m, 7H). **¹³C-NMR** (101 MHz, DMSO-*d*₆): δ (ppm) -4.6, 17.9, 25.5, 73.8, 119.3, 126.2, 126.6, 127.6, 128.0, 138.7, 145.9, 153.8. **HRMS** (APCI): *m/z* [M]⁺ calcd. for [C₁₉H₂₆O₂Si]⁺ 314.1697, found 314.1712. C₁₉H₂₆O₂Si (314.50).



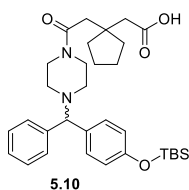
1-((3-((*tert*-Butyldimethylsilyl)oxy)phenyl)(phenyl)methyl)piperazine (5.7). (3-((*tert*-Butyldimethylsilyl)oxy)phenyl)(phenyl)methanol (**5.3**) (260 mg, 0.827 mmol) was dissolved in CH₂Cl₂ (6 mL), Et₃N (0.40 mL, 2.88 mmol) was added and the mixture was cooled in an ice bath. Under stirring, methanesulfonyl chloride (96 μL, 1.24 mmol) in CH₂Cl₂ (1 mL) was dropped to the mixture. After 2 h the reaction mixture was allowed to warm to rt and stirred for 3 h. Then, 1 N NaOH (10 mL) was added and the product was extracted from the aqueous phase with CH₂Cl₂. The combined organic phases were dried over Na₂SO₄ and the solvent was evaporated. The residue was dissolved in acetonitrile (10 mL), piperazine (420 mg, 4.88 mmol) was added and the reaction mixture was treated in the microwave device (70 °C, 30 min). The organic solvent was evaporated, and the crude product was purified by column chromatography (eluent: CH₂Cl₂/MeOH/NH₃ aq 90:9:1) to give **5.7** as an oil (105 mg, 0.274 mmol, 62%). **HRMS** (ESI): *m/z* [M+H]⁺ calcd. for [C₂₃H₃₅N₂OSi]⁺ 383.2513, found 383.2520. C₂₃H₃₄N₂OSi (382.62).



1-((4-((*tert*-Butyldimethylsilyl)oxy)phenyl)(phenyl)methyl)piperazine (5.8). (4-((*tert*-Butyldimethylsilyl)oxy)phenyl)(phenyl)methanol (**5.6**) (140 mg, 0.445 mmol) was dissolved in CH₂Cl₂ (5 mL), Et₃N (0.20 mL, 1.44 mmol) was added and the mixture was cooled in an ice bath. Under stirring, methanesulfonyl chloride (56 μL, 0.723 mmol) in CH₂Cl₂ (1 mL) was added to the mixture. After 2 h the reaction mixture was allowed warm to rt and stirred for 3 h. Then, 1 N NaOH (10 mL) was added to the mixture and the product was extracted from the aqueous phase with CH₂Cl₂. The combined organic phases were dried over Na₂SO₄ and the organic solvent was evaporated. The residue was dissolved in acetonitrile (10 mL) and piperazine (280 mg, 3.25 mmol) was added and the reaction mixture was treated in the microwave device (70 °C, 30 min). The organic solvent was evaporated, and the crude product was purified by column chromatography (eluent: CH₂Cl₂/MeOH/NH₃ aq. 90:9:1) to give **5.8** as an oil (105 mg, 0.274 mmol, 62%). **¹H-NMR** (400 MHz, DMSO-*d*₆): δ (ppm) 0.14 (s, 6H), 0.91 (s, 9H), 2.12-2.45 (m, 4H), 2.38 (s, 1H), 2.62-2.77 (m, 4H), 4.16 (s, 1H), 6.71-6.78 (m, 2H), 7.12-7.18 (m, 1H), 7.23-7.29 (m, 4H), 7.34-7.40 (m, 2H). **¹³C-NMR** (101 MHz, DMSO-*d*₆): δ (ppm) -4.6, 17.8, 25.5, 45.7, 52.7, 75.1, 119.5, 126.6, 127.6, 128.4, 128.8, 135.5, 143.1, 153.7. **HRMS** (ESI): *m/z* [M+H]⁺ calcd. for [C₂₃H₃₅N₂OSi]⁺ 383.2513, found 383.2517. C₂₃H₃₄N₂OSi (382.62).

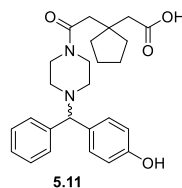


(2S)-N²-(2-{1-[2-(4-((3-Hydroxyphenyl)(phenyl)methyl)piperazin-1-yl)-2-oxoethyl]cyclopentyl}acetyl)[2-(3,5-dioxo-1,2-diphenyl-1,2,4-triazolidin-4-yl)ethyl]argininamide bis(hydrotrifluoroacetate) (5.9). Compound **5.9** was prepared according to *general procedure A* and the reactants (S)-2-(1-(2-((1-((2-(3,5-dioxo-1,2-diphenyl-1,2,4-triazolidin-4-yl)ethyl)amino)-1-oxo-5(2-((2,2,4,6,7-pentamethyl-2,3-dihydrobenzofuran-5-yl)sulfonyl)guanidino)pentan-2-yl)amino)-2-oxoethyl)cyclopentyl)acetic acid (**4.15**) (77.9 mg, 89.2 μmol), EDC·HCl (27.2 mg, 141.9 μmol), HOBT (13.9 mg, 102.9 μmol) and 1-((3-((tert-Butyldimethylsilyl)oxy)phenyl)(phenyl)methyl)piperazine (**5.7**) (32.6 mg, 85.2 μmol). Purification by preparative HPLC (gradient: 0-30 min, A/B 79:21–57:43, *t_R* = 15 min) gave **4.1** as a fluffy white solid (15.4 mg, 14.0 μmol, 16%). **¹H-NMR** (600-MHz, DMSO-*d*₆): δ (ppm) 1.33-1.69 (m, 13H), 2.23 (m, 1H), 2.31-2.39 (m, 1H), 2.42-2.49 (m, 1H, interfering with solvent residual peak), 2.56-2.67 (m, 1H), 2.64-3.07 (m, 5H), 3.27-3.33 (m, 1H), 3.35-3.40 (m, 1H), 3.41-4.10 (m, 6H), 4.11-4.18 (m, 1H), 6.86-7.48 (m, 21H), 7.58 (br s, 4H, interfering with surrounding signals), 7.64-7.68 (m, 1H), 7.92-7.98 (m, 1H), 8.18-8.24 (m, 1H). One proton signal was not apparent ((C₆H₄OH)(Ph)CH₂-N-piperazine). **¹³C-NMR** (150 MHz, DMSO-*d*₆): δ (ppm) 23.3 (two carbon signals), 25.1, 28.8, 36.2 (2 carb.), 37.3, 37.5, 38.6, 39.6 (overlaid by solvent residual peak), 40.4, 42.6, 43.9, 51.2, 51.5, 52.0, 74.0, 113.6, 115.5 (TFA), 117.5 (TFA), 122.7, 126.7 (2 carb.), 127.9 (2 carb.), 129.0 (3 carb.), 129.2, 136.5, 152.6, 156.8, 158.6 (q, *J* = 33.7 Hz) (TFA), 117.2, 171.3, 172.0. **RP-HPLC** (220 nm): 97% (*t_R* = 12.9 min, *k* = 4.0). **HRMS** (ESI): *m/z* [M+H]⁺ calcd. for [C₄₈H₅₉N₁₀O₆]⁺ 871.4614, found 871.4618. C₄₈H₅₈N₁₀O₆ × C₄H₂F₆O₄. (870.06 + 228.04).

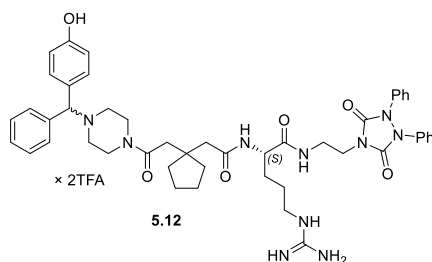


2-(1-(2-(4-((tert-Butyldimethylsilyl)oxy)phenyl)(phenyl)methyl)piperazin-1-yl)-2-oxoethyl)cyclopentyl)acetic acid (5.10). 1-((4-((tert-Butyldimethylsilyl)oxy)phenyl)(phenyl)methyl)piperazine (**5.8**) (155 mg, 0.405 mmol) was dissolved in CH₂Cl₂ (5 mL) and cooled using an ice-bath followed by addition of 3,3-tetramethyleneglutaric anhydride (**4.14**) (90 mg, 0.535 mmol) dissolved in CH₂Cl₂ (1 mL). After 2 h, the mixture was allowed to warm to rt and stirring was continued overnight. The solvent was evaporated, and the crude product was purified by column chromatography (eluent: CH₂Cl₂/MeOH 95:5) to give **5.10** as an oil (141 mg, 0.256 mmol, 63%). **¹H-NMR** (400 MHz, DMSO-*d*₆): δ (ppm) 0.14 (s, 6H), 0.91 (s, 9H), 1.49-1.57 (m, 8H), 2.17-2.28 (m, 4H), 2.42 (s, 2H), 2.47 (s, 2H, interfering with solvent residual peak), 3.67-3.52 (m, 4H), 4.22 (s, 1H), 6.73-6.78 (m, 2H), 7.14-7.21 (m, 1H), 7.24-7.31 (m, 4H), 7.37-7.42 (m, 2H), 12.0 (s, 1H). **¹³C-NMR** (101 MHz, DMSO-*d*₆): δ (ppm) -4.6, 17.8, 23.5, 23.7, 25.5,

36.8, 37.5, 40.9, 41.7, 43.0, 74.1, 119.7, 126.8, 127.5, 128.5, 128.8, 135.1, 142.8, 153.9, 169.6, 173.5.
HRMS (ESI): m/z $[M+H]^+$ calcd. for $[C_{32}H_{47}N_2O_4Si]^+$ 551.3300, found 551.3303. $C_{32}H_{46}N_2O_4Si$. (550.82).

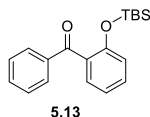


2-(1-(2-(4-((4-Hydroxyphenyl)(phenyl)methyl)piperazin-1-yl)-2-oxoethyl)cyclopentyl)acetic acid (5.11). 2-(1-(2-(4-((*tert*-Butyldimethylsilyloxy)phenyl)(phenyl)methyl)piperazin-1-yl)-2-oxoethyl)-cyclopentyl)acetic acid (**5.10**) (91 mg, 0.165 mmol) was dissolved in TBAF (1.1 M) in THF (3 mL, 3.3 mmol) and stirred at rt for 3 h. The organic solvent was evaporated, and the crude product was purified by column chromatography (eluent: CH_2Cl_2 /methanol 90:10) to give **5.11** as an oil (72 mg, 0.165 mmol, 100%). **¹H-NMR** (400 MHz, $DMSO-d_6$): δ (ppm) 1.46-1.55 (m, 8H), 2.17-2.30 (m, 4H), 2.42 (s, 2H), 2.48 (s, 2H, interfering with solvent residual peak), 2.70-2.82 (m, 4H), 4.16 (s, 1H), 6.64-6.73 (m, 2H), 7.14 (m, 3H), 7.25-7.32 (m, 2H), 7.36-7.43 (m, 2H), 9.30 (br s, 1H). One exchangeable proton signal (-COOH or -OH) was not apparent. **¹³C-NMR** (101 MHz, $DMSO-d_6$): δ (ppm) 20.1, 24.0, 25.5, 37.9, 42.2, 43.5, 52.6, 74.4, 115.7, 127.2, 127.9, 128.9, 129.1, 133.1, 143.7, 156.8, 170.0, 174.0. **HRMS** (ESI): m/z $[M+H]^+$ calcd. for $[C_{26}H_{33}N_2O_4]^+$ 437.2435, found 437.2446. $C_{26}H_{32}N_2O_4$ (436.55).

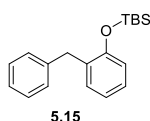


(2S)-N²-(2-{1-[2-(4-((4-Hydroxyphenyl)(phenyl)methyl)piperazin-1-yl)-2-oxoethyl]cyclopentyl}acetyl)[2-(3,5-dioxo-1,2-diphenyl-1,2,4-triazolidin-4-yl)ethyl]argininamide bis(hydrotrifluoroacetate) (5.12). Compound **5.12** was prepared according to *general procedure A* and the reactants 2-(1-(2-(4-((4-hydroxyphenyl)(phenyl)methyl)piperazin-1-yl)-2-oxoethyl)cyclopentyl)acetic acid (**5.11**) (30.0 mg, 54.5 μ mol), EDC·HCl (12.7 mg, 66.2 μ mol), HOBT (12.6 mg, 93.3 μ mol) and (*S*)-[2-(3,5-dioxo-1,2-diphenyl-1,2,4-triazolidin-4-yl)ethyl]argininamid bis(hydrotrifluoroacetate) (**4.16**) (40.9 mg, 60.1 μ mol). Additionally, DIPEA (19 μ L, 109 μ mol) was added to the solution of **4.16** in DMF. Purification by preparative HPLC (gradient: 0-30 min, A/B 71:29–38:62, t_R = 10 min) gave **5.12** as a fluffy white solid (15.8 mg, 14.4 μ mol, 24%). **¹H-NMR** (600 MHz, $DMSO-d_6$): δ (ppm) 1.32-1.68 (m, 13H), 2.19-2.26 (m, 1H), 2.31-2.38 (m, 1H), 2.43-2.48 (m, 1H, interfering with solvent residual peak), 2.54-2.60 (m, 1H), 2.63-3.27 (m, 6H), 3.27-3.33 (m, 1H), 3.35-3.41 (m, 1H), 3.51-3.61 (m, 5H, interfering with water signal), 4.12-4.16 (m, 1H), 5.38 (br s, 1H), 6.76 (br s, 2H), 6.86-7.62 (m, 22H), 7.68 (br s, 1H), 7.95 (d, J = 7.6 Hz, 1H), 8.22 (t, J = 5.5 Hz, 1H), 9.72 (br s, 1H). **¹H-NMR** (600 MHz, MeOH- d_4): δ (ppm) 1.44-1.94 (m, 13H), 2.24-2.33 (m, 1H), 2.46-2.63 (m, 3H), 2.84-3.25 (m, 6H), 3.41-3.47 (m, 1H), 3.50-4.13 (m, 6H), 4.20-4.27 (m, 1H), 5.17 (br s, 1H), 6.82-6.89 (m, 2H), 7.18-7.25 (m, 2H), 7.29-7.50 (m, 13H), 7.56-7.63 (m, 2H). **¹³C-NMR** (150 MHz, MeOH- d_4): δ (ppm) 24.60, 24.64, 26.3, 30.1 (two carbon signals), 38.3, 39.3,

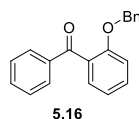
39.5, 39.6, 39.9 (2 carb.), 41.2, 41.9, 44.4 (2 carb.), 45.6, 52.6, 52.9, 54.0, 76.7 (2 carb.), 117.3, 119.2, 142.3, 124.4, 128.3, 129.05, 129.06, 130.1, 130.23, 130.30, 130.7, 130.98, 131.00, 137.7 (2 carb.), 154.5, 158.6, 159.8, 162.7 (TFA), 163.0 (TFA), 172.9, 174.69, 174.73. **RP-HPLC** (220 nm): 97% ($t_R = 12.3$ min, $k = 3.8$). **HRMS** (ESI): m/z $[M+H]^+$ calcd. for $[C_{48}H_{59}N_{10}O_6]^+$ 871.4619, found 871.4615. $C_{48}H_{58}N_{10}O_6 \times C_4H_2F_6O_4$ (870.06 + 228.04).



(2-((tert-Butyldimethylsilyloxy)phenyl)(phenyl)methanone (5.13). (2-Hydroxyphenyl)(phenyl)methanone (**4.42**) (500 mg, 2.52 mmol) was dissolved in CH_2Cl_2 (15 mL), Et_3N (0.70 mL, 5.05 mmol) was added and the mixture was cooled in an ice bath. Under stirring, *tert*-butyldimethylsilyl chloride (1.16 g, 7.70 mmol) in CH_2Cl_2 (10 mL) was dropped slowly into the mixture over a time period of 1 h. The reaction mixture was allowed to warm to rt and stirred overnight. The organic solvent was evaporated, and the crude product was purified by column chromatography (eluent: light petroleum/ethyl acetate 95:5) to give **5.13** as an oil (670 mg, 2.14 mmol, 85%). **¹H-NMR** (400 MHz, $DMSO-d_6$): δ (ppm) 0.24 (s, 6H), 0.95 (s, 9H), 6.97-7.02 (m, 2H), 7.51-7.57 (m, 2H), 7.61-7.73 (m, 5H). **¹³C-NMR** (101 MHz, $DMSO-d_6$): δ (ppm) -4.8, 17.4, 25.0, 119.4, 121.4, 128.5, 129.26, 129.31, 131.1, 131.9, 133.3, 137.1, 152.4, 196.1. **HRMS** (APCI): m/z $[M+H]^+$ calcd. for $[C_{19}H_{25}O_2Si]^+$ 313.1618, found 313.1617. $C_{19}H_{24}O_2Si$ (312.48).

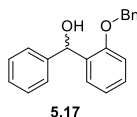


(2-Benzyloxy)(tert-butyl)dimethylsilane (5.15). (2-((tert Butyldimethylsilyloxy)phenyl)(phenyl)methanone (**5.13**) (3.05 g, 9.76 mmol) was dissolved in MeOH (150 mL). Palladium on activated charcoal (Pd/C; 340 mg) was added and hydrogen (H_2) was bubbled (balloon) through the reaction, whilst stirring at rt. The reaction mixture was filtered, and the organic solvent evaporated. The crude product was purified by column chromatography (eluent: light petroleum/ethyl acetate 95:5) to give **5.15** as an oil (2.31 g, 7.74 mmol, 79%). **¹H-NMR** (400 MHz, $DMSO-d_6$): δ (ppm) 0.19 (s, 6H), 0.91 (s, 9H), 3.91 (s, 2H), 6.81-6.91 (m, 2H), 7.03-7.17 (m, 5H), 7.20-7.27 (m, 2H). **¹³C-NMR** (101 MHz, $DMSO-d_6$): δ (ppm) -4.4, 17.8, 25.5, 35.3, 118.3, 121.1, 125.7, 127.3, 128.1, 128.4, 130.8, 131.0, 140.7, 152.9. **HRMS** (APCI): m/z $[M+H]^+$ calcd. for $[C_{19}H_{27}O_2Si]^+$ 299.1826, found 299.1837. $C_{19}H_{26}OSi$ (298.50).

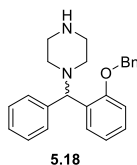


(2-(Benzyloxy)phenyl)(phenyl)methanone (5.16).²¹ (2-Hydroxyphenyl)(phenyl)methanone (**4.42**) (1.00 g, 5.04 mmol) was dissolved in acetonitrile (10 mL) and K_2CO_3 (2.12 g, 15.3 mmol) was added. After addition of benzyl bromide (0.80 mL, 6.74 mmol) the reaction mixture was treated in the microwave device (80 °C, 1 h). The organic solvent was evaporated, and the crude product was purified by column chromatography (eluent: light petroleum/ethyl acetate 95:5 to 90:10 to 75:25) to give **5.16** as a white

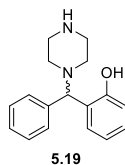
solid (1.02 g, 3.54 mmol, 70%). **¹H-NMR** (400 MHz, DMSO-*d*₆): δ (ppm) 5.06 (s, 2H), 6.93-7.00 (m, 2H), 7.08-7.15 (m, 1H), 7.16-7.22 (m, 3H), 7.24-7.29 (m, 1H), 7.36-7.42 (m, 1H), 7.49-7.58 (m, 3H), 7.62-7.69 (m, 1H), 7.69-7.74 (m, 2H). **¹³C-NMR** (101-MHz, DMSO-*d*₆): δ (ppm) 69.3, 113.1, 120.9, 126.8, 127.5, 128.1, 128.6, 128.8, 129.0, 129.1, 132.1, 133.2, 136.4, 137.5, 155.7, 196.0. **HRMS** (ESI): *m/z* [M+H]⁺ calcd. for [C₂₀H₁₇O₂]⁺ 289.1223, found 289.1225. C₂₀H₁₆O₂ (288.35).



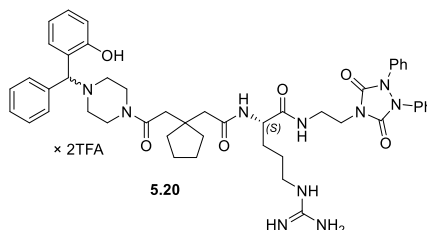
(2-(Benzyloxy)phenyl)(phenyl)methanol (5.17). (2-(Benzyloxy)phenyl)(phenyl)methanone (**5.16**) (0.45 g, 1.56 mmol) was dissolved in methanol (10 mL) and sodium borohydride (0.19 g, 5.02 mmol) was added portion wise and the mixture was stirred and cooled using an ice bath. Then, the reaction mixture was allowed to warm to rt and stirred for 2 h. The organic solvent was evaporated, and the crude product was purified by column chromatography (eluent: light petroleum/ethyl acetate 90:10) to give **5.17** as an oil (0.43 g, 1.48 mmol, 95%). **¹H-NMR** (400 MHz, DMSO-*d*₆): δ (ppm) 5.09 (s, 2H), 5.68 (d, *J* = 4.2 Hz, 1H), 6.03 (d, *J* = 4.1 Hz, 1H), 6.91-7.06 (m, 2H), 7.15-7.40 (m, 11H), 7.49-7.60 (m, 1H). **¹³C-NMR** (101 MHz, DMSO-*d*₆): δ (ppm) 68.1, 69.2, 111.8, 120.5, 126.51, 126.55, 127.4, 127.69, 127.74, 127.79, 128.3, 133.8, 137.2, 145.3, 154.4. One aromatic carbon was not apparent. **HRMS** (ESI): *m/z* [M+Na]⁺ calcd. for [C₂₀H₁₈O₂Na]⁺ 313.1199, found 313.1198. C₂₀H₁₈O₂ (290.36).



1-((2-(Benzyloxy)phenyl)(phenyl)methyl)piperazine (5.18). (2-(Benzyloxy)phenyl)(phenyl)methanol (**5.17**) (290 mg, 0.999 mmol) was dissolved in CH₂Cl₂ (5 mL), Et₃N (0.40 mL, 2.89 mmol) was added and the mixture was cooled using an ice bath. Under stirring, methanesulfonyl chloride (0.20 mL, 2.58 mmol) was added. The reaction mixture was allowed to warm to rt and stirred for 2 h. Then, 1 N NaOH (10 mL) was added. The product was extracted from the aqueous phase with CH₂Cl₂ (3x 10 mL) and the combined organic phases were dried over Na₂SO₄ and the solvent was evaporated. The residue was dissolved in acetonitrile (10 mL) and piperazine (390 mg, 4.53 mmol) was added. The reaction mixture was treated in the microwave device (85 °C, 45 min) and the organic solvent was evaporated. The crude product was purified by column chromatography (eluent: CH₂Cl₂/methanol/NH₃ aq. 90:9:1) to give **5.18** as an oil (190 mg, 0.53 mmol, 53%). **¹H-NMR** (400 MHz, DMSO-*d*₆): δ (ppm) 2.12-2.34 (m, 4H), 2.65-2.75 (m, 4H), 4.72 (s, 1H, interfering with water signal), 5.05-5.14 (m, 2H), 6.91-7.01 (m, 2H), 7.09-7.18 (m, 2H), 7.20-7.28 (m, 2H), 7.29-7.37 (m, 3H), 7.37-7.43 (m, 4H), 7.55-7.62 (m, 1H). One exchangeable proton signal (NH-piperazine) was not apparent. **¹³C-NMR** (101 MHz, DMSO-*d*₆): δ (ppm) 45.6, 52.7, 67.2, 69.4, 112.5, 120.8, 126.6, 127.4, 127.5, 127.6, 127.7, 128.1, 128.2, 128.4, 130.7, 137.2, 142.3, 155.6. **HRMS** (ESI): *m/z* [M+Na]⁺ calcd. for [C₂₄H₂₆N₂O₂Na]⁺ 381.1937, found 381.1932. C₂₄H₂₆N₂O (358.49).

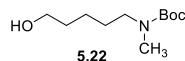


2-(Phenyl(piperazin-1-yl)methyl)phenol (5.19).²² 1-((2-(Benzyloxy)phenyl)(phenyl)methyl)piperazine (**5.18**) (168 mg, 0.469 mmol) was dissolved in methanol (5 mL) and Pd/C (17 mg) was added and stirred in a reaction vessel under hydrogen atmosphere (10 bar) at rt overnight. The reaction was filtered, and the organic solvent was evaporated to give **5.19** as an oil (90 mg, 0.206 mmol, 44%). **¹H-NMR** (400 MHz, DMSO-*d*₆): δ (ppm) 2.89-2.46 (m, 4H), 2.64-2.83 (m, 4H), 4.61 (s, 1H), 6.67-6.76 (m, 2H), 6.98-7.05 (m, 1H), 7.14-7.24 (m, 3H), 7.27-7.31 (m, 2H), 7.39-7.43 (m, 1H), 11.01 (br s, 1H). One exchangeable proton (NH-piperazine) signal was not apparent. **¹³C-NMR** (101 MHz, DMSO-*d*₆): δ (ppm) 45.5, 52.2, 71.8, 115.9, 119.0, 120.8, 127.2, 127.7, 128.1, 128.5 (two carbon signals), 141.1, 155.7. **HRMS** (ESI): *m/z* [M+H]⁺ calcd. for [C₁₇H₂₁N₂O]⁺ 269.1648, found 269.1651. C₁₇H₂₀N₂O (268.36).

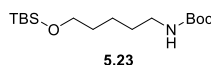


(2S)-N^ε-(2-{1-[2-(4-((2-Hydroxyphenyl)(phenyl)methyl)piperazin-1-yl)-2-oxoethyl]cyclopentyl}-acetyl)[2-(3,5-dioxo-1,2-diphenyl-1,2,4-triazolidin-4-yl)ethyl]argininamide bis(hydrotrifluoroacetate) (5.20). Compound **5.20** was prepared according to *general procedure A* and the reactants (S)-2-(1-(2-((1-(2-((2-(3,5-dioxo-1,2-diphenyl-1,2,4-triazolidin-4-yl)ethyl)amino)-1-oxo-5(2-((2,2,4,6,7-pentamethyl-2,3-dihydrobenzo-furan-5-yl)sulfonyl)guanidino)pentan-2-yl)amino)-2-oxoethyl)cyclopentyl)acetic acid (**4.15**) (200.8 mg, 230.0 μmol), EDC·HCl (64.6 mg, 337.0 μmol), HOBT (43.9 mg, 324.7 μmol) and 2-(phenyl(piperazin-1-yl)methyl)phenol (**5.19**) (60.0 mg, 223.6 μmol). Purification by preparative HPLC (gradient: 0-30 min, A/B 71:29–47:53, *t_R* = 13 min) gave **5.20** as a fluffy white solid (20.7 mg, 18.8 μmol, 8.4%). **¹H-NMR** (600 MHz, DMSO-*d*₆): δ (ppm) 1.30-1.72 (m, 13H), 2.20-2.26 (m, 1H), 2.32-2.39 (m, 1H), 2.43-2.48 (m, 1H, interfering with solvent residual peak), 2.55-2.62 (m, 1H), 2.64-3.07 (m, 6H), 3.27-3.34 (m, 1H), 3.35-3.41 (m, 1H), 3.54-3.66 (m, 5H, interfering with water signal), 4.10-4.18 (m, 1H), 5.32 (br s, 1H), 6.80-6.91 (m, 2H), 6.95-7.59 (m, 22H), 7.72 (t, *J* = 5.5 Hz, 1H), 7.91-7.99 (m, 1H), 8.22 (t, *J* = 5.9 Hz, 1H), 10.37 (br s, 1H). **¹H-NMR** (600 MHz, MeOH-*d*₄): δ (ppm) 1.42-1.91 (m, 13H), 2.24-2.31 (m, 1H), 2.48-2.64 (m, 3H), 2.90-3.20 (m, 5H), 3.20-3.30 (m, 1H, interfering with solvent residual peak), 3.39-3.45 (m, 1H), 3.53-3.61 (m, 1H), 3.62-4.19 (m, 5H), 4.21-4.28 (m, 1H), 5.52 (s, 0.5H), 5.53 (s, 0.5H, interfering with previous signal), 6.89-6.97 (m, 2H), 7.18-7.27 (m, 3H), 7.29-7.47 (m, 12H), 7.67-7.72 (m, 2H). **¹³C-NMR** (150 MHz, DMSO-*d*₆): δ (ppm) 23.3 (two carbon signals), 25.1, 28.8, 36.2 (2 carb.), 37.27, 37.31, 37.5, 38.6, 39.6 (overlaid by solvent residual peak), 40.4, 42.7, 34.92, 51.1, 51.4, 52.0, 69.0, 116.00 (TFA), 116.05, 117.97 (TFA), 122.7, 126.7 (2 carb.), 128.2, 128.3, 128.9, 129.0, 136.6, 152.6, 154.9, 156.8, 158.5 (q, *J* = 32.0 Hz) (TFA), 170.2, 171.3, 172.0. **¹³C-NMR** (150 MHz, MeOH-*d*₄) δ (ppm) 24.58, 24.62, 26.32, 26.33, 30.1, 30.2, 38.2, 38.3, 39.2, 39.29, 39.33, 39.3, 39.49, 39.51, 40.0, 41.2, 41.3, 41.9, 44.0, 44.31, 44.35, 45.60, 45.63, 52.6, 52.7, 52.8, 52.9, 53.97,

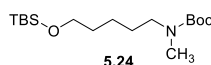
54.04, 73.77, 73.81, 117.4, 121.80, 121.82, 122.2, 124.31, 124.32, 128.2, 129.66, 129.69, 130.2, 130.50, 130.55, 130.56, 130.7 (two carbon signals), 131.8, 136.18, 136.24, 137.66, 137.68, 154.5, 155.55, 155.57, 158.6, 162.7 (TFA), 172.94, 172.97, 174.67, 174.72, 174.74. **RP-HPLC** (220 nm): 98% ($t_R = 13.2$ min, $k = 4.1$). **HRMS** (ESI): m/z $[M+H]^+$ calcd. for $[C_{48}H_{59}N_{10}O_6]^+$ 871.4614, found 871.4620. $C_{48}H_{58}N_{10}O_6 \times C_4H_2F_6O_4$ (871.06 + 228.04).



tert-Butyl (5-hydroxypentyl)(methyl)carbamate (5.22).²³ *tert*-Butyl (5-((*tert*-butyldimethylsilyl)oxy)pentyl)(methyl)carbamate (**5.24**) (3.38 g, 10.2 mmol) was dissolved in THF (150 mL). TBAF (1.1 M) in THF (15 mL, 16.5 mmol) was added and the reaction mixture stirred at rt for 4 h. The organic solvent was evaporated, and the crude product was purified by column chromatography (eluent: light petroleum/ethyl acetate 1:2) to give **5.22** as an oil (1.10 g, 5.1 mmol, 50%). **¹H-NMR** (400 MHz, DMSO- d_6): δ (ppm) 1.16-1.30 (m, 2H), 1.38 (s, 9H), 1.40-1.49 (m, 4H), 2.74 (s, 3H), 3.13 (t, $J = 7.1$ Hz, 2H), 3.38 (t, $J = 6.4$ Hz, 2H), 4.35 (br s, 1H). **¹³C-NMR** (101 MHz, DMSO- d_6): δ (ppm) 22.6, 27.2, 28.1, 32.2, 33.6, 48.0, 60.6, 78.2, 154.8. **HRMS** (ESI): m/z $[M+H]^+$ calcd. for $[C_{11}H_{24}NO_3]^+$ 218.1751, found 218.1749. $C_{11}H_{23}NO_3$ (217.31).

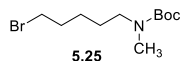


tert-Butyl (5-((tert-butyldimethylsilyl)oxy)pentyl)carbamate (5.23).²⁴ *tert*-Butyl (5-hydroxypentyl)carbamate (**4.34**) (6.12 g, 30.1 mmol) was dissolved in CH_2Cl_2 (200 mL), Et_3N (8.5 mL, 61.3 mmol) was added and the mixture was cooled in an ice bath. Under stirring, *tert*-butyldimethylsilylchlorid (5.51 g, 36.6 mmol) in CH_2Cl_2 (100 mL) was dropped slowly into the mixture over a time period of 1 h. The reaction mixture was allowed to warm to rt and stirred for 12 h. The organic solvent was evaporated, and the crude product was purified by column chromatography (eluent: light petroleum/ethyl acetate 95:5) to give **5.23** as a white solid (9.11 g, 28.7 mmol, 95%). **¹H-NMR** (400 MHz, DMSO- d_6): δ (ppm) 0.02 (s, 6H), 0.86 (s, 9H), 1.20-1.34 (m, 3H), 1.36 (s, 9H), 1.38-1.47 (m, 3H), 2.85-2.93 (m, 2H), 3.55 (t, $J = 6.4$ Hz, 2H), 6.73 (t, $J = 5.2$ Hz, 1H). **¹³C-NMR** (101 MHz, DMSO- d_6): δ (ppm) -5.4, 17.9, 22.6, 25.77, 25.80, 28.2, 29.3, 32.0, 62.4, 77.2, 155.5. **HRMS** (APCI): m/z $[M+H]^+$ calcd. for $[C_{16}H_{36}NO_3Si]^+$ 318.2459, found 318.2466. $C_{16}H_{35}NO_3Si$ (317.55).

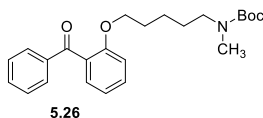


tert-Butyl (5-((tert-butyldimethylsilyl)oxy)pentyl)(methyl)carbamate (5.24). *tert*-Butyl (5-((*tert*-butyldimethylsilyl)oxy)pentyl)carbamate (**5.23**) (7.04 g, 22.2 mmol) was dissolved in THF (175 mL) and cooled using an ice bath. Sodium hydride (1.88 g, 47.0 mmol, 60%, dispersion in mineral oil) was added portionwise to the reaction mixture and stirred for 15 min. Then, MeI (2.80 mL, 45.0 mmol) was dropped into the mixture. After 1 h, the reaction mixture was allowed to warm to rt and stirred for 1 day. The solvent was evaporated, and the residue was dissolved in a saturated ammonium chloride solution (500 mL). The product was extracted from the aqueous phase with ethyl acetate (3x 500 mL) and the combined organic phases were dried over sodium sulfate and the organic solvent was evaporated. The crude product was purified by column chromatography (eluent: light petroleum/ethyl acetate 95:5) to

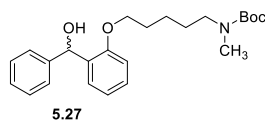
give **5.24** as a colourless oil (3.84 g, 11.6 mmol, 52%). **¹H-NMR** (400 MHz, DMSO-*d*₆): δ (ppm) 0.02 (s, 6H), 0.85 (s, 9H), 1.19-1.30 (m, 2H), 1.38 (s, 9H), 1.40-1.50 (m, 4H), 2.74 (s, 3H), 3.14 (t, *J* = 7.0 Hz, 2H), 3.57 (t, *J* = 6.2 Hz, 2H). **¹³C-NMR** (101 MHz, DMSO-*d*₆): δ (ppm) -4.9, 18.4, 22.9, 26.3, 27.2, 27.5, 28.5, 32.4, 34.0, 62.8, 78.6, 155.2. **HRMS** (ESI): *m/z* [M+H]⁺ calcd. for [C₁₇H₃₈NO₃Si]⁺ 332.2615, found 332.2626. C₁₇H₃₇NO₃Si (331.57).



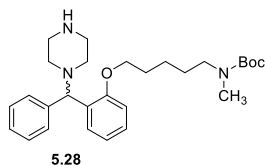
tert-Butyl (5-bromopentyl)(methyl)carbamate (5.25).²³ *tert*-Butyl (5-hydroxypentyl)(methyl)carbamate (**5.24**) (1.07 g, 4.92 mmol) and PPh₃ (1.86 g, 7.09 mmol) were dissolved in THF (50 mL) and the mixture was cooled in an ice bath. Under stirring, carbon tetrabromide (2.36 g, 7.12 mmol) in THF (50 mL) was added dropwise to the mixture and stirred for 1 h. Then, the reaction mixture was allowed to warm to rt. After 3 h, PPh₃ (1.84 g, 7.02 mmol) and carbon tetrabromide (2.35 g, 7.09 mmol) were added to the reaction mixture, which was stirred at rt overnight. The organic solvent was evaporated, and the crude product was purified by column chromatography (eluent: CH₂Cl₂/ethyl acetate 1:0 to 9:1) to give **5.25** as an oil (1.35 g, 4.82 mmol, 98%). **¹H-NMR** (400 MHz, DMSO-*d*₆): δ (ppm) 1.29-1.42 (m, 11H), 1.42-1.51 (m, 2H), 1.76-1.87 (m, 2H), 2.75 (s, 3H), 3.15 (t, *J* = 7.0 Hz, 2H), 3.52 (t, *J* = 6.8 Hz, 2H). **¹³C-NMR** (101 MHz, DMSO-*d*₆): δ (ppm) 24.6, 28.0, 31.8, 33.5, 35.0, 40.2 (overlaid by solvent residual peak), 47.8, 78.2, 154.7. **HRMS** (APCI): *m/z* [M+H]⁺ calcd. for [C₁₁H₂₃BrNO₂]⁺ 280.0907, found 280.0908. C₁₁H₂₂BrNO₂ (280.21).



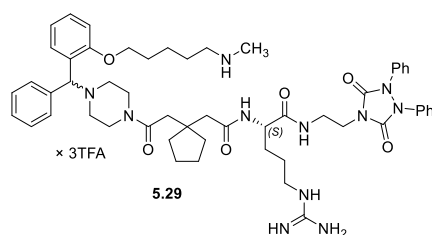
tert-Butyl (5-(2-benzoylphenoxy)pentyl)(methyl)carbamate (5.26). (2-Hydroxyphenyl)(phenyl)-methanone (**4.42**) (0.43 g, 2.17 mmol) was dissolved in DMF (5 mL) and K₂CO₃ (0.59 g, 4.27 mmol) was added and the mixture was stirred at rt for 5 min. Under stirring, *tert*-butyl (5-bromopentyl)carbamate (**5.25**) (0.69 g, 18.1 mmol) was added to the mixture and stirred at rt for 24 h. The reaction mixture was poured in water (200 mL) and the crude product was extracted from the aqueous phase with ethyl acetate (3x 150 mL). The combined organic phases were dried over sodium sulfate and the organic solvent was evaporated. The crude product was purified by column chromatography (eluent: light petroleum/ethyl acetate 8:2) to give **5.26** as a yellow oil (0.45 g, 1.17 mmol, 52%). **¹H-NMR** (400 MHz, DMSO-*d*₆): δ (ppm) 1.17-1.25 (m, 2H), 1.29-1.41 (m, 13H), 2.68 (s, 3H), 2.95 (t, *J* = 7.2 Hz, 2H), 3.88 (t, *J* = 5.9 Hz, 2H), 7.03-7.10 (m, 1H), 7.11-7.16 (m, 1H), 7.32-7.37 (m, 1H), 7.47-7.52 (m, 3H), 7.61-7.68 (m, 3H). **¹³C-NMR** (101 MHz, DMSO-*d*₆): δ (ppm) 25.2, 26.5, 26.8, 28.0, 33.6, 47.8, 67.6, 78.1, 112.6, 120.5, 128.4, 128.5, 129.9, 129.0, 132.2, 132.9, 137.8, 154.7, 156.2, 196.0. **HRMS** (ESI): *m/z* [M+Na]⁺ calcd. for [C₂₄H₃₁NO₄Na]⁺ 420.2145, found 420.2165. C₂₄H₃₁NO₄ (397.52).



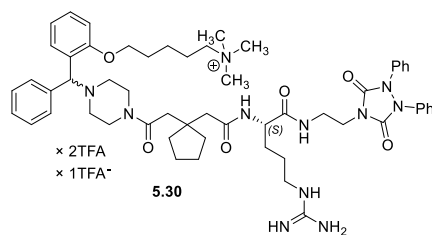
tert-Butyl (5-(2-(hydroxy(phenyl)methyl)phenoxy)pentyl)(methyl)carbamate (5.27). *tert*-Butyl (5-(2-benzoylphenoxy)pentyl)(methyl)carbamate (**5.26**) (0.246 g, 0.619 mmol) was dissolved in methanol (15 mL) and NaBH₄ (64.3 mg, 1.70 mmol) was added portion wise and stirred at rt for 4 h. The organic solvent was evaporated, and the crude product was purified by column chromatography (eluent: light petroleum/ethyl acetate 7:3) to give **5.27** as a yellow oil (0.247 g, 0.619 mmol, 100%). **¹H-NMR** (400 MHz, DMSO-*d*₆): δ (ppm) 1.29-1.36 (m, 2H), 1.39 (s, 9H), 1.44-1.56 (m, 2H), 1.66-1.75 (m, 2H), 2.76 (s, 3H), 3.15 (t, *J* = 7.1 Hz, 2H), 3.91 (t, *J* = 6.3 Hz, 2H), 5.62 (d, *J* = 4.3 Hz, 1H), 5.97 (d, *J* = 4.3 Hz, 1H), 6.87-6.97 (m, 2H), 7.13-7.20 (m, 2H), 7.22-7.28 (m, 2H), 7.30-7.35 (m, 2H), 7.52-7.57 (m, 1H). **¹³C-NMR** (101 MHz, DMSO-*d*₆): δ (ppm) 22.7, 26.8, 27.1, 28.1, 28.5, 40.0 (overlaid by solvent residual peak), 67.3, 68.2, 78.2, 111.2, 120.1, 126.3, 126.4, 126.5, 127.7, 133.7, 145.4, 154.78, 154.80, 170.3. **HRMS** (ESI): *m/z* [M+Na]⁺ calcd. for [C₂₄H₃₃NO₄Na]⁺ 422.2302, found 422.2300. C₂₄H₃₃NO₄ (399.53).



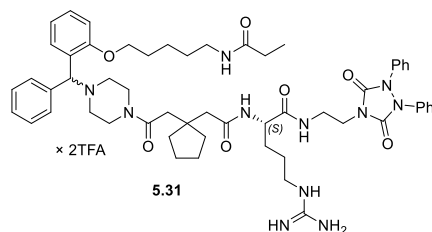
tert-Butyl methyl(5-(2-(phenyl(piperazin-1-yl)methyl)phenoxy)pentyl)carbamate (5.28). *tert*-Butyl (5-(2-(hydroxy(phenyl)methyl)phenoxy)pentyl)(methyl)carbamate (**5.27**) (150 mg, 0.375 mmol) was dissolved in CH₂Cl₂ (10 mL), Et₃N (200 μL, 1.44 mmol) was added and the mixture was cooled in an ice bath. Under stirring, methanesulfonyl chloride (45 μL, 0.563 mmol) was added to the mixture. After 3 h, 1 N NaOH (15 mL) was added to the reaction mixture. The compound was extracted from the aqueous phase with CH₂Cl₂ (3x) and the combined organic phases were dried over Na₂SO₄ and the organic solvent was evaporated. The residue was dissolved in acetonitrile (10 mL) and piperazine (230 mg, 2.67 mmol) was added. The reaction mixture was treated in the microwave device (70 °C, 45 min) and the organic solvent was evaporated. The crude product was purified by column chromatography (eluent: CH₂Cl₂/MeOH/NH₃ aq. 90:9:1) to give **5.28** as a yellow oil (140 mg, 0.299 mmol, 80%). **¹H-NMR** (400 MHz, DMSO-*d*₆): δ (ppm) 1.32-1.46 (m, 11H), 1.50-1.61 (m, 2H), 1.72-1.81 (m, 2H), 2.11-2.33 (m, 4H), 2.66-2.74 (m, 4H), 3.20 (t, *J* = 6.8 Hz, 2H), 3.29 (s, 3H), 3.88-3.96 (m, 2H), 4.66 (s, 1H), 6.86-6.94 (m, 2H), 7.07-7.19 (m, 2H), 7.21-7.28 (m, 2H), 7.30-7.38 (m, 2H), 7.53-7.58 (m, 1H). One exchangeable proton signal (NH-piperazine) was not apparent. **¹³C-NMR** (101 MHz, DMSO-*d*₆): δ (ppm) 33.8, 38.3, 39.9 (overlaid by solvent residual peak), 40.1 (overlaid by solvent residual peak), 43.9, 56.6, 58.9, 62.5, 63.8, 78.2, 88.8, 122.2, 130.9, 137.0, 138.0, 138.4, 138.6, 138.9, 139.0, 141.6, 153.5, 165.7. **HRMS** (ESI): *m/z* [M+Na]⁺ calcd. for [C₂₈H₄₁N₃O₃Na]⁺ 490.3040, found 490.3033. C₂₈H₄₁N₃O₃ (467.65).



(2S)-N¹-(2-{1-[2-(4-((2-((5-(methylamino)pentyl)oxy)phenyl)(phenyl)methyl)piperazin-1-yl]-2-oxoethyl]cyclopentyl}acetyl)[2-(3,5-dioxo-1,2-diphenyl-1,2,4-triazolidin-4-yl)ethyl]argininamide tris(hydrotrifluoroacetate) (5.29). Compound **5.29** was prepared according to *general procedure A* and the reactants (S)-2-(1-(2-((1-((2-(3,5-dioxo-1,2-diphenyl-1,2,4-triazolidin-4-yl)ethyl)amino)-1-oxo-5(2-((2,2,4,6,7-pentamethyl-2,3-dihydrobenzofuran-5-yl)sulfonyl)guanidino)pentan-2-yl)amino)-2-oxoethyl)cyclopentyl)acetic acid (**4.15**) (89.9 mg, 97.0 μmol), EDC·HCl (22.4 mg, 116.8 μmol), HOBT (19.3 mg, 142.8 μmol) and *tert*-butyl methyl(5-(2-(phenyl(piperazin-1-yl)methyl)phenoxy)pentyl)-carbamate (**5.28**) (44.7 mg, 95.6 μmol). Purification by preparative HPLC (gradient: 0-30 min, A/B 81:19–38:62, *t_R* = 14 min) gave **5.29** as a fluffy white solid (24.5 mg, 18.7 μmol, 20%). **¹H-NMR** (600 MHz, DMSO-*d*₆): δ (ppm) 1.33-1.71 (m, 17H), 1.72-1.80 (m, 2H), 2.20-2.27 (m, 1H), 2.31-2.38 (m, 1H), 2.42-2.48 (m, 1H), 2.55-2.60 (m, 4H), 2.85-2.92 (m, 2H), 2.95-3.04 (m, 2H), 3.26-3.33 (m, 1H), 3.35-3.41 (m, 1H), 3.46-3.74 (m, 5H), 3.89-4.06 (m, 6H), 4.12-4.16 (m, 1H), 5.30 (br s, 1H), 6.70-8.10 (m, 26H), 8.15-8.30 (m, 1H), 8.64 (br s, 2H). **¹H-NMR** (600 MHz, MeOH-*d*₄): δ (ppm) 1.46-1.79 (m, 17H), 1.81-1.94 (m, 2H), 2.24-2.32 (m, 1H), 2.45-2.64 (m, 3H), 2.68 (s, 3H), 2.78-3.23 (m, 8H), 3.41-3.47 (m, 1H), 3.50-3.56 (m, 1H), 3.66-3.90 (m, 5H), 4.01-4.13 (m, 2H), 4.17-4.27 (m, 1H), 5.55 (br s, 1H), 7.02-7.10 (m, 2H), 7.19-7.24 (m, 2H), 7.30-7.44 (m, 12H), 7.52-7.58 (m, 2H), 7.70-7.74 (m, 1H). **¹³C-NMR** (150 MHz, DMSO-*d*₆): δ (ppm) 22.4, 23.3, 25.01, 25.09, 28.1, 28.9, 32.4, 36.2 (two carbon signals), 37.2, 37.3, 37.4, 38.6, 39.6 (overlaid by solvent residual peak), 40.4, 42.7, 44.0, 48.1, 51.3, 51.6, 52.0, 67.0, 67.4, 112.4, 113.9 (TFA), 115.9 (TFA), 117.9 (TFA), 120.8, 122.7, 126.7, 127.1, 128.5, 128.7, 129.0, 136.6, 152.6, 155.8, 156.9, 158.6 (q, *J* = 32.4 Hz) (TFA), 170.1, 171.3, 172.04, 172.05. **¹³C-NMR** (150 MHz, MeOH-*d*₄): δ (ppm) 24.00, 24.01, 24.60, 24.64, 24.65, 26.31, 26.32, 26.8 (two carbon signals), 29.6 (2 carb.), 30.03, 30.05, 33.6, 38.32, 38.34, 39.2, 39.3, 39.39, 39.42, 39.9 (2 carb.), 41.20, 41.24, 41.9, 44.38, 44.41, 45.66, 45.69, 50.2, 52.79, 52.85, 54.01, 54.06, 69.0, 69.9, 113.7, 117.2 (TFA), 119.1, 122.4, 124.23, 124.25, 128.22, 128.24, 128.60, 128.63, 129.96, 130.02, 130.2, 130.3, 131.4, 137.70, 137.71, 154.5, 157.38, 157.41, 158.6, 162.9 (TFA), 172.91, 172.92, 174.7, 174.7 (2 carb.). **RP-HPLC** (220 nm): 95% (*t_R* = 12.0 min, *k* = 3.7). **HRMS** (ESI): *m/z* [M+H]⁺ calcd. for [C₅₄H₇₂N₁₁O₆]⁺ 970.5662, found 970.5672. C₅₄H₇₁N₁₁O₆ × C₆H₃F₉O₆. (969.56 + 342.07).

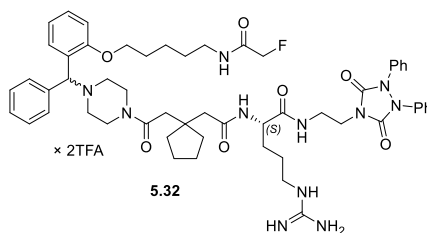


(2S)-N^α-(2-{1-[2-(4-((2-((5-(Trimethylaminio)pentyl)oxy)phenyl)(phenyl)methyl)piperazin-1-yl]-2-oxoethyl]cyclopentyl}acetyl)[2-(3,5-dioxo-1,2-diphenyl-1,2,4-triazolidin-4-yl)ethyl]argininamide bis(hydrotrifluoroacetate) trifluoroacetate (5.30). (2S)-N^α-(2-{1-[2-(4-((2-((5-Aminopentyl)oxy)phenyl)(phenyl)methyl)piperazin-1-yl]-2-oxoethyl]-cyclopentyl}acetyl)[2-(3,5-dioxo-1,2-diphenyl-1,2,4-triazolidin-4-yl)ethyl]argininamide tris(hydrotrifluoro-acetate) (4.50) (21.5 mg, 16.2 μmol) was dissolved in DMF (200 μL) and K₂CO₃ (13.9 mg, 363.8 μmol) was added. Methyl 4-nitrobenzenesulfonate (7.6 mg, 34.99 μmol) was added to the mixture and stirred at rt for 2 h. Then, 10% aq TFA (10 equiv.) was added and the mixture was directly purified by preparative HPLC (gradient: 0-30 min, A/B 71:29–57:43, t_R = 12 min) to give **5.29** as a fluffy white solid (12.9 mg, 9.62 μmol, 59%). ¹H-NMR (600 MHz, DMSO-*d*₆): δ (ppm) 1.36-1.82 (m, 19H), 2.19-2.25 (m, 1H), 2.30-2.36 (m, 1H), 2.39-2.47 (m, 1H, interfering with solvent residual peak), 2.55-2.59 (m, 1H, interfering with solvent residual peak), 2.92-3.15 (m, 10H), 3.26-3.40 (m, 5H), 3.42-3.64 (m, 5H), 3.89-4.19 (m, 7H), 5.63 (br s, 1H), 6.92-7.55 (m, 23H), 7.62-7.80 (m, 2H), 7.92-8.05 (m, 1H), 8.18-8.26 (m, 1H). ¹H-NMR (400 MHz, MeOH-*d*₄): δ (ppm) 1.45-1.94 (m, 19H), 2.24-2.30 (m, 1H), 2.46-2.55 (m, 2H), 2.58-2.64 (m, 1H), 2.66-3.19 (m, 15H), 3.31-3.34 (m, 2H, interfering with solvent residual peak), 3.41-3.49 (m, 1H), 3.51-3.59 (m, 1H), 3.61-3.99 (m, 5H), 4.02-4.15 (m, 2H), 4.21-4.27 (m, 1H), 5.44 (br s, 1H), 7.02-7.09 (m, 2H), 7.19-7.24 (m, 2H), 7.30-7.43 (m, 12H), 7.50-7.56 (m, 2H), 7.68-7.72 (m, 1H). ¹³C-NMR (150 MHz, DMSO-*d*₆): δ (ppm) 21.8, 22.4, 23.3, 25.00, 25.07, 28.2, 28.9, 32.4, 36.2, 37.2, 37.4, 38.6, 39.6 (overlaid by solvent residual peak), 40.4, 42.1, 42.7, 44.0, 48.1, 51.4, 51.8, 51.9, 52.2, 65.2, 67.3, 112.3, 116.0 (TFA), 117.9 (TFA), 120.7, 122.6, 126.7 (two carbon signals), 127.2, 128.3, 129.0, 136.5, 152.6, 155.8, 156.8, 158.3 (q, *J* = 32.0 Hz) (TFA), 170.1, 171.3, 172.0. **RP-HPLC** (220 nm): 99% (t_R = 11.5 min, *k* = 3.5). **HRMS** (ESI): *m/z* [M]⁺ calcd. for [C₅₆H₇₆N₁₁O₆]⁺ 998.5975, found 998.5969. C₅₆H₇₆N₁₁O₆⁺ × C₆H₂F₉O₆ (999.29 + 228.05 + 113.02).



(2S)-N^α-(2-{1-[2-(4-(Phenyl(2-((5-propionamidopentyl)oxy)phenyl)methyl)piperazin-1-yl]-2-oxoethyl]cyclopentyl}acetyl)[2-(3,5-dioxo-1,2-diphenyl-1,2,4-triazolidin-4-yl)ethyl]argininamide bis(hydrotrifluoroacetate) (5.31). (2S)-N^α-(2-{1-[2-(4-((2-((5-Aminopentyl)oxy)phenyl)(phenyl)methyl)piperazin-1-yl]-2-oxoethyl]cyclopentyl}acetyl)[2-(3,5-dioxo-1,2-diphenyl-1,2,4-triazolidin-4-yl)ethyl]argininamide tris(hydrotrifluoro-acetate) (4.50) (15.2 mg, 11.7 μmol) and DIPEA (6 μL, 35.3 μmol) was dissolved in DMF (0.5 mL) and stirred at rt for 5 min. Succinimidyl propionate (2.44) (2 mg, 11.7 μmol)

was added and the reaction mixture was stirred at rt for 3 h. Then, 10% aq TFA (10 equiv.) was added and the mixture was purified directly by preparative HPLC (gradient: 0-30 min, A/B 76:24–38:62, $t_R = 20$ min) to give **5.31** as a fluffy white solid (14.0 mg, 10.8 μ mol, 92%). **¹H-NMR** (600 MHz, DMSO-*d*₆): δ (ppm) 0.97 (t, $J = 7.6$ Hz, 3H), 1.33-1.64 (m, 17H), 1.70-1.77 (m, 2H), 2.04 (q, $J = 7.6$ Hz, 2H), 2.19-2.24 (m, 1H), 2.29-2.36 (m, 1H), 2.41-2.47 (m, 1H, interfering with solvent residual peak), 2.52-2.60 (m, 1H, interfering with solvent residual peak), 2.94-3.02 (m, 2H), 3.03-3.10 (m, 2H), 3.26-3.32 (m, 2H), 3.33-3.39 (m, 1H), 3.39-3.62 (m, 5H), 3.83-4.05 (m, 5H), 4.11-4.16 (m, 1H), 5.74 (br s, 1H), 6.79-7.82 (m, 26H), 8.18-8.25 (m, 1H), 7.95 (d, $J = 6.8$ Hz, 1H). **¹H-NMR** (600 MHz, MeOH-*d*₄): δ (ppm) 1.11 (t, $J = 7.6$ Hz, 3H, -NCOCH₂CH₃ the triplet is overlaid by a second triplet, because two diastereomers are evident in the spectra), 1.43-1.95 (m, 19H), 2.17 (q, $J = 7.6$ Hz, 2H), 2.26-2.33 (m, 1H), 2.46-2.67 (m, 3H), 2.87-3.29 (m, 8H, interfering with solvent residual peak), 3.41-3.48 (m, 1H), 3.53-3.61 (m, 1H), 3.62-3.99 (m, 5H), 4.01-4.08 (m, 1H), 4.08-4.15 (m, 1H), 4.20-4.28 (m, 1H), 5.65 (s, 0.5H), 5.66 (s, 0.5H), 7.05-7.12 (m, 2H), 7.18-7.26 (m, 2H), 7.30-7.49 (m, 12H), 7.55-7.60 (m, 2H), 7.67-7.72 (m, 1H). **¹³C-NMR** (150 MHz, DMSO-*d*₆): δ (ppm) 10.0, 23.1, 23.3, 24.3, 24.9, 25.1, 25.2, 28.3, 28.6, 28.9, 29.8, 31.5, 36.2, 37.2, 37.3, 37.4, 38.3, 38.6, 39.6 (overlaid by solvent residual peak), 40.4, 42.7, 44.0, 49.8, 51.3, 51.9, 54.2, 66.9, 67.7, 112.3, 116.0 (TFA), 117.9 (TFA), 120.7, 122.6, 126.6, 127.2, 128.6, 129.0, 136.6, 152.6, 155.8, 156.8, 158.3 (q, $J = 32.4$ Hz), 170.1, 171.3, 171.99, 172.01, 172.7. **RP-HPLC** (220 nm): 100% ($t_R = 14.3$ min, $k = 3.6$). **HRMS** (ESI): m/z [M+H]⁺ calcd. for [C₅₆H₇₄N₁₁O₇]⁺ 1012.5767, found 1012.5776. C₅₆H₇₃N₁₁O₇ × C₄H₂F₆O₄ (1011.57 + 228.04).



(2S)-N^α-(2-{1-[2-(4-(Phenyl(2-((5-(2-fluoroacetamido)pentyl)oxy)phenyl)methyl)piperazin-1-yl]-2-oxo-ethyl]cyclopentyl}acetyl)[2-(3,5-dioxo-1,2-diphenyl-1,2,4-triazolidin-4-yl)ethyl]argininamide bis(hydrotrifluoroacetate) (5.32). A freshly prepared solution of 2-fluoroacetic acid (**2.44**) (1.8 mg, 23.1 μ mol), EDC·HCl (5.3 mg, 27.6 μ mol), HOBT (10.3 mg, 76.2 μ mol) in DMF (0.5 mL) was added dropwise to a solution of (2S)-N^α-(2-{1-[2-(4-((2-((5-aminopentyl)oxy)phenyl)(phenyl)methyl)-piperazin-1-yl]-2-oxoethyl]cyclopentyl}acetyl)[2-(3,5-dioxo-1,2-diphenyl-1,2,4-triazolidin-4-yl)ethyl]-argininamide tris(hydrotrifluoroacetate) (**4.50**) (34.9 mg, 26.9 μ mol) and DIPEA (20 μ L, 117.6 μ mol) in DMF (1 mL). The reaction mixture was stirred at rt for 2-3 h. The product was purified by preparative HPLC (gradient: 0-30 min, A/B 85:15–38:62, $t_R = 20$ min) to give **5.32** as a fluffy white solid (13.9 mg, 11.2 μ mol, 42%). **¹H-NMR** (600 MHz, DMSO-*d*₆): δ (ppm) 1.33-1.68 (m, 17H), 1.70-1.82 (m, 2H), 2.17-2.26 (m, 1H), 2.29-2.39 (m, 1H), 2.41-2.49 (m, 1H, interfering with solvent residual peak), 2.53-2.69 (m, 2H, interfering with solvent residual peak), 2.94-3.05 (m, 3H), 3.10-3.22 (m, 3H), 3.27-3.32 (m, 1H), 3.34-3.39 (m, 1H), 3.43-3.85 (m, 5H), 3.87-4.04 (m, 3H), 4.12-4.16 (m, 1H, interfering with water signal), 4.77 (d, $J = 47.1$ Hz, 2H), 5.72 (br s, 1H), 6.76-7.86 (m, 25H), 7.95 (d, $J = 7.2$ Hz, 1H), 8.13-8.29 (m, 2H). **¹H-NMR** (600 MHz, MeOH-*d*₄): δ (ppm) 1.44-1.82 (m, 17H), 1.83-1.90 (m, 2H), 2.24-2.31 (m, 1H), 2.47-2.62 (m, 3H), 2.69-3.23 (m, 6H), 3.24-3.29 (m, 1H, interfering with solvent residual peak), 3.31-

3.35 (m, 1H), 3.41-3.48 (m, 1H), 3.50-3.57 (m, 1H), 3.60-3.99 (m, 5H), 4.00-4.06 (m, 1H), 4.07-4.14 (m, 1H), 4.21-4.28 (m, 1H), 4.76 (d, $J = 47.1$ Hz, 2H, $-\text{CH}_2\text{F}$, the doublet is overlaid by a second doublet, because two diastereomers are evident in the spectra), 5.53 (br s, 1H), 7.02-7.09 (m, 2H), 7.18-7.24 (m, 2H), 7.29-7.45 (m, 12H), 7.51-7.58 (m, 2H), 7.64-7.69 (m, 1H). **$^{13}\text{C-NMR}$** (150 MHz, $\text{DMSO-}d_6$): δ (ppm) 22.9, 23.3, 25.1, 28.3, 28.78, 28.84, 36.15, 36.17, 37.23, 37.27, 37.43, 37.97, 38.7, 39.6 (overlaid by solvent residual peak), 40.4, 42.7, 43.9, 51.2, 51.5, 51.9, 67.6, 80.0 (d, $J = 180.2$ Hz), 112.5, 113.7 (TFA), 115.7 (TFA), 117.7 (TFA), 120.8, 122.6, 126.7 (two carbon signals), 127.0 (2 carb.), 128.4, 129.0, 136.5, 152.6, 155.8, 156.8, 158.4 (q, $J = 32.9$ Hz) (TFA), 166.9 (d, $J = 18.1$ Hz), 170.1, 171.3, 171.98, 172.00. **RP-HPLC** (220 nm): 100% ($t_R = 13.6$ min, $k = 4.3$). **HRMS** (ESI): m/z $[\text{M}+\text{H}]^+$ calcd. for $[\text{C}_{55}\text{H}_{71}\text{FN}_{11}\text{O}_7]^+$ 1016.5516, found 1016.5507. $\text{C}_{55}\text{H}_{70}\text{FN}_{11}\text{O}_7 \times \text{C}_4\text{H}_2\text{F}_6\text{O}_4$ (1015.54 + 228.04).

5.4.3. Investigation of the chemical stability of compounds 4.23, 4.24, 4.27, 5.9, 5.30 and 5.32

cf. 4.4.4.

5.4.4. Pharmacological methods: cell culture, radioligand competition binding assay in HEK293T $\beta\text{Arr}2 + \text{Y}_2\text{R}$ cells, BRET based binding assay and β -arrestin2 recruitment assay (Y_2R), radioligand binding assay for hY_1R , hY_4R and hY_5R

5.4.4.1. Cell culture

cf. 4.4.5.1.

5.4.4.2. Radioligand competition binding assay in HEK293 $\beta\text{Arr}2 + \text{Y}_2\text{R}$ cells

cf. 4.4.5.3.

5.4.4.3. BRET based binding assay

cf. 4.4.5.6.

5.4.4.4. β -Arrestin2 recruitment assay (Y_2R)

cf. 4.4.5.4.

5.4.4.5. Radioligand binding assay for hY_1R , hY_4R and hY_5R

cf. 4.4.5.8.

5.4.5. Data analysis

cf. 4.4.6.

5.5. References

1. Doods, H.; Gaida, W.; Wieland, H. A.; Dollinger, H.; Schnorrenberg, G.; Esser, F.; Engel, W.; Eberlein, W.; Rudolf, K. BIIE0246: A selective and high affinity neuropeptide Y Y₂ receptor antagonist. *Eur. J. Pharm.* **1999**, *384*, R3-R5.
2. Pluym, N.; Baumeister, P.; Keller, M.; Bernhardt, G.; Buschauer, A. [³H]UR-PLN196: A Selective Nonpeptide Radioligand and Insurmountable Antagonist for the Neuropeptide Y Y₂ Receptor. *ChemMedChem* **2013**, *8*, 587-593.
3. Pluym, N. Application of the Guanidine-Acylguanidine Bioisosteric Approach to NPY Y₂ Receptors Antagonists: Bivalent, Radiolabeled and Fluorescent Pharmacological Tools. PhD Thesis, University of Regensburg, 2011.
4. Baumeister, P. Molecular tools for G-Protein Coupled Receptors: Synthesis, Pharmacological Characterization and [³H]-Labeling of Subtype-selective Ligands for Histamine H₄ and NPY Y₂ Receptors. PhD Thesis, University of Regensburg, 2014.
5. Brennauer, A.; Keller, M.; Freund, M.; Bernhardt, G.; Buschauer, A. Decomposition of 1-(ω-aminoalkanoyl)guanidines under alkaline conditions. *Tetrahedron Lett.* **2007**, *48*, 6996-6999.
6. Dautzenberg, F. M. Stimulation of neuropeptide Y-mediated calcium responses in human SMS-KAN neuroblastoma cells endogenously expressing Y₂ receptors by co-expression of chimeric G proteins. *Biochem. Pharmacol.* **2005**, *69*, 1493-1499.
7. Appel, R. Tertiary Phosphane/Tetrachloromethane, a Versatile Reagent for Chlorination, Dehydration, and P-N Linkage. *Angew. Chem., Int. Ed. Engl.* **1975**, *14*, 801-811.
8. Buschmann, J.; Seiler, T.; Bernhardt, G.; Keller, M.; Wifling, D. Argininamide-type neuropeptide Y Y₁ receptor antagonists: the nature of N^ω-carbamoyl substituents determines Y₁R binding mode and affinity. *RSC Med. Chem.* **2020**, *11*, 274-282.
9. Ziemek, R.; Brennauer, A.; Schneider, E.; Cabrele, C.; Beck-Sickinger, A. G.; Bernhardt, G.; Buschauer, A. Fluorescence- and luminescence-based methods for the determination of affinity and activity of neuropeptide Y₂ receptor ligands. *Eur. J. Pharm.* **2006**, *551*, 10-18.
10. Felixberger, J. Luciferase complementation for the determination of arrestin recruitment: Investigation at histamine and NPY receptors. PhD Thesis, University of Regensburg, 2014.
11. Keller, M.; Weiss, S.; Hutzler, C.; Kuhn, K. K.; Mollereau, C.; Dukorn, S.; Schindler, L.; Bernhardt, G.; König, B.; Buschauer, A. N^ω-Carbamoylation of the Argininamide Moiety: An Avenue to Insurmountable NPY Y₁ Receptor Antagonists and a Radiolabeled Selective High-Affinity Molecular Tool ([³H]UR-MK299) with Extended Residence Time. *J. Med. Chem.* **2015**, *58*, 8834-8849.
12. Ziemek, R.; Schneider, E.; Kraus, A.; Cabrele, C.; Beck-Sickinger, A. G.; Bernhardt, G.; Buschauer, A. Determination of Affinity and Activity of Ligands at the Human Neuropeptide Y Y₄ Receptor by Flow Cytometry and Aequorin Luminescence. *J. Recept. Signal Transduct. Res.* **2007**, *27*, 217-233.
13. Kuhn, K. K.; Ertl, T.; Dukorn, S.; Keller, M.; Bernhardt, G.; Reiser, O.; Buschauer, A. High Affinity Agonists of the Neuropeptide Y (NPY) Y₄ Receptor Derived from the C-Terminal Pentapeptide of Human Pancreatic Polypeptide (hPP): Synthesis, Stereochemical Discrimination, and Radiolabeling. *J. Med. Chem.* **2016**, *59*, 6045-6058.

14. Moser, C.; Bernhardt, G.; Michel, J.; Schwarz, H.; Buschauer, A. Cloning and functional expression of the hNPY Y₅ receptor in human endometrial cancer (HEC-1B) cells. *Can. J. Physiol. Pharmacol.* **2000**, *78*, 134-42.
15. Wodtke, R.; Hauser, C.; Ruiz-Gómez, G.; Jäckel, E.; Bauer, D.; Lohse, M.; Wong, A.; Pufe, J.; Ludwig, F.-A.; Fischer, S.; Hauser, S.; Greif, D.; Pisabarro, M. T.; Pietzsch, J.; Pietzsch, M.; Löser, R. N^ε-Acryloyllysine Piperazides as Irreversible Inhibitors of Transglutaminase 2: Synthesis, Structure–Activity Relationships, and Pharmacokinetic Profiling. *J. Med. Chem.* **2018**, *61*, 4528-4560.
16. Fulmer, G. R.; Miller, A. J. M.; Sherden, N. H.; Gottlieb, H. E.; Nudelman, A.; Stoltz, B. M.; Bercaw, J. E.; Goldberg, K. I. NMR Chemical Shifts of Trace Impurities: Common Laboratory Solvents, Organics, and Gases in Deuterated Solvents Relevant to the Organometallic Chemist. *Organometallics* **2010**, *29*, 2176-2179.
17. Dollinger, H.; Esser, F.; Mihm, G.; Rudolf, K.; Schnorrenberg, G.; Gaida, W.; Doods, N. H. Neue substituierte Aminosäurederivate, Verfahren zu ihrer Herstellung und diese Verbindungen enthaltene pharmazeutische Zusammensetzungen. DE19816929A1, 1998.
18. Brennauer, A. Acylguanidines as bioisosteric groups in argininamide-type neuropeptide Y Y₁ and Y₂ receptor antagonists: synthesis, stability and pharmacological activity. PhD Thesis, University of Regensburg, 2006.
19. Sugiyama, K.; Yamada, T. Precise Synthesis and Surface Characterization of End-Functionalized Polystyrene with Perfluoroalkyl Group via Ionic Bond Formation of Diethylamino End-Group with Perfluoroalkylcarboxylic Acid. *Macromol. Chem. Phys.* **2017**, *218*, 1600444.
20. Misawa, T.; Dodo, K.; Ishikawa, M.; Hashimoto, Y.; Sagawa, M.; Kizaki, M.; Aoyama, H. Structure–activity relationships of benzhydrol derivatives based on 1'-acetoxychavicol acetate (ACA) and their inhibitory activities on multiple myeloma cell growth via inactivation of the NF- κ B pathway. *Bioorg. Med. Chem.* **2015**, *23*, 2241-2246.
21. Soldi, C.; Lamb, K. N.; Squitieri, R. A.; González-López, M.; Di Maso, M. J.; Shaw, J. T. Enantioselective Intramolecular C–H Insertion Reactions of Donor–Donor Metal Carbenoids. *J. Am. Chem. Soc.* **2014**, *136*, 15142-15145.
22. Schlienger, N.; Bryce, M. R.; Hansen, T. K. The Boronic Mannich Reaction in a Solid-Phase Approach. *Tetrahedron* **2000**, *56*, 10023-10030.
23. Wagner, S.; Buchgraber, P.; Klar, U.; Christ, C.; Fernandez-Montalvan, A. E.; Möwes, M.; Lienau, P.; Eis, K.; Sack, U.; Mönning, U.; Scholz, A.; Kuhnke, J.; Thede, K.; Werbeck, N.; Serrano-Wu, M.; Lemke, C.; McKinney, D.; Fitzgerald, M.; Nasveschuk, C.; Lazarski, K.; Ferrara, S. J.; Furst, L.; Wei, G.; Mccarren, P. R. Macrocyclic indole derivatives. WO2017198341A1, 2017.
24. Hernández, J. N.; Ramírez, M. A.; Martín, V. S. A New Selective Cleavage of N,N-Dicarbamoyl-Protected Amines Using Lithium Bromide. *J. Org. Chem.* **2003**, *68*, 743-746.

Chapter 6

Synthesis and pharmacological investigation of substituted (*R,R*)-diaminocyclohexanes as potential non-peptide ligands for the hY₄R

Note: I gratefully acknowledge the support of my research students (Forschungspraktikanten) Florian Fricke and Maria Deichner during synthesis.

Thanks are due to Dr. Stefanie Dukorn, Susanne Bollwein and Dita Fritsch for excellent technical assistance (cultivation of cells).

X-ray crystallography of compounds (*R*)-**6.17** and (*R,R,S*)-**6.6b** were performed by the Central Analytical Services (Faculty of Chemistry and Pharmacy).

6.1. Introduction

The NPY hY₄ receptor shows higher affinity to pancreatic polypeptide (PP) compared to NPY and is therefore, in this respect, different from the other receptor subtypes (hY₁R, hY₂R and hY₅R).¹ Furthermore, the Y₄R is a potential target for the treatment of obesity, because of its physiological role in regulation of appetite and gut function.^{2,3} Therefore, there is an interest in small molecule Y₄R ligands, particularly agonists and positive allosteric modulators.³⁻¹³ During the last decade, several non-peptide Y₄R ligands have been reported in literature (Figure 6.1 and Table 6.1).⁴⁻¹¹

The bivalent ligand (*R,R*)-**6.1**, representing a dimer of the Y₁R antagonist BIBP-3226, showed, in addition to Y₁R binding, moderate to high affinity ($pK_i = 6.9$) and antagonism ($pK_b = 7.7$).⁴ Notably, the optical antipode of (*R,R*)-**6.1**, i.e. (*S,S*)-**6.1** (Figure 6.1), proved to be a Y₄R selective antagonist.⁴ An imidazolepropylguanidine-type histamine receptor ligand (**6.2**), developed in our group, showed affinity and antagonism towards the hY₄R,⁵ but further investigations revealed cytotoxicity at a concentration of 10 μ M.¹⁴ The cytotoxic effects of compound **6.2** were determined in a kinetic crystal violet based chemosensitivity assay using HT-29 carcinoma cells over a period of 200 h.¹⁴

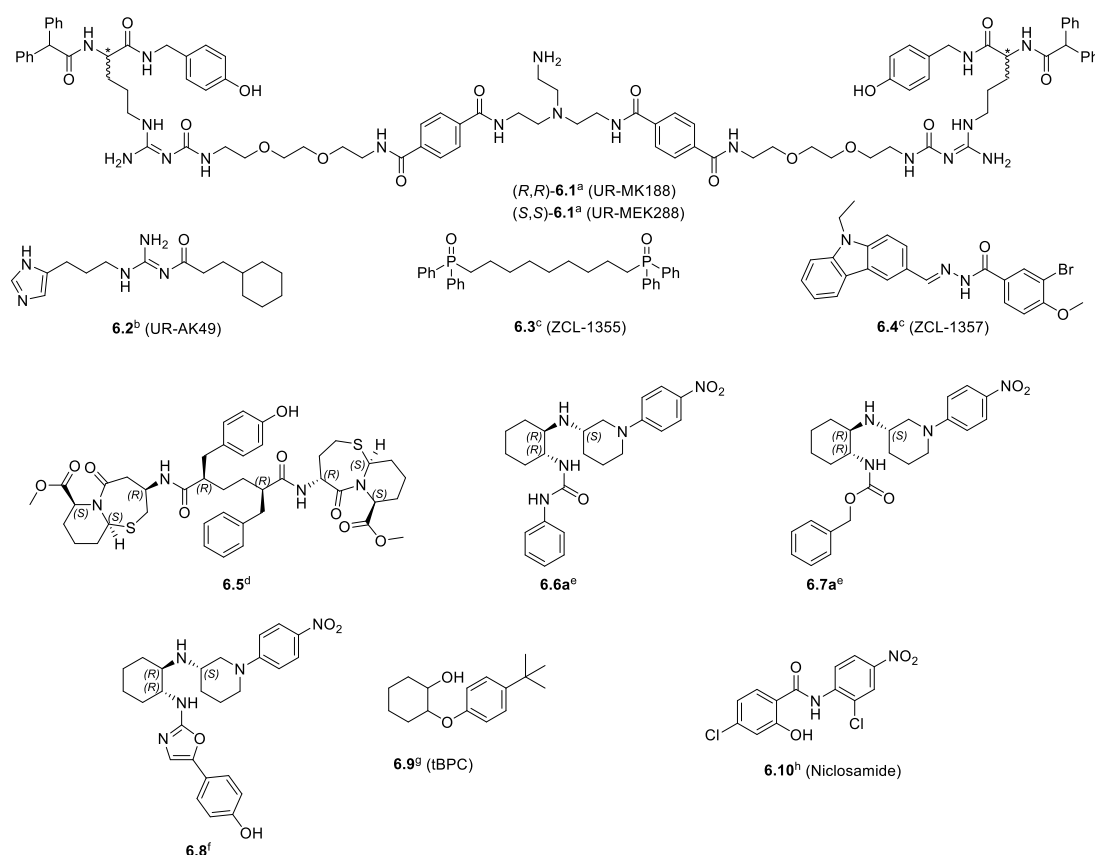


Figure 6.1. Structures of reported non-peptide antagonists (**6.1** and **6.2**), agonists (**6.3-6.8**) and modulators (**6.9** and **6.10**) of the NPY Y₄R (for Y₄R affinities, potencies or antagonistic activities see Table 6.1). References: (a) Keller et al.,⁴ (b) Ziemek et al.,⁵ (c) Kang et al.,⁶ (d) Sun et al.,⁷ (e) Ewing et al.,⁸ (f) Ewing et al.,⁹ (g) Schubert et al.,¹¹ (h) Sliwoski et al.¹⁰

Recently, a series of Y₄R agonists (e.g. **6.3** and **6.4**), which showed moderate potencies, were discovered by computer aided drug design.⁶ These agonists with micromolar potency were investigated in a cAMP assay (prevention of forskolin stimulated transformation from ATP to cAMP) in HEK293/NPY4R cells.

Moreover, Chongqing et al.⁷ and Ewing et al.^{8, 9} have reported a series of adipic acids (**6.5**) and (*R,R*)-diaminocyclohexanes ((*R,R,S*)-**6.6a** and (*R,R,S*)-**6.7a**) that were considered as agonists, antagonists or modulators of the hY₄R. According to the data (procedures) given in the patents, these ligands should be considered as agonists. These compounds were investigated in a cAMP assay (prevention of forskolin stimulated transformation from ATP to cAMP) in CHO cells. The affinities of compounds **6.3-6.8** for Y₄R are not reported in literature.

Table 6.1. Reported Y₄R binding data (p*K_i*), agonistic potencies (pEC₅₀) or antagonistic activities (p*K_b*) of reported Y₄R agonists, antagonists or modulators (structures see Figure 6.1).

Compound	Ref.	p <i>K_i</i>	pEC ₅₀ /p <i>K_b</i>
(<i>R,R</i>)- 6.1 (UR-M188)	a	6.89	7.70
(<i>S,S</i>)- 6.1 (UR-MEK288)	a	6.59	7.57
6.2	b	4.17	3.88
6.3	c	n.a.	4.21
6.4	c	n.a.	4.19
6.5	d	n.a.	8.30
6.6a	e	n.a.	7.09
6.7a	e	n.a.	n.a.
6.8	f	n.a.	9.00
6.9 (tBPC)	g	<4.52	5.29
6.10 (Niclosamide)	h	n.a.	6.21

References: (a) Keller et al.;⁴ these authors reported *K_i* values (affinities determined in a flow cytometric binding assay using Cy5-[K⁴]-hPP (*c_{final}* = 3 nM, *K_d* = 5.6 nM) and *K_b* values (antagonistic activities determined in an aequorin assay in intact CHO-hY₄-G_{q15}-mtAEQ cells. Aequorin Ca²⁺ mobilization was induced by 100 nM hPP (EC₅₀ = 15.5 nM), after pre-incubation of the cells with the antagonists for 15 min). (b) Ziemek et al.;⁵ these authors reported p*K_i* values (affinities determined in a flow cytometric binding assay using Cy5-[K⁴]-hPP (*c_{final}* = 3 nM, *K_d* = 5.6 nM) and p*K_b* values (antagonistic activities determined in an aequorin assay in intact CHO-hY₄-G_{q15}-mtAEQ cells. Aequorin Ca²⁺ mobilization was induced by 100 nM hPP (pEC₅₀ = 8.07), after pre-incubation of the cells with the antagonists for 15 min). (c) Kang et al.;⁶ these authors reported EC₅₀ values (potencies were determined in a cAMP assay in HEK293/NPY4R cells). (d) Sun et al.;⁷ these authors reported EC₅₀ values (potencies were determined in a cAMP assay in CHO cells). (e) Ewing et al.;⁸ these authors reported EC₅₀ values (potencies were determined in a cAMP assay in CHO cells). (f) Ewing et al.;⁹ these authors reported EC₅₀ values (potencies were determined in a cAMP assay in CHO cells). (g) Schubert et al.;¹¹ these authors reported EC₅₀ value (modulation was investigated through potentiation of a PP EC₂₀ signal response by increasing concentrations of **6.9** in a Ca²⁺ assay in COS7_Y₄R-eYFP_Δ6Gα_{q14}-myr cells). (h) Sliwoski et al.;¹⁰ these authors reported pEC₅₀ value (modulation was investigated through potentiation of a PP EC₂₀ signal response by increasing concentrations of **6.9** in an inositol phosphate accumulation assay in COS7_Y₄R-eYFP_Δ6Gα_{q14}-myr cells). Reported *K_i* values (EC₅₀ or *K_b*) were converted to p*K_i* values (pEC₅₀, or p*K_b*). n.a. not applicable. *K_b* values given in italics.

Lately, the development of positive (PAM) or negative (NAM) allosteric GPCR modulators has emerged as an approach in drug discovery for an improved treatment of various diseases (possible reduction of

adverse effects).^{15, 16} The group of Beck-Sickinger reported tBPC (**6.9**) and niclosamide (**6.10**) as the first allosteric modulators for the NPY Y₄R.^{10, 11} The pEC₅₀ value of **6.9** (Table 6.1) was determined in an inositol phosphate accumulation assay through potentiation of a PP EC₂₀ response as well as the effect on the pEC₅₀ value of PP in presence of 30 μM **6.10** (shown in bar chart and concentration response curves).¹⁰ Additionally, the pEC₅₀ value of **6.9** was determined in a Ca²⁺ assay through potentiation of a PP EC₂₀ response, and an effect on potency in a β-arrestin2 recruitment assay was reported.¹¹

In this chapter, the synthesis of the reported potential Y₄R agonists (*R,R,S**)-**6.6a** and (*R,R,S**)-**6.7a**, as well as the literature Y₄R modulator tBPC (**6.9**) are described, along with an evaluation of their activities at the NPY Y₄R (competition binding studies). Moreover, several derivatives of (*R,R,S**)-**6.6a** and (*R,R,S**)-**6.7a** were synthesized and investigated with respect to Y₄R binding. Selected compounds, including the putative Y₄R PAM niclosamide (**6.10**), were investigated in an aequorin Ca²⁺ assay. Additionally, the cytotoxicity of a set of compounds was investigated by ethidium bromide/acridine orange staining.

6.2. Results and discussion

6.2.1. Annotation concerning stereochemistry

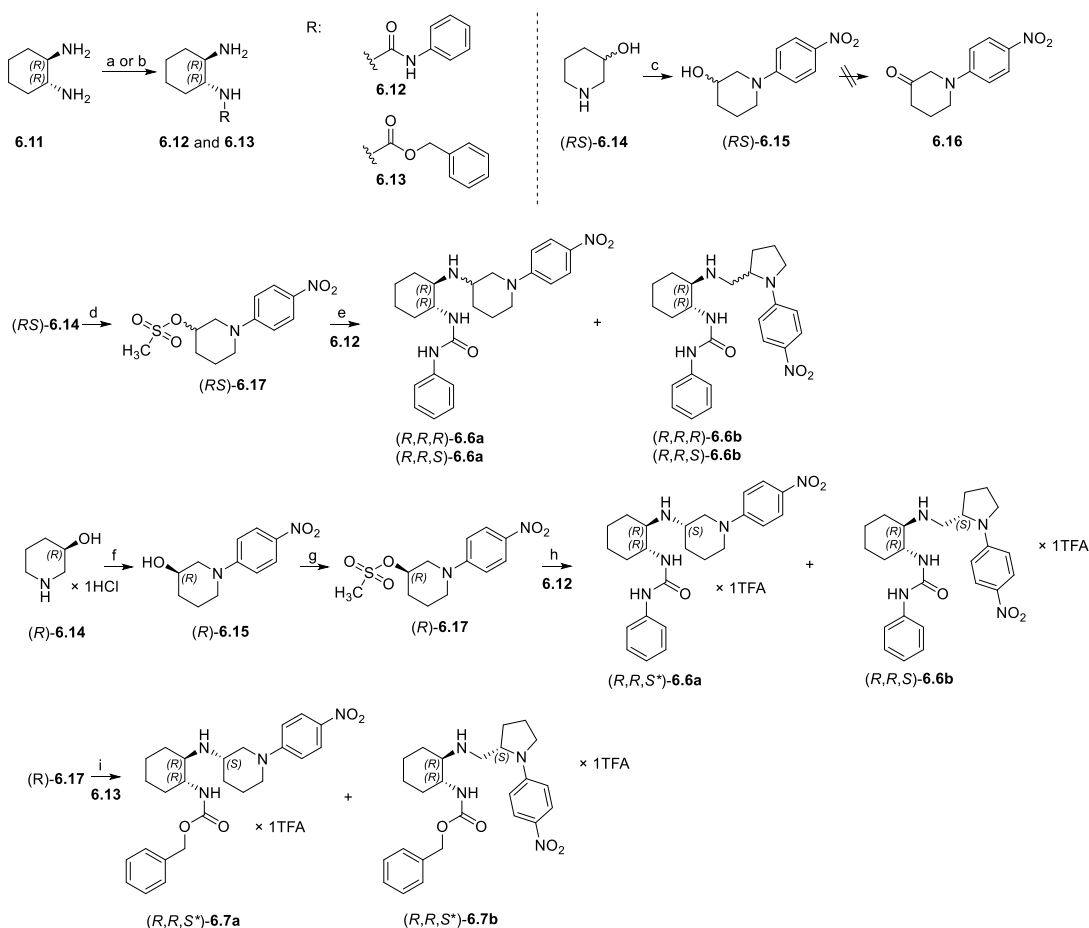
Annotation concerning stereochemistry of (*R,R,S**)-**6.6a**, (*R,R,S**)-**6.7a**, (*R,R,S**)-**6.7b**: the absolute configurations of the stereogenic centres of the (1*R*,2*R*)-diaminocyclohexane moiety are known, whereas the stereogenic centres in the piperidine or pyrrolidine moiety were defined as *R** or *S**, as the absolute configuration could not be elucidated by X-ray crystallography.

Annotation concerning the stereochemistry of (*S**)-**6.18a** and (*S**)-**6.18b**: the absolute configuration of the stereogenic centres could not be elucidated by X-ray crystallography, therefore the absolute configuration was defined as *R** or *S**.

6.2.2. Synthesis

(*R,R*)-Diaminocyclohexane (**6.11**) was derivatized at one of the two amine groups by use of isocyanatobenzene and *N*-(benzyloxycarbonyloxy)succinimide to form urea **6.12** and carbamate **6.13**, respectively. Target compounds (*R,R,S*)-**6.6a** and (*R,R,S*)-**6.7a** were synthesized according to Ewing et al.^{8, 9} with minor modifications (Scheme 6.1): in these patents several different synthesis routes are described to afford target compounds (*R,R,S*)-**6.6a** and (*R,R,S*)-**6.7a**, however the reported experimental part is limited to a few representative examples. One synthesis route in the patent started from a racemic mixture of piperidine-3-ol ((*RS*)-**6.14**) to form arylamine (*RS*)-**6.15** from (*RS*)-**6.14** and 1-bromo-4-nitrophenylbenzene catalysed by CuI and *L*-proline (Ullmann-type¹⁷) in good yields. In the patents^{8, 9} the hydroxyl group of (*RS*)-**6.15** was oxidized to a ketone **6.16** by use of pyridine-sulfur trioxide complex in DMSO (Parikh-Doering oxidation¹⁸). The next step of the synthesis was intended to be the coupling of ketone **6.16** and (*R,R*)-diaminocyclohexane (**6.11**) by use of sodium triacetoxyborohydride (reductive amination) and subsequent coupling with isocyanatobenzene and *N*-(benzyloxycarbonyloxy)succinimide to obtain (*R,R,S*)-**6.6a** and (*R,R,S*)-**6.7a**, respectively. In this work, the ketone **6.16** could not be obtained from the secondary alcohol (*RS*)-**6.15** by use of pyridine-sulfur trioxide complex in DMSO or other oxidizing agents like K₂Cr₂O₇, CrO₃, MnO₂ or KMnO₄. Therefore, the alcohol (*RS*)-**6.14**

was mesylated and (*RS*)-**6.17** was obtained in good yield after crystallization. The mesylate (*RS*)-**6.17** was used to alkylate amine **6.12** in a S_N reaction under microwave irradiation (120 °C, 1 h) to obtain a diastereomeric mixture of compound **6.6a**, under applied conditions, a mixture of the diastereomeric structural isomers **6.6b** was evident (Scheme 6.1, RP-HPLC chromatograms shown in Figure 6.2 A, 6.2 C). The formation of a highly reactive aziridine ring system at higher temperatures give rise to the mixture of products. Additionally, there is also the potential for neighbouring group participation, which could further complicate the stereochemical outcome of this transformation.



Scheme 6.1. Synthesis of the (*R,R*)-diaminocyclohexane derivatives (*R,R,S**)-**6.6a** and (*R,R,S**)-**6.7a**. Reagents and conditions: (a) isocyanatobenzene, CH_2Cl_2 , 16%; (b) *N*-(benzyloxycarbonyloxy)succinimide, CH_2Cl_2 , 64%; (c) 1-bromo-4-nitrobenzene, *L*-proline, CuI, K_2CO_3 , DMSO, 85%; (d) methanesulfonyl chloride, Et_3N , CH_2Cl_2 , 62%; (e) acetonitrile, microwave device (120 °C, 1 h), yield was determined; (f) 1-bromo-4-nitrobenzene, *L*-proline, CuI, K_2CO_3 , DMSO, 81%; (g) methanesulfonyl chloride, Et_3N , CH_2Cl_2 , 74%; (h) acetonitrile, microwave device (120 °C, 1 h), 5% ((*R,R,S**)-**6.6a**) and 9% ((*R,R,S*)-**6.6b**); (i) acetonitrile, microwave device (120 °C, 1 h), 3% ((*R,R,S**)-**6.7a**) and 8% ((*R,R,S**)-**6.7b**).

To circumvent the required separation of diastereomers, the starting material was changed from the racemate (*RS*)-**6.14** to the enantiomerically pure building block (*R*)-piperidine-3-ol ((*R*)-**6.14**). (*R*)-**6.14** was coupled with 1-bromo-4-nitrobenzene in an Ullman-type reaction to form (*R*)-1-(4-nitrophenyl)piperidine-3-ol ((*R*)-**6.15**). The secondary alcohol (*R*)-**6.15** was transformed to the mesylate (*R*)-**6.17**, which was then coupled with the (*R,R*)-diaminocyclohexane derivatives **6.12** and **6.13**, respectively, under microwave irradiation to form compounds (*R,R,S**)-**6.6a**, (*R,R,S*)-**6.6b**, (*R,R,S**)-**6.7a** and (*R,R,S**)-**6.7b**. The structural isomers of (*R,R,S**)-**6.6a** and (*R,R,S**)-**6.7a** were separated by preparative HPLC. The stereochemistry of constitutional isomer (*R,R,S*)-**6.6b**, was elucidated by X-ray

crystallography (Figure 6.3): a methanolic solution of the hydrochloride of (*R,R,S*)-**6.6** in methanol was allowed to vaporize at ambient temperature to obtain crystals suitable for X-ray crystallographic analysis.

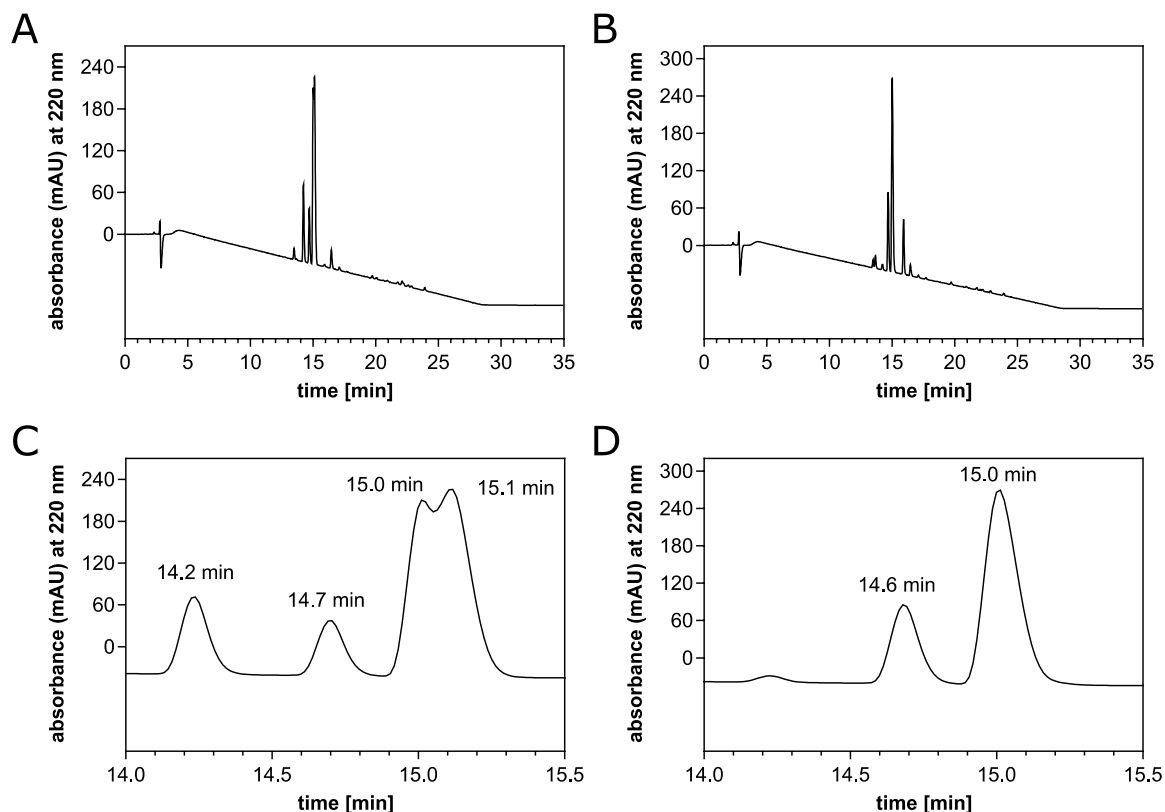


Figure 6.2. RP-HPLC (Method A, 220 nm) chromatograms (A-D) of alkylation of amine **6.12** by mesylate (*RS*)-**6.17** (A, C) and (*R*)-**6.17** (B, D). $t_R((R,R,S^*)\text{-6.6a}) = 14.6$ min and $t_R((R,R,S^*)\text{-6.6a}) = 15.0$ min

Interestingly, the structural isomers (*R,R,S*)-**6.6b** and (*R,R,S**)-**6.7b** (containing a pyrrolidine ring rather than the piperidine moiety of (*R,R,S**)-**6.6a** and (*R,R,S**)-**6.7a**) were the main products of the substitution reactions (see RP-HPLC chromatograms shown in Figure 6.2 C, D). For the formation of (*R,R,S*)-**6.6b** and (*R,R,S**)-**6.7b** an S_N2 -like reaction can be alternatively assumed, because using the enantiomerically pure mesylate (*R*)-**6.17** led to a decrease in side products (Figure 6.2 C).

(*R*)-**6.17** was coupled with the non-chiral amine **2.36** under microwave irradiation. Subsequent Boc deprotection using TFA gave a mixture of structural isomers (*S**)-**6.18a** and (*S**)-**6.18b** (Scheme 6.2). The desired product of substitution (S_N2 -like) reaction between amine **2.36** and (*R*)-**6.17** is amine (*S**)-**6.18a**, however the structural isomer (*S**)-**6.18b** was evident in the reaction mixture. Further investigation should focus on configuration determination of stereogenic centres by X-ray crystallography. Furthermore, the presence of enantiomers of (*S**)-**6.18a** and (*S**)-**6.18b** needs to be considered, especially if non- S_N2 mechanisms are involved (or double S_N2 via the aziridine) that would lead to a retention of configuration.

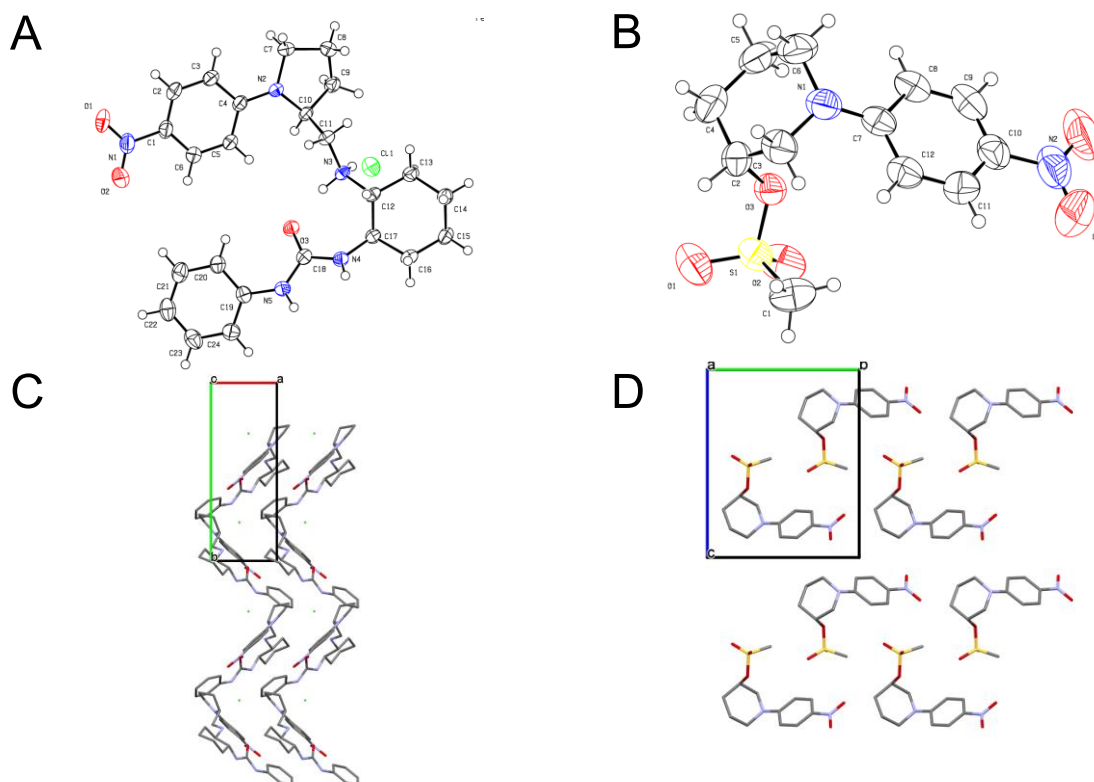
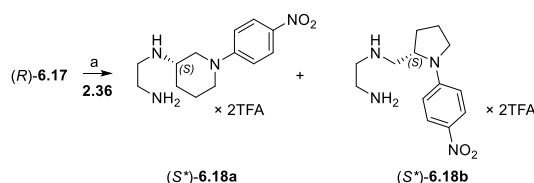


Figure 6.3. Platon plots (A-B) and stereoview of a unit cell (C-D) of (*R,R,S*)-**6.6b** (A-C) and (*R*)-**6.17** (B-D). Platon plot (Platon version 13/08/2017) of (*R,R,S*)-**6.6b** (50% probability ellipsoids) (A). Platon plot (Platon version 22/12/2019) of (*R*)-**6.17** (50% probability of ellipsoids) (B). Stereoview of molecular packing (Mercury 3.7) in the unit cell of (*R,R,S*)-**6.6b** with view along *c* axis, hydrogens not shown (C). Stereoview of molecular packing (Mercury 3.7) in the unit cell of (*R*)-**6.17** with view along *a* axis, hydrogens not shown (D). (*R,R,S*)-**6.6b** was used as HCl salt for crystallization.

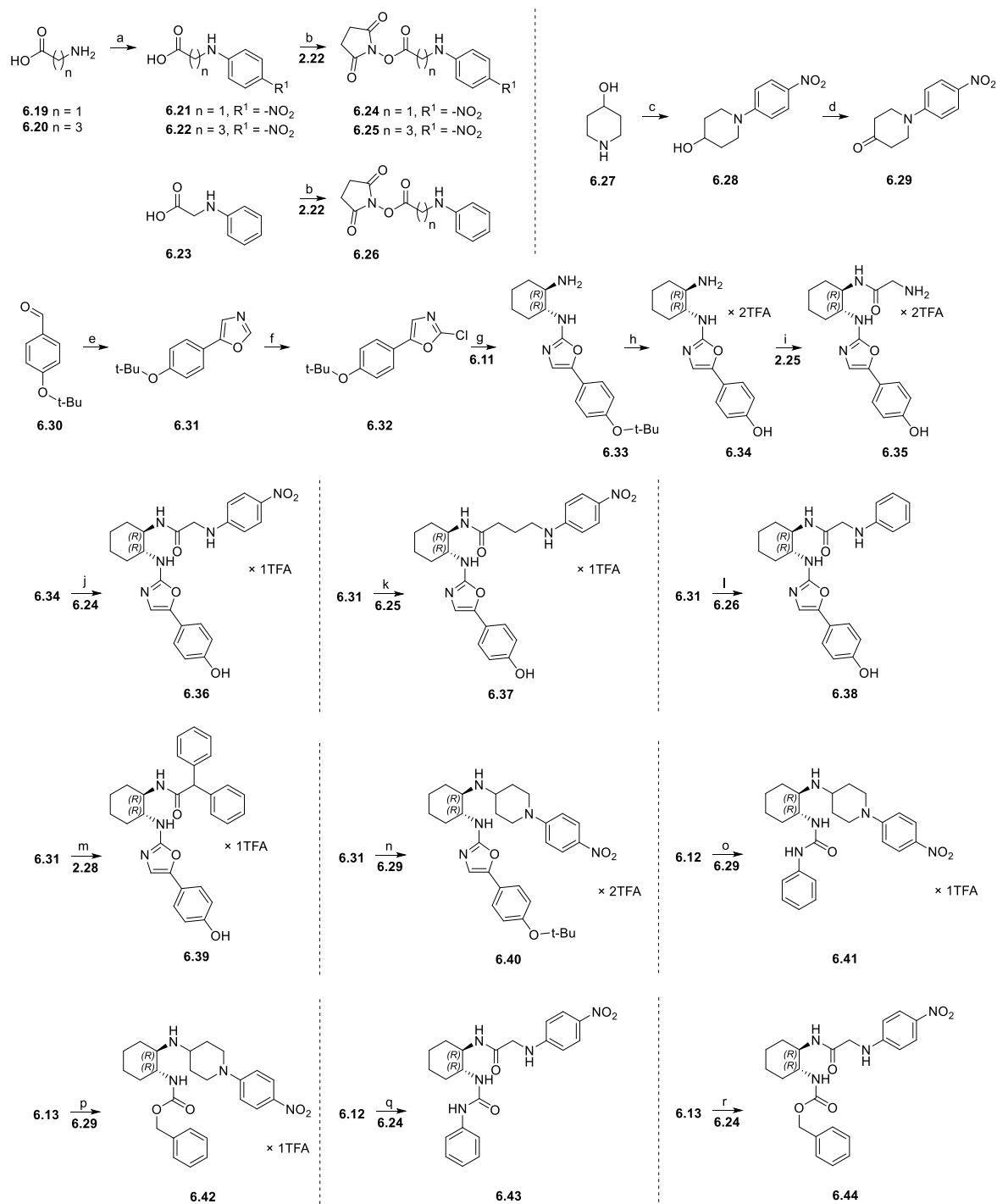
The amino groups of glycine (**6.19**) and γ -aminobutyric acid (**6.20**) were coupled with 1-fluoro-4-nitrobenzene to form **6.21** and **6.22**, respectively. The amino-functionalized carboxylic acids (**6.21-6.23**) were transformed to the respective succinimidyl esters **6.24-6.26** (Scheme 6.3).

Arylamine **6.28** was synthesized from piperidine-4-ol (**6.27**) and 1-bromo-4-nitrobenzene in an Ullmann-type reaction (compare with Scheme 6.1, compound (*RS*)-**6.15**). The secondary alcohol **6.28** was converted to the respective ketone in a Parikh-Doering oxidation (Scheme 6.3) in moderate yield.



Scheme 6.2. Synthesis of compounds (*S*^{*})-**6.18a** and (*S*^{*})-**6.18b**. Reagents and conditions: (a) acetonitrile, microwave device (120 °C, 1 h), 2% ((*S*^{*})-**6.18a**) and 3% ((*S*^{*})-**6.18b**).

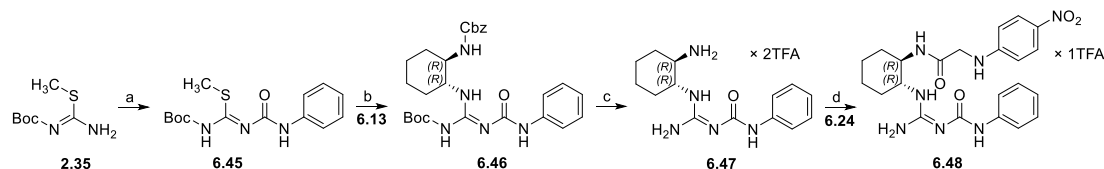
Intermediate **6.31** was synthesized from benzaldehyde **6.30** and 1-((isocyanomethyl)sulfonyl)-4-methylbenzene (van Leusen oxazole synthesis¹⁹) in good yield. The oxazole **6.31** derivative was converted to the respective chloride **6.32**, which was coupled with amine **6.11** under microwave irradiation (130 °C, 1 h) to give **6.33** in moderate yield. The removal of the *tert*-butyl group of **6.33** by treatment with TFA gave **6.34** after purification by preparative HPLC (Scheme 6.3).



Scheme 6.3. Synthesis of substituted (*R,R*)-diaminocyclohexanes **6.34** and **6.35-6.44**. Reagents and conditions: (a) 1-fluoro-4-nitrobenzene, Na₂CO₃, dioxane/H₂O, 70 °C, overnight, 55-82%; (b) DCC, DMF, rt, overnight, 63-89%; (c) 1-bromo-4-nitrobenzene, *L*-proline, CuI, K₂CO₃, DMSO, 65 °C, 2 d, 88%; (d) pyridine sulfur-trioxide complex, Et₃N, DMSO, 50%; (e) 1-((isocyanomethyl)sulfonyl)-4-methylbenzene, K₂CO₃, MeOH, reflux, 4 h, 77%; (f) (1) *n*-BuLi, THF, -78 °C, (2) C₂Cl₆, -78 °C, 88%; (g) K₂CO₃, microwave device (130 °C, 45 min), 47%; (h) CH₂Cl₂/TFA 1:1, 46%; (i) (1) CH₂Cl₂, DIPEA, (2) CH₂Cl₂/TFA 1:1, 51%; (j) DIPEA, DMF, rt, 3 h, 39%; (k) DIPEA, DMF, rt, 3 h, 32%; (l) DIPEA, DMF, rt, 3 h, 25%; (m) DIPEA, DMSO, rt, 2 h, 17%; (n) (1) CH₂Cl₂, AcOH, Na₂SO₄ (anhydrous), (2) NaBH(OAc)₃, 10%; (o) (1) CH₂Cl₂, AcOH, Na₂SO₄ (anhydrous), (2) NaBH(OAc)₃, 14%; (p) (1) CH₂Cl₂, AcOH, Na₂SO₄ (anhydrous), (2) NaBH(OAc)₃, 10%; (q) CH₂Cl₂, DIPEA, 51%; (r) DMF, DIPEA, 12%.

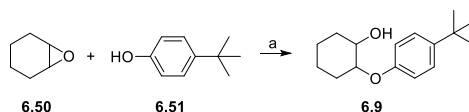
Compound **6.35** was synthesized by amide coupling between amine **6.34** and succinimidyl ester **2.25** followed by Boc deprotection with TFA. The target compounds **6.36-6.39** were synthesized by treatment

of **6.34** with the succinimidyl esters **2.28** or **6.24-6.26**. Compounds **6.40-6.42** were synthesized from ketone **6.29** and amines **6.12**, **6.13** or **6.31** by formation of the imines and subsequent reduction (reductive amination) to give the respective amines **6.40-6.42** (Scheme 6.3). Succinimidyl ester **6.24** was used for amide bond formation between amines **6.12** and **6.13** to obtain compounds **6.43** and **6.44** (Scheme 6.3).



Scheme 6.4. Synthesis of the *(R,R)*-aminocyclohexylcarbamoylguanidines **6.47** and **6.48**. Reagents and conditions: (a) isocyanatobenzene, CH_2Cl_2 , 55%; (b) HgCl_2 , DIPEA, CH_2Cl_2 , 50%; (c) (1) Pd/C, MeOH, (2) $\text{CH}_2\text{Cl}_2/\text{TFA}$ 1:1, 20%; (d) DIPEA, DMSO, rt, 2 h, 40%.

Isocyanatobenzene was treated with **2.35** to form the guanidinylation reagent **6.45** in moderate yield (Scheme 6.4). Compound **6.46** was obtained by guanidinylation of *(R,R)*-diaminocyclohexane derivative **6.13** with **6.45**. The *(R,R)*-aminocyclohexylcarbamoylguanidine **6.47** was obtained after removal of the Cbz group by hydrogenation, and subsequent cleavage of the Boc group by treatment with TFA. Further derivatization of **6.47** by amide bond formation using succinimidylester **6.24** gave **6.48** in moderate yield.



Scheme 6.5. Synthesis of **6.9** (tBPC). Reagents and conditions: (a) CsCO_3 , DMF, 110 °C, overnight, 74%.

Finally, cyclohexene oxide (**6.50**) and the phenol **6.51** were coupled (S_N reaction) to give *trans*-2-(4-(*tert*-butyl)phenoxy)cyclohexan-1-ol (**6.9**) in good yields (Scheme 6.5).

6.2.3. Pharmacological methods: investigation of test compounds in a radioligand binding assay, an aequorin Ca^{2+} assay and a cytotoxicity assay (live/dead staining).

Compounds *(R,R,S^*)*-**6.6a**, *(R,R,S)*-**6.6b**, *(R,R,S^*)*-**6.7a**, *(R,R,S^*)*-**6.7b**, **6.9**, **6.10**, **6.12**, **6.13**, *(S^*)*-**6.18a**, *(S^*)*-**6.18b**, **6.34-6.44**, **6.47** and **6.48** were investigated in competition binding studies. Selected compounds (*(R,R,S)*-**6.6b**, *(R,R,S^*)*-**6.7b**, niclosamide (**6.10**) and **6.36**) were additionally investigated in the aequorin Ca^{2+} assay to elucidate modulatory effects on the action of hPP. The cytotoxicity of compounds **2.68**, *(R,R,S)*-**6.6b**, *(R,R,S^*)*-**6.7b** and niclosamide (**6.10**) was investigated by ethidium bromide/acridine orange staining of CHO-hY₄R-G_{q15}-mtAEQ cells.

6.2.3.1. Displacement studies of investigated compounds in a radioligand competition binding assay in CHO-hY₄R-G_{q15}-mtAEQ cells

A competition binding assay was performed according to the literature²⁰ in living CHO-hY₄R-G_{q15}-mtAEQ cells⁵ using [³H]UR-KK200 ($C_{\text{final}} = 1.0 \text{ nM}$, $K_d = 0.67 \text{ nM}^{20}$) as radioligand in sodium-free binding buffer (Table 6.2). The inhibitory effect of all investigated compounds ((*R,R,S**)-**6.6a**, (*R,R,S*)-**6.6b**, (*R,R,S**)-**6.7a**, (*R,R,S**)-**6.7b**, **6.9**, **6.10**, **6.12**, **6.13**, (*S**)-**6.18a**, (*S**)-**6.18b**, **6.34-6.44**, **6.47** and **6.48**) on Y₄R binding of [³H]UR-KK200 was determined for three concentrations (3 μM, 10 μM and 30 μM). The investigation of higher concentrations was not feasible due to solubility limitations of the test compounds and possible cytotoxicity.

Ewing et al.⁸ described the compounds (*R,R,S**)-**6.6a** and (*R,R,S**)-**6.7a** as Y₄R agonists, antagonists or modulators, but only EC₅₀ values obtained from a functional cAMP assay were reported.

Table 6.2. hY₄R affinities (pK_i) of synthesized (*R,R*)-diaminocyclohexane derivatives, as determined by competition binding assays with [³H]UR-KK200.

Compound	pK_i^a	Compound	pK_i^a
(<i>R,R,S*</i>)- 6.6a	<4.52	6.36	<4.52
(<i>R,R,S</i>)- 6.6b	<4.52	6.37	<4.52
(<i>R,R,S*</i>)- 6.7a	<5.00	6.38	<4.52
(<i>R,R,S*</i>)- 6.7b	<4.52	6.39	<4.52
6.9 (tBPC)	<4.52	6.40	<4.52
6.10 (Niclosamide)	<4.52	6.41	<4.52
6.12	<4.52	6.42	<4.52
6.13	<4.52	6.43	<5.00
(<i>S*</i>)- 6.18a	<4.52	6.44	<5.00
(<i>S*</i>)- 6.18b	<4.52	6.47	<4.52
6.34	<4.52	6.48	<4.52
6.35	<4.52		

Radioligand competition binding assay with [³H]UR-KK200 ($C_{\text{final}} = 1.0 \text{ nM}$, $K_d = 0.67 \text{ nM}^{20}$) in intact CHO-hY₄R-G_{q15}-mtAEQ cells.²⁰ At least two independent experiments (each performed in triplicate) were performed.

It should be mentioned at this point that work in our group has described a discrepancy between potency (pEC_{50}) and affinity (pK_i) of agonists at the hY₄R.^{20, 21} The apparent higher affinity of agonists compared with their potency was explained by the absence of sodium in the binding buffer used for radioligand competition binding experiments at hY₄R.^{20, 21} The phenomenon of a negative allosteric modulatory effect of sodium ions has also been reported in literature, and shown for other GPCRs (e.g. μOR,²²

A_{2A}R,²³ and β₁AR²⁴), whilst sodium cations stabilize the inactive state of the receptor. Whereas (*R,R,S**)-**6.6a**, (*R,R,S*)-**6.6b** and (*R,R,S**)-**6.6b** showed no apparent affinity for the hY₄R, (*R,R,S**)-**6.7a** displaced ca. 50% of the radioligand at a concentration of 30 μM.

tBPC (**6.9**) and niclosamide (**6.10**) demonstrated no Y₄R affinity. Whilst, the results of these experiments were in agreement with the literature,^{10, 11} these compounds (**6.9** and **6.10**) have been reported to act as modulators in functional Y₄R assays using PP as agonist.

The (*R,R*)-diaminocyclohexanes **6.12**, **6.13**, **6.34**, **6.35** and **6.47**, as well as ethane-1,2-diamines **6.18a** and **6.18b** (series of substituted diamines) showed no affinity at the hY₄R.

Further derivatization of (*R,R*)-diaminocyclohexanes **6.12**, **6.13** and **6.34**, resulting in compounds **6.36**-**6.44** (*cf.* Scheme 6.3), did not enhance Y₄R affinity. Compounds **6.43** and **6.44** demonstrated no increased affinity compared to the other investigated compounds ((*R,R,S**)-**6.6a**, (*R,R,S*)-**6.6b**, (*R,R,S**)-**6.7a**, (*R,R,S**)-**6.7b**, **6.9**, **6.10**, **6.12**, **6.13**, (*S**)-**6.18a**, (*S**)-**6.18b**, **6.34**-**6.42**, **6.47** and **6.48**), but were not soluble at concentrations higher than 10 μM.

The introduction of a carbamoyl guanidine at the (*R,R*)-diaminocyclohexane moiety led to compounds **6.47** and **6.48**, which also showed no Y₄R binding.

6.2.3.2. Modulatory effects of test compounds on the action of hPP in an aequorin Ca²⁺ assay

The aequorin Ca²⁺ assay was performed as previously described by Ziemek et al⁵ with minor modifications: on the day of the experiment the CHO-hY₄R-G_{q15}-mtAEQ cells were scraped from the culture flask rather than trypsination. The studied compounds (at a final concentration of 30 μM) were incubated with CHO-hY₄R-G_{q15}-mtAEQ cells for 30 min.

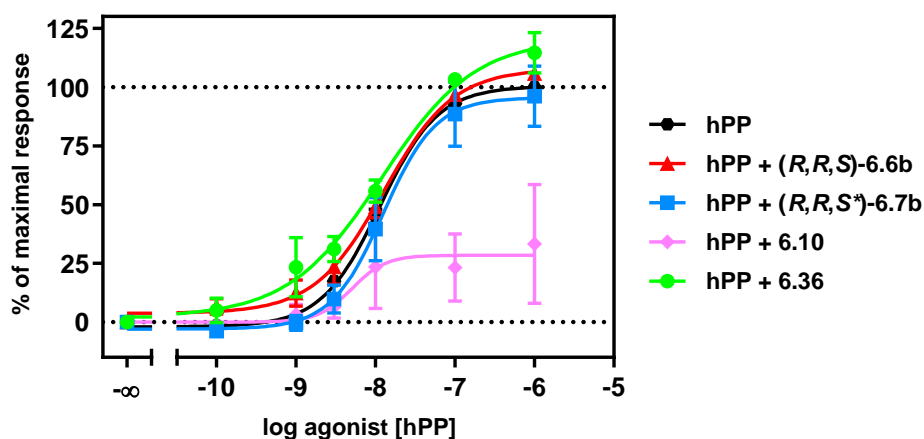


Figure 6.4. hY₄R agonism of hPP + 0.5% DMSO and hPP in the presence of compounds (*R,R,S*)-**6.6b**, (*R,R,S**)-**6.7b**, niclosamide (**6.10**) and **6.36** (*C*_{final} = 30 μM) determined in an aequorin Ca²⁺ assay in live CHO-hY₄R-G_{q15}-mtAEQ cells. Data are presented as means ± SEM from at least two independent experiments, each performed in triplicate.

The aequorin Ca²⁺ assay was performed using intact CHO-hY₄R-G_{q15}-mtAEQ cells to study the potential modulatory effects of (*R,R,S*)-**6.6b**, (*R,R,S**)-**6.7b**, niclosamide (**6.10**) and **6.36** on the action of hPP at the Y₄R. For this purpose, the stimulatory effect of hPP was investigated in the absence (0.5% DMSO) and in the presence of (*R,R,S*)-**6.6b**, (*R,R,S**)-**6.7b**, niclosamide (**6.10**) or **6.36**, used at a concentration of 30 μM. Moreover, all investigated compounds showed no intrinsic activity at a concentration of 30 μM

in the aequorin Ca²⁺ assay. The CHO-hY₄R-G_{qi5}-mtAEQ cells were pre-incubated with the studied compounds for 30 min prior to addition of hPP.

Concentration effect curves of hPP are shown in Figure 6.3 and corresponding pEC₅₀ values are summarized in Table 6.3. The determined pEC₅₀ value of hPP was in good agreement with literature data,⁵ and its intrinsic activity was not influenced in the presence of compounds (*R,R,S*)-**6.6b** and (*R,R,S**)-**6.7b**. Niclosamide (**6.10**) was described in literature as a positive allosteric modulator (PAM) at the hY₄R.¹⁰ In the presence of **6.10** (C_{final} = 30 μM) the concentration effect curve of hPP was left shifted and no effect on the maximal response of hPP was observed in an inositol phosphate accumulation assay (in COS7_Y₄R-eYFP_Δ6Gα_{qi4}-myr cells) as reported by Sliwowski et al.¹⁰

In the aequorin Ca²⁺ assay, the endogenous agonist hPP showed a slight decrease in potency and depression of intrinsic activity in the presence of **6.10** (Table 6.3). The obtained results must be scrutinized as a cytotoxic effect cannot be excluded (6.2.2.3.) (Note: **6.10** has been reported^{25, 26} to be cytotoxic). Beside the use as an oral anthelmintic drug, niclosamide has been reported to induce cell death in several cancer cell lines (e.g. MCF-7).^{25, 26}

Whilst the substituted (*R,R*)-diaminocyclohexane **6.36** caused no shift in potency (pEC₅₀) of hPP, the intrinsic activity (α) of hPP was marginally increased by ca. 25%. The effect of compound **6.36** on the intrinsic activity of hPP might be too small to unambiguously classify compound **6.36** a modulator at the NPY Y₄R. Further investigations in additional functional assays are required.

Table 6.3. Potencies (pEC₅₀) and intrinsic activities (α) of hPP determined in the aequorin Ca²⁺ assay in the presence of selected compounds (*R,R,S*)-**6.6b**, (*R,R,S**)-**6.7b**, niclosamide (**6.10**) and **6.36** at a concentration of 30 μM.

compound	pEC ₅₀ ± SEM ^a	α ± SEM ^b	N
hPP + 0.5% DMSO	7.95 ± 0.05	1	3
hPP + (<i>R,R,S</i>)- 6.6b	7.91 ± 0.08	1.09 ± 0.03	3
hPP + (<i>R,R,S*</i>)- 6.7b	7.87 ± 0.10	0.96 ± 0.12	3
hPP + niclosamide (6.10)	8.29 ± 0.02	0.28 ± 0.20	2
hPP + 6.36	7.89 ± 0.07	1.27 ± 0.12	3

^aAequorin Ca²⁺ mobilization assay in living CHO-hY₄R-G_{qi5}-mtAEQ cells. ^bEfficacies (intrinsic activity, α) were calculated from the maximum response relative to 1 μM hPP + 0.5% DMSO (α = 1). Mean values ± SEM from at least N independent experiments, each performed in triplicate.

6.2.3.3. Investigation of cytotoxicity by ethidium bromide/acridine orange staining

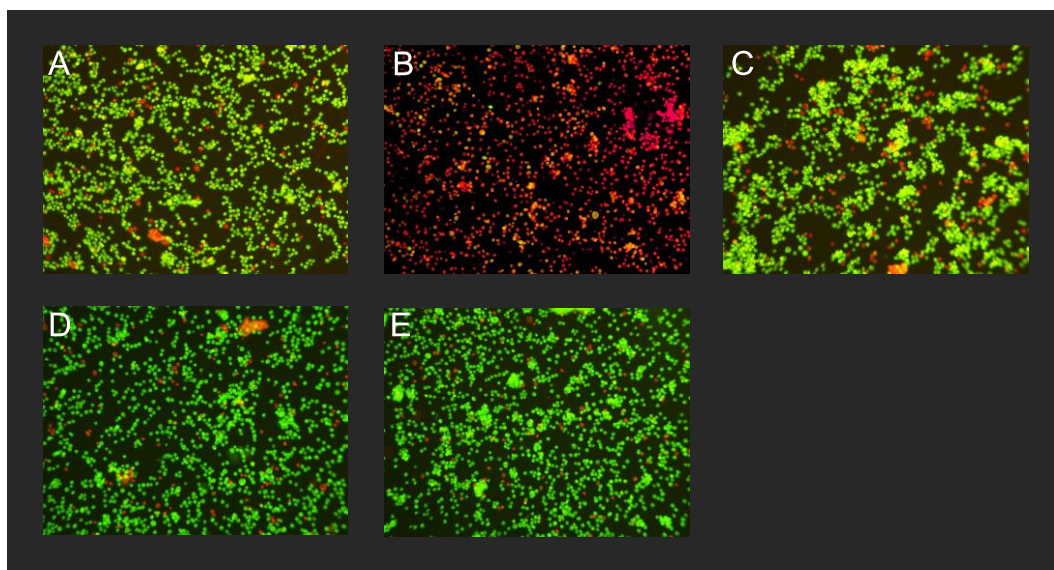


Figure 6.5. (A-E) Ethidium bromide/acridine orange staining of CHO-hY₄R-G_{q15}-mtAEQ cells (A-E). CHO-hY₄R-G_{q15}-mtAEQ cells were incubated for 30 min with (A) 3% DMSO and 30 μ M of (B) niclosamide (**6.10**), (C) **2.68**, (D) (***R,R,S***-**6.6b**) and (E) (***R,R,S****-**6.6b**). Images were acquired with an Olympus BH-2 microscope using a planachromat objective (10x), filter (Fluorescein) and a DCM-510 ocular microscope camera (Software: ScopePhoto 3.0).

The cytotoxicity of compounds **2.68**, (***R,R,S***-**6.6b**), (***R,R,S****-**6.7b**) and niclosamide (**6.10**) in CHO-hY₄R-G_{q15}-mtAEQ cells was investigated by ethidium bromide/acridine orange staining (Figure 6.5). In contrast to the aequorin Ca²⁺ assay procedure, CHO-hY₄R-G_{q15}-mtAEQ cells were detached by trypsinization (not by scratching) and were resuspended in buffer containing 10% FCS.

Live cells with an intact membrane/membrane potential exclude ethidium bromide, whereas acridine orange penetrates across intact cell membranes and intercalates with the DNA. As a consequence nuclei of live cells, show green fluorescence. Both live and dead cells show membrane permeability for acridine orange, whilst ethidium bromide only show membrane permeability in dead cells, allowing one to distinguish between vital (green) and dead (orange/red) cells by microscopy.²⁷

Compounds **2.68**, (***R,R,S***-**6.6b**) and (***R,R,S****-**6.7b**) did not damage cells. Niclosamide (**6.10**) induced cell death at a concentration of 30 μ M after incubation for 30 min. The results from the ethidium bromide/acridine orange staining helped to explain data obtained from the aequorin Ca²⁺ assay (6.2.2.2.). Obviously, this cytotoxic effect of **6.10** led to the apparent decrease in intrinsic activity of hPP (Table 6.3).

6.3. Conclusion

Compounds (***R,R,S****-**6.6a**) and (***R,R,S***-**6.7a**), previously described by Ewing et al,⁸ were synthesized and pharmacologically characterized in radioligand competition binding studies. (***R,R,S****-**6.6a**) and (***R,R,S***-**6.7a**) showed no affinity towards hY₄R, therefore compounds (***R,R,S****-**6.6a**) and (***R,R,S***-**6.7a**) were not investigated in functional assays.

During the synthesis of compounds (***R,R,S****-**6.6a**) and (***R,R,S***-**6.7a**) structural isomers were evident in the last synthesis step. The reaction could be stereochemically controlled by use of enantiomerically

pure mesylate (*(R)*-**6.17**), whereas structural isomers of (*R,R,S**)-**6.6a** and (*R,R,S*)-**6.7a** are still evident as main products. Further investigations could focus on mechanism and optimization of reaction conditions to avoid structural isomers. The formation of structural isomers was not described by Ewing et al.,^{8, 9} because they used a reductive amination route on the 1-(4-nitrophenyl)piperidin-3-on, which does not allow for aziridine formation.

A series of compounds with a (*R,R*)-diaminocyclohexane moiety (*(R,R,S*)*-**6.6a**, (*R,R,S*)-**6.6b**, (*R,R,S**)-**6.7a**, (*R,R,S**)-**6.7b**, **6.12**, **6.13**, **6.34-6.44**, **6.47**, **6.48** and a 1,2-ethanediamine moiety (*(S*)*-**6.18a**, (*S**)-**6.18b**) were synthesized and investigated in competition binding studies, but none showed Y₄R affinity.

Niclosamide (**6.10**) and selected compounds (*(R,R,S)*-**6.6b**, (*R,R,S**)-**6.7b** and **6.36**) were further investigated in the aequorin Ca²⁺ assay with respect to a modulatory effects on the action of hPP. The reported positive allosteric modulation by niclosamide (**6.10**) was not obvious in the aequorin Ca²⁺ assay, rather a decrease in intrinsic affinity was observed, which was likely caused by the cytotoxicity of **6.10**. Compounds (*R,R,S*)-**6.6b** and (*R,R,S**)-**6.7b** showed no modulatory effect in the aequorin Ca²⁺ assay on the action of hPP. Additionally, the increase in intrinsic activity of hPP induced by compound **6.36** was too less pronounced to definitively classify this compound as a modulator. To shed light on this question further investigations in different functional assays (G-protein mediated) are needed.

Finally, the modulatory effect of **6.10** was not obvious in the aequorin Ca²⁺ assay, but further investigations are required for the evaluation of modulators at the Y₄R. Firstly, another functional assay could be performed (e.g. miniG protein recruitment, β-arrestin2 recruitment assay) for the investigation of the modulatory effect on hPP. Secondly, the setup of the aequorin assay could be changed (e.g. potentiation of a PP EC₂₀ response in the presence of increasing concentrations of the modulator).

As results were disappointing, the synthesis of additional analogs and further in depth functional characterization of the compounds described in this chapter were discontinued. Compound **6.9** was published in the later stages of this thesis and therefore not functionally characterized. The recently resolved crystal structure²⁸ of the hY₁R in complex with UR-MK299 (**2.2**) could be the basis for a homology model of the hY₄R to aid in the search for new non-peptide ligands with affinity to the hY₄R.

6.4. Experimental section

6.4.1. General experimental conditions

The following reagents and solvents (analytical grade) were purchased from commercial suppliers and used without further purification: CH₂Cl₂, glycine, DMF, DMSO, MeOH, methanesulfonyl chloride (Fisher Scientific, Schwerte, Germany); 1-((isocyanomethyl)sulfonyl)-4-methylbenzene (Acros Organics, Schwerte, Germany); DCC, TFA, pyridine-sulfur trioxide complex, palladium on activated charcoal (Pd/C), n-BuLi, NaBH(OAc)₃, acetic acid, HgCl₂, isocyanatobenzene, 1-fluoro-4-nitrobenzene, 1-bromo-4-nitrobenzene, CuI (*RS*)-**6.14**, **6.23**, **6.27**, (Sigma Aldrich, München, Germany); C₂Cl₆, **6.51** (TCI, Eschborn, Germany); DIPEA, **2.36**, (*R*)-pyridine-3-ol hydrochlorid ((*R*)-**6.14**·HCl) (Abcr, Karlsruhe, Germany); *L*-proline, dioxane, Et₃N, K₂CO₃, NaBH₄, Na₂SO₄, MgSO₄ (Merck, Darmstadt, Germany); (*R,R*)-diaminocyclohexane (Ark Pharm, Arlington Heights, USA), conc. HCl (VWR Chemicals, Darmstadt, Germany); Ammonium hydroxide (Carl Roth, Karlsruhe, Germany). For pharmacological characterization, hPP was purchased from Synpeptide (Shanghai, China).

Compounds **2.25**²⁹ and **2.28**³⁰ were synthesized as described previously in the literature (*cf.* Chapter 2).

Column chromatography was performed using Merck Gerduran 60 silica gel (0.063-0.200 mm) or Merck flash silica gel 60 (0.040-0.063 mm). For thin layer chromatography, TLC sheets ALUGRAM Xtra SIL G/UV254 from Macherey-Nagel GmbH & Co. KG (Düren, Germany) were used. Compounds were detected by irradiation with UV light (254 nm), and staining was performed with ninhydrin.

Acetonitrile (HPLC grade), used for HPLC, was purchased from Sigma-Aldrich. Millipore water was used for eluents for analytical and preparative HPLC. Compounds (*R,R,S**)-**6.6a**, (*R,R,S*)-**6.6b**, (*R,R,S**)-**6.7a**, (*R,R,S**)-**6.7b**, **6.9**, **6.12**, **6.13**, **6.34-6.38** and **6.42** were purified by a preparative HPLC-system from Knauer (Berlin, Germany) consisting of two pumps K-1800 and a detector K-2001 (HPLC A). A Kinetex XB C18, 5 µm, 250 x 21 mm (Phenomenex, Aschaffenburg, Germany) served as RP-column at a flow rate of 18 mL/min. Compounds (*S**)-**6.18a**, (*S**)-**6.18b**, **6.39-6.41**, **6.44**, **6.47** and **6.48** were purified by a preparative HPLC-system from Waters (Eschborn, Germany) consisting of a Binary Gradient Module (Waters 2545), a detector (Waters 2489 UV/visible Detector), a manual injector (Waters Prep inject) and a collector (Waters Fraction Collector III) (HPLC B). A Kinetex XB C18, 5 µm, 250 x 21 mm (Phenomenex) served as RP-column at a flow rate of 20 mL/min. All injected solutions were filtered with syringe filters (0.45 µm). The mobile phase contained the solvents A (0.1% aq TFA) and B (acetonitrile). The detection wavelength was 220 nm. The eluates, containing isolated compounds, were lyophilized using a Christ alpha 2-4 LD (Martin Christ Gefriertrocknungsanlagen, Osterode am Harz, Germany) or a Scanvac CoolSafe 100-9 (Labogene, Allerød, Denmark) lyophilization apparatus equipped with a Vacuubrand RZ rotary vane vacuum pump (Vacuubrand, Wertheim, Germany).

The purity of compounds (*R,R,S**)-**6.7a**, (*R,R,S*)-**6.7b**, **6.9**, **6.12**, **6.13**, (*S**)-**6.18a**, (*S**)-**6.18b**, **6.34**, **6.36-6.44**, **6.47** and **6.48** was determined by analytical HPLC (RP-HPLC) on a 1100 series system from Agilent Technologies (Santa Clara, CA USA) composed of a Degasser (G1379A), a Binary Pump (G1312A), a Diode Array Detector (G1315A), a thermostated Column Compartment (G1316A) and an Autosampler (G1329A). A Phenomenex Kinetex 5u XB-C18 100A, 250 x 4.6 mm was used as stationary phase. The flow rate was 1 mL/min, the oven temperature was set to 30 °C and the injection volume

was 50 μ L. Mixtures of solvents A (0.1% aq TFA) and B (acetonitrile) were used as mobile phase. The following gradient was applied (Method A): 0-25 min, A/B 90:10–5:95; 25-35 min, 5:95. Analytical HPLC analysis of compounds (*R,R,S*^{*})-**6.7a**, (*R,R,S*^{*})-**6.7b** and **6.35** was performed on a system from Merck-Hitachi composed of a Pump (L-6200A), an Interface (D600 IF), an Autosampler (AS-2000) and an UV-Detector (L-4000A). A Phenomenex Kinetex 5u XB-C18 100A, 250 x 4.6 mm (Phenomenex) was used as stationary phase. The flow rate was 0.8 mL/min, the oven temperature was set to 30 °C, the detection wavelength was set to 220 nm and the injection volume was 35 μ L. A mixture of solvents A (0.05% aq TFA) and B (acetonitrile supplemented with 0.05% TFA) was used as mobile phase. The following gradient was applied (Method B): 0-25 min, A/B 90:10–5:95; 25-35 min, 5:95.

Microwave reactions were carried out on a Biotage Initiator 2.0 microwave device (Biotage, Uppsala, Sweden) using pressure stable sealed 10-20 mL vessels.

Deuterated solvents for NMR spectroscopy (DMSO-*d*₆, MeOH-*d*₄, CDCl₃) were obtained from Deutero (Kastellaun, Germany) in ampoules (1 mL). NMR spectra were recorded on a Bruker Avance 300 (¹H, 300 MHz; ¹³C, 75 MHz), a Bruker Avance III 400 (¹H, 400 MHz; ¹³C, 101 MHz) and a Bruker Avance 600 with cryogenic probe (¹H, 600 MHz; ¹³C, 150 MHz) (Bruker, Karlsruhe, Germany). Chemical shifts are given in ppm and were referenced to the solvent residual peak (DMSO-*d*₆, at 2.50 ppm (¹H-NMR) and at 39.52 ppm (¹³C-NMR); CDCl₃, at 7.26 ppm (¹H-NMR) and at 77.16 ppm (¹³C-NMR)).³¹ The coupling constants (*J*) are given in Hertz (Hz). The splitting of the signals is described as follows: s = singlet, bs = broad singlet, d = doublet, t = triplet, q = quartet, m = multiplet.

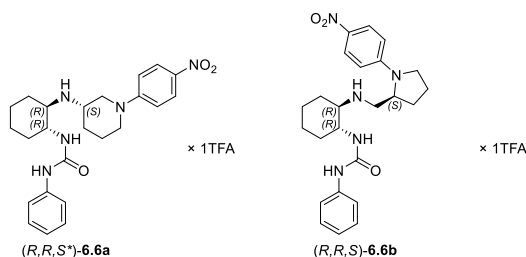
Mass spectrometry (HRMS) analysis was performed either on an Agilent 6540 UHD Accurate-Mass Q-TOF LC/MS system (Agilent Technologies) using an electrospray source (ESI) or on an Agilent GC7890A GC/MS system (Agilent Technologies) using an atmospheric pressure chemical ionization (APCI) source.

Elemental analysis was performed on a Vario micro cube (Elementar, Langenselbold, Germany).

Stock solutions were prepared in DMSO at concentrations 10 mM.

6.4.2. Synthesis protocols and analytical data

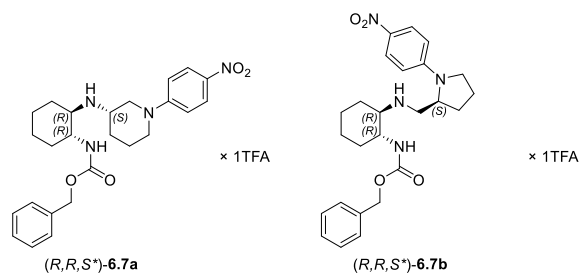
Compounds **6.12**, **6.13** were purified by preparative HPLC and obtained as their TFA salts (used to prepare stock solutions for the pharmacological characterization). For synthesis of compounds (*R,R,S*^{*})-**6.6a**, (*R,R,S*)-**6.6b**, (*R,R,S*^{*})-**6.7a**, (*R,R,S*^{*})-**6.7b** and **6.41-6.44** the free base of **6.12** and **6.13** was used.



1-((1*R*,2*R*)-2-(((*S*^{*})-1-(4-Nitrophenyl)piperidin-3-yl)amino)-cyclohexyl)-3-phenylurea hydrotrifluoroacetate ((*R*,*R*,*S*^{*})-6.6a)⁸ and 1-((1*R*,2*R*)-2-(((*S*)-1-(4-nitrophenyl)pyrrolidine-2-yl)methyl)-amino)cyclohexyl)-3-phenylurea hydrotrifluoroacetate ((*R*,*R*,*S*)-6.6b). 1-((1*R*,2*R*)-2-Aminocyclohexyl)-3-phenylurea (6.12**) (164 mg, 703 μ mol) and (*R*)-1-(4-nitrophenyl)piperidin-3-yl methane-sulfonate ((*R*)-**6.17**) (211 mg, 703 μ mol) were dissolved in acetonitrile (10 mL) in a 20 mL reaction tube and heated in a microwave device (100 °C, 1 h). The organic solvent was evaporated and the crude mixture was purified by column chromatography (eluent: CH₂Cl₂/MeOH/NH₃ ag 90:9:1) and then by preparative HPLC A (gradient: 0-30 min, A/B 68:32–52:48, t_R ((*R*,*R*,*S*^{*})-**6.6a**) = 12 min, t_R ((*R*,*R*,*S*^{*})-**6.6a**) = 13 min) to isolate (*R*,*R*,*S*^{*})-**6.6a** and (*R*,*R*,*S*)-**6.6b** as fluffy yellow solids, respectively ((*R*,*R*,*S*^{*})-**6.6a**: 19.4 mg, 35 μ mol, 5%; (*R*,*R*,*S*)-**6.6b**: 34.2 mg, 61.6 μ mol, 9%).**

(*R*,*R*,*S*^{*})-**6.6a**: **¹H-NMR** (600 MHz, DMSO-*d*₆): δ (ppm) 1.22-1.34 (m, 2H), 1.36-1.50 (m, 2H), 1.51-1.60 (m, 1H), 1.66-1.81 (m, 4H), 1.88-1.94 (m, 1H), 2.08-2.16 (m, 2H), 2.96-3.04 (m, 1H), 3.14-3.22 (m, 1H), 3.30-3.41 (m, 2H), 3.62-3.68 (m, 1H), 3.85-3.92 (m, 1H), 4.12-4.19 (m, 1H), 6.87-6.97 (m, 2H), 7.02-7.08 (m, 2H), 7.18-7.26 (m, 2H), 7.37-7.44 (m, 2H), 8.02-8.08 (m, 2H), 8.36 (br s, 1H), 8.87 (br s, 1H), 9.15 (s, 1H). **¹³C-NMR** (150 MHz, DMSO-*d*₆): δ (ppm) 22.2, 23.1, 23.8, 25.8, 27.1, 31.6, 46.9, 48.8, 50.0, 50.6, 58.1, 113.0, 117.7, 121.3, 125.7, 128.6, 137.0, 140.1, 154.1, 155.9. **RP-HPLC** (Method B, 220 nm): 94% (t_R = 17.9 min, k = 5.2). **HRMS** (ESI): m/z [M+H]⁺ calcd. for [C₂₄H₃₂N₅O₃]⁺ 438.2500, found 438.2507. C₂₄H₃₁N₅O₃ × C₂HF₃O₂ (437.54 + 114.02).

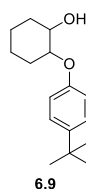
(*R*,*R*,*S*)-**6.6b**: **¹H-NMR** (600 MHz, DMSO-*d*₆): δ (ppm) 1.21-1.30 (m, 2H), 1.31-1.40 (m, 1H), 1.46-1.55 (m, 1H), 1.64-1.75 (m, 2H), 1.86-2.04 (m, 3H), 2.06-2.18 (m, 3H), 2.91-2.98 (m, 1H), 3.06-3.16 (m, 2H), 3.16-3.25 (m, 1H), 3.49-3.54 (m, 1H), 3.72-3.79 (m, 1H), 4.23-4.28 (m, 1H), 6.76-6.83 (m, 3H), 6.90-6.94 (m, 1H), 7.22-7.26 (m, 2H), 7.42-7.46 (m, 2H), 8.04 (d, J = 9.5 Hz, 2H), 8.40 (br s, 1H), 8.90 (br s, 1H), 9.05 (br s, 1H). **¹³C-NMR** (150 MHz, DMSO-*d*₆): δ (ppm) 21.9, 23.5, 24.1, 26.4, 28.2, 32.3, 42.8, 48.0, 49.2, 55.2, 61.0, 111.5, 117.7, 121.3, 125.9, 128.7, 136.3, 140.3, 151.1, 155.5, 158.6 (q J = 34.3 Hz) (TFA). **RP-HPLC** (Method B, 220 nm): 95% (t_R = 18.4 min, k = 5.4). **HRMS** (ESI): m/z [M+H]⁺ calcd. for [C₂₄H₃₂N₅O₃]⁺ 438.2500, found 438.2519. C₂₄H₃₁N₅O₃ × C₂HF₃O₂ (437.54 + 114.02).



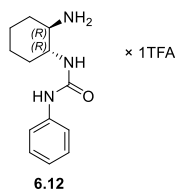
Benzyl ((1*R*,2*R*)-2-(((*S*^{*})-1-(4-nitrophenyl)piperidin-3-yl)amino)cyclohexyl)carbamate hydrotrifluoroacetate⁸ ((*R,R,S*^{*})-6.7a) and benzyl ((1*R*,2*R*)-2-(((*S*^{*})-1-(4-nitrophenyl)pyrrolidin-2-yl)methyl)amino)cyclohexyl)carbamate hydrotrifluoroacetate ((*R,R,S*^{*})-6.7b): Benzyl ((1*R*,2*R*)-2-aminocyclohexyl)carbamate (**6.13**) (150 mg, 604 μmol) and (*R*)-1-(4-nitrophenyl)piperidin-3-yl methanesulfonate ((*R*)-**6.17**) (181 mg, 603 μmol) were dissolved in acetonitrile (10 mL) in a 20 mL reaction tube and heated in a microwave device (100 °C, 1 h). The organic solvent was evaporated and the crude mixture was purified by column chromatography (eluent: CH₂Cl₂/MeOH/NH₃ ag 90:9:1) and then by preparative HPLC A (gradient: 0-30 min, A/B 62:38–52:48, *t_R*((*R,R,S*^{*})-**6.6a**) = 10 min, *t_R*((*R,R,S*^{*})-**6.7b**) = 11 min) to isolate (*R,R,S*^{*})-**6.7a** and (*R,R,S*^{*})-**6.7b** as fluffy yellow solids, respectively ((*R,R,S*^{*})-**6.7a**: 12 mg, 21 μmol, 3%; (*R,R,S*^{*})-**6.7b**: 26 mg, 46 μmol, 8%).

(*R,R,S*^{*})-**6.7a**: **¹H-NMR** (600 MHz, DMSO-*d*₆): δ (ppm) 1.17-1.42 (m, 4H), 1.47-1.57 (m, 1H), 1.57-1.74 (m, 3H), 1.77-1.91 (m, 2H), 2.08-2.17 (m, 2H), 2.89-2.98 (m, 1H), 3.06-3.18 (m, 1H), 3.21-3.34 (m, 2H), 3.45-3.57 (m, 1H, interfering with water signal), 4.02 (d, *J* = 13.2 Hz, 1H), 4.21 (d, *J* = 12.9 Hz, 1H), 4.99 (d, *J* = 12.5 Hz, 1H), 5.13 (d, *J* = 12.5 Hz, 1H), 7.04 (d, *J* = 9.4 Hz, 2H), 7.30-7.34 (m, 1H), 7.35-7.38 (m, 4H), 7.47 (d, *J* = 8.8 Hz, 1H), 8.08 (d, *J* = 9.4 Hz, 2H), 8.22 (br s, 1H), 8.85 (br s, 1H). **¹³C-NMR** (150 MHz, DMSO-*d*₆): δ (ppm) 22.6, 23.3, 23.8, 26.1, 27.1, 32.0, 47.0, 48.7, 50.0, 52.1, 56.8, 65.8, 112.9, 125.8, 127.8, 127.9, 128.4, 136.7, 137.0, 153.9, 156.2. **RP-HPLC** (Method A, 220 nm): 95% (*t_R* = 14.9 min, *k* = 4.8). **HRMS** (ESI): *m/z* [M+H]⁺ calcd. for [C₂₅H₃₃N₄O₄]⁺ 453.2496, found 453.2504. C₂₅H₃₂N₄O₄ × C₂HF₃O₂ (452.56 + 114.02).

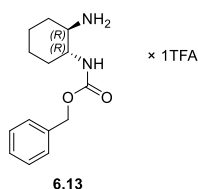
(*R,R,S*^{*})-**6.7b**: **¹H-NMR** (600 MHz, DMSO-*d*₆): δ (ppm) 1.15-1.27 (m, 2H), 1.27-1.36 (m, 1H), 1.45-1.53 (m, 1H), 1.61-1.67 (m, 1H), 1.68-1.75 (m, 1H), 1.83-1.89 (m, 1H), 1.90-2.08 (m, 3H), 2.08-2.14 (m, 2H), 2.91-3.02 (m, 2H), 3.05-3.123 (m, 1H), 3.18-3.25 (m, 1H), 3.47-3.52 (m, 1H), 3.58-3.65 (m, 1H), 4.25-4.31 (m, 1H), 5.01 (d, *J* = 12.5 Hz, 1H), 5.10 (d, *J* = 12.5 Hz, 1H), 6.82 (d, *J* = 9.4 Hz, 2H), 7.30-7.35 (m, 1H), 7.35-7.39 (m, 4H), 7.48 (d, *J* = 9.0 Hz, 1H), 8.06 (d, *J* = 9.4 Hz, 2H), 8.62 (br s, 1H), 9.11 (br s, 1H). **¹³C-NMR** (150 MHz, DMSO-*d*₆): δ (ppm) 21.9, 23.6, 23.8, 26.4, 28.3, 32.2, 42.9, 47.9, 50.6, 55.2, 59.9, 65.8, 111.6, 116.1 (q, *J* = 29.8 Hz) (TFA), 125.9, 127.8, 127.9, 128.4, 136.3, 136.8, 151.1, 156.0, 158.4 (q, *J* = 31.7 Hz) (TFA). **RP-HPLC** (Method A, 220 nm): 96% (*t_R* = 15.3 min, *k* = 5.0). **HRMS** (ESI): *m/z* [M+H]⁺ calcd. for [C₂₅H₃₃N₄O₄]⁺ 453.2496, found 453.2502. C₂₅H₃₂N₄O₄ × C₂HF₃O₂ (452.56 + 114.02).



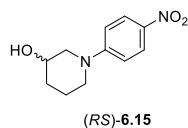
trans-2-(4-(*tert*-Butyl)phenoxy)cyclohexan-1-ol (6.9).^{32, 33} 4-*tert*-Butylphenol (**6.51**) (0.53 g, 3.53 mmol) was dissolved in DMF (15 mL) and CsCO₃ (2.26 g, 6.94 mmol) was added. After addition of cyclohexene oxide (**6.50**) (0.35 mL, 3.46 mmol), the reaction mixture was stirred at 110 °C overnight. The reaction mixture was allowed to warm to rt and poured in water (25 mL). The crude product was extracted from the aqueous phase with ethyl acetate (3x 120 mL). The combined organic phases were dried over Na₂SO₄ and the organic solvent was evaporated. The crude product was purified by column chromatography (eluent: light petroleum/ethyl acetate 90:10) and, subsequently, by preparative HPLC A (gradient: 0-35 min, A/B 55:45–25:75, *t_R* = 15 min) to give **6.9** as a fluffy white solid (650 mg, 2.62 mmol, 74%). **¹H-NMR** (400 MHz, CDCl₃): δ (ppm) 1.22-1.47 (m, 13H), 1.69-1.80 (m, 2H), 2.06-2.21 (m, 2H), 2.59 (s, 1H), 3.67-3.75 (m, 1H), 3.93-4.01 (m, 1H), 6.86-6.92 (m, 2H), 7.27-7.33 (m, 2H). **¹³C-NMR** (101 MHz, CDCl₃): δ (ppm) 24.05, 24.13, 29.4, 31.6, 32.1, 34.2, 73.6, 82.4, 116.0, 126.4, 144.1, 155.7. **RP-HPLC** (Method A, 220 nm): 100% (*t_R* = 22.1 min, *k* = 7.5). **HRMS** (APCI): *m/z* [M+NH₄]⁺ calcd. for [C₁₆H₂₈NO₂]⁺ 266.2115, found 266.2115. C₁₆H₂₄O₂ (248.37).



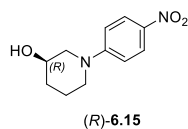
1-((1*R*,2*R*)-2-Aminocyclohexyl)-3-phenylurea hydrotrifluoroacetate (6.12).³⁴ (*R,R*)-Diaminocyclohexane (**6.11**) (1.24 g, 10.9 mmol) was dissolved in CH₂Cl₂ (100 mL) and stirred at -25 °C. Under stirring, isocyanatobenzene (0.85 mL, 7.85 mmol) in CH₂Cl₂ (50 mL) was added dropwise to the reaction mixture. Then, the reaction mixture was allowed to warm to rt and stirred overnight. CH₂Cl₂ (100 mL) was added to the reaction mixture and the solution was filtered. The filtrate was washed with a saturated solution of Na₂CO₃ (3x 200 mL) and the organic solvent was evaporated. The crude product was purified by column chromatography (eluent: CH₂Cl₂/MeOH/NH₃ aq 90:9:1) and, subsequently, by preparative HPLC A (gradient: 0-35 min, A/B 85:15–28:72, *t_R* = 5 min) to give **6.12** as a fluffy white solid (0.45 g, 1.29 mmol, 16%). **¹H-NMR** (600 MHz, DMSO-*d*₆): δ (ppm) 1.21-1.42 (m, 4H), 1.65-1.73 (m, 2H), 1.82-1.88 (m, 1H), 1.95-2.01 (m, 1H), 2.83-2.91 (m, 1H), 3.51-3.59 (m, 1H), 6.83 (d, *J* = 8.4 Hz, 1H), 6.87-6.91 (m, 1H), 7.19-7.25 (m, 2H), 7.41-7.46 (m, 2H), 7.88 (br s, 3H), 8.98 (s, 1H). **¹³C-NMR** (150 MHz, DMSO-*d*₆): δ (ppm) 23.4, 24.3, 29.5, 31.7, 50.8, 54.2, 116.0 (TFA), 117.7, 118.0 (TFA), 119.9, 128.7, 140.6, 155.4, 158.9 (q, *J* = 32.2 Hz) (TFA). **RP-HPLC** (Method A, 220 nm): 100% (*t_R* = 9.7 min, *k* = 2.8). **HRMS** (ESI): *m/z* [M+H]⁺ calcd. for [C₁₃H₂₀N₃O]⁺ 234.1601, found 234.1604. C₁₃H₁₉N₃O × C₂HF₃O₂. (233.32 + 114.02).



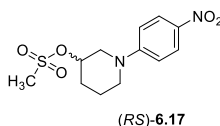
Benzyl ((1*R*,2*R*)-2-aminocyclohexyl)carbamate hydrotrifluoroacetate (6.13).³⁵ (*R,R*)-Diaminocyclohexane (**6.11**) (1.06 g, 9.28 mmol) was dissolved in CH₂Cl₂ (200 mL) and stirred at -20 °C. Under stirring, *N*-(benzyloxycarbonyloxy)succinimide (1.69 g, 6.78 mmol) in CH₂Cl₂ (100 mL) was added dropwise to the reaction mixture. Then, the reaction mixture was allowed to warm to rt and stirred overnight. The organic phase was washed with 1N NaOH (2x 250 mL), brine (1x 250 mL) and the organic solvent was evaporated. The crude product was purified by column chromatography (eluent: CH₂Cl₂/MeOH/NH₃ aq 90:9:1) and, subsequently, by preparative HPLC A (gradient: 0-35 min, A/B 76:24–28:72, *t_R* = 7 min) to give **6.13** as a fluffy white solid (1.58 g, 4.36 mmol, 64%). **¹H-NMR** (600 MHz, DMSO-*d*₆): δ (ppm) 1.15-1.40 (m, 4H), 1.61-1.73 (m, 2H), 1.78-1.91 (m, 1H), 1.96-2.04 (m, 1H), 2.83-2.88 (m, 1H), 3.34-3.44 (m, 1H), 4.99 (d, *J* = 12.4 Hz, 1H), 5.08 (d, *J* = 12.4 Hz, 1H), 7.30-7.34 (m, 1H), 7.35-7.40 (m, 5H), 7.96 (br s, 3H). **¹³C-NMR** (150 MHz, DMSO-*d*₆): δ (ppm) 23.4, 24.1, 29.4, 31.5, 52.3, 53.3, 65.6, 116.2 (TFA), 118.2 (TFA), 127.8 (two carbon signals), 128.3, 136.9, 156.0, 158.2 (q, *J* = 31.4 Hz) (TFA). **RP-HPLC** (Method A, 220 nm): 98% (*t_R* = 8.4 min, *k* = 2.3). **HRMS** (ESI): *m/z* [M+H]⁺ calcd. for [C₁₄H₂₁N₂O₂]⁺ 249.1598, found 249.1601. C₁₄H₂₀N₂O₂ × C₂HF₃O₂ (248.33 + 114.02).



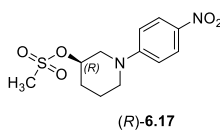
(*RS*)-1-(4-Nitrophenyl)piperidin-3-ol ((*RS*)-6.15).⁹ (*RS*)-Piperidine-3-ol (**6.14**) (5.01 g, 49.5 mmol) and 1-bromo-4-nitrobenzene (12.02 g, 59.5 mmol) were dissolved in DMSO (100 mL). Additionally, *L*-proline (1.16 g, 10.1 mmol), CuI (0.981 g, 5.15 mmol) and K₂CO₃ (14.06 g, 101.7 mmol) were added to the reaction mixture, which was stirred at 65 °C for 2 d. Then, the reaction mixture was poured into ethyl acetate (700 mL). The organic phase was washed with water (6x 600 mL), dried over MgSO₄ and the organic solvent was evaporated. The crude product was purified by column chromatography (eluent: light petroleum/ethyl acetate 1:2) to obtain (*RS*)-**6.14** as an orange crystalline solid (9.31 g, 41.9 mmol, 85%). **Anal. calcd.** for C₁₁H₁₄N₂O₃: C 59.45, H 6.35, N 12.61, found: C 59.46, H 6.28, N 12.48. **¹H-NMR** (600 MHz, CDCl₃): δ (ppm) 1.61-1.71 (m, 2H), 1.76-1.96 (m, 2H), 1.98-2.05 (m, 1H), 3.17-3.22 (m, 1H), 3.22-3.27 (m, 1H), 3.49-3.55 (m, 1H), 3.69-3.74 (m, 1H), 3.87-3.93 (m, 1H), 6.84 (d, *J* = 9.4 Hz, 2H), 8.10 (d, *J* = 9.4 Hz, 2H). **¹³C-NMR** (151 MHz, CDCl₃): δ (ppm) 22.1, 32.8, 47.8, 54.7, 66.3, 113.1, 126.2, 138.3, 155.2. **HRMS** (ESI): *m/z* [M+H]⁺ calcd. for [C₁₁H₁₅N₂O₃]⁺ 223.1077, found 223.1081. C₁₁H₁₄N₂O₃ (222.24).



(R)-1-(4-Nitrophenyl)piperidin-3-ol ((R)-6.15). (*R*)-Piperidine-3-ol·HCl (3.12 g, 23.3 mmol) ((*R*)-6.14·HCl) and 1-bromo-4-nitrobenzene (5.83 g, 28.9 mmol) were dissolved in DMSO (60 mL). Additionally, *L*-proline (0.556 g, 4.83 mmol), CuI (0.430 g, 2.26 mmol) and K₂CO₃ (10.77 g, 77.9 mmol) were added to the reaction mixture that was stirred at 65 °C for 2 d. The reaction mixture was poured into water (500 mL). The crude product was extracted from the aqueous phase with ethyl acetate (3x 300 mL), dried over MgSO₄ and the organic solvent was evaporated. The crude product was purified by column chromatography (eluent: light petroleum/ethyl acetate 1:2) to obtain (*R*)-6.14 as an orange crystalline solid (4.21 g, 18.9 mmol, 81%). ¹H-NMR (300 MHz, CDCl₃): δ (ppm) 1.55-1.72 (m, 2H), 1.83-2.10 (m, 2H), 2.30 (br s, 1H), 3.14-3.30 (m, 2H), 3.47-3.60 (m, 1H), 3.70-3.77 (m, 1H), 3.84-3.94 (m, 1H), 6.80 (d, *J* = 9.5 Hz, 2H), 8.04 (d, *J* = 9.5 Hz, 2H). ¹³C-NMR (75 MHz, CDCl₃): δ (ppm) 22.0, 32.6, 47.6, 54.5, 66.2, 112.9, 126.2, 137.9, 155.1. HRMS (ESI): *m/z* [M+H]⁺ calcd. for [C₁₁H₁₅N₂O₃]⁺ 223.1077, found 223.1077. C₁₁H₁₄N₂O₃ (222.24).

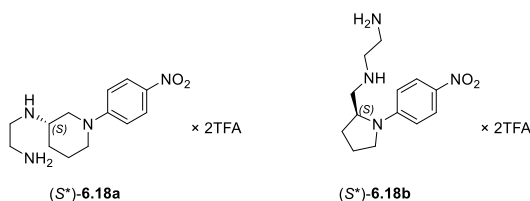


(RS)-1-(4-Nitrophenyl)piperidin-3-yl methanesulfonate ((RS)-6.17). (*RS*)-1-(4-Nitrophenyl)piperidin-3-ol ((*RS*)-6.14) (2.06 g, 9.27 mmol) was dissolved in CH₂Cl₂ (70 mL) and Et₃N (1.90 mL, 13.7 mmol) was added and the mixture was stirred and cooled in an ice bath. Under stirring, methanesulfonyl chloride (1.10 mL, 14.2 mmol) in CH₂Cl₂ (30 mL) was dropped slowly into the reaction mixture. The reaction mixture was stirred at rt for 2 h. Then, CH₂Cl₂ (100 mL) was added into the reaction mixture. The organic phase was washed with 0.5 N HCl (2x 200 mL), saturated NaHCO₃ solution (2x 200 mL), brine (1x 200 mL) and the organic phase was dried over MgSO₄. The organic solvent was removed by evaporation, the residue was taken up in CH₂Cl₂ and crystallization, initiated by the addition of light petroleum, afforded (*RS*)-6.19 as dark yellow crystals (1.72 g, 5.73 mmol, 62%). **Anal. calcd.** for C₁₂H₁₆N₂O₅S: C 47.99, H 5.37, N 9.33, S 10.67, found: C 48.09, H 5.29, N 9.24, S 10.65. ¹H-NMR (600 MHz, CDCl₃): δ (ppm) 1.70-1.80 (m, 1H), 1.93-2.02 (m, 2H), 2.08-2.19 (m, 1H), 3.03 (s, 3H), 3.33-3.41 (m, 1H), 3.47-3.53 (m, 1H), 3.56-3.61 (m, 1H), 3.78-3.83 (m, 1H), 4.81-4.88 (m, 1H), 6.86 (d, *J* = 9.4 Hz, 2H), 8.11 (d, *J* = 9.4 Hz, 2H). ¹³C NMR (151 MHz, CDCl₃): δ (ppm) 21.8, 30.4, 38.8, 47.5, 52.3, 74.6, 113.3, 126.2, 138.8, 154.5. HRMS (ESI): *m/z* [M+H]⁺ calcd. for [C₁₂H₁₇N₂O₅S]⁺ 301.0853, found 301.0858. C₁₂H₁₆N₂O₅S (300.33).



(R)-1-(4-Nitrophenyl)piperidin-3-yl methanesulfonate ((R)-6.17). (*R*)-1-(4-Nitrophenyl)piperidin-3-ol ((*R*)-6.14) (2.13 g, 9.58 mmol) was dissolved in CH₂Cl₂ (70 mL) and Et₃N (1.90 mL, 13.7 mmol) was added and the mixture was stirred and cooled in an ice bath. Under stirring, methanesulfonyl chloride

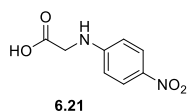
(1.05 mL, 13.6 mmol) in CH₂Cl₂ (30 mL) was dropped slowly into the reaction mixture. The reaction mixture was stirred at rt for 2 h. Then, the organic phase was washed with 0.5 N HCl (2x 200 mL), saturated NaHCO₃ solution (2x 200 mL), brine (1x 200 mL) and the organic phase was dried over MgSO₄. The organic solvent was removed by evaporation, the residue was taken up in CH₂Cl₂ and crystallization, initiated by the addition of light petroleum, afforded (*R*)-**6.19** as dark yellow crystals (2.14 g, 7.13 mmol, 74%). **¹H-NMR** (300 MHz, CDCl₃): δ (ppm) 1.61-1.80 (m, 1H), 1.87-2.04 (m, 2H), 2.05-2.15 (m, 1H), 3.03 (s, 3H), 3.29-3.42 (m, 1H), 3.44-3.67 (m, 2H), 3.76-3.86 (m, 1H), 4.79-4.89 (m, 1H), 6.84 (d, *J* = 9.5 Hz, 2H), 8.09 (d, *J* = 9.5 Hz, 2H). **¹³C-NMR** (75 MHz, CDCl₃): δ (ppm) 21.8, 30.4, 38.7, 47.4, 52.2, 74.7, 113.2, 126.2, 138.6, 154.5. **HRMS** (ESI): *m/z* [M+H]⁺ calcd. for [C₁₂H₁₇N₂O₅S]⁺ 301.0853, found 301.0851. C₁₂H₁₆N₂O₅S (300.33).



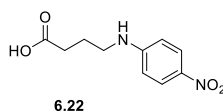
(*S*^{*})-*N*'-(1-(4-Nitrophenyl)piperidin-3-yl)ethane-1,2-diamine ((*S*^{*})-6.18a**) and (*S*^{*})-*N*'-((1-(4-nitrophenyl)pyrrolidine-2-yl)methyl)ethane-1,2-diamin ((*S*^{*})-**6.18b**).** *tert*-Butyl (2-aminoethyl)carbamate (**2.36**) (240 mg, 1.50 mmol) and (*R*)-1-(4-nitrophenyl)piperidin-3-yl methanesulfonate ((*R*)-**6.17**) (400 mg, 1.33 mmol) were dissolved in acetonitrile (10 mL) in a 20 mL reaction tube and heated in a microwave device (120 °C, 1 h). The organic solvent was evaporated and the crude mixture was purified by column chromatography (eluent: CH₂Cl₂/MeOH 90:10). The purified product was dissolved in CH₂Cl₂ (5 mL) and TFA (5 mL) was added dropwise to the mixture and stirred at rt overnight. The organic solvent was evaporated and the residue was dissolved in CH₂Cl₂ (10 mL) and the organic solvent was evaporated (3x). The crude product was purified by preparative HPLC B (gradient: 0-30 min, A/B 66:34–38:62, *t_R*((*S*^{*})-**6.18a**) = 12 min, *t_R*((*S*^{*})-**6.18b**) = 13 min) to isolate (*S*^{*})-**6.18a** and (*S*^{*})-**6.18b** as fluffy yellow solids ((*S*^{*})-**6.18a**: 11.4 mg, 23.2 μmol, 2%; (*S*^{*})-**6.18b**: 21.4 mg, 43.5 μmol, 3%).

(*S*^{*})-6.18a****: **¹H-NMR** (600 MHz, DMSO-*d*₆): δ (ppm) 1.52-1.62 (m, 1H), 1.63-1.72 (m, 1H), 1.80-1.89 (m, 1H), 2.06-2.14 (m, 1H), 3.10-3.21 (m, 3H), 3.23-3.40 (m, 4H), 3.78-3.86 (m, 1H), 4.04-4.14 (m, 1H), 7.06-7.11 (m, 2H), 7.90-9.60 (m, 7H). **¹³C-NMR** (150 MHz, DMSO-*d*₆): δ (ppm) 21.9, 26.1, 35.4, 41.4, 46.9, 48.5, 52.5, 113.3, 116.0 (TFA), 118.0 (TFA), 125.7, 137.3, 154.3, 158.8 (q, *J* = 31.1 Hz) (TFA). **RP-HPLC** (Method A, 220 nm): 98% (*t_R* = 7.5 min, *k* = 1.9). **HRMS** (ESI): *m/z* [M+H]⁺ calcd. for [C₁₃H₂₁N₄O₂]⁺ 265.1659, found 265.1660. C₁₃H₂₀N₄O₂ × C₄H₂F₆O₄ (264.33 + 228.04).

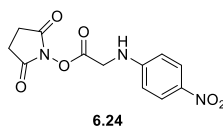
(*S*^{*})-6.18b****: **¹H-NMR** (600 MHz, DMSO-*d*₆): δ (ppm) 1.94-2.12 (m, 3H), 2.15-2.21 (m, 1H), 2.99-3.06 (m, 2H), 3.17-3.32 (m, 5H), 3.49-3.54 (m, 1H), 4.15-4.22 (m, 1H), 6.78-6.84 (m, 2H), 7.98-9.92 (m, 7H). **¹³C-NMR** (150 MHz, DMSO-*d*₆): δ (ppm) 22.1, 28.0, 35.3, 44.9, 47.1, 48.1, 55.4, 111.7, 117.0 (q, *J* = 297.9 Hz) (TFA), 125.8, 136.3, 151.2, 159.1 (q, *J* = 32.1 Hz) (TFA). **RP-HPLC** (Method A, 220 nm): 98% (*t_R* = 7.9 min, *k* = 2.0). **HRMS** (ESI): *m/z* [M+H]⁺ calcd. for [C₁₃H₂₁N₄O₂]⁺ 265.1659, found 265.1661. C₁₃H₂₀N₄O₂ × C₄H₂F₆O₄ (264.33 + 228.04).



(4-Nitrophenyl)glycine (6.21).^{36, 37} Glycine (3.78 g, 50.4 mmol) (**6.19**), 1-fluoro-4-nitrobenzene (3.55 g, 25.2 mmol) and Na_2CO_3 (4.89 g, 46.1 mmol) were dissolved in a mixture of dioxane (42 mL) and water (7 mL) and stirred at 70 °C overnight. The reaction mixture was allowed to cool to rt and poured in water (100 mL). The aqueous phase was washed with ethyl acetate (3x 100 mL) and then acidified with 1N HCl. (Addition of 1N HCl was continued until no further orange solid precipitated). The compound was extracted from the aqueous phase with ethyl acetate (3x 200 mL) and the combined organic phases were dried over MgSO_4 . Then, the organic solvent was evaporated and **6.21** was obtained as an orange solid that was used in the next step without further purification (2.73 g, 13.9 mmol, 55%). **Anal. calcd.** for $\text{C}_8\text{H}_8\text{N}_2\text{O}_4$: C 48.98, H 4.11, N 14.28, found: C 48.98, H 4.28, N 14.18. **$^1\text{H-NMR}$** (300 MHz, $\text{DMSO-}d_6$): δ (ppm) 7.98 (d, $J = 6.0$ Hz, 2H), 6.66 (d, $J = 9.4$ Hz, 2H), 7.47 (t, $J = 6.0$ Hz, 1H), 8.00 (d, $J = 9.4$ Hz, 2H), 12.83 (br s, 1H). **$^{13}\text{C-NMR}$** (75 MHz, $\text{DMSO-}d_6$): 44.0, 111.2, 126.1, 136.3, 154.3, 171.5. **HRMS** (ESI): m/z $[\text{M}+\text{H}]^+$ calcd. for $[\text{C}_8\text{H}_9\text{N}_2\text{O}_4]^+$ 197.0557, found 197.0556. $\text{C}_8\text{H}_8\text{N}_2\text{O}_4$ (196.16).

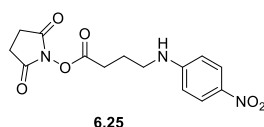


4-((4-Nitrophenyl)amino)butanoic acid (6.22).^{37, 38} 4-((4-Nitrophenyl)amino)butanoic acid (7.03 g, 68.2 mmol) (**6.20**), 1-fluoro-4-nitrobenzene (4.80 g, 34.0 mmol) and Na_2CO_3 (9.96 g, 94.0 mmol) were dissolved in a mixture of dioxane (15 mL) and water (85 mL) and stirred at 70 °C overnight. The reaction mixture was allowed to cool to rt and poured into water (200 mL). The aqueous phase was washed with ethyl acetate (3x 250 mL) and then acidified with 0.5 N H_2SO_4 . (Addition of 0.5 N H_2SO_4 was continued until no further orange solid precipitated). The compound was extracted from the aqueous phase with ethyl acetate (3x 200 mL) and the combined organic phases were dried over MgSO_4 . Then, the organic solvent was evaporated and **6.23** was obtained as an orange solid that was used in the next step without further purification (6.26 g, 27.9 mmol, 82%). **$^1\text{H-NMR}$** (300 MHz, $\text{DMSO-}d_6$): δ (ppm) 1.70-1.85 (m, 2H), 2.33 (t, $J = 7.4$ Hz, 2H), 3.11-3.20 (m, 2H), 6.63 (d, $J = 9.3$ Hz, 2H), 7.34 (t, $J = 5.4$ Hz, 1H), 7.98 (d, $J = 9.3$ Hz, 2H), 12.15 (br s, 1H). **$^{13}\text{C-NMR}$** (75 MHz, $\text{DMSO-}d_6$): δ (ppm) 23.8, 31.0, 41.7, 110.8, 126.3, 135.6, 154.6, 174.2. **HRMS** (ESI): m/z $[\text{M}+\text{Na}]^+$ calcd. for $[\text{C}_{10}\text{H}_{12}\text{N}_2\text{O}_4\text{Na}]^+$ 247.0689, found 247.0695. $\text{C}_{10}\text{H}_{12}\text{N}_2\text{O}_4$ (224.22).

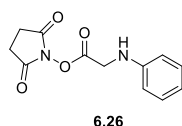


Succinimidyl (4-nitrophenyl)glycinate (6.24). (4-Nitrophenyl)glycine (2.16 g, 11.0 mmol) (**6.21**) and *N*-hydroxysuccinimide (**2.22**) (1.31 g, 11.4 mmol) were dissolved in DMF (30 mL) and the reaction mixture was stirred at rt. Under stirring, a solution of DCC (2.62 g, 12.7 mmol) in DMF (5 mL) was added dropwise into the mixture and the reaction mixture was stirred at rt overnight. The precipitate was removed by filtration, and washed with DMF (50 mL). The combined organic (DMF) phases were poured into water (1.5 L) and the compound was extracted from the aqueous phase with ethyl acetate (3x

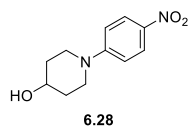
250 mL). The combined organic phases (ethyl acetate) were dried over Na₂SO₄ and the organic solvent was evaporated. The residue was dissolved in CH₂Cl₂ (insoluble components were filtered off) and the organic solvent was evaporated to give **6.24** as a bright yellow solid (2.02 g, 6.89 mmol, 63%). **¹H-NMR** (300 MHz, DMSO-*d*₆): δ (ppm) 2.82 (s, 4H), 4.63 (d, *J* = 6.6 Hz, 2H), 6.74 (d, *J* = 9.3 Hz, 2H), 7.73 (t, *J* = 6.6 Hz, 1H), 8.03 (d, *J* = 9.3 Hz, 2H). **¹³C-NMR** (75 MHz, DMSO-*d*₆): 25.5, 41.9, 111.6, 126.0, 137.2, 153.6, 167.0, 170.1. **HRMS** (ESI): *m/z* [M+H]⁺ calcd. for [C₁₂H₁₂N₃O₆]⁺ 294.0721, found 294.0729. C₁₂H₁₁N₃O₆ (293.24).



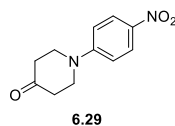
Succinimidyl 4-((4-nitrophenyl)amino)butanoate (6.25). 4-((4-Nitrophenyl)amino)butanoic acid (**6.22**) (1.02 g, 4.55 mmol) and *N*-hydroxysuccinimide (**2.22**) (0.57 g, 4.95 mmol) were dissolved in DMF (30 mL). Under stirring, a solution of DCC (1.06 g, 5.14 mmol in DMF (5 mL) was added dropwise into the mixture and the reaction mixture was stirred at rt overnight. The precipitate was removed by filtration and washed with DMF (50 mL). The combined organic (DMF) phases were poured into water (1.5 L) and the compound was extracted from the aqueous phase with ethyl acetate (3x 250 mL). The combined organic phases (ethyl acetate) were dried over Na₂SO₄ and the solvent was evaporated. The residue was dissolved in CH₂Cl₂ (insoluble components were filtered off) and the solvent was evaporated to give **6.25** as a bright yellow solid (1.30 g, 4.05 mmol, 89%). **¹H-NMR** (400 MHz, DMSO-*d*₆): δ (ppm) 1.86-1.96 (m, 2H), 2.78-2.85 (m, 6H), 3.21-3.28 (m, 2H), 3.62-6.69 (m, 2H), 7.35 (t, *J* = 5.5 Hz, 1H), 7.97-8.04 (m, 2H). **¹³C-NMR** (101 MHz, DMSO-*d*₆): δ (ppm) 23.6, 25.5, 27.8, 41.1, 110.8, 126.3, 135.8, 154.4, 168.8, 170.3. **HRMS** (ESI): *m/z* [M+H]⁺ calcd. for [C₁₄H₁₆N₃O₆]⁺ 322.1034, found 322.1044. C₁₄H₁₅N₃O₆ (321.29).



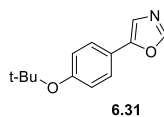
Succinimidyl phenylglycinate (6.26). DCC (1.55 g, 7.51 mmol) in CH₂Cl₂ (15 mL) was added dropwise into an ice-cold solution of phenylglycine (**6.23**) (1.04 g, 6.88 mmol) and *N*-hydroxysuccinimide (**2.22**) (0.78 g, 6.78 mmol) in CH₂Cl₂ (50 mL). The reaction mixture was allowed to warm to rt and stirred overnight. The precipitated solid was removed by filtration and washed with CH₂Cl₂. The filtrate was evaporated, and the residue was dissolved in CH₂Cl₂. The organic phase (insoluble components were filtered off) was evaporated to give **6.26** as a dark yellow solid (0.647 g, 2.61 mmol, 38%). **¹H-NMR** (300 MHz, DMSO-*d*₆): δ (ppm) 2.81 (s, 4H), 4.35 (d, *J* = 6.7 Hz, 2H), 6.29 (t, *J* = 6.7 Hz, 1H), 6.55-6.67 (m, 3H), 7.04-7.17 (m, 2H). **¹³C-NMR** (75 MHz, DMSO-*d*₆): δ (ppm) 25.5, 42.4, 112.3, 116.9, 128.9, 147.4, 167.9, 170.2. **HRMS** (ESI): *m/z* [M+H]⁺ calcd. for [C₁₂H₁₃N₂O₄]⁺ 249.0870, found 249.0871. C₁₂H₁₂N₂O₄ (248.24).



1-(4-Nitrophenyl)piperidin-4-ol (6.28).^{9, 39} Piperidin-4-ol (**6.27**) (3.60 g, 35.6 mmol) and 1-bromo-4-nitro-benzene (9.10 g, 45.0 mmol) were dissolved in DMSO (100 mL). Additionally, *L*-proline (0.80 g, 6.95 mmol), CuI (0.80 g, 4.20 mmol) and K₂CO₃ (17.64 g, 127.6 mmol) were added to the reaction mixture, which was stirred at 65 °C for 2 d. The reaction mixture was poured in water (1 L) and the product was extracted from the aqueous phase with ethyl acetate (3x 500 mL), dried over MgSO₄ and the organic solvent was evaporated. The crude product was purified by column chromatography (eluent: light petroleum/ethyl acetate 1:2 to 1:3 to 0:1) to give **6.28** as a yellow crystalline solid (6.94 g, 31.22 mmol, 88%). **¹H-NMR** (300 MHz, DMSO-*d*₆): δ (ppm) 1.32-1.49 (m, 2H), 1.73-1.88 (m, 2H), 3.12-3.30 (m, 2H), 3.66-3.90 (m, 3H), 4.79 (d, *J* = 4.1 Hz, 1H), 6.99 (d, *J* = 9.5 Hz, 2H), 8.01 (d, *J* = 9.5 Hz, 2H). **¹³C-NMR** (75 MHz, DMSO-*d*₆): δ (ppm) 33.5, 44.4, 65.5, 112.4, 125.9, 136.1, 154.3. **HRMS** (ESI): *m/z* [M+H]⁺ calcd. for [C₁₁H₁₅N₂O₃]⁺ 223.1077, found 223.1081. C₁₁H₁₄N₂O₃ (222.24).

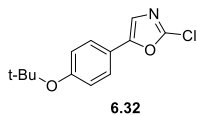


1-(4-Nitrophenyl)piperidin-4-one (6.29).^{9, 40} 1-(4-Nitrophenyl)piperidin-4-ol (**6.28**) (1.00 g, 4.50 mmol) was dissolved in DMSO (20 mL) and Et₃N (3.20 mL, 23.1 mmol) was added to the reaction mixture. Under stirring, pyridine-sulfur trioxide complex (3.57 g, 22.4 mmol) in DMSO (15 mL) was dropped slowly into the mixture. Then, the reaction mixture was poured into ethyl acetate (400 mL). The organic phase was washed with water (6x 500 mL), brine (1x 500 mL) and dried over Na₂SO₄. The organic solvent was evaporated, and the crude product was purified by column chromatography (eluent: light petroleum/ethyl acetate 1:1 to 1:2) to give **6.29** as a yellow amorphous solid (0.51 g, 2.27 mmol, 50%). **¹H-NMR** (300 MHz, CDCl₃): δ (ppm) 2.62 (t, *J* = 6.3 Hz, 4H), 3.82 (t, *J* = 6.3 Hz, 4H), 6.84 (d, *J* = 9.4 Hz, 2H), 8.14 (d, *J* = 9.4 Hz, 2H). **¹³C-NMR** (101 MHz, DMSO-*d*₆): δ (ppm) 39.4 (overlaid by solvent residual peak), 44.4, 112.0, 125.9, 136.6, 153.4, 207.2. **HRMS** (EIC): *m/z* [M]⁺ calcd. for [C₁₁H₁₂N₂O₃]⁺ 220.0842 found, 220.0840. C₁₁H₁₂N₂O₃ (220.23).

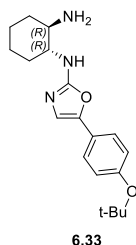


5-(4-(*tert*-Butoxy)phenyl)oxazole (6.31).⁹ 4-(*tert*-Butoxy)benzaldehyde (**6.30**) (2.0 mL, 11.4 mmol), 1-((isocyanomethyl)sulfonyl)-4-methylbenzene (2.46 g, 12.6 mmol) and K₂CO₃ (3.20 g, 23.2 mmol) were dissolved in methanol (20 mL) and refluxed for 4 h. The organic solvent was evaporated, and water was added (50 mL) to the residue. The product was extracted from the aqueous phase with ethyl acetate (3x 50 mL), the combined organic phases were dried over MgSO₄ and the organic solvent was evaporated. The crude product was purified by column chromatography (eluent: light petroleum/ethyl acetate 1:0 to 4:1) to give **6.31** as a pale-yellow solid (1.74 g, 8.73 mmol, 77%). **Anal. calcd.** for C₁₃H₁₅NO₂: C 71.87, H 6.96, N 6.45, found: C 71.94, H 6.93, N 6.16. **¹H-NMR** (600 MHz, CDCl₃): δ

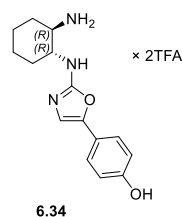
(ppm) 1.37 (s, 9H), 7.04 (d, $J = 8.7$ Hz, 2H), 7.26 (s, 1H, interfering with solvent residual peak), 7.56 (d, $J = 8.7$ Hz, 2H), 7.88 (s, 1H). **¹³C-NMR** (151 MHz, CDCl₃): δ (ppm) 29.0, 79.3, 120.7, 123.0, 124.5, 125.4, 150.2, 151.7, 156.2. **HRMS** (EIC): m/z [M]⁺ calcd. for [C₁₃H₁₅NO₂]⁺ 217.1097, found 217.1100. C₁₃H₁₅NO₂ (217.27).



5-(4-(*tert*-Butoxy)phenyl)-2-chlorooxazole (6.32).⁹ 5-(4-(*tert*-Butoxy)phenyl)oxazole (**6.31**) (3.53 g, 16.2 mmol) was dissolved in dry THF (40 mL) and stirred at -78 °C (dry ice/acetone). After addition of *n*-BuLi (7.1 mL, 76.8 mmol) the solution turned red and the reaction mixture was stirred for 2 h. Under stirring, C₂Cl₆ (5.95 g, 25.1 mmol) was added into the reaction mixture, which was stirred at -78 °C for 2 h. The reaction mixture was allowed to warm to rt and then poured into a mixture of ice and water (200 mL). The compound was extracted from the aqueous phase with ethyl acetate (3x 150 mL), the combined organic phases were dried over MgSO₄ and the organic solvent was evaporated. The crude product was purified by column chromatography (eluent: light petroleum/ethyl acetate 1:0 to 9:1 to 8:2) to give **6.32** as a yellow oil (3.59 g, 14.3 mmol, 88%). **Anal. calcd.** for C₁₃H₁₅ClNO₂: C 62.03, H 5.61, N 5.56, found: C 62.41, H 6.05, N 5.16. **¹H-NMR** (600 MHz, CDCl₃): δ (ppm) 1.38 (s, 9H), 7.04 (d, $J = 8.6$ Hz, 2H), 7.19 (s, 1H), 7.49 (d, $J = 8.6$ Hz, 2H). **¹³C-NMR** (151 MHz, CDCl₃): δ (ppm) 29.0, 79.4, 122.1, 122.5, 124.4, 125.1, 145.8, 154.0, 156.5. **HRMS** (ESI): m/z [M+H]⁺ calcd. for [C₁₃H₁₅ClNO₂]⁺ 252.0786, found 252.0792. C₁₃H₁₄ClNO₂ (251.71).

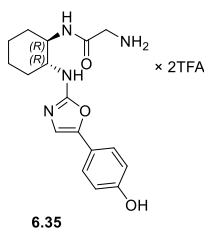


(1*R*,2*R*)-*N'*-(5-(4-(*tert*-Butoxy)phenyl)oxazol-2-yl)cyclohexane-1,2-diamine (6.33). (*R,R*)-Diaminocyclohexane (**6.11**) (4.67 g, 40.9 mmol) and 5-(4-(*tert*-butoxy)phenyl)-2-chlorooxazole (**6.32**) (2.06 g, 8.18 mmol) were dissolved in DMF (30 mL) and K₂CO₃ (4.50 g, 32.6 mmol) was added. The reaction mixture (suspension) was split into three 20 mL reaction tubes (3x 10 mL) and heated in a microwave device (130 °C, 45 min). The combined reaction mixtures were poured into ethyl acetate (300 mL), then washed with water (3x 300 mL) and brine (1x 300 mL). The organic phase was dried over MgSO₄ and the organic solvent was evaporated. The crude product was purified by column chromatography (eluent: CH₂Cl₂/MeOH 90:10 to 50:50) to give **6.33** as a solid (1.27 g, 3.84 mmol, 47%). **¹H-NMR** (300 MHz, DMSO-*d*₆): δ (ppm) 1.15-1.25 (m, 4H), 1.29 (s, 9H), 1.59-1.75 (m, 2H), 1.86-1.95 (m, 1H), 1.95-2.05 (m, 1H), 2.61-2.76 (m, 1H), 3.14-3.29 (m, 1H), 4.00 (br s, 2H, interfering with water signal), 6.93-7.02 (m, 2H), 7.12 (s, 1H), 7.32-7.42 (m, 3H). **¹³C-NMR** (75 MHz, DMSO-*d*₆): δ (ppm) 24.3, 24.6, 28.6, 31.6, 32.9, 53.6, 58.0, 78.2, 121.7, 122.8, 123.8, 124.2, 143.1, 153.5, 160.6. **HRMS** (ESI): m/z [M+H]⁺ calcd. for [C₁₉H₂₈N₃O₂]⁺ 330.2176, found 330.2178. C₁₉H₂₇N₃O₂ (329.44).



4-(2-(((1*R*,2*R*)-2-Aminocyclohexyl)amino)oxazol-5-yl)phenol bis(hydrotrifluoroacetate) (6.34).

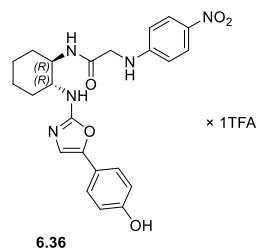
(1*R*,2*R*)-*N*'-(5-(4-(*tert*-Butoxy)phenyl)oxazol-2-yl)cyclohexane-1,2-diamine (**6.33**) (0.346 g, 1.05 mmol) was dissolved in CH₂Cl₂ (10 mL) and the mixture was stirred and cooled in an ice bath. Under stirring, TFA (10 mL) was added dropwise to the mixture. After 1 h, the mixture was allowed to warm to rt and stirred overnight. The solvent was evaporated, and the crude product was purified by preparative HPLC A (gradient: 0-30 min, A/B 85:15–66:34, *t_R* = 9 min) to give **6.34** as a fluffy white solid (243 mg, 0.485 mmol, 46%). **¹H-NMR** (600 MHz, DMSO-*d*₆): δ (ppm) 1.19-1.31 (m, 2H), 1.33-1.46 (m, 2H), 1.66-1.75 (m, 2H), 1.97-2.06 (m, 2H), 2.99-3.08 (m, 1H), 3.52-3.61 (m, 1H), 6.79-6.83 (m, 2H), 7.28 (s, 1H), 7.34-7.39 (m, 2H), 8.07 (br s, 3H), 8.39 (br s, 1H), 9.67 (br s, 1H). One exchangeable proton signal was not apparent. **¹³C-NMR** (150 MHz, DMSO-*d*₆): δ (ppm) 23.4, 24.0, 29.5, 31.2, 53.2, 54.6, 115.2, 115.8, 116.4 (q, *J* = 294.9 Hz) (TFA), 118.6, 124.4, 144.5, 157.2, 158.3, 158.6 (q, *J* = 33.8 Hz) (TFA). **RP-HPLC** (Method A, 220 nm): 97% (*t_R* = 6.9 min, *k* = 1.7). **HRMS** (ESI): *m/z* [M+H]⁺ calcd. for [C₁₅H₂₀N₃O₂]⁺ 274.1550, found 274.1558. C₁₅H₁₉N₃O₂ × C₄H₂F₆O₄ (273.34 + 228.04).



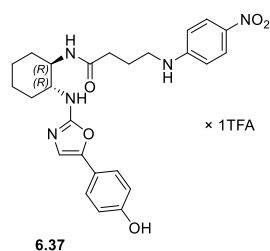
2-Amino-*N*-(((1*R*,2*R*)-2-((5-(4-hydroxyphenyl)oxazol-2-yl)amino)cyclohexyl)acetamide bis(dihydrotrifluoroacetate) (6.35).

4-(2-(((1*R*,2*R*)-2-Aminocyclohexyl)amino)oxazol-5-yl)phenol bis(hydrotrifluoroacetate) (**6.34**) (94.0 mg, 188 μmol) was dissolved in CH₂Cl₂ (5 mL) and DIPEA (42 μL, 247 μmol) was added to the mixture. The reaction mixture was stirred at rt for 2 min. Under stirring, succinimidyl *N*-Boc-glycinate (**2.25**) (124 mg, 455 μmol) was added to the mixture and the reaction mixture stirred at rt for 5 min. Then, the organic solvent was evaporated and the crude product was purified by column chromatography (eluent: CH₂Cl₂/MeOH 9:1). The purified product was dissolved in CH₂Cl₂ (1.5 mL), the solution was cooled to 0 °C and a mixture of CH₂Cl₂ (1 mL) and TFA (1 mL) was added dropwise. After 1 h, the mixture was allowed to warm to rt and stirred overnight. The solvent was evaporated, and the crude product was purified by preparative HPLC A (gradient: 0-30 min, A/B 85:15–66:34, *t_R* = 11 min) to afford **6.35** as a fluffy white solid (45.0 mg, 109 μmol, 51%). **¹H-NMR** (600 MHz, DMSO-*d*₆): δ (ppm) 1.22-1.32 (m, 3H), 1.35-1.44 (m, 1H), 1.64-1.72 (m, 2H), 1.87-1.94 (m, 1H), 2.00-2.07 (m, 1H), 3.33-3.53 (m, 3H), 3.67-3.75 (m, 1H), 6.79-6.84 (m, 2H), 7.34-7.39 (m, 3H), 8.00 (br s, 3H), 8.36-8.41 (m, 1H), 8.60 (s, 1H), 9.79 (br s, 1H). One exchangeable proton signal was not apparent. **¹³C-NMR** (150 MHz, DMSO-*d*₆): δ (ppm) 24.0, 31.4, 31.7, 40.06, 40.10, 51.9, 55.8, 115.8, 116.6 (q, *J* = 296.0 Hz) (TFA), 118.1, 124.5, 144.2, 157.4, 158.1, 158.5 (q, *J* = 32.2 Hz) (TFA), 165.5. **RP-HPLC** (Method B,

220 nm): 95% ($t_R = 10.2$ min, $k = 2.5$). **HRMS** (ESI): m/z $[M+H]^+$ calcd. for $[C_{17}H_{23}N_4O_3]^+$ 331.1765, found 331.1766. $C_{17}H_{22}N_4O_3 \times C_4H_2F_6O_4$ (330.39 + 228.04).

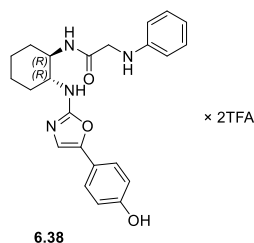


***N*-((1*R*,2*R*)-2-((5-(4-Hydroxyphenyl)oxazol-2-yl)amino)cyclohexyl)-2-((4-nitrophenyl)amino)-acetamide hydrotrifluoroacetate (6.36)**. 4-(2-(((1*R*,2*R*)-2-Aminocyclohexyl)amino)oxazol-5-yl)phenol bis(hydrotrifluoroacetate) (**6.34**) (34.2 mg, 68.2 μ mol) was dissolved in DMF (100 μ L) and DIPEA (31 μ L, 182.3 μ mol) was added to the solution and stirred at rt for 5 min. Under stirring, succinimidyl (4-nitrophenyl)glycinate (**6.24**) (40.6 mg, 138.5 μ mol) was added into the reaction mixture and stirred at rt for 3 h. The mixture was purified by preparative HPLC A (gradient: 0-30 min, A/B 81:19–57:43, $t_R = 21$ min) to give **6.36** as a fluffy yellow solid (15.0 mg, 26.5 μ mol, 39%). **¹H-NMR** (600 MHz, DMSO- d_6): δ (ppm) 1.21-1.43 (m, 4H), 1.65-1.75 (m, 2H), 1.83-1.91 (m, 1H), 1.99-2.05 (m, 1H), 3.44-3.53 (m, 1H), 3.67-3.77 (m, 3H), 6.47 (d, $J = 8.0$ Hz, 2H), 6.80-6.83 (m, 2H), 7.34-7.37 (m, 2H), 7.39 (s, 1H), 7.44 (br s, 1H), 7.82-7.86 (m, 2H), 8.07 (d, $J = 8.5$ Hz, 1H), 8.90 (br s, 1H), 8.79 (br s, 1H). One exchangeable proton signal was not apparent. **¹³C-NMR** (150 MHz, DMSO- d_6): δ (ppm) 16.7, 18.1, 24.2, 31.6, 31.8, 45.8, 52.0, 53.6, 56.2, 111.0, 115.4 (TFA), 115.8, 117.4 (TFA), 117.6, 124.6, 125.8, 136.2, 144.1, 154.2, 157.6, 158.3 (q, $J = 35.0$ Hz) (TFA), 168.6. **RP-HPLC** (Method A, 220 nm): 98% ($t_R = 12.2$ min, $k = 3.7$). **HRMS** (ESI): m/z $[M+H]^+$ calcd. for $[C_{23}H_{26}N_5O_5]^+$ 452.1928, found 452.1928. $C_{23}H_{25}N_5O_5$ (451.48 + 114.02).

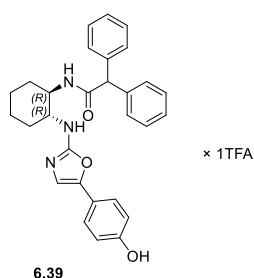


***N*-((1*R*,2*R*)-2-((5-(4-Hydroxyphenyl)oxazol-2-yl)amino)cyclohexyl)-4-((4-nitrophenyl)amino)-butanamide hydrotrifluoroacetate (6.37)**. 4-(2-(((1*R*,2*R*)-2-Aminocyclohexyl)amino)oxazol-5-yl)phenol bis(hydrotrifluoroacetate) (**6.34**) (35.3 mg, 70.4 μ mol) was dissolved in DMF (100 μ L) and DIPEA (31 μ L, 182.3 μ mol) was added to the mixture. The mixture was stirred at rt for 5 min. Under stirring, succinimidyl 4-((4-nitrophenyl)amino)butanoate (**6.25**) (45.3 mg, 148.4 μ mol) was added to the reaction mixture. Then, the reaction mixture was stirred at rt for 3 h. The mixture was purified by preparative HPLC A (gradient: 0-30 min, A/B 81:19–57:43, $t_R = 21$ min) to give **6.37** as a fluffy yellow solid (13.31 mg, 22.4 μ mol, 32%). **¹H-NMR** (600 MHz, DMSO- d_6): δ (ppm) 1.18-1.34 (m, 3H), 1.34-1.46 (m, 1H), 1.60-1.74 (m, 4H), 1.80-1.88 (m, 1H), 1.98-2.09 (m, 2H), 2.10-2.20 (m, 1H), 2.93-3.05 (m, 2H), 3.38-3.48 (m, 1H), 3.63-3.74 (m, 1H), 6.48-6.54 (m, 2H), 6.78-6.82 (m, 2H), 7.22 (br s, 1H), 7.33-7.37 (m, 2H), 7.43 (s, 1H), 7.89 (d, $J = 8.5$ Hz, 1H), 7.92 (d, $J = 9.3$ Hz, 2H), 8.91 (br s, 1H), 9.82 (br s, 1H).

One exchangeable proton signal was not apparent. $^{13}\text{C-NMR}$ (150 MHz, $\text{DMSO-}d_6$): δ (ppm) 24.18, 24.24, 24.4, 31.5, 31.7, 32.7, 41.8, 51.8, 56.7, 110.6, 112.4, 115.6 (TFA), 115.8, 117.6 (TFA), 117.63, 124.7, 126.2, 135.5, 144.1, 154.4, 157.6, 157.7, 158.4 (q, $J = 32.9$ Hz) (TFA), 170.2. **RP-HPLC** (Method A, 220 nm): 97% ($t_R = 12.2$ min, $k = 3.7$). **HRMS** (ESI): m/z $[\text{M}+\text{H}]^+$ calcd. for $[\text{C}_{25}\text{H}_{30}\text{N}_5\text{O}_5]^+$ 480.2241, found 480.2249. $\text{C}_{25}\text{H}_{29}\text{N}_5\text{O}_5 \times \text{C}_2\text{HF}_3\text{O}_2$ (479.54 + 114.02).

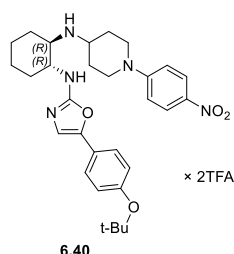


***N*-((1*R*,2*R*)-2-((5-(4-Hydroxyphenyl)oxazol-2-yl)amino)cyclohexyl)-2-(phenylamino)acetamide bis(hydrotrifluoroacetate) (6.38).** 4-(2-(((1*R*,2*R*)-2-Aminocyclohexyl)amino)oxazol-5-yl)phenol bis(hydro-trifluoroacetate) (**6.34**) (34.2 mg, 68.2 μmol) was dissolved in DMF (100 μL) and DIPEA (31 μL , 182.3 μmol) was added to the mixture. The reaction mixture was stirred at rt for 5 min. Under stirring, succinimidyl phenylglycinate (**6.26**) (37.1 mg, 149.5 μmol) was added and the reaction mixture was stirred at rt for 3 h. The mixture was purified by preparative HPLC A (gradient: 0-30 min, A/B 71:29–57:43, $t_R = 10$ min) to give **6.38** as a fluffy white solid (10.75 mg, 16.9 μmol , 25%). $^1\text{H-NMR}$ (600 MHz, $\text{DMSO-}d_6$): δ (ppm) 1.18-1.44 (m, 4H), 1.62-1.76 (m, 2H), 1.79-1.85 (m, 1H), 1.97-2.03 (m, 1H), 3.46-3.57 (m, 3H), 3.68-3.76 (m, 1H), 5.44 (br s, 3H), 6.38-6.45 (m, 3H), 6.84-6.88 (m, 2H), 6.90-6.95 (m, 2H), 7.38-7.41 (m, 2H), 7.44 (s, 1H), 7.88 (d, $J = 8.7$ Hz, 1H), 9.21 (br s, 1H), 9.88 (br s, 1H). $^{13}\text{C-NMR}$ (150 MHz, $\text{DMSO-}d_6$): δ (ppm) 24.11, 24.18, 31.6, 31.7, 47.2, 51.8, 56.1, 110.0, 112.2, 115.3 (TFA), 115.9, 116.5, 117.3 (TFA), 117.4, 124.8, 128.7, 144.2, 148.2, 157.1, 157.8, 158.3 (q, $J = 34.3$ Hz) (TFA), 170.2. **RP-HPLC** (Method A, 220 nm): 97% ($t_R = 11.0$ min, $k = 3.3$). **HRMS** (ESI): m/z $[\text{M}+\text{H}]^+$ calcd. for $[\text{C}_{23}\text{H}_{27}\text{N}_4\text{O}_3]^+$ 407.2078, found 407.2081. $\text{C}_{23}\text{H}_{26}\text{N}_4\text{O}_3$ (406.49 + 228.04).

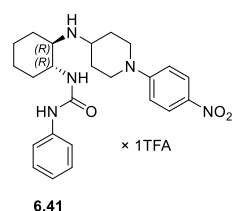


***N*-((1*R*,2*R*)-2-((5-(4-Hydroxyphenyl)oxazol-2-yl)amino)cyclohexyl)-2,2-diphenylacetamide hydrotrifluoroacetate (6.39).** 4-(2-(((1*R*,2*R*)-2-Aminocyclohexyl)amino)oxazol-5-yl)phenol bis(hydrotrifluoroacetate) (**6.34**) (30.0 mg, 109.8 μmol) was dissolved in DMSO (500 μL) and DIPEA (50 μL , 294 μmol) was added to the mixture. The mixture was stirred at rt for 5 min. Under stirring, succinimidyl diphenylacetate (**2.28**) (31 mg, 102 μmol) was added and the reaction mixture was stirred at rt for 2 h. The mixture was purified by preparative HPLC B (gradient: 0-30 min, A/B 66:34–47:53, $t_R = 7$ min) to give **6.39** as a fluffy white solid (11.0 mg, 18.9 μmol , 17%). $^1\text{H-NMR}$ (600 MHz, $\text{DMSO-}d_6$): δ (ppm) 1.20-1.30 (m, 3H), 1.30-1.39 (m, 1H), 1.62-1.71 (m, 2H), 1.78-1.84 (m, 1H), 1.94-2.01 (m, 1H), 3.40-3.48 (m, 1H), 3.65-3.73 (m, 1H), 4.82 (s, 1H), 6.82-6.86 (m, 2H), 6.94-6.99 (m, 1H), 7.00-7.08 (m, 4H), 7.17-7.29

(m, 6H), 7.32-7.36 (m, 2H), 8.24 (d, $J = 8.5$ Hz, 1H), 8.40 (br s, 1H), 9.75 (s, 1H). One exchangeable proton signal was not apparent. ¹³C-NMR (150 MHz, DMSO-*d*₆): δ (ppm) 24.2, 31.74, 31.77, 52.1, 56.4, 56.7, 115.8, 115.9 (TFA), 117.9 (TFA), 124.4, 126.2, 126.6, 127.9, 128.15, 128.16, 128.5, 140.1, 140.2, 143.9, 157.1, 158.0 (TFA), 158.2 (TFA), 170.8. **RP-HPLC** (Method A, 220 nm): 98% ($t_R = 14.3$ min, $k = 4.5$). **HRMS** (ESI): m/z [M+H]⁺ calcd. for [C₂₉H₃₀N₃O₃]⁺ 468.2282, found 468.2289. C₂₉H₂₉N₃O₃ × C₂HF₃O₂ (467.57 + 114.02).

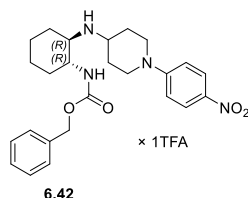


(1*R*,2*R*)-*N*¹-(5-(4-(*tert*-Butoxy)phenyl)oxazol-2-yl)-*N*²-(1-(4-nitrophenyl)piperidin-4-yl)cyclohexane-1,2-diamine bis(hydrotrifluoroacetate) (6.40). (1*R*,2*R*)-*N*¹-(5-(4-(*tert*-Butoxy)phenyl)oxazol-2-yl)cyclohexane-1,2-diamine (**6.33**) (88 mg, 267 μ mol) and 1-(4-nitrophenol)piperidin-4-one (**6.29**) (60 mg, 273 μ mol) were dissolved in CH₂Cl₂ (5 mL). Under stirring, acetic acid (16 μ L, 280 μ mol) and anhydrous Na₂SO₄ were added to the mixture. Then, the mixture was vigorously stirred at rt for 1 h. NaBH(OAc)₃ (228 mg, 1.08 mmol) was added to the reaction mixture and the mixture was stirred at rt for 4 h. After addition of CH₂Cl₂ (50 mL) the reaction mixture was washed with water (2x 50 mL), brine (1x 50 mL) and the organic solvent was dried over Na₂SO₄. The organic solvent was evaporated. Then, the crude product was purified by column chromatography (eluent: CH₂Cl₂/MeOH/NH₃ aq 90:9:1) and, subsequently, by preparative HPLC B (gradient: 0-30 min, A/B 57:43–38:62, $t_R = 8$ min) to give **6.41** as a fluffy bright yellow solid (20.0 mg, 26.3 μ mol, 10%). ¹H-NMR (600 MHz, DMSO-*d*₆): δ (ppm) 1.21-1.36 (m, 12H), 1.36-1.47 (m, 2H), 1.49-1.58 (m, 1H), 1.68-1.82 (m, 3H), 1.93-1.99 (m, 1H), 1.99-2.05 (m, 1H), 2.06-2.13 (m, 1H), 2.21-2.29 (m, 1H), 3.00-3.12 (m, 2H), 3.18-3.25 (m, 1H), 3.55-3.67 (m, 2H), 4.13-4.22 (m, 2H), 6.97-7.00 (m, 2H), 7.04-7.09 (m, 2H), 7.22 (s, 1H), 7.38-7.42 (m, 2H), 7.63 (d, $J = 8.6$ Hz, 1H), 7.96 (br s, 1H, interfering with next listed signal), 8.04-8.07 (m, 2H), 8.78 (br s, 1H). ¹³C-NMR (150 MHz, DMSO-*d*₆): δ (ppm) 23.4, 23.9, 26.2, 27.0, 27.7, 28.5, 31.6, 45.2, 45.4, 51.7, 54.0, 56.4, 78.3, 112.8, 120.6, 123.1, 123.2, 124.0, 125.9, 136.7, 144.0, 153.9, 154.0, 158.1 (q $J = 43.5$ Hz) (TFA), 159.7. **RP-HPLC** (Method A, 220 nm): 95% ($t_R = 16.0$ min, $k = 5.2$). **HRMS** (ESI): m/z [M+H]⁺ calcd. for [C₃₀H₄₀N₅O₄]⁺ 534.3075, found 534.3080. C₃₀H₃₉N₅O₄ × C₄H₂F₆O₄ (533.67 + 228.04).

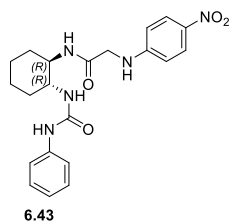


1-((1*R*,2*R*)-2-((1-(4-Nitrophenyl)piperidin-4-yl)amino)cyclohexyl)-3-phenylurea hydrotrifluoroacetate (6.41). 1-((1*R*,2*R*)-2-Aminocyclohexyl)-3-phenylurea (**6.12**) (91 mg, 390 μ mol) and 1-(4-nitrophenol)piperidin-4-one (**6.29**) (91 mg, 413 μ mol) were dissolved in CH₂Cl₂ (5 mL). Under stirring, acetic acid (23 μ L, 402 μ mol) and anhydrous Na₂SO₄ were added to the mixture. Then, the reaction

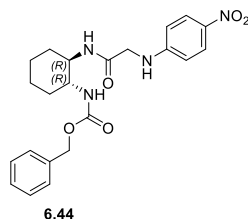
mixture was vigorously stirred at rt for 1 h. $\text{NaBH}(\text{OAc})_3$ (270 mg, 1.27 mmol) was added to the reaction mixture and stirred at rt for 4 h. After addition of CH_2Cl_2 (50 mL) the reaction mixture was washed with water (2x 50 mL), brine (1x 50 mL) and the organic solvent was dried over Na_2SO_4 . Then, the organic solvent was evaporated. The crude product was purified by column chromatography (eluent: $\text{CH}_2\text{Cl}_2/\text{MeOH}/\text{NH}_3$ aq 90:9:1) and, subsequently, by preparative HPLC B (gradient: 0-30 min, A/B 66:34–38:62, $t_R = 8$ min) to give **6.41** as a fluffy bright yellow solid (30.0 mg, 54.4 μmol , 14%). **$^1\text{H-NMR}$** (600 MHz, $\text{DMSO-}d_6$): δ (ppm) 1.21-1.48 (m, 4H), 1.52-1.61 (m, 1H), 1.67-1.79 (m, 3H), 1.86-1.92 (m, 1H), 1.99-2.09 (m, 2H), 2.14-2.20 (m, 1H), 3.01-3.08 (m, 2H), 3.09-3.17 (m, 1H), 3.53-3.60 (m, 1H), 3.60-3.67 (m, 1H), 4.11-4.18 (m, 2H), 6.86-6.90 (m, 1H), 7.00 (d, $J = 8.3$ Hz, 1H), 7.03-7.06 (m, 2H), 7.17-7.44 (m, 2H), 7.40-7.44 (m, 2H), 8.02-8.06 (m, 2H), 8.07-8.15 (m, 1H), 8.70 (br s, 1H), 9.20 (s, 1H). **$^{13}\text{C-NMR}$** (150 MHz, $\text{DMSO-}d_6$): δ (ppm) 23.2, 23.9, 26.3, 27.3, 27.6, 31.9, 45.2, 45.4, 50.7, 52.2, 57.5, 112.8, 116.1 (TFA), 117.7, 118.1 (TFA), 121.3, 125.9, 128.6, 136.7, 140.3, 153.9, 155.9, 158.8 (q, $J = 32.2$ Hz) (TFA). **RP-HPLC** (Method A, 220 nm): 95% ($t_R = 16.7$ min, $k = 5.4$). **HRMS** (ESI): m/z $[\text{M}+\text{H}]^+$ calcd. for $[\text{C}_{24}\text{H}_{32}\text{N}_5\text{O}_3]^+$ 438.2500, found 438.2507. $\text{C}_{24}\text{H}_{31}\text{N}_5\text{O}_3 \times \text{C}_2\text{H}_1\text{F}_3\text{O}_2$ (437.54 + 114.02).



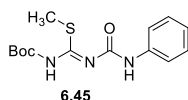
Benzyl ((1*R*,2*R*)-2-((1-(4-nitrophenyl)piperidin-4-yl)amino)cyclohexyl)carbamate hydrotrifluoroacetate (6.42). Benzyl ((1*R*,2*R*)-2-aminocyclohexyl)carbamate (**6.13**) (107 mg, 431 μmol) and 1-(4-nitrophenyl)piperidin-4-one (**6.29**) (93 mg, 422 μmol) were dissolved in CH_2Cl_2 (5 mL). Under stirring, acetic acid (23 μL , 402 μmol) and anhydrous Na_2SO_4 were added to the mixture. Then, the reaction mixture was and vigorously stirred at rt for 1 h. $\text{NaBH}(\text{OAc})_3$ (271 mg, 1.28 mmol) was added to the reaction mixture and stirred at rt for 4 h. After addition of CH_2Cl_2 (50 mL) the reaction mixture was washed with water (2x 50 mL), brine (1x 50 mL) and the organic solvent was dried over Na_2SO_4 . Then, the organic solvent was evaporated. The crude product was purified by column chromatography (eluent: $\text{CH}_2\text{Cl}_2/\text{MeOH}/\text{NH}_3$ aq 90:9:1) and, subsequently, by preparative HPLC A (gradient: 0-30 min, A/B 67:33–38:62, $t_R = 13$ min) to give **6.42** as a fluffy bright yellow solid (22.8 mg, 40.2 μmol , 10%). **$^1\text{H-NMR}$** (600 MHz, $\text{DMSO-}d_6$): δ (ppm) 1.18-1.27 (m, 2H), 1.27-1.42 (m, 2H), 1.48-1.57 (m, 1H), 1.63-1.89 (m, 4H), 1.93-2.05 (m, 2H), 2.16-2.22 (m, 1H), 2.97-3.14 (m, 3H), 3.44-3.52 (m, 1H), 3.53-3.62 (m, 1H), 4.13-4.19 (m, 2H), 4.96 (d, $J = 12.4$ Hz, 1H), 5.12 (d, $J = 12.4$ Hz, 1H), 7.07 (d, $J = 9.6$ Hz, 2H), 7.29-7.33 (m, 1H), 7.34-7.42 (m, 5H), 7.94 (t, $J = 9.5$ Hz, 1H), 8.07 (d, $J = 9.2$ Hz, 2H), 8.76 (br s, 1H). **$^{13}\text{C-NMR}$** (150 MHz, $\text{DMSO-}d_6$): δ (ppm) 23.3, 23.8, 26.3, 27.0, 27.6, 32.0, 45.2, 45.4, 51.8, 51.9, 56.1, 65.7, 112.8, 115.8 (TFA), 117.8 (TFA), 125.9, 127.9, 128.4, 136.7, 153.9, 156.0, 158.11 (q, $J = 32.1$ Hz) (TFA). **RP-HPLC** (Method A, 220 nm): 95% ($t_R = 14.6$ min, $k = 4.6$). **HRMS** (ESI): m/z $[\text{M}+\text{Na}]^+$ calcd. for $[\text{C}_{25}\text{H}_{32}\text{N}_4\text{O}_4\text{Na}]^+$ 475.2316, found 475.2319. $\text{C}_{25}\text{H}_{32}\text{N}_4\text{O}_4 \times \text{C}_2\text{HF}_3\text{O}_2$ (452.56 + 114.02).



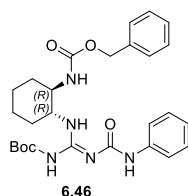
2-((4-Nitrophenyl)amino)-*N*-((1*R*,2*R*)-2-(3-phenylureido)cyclohexyl)acetamide (6.43). 1-((1*R*,2*R*)-2-aminocyclohexyl)-3-phenylurea (**6.12**) (50.0 mg, 214 μ mol) was dissolved in CH₂Cl₂ (8 mL) and DIPEA (73 μ L, 429 μ mol) was added to the mixture. The mixture was stirred at rt for 5 min. Under stirring, succinimidyl (4-nitrophenyl)glycinate (**6.24**) (75.7 mg, 258 μ mol) was added to the reaction mixture and stirred at rt for 2 h. Then, the organic solvent was evaporated, and the crude product was purified by column chromatography (eluent: CH₂Cl₂/MeOH/NH₃ aq 90:9:1) to obtain **6.43** as a yellow solid (45.0 mg, 109 μ mol, 51%). **¹H-NMR** (600 MHz, DMSO-*d*₆): δ (ppm) 1.18-1.32 (m, 4H), 1.61-1.69 (m, 2H), 1.78-1.84 (m, 1H), 1.90-1.95 (m, 1H), 3.40-3.47 (m, 1H), 3.50-3.58 (m, 1H), 3.71-3.81 (m, 2H), 5.94 (d, *J* = 7.8 Hz, 1H), 6.53 (d, *J* = 8.4 Hz, 2H), 6.86 (t, *J* = 7.3 Hz, 1H), 7.16-7.22 (m, 2H), 7.35 (d, *J* = 7.8 Hz, 2H), 7.43 (br s, 1H), 7.81 (d, *J* = 9.2 Hz, 2H), 8.00 (d, *J* = 8.4 Hz, 1H), 8.48 (s, 1H). **¹³C-NMR** (150 MHz, DMSO-*d*₆): δ (ppm) 24.3, 24.5, 31.9, 32.7, 45.8, 52.3, 52.4, 111.1, 117.3, 120.9, 125.9, 128.6, 136.2, 140.5, 154.4, 155.1, 168.1. **RP-HPLC** (Method A, 220 nm): 98% (*t*_R = 15.5 min, *k* = 5.0). **HRMS** (ESI): *m/z* [M+H]⁺ calcd. for [C₂₁H₂₆N₅O₄]⁺ 412.1979, found 412.1985. C₂₁H₂₅N₅O₄ (411.46).



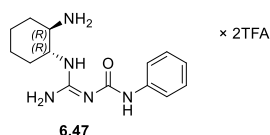
Benzyl ((1*R*,2*R*)-2-(2-((4-nitrophenyl)amino)acetamido)cyclohexyl)carbamate (6.44). Benzyl ((1*R*,2*R*)-2-aminocyclohexyl)carbamate (**6.13**) (44.0 mg, 177 μ mol) was dissolved in DMF (400 μ L) and DIPEA (100 μ L, 588 μ mol) was added to the mixture. Then, the reaction mixture was stirred at rt for 5 min. Under stirring, succinimidyl (4-nitrophenyl)glycinate (**6.24**) (65 mg, 22 μ mol) was added to the mixture and the reaction mixture was stirred at rt for 2 h. The mixture was purified by preparative HPLC B (gradient: 0-30 min, A/B 67:33–47:53, *t*_R = 7 min) to give **6.44** as a fluffy bright yellow solid (9.4 mg, 22 μ mol, 12%). **¹H-NMR** (600 MHz, DMSO-*d*₆): δ (ppm) 1.13-1.28 (m, 4H), 1.59-1.68 (m, 2H), 1.76-1.85 (m, 2H), 3.23-3.31 (m, 1H), 3.50-3.58 (m, 1H), 3.64-3.79 (m, 2H), 4.87-4.99 (m, 2H), 6.59 (d, *J* = 8.3 Hz, 2H), 7.04 (d, *J* = 8.6 Hz, 1H), 7.24-7.37 (m, 5H), 7.44 (t, *J* = 5.9 Hz, 1H), 7.89 (d, *J* = 8.3 Hz, 1H), 7.96 (d, *J* = 9.4 Hz, 2H). **¹³C-NMR** (150 MHz, DMSO-*d*₆): δ (ppm) 24.3, 24.4, 31.8, 32.0, 45.7, 52.3, 53.7, 65.1, 111.2, 125.9, 127.5, 127.7, 128.3, 136.2, 137.2, 154.3, 155.9, 168.2. **RP-HPLC** (Method A, 220 nm): 97% (*t*_R = 17.7 min, *k* = 5.8). **HRMS** (ESI): *m/z* [M+H]⁺ calcd. for [C₂₂H₂₇N₄O₅]⁺ 427.1976, found 427.1980. C₂₂H₂₆N₄O₅ (426.47).



***N*-tert-Butoxycarbonyl-*N'*-[phenyl]aminocarbonyl-*S*-methylisothiourea (6.45).** *N*-Boc-*S*-methylisothiourea (**2.35**) (1.16 g, 6.10 mmol) was dissolved in CH₂Cl₂ (20 mL) and stirred at 0 °C. Under stirring, isocyanatobenzene (0.75 mL, 6.93 mmol) in CH₂Cl₂ (5 mL) was added dropwise to the reaction mixture. Then, the reaction mixture was allowed to warm up to rt and stirred overnight. The organic solvent was evaporated, and the residue was dissolved in CH₂Cl₂ and evaporated (2x). The crude product was purified by column chromatography (eluent: CH₂Cl₂) to give **6.45** as a white solid (1.03 g, 3.33 mmol, 55%). **¹H-NMR** (300 MHz, DMSO-*d*₆): δ (ppm) 1.46 (s, 9H), 2.40 (s, 3H), 6.99-7.08 (m, 1H), 7.23-7.35 (m, 2H), 7.59-7.67 (m, 2H), 9.87 (s, 1H), 12.05 (s, 1H). **¹³C-NMR** (75 MHz, DMSO-*d*₆): δ (ppm) 13.8, 27.6, 82.4, 119.2, 123.0, 128.6, 139.0, 150.1, 159.3, 166.0. **HRMS** (ESI): *m/z* [M+Na]⁺ calcd. for [C₁₄H₁₉N₃O₃SNa]⁺ 332.1039, found 332.1044. C₁₄H₁₉N₃O₃S (309.38).

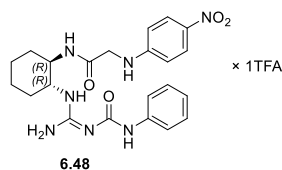


Benzyl ((1*R*,2*R*)-2-(3-(2-*tert*-butoxycarbonyl)(phenylcarbamoyl)guanidino)cyclohexyl)carbamate (6.46). Benzyl ((1*R*,2*R*)-2-aminocyclohexyl)carbamate (**6.13**) (0.35 g, 1.41 mmol) and *N*-*tert*-butoxycarbonyl-*N'*-[benzene]aminocarbonyl-*S*-methylisothiourea (**6.45**) (0.49 g, 1.58 mmol) were dissolved in CH₂Cl₂ (10 mL). Under stirring, HgCl₂ (0.57 g, 2.10 mmol) and DIPEA (0.60 mL, 3.53 mmol) were added and the mixture was stirred at rt for 4 h. The solid was separated by filtration and the filtrate was evaporated. The crude product was purified by column chromatography (eluent: light petroleum/ethyl acetate 5:1) to give **6.46** as an oil (0.36 g, 70.6 μmol, 50%). **¹H-NMR** (400 MHz, DMSO-*d*₆): δ (ppm) 1.22-1.34 (m, 4H), 1.41-1.46 (m, 9H, due two slow rotation of C-N bond of Boc group two inferring signals (singulets) were evident in the spectra), 1.59-1.75 (m, 2H), 1.78-1.92 (m, 1H), 2.09-2.14 (m, 1H), 3.37-3.51 (m, 1H), 3.73-3.93 (m, 1H), 4.90 (d, *J* = 12.9 Hz, 1H), 5.11 (d, *J* = 12.9 Hz, 1H), 6.91-6.97 (m, 1H), 7.20-7.39 (m, 8H), 7.58 (d, *J* = 7.8 Hz, 2H), 7.97-8.14 (m, 1H), 9.20 (s, 1H), 12.17 (s, 1H). **¹³C-NMR** (151 MHz, DMSO-*d*₆): δ (ppm) 24.3, 27.6, 28.1, 30.7, 31.5, 53.8, 64.9, 82.4, 118.7, 121.9, 127.0, 127.3, 127.5, 128.2, 128.4, 128.8, 137.4, 140.1, 152.1, 155.9, 162.5. **HRMS** (ESI): *m/z* [M+Na]⁺ calcd. for [C₂₇H₃₅N₅O₅Na]⁺ 532.2530, found 532.2534. C₂₇H₃₅N₅O₅ (509.61).



1-(Amino(((1*R*,2*R*)-2-aminocyclohexyl)amino)methylene)-3-phenylurea bis(hydrotrifluoroacetate) (6.47). Compound **6.46** (173 mg, 0.339 mmol) was dissolved in MeOH (10 mL) and palladium on activated charcoal (Pd/C) (30 mg) was added. A constant stream of hydrogen (H₂) was bubbled through the reaction mixture at rt for 1 h. The catalyst Pd/C was removed by filtration and the organic solvent was evaporated. The residue was dissolved in CH₂Cl₂ (5 mL) and stirred under ice bath cooling.

Under stirring, TFA (5 mL) was dropped into the reaction mixture. The organic solvent was evaporated and CH₂Cl₂ (10 mL) was added. Then, the organic solvent was evaporated and the crude product was purified by preparative HPLC B (gradient: 0-30 min, A/B 71:29–38:62, *t_R* = 14 min) to give **6.47** as a fluffy white solid (34.5 mg, 68.5 μmol, 20%). **¹H-NMR** (600 MHz, DMSO-*d*₆): δ (ppm) 1.22-1.48 (m, 4H), 1.67-1.77 (m, 2H), 1.92-1.99 (m, 1H), 2.01-2.07 (m, 1H), 3.17-3.30 (m, 1H), 3.67-3.78 (m, 1H), 7.06-7.18 (m, 1H), 7.35 (t, *J* = 7.5 Hz, 2H), 7.47 (d, *J* = 7.5 Hz, 2H), 8.13 (s, 3H), 8.68 (s, 2H), 9.04 (s, 1H), 10.09 (s, 1H), 10.77 (s, 1H). **¹³C-NMR** (150 MHz, DMSO-*d*₆): δ (ppm) 23.0, 23.5, 29.5, 31.1, 52.4, 52.9, 117.0 (q, *J* = 298.2 Hz) (TFA), 119.7, 124.0, 129.0, 137.5, 151.6, 153.7, 159.1 (q, *J* = 32.1 Hz) (TFA). **RP-HPLC** (Method A, 220 nm): 98% (*t_R* = 8.0 min, *k* = 2.1). **HRMS** (ESI): *m/z* [M+H]⁺ calcd. for [C₁₄H₂₂N₅O]⁺ 276.1819, found 276.1822. C₁₄H₂₁N₅O × C₄H₂F₆O₄ (275.36 + 228.04).



2-((4-Nitrophenyl)amino)-*N*-((1*R*,2*R*)-2-(2-(phenylcarbamoyl)guanidino)cyclohexyl)acetamide hydrotrifluoroacetate (6.48). 1-(Amino(((1*R*,2*R*)-2-aminocyclohexyl)amino)methylene)-3-phenylurea bis(hydrotrifluoroacetate) (**6.47**) (32.65 mg, 64.86 μmol) was dissolved in DMSO (1 mL) and DIPEA (37 μL, 212 μmol) was added. Under stirring, succinimidyl (4-nitrophenyl)glycinate (**6.24**) (25.73 mg, 87.74 μmol) was added to the reaction mixture. The reaction mixture was shaken in a microcentrifuge tube (1.5 mL) at rt for 2 h. The crude product was purified by preparative HPLC B (gradient: 0-30 min, A/B 71:29–38:62, *t_R* = 14 min) to give **6.48** as a fluffy bright yellow solid (14.79 mg, 26.06 μmol, 40%). **¹H-NMR** (600 MHz, DMSO-*d*₆): δ (ppm) 1.21-1.40 (m, 4H), 1.62-1.72 (m, 2H), 1.77-1.85 (m, 1H), 1.92-2.00 (m, 1H), 3.48-3.59 (m, 1H), 3.70-3.85 (m, 3H), 6.51-6.64 (m, 2H), 7.10 (t, *J* = 7.20 Hz, 1H), 7.33 (t, *J* = 7.6 Hz, 2H), 7.38-7.55 (m, 3H), 7.94 (d, *J* = 9.0 Hz, 2H), 8.10 (d, *J* = 8.2 Hz, 1H), 8.54 (br s, 2H), 8.71-8.80 (m, 1H), 9.89 (s, 1H), 10.20 (br s, 1H). **¹³C-NMR** (150 MHz, DMSO-*d*₆): δ (ppm) 23.7, 24.0, 31.1, 31.6, 45.8, 51.2, 54.4, 111.0, 116.1 (TFA), 118.1 (TFA), 119.7, 123.9, 125.8, 128.9, 136.4, 137.4, 151.5, 153.1, 154.3, 159.1 (q, *J* = 31.7 Hz) (TFA), 168.8. **RP-HPLC** (Method A, 220 nm): 99% (*t_R* = 12.9 min, *k* = 4.0). **HRMS** (ESI): *m/z* [M+H]⁺ calcd. for [C₂₂H₂₈N₇O₄]⁺ 454.2197, found 454.2202. C₂₂H₂₇N₇O₄ × C₂HF₃O₂ (453.50 + 114.02).

6.4.3. X-Ray crystallography of compounds (*R,R,S*)-**6.6b** and (*R*)-**6.17**

6.4.3.1. X-Ray crystallography of compounds (*R,R,S*)-**6.6b**

Single clear yellow prism crystals of (*R,R,S*)-**6.6b** were obtained according to following procedure: the TFA salt of (*R,R,S*)-**6.6b** (15 mg) was dissolved in methanol (2 mL) and HCl in methanol (TCI, Eschborn, Germany; 5-10%; 3 mL) was added and the volatiles were evaporated (4x). The obtained residue was dried in vacuo and dissolved in methanol (1 mL). The solution was allowed to slowly concentrate at ambient temperature.

Table 6.4. Crystal data and structure refinement of (*R,R,S*)-**6.6b**

Formula	C ₂₄ H ₃₂ ClN ₅ O ₃	Z	2
$D_{calc.} / \text{g cm}^{-3}$	1.289	Z'	1
μ / mm^{-1}	1.222	Wavelength/Å	1.39222
Formula Weight	473.99	Radiation type	Cu K β
Colour	clear yellow	$\Theta_{min} / ^\circ$	3.818
Shape	plate	$\Theta_{max} / ^\circ$	58.863
Size / mm ³	0.18x0.15x0.06	Measured Refl.	30702
T / K	122.96(11)	Independent Refl.	4660
Crystal System	monoclinic	Reflections Used	4310
Flack Parameter	-0.005(6)	R_{int}	0.0427
Hooft Parameter	-0.009(6)	Parameters	298
Space Group	P2 ₁	Restraints	1
a / Å	5.5823(2)	Largest Peak	0.215
b / Å	15.1245(4)	Deepest Hole	-0.194
c / Å	14.5029(4)	Goof	1.072
$\alpha / ^\circ$	90	wR ₂ (all data)	0.0732
$\beta / ^\circ$	94.173(2)	wR ₂	0.0707
$\gamma / ^\circ$	90	R ₁ (all data)	0.0366
V / Å ³	1221.23(6)	R ₁	0.0317

A suitable crystal (0.18x0.15x0.06) mm³ was selected and mounted on a MiTeGen holder (Jena Bioscience, Jena, Germany) with oil using a GV1000 diffractometer (Agilent Technologies, Santa Clara, USA) with Titan S2 CCD detector. The crystal was kept at $T = 122.96(11)$ K during data collection. The structure was solved with the ShelXT⁴¹ solution program using the intrinsic phasic methods and by using Olex2⁴² as the graphical interface. The model was refined with ShelXL⁴³ (version 2016/6) using full matrix least squares minimization.

Data were measured using ω scans and Cu K β radiation. The total number of runs and images was based on the strategy calculation from the program CrysAlisPro (Agilent Technologies). The maximum resolution that was achieved was $\Theta = 58.863$. Cell parameters were retrieved using the CrysAlisPro

(Agilent Technologies) software and refined using CrysAlisPro (Agilent Technologies) on 13758 reflections, 45% of the observed reflections. Data reduction was performed using the CrysAlisPro (Agilent Technologies) software, which corrects for Lorentz polarisation. The final completeness is 99.90% out to 58.863° in Θ . The absorption coefficient μ of this material is 1.222 mm⁻¹ at this wavelength ($\lambda = 1.39222$) and the minimum and maximum transmissions are 0.823 and 1.000. The Flack parameter was refined to -0.005(6). Determination of absolute structure using Bayesian statistics on Bijvoet differences using the Olex2 results in -0.009(6).

Crystal data of (*R,R,S*)-**6.6b** see 8.5.3.1.: Fractional atomic coordinates ($\times 10^4$) and equivalent isotropic displacement parameters ($\text{\AA}^2 \times 10^3$) for (*R,R,S*)-**6.6a**. U_{eq} is defined as 1/3 of the trace of the orthogonalised U_{ij} (cf. Table 8.3). Anisotropic displacement parameters ($\times 10^4$) for (*R,R,S*)-**6.6a**. The anisotropic displacement factor exponent takes the form: $-2\pi^2[h^2a^{*2} \times U_{11} + \dots + 2hka^* \times b^* \times U_{12}]$ (cf. Table 8.4). Bond lengths in \AA for (*R,R,S*)-**6.6a** (cf. Table 8.5). Bond angles in ° for (*R,R,S*)-**6.6a** (cf. Table 8.6) and hydrogen fractional atomic coordinates ($\times 10^4$) and equivalent isotropic displacement parameters ($\text{\AA}^2 \times 10^3$) for (*R,R,S*)-**6.6a**. U_{eq} is defined as 1/3 of the trace of the orthogonalised U_{ij} (cf. Table 8.7).

6.4.3.2. X-Ray crystallography of (*R*)-**6.17**

Single clear yellow prism crystals of (*R*)-**6.17** were obtained according to following procedure: cf. 6.4.2. synthesis protocols and analytical data

Table 6.5. Crystal data and structure refinement of (*R*)-**6.17**

Formula	C ₁₂ H ₁₆ N ₂ O ₅ S	Z	2
$D_{calc} / \text{g cm}^{-3}$	1.421	Z'	1
μ / mm^{-1}	2.258	Wavelength/ \AA	1.54184
Formula Weight	300.33	Radiation type	Cu K α
Colour	clear yellow	$\theta_{min} / ^\circ$	3.461
Shape	prism	$\theta_{max} / ^\circ$	76.344
Size / mm ³	0.29×0.11×0.10	Measured Refl.	8519
T / K	294(4)	Independent Refl.	2888
Crystal System	monoclinic	Refl's with I > 2(I)	2761
Flack Parameter	-0.004(8)	R_{int}	0.0180
Hooft Parameter	-0.006(6)	Parameters	183
Space Group	$P2_1$	Restraints	1
a / \AA	5.32850(10)	Largest Peak	0.130
b / \AA	10.3138(3)	Deepest Hole	-0.125

Table 6.5 continued.

$c / \text{\AA}$	12.9123(4)	Goof	1.039
$\alpha / ^\circ$	90	wR_2 (all data)	0.0800
$\beta / ^\circ$	98.477(3)	wR_2	0.0782
$\gamma / ^\circ$	90	R_1 (all data)	0.0294
$V / \text{\AA}^3$	701.87(3)	R_1	0.0279

A suitable crystal with dimensions (0.29×0.11×0.10) mm³ was selected and mounted on a MiTeGen holder (Jena Bioscience) with oil using a SuperNova diffractometer (Agilent Technologies) with Atlas CCD detector. The crystal was kept at a $T = 294(4)$ K during data collection. The structure was solved with the ShelXT⁴¹ solution program using dual methods and by using Olex2⁴² as the graphical interface. The model was refined with ShelXL⁴³ (version 2018/3) using full matrix least squares minimization on F^2 .

Data were measured using ω scans and Cu K α radiation. The diffraction pattern was indexed and the total number of runs and images was based on the strategy calculation from the program CrysAlisPro 1.171.41.47a (Rigaku Europe, Neu-Isenburg, Germany). The maximum resolution that was achieved was $\theta = 76.344^\circ$. The diffraction pattern was indexed and the total number of runs and images was based on the strategy calculation from the program CrysAlisPro 1.171.41.47a (Rigaku Europe). The unit cell was refined using CrysAlisPro 1.171.41.47a (Rigaku Europe) on 5092 reflections, 60% of the observed reflections. Data reduction, scaling and absorption corrections were performed using CrysAlisPro 1.171.41.47a (Rigaku Europe). The final completeness is 99.90% out to 76.344° in θ . A gaussian absorption correction was performed using CrysAlisPro 1.171.41.47a (Rigaku Europe). The absorption coefficient μ of this material is 2.258 mm⁻¹ at this wavelength ($\lambda = 1.54184 \text{ \AA}$) and the minimum and maximum transmissions are 0.699 and 1.000. The Flack parameter was refined to -0.004(8). Determination of absolute structure using Bayesian statistics on Bijvoet differences using the Olex2 results in -0.006(6).

Crystal data of (R)-**6.17** see 8.5.3.2.: Fractional atomic coordinates ($\times 10^4$) and equivalent isotropic displacement parameters ($\text{\AA}^2 \times 10^3$) for (R)-**6.17**. U_{eq} is defined as 1/3 of the trace of the orthogonalised U_{ij} (cf. Table 8.8), anisotropic displacement parameters ($\times 10^4$) for (R)-**6.17**. The anisotropic displacement factor exponent takes the form: $-2\pi^2[h^2a^{*2} \times U_{11} + \dots + 2hka^* \times b^* \times U_{12}]$ (cf. Table 8.9), bond lengths in \AA for (R)-**6.17** (cf. Table 8.10), bond angles in $^\circ$ for (R)-**6.17** (cf. Table 8.11), torsion angles in $^\circ$ for (R)-**6.17** (cf. Table 8.12) and hydrogen fractional atomic coordinates ($\times 10^4$) and equivalent isotropic displacement parameters ($\text{\AA}^2 \times 10^3$) for (R)-**6.17**. U_{eq} is defined as 1/3 of the trace of the orthogonalised U_{ij} (cf. Table 8.13).

6.4.4. Pharmacological methods: cell culture, radioligand competition binding assay in CHO-hY₄R-G_{qi5}-mtAEQ cells, aequorin Ca²⁺ assay, ethidium bromide/acridine orange staining (live/dead staining)

6.4.4.1. Cell culture

Cultivation of CHO-hY₄R-G_{qi5}-mtAEQ cells was performed according to literature.⁵ CHO-hY₄R-G_{qi5}-mtAEQ cells were cultivated in nutrient mixture Ham's F12 medium (Sigma Aldrich) at 37 °C in a water saturated atmosphere containing 5% CO₂. Ham's F12 medium was supplemented with G418 (Merck Biochrom; 400 µg/mL), hygromycin (InvivoGen, San Diego, USA; 250 µg/mL), zeocin (InvivoGen, San Diego, USA; 250 µg/mL) and 10% (v/v) FCS (Merck Biochrom, Darmstadt, Germany).

Routinely performed examinations for mycoplasma contamination using the Venor GeM Mycoplasma Detection Kit (Minerva Biolabs, Berlin, Germany) were negative for all cell types.

6.4.4.2. Radioligand competition binding assay in CHO-hY₄R-G_{qi5}-mtAEQ cells

The synthesis of [³H]UR-KK200 ($C_{\text{final}} = 1.0$ nM, $K_d = 0.67$ nM) was described previously.²⁰ The equilibrium competition binding experiments were performed in intact CHO-hY₄R-G_{qi5}-mtAEQ cells as described in the literature.²⁰

On the day of the experiment cells were scraped off the culture flask, resuspended in sodium-free buffer (25 mM HEPES, 2.5 mM CaCl₂, 1 mM MgCl₂, pH 7) containing 1% BSA and 0.1 mg/mL of bacitracin and a density of 500,000 cells/mL was adjusted. Increasing concentrations (10-fold concentrated compared to final assay concentration) of investigated ligands (20 µL) were added to the Primaria 96-well plate (Corning Life Science, Oneonta, USA). The radioligand solution (10-fold concentrated compared to $C_{\text{final}} = 1$ nM) was added in every well and subsequently 160 µL of the prepared cell suspension (500,000 cells/mL) was added. All dilutions of radio- and investigated ligands were prepared in sodium-free buffer (25 mM HEPES, 2.5 mM CaCl₂, 1 mM MgCl₂, pH 7) containing 1% BSA and 0.1 mg/mL of bacitracin. After incubation at rt for 90 min, the bound and free radioligand ([³H]UR-KK200) were separated by filtration through glass microfiber filters (GF/C filters) (Whatman, Maidstone, UK) by use of Brandel Harvester (Brandel, Gaithersburg, USA). Before use, the GF/C filters were treated with 0.3% polyethyleneimine solution for 20 min. The filter was stamped out (every well) and transferred to a 96-well plate 1450-401 (Perkin-Elmer, Rodgau, Germany). Before measuring the radioactivity (dpm) with a MicroBeta2 plate counter (Perkin-Elmer, Rodgau, Germany), 200 µl of a scintillation cocktail (Rotiscint eco plus) was added and the plates were shaken in the dark for at least 3 h.

Non-specific binding was determined in the presence of a 200-fold excess of hPP and total binding in buffer (At least one triplicate of non-specific and total binding was determined on every plate).

6.4.4.3. Aequorin Ca²⁺ assay

The aequorin Ca²⁺ assay was performed in CHO-hY₄R-G_{qi5}-mtAEQ cells as described in literature⁵ with minor modifications: on the day of the experiment the CHO-hY₄R-G_{qi5}-mtAEQ cells were scraped from

the culture flask rather than trypsination. The studied compounds (at a final concentration of 30 μM) were incubated with CHO-hY₄R-G_{q15}-mtAEQ cells for 30 min.

The procedure was as follows: on the same day of the experiment, CHO-hY₄R-G_{q15}-mtAEQ cells were scraped of the culture flask and resuspended in loading buffer (120 mM NaCl, 5 mM KCl, 2 mM MgCl₂, 1.5 mM CaCl₂, 25 mM HEPES and 10 glucose, pH 7.4). A density of $1 \cdot 10^7$ cells/mL was adjusted and coelenterazine h (Biotrend, Köln, Germany; c = 1 mM in methanol) was added ($c_{\text{final}} = 2 \mu\text{M}$) followed by incubation in the dark for 2 h. The cell suspension was diluted with loading buffer (120 mM NaCl, 5 mM KCl, 2 mM MgCl₂, 1.5 mM CaCl₂, 25 mM HEPES and 10 glucose, pH 7.4) containing 1% BSA and 0.1 mg/mL of bacitracin to obtain a cell density of 500,000 cells/mL and the cell suspension was kept under gentle stirring in the dark for further 3 h. Then, ligands (*R,R,S*)-**6.6b**, (*R,R,S**)-**6.7b**, niclosamide (**6.10**) or **6.36** ($c_{\text{final}} = 30 \mu\text{M}$) were added to the cell suspension, followed by incubation under gentle stirring in the dark for 30 min. This suspension (162 μL) was added (with injection unit of GENios Pro plate reader) to increasing concentrations of hPP (18 μL) in a white 96-well plate (Greiner Bio-One, Frickenhausen, Germany). The luminescence was recorded for 43 s, before adding (with injection unit) 20 μL of a 1% Triton-X-100 solution (the luminescence was recorded for additional 22 s). Dilutions of compounds (*R,R,S*)-**6.6b**, (*R,R,S**)-**6.7b**, niclosamide (**6.10**), **6.36** and hPP were prepared in buffer (120 mM NaCl, 5 mM KCl, 2 mM MgCl₂, 1.5 mM CaCl₂, 25 mM HEPES and 10 glucose, pH 7.4) containing 1% BSA and 0.1 mg/mL of bacitracin.

On every experiment day (*R,R,S*)-**6.6b**, (*R,R,S**)-**6.7b**, niclosamide (**6.10**) and **6.36** were investigated in a concentration of 30 μM without hPP. Additionally, a dose response curve of hPP (0.5% DMSO) was investigated in the absence of (*R,R,S*)-**6.6b**, (*R,R,S**)-**6.7b**, niclosamide (**6.10**) and **6.36**. The plates were measured using a GENios Pro (Tecan, Grödig, Austria) plate reader.

6.4.4.4. Ethidium bromide/acridine orange staining (live/dead staining)

On the same day of the experiment, CHO-hY₄R-G_{q15}-mtAEQ cells were detached by trypsinization and resuspended in buffer (120 mM NaCl, 5 mM KCl, 2 mM MgCl₂, 1.5 mM CaCl₂, 25 mM HEPES and 10 glucose, pH 7.4) containing 5% FCS and 0.1 mg/mL of bacitracin. The cell density was adjusted to 500,000 cells/mL. The CHO-hY₄R-G_{q15}-mtAEQ cells were incubated with compounds **2.68**, (*R,R,S*)-**6.6b**, (*R,R,S**)-**6.7b** and niclosamide (**6.10**) (each 30 μM , 2 mL) in the dark for 30 min. A cell suspension, which contained the same amount of DMSO served as control. Then, the cell suspensions were resuspended in PBS (1 mL) and 200 μL of ethidium bromide/acridine orange solution (50 $\mu\text{g/mL}$ ethidium bromide and 50 $\mu\text{g/mL}$ acridine orange in PBS) was added for staining (the solutions were incubated in the dark for 10 min). The cell viability was determined with an Olympus BH-2 microscope (Olympus, Hamburg, Germany) with a planachromat 10x objective (Olympus; NA 0.25), filter (Fluorescein, Olympus) and a DCM-510 ocular microscope camera (OCS.tec, Neuching, Germany). Following software was used: ScopePhoto 3.0 (ScopeTeck, Hangzhou, Zhejiang Province, PR China)

6.4.5. Data analysis

The retention factor k was calculated according to the following equation: $k = (t_R - t_0)/t_0$ (t_R = retention time; t_0 = dead time).

Data obtained from aequorin Ca²⁺ assay were processed following literature⁵ procedures: the area under the curve (AUC) of emitted luminescence peak, caused by agonist hPP, and emitted luminescence caused by unloading the remaining aequorin by cell lysis (addition of Triton X solution) were determined using Sigma Plot 12.5 (Systat Software, Chicago, USA). The fractional luminescence was normalized (100% = fractional bioluminescence obtained from 1 μM hPP, 0% = basal effect in the absence of hPP, GraphPad Prism 8.0). Relative responses were plotted as % against log(hPP) and analyzed by four-parameter logistic fits (GraphPad Prism version 8.0) to obtain pEC₅₀ values. Efficacies α were calculated from the maximum response relative to 1 μM hPP ($\alpha = 1$).

6.5. References

1. Lundell, I.; Blomqvist, A. G.; Berglund, M. M.; Schober, D. A.; Johnson, D.; Statnick, M. A.; Gadski, R. A.; Gehlert, D. R.; Larhammar, D. Cloning of a human receptor of the NPY receptor family with high affinity for pancreatic polypeptide and peptide YY. *J Biol Chem* **1995**, *270*, 29123-29128.
2. Zhang, L.; Bijker, M. S.; Herzog, H. The neuropeptide Y system: Pathophysiological and therapeutic implications in obesity and cancer. *Pharmacol. Ther.* **2011**, *131*, 91-113.
3. Yulyaningsih, E.; Zhang, L.; Herzog, H.; Sainsbury, A. NPY receptors as potential targets for anti-obesity drug development. *Br. J. Pharmacol.* **2011**, *163*, 1170-1202.
4. Keller, M.; Kaske, M.; Holzammer, T.; Bernhardt, G.; Buschauer, A. Dimeric argininamide-type neuropeptide Y receptor antagonists: Chiral discrimination between Y₁ and Y₄ receptors. *Bioorg. Med. Chem.* **2013**, *21*, 6303-6322.
5. Ziemek, R.; Schneider, E.; Kraus, A.; Cabrele, C.; Beck-Sickinger, A. G.; Bernhardt, G.; Buschauer, A. Determination of Affinity and Activity of Ligands at the Human Neuropeptide Y Y₄ Receptor by Flow Cytometry and Aequorin Luminescence. *J. Recept. Signal Transduct. Res.* **2007**, *27*, 217-233.
6. Kang, N.; Wang, X.-L.; Zhao, Y. Discovery of small molecule agonists targeting neuropeptide Y₄ receptor using homology modeling and virtual screening. *Chem Biol Drug Des* **2019**, *94*, 2064-2072.
7. Sun, C.; Ewing, W. R.; Bolton, S. A.; Gu, Z.; Huang, Y.; Murugesan, N.; Zhu, Y. Substituted adipic acid amides and uses thereof. WO 2012/125622 A1, 2012.
8. Ewing, W. R.; Zhu, Y.; Sun, C.; Huang, Y.; Sivasamban, M.; Karatholuvhu. Diaminocyclohexane compounds and uses thereof. US 2013/0184262 A1, 2013.
9. Ewing, W. R.; Zhu, Y.; Sun, C.; Huang, Y.; Sivasamban, M.; Karatholuvhu; Bolton, S. A.; Pasunoori, L.; Mandal, S. K.; Sher, P. M. Diaminocyclohexane compounds and uses thereof. US 2013/0184284 A1, 2013.
10. Sliwoski, G.; Schubert, M.; Stichel, J.; Weaver, D.; Beck-Sickinger, A. G.; Meiler, J. Discovery of Small-Molecule Modulators of the Human Y₄ Receptor. *PLOS ONE* **2016**, *11*, e0157146.
11. Schubert, M.; Stichel, J.; Du, Y.; Tough, I. R.; Sliwoski, G.; Meiler, J.; Cox, H. M.; Weaver, C. D.; Beck-Sickinger, A. G. Identification and Characterization of the First Selective Y₄ Receptor Positive Allosteric Modulator. *J. Med. Chem.* **2017**, *60*, 7605-7612.
12. Balasubramaniam, A.; Mullins, D. E.; Lin, S.; Zhai, W.; Tao, Z.; Dhawan, V. C.; Guzzi, M.; Knittel, J. J.; Slack, K.; Herzog, H.; Parker, E. M. Neuropeptide Y (NPY) Y₄ Receptor Selective Agonists Based on NPY(32-36): Development of an Anorectic Y₄ Receptor Selective Agonist with Picomolar Affinity. *J. Med. Chem.* **2006**, *49*, 2661-2665.
13. Sainsbury, A.; Shi, Y.-C.; Zhang, L.; Aljanova, A.; Lin, Z.; Nguyen, A. D.; Herzog, H.; Lin, S. Y₄ receptors and pancreatic polypeptide regulate food intake via hypothalamic orexin and brain-derived neurotrophic factor dependent pathways. *Neuropeptides* **2010**, *44*, 261-268.
14. Kaske, M. In Search for Potent and Selective NPY Y₄ Receptor Ligands: Acylguanidines, Argininamides and Peptide Analogs. PhD Thesis, University of Regensburg, 2012.

15. Wootten, D.; Christopoulos, A.; Sexton, P. M. Emerging paradigms in GPCR allostery: implications for drug discovery. *Nat. Rev. Drug Discov.* **2013**, *12*, 630-644.
16. Christopoulos, A. Advances in G Protein-Coupled Receptor Allostery: From Function to Structure. *Mol. Pharmacol.* **2014**, *86*, 463.
17. Xie, X.; Cai, G.; Ma, D. CuI/I-Proline-Catalyzed Coupling Reactions of Aryl Halides with Activated Methylene Compounds. *Org. Lett.* **2005**, *7*, 4693-4695.
18. Parikh, J. R.; Doering, W. v. E. Sulfur trioxide in the oxidation of alcohols by dimethyl sulfoxide. *J. Am. Chem. Soc.* **1967**, *89*, 5505-5507.
19. van Leusen, A. M.; Hoogenboom, B. E.; Siderius, H. A novel and efficient synthesis of oxazoles from tosylmethylisocyanide and carbonyl compounds. *Tetrahedron Lett.* **1972**, *13*, 2369-2372.
20. Kuhn, K. K.; Ertl, T.; Dukorn, S.; Keller, M.; Bernhardt, G.; Reiser, O.; Buschauer, A. High Affinity Agonists of the Neuropeptide Y (NPY) Y₄ Receptor Derived from the C-Terminal Pentapeptide of Human Pancreatic Polypeptide (hPP): Synthesis, Stereochemical Discrimination, and Radiolabeling. *J. Med. Chem.* **2016**, *59*, 6045-6058.
21. Dukorn, S.; Littmann, T.; Keller, M.; Kuhn, K.; Cabrele, C.; Baumeister, P.; Bernhardt, G.; Buschauer, A. Fluorescence- and Radiolabeling of [Lys⁴,Nle^{17,30}]hPP Yields Molecular Tools for the NPY Y₄ Receptor. *Bioconjug. Chem.* **2017**, *28*, 1291-1304.
22. Huang, W.; Manglik, A.; Venkatakrisnan, A. J.; Laeremans, T.; Feinberg, E. N.; Sanborn, A. L.; Kato, H. E.; Livingston, K. E.; Thorsen, T. S.; Kling, R. C.; Granier, S.; Gmeiner, P.; Husbands, S. M.; Traynor, J. R.; Weis, W. I.; Steyaert, J.; Dror, R. O.; Kobilka, B. K. Structural insights into μ -opioid receptor activation. *Nature* **2015**, *524*, 315-321.
23. Liu, W.; Chun, E.; Thompson, A. A.; Chubukov, P.; Xu, F.; Katritch, V.; Han, G. W.; Roth, C. B.; Heitman, L. H.; IJzerman, A. P.; Cherezov, V.; Stevens, R. C. Structural Basis for Allosteric Regulation of GPCRs by Sodium Ions. *Science* **2012**, *337*, 232-236.
24. Miller-Gallacher, J. L.; Nehmé, R.; Warne, T.; Edwards, P. C.; Schertler, G. F. X.; Leslie, A. G. W.; Tate, C. G. The 2.1 Å Resolution Structure of Cyanopindolol-Bound β_1 -Adrenoceptor Identifies an Intramembrane Na⁺ Ion that Stabilises the Ligand-Free Receptor. *PLOS ONE* **2014**, *9*, e92727.
25. Li, Y.; Li, P.-K.; Roberts, M. J.; Arend, R. C.; Samant, R. S.; Buchsbaum, D. J. Multi-targeted therapy of cancer by niclosamide: A new application for an old drug. *Cancer Lett.* **2014**, *349*, 8-14.
26. Deitrick, J.; Pruitt, W. M. Chapter Two - Wnt/ β Catenin-Mediated Signaling Commonly Altered in Colorectal Cancer. In *Progress in Molecular Biology and Translational Science*, Pruitt, K., Ed. Academic Press: 2016; Vol. 144, pp 49-68.
27. Liu, K.; Liu, P. C.; Liu, R.; Wu, X. Dual AO/EB staining to detect apoptosis in osteosarcoma cells compared with flow cytometry. *Med Sci Monit Basic Res* **2015**, *21*, 15-20.
28. Yang, Z.; Han, S.; Keller, M.; Kaiser, A.; Bender, B. J.; Bosse, M.; Burkert, K.; Kogler, L. M.; Wifling, D.; Bernhardt, G.; Plank, N.; Littmann, T.; Schmidt, P.; Yi, C.; Li, B.; Ye, S.; Zhang, R.; Xu, B.; Larhammar, D.; Stevens, R. C.; Huster, D.; Meiler, J.; Zhao, Q.; Beck-Sickingler, A. G.; Buschauer, A.; Wu, B. Structural basis of ligand binding modes at the neuropeptide Y Y₁ receptor. *Nature* **2018**, *556*, 520-524.

29. Laurent, S.; Botteman, F.; Elst, L. V.; Muller, R. N. Relaxivity and Transmetallation Stability of New Benzyl-Substituted Derivatives of Gadolinium DTPA Complexes. *Helv. Chim. Acta* **2004**, *87*, 1077-1089.
30. Keller, M.; Pop, N.; Hutzler, C.; Beck-Sickinger, A. G.; Bernhardt, G.; Buschauer, A. Guanidine–Acyguanidine Bioisosteric Approach in the Design of Radioligands: Synthesis of a Tritium-Labeled N^G-Propionylargininamide ([³H]-UR-MK114) as a Highly Potent and Selective Neuropeptide Y Y₁ Receptor Antagonist. *J. Med. Chem.* **2008**, *51*, 8168-8172.
31. Gottlieb, H. E.; Kotlyar, V.; Nudelman, A. NMR Chemical Shifts of Common Laboratory Solvents as Trace Impurities. *J. Org. Chem.* **1997**, *62*, 7512-7515.
32. Basavaiah, D.; Krishna, P. R.; Bharathi, T. K. A convenient enantioselective synthesis of trans-2-aryloxycyclohexan-1-ols using pig liver acetone powder (PLAP) as biocatalyst. *Tetrahedron: Asymmetry* **1995**, *6*, 439-454.
33. Naidu, A. B.; Ganapathy, D.; Sekar, G. Copper(I)-Catalyzed Intramolecular Caryl-O Bond-Forming Cyclization for the Synthesis of 1,4-Benzodioxines and Its Application in the Total Synthesis of Sweetening Isovanillins. *Synthesis* **2010**, 2010, 3509-3519.
34. Bied, C.; Moreau, J. J. E.; Wong Chi Man, M. Chiral amino-urea derivatives of (1R,2R)-1,2-diaminocyclohexane as ligands in the ruthenium catalysed asymmetric reduction of aromatic ketones by hydride transfer. *Tetrahedron: Asymmetry* **2001**, *12*, 329-336.
35. Minarini, A.; Marucci, G.; Bellucci, C.; Giorgi, G.; Tumiatti, V.; Bolognesi, M. L.; Matera, R.; Rosini, M.; Melchiorre, C. Design, synthesis, and biological evaluation of pirenzepine analogs bearing a 1,2-cyclohexanediamine and perhydroquinoxaline units in exchange for the piperazine ring as antimuscarinics. *Bioorg. Med. Chem.* **2008**, *16*, 7311-7320.
36. Specklin, S.; Decuypere, E.; Plougastel, L.; Aliani, S.; Taran, F. One-Pot Synthesis of 1,4-Disubstituted Pyrazoles from Arylglycines via Copper-Catalyzed Sydnone–Alkyne Cycloaddition Reaction. *J. Org. Chem.* **2014**, *79*, 7772-7777.
37. Downham, R.; Sibley, G. E. M.; Payne, L. J.; Edwards, P.; Davies, G. M. 2-[(2-Substituted)-Indolizin-3-yl]-2-oxo-acetamide derivatives as antifungal agents. US 8,604,029 B2, 2013.
38. Sedlák, M.; Hejtmánková, L.; Kašparová, P.; Kaválek, J. Kinetics and mechanism of formation and decomposition of substituted 1-phenylpyrrolidin-2-ones in basic medium. *J. Phys. Org. Chem.* **2002**, *15*, 165-173.
39. Taylor, E. C.; Skotnicki, J. S. A Convenient Synthesis of 1-Aryl-4-piperidones. *Synthesis* **1981**, 1981, 606-608.
40. Samuels, H. H.; Abagyan, R.; Schapira, M.; Totrov, M.; Raaka, B. M.; Wilson, S. R.; Fan, L.; Zhou, Z. Hydrazide compounds as thyroid hormone receptor modulators and uses thereof. US 8,394,811 B2, 2013.
41. Sheldrick, G. SHELXT - Integrated space-group and crystal-structure determination. *Acta Cryst.* **2015**, *71*, 3-8.
42. Dolomanov, O. V.; Bourhis, L. J.; Gildea, R. J.; Howard, J. A. K.; Puschmann, H. OLEX2: a complete structure solution, refinement and analysis program. *J. Appl. Crystallogr.* **2009**, *42*, 339-341.
43. Sheldrick, G. Crystal structure refinement with SHELXL. *Acta Crystallogr. C.* **2015**, *71*, 3-8.

Chapter 7

Summary

Note: Prior to the submission of the thesis parts of this chapter were published in cooperation with partners (schemes, tables, figures and text may differ from published version): Buschmann, J.; Seiler, T.; Bernhardt, G.; Keller, M.; Wifling, D. Argininamide-type neuropeptide Y Y₁ receptor antagonists: the nature of N^ω-carbamoyl substituents determines Y₁R binding mode and affinity. *RSC Med. Chem.* **2020**, 11, 274-282 DOI: 10.1039/C9MD00538B – adopted by permission of The Royal Society of Chemistry

cf. note of Chapter 2

Neuropeptide Y (NPY), peptide YY (PYY) and pancreatic polypeptide (PP) share similarities, such as a sequence comprising 36 amino acids and an amidated C-terminus, which activate NPY receptors. These receptors belong to class A (rhodopsin-like receptors) of G-protein coupled receptors (GPCRs),¹ which are distributed in the central nervous system (CNS) and as well in the periphery.² In humans four (Y₁R, Y₂R, Y₄R and Y₅R) different subtypes are functional and their stimulation leads to several biological effects, which are involved in several dysfunctions such as dislocation of energy homeostasis, seizure, neurodegeneration and psychotic disorders.²⁻⁴ Furthermore, the overexpression of NPY receptors in different tumours (e.g. overexpression of Y₁R in breast cancer) make them a promising target for cancer imaging and therapy.⁵

The (*R*)-argininamide-type Y₁R antagonist UR-MK299 (**2.2**) was recently co-crystallized with the hY₁R and revealed that the *N*^ω-carbamoyl substituent (van der Waals volume: 139 Å³) is deeply buried in the receptor, occupying a hydrophobic pocket that is not completely filled.^{6, 7} (*R*)-Argininamides **2.53-2.76** and **2.78**, derived from **2.2** and **2.3** were synthesized and pharmacologically characterized (e.g. radioligand competition binding assay, Fura-2 Ca²⁺ assay). The propionyl group in **2.2** was replaced by several acyl residues (cyclic, acyclic and aromatic). In addition the ethylene spacer in **2.2** was replaced by a propylene spacer bearing acetyl or propionyl moieties. A decrease in Y₁R affinity was observed with increasing size of the carbamoyl residue (minimal p*K*_i = 5.67). When the van der Waals volume (212 Å³) of the side chain reached a critical size, the binding mode of argininamide-type ligands inverted and the carbamoyl side chain was located at the surface of the receptor. These findings were supported by induced-fit docking and molecular dynamics simulations (*cf.* Chapter 2).

Additionally, selected (*R*)-argininamides **2.1**, **2.2**, **2.56-2.59**, **2.61** and **2.65** were investigated in a β-arrestin2 recruitment assay. Compounds **2.58**, **2.68** and **2.72** were supposed to share a similar binding mode to **2.2**, however the increasing size of the carbamoyl residue of these ligands did not result in hY₄R and hY₅R binding. Additionally, potential irreversibly binding compounds **2.60** and **2.63** identified by model chemical reactivity experiments with 2-mercaptoethanol were investigated in saturation binding experiments with [³H]**2.2** as radioligand. However, covalent binding of **2.60** and **2.63** to the hY₁R could neither be confirmed nor excluded (*cf.* Chapter 3).

The (*S*)-argininamide BIIE-0246 (**4.1**) was the first selective hY₂R antagonist known from the literature⁸ and acylation of the guanidine group of **4.1** led to [³H]UR-PLN196 ([³H]**4.2**),⁹ which was the first non-peptide hY₂R radioligand synthesized in our group. In a further project, the replacement of the benzoazepinone moiety of **4.1** by an amino functionalized benzhydryl group led to compounds **4.50** and **4.51** with binding affinities in the nanomolar range. Derived from **4.50**, the red-emitting fluorescent ligand UR-jb264 (**4.58**) was synthesized. **4.58** was successfully used in a BRET based binding assay as an alternative to radioligand binding with [³H]propionyl-pNPY as a tracer for the determination of binding constants of Y₂R ligands. Additionally, **4.58** was applied in confocal microscopy (*cf.* Chapter 4).

Compound **4.23** derived from (*S*)-argininamide **4.5** is the cold form of a potential radioligand. To explore the feasibility of future tritium labelling of **4.23** by methylation (e.g. with methyl iodide or methyl nosylate) in the last synthetic step, the phenolic precursor **5.20** was synthesized. Furthermore, the amine precursor **4.50** was propionylated (**5.31**), 2-fluoroacetylated (**5.32**), mono- (**5.29**) and tri- (**5.30**) alkylated to obtain additional cold forms of potential radioligands (*cf.* Chapter 5).

Ewing et al.^{10, 11} reported a series of (*R,R*)-diaminocyclohexanes, which were classified as agonists antagonists or modulators. These authors evaluated just a subset of compounds at the hY₄R in a cAMP accumulation assay. In a third project, selected compounds were synthesized and investigated in competition binding experiments at the hY₄R, established in our group. Unfortunately, the compounds showed no affinity in competition binding experiments. Additionally, selected compounds were investigated in an aequorin assay and showed neither potency nor modulatory effects on the action of hPP. Niclosamide (**6.10**) was described as the first allosteric modulator at the hY₄R,¹² but the reported results could not be reproduced in the aequorin assay using live CHO-hY₄-G_{q15}-mtAEQ cells. Live/dead staining of the cells revealed that niclosamide (**6.10**) proved to be cytotoxic at the used concentrations, compromising the results of functional assays with live cells (*cf.* Chapter 6).

First and foremost, this thesis contributes to a deeper insight on the binding mode of *N*^ω-carbamoylated (*R*)-argininamide at Y₁R, which may help to design and prepare further novel molecular tools such as fluorescence labelled or PET ligands. Furthermore, the synthesis of amine precursor **4.50** enables the synthesis of fluorescent ligand **4.58**, which could be used for the determination of binding constants of non-labelled compounds.

References

1. Joost, P.; Methner, A. Phylogenetic analysis of 277 human G-protein-coupled receptors as a tool for the prediction of orphan receptor ligands. *Genome Biol* **2002**, *3*, research0063.1.
2. Reichmann, F.; Holzer, P. Neuropeptide Y: A stressful review. *Neuropeptides* **2016**, *55*, 99-109.
3. Michel, M. C.; Beck-Sickinger, A.; Cox, H.; Doods, H. N.; Herzog, H.; Larhammar, D.; Quirion, R.; Schwartz, T.; Westfall, T. XVI. International Union of Pharmacology recommendations for the nomenclature of neuropeptide Y, peptide YY, and pancreatic polypeptide receptors. *Pharmacol. Rev.* **1998**, *50*, 143-50.
4. Zhang, L.; Bijker, M. S.; Herzog, H. The neuropeptide Y system: Pathophysiological and therapeutic implications in obesity and cancer. *Pharmacol. Ther.* **2011**, *131*, 91-113.
5. Li, J.; Tian, Y.; Wu, A. Neuropeptide Y receptors: a promising target for cancer imaging and therapy. *Regener. Biomater.* **2015**, *2*, 215-219.
6. Yang, Z.; Han, S.; Keller, M.; Kaiser, A.; Bender, B. J.; Bosse, M.; Burkert, K.; Kogler, L. M.; Wifling, D.; Bernhardt, G.; Plank, N.; Littmann, T.; Schmidt, P.; Yi, C.; Li, B.; Ye, S.; Zhang, R.; Xu, B.; Larhammar, D.; Stevens, R. C.; Huster, D.; Meiler, J.; Zhao, Q.; Beck-Sickinger, A. G.; Buschauer, A.; Wu, B. Structural basis of ligand binding modes at the neuropeptide Y Y₁ receptor. *Nature* **2018**, *556*, 520-524.
7. Keller, M.; Weiss, S.; Hutzler, C.; Kuhn, K. K.; Mollereau, C.; Dukorn, S.; Schindler, L.; Bernhardt, G.; König, B.; Buschauer, A. N^ω-Carbamoylation of the Argininamide Moiety: An Avenue to Insurmountable NPY Y₁ Receptor Antagonists and a Radiolabeled Selective High-Affinity Molecular Tool ([³H]UR-MK299) with Extended Residence Time. *J. Med. Chem.* **2015**, *58*, 8834-8849.
8. Doods, H.; Gaida, W.; Wieland, H. A.; Dollinger, H.; Schnorrenberg, G.; Esser, F.; Engel, W.; Eberlein, W.; Rudolf, K. BIIE0246: A selective and high affinity neuropeptide Y Y₂ receptor antagonist. *Eur. J. Pharm.* **1999**, *384*, R3-R5.
9. Pluym, N.; Baumeister, P.; Keller, M.; Bernhardt, G.; Buschauer, A. [³H]UR-PLN196: A Selective Nonpeptide Radioligand and Insurmountable Antagonist for the Neuropeptide Y Y₂ Receptor. *ChemMedChem* **2013**, *8*, 587-593.
10. Ewing, W. R.; Zhu, Y.; Sun, C.; Huang, Y.; Sivasamban, M.; Karatholuvhu. Diaminocyclohexane compounds and uses thereof. US 2013/0184262 A1, 2013.
11. Ewing, W. R.; Zhu, Y.; Sun, C.; Huang, Y.; Sivasamban, M.; Karatholuvhu; Bolton, S. A.; Pasunoori, L.; Mandal, S. K.; Sher, P. M. Diaminocyclohexane compounds and uses thereof. US 2013/0184284 A1, 2013.
12. Sliwoski, G.; Schubert, M.; Stichel, J.; Weaver, D.; Beck-Sickinger, A. G.; Meiler, J. Discovery of Small-Molecule Modulators of the Human Y₄ Receptor. *PLOS ONE* **2016**, *11*, e0157146.

Chapter 8

Appendix

Note: Prior to the submission of the thesis parts of this chapter (*cf.* 8.1.) were published in cooperation with partners (schemes, tables, figures and text may differ from published version): Buschmann, J.; Seiler, T.; Bernhardt, G.; Keller, M.; Wifling, D. Argininamide-type neuropeptide Y Y₁ receptor antagonists: the nature of *N*^ω-carbamoyl substituents determines Y₁R binding mode and affinity. *RSC Med. Chem.* **2020**, 11, 274-282 DOI: 10.1039/C9MD00538B – adopted by permission of The Royal Society of Chemistry

cf. note of Chapter 2

8.1. Chapter 2

8.1.1. Supplementary figure 8.1

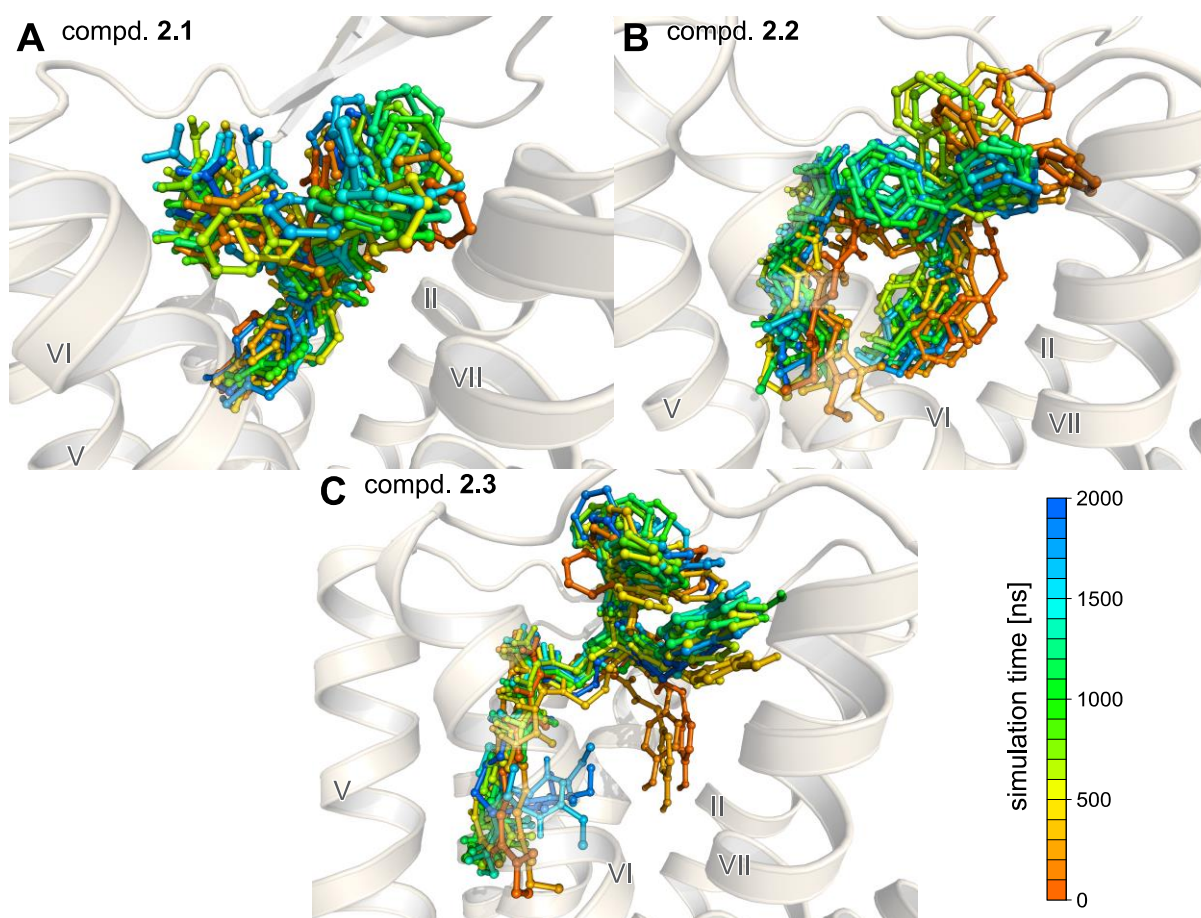


Figure 8.1. Time-course illustrations of the 2- μ s MD simulations of the Y₁R (inactive state, PDB ID: 5ZBQ¹) bound to **2.1** (A), **2.2** (B) or **2.3** (C) showing superimposed snapshots collected every 100 ns.

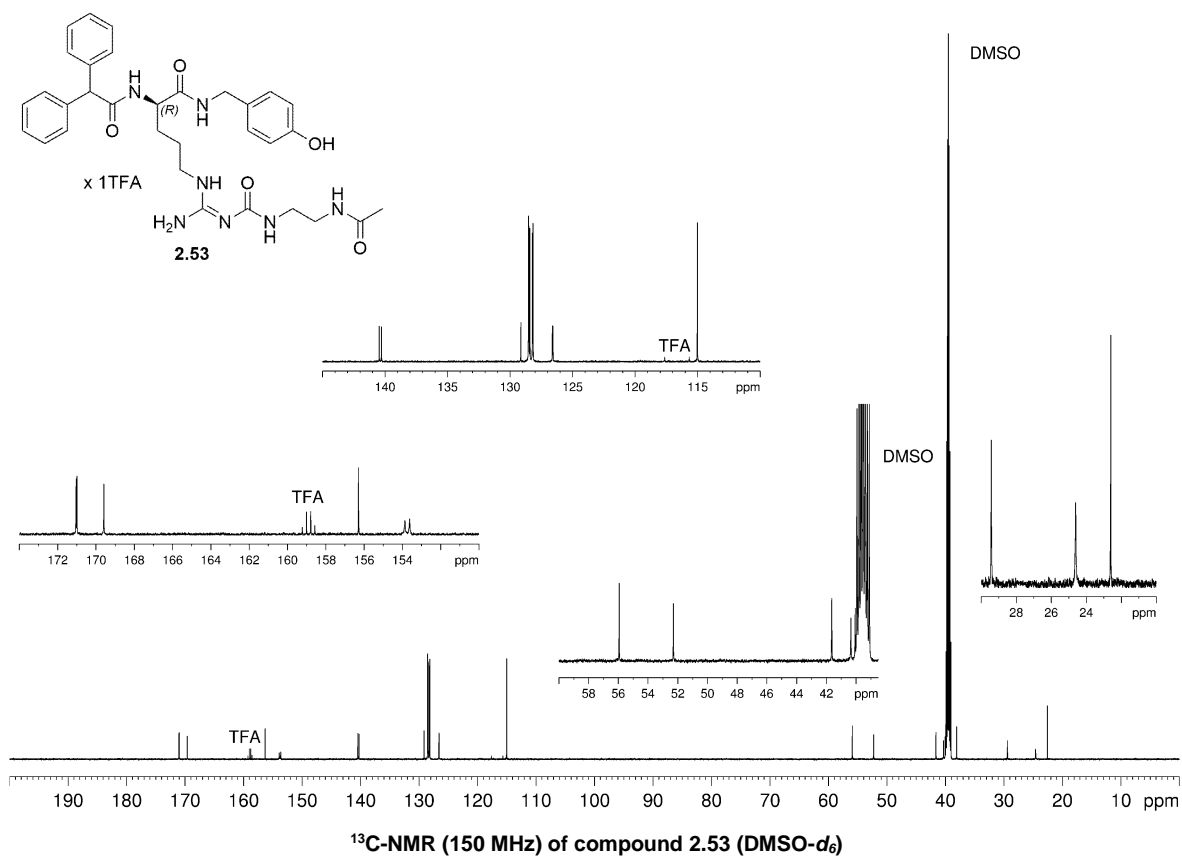
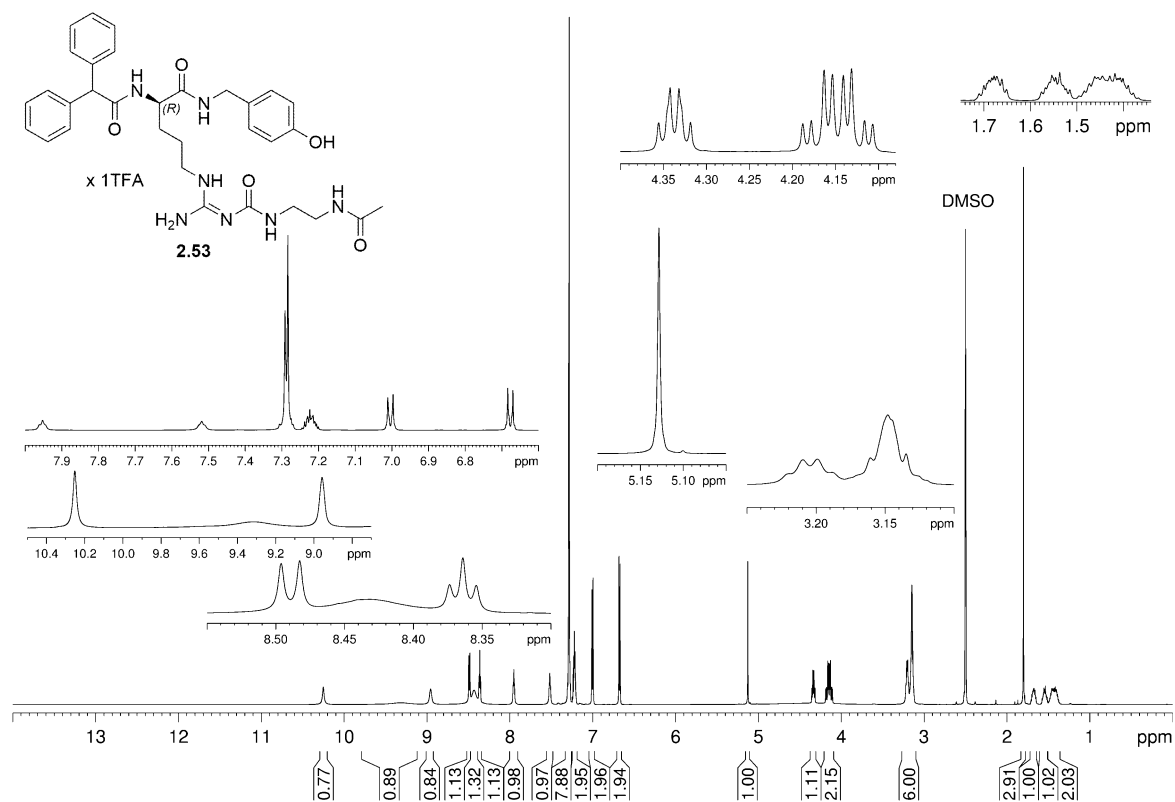
8.1.2. Supplementary table 8.1

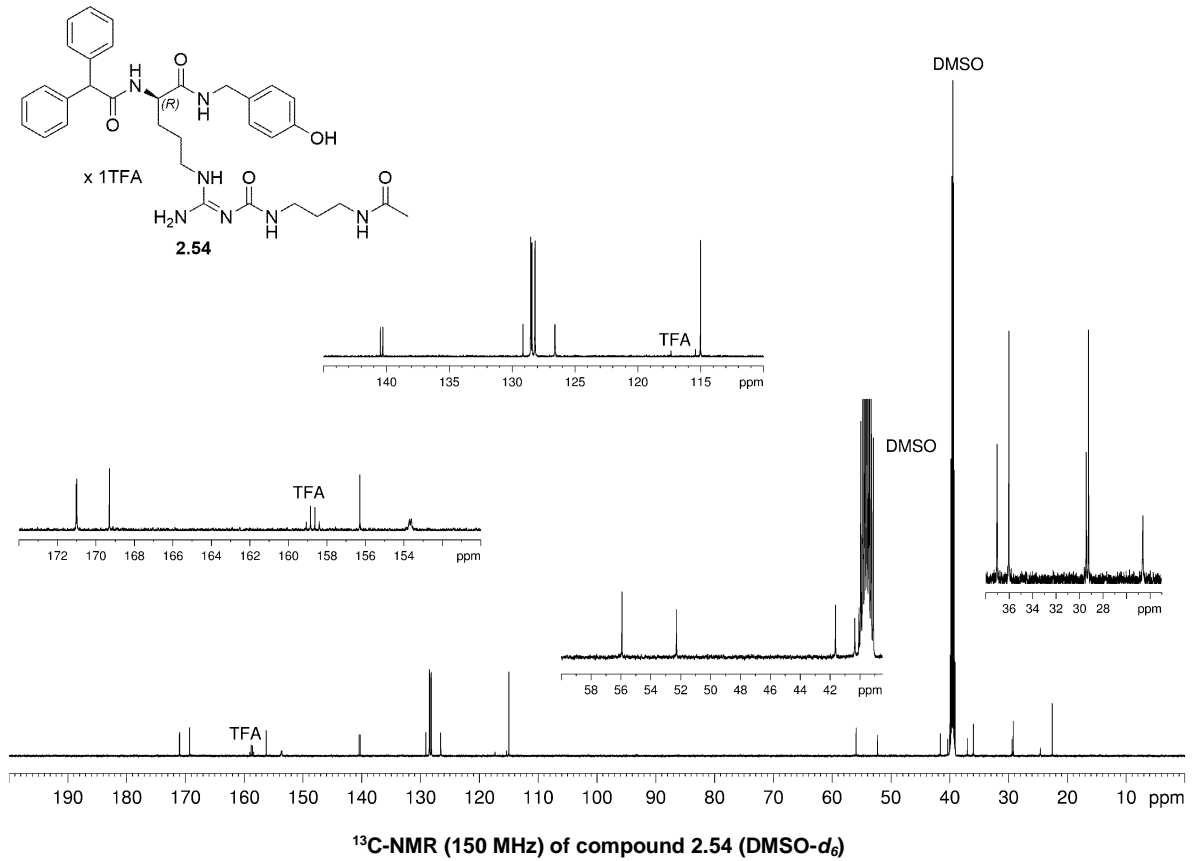
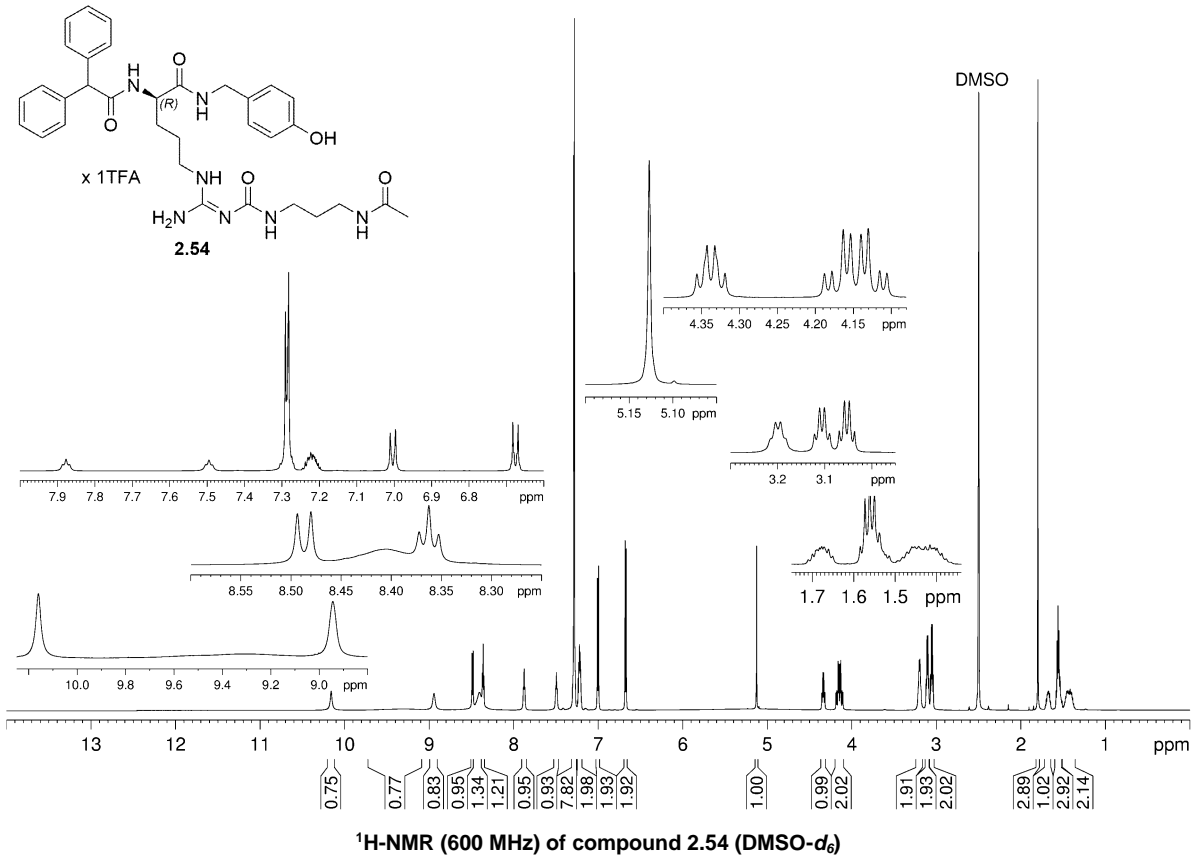
Table 8.1. Slope factors (Hill slope) of compounds **2.53-2.76** and **2.78** determined by equilibrium competition binding with [³H]**2.2** and in the Fura-2 Ca²⁺ assay, respectively.

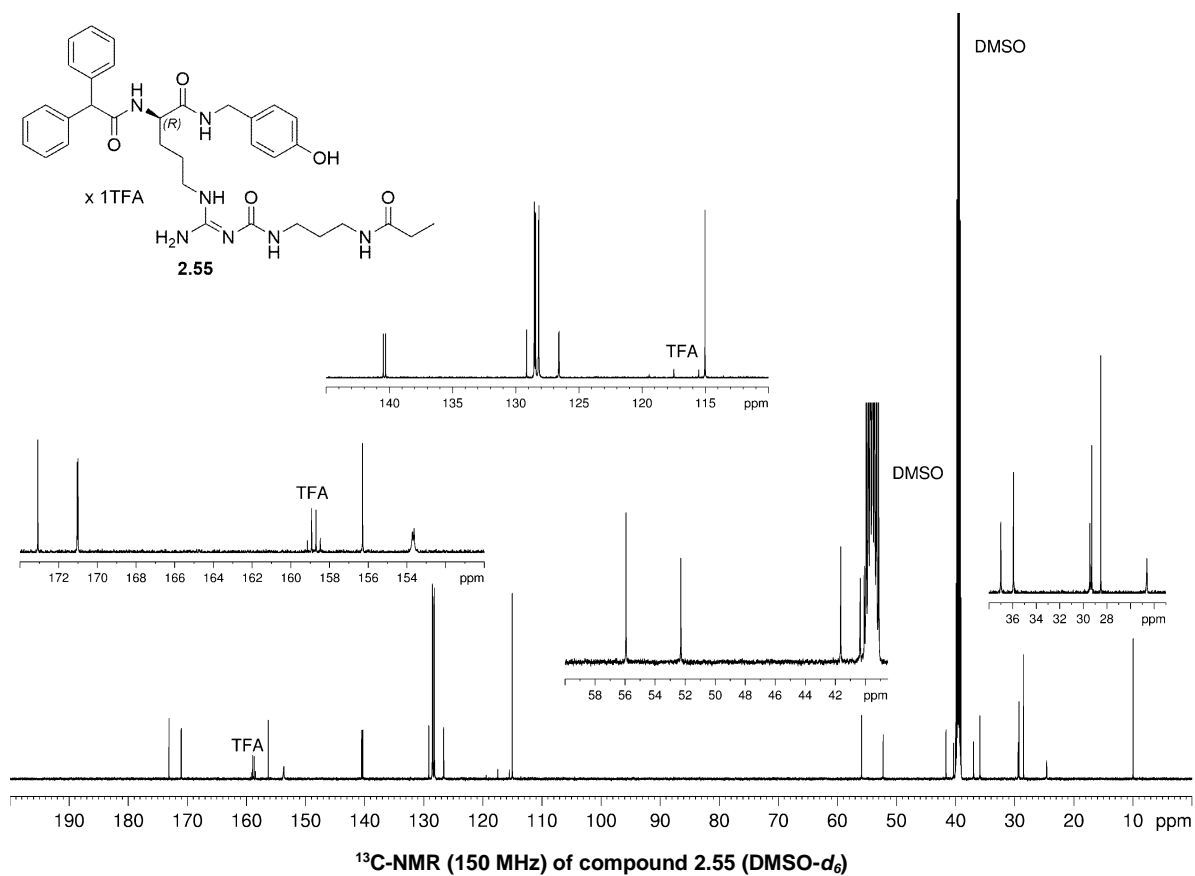
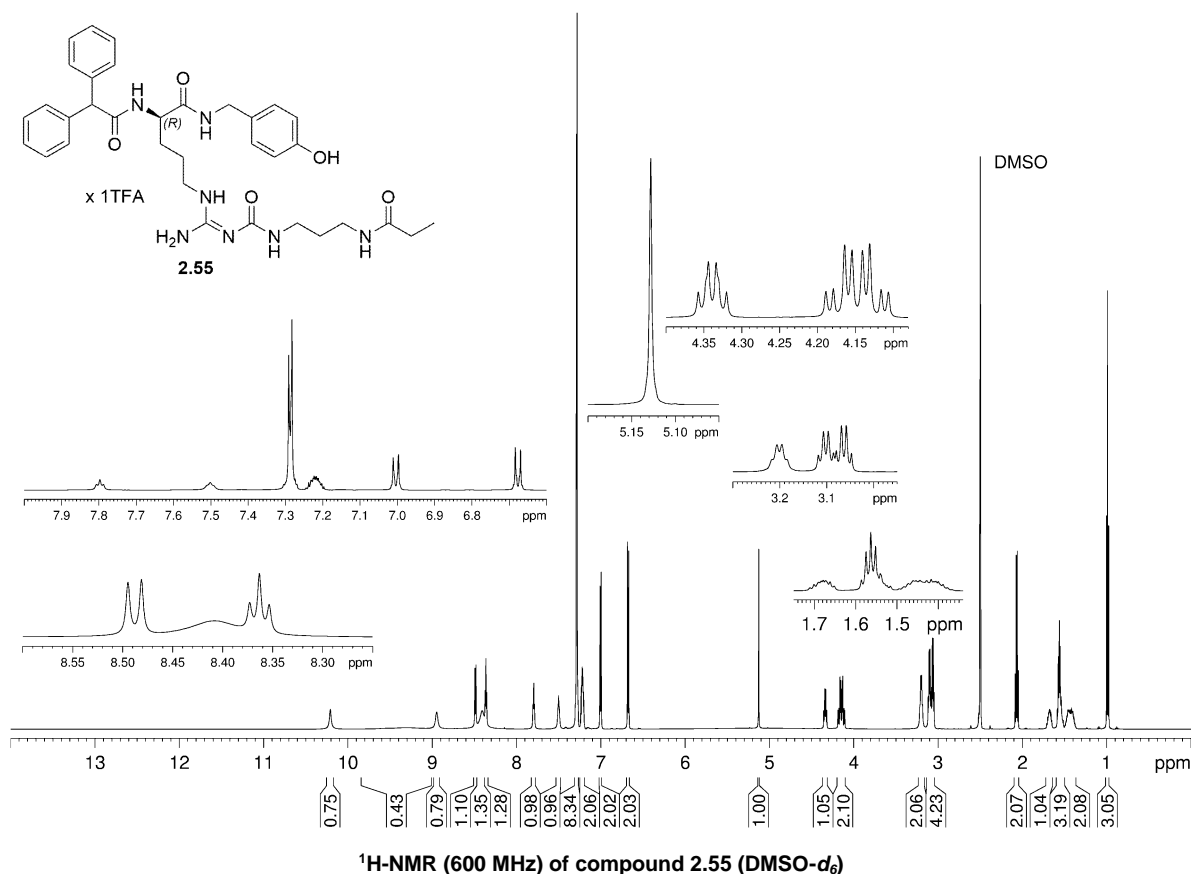
com- pound	slope ± SEM ^a (competition binding)	slope ± SEM ^b (Fura-2 Ca ²⁺)	com- pound	slope ± SEM ^a (competition binding)	slope ± SEM ^b (Fura-2 Ca ²⁺)
2.53	-1.05 ± 0.07	n.d.	2.66	-1.17 ± 0.08	-1.17 ± 0.11
2.54	-1.06 ± 0.03	n.d.	2.67	-0.97 ± 0.05	-1.30 ± 0.21
2.55	-0.97 ± 0.10	n.d.	2.68	-1.02 ± 0.09	-0.96 ± 0.07
2.56	-1.27 ± 0.10	-2.36 ± 0.09**	2.69	-1.00 ± 0.07	-1.07 ± 0.24
2.57	-1.25 ± 0.06*	-1.92 ± 0.09**	2.70	-1.03 ± 0.14	-1.13 ± 0.30
2.58	-1.08 ± 0.08	-2.17 ± 0.15**	2.71	-1.00 ± 0.04	-1.02 ± 0.05
2.59	-1.17 ± 0.03*	-1.74 ± 0.22*	2.72	-0.98 ± 0.07	-1.19 ± 0.12
2.60	-1.03 ± 0.09	-1.79 ± 0.29	2.73	-0.91 ± 0.16	-0.99 ± 0.07
2.61	-1.02 ± 0.01	-0.79 ± 0.07	2.74	-0.90 ± 0.03*	-0.83 ± 0.01**
2.62	-1.01 ± 0.08	-1.39 ± 0.21	2.75	-0.89 ± 0.06	-0.86 ± 0.12
2.63	-1.10 ± 0.18	-1.27 ± 0.16	2.76	-0.82 ± 0.08	-1.00 ± 0.11
2.64	-0.89 ± 0.05	-0.69 ± 0.07*	2.78	-1.17 ± 0.03*	n.d.
2.65	-0.81 ± 0.07	-0.83 ± 0.04			

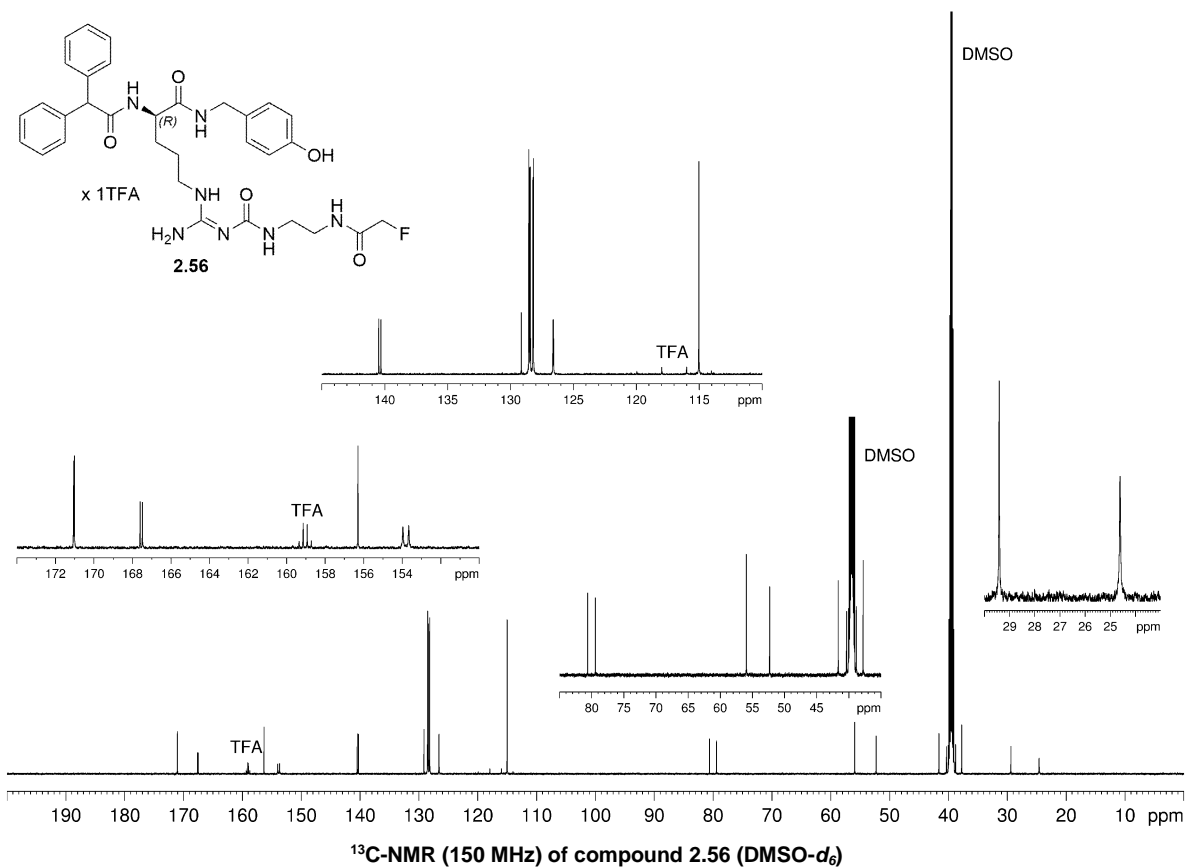
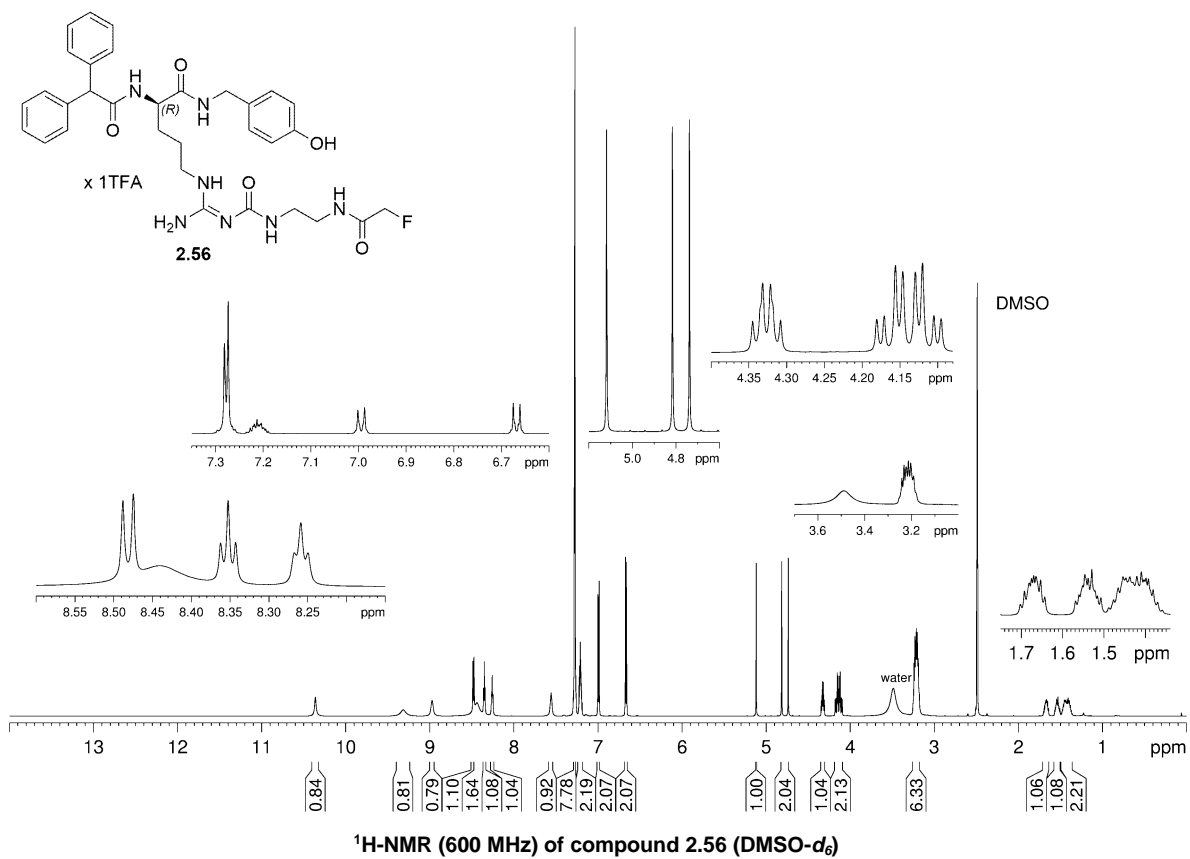
^aSlope factors of the four-parameter logistic fit (GraphPad Prism 8) obtained from analysis of radioligand competition binding data. Mean values ± SEM from at least three independent experiments, each performed in triplicate. ^bSlope factors of the four-parameter logistic fit (GraphPad Prism 8) obtained from analysis of the Fura-2 Ca²⁺ data. Mean values ± SEM from at least three independent experiments performed in singlet. *Slope significantly different from unity, $P \leq 0.05$ (one sample, two-tailed t-test).

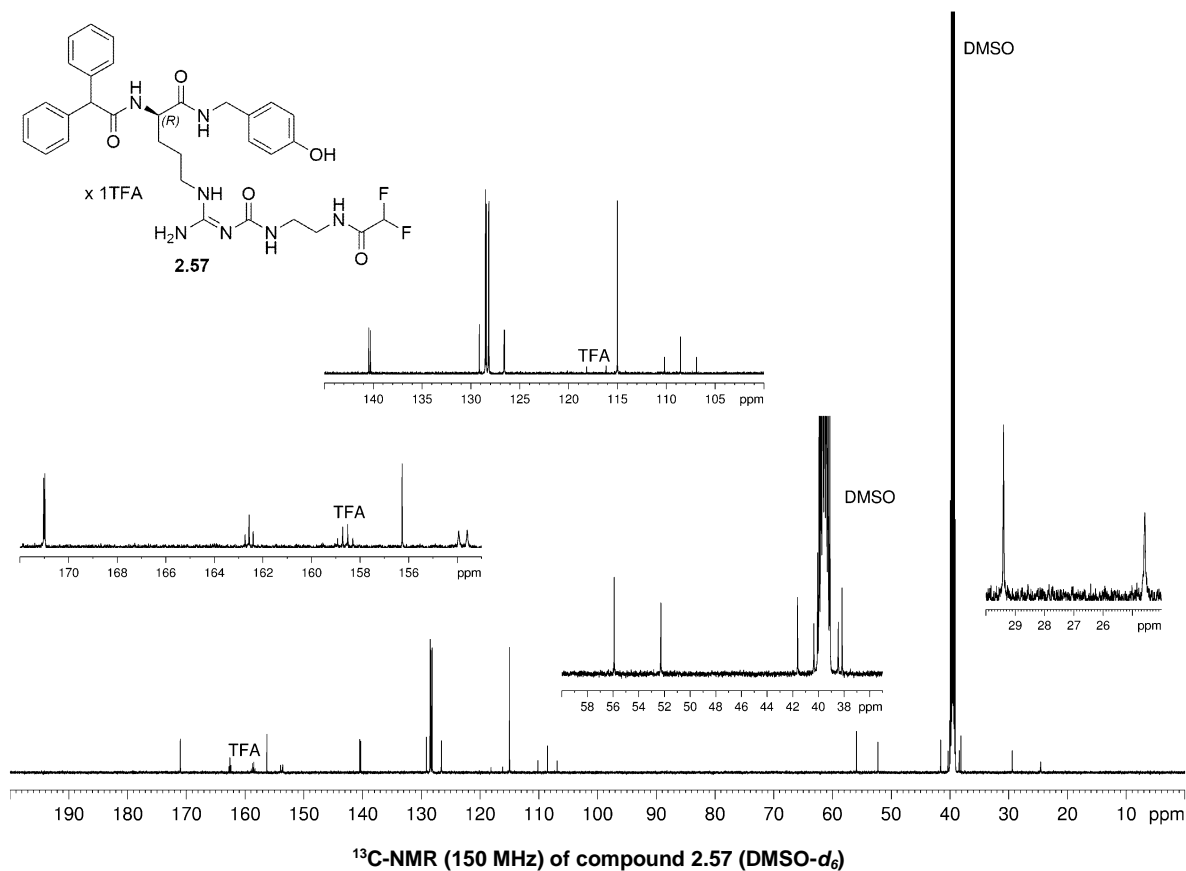
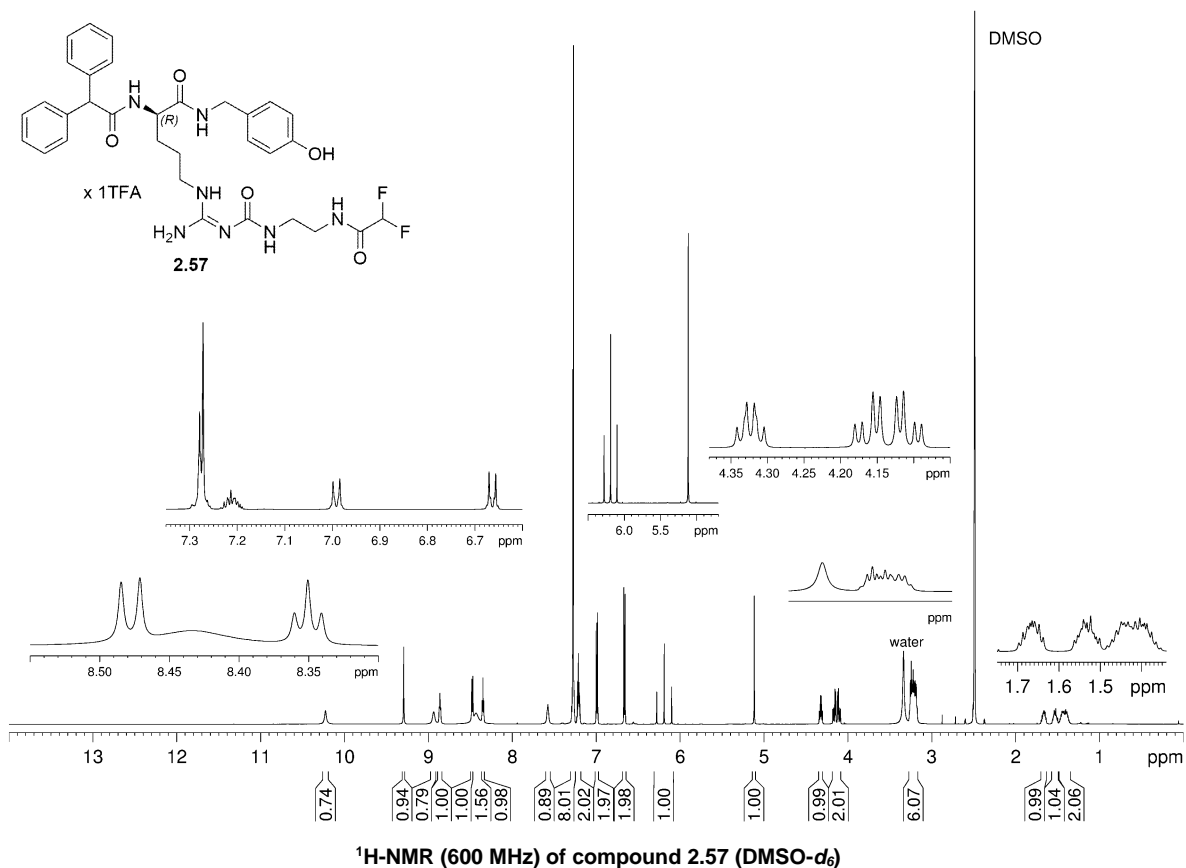
**Slope significantly different from unity, $P \leq 0.01$ (one sample, two-tailed t-test). n.d.: not determined.

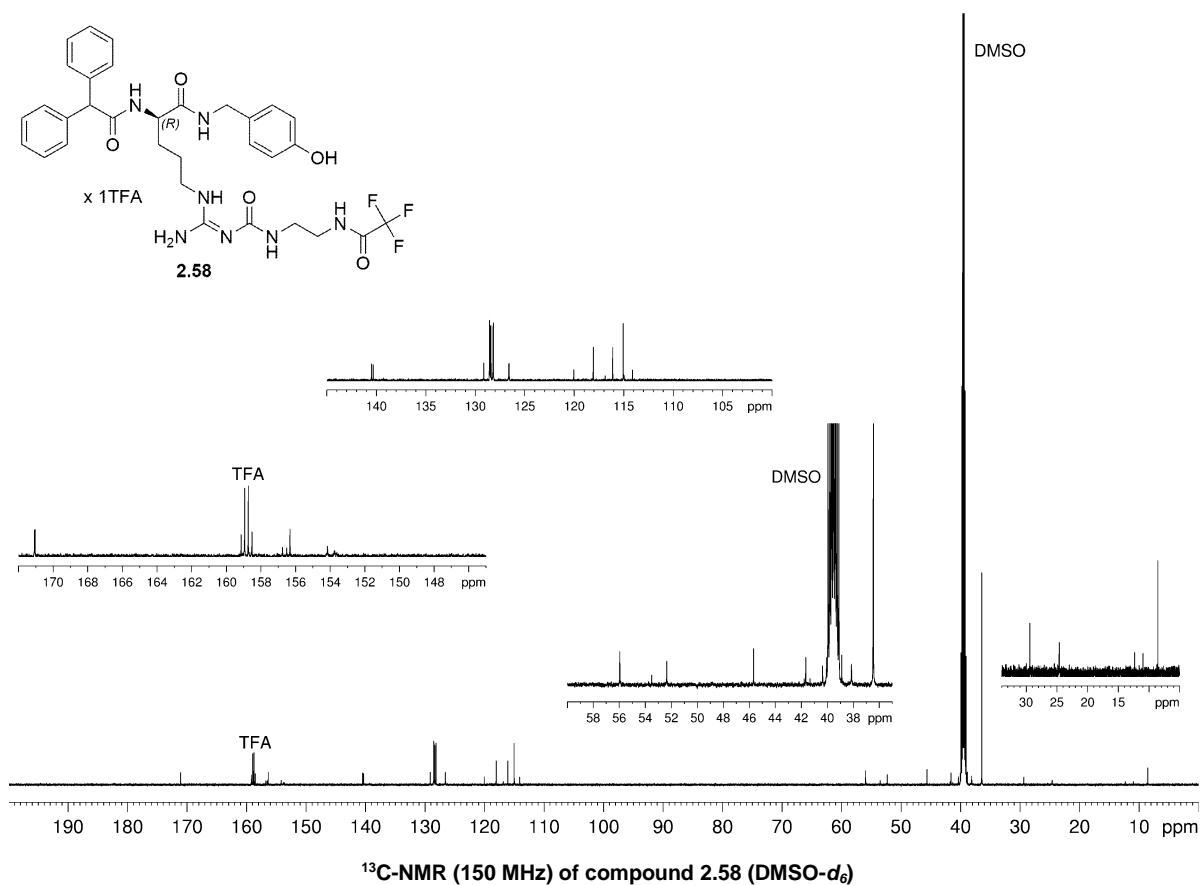
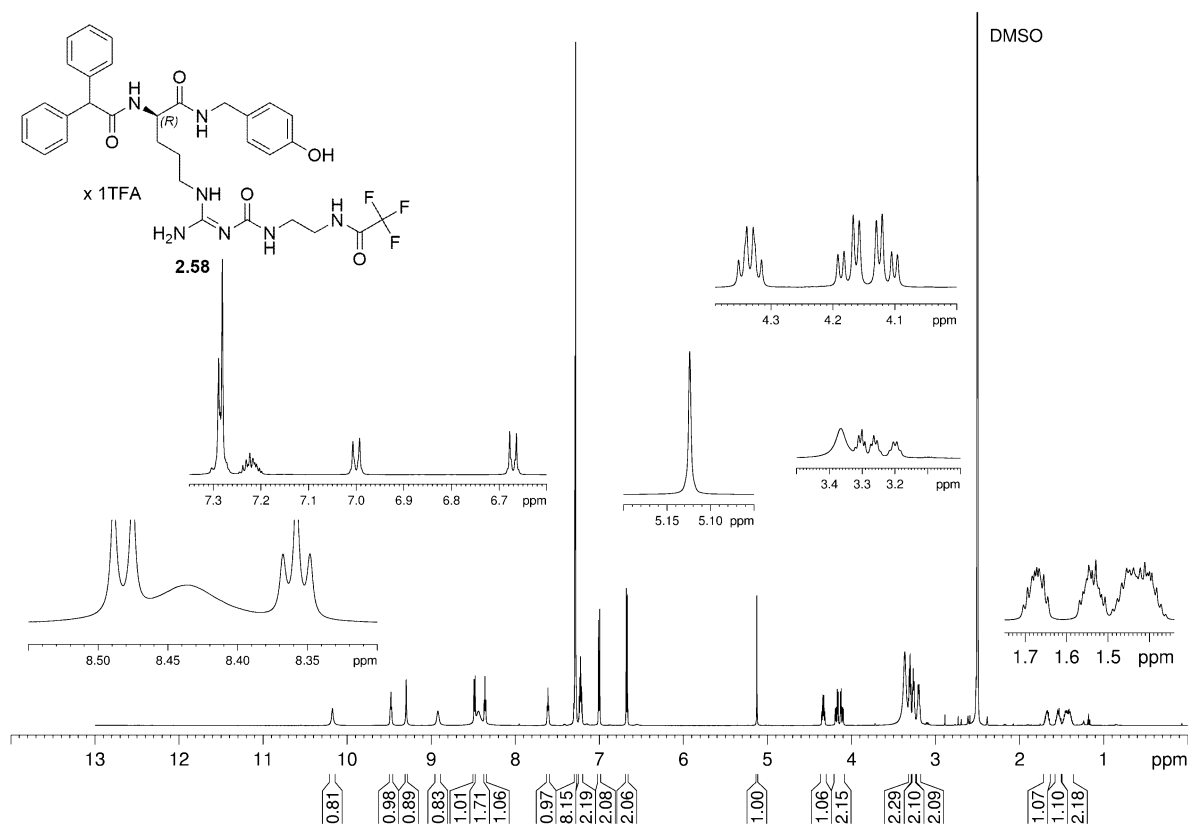
8.1.3. $^1\text{H-NMR}$ and $^{13}\text{C-NMR}$ spectra of compounds 2.53-2.76

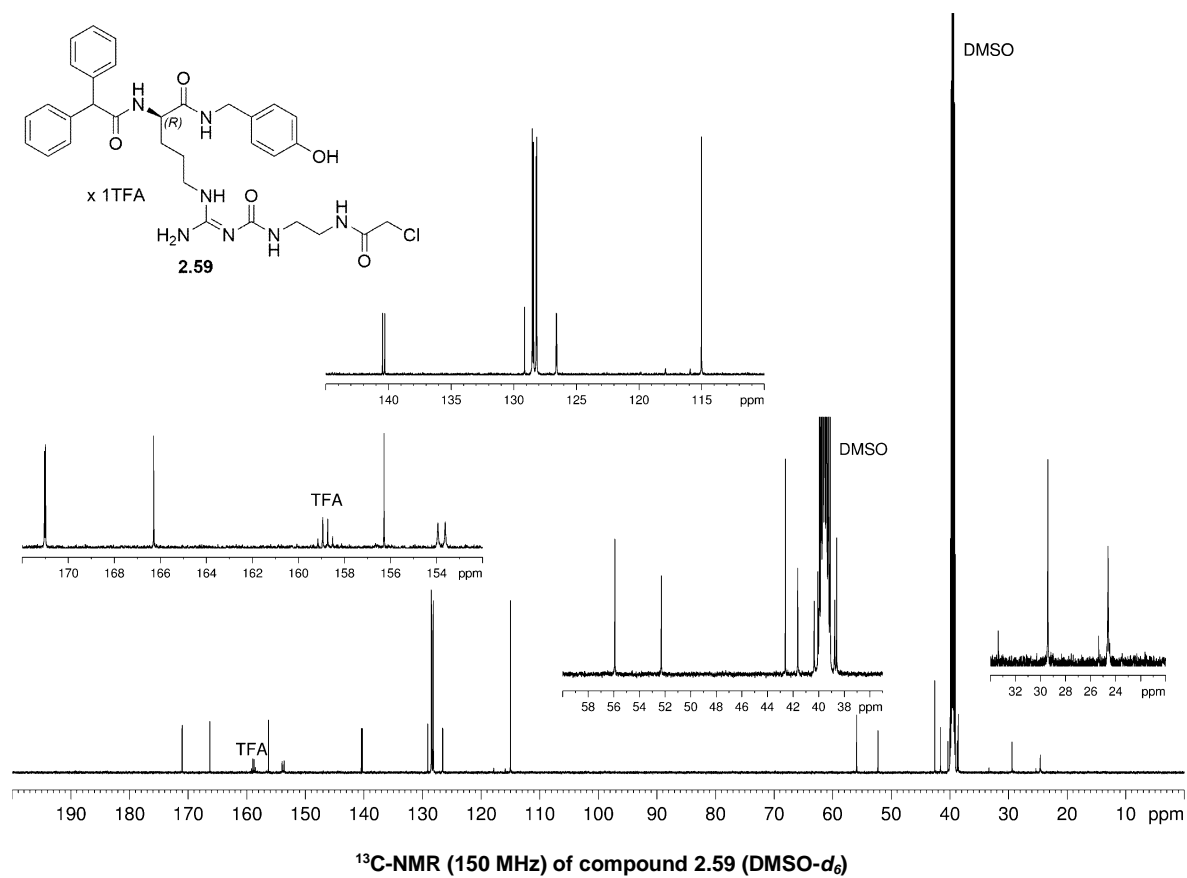
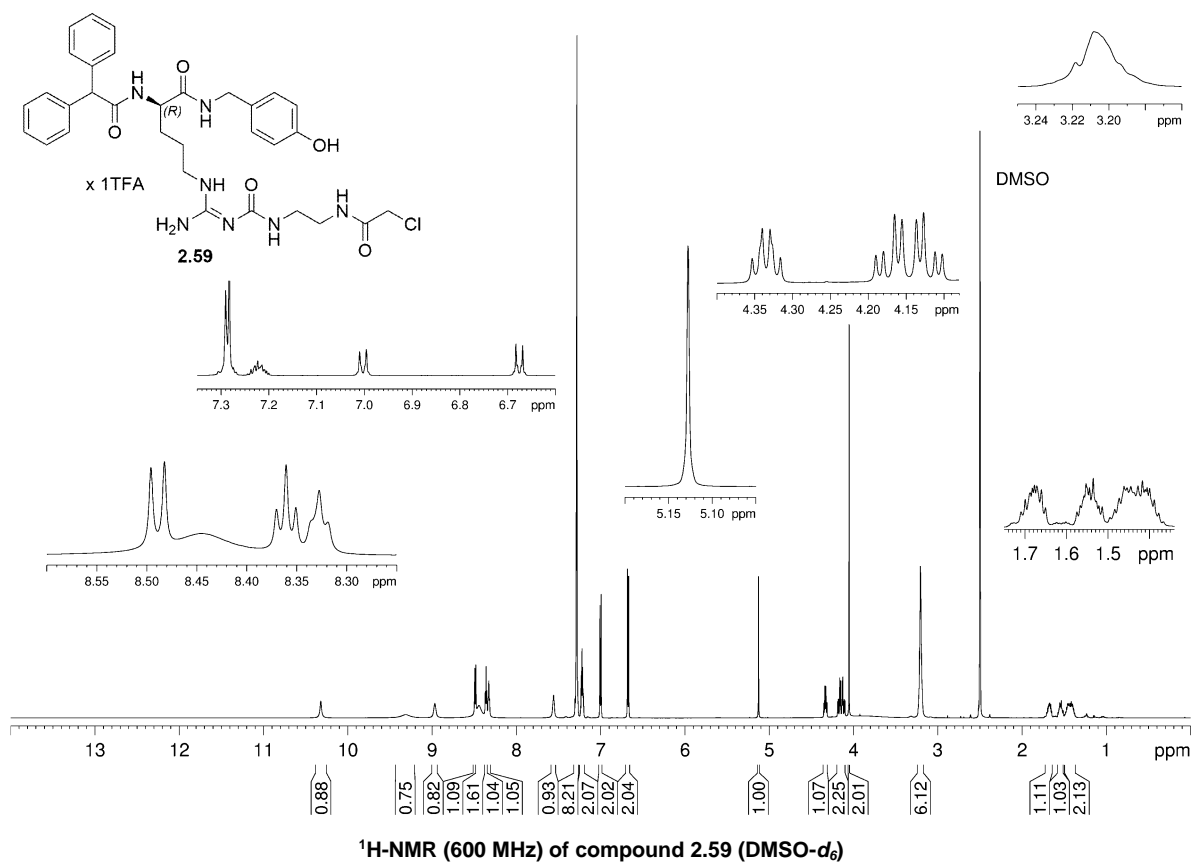


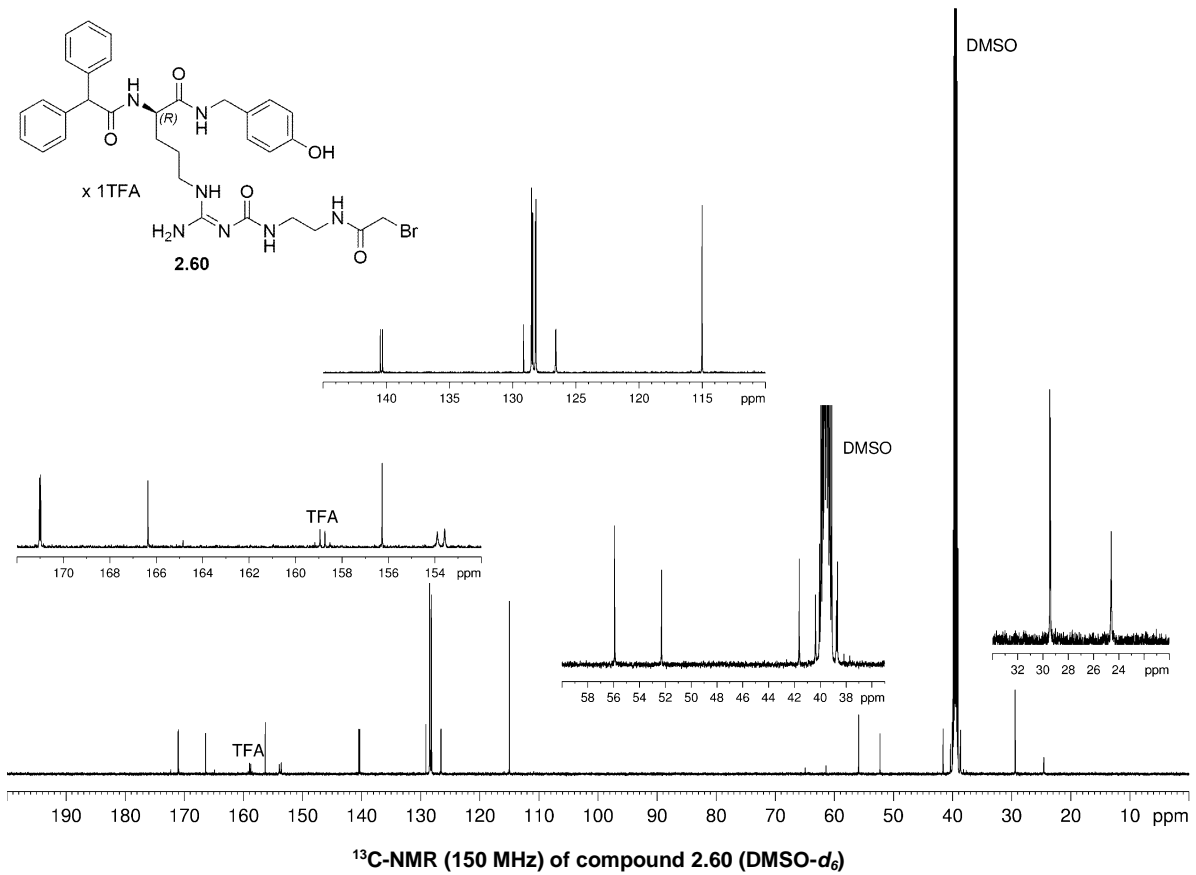
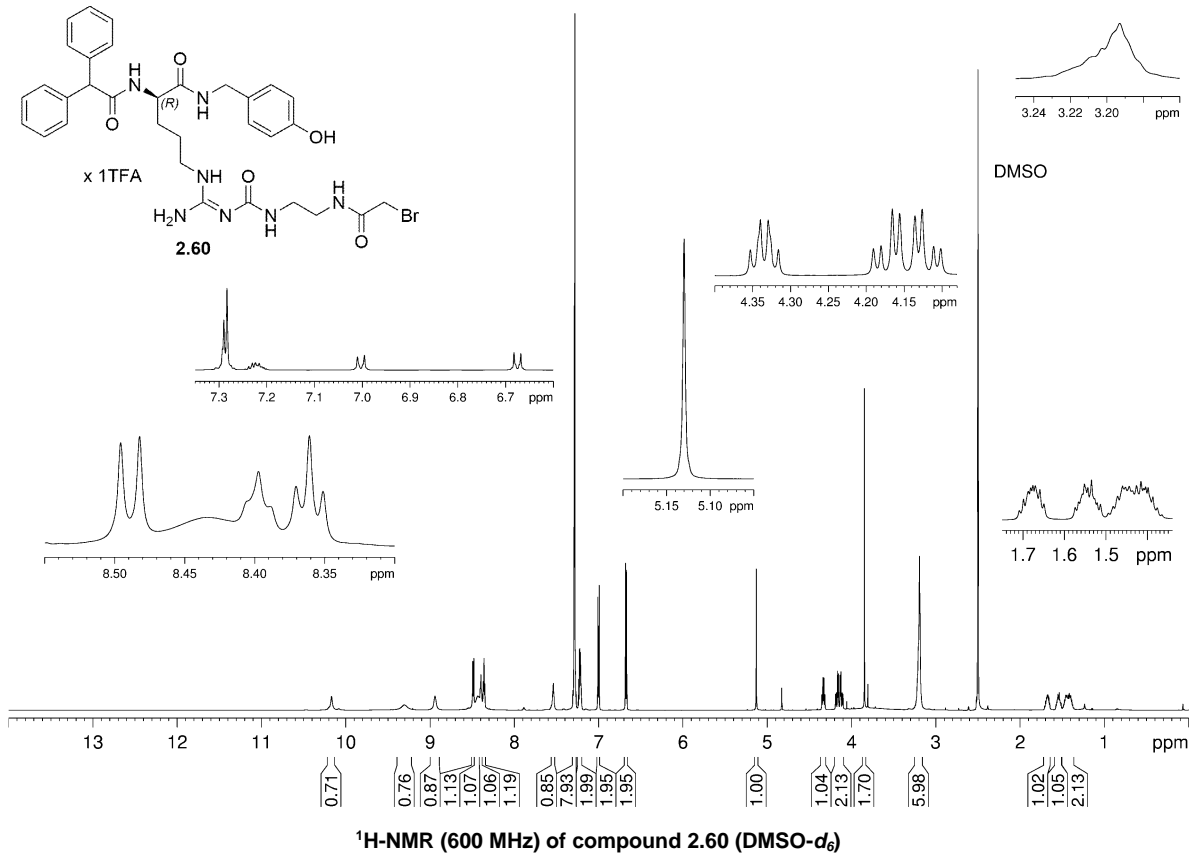


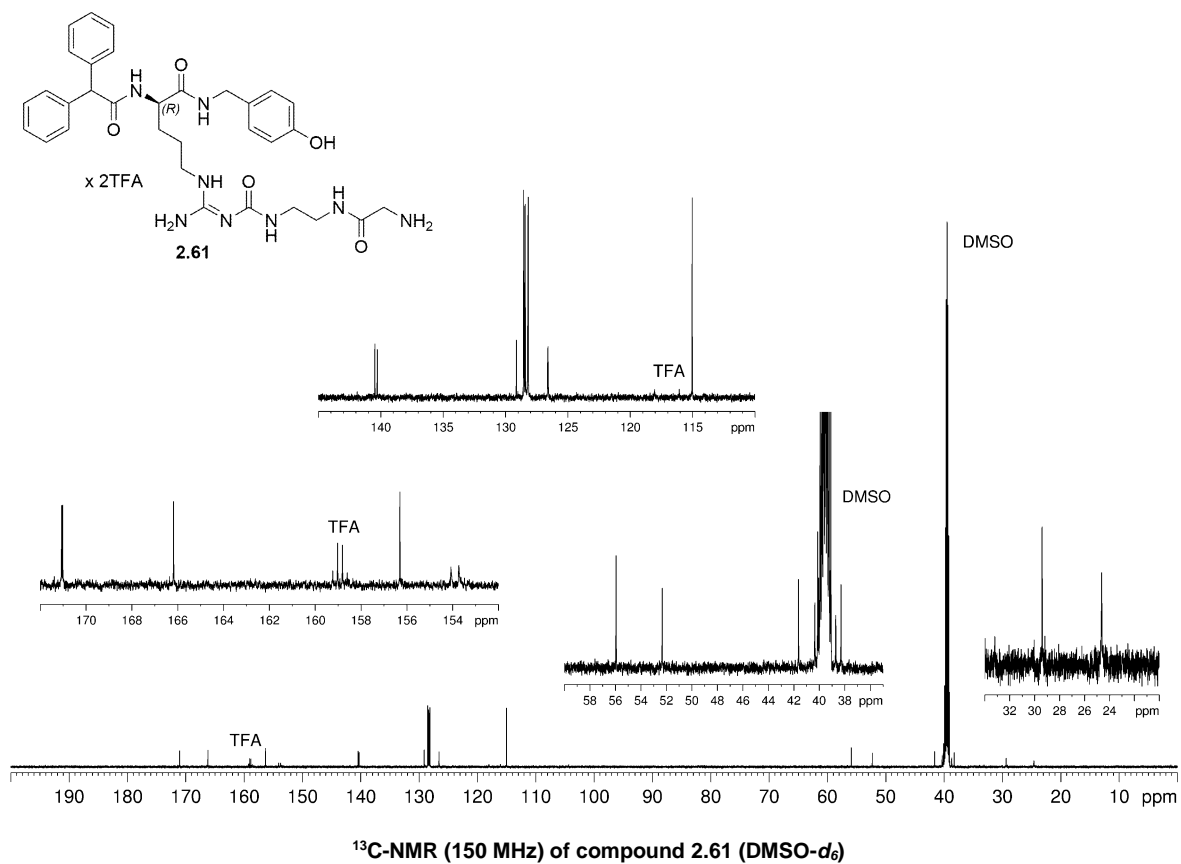
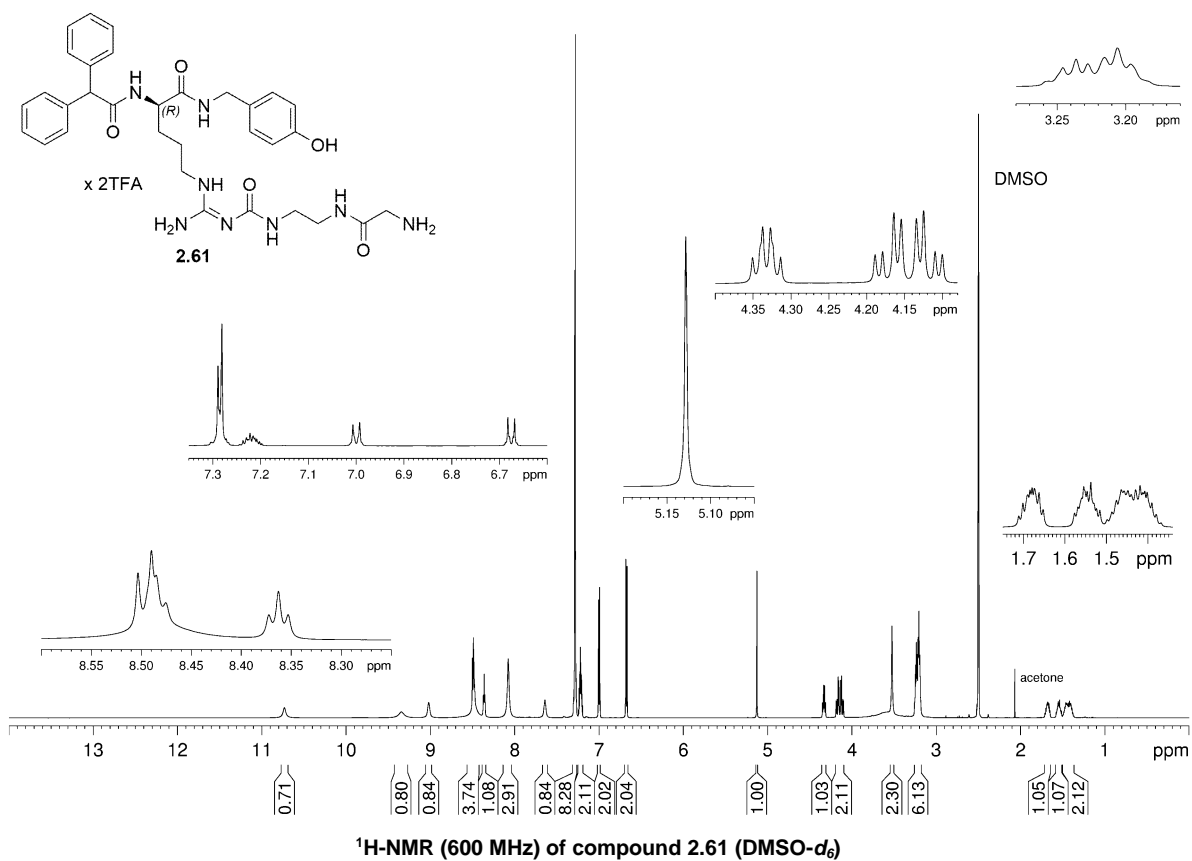


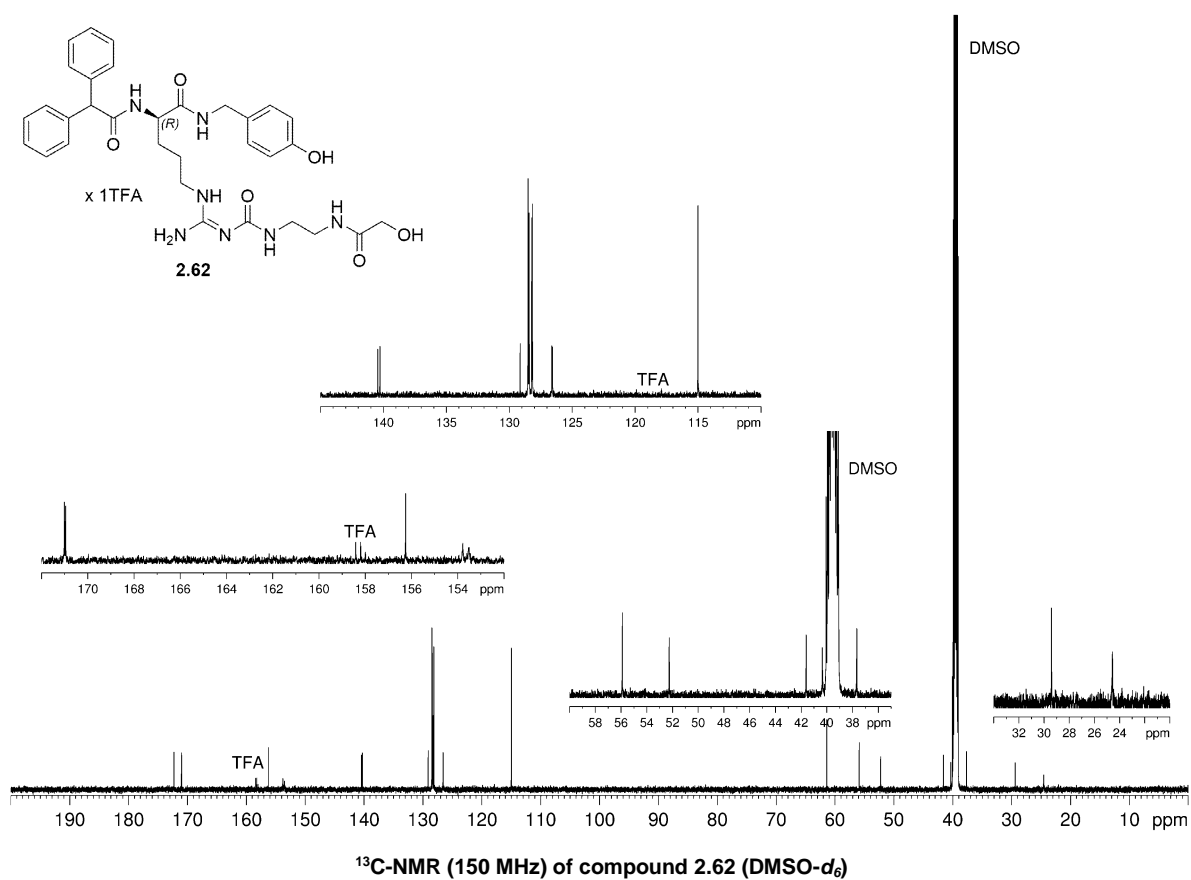
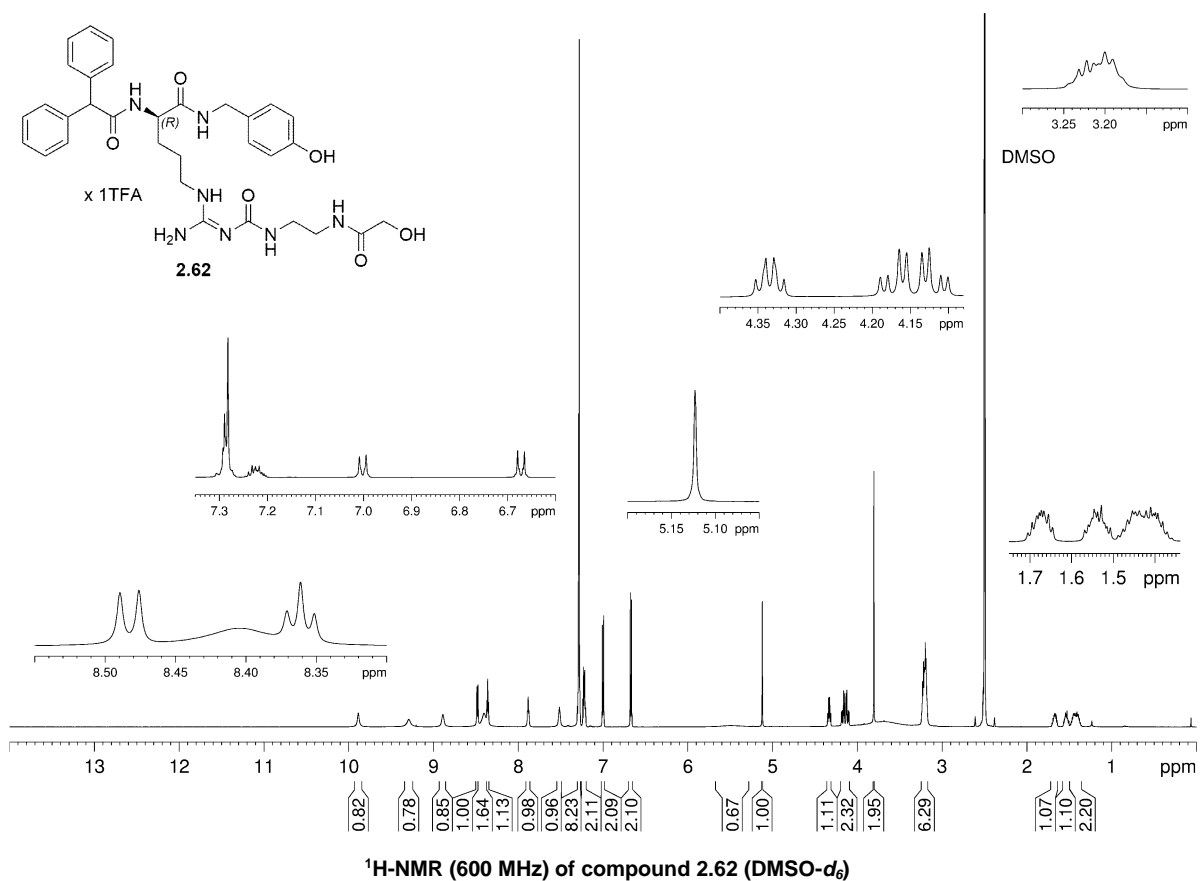


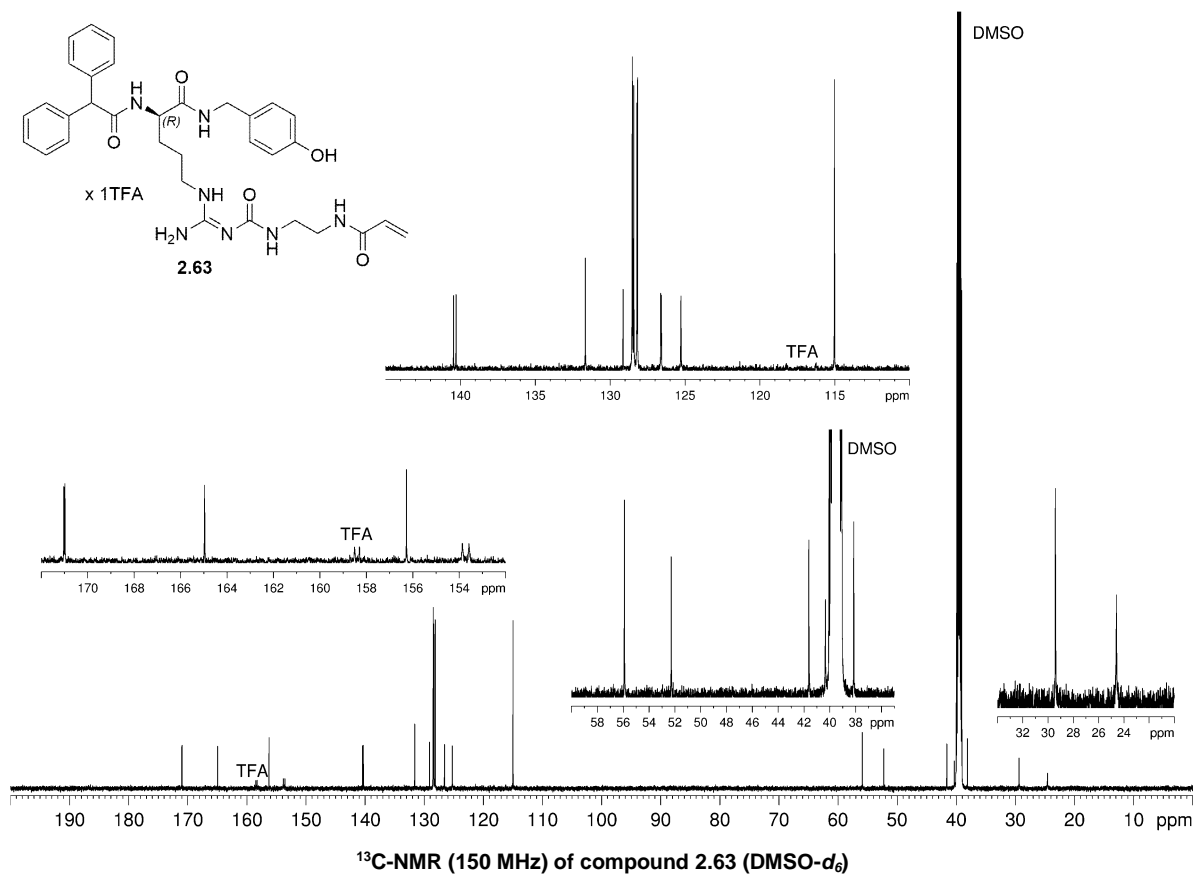
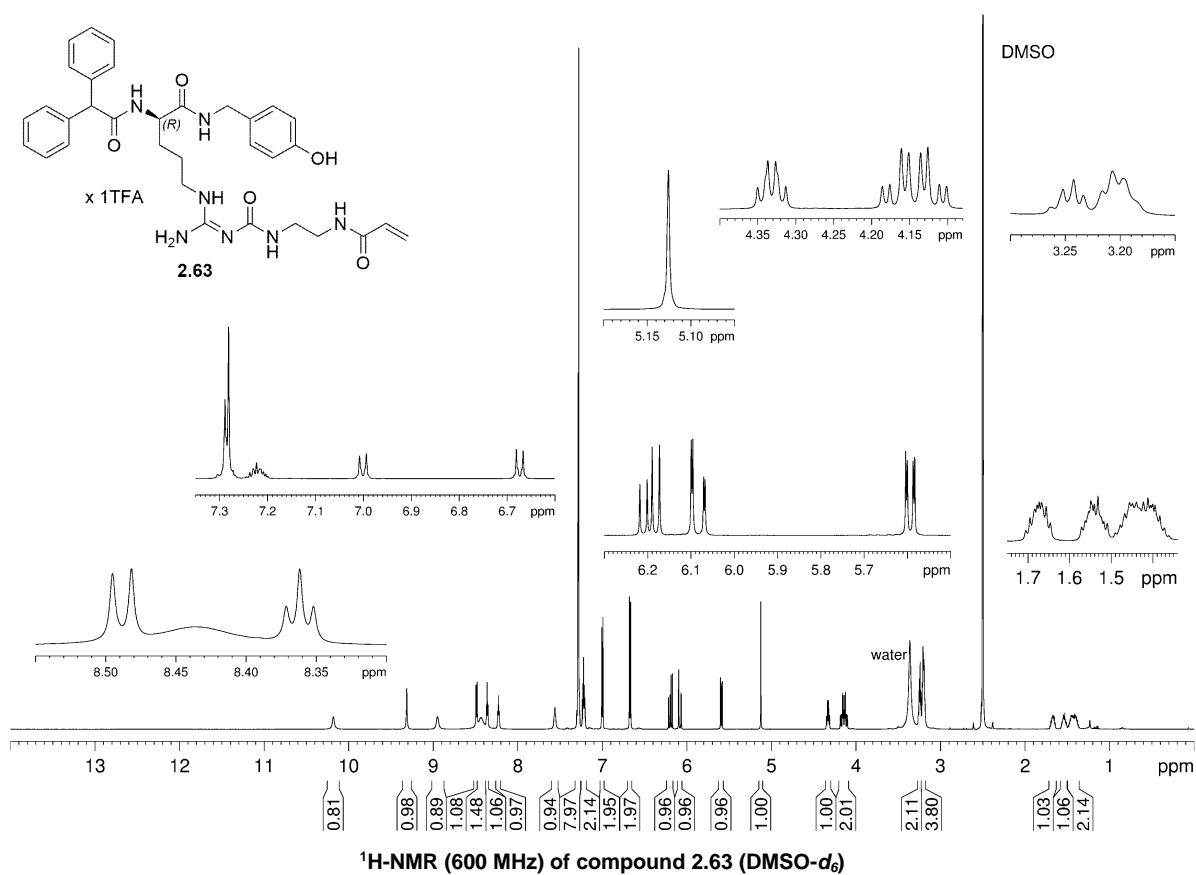


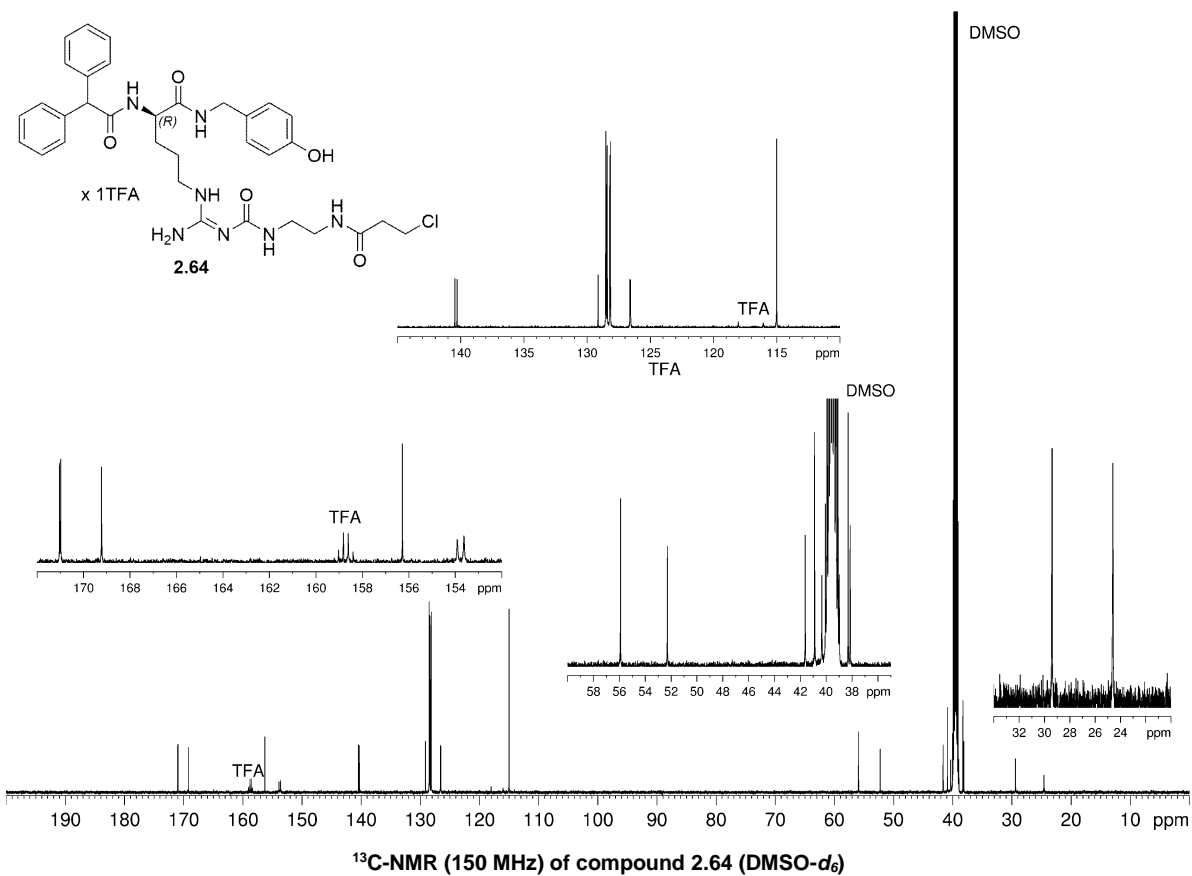
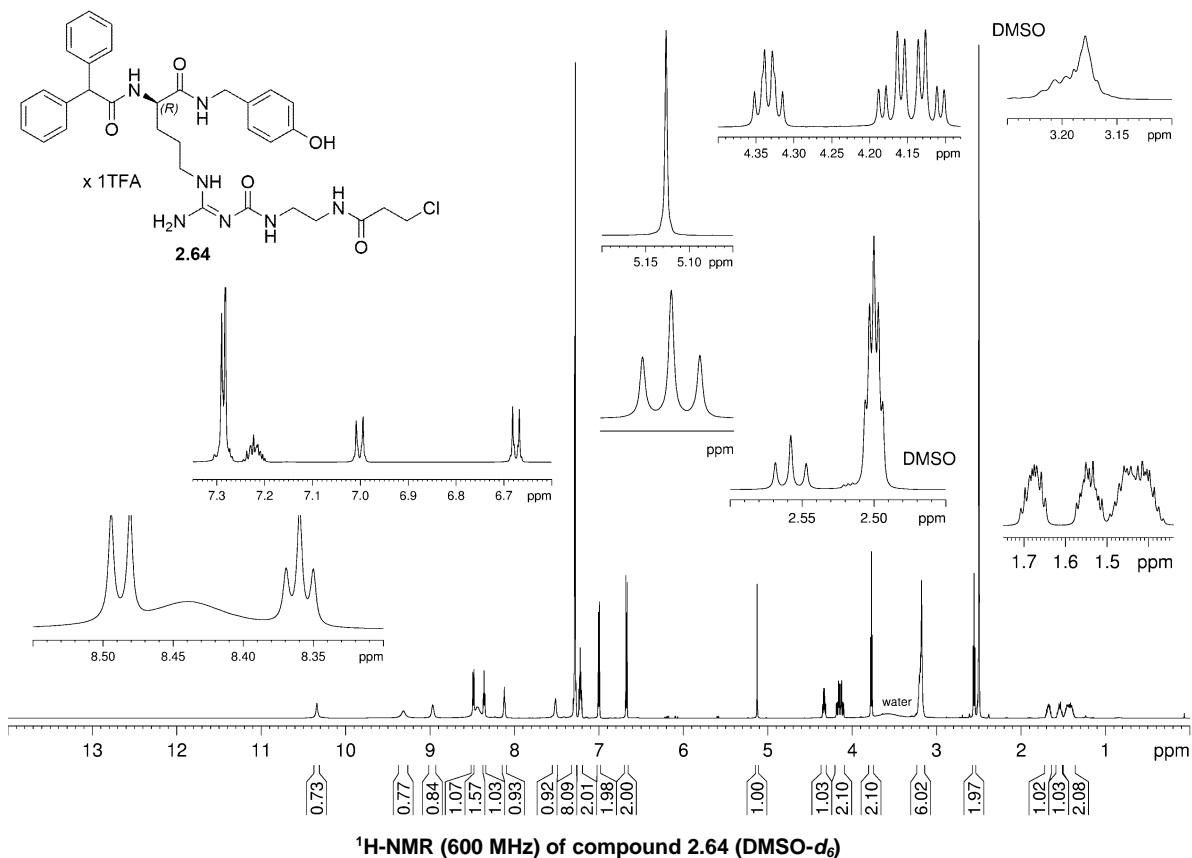


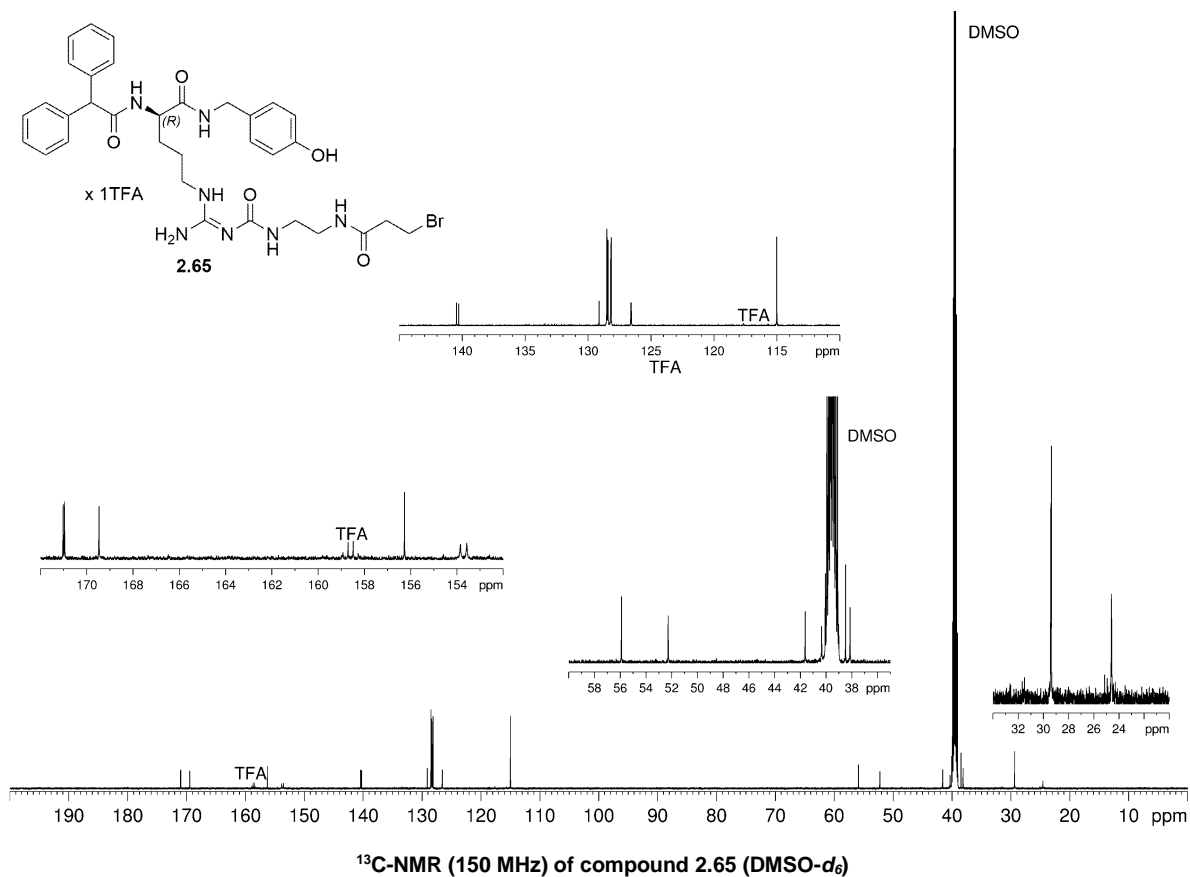
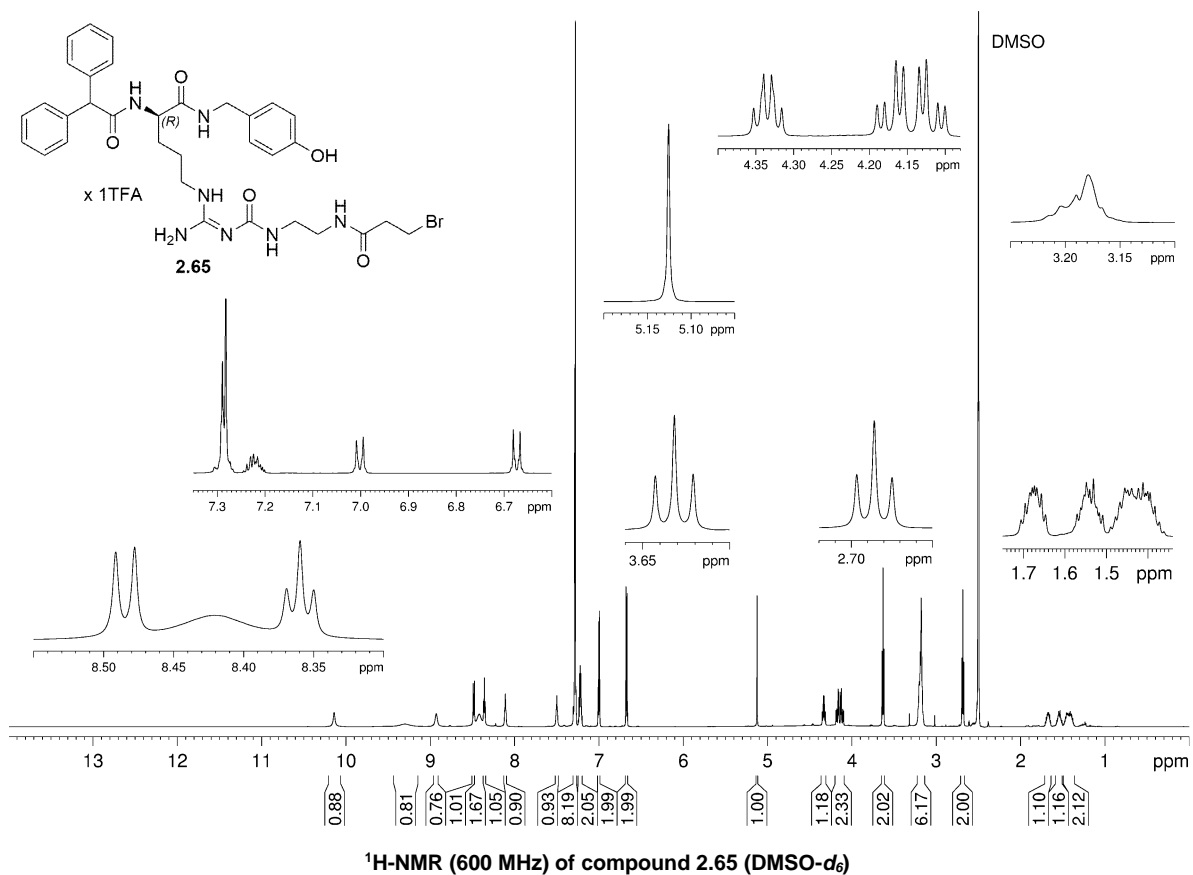


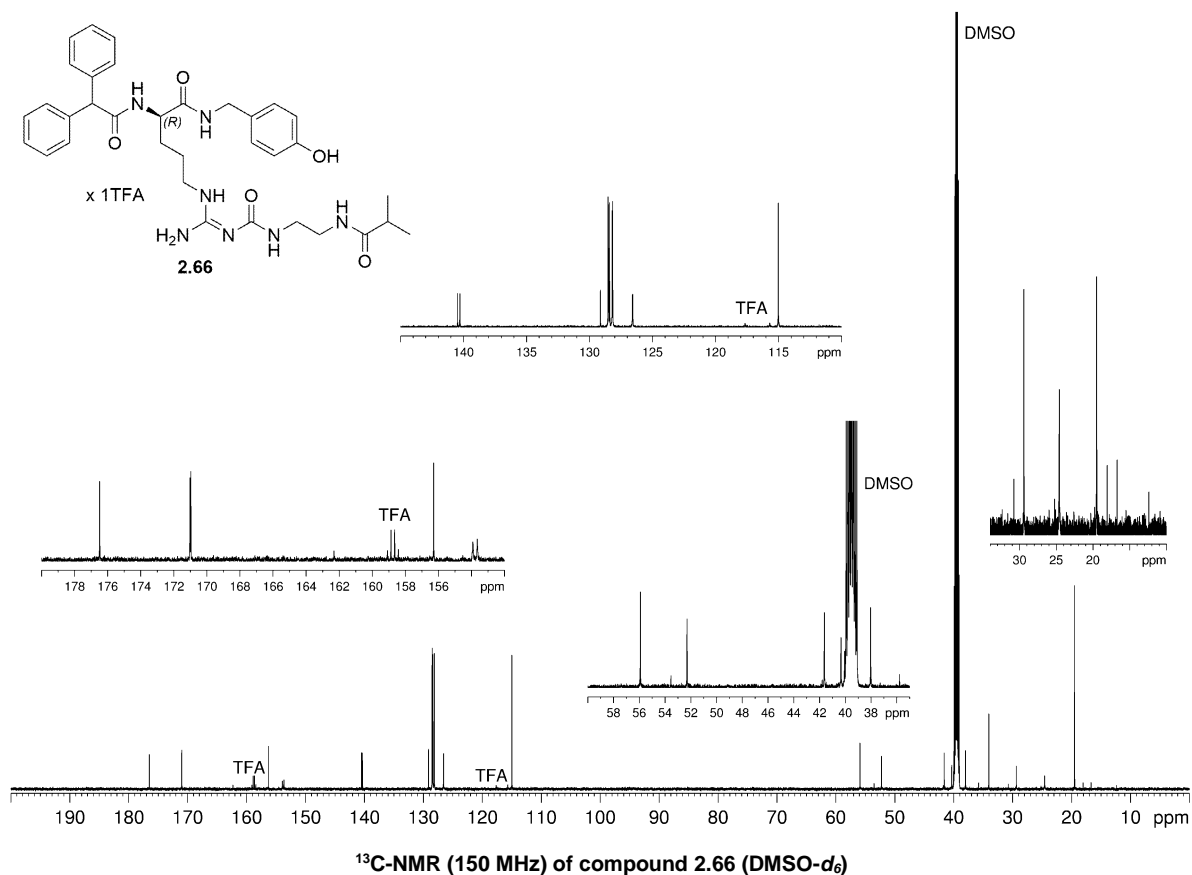
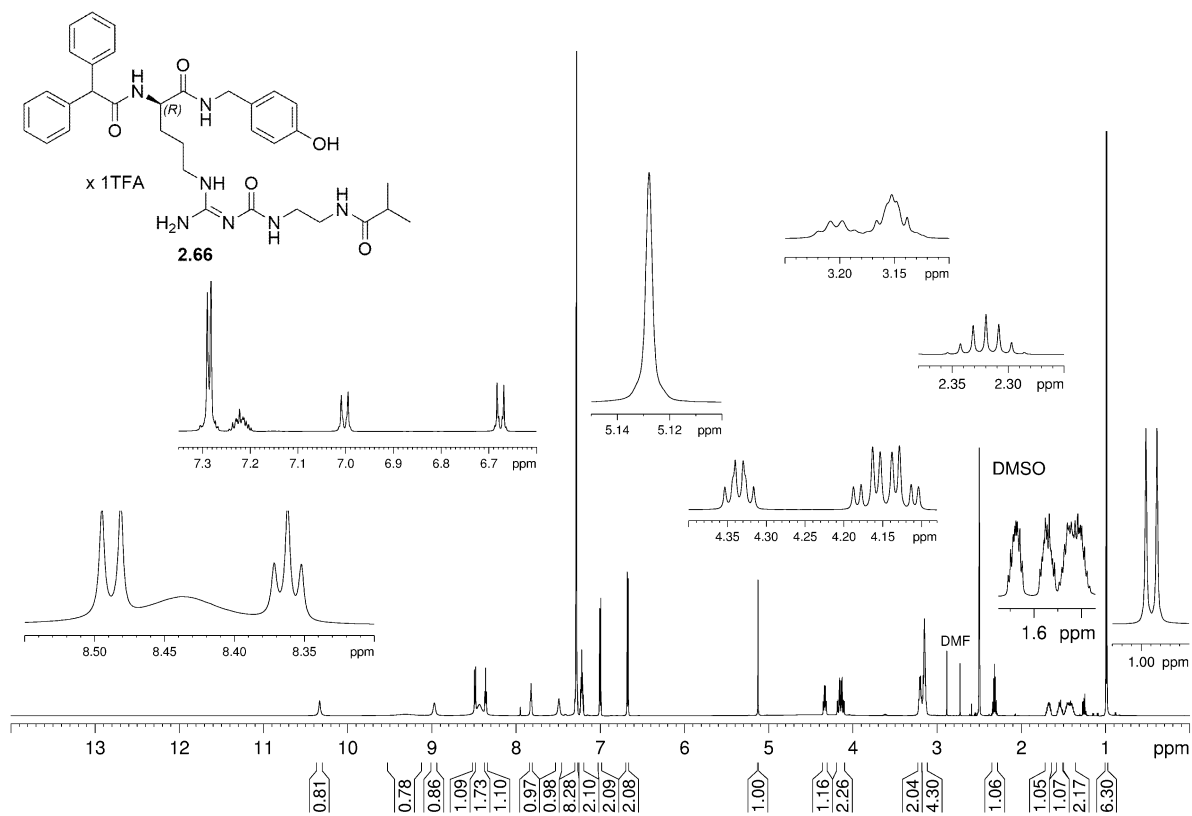


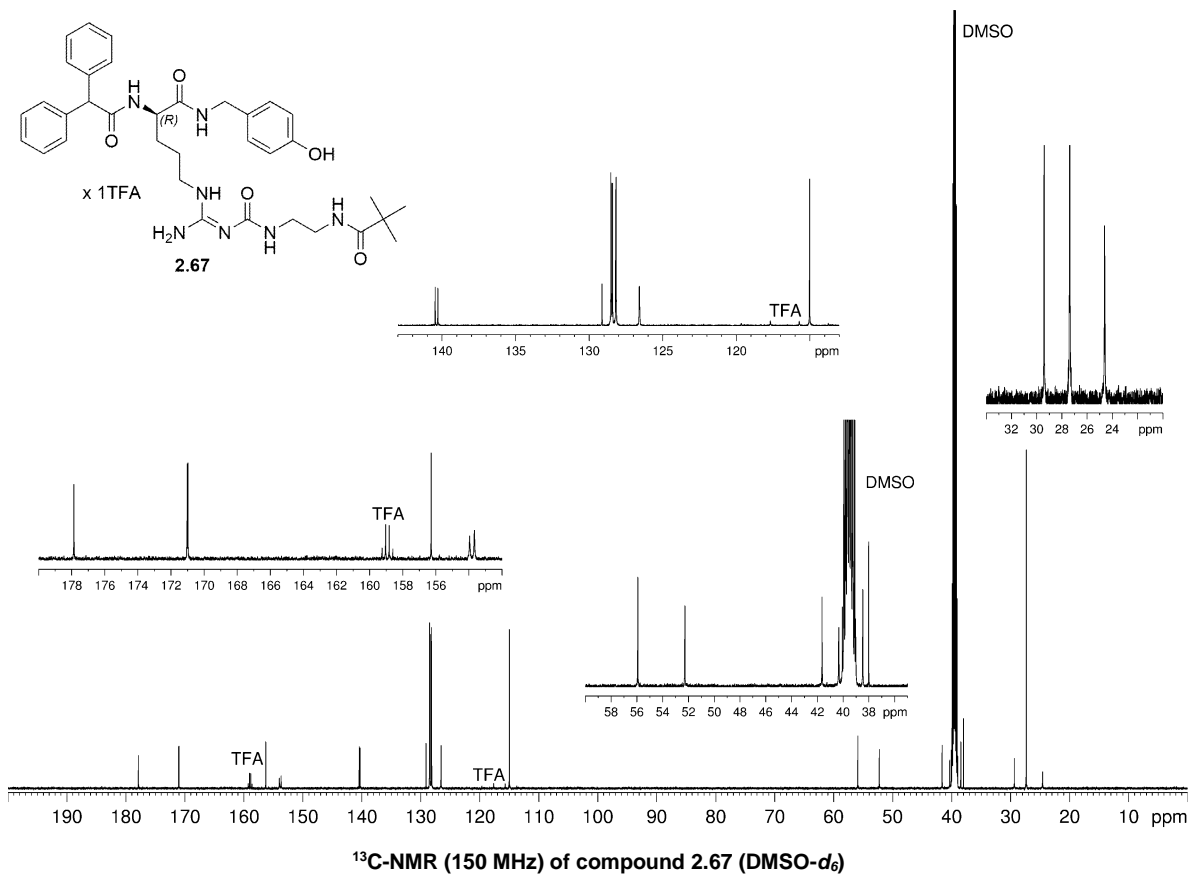
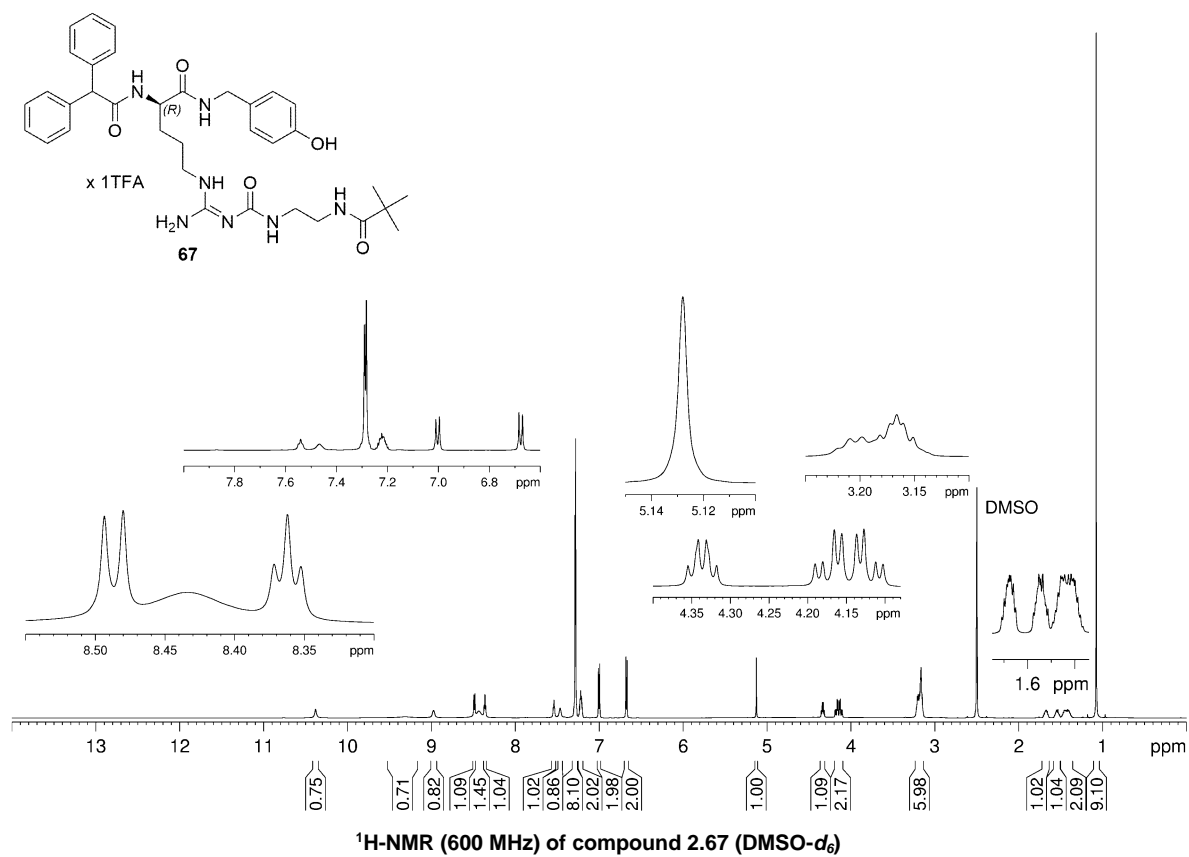


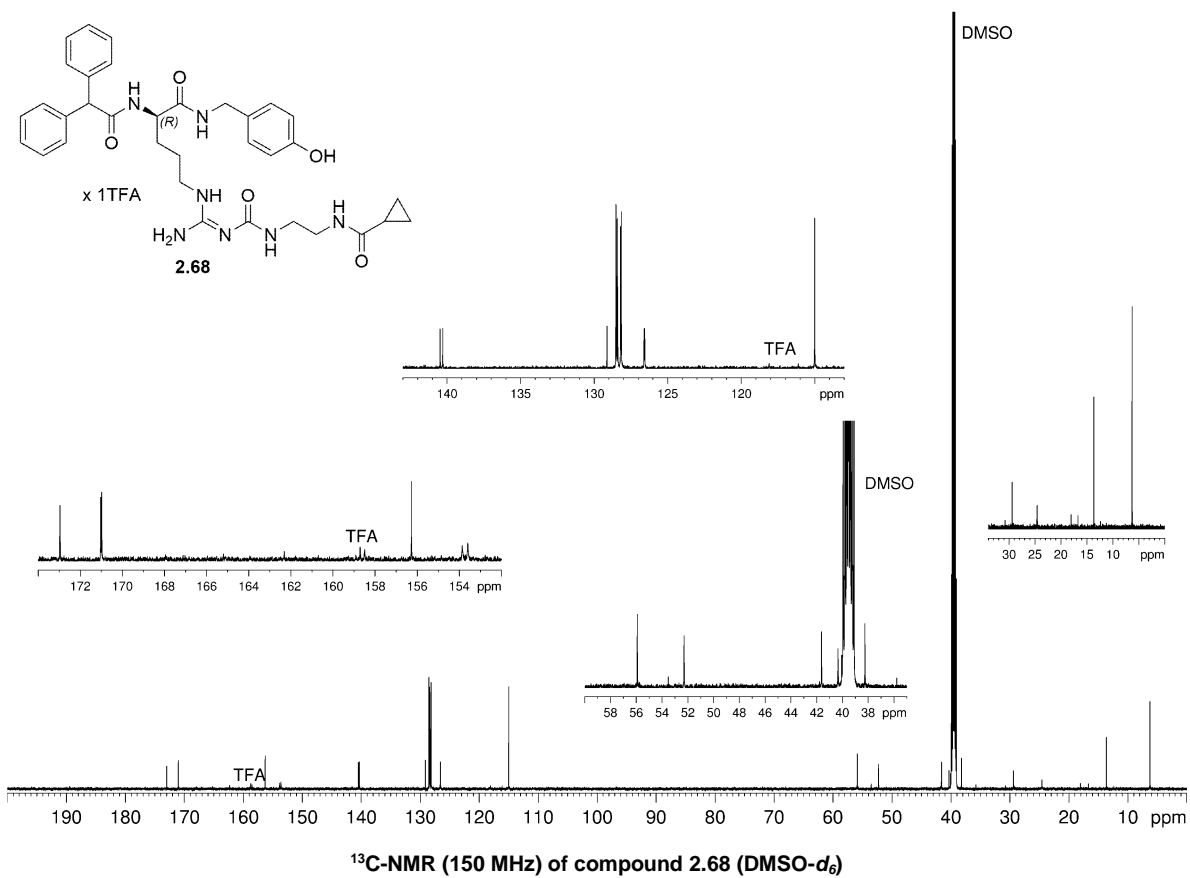
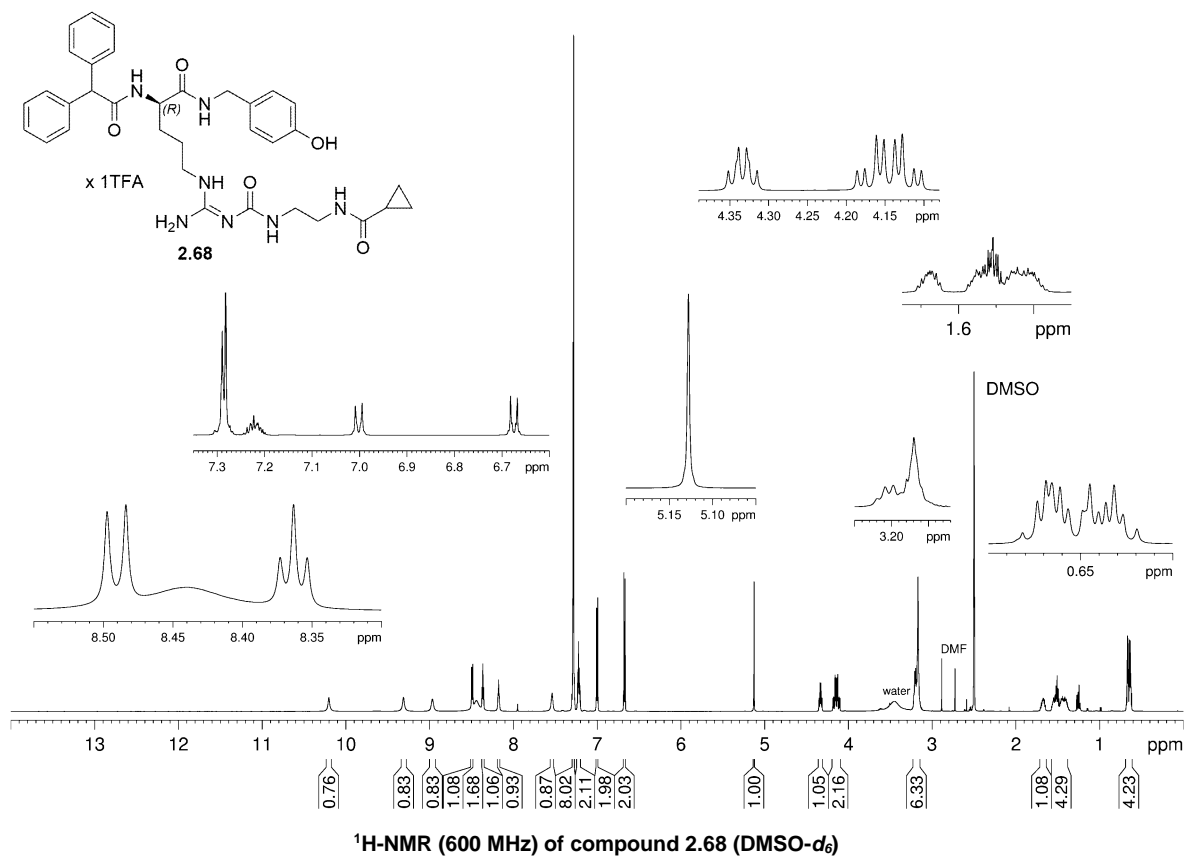


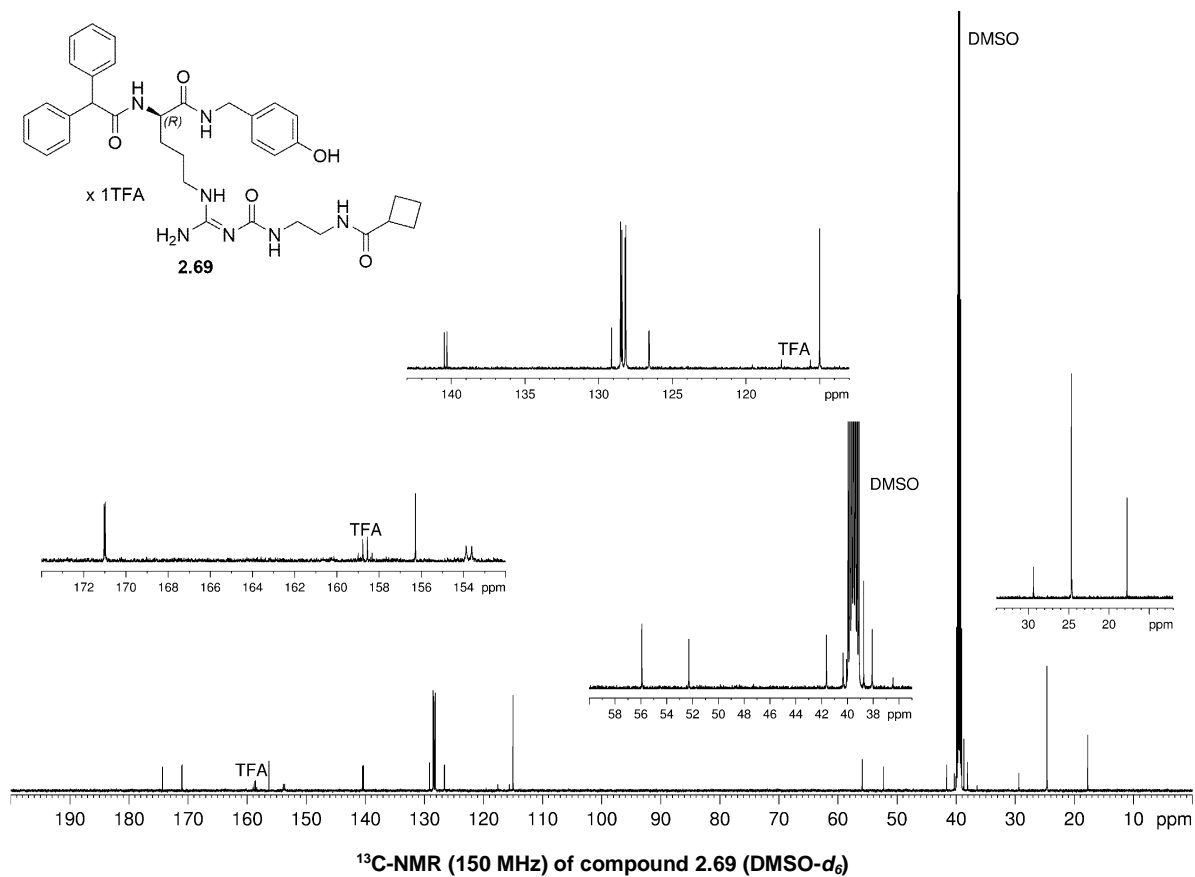
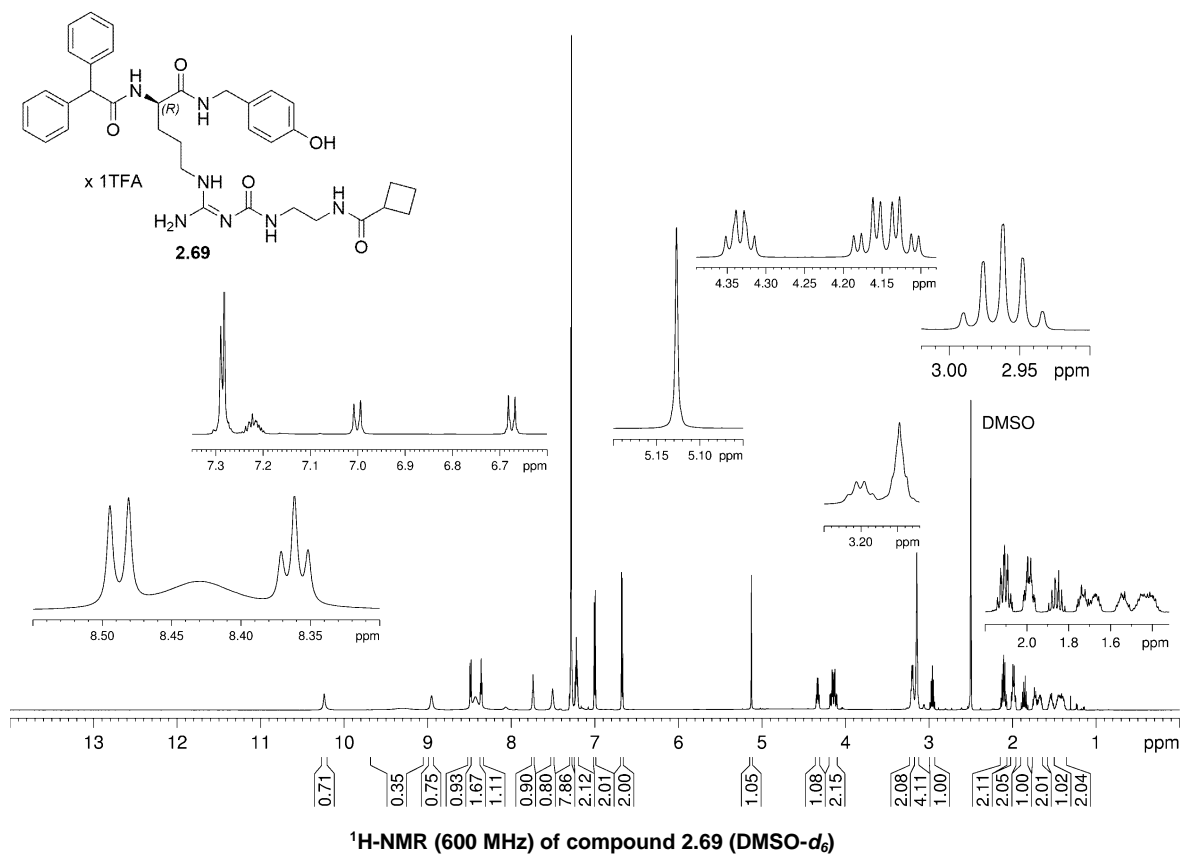


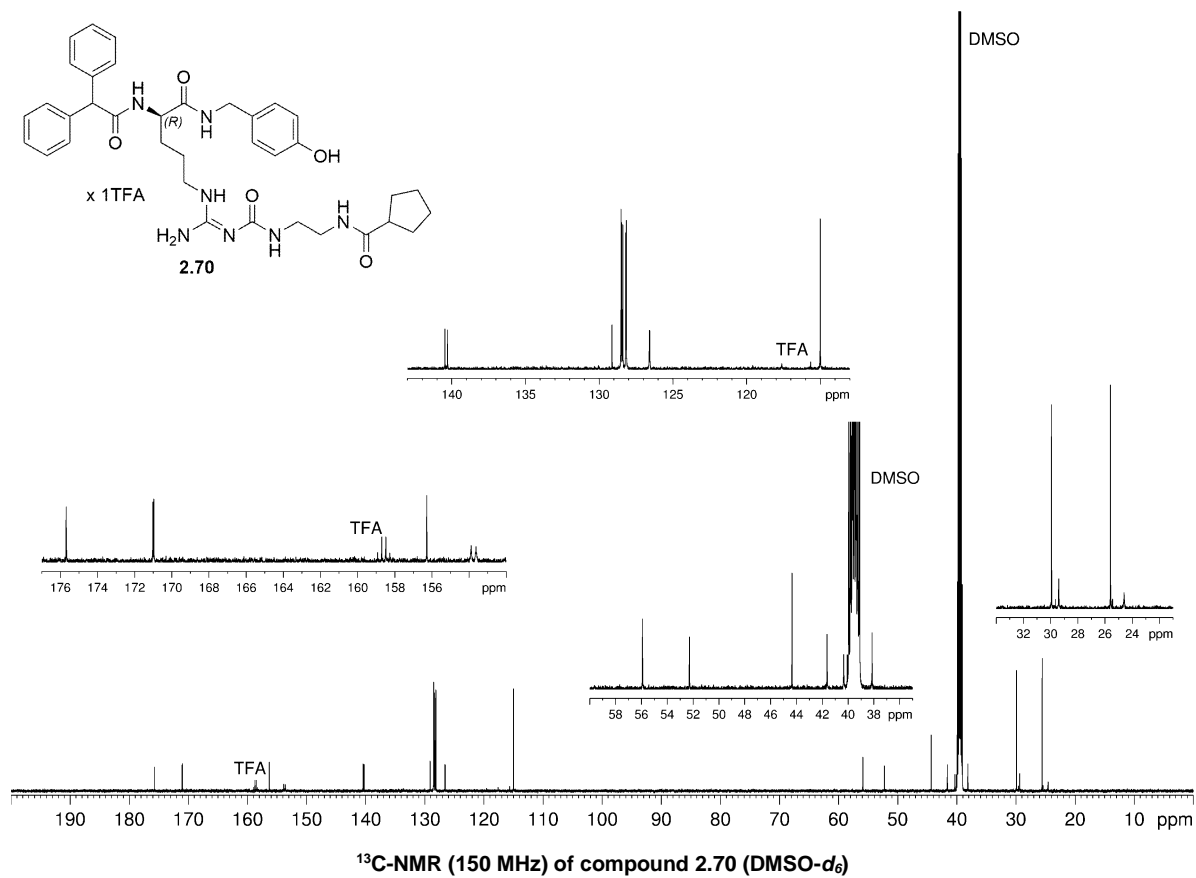
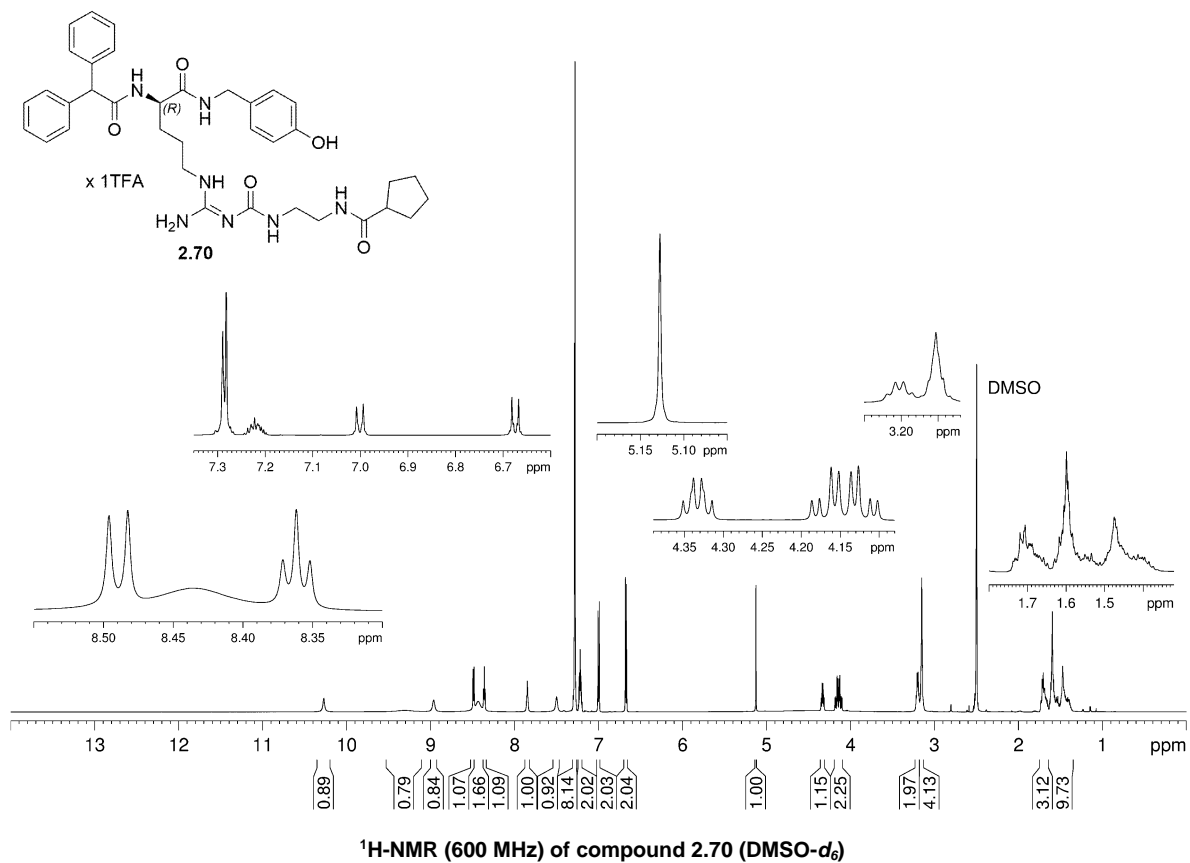


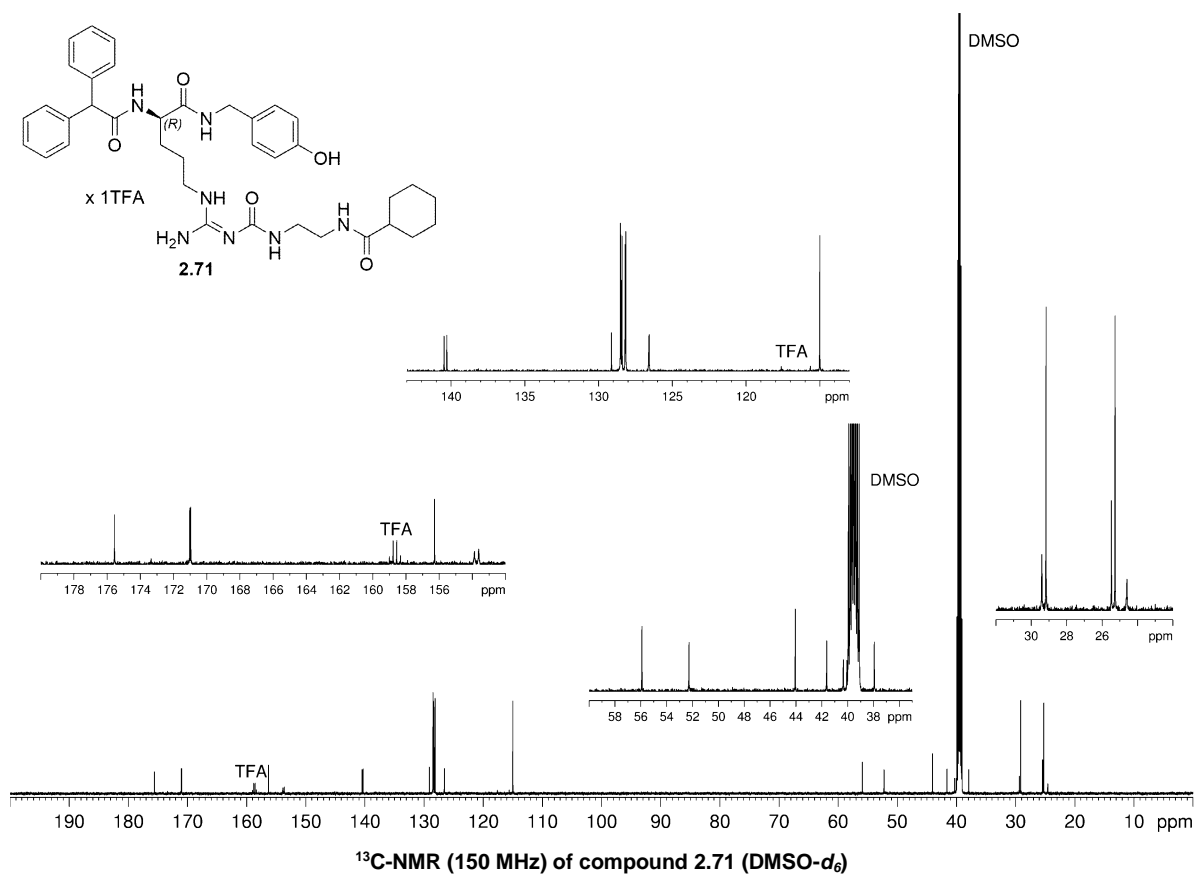
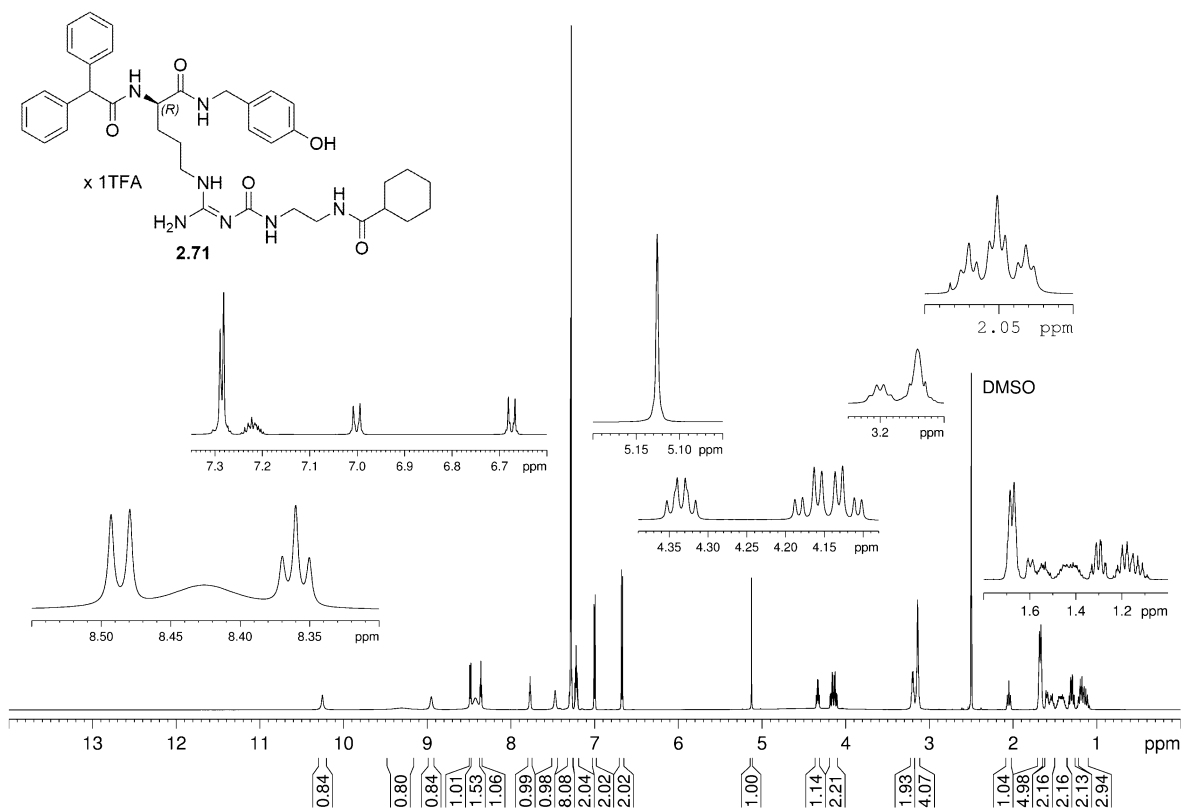


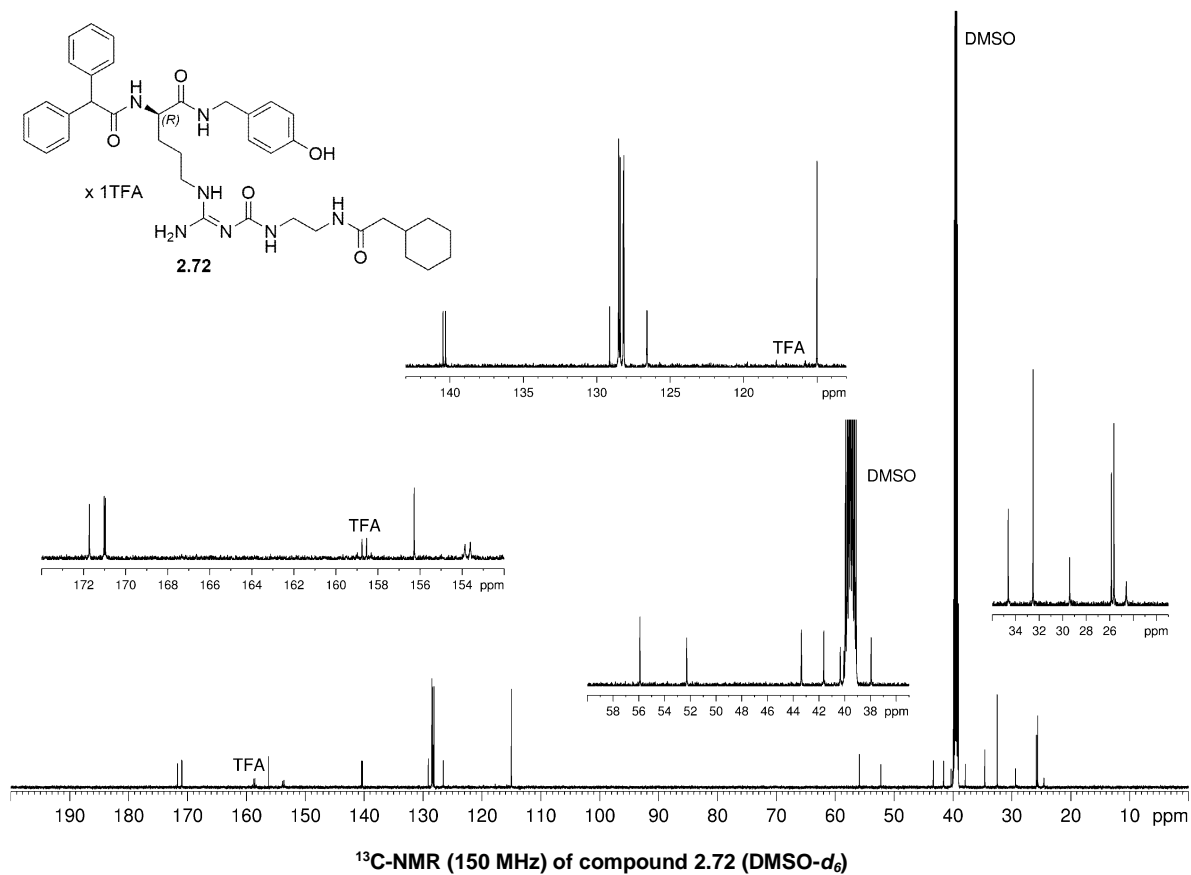
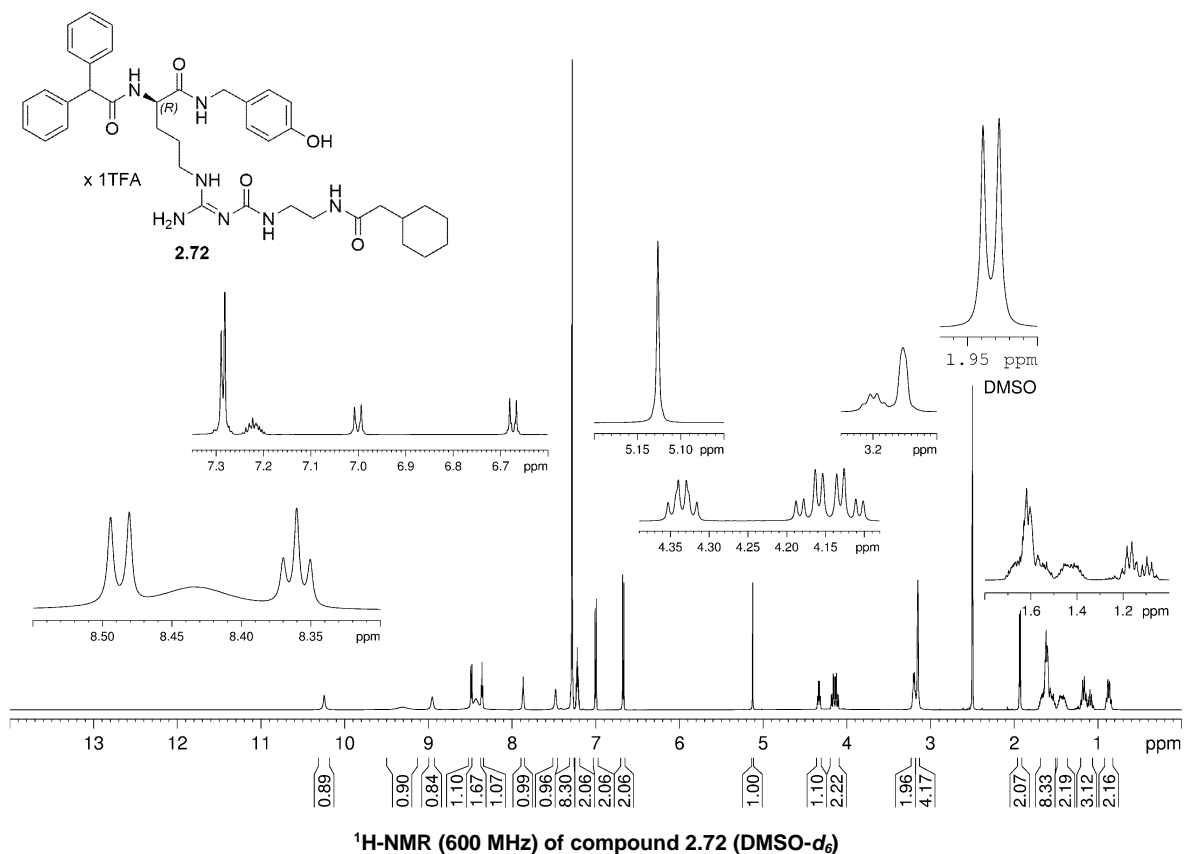


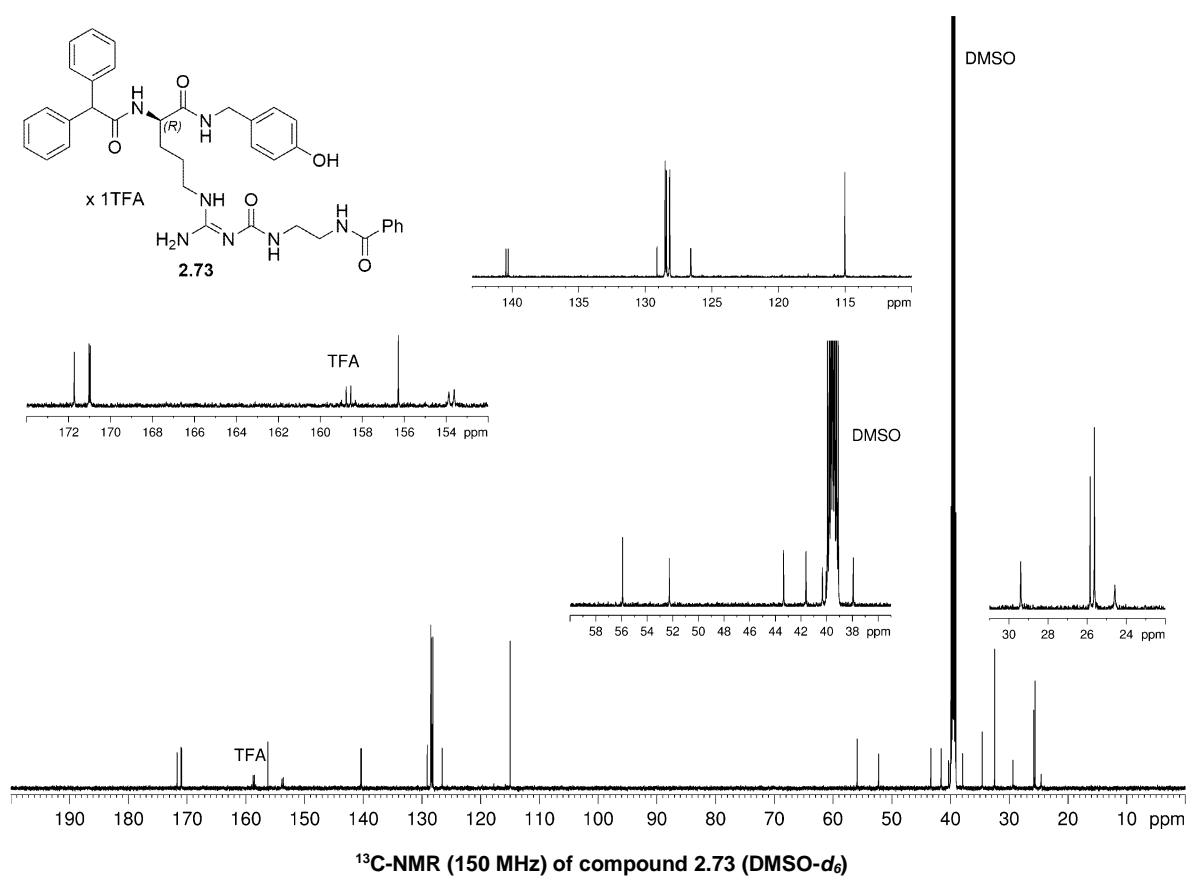
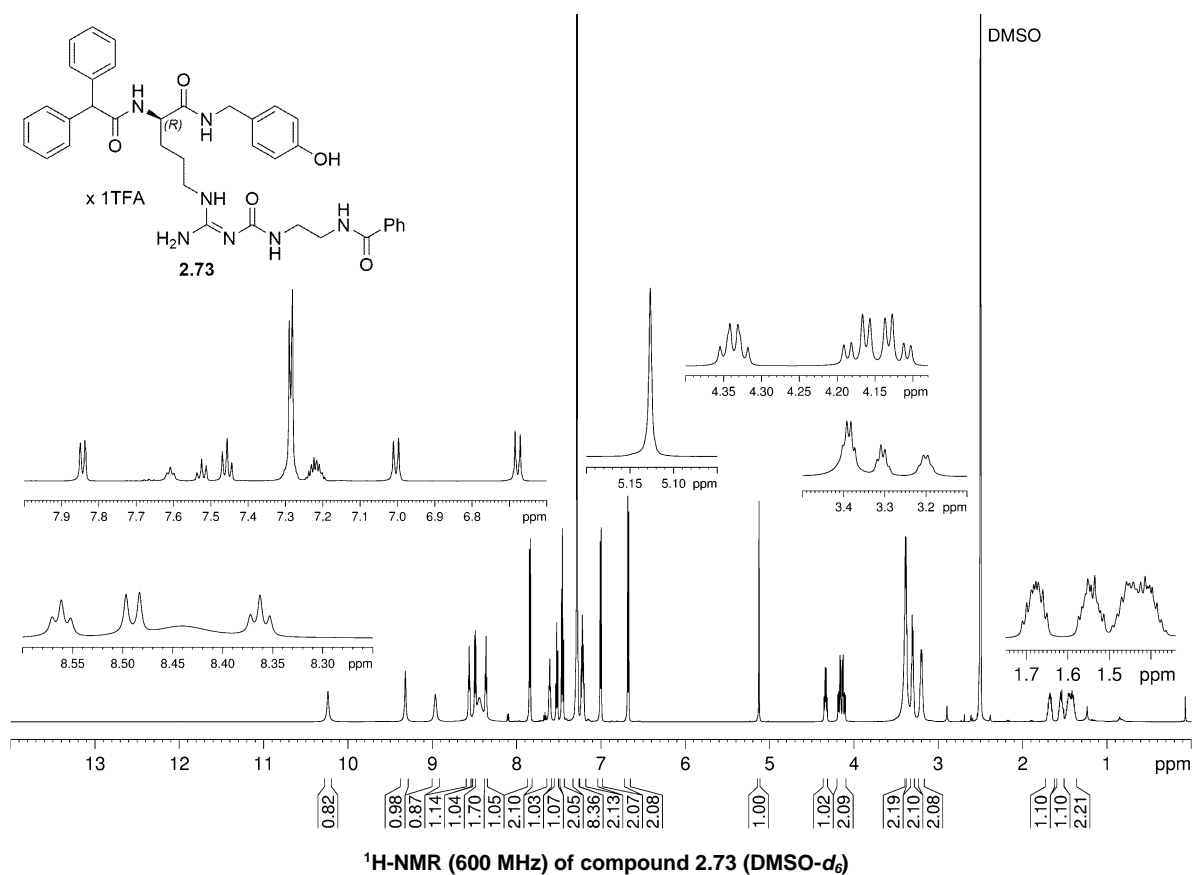


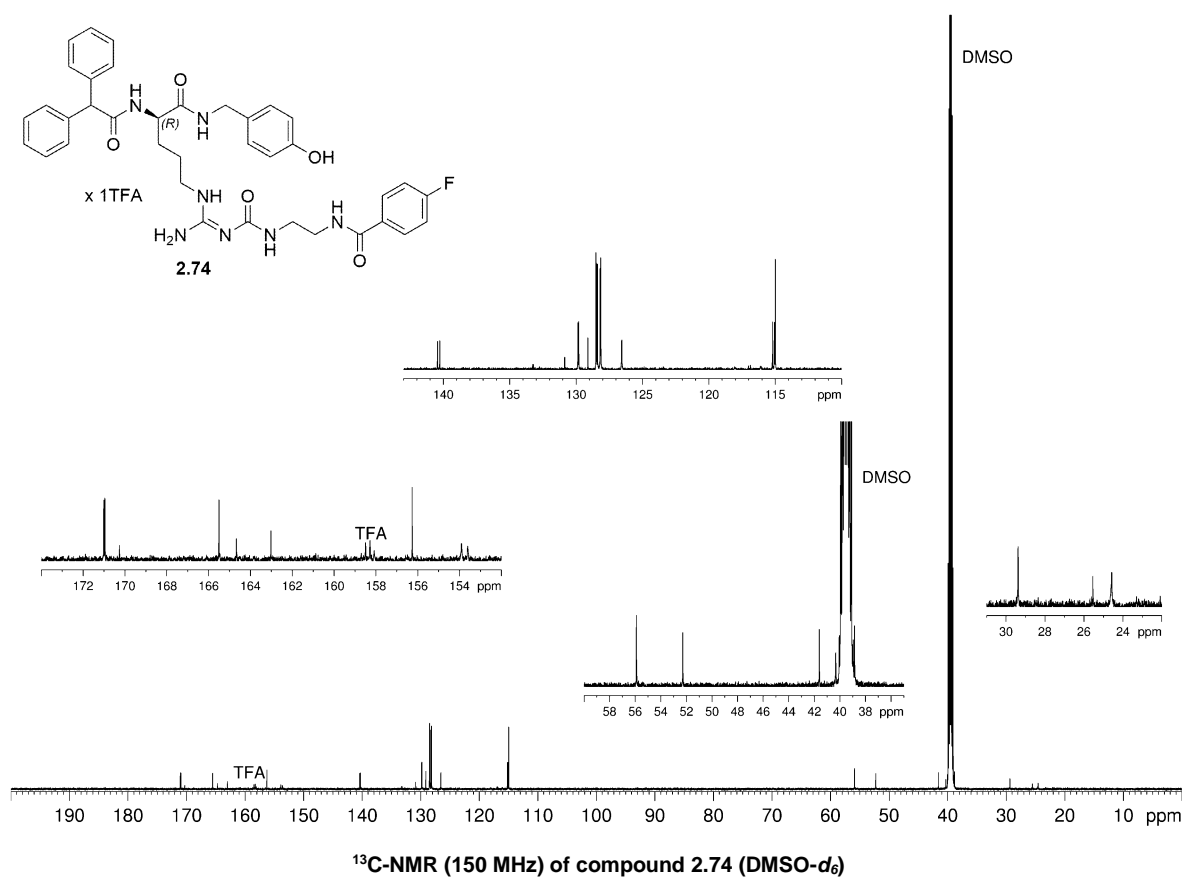
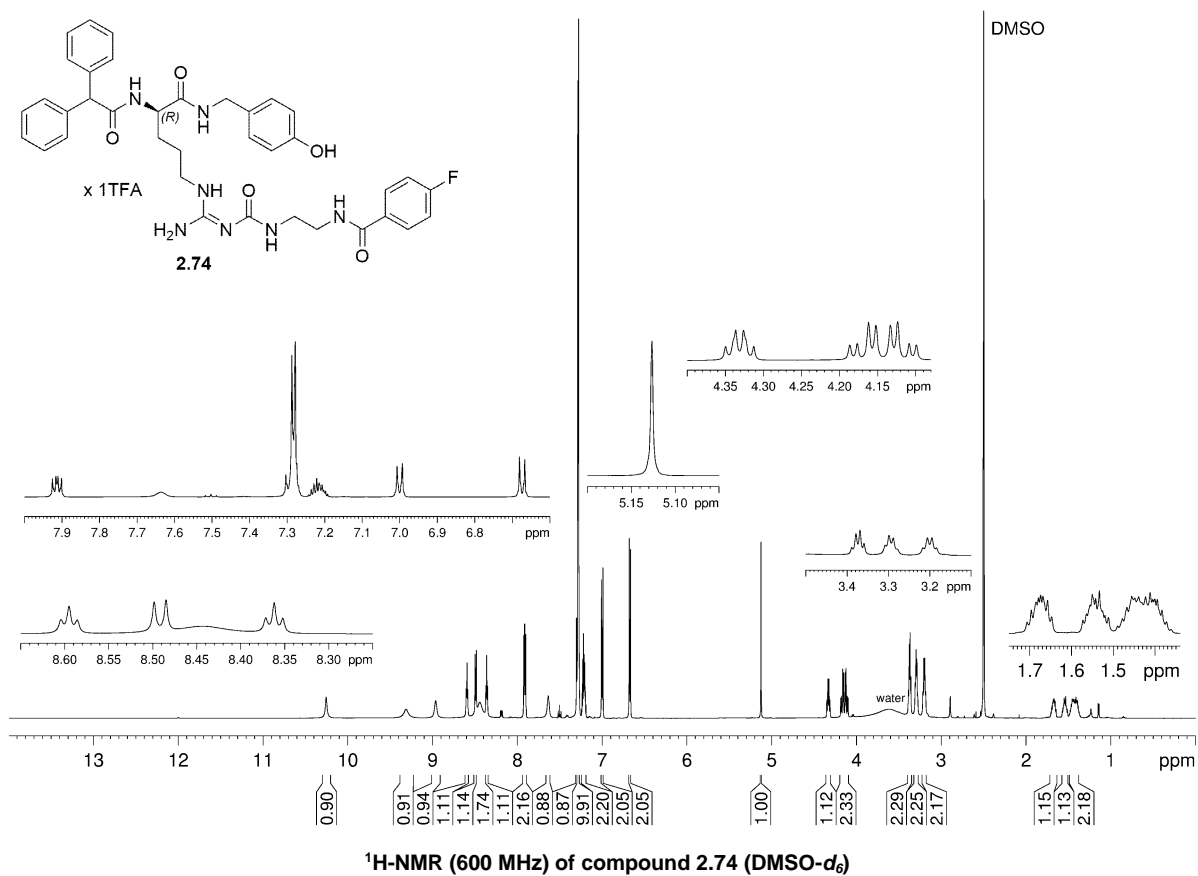


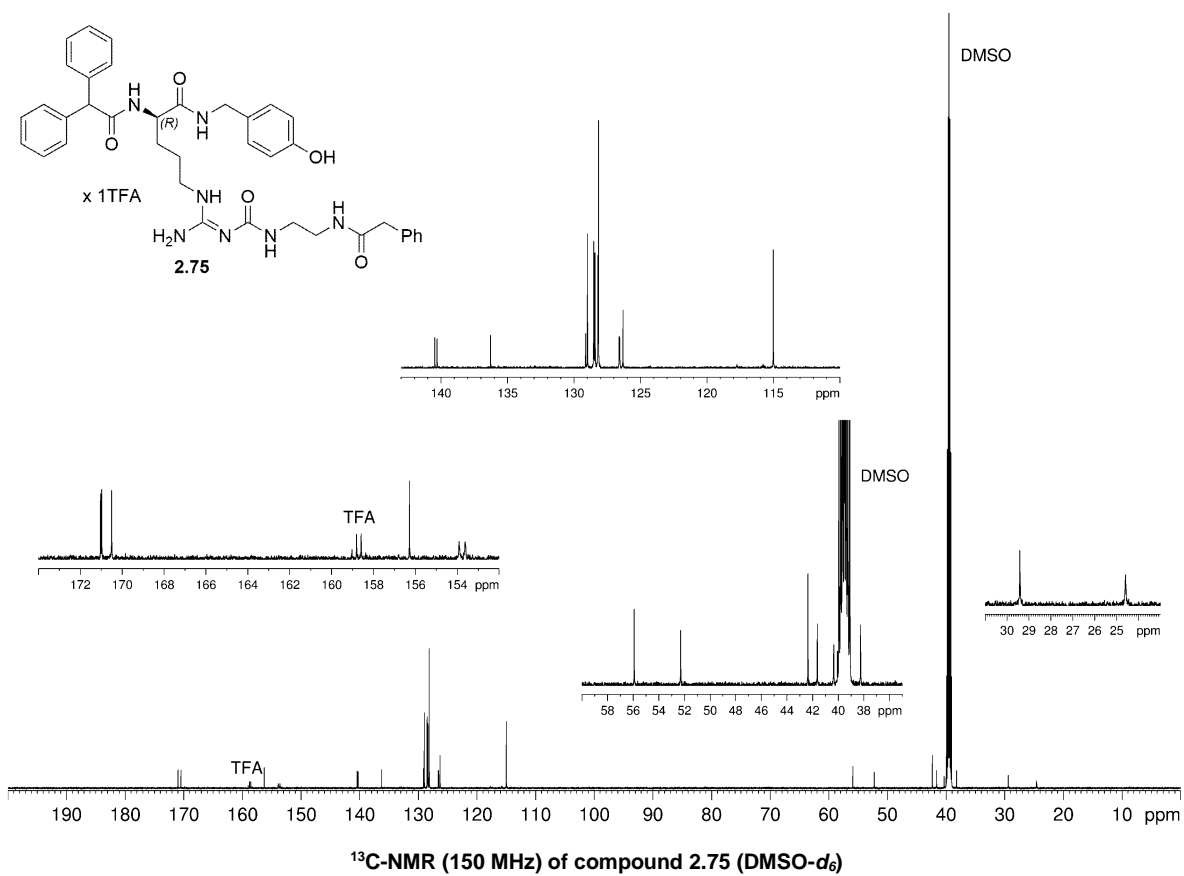
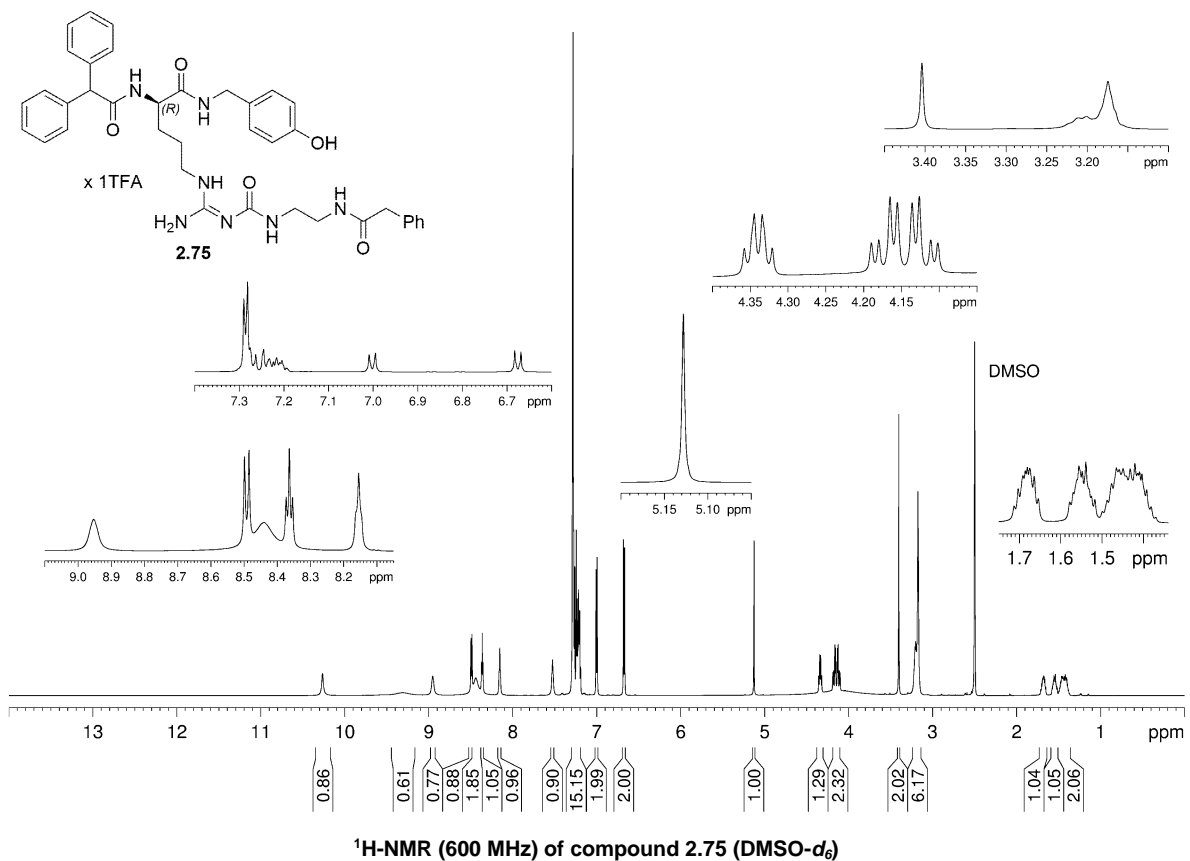


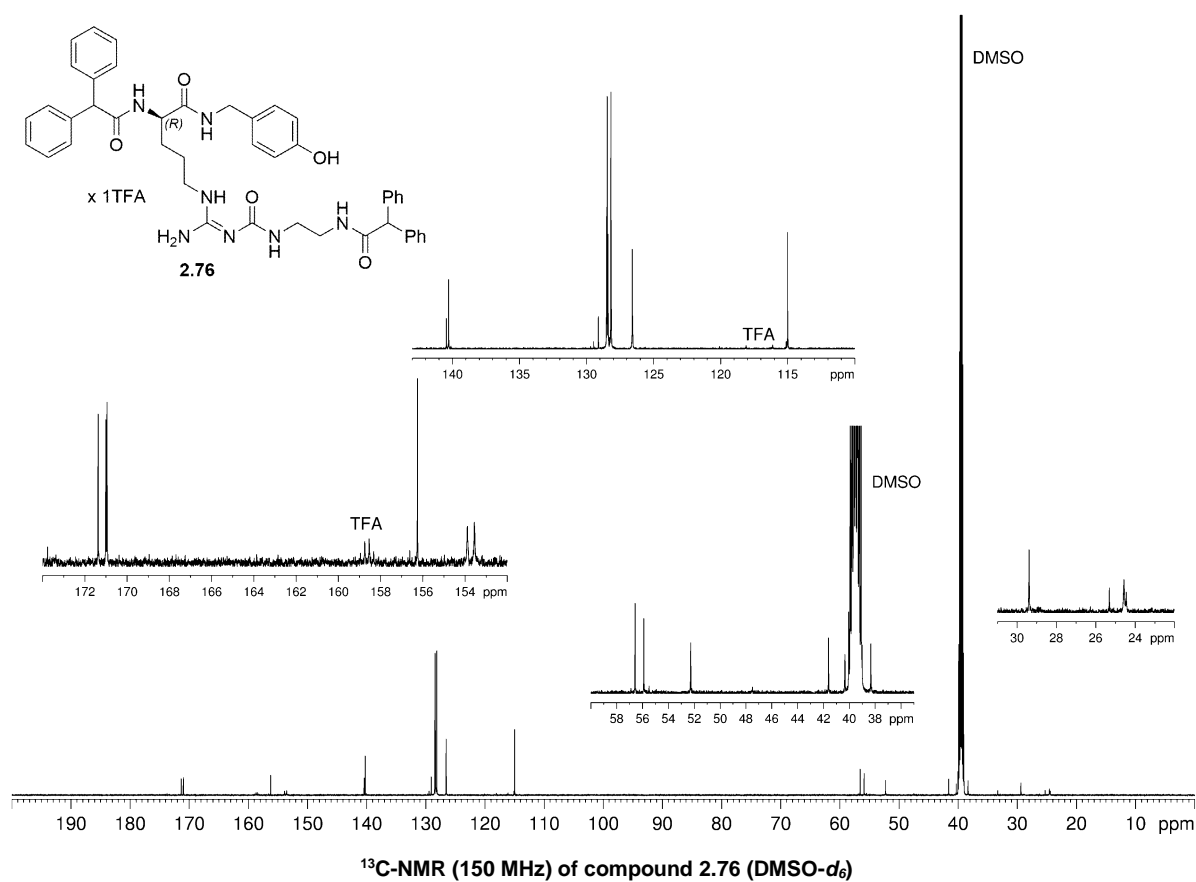
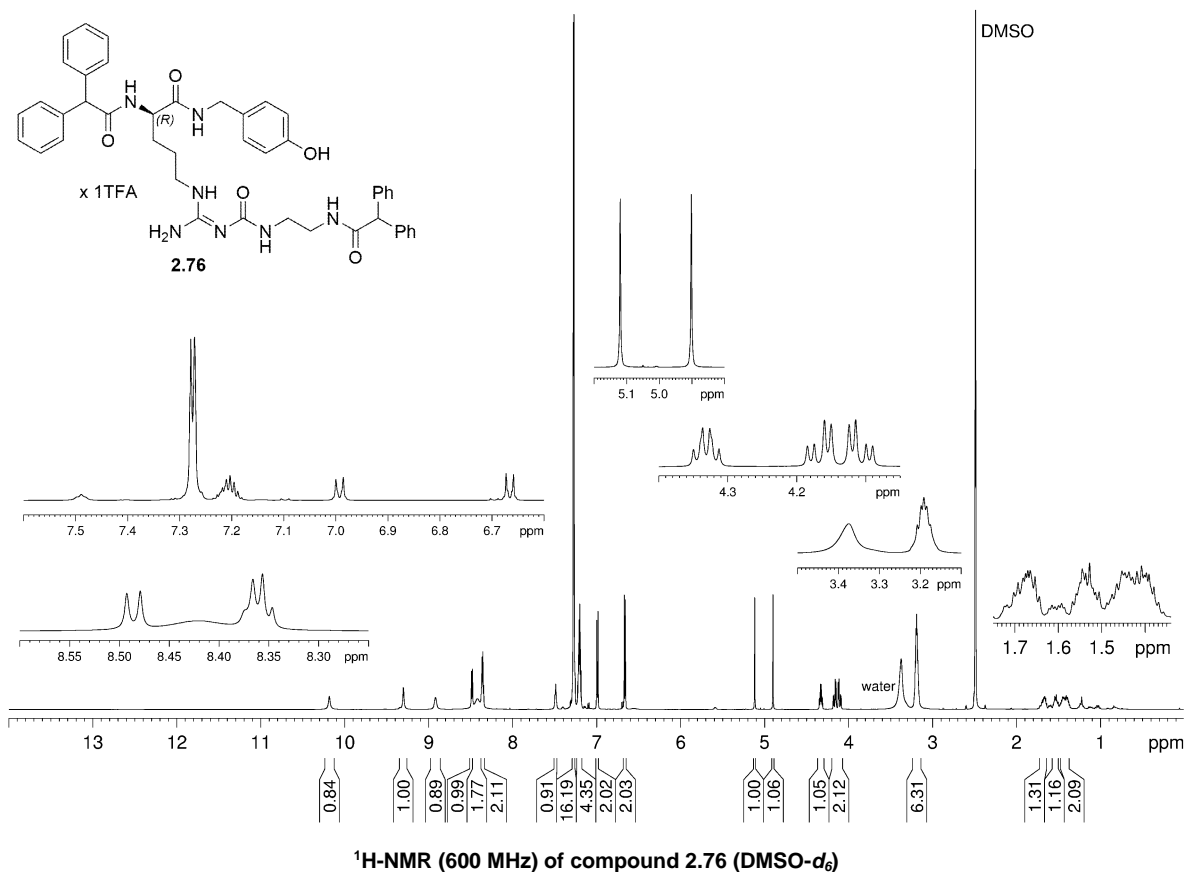




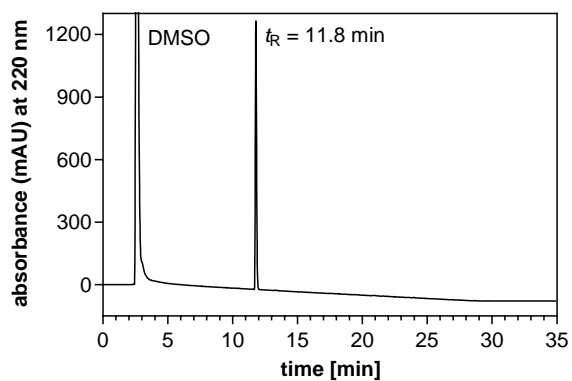




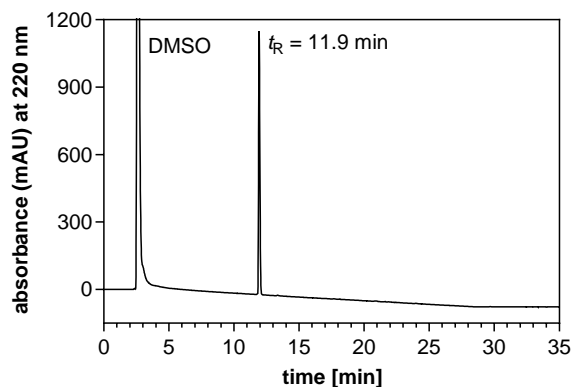




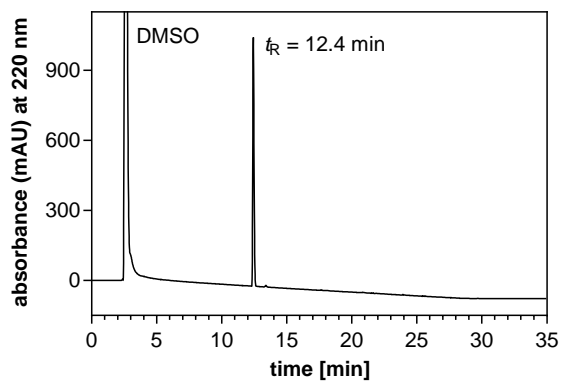
8.1.4. RP-HPLC purity chromatograms (220 nm) of compounds 2.53-2.76 and 2.78



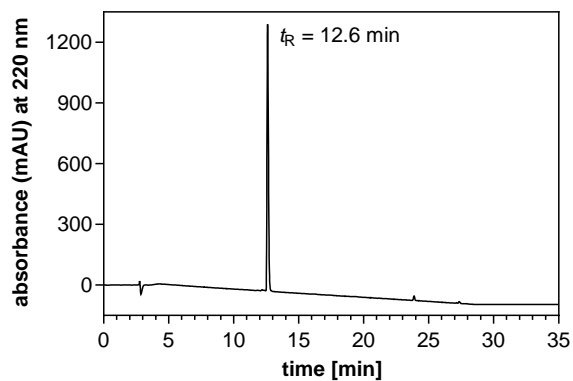
RP-HPLC (220 nm) chromatogram of 2.53



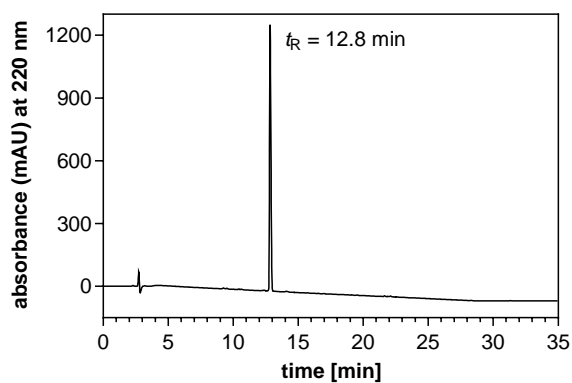
RP-HPLC (220 nm) chromatogram of 2.54



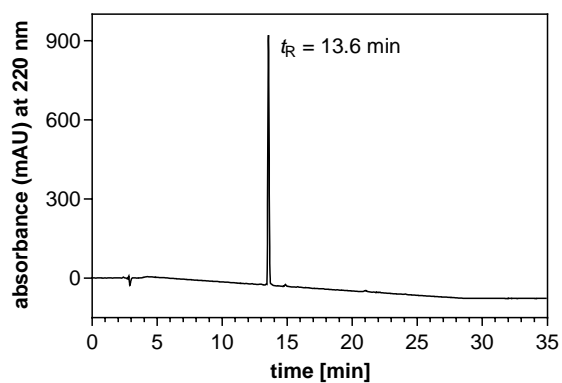
RP-HPLC (220 nm) chromatogram of 2.55



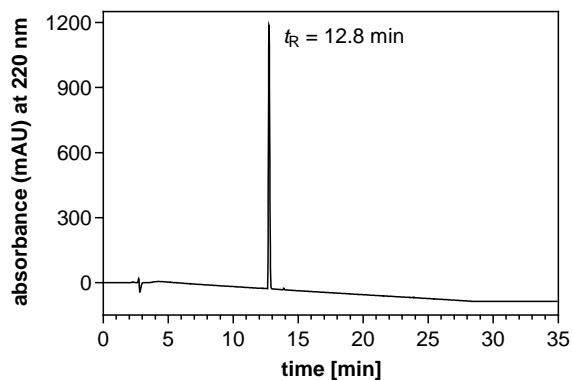
RP-HPLC (220 nm) chromatogram of 2.56



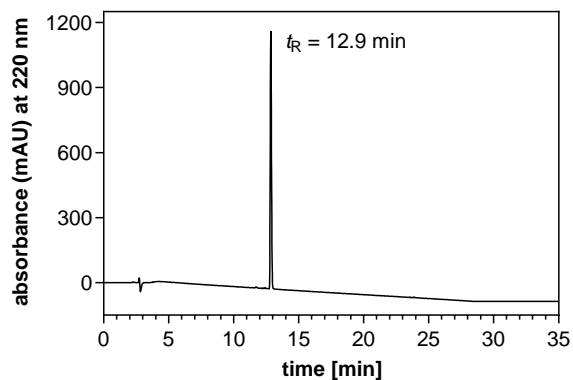
RP-HPLC (220 nm) chromatogram of 2.57



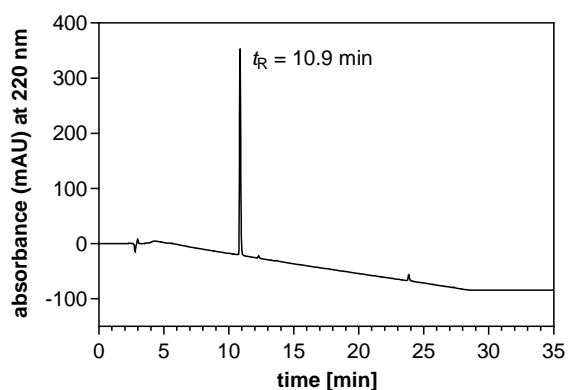
RP-HPLC (220 nm) chromatogram of 2.58



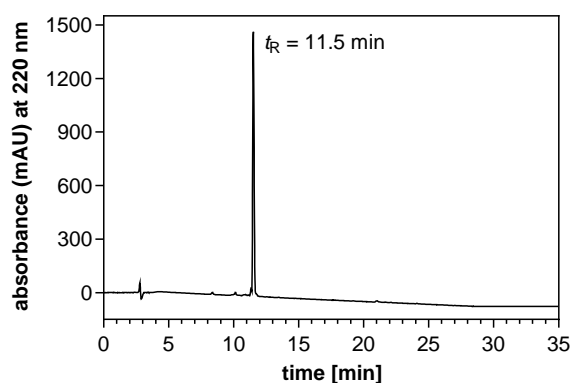
RP-HPLC (220 nm) chromatogram of 2.59



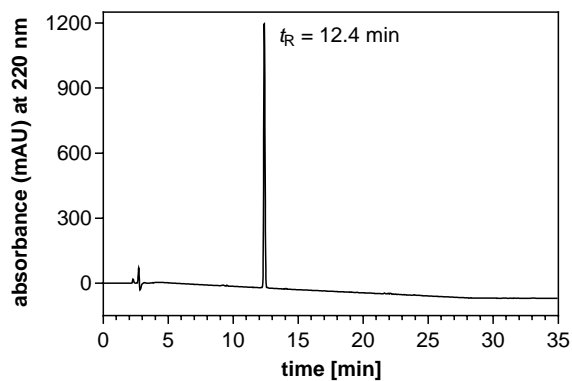
RP-HPLC (220 nm) chromatogram of 2.60



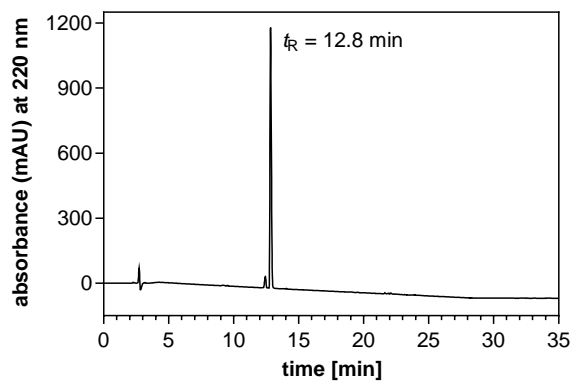
RP-HPLC (220 nm) chromatogram of 2.61



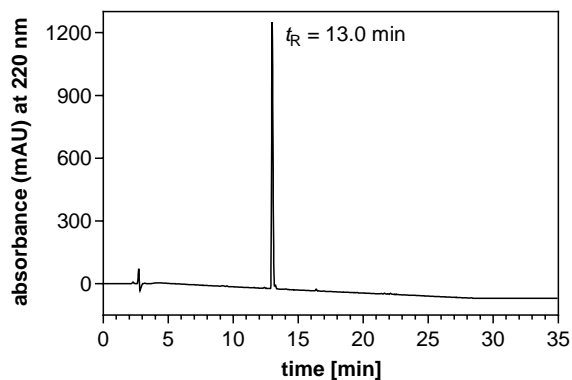
RP-HPLC (220 nm) chromatogram of 2.62



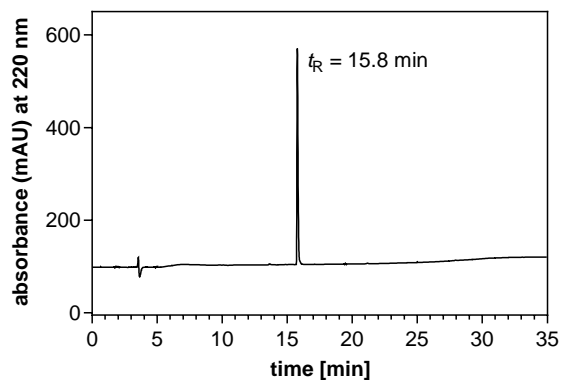
RP-HPLC (220 nm) chromatogram of 2.63



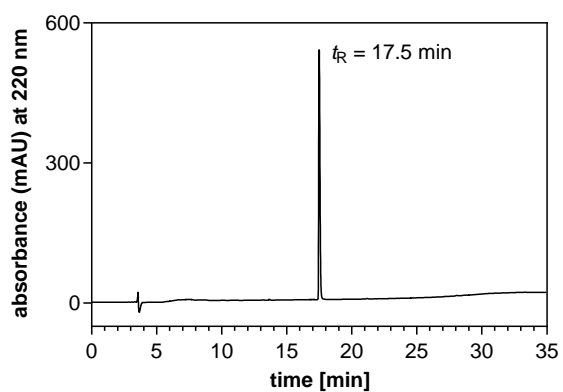
RP-HPLC (220 nm) chromatogram of 2.64



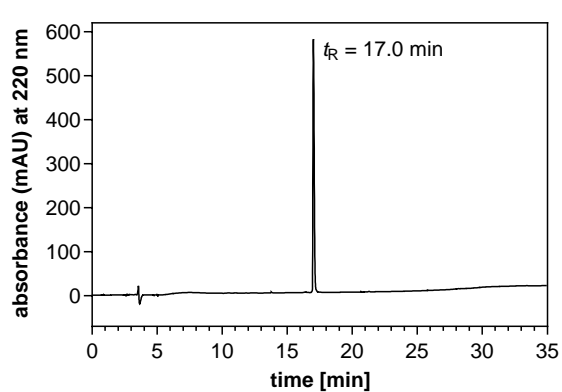
RP-HPLC (220 nm) chromatogram of 2.65



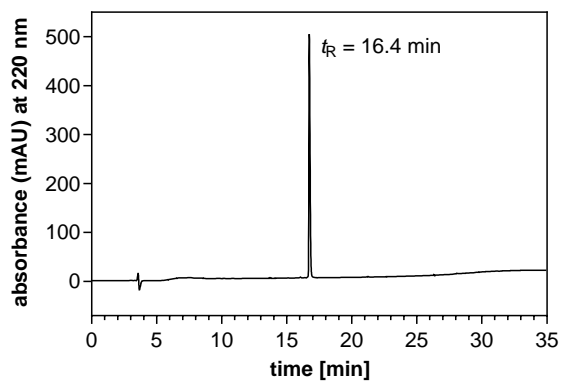
RP-HPLC (220 nm) chromatogram of 2.66



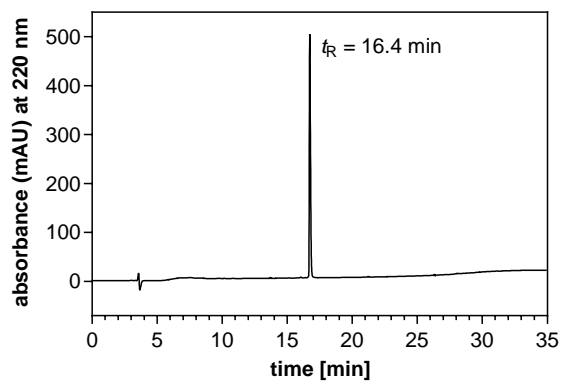
RP-HPLC (220 nm) chromatogram of 2.67



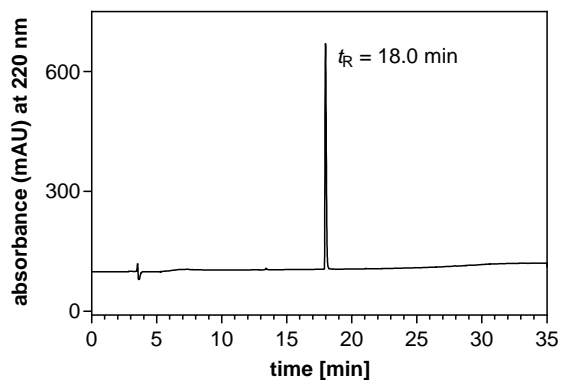
RP-HPLC (220 nm) chromatogram of 2.68



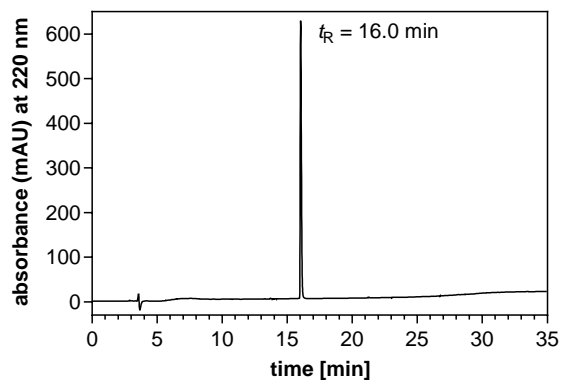
RP-HPLC (220 nm) chromatogram of 2.69



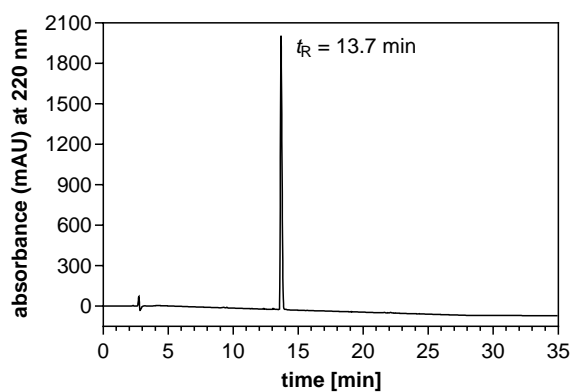
RP-HPLC (220 nm) chromatogram of 2.70



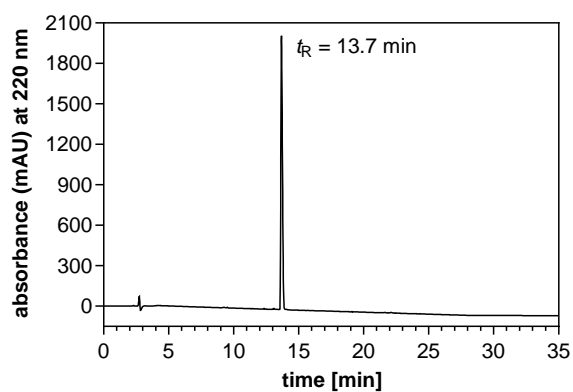
RP-HPLC (220 nm) chromatogram of 2.71



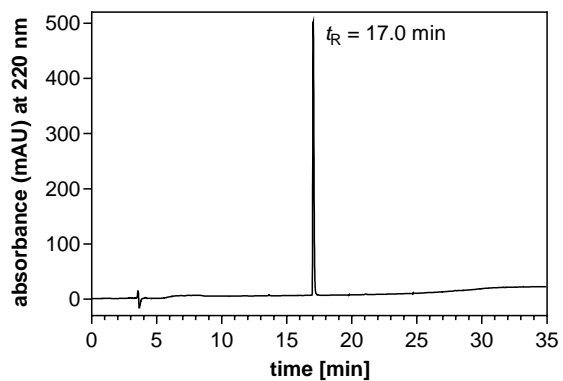
RP-HPLC (220 nm) chromatogram of 2.72



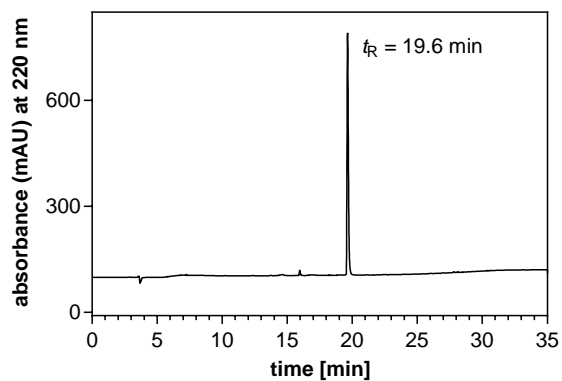
RP-HPLC (220 nm) chromatogram of 2.73



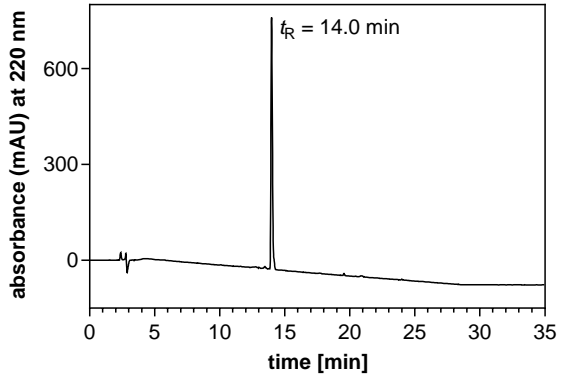
RP-HPLC (220 nm) chromatogram of 2.74



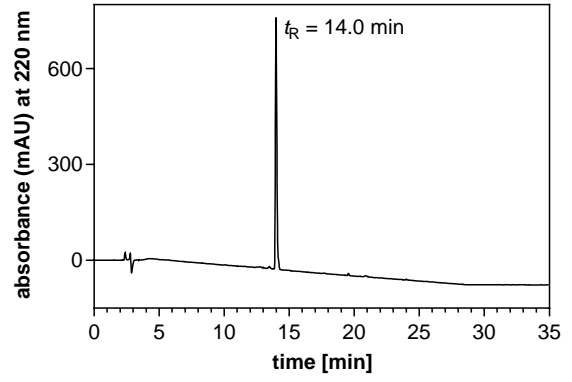
RP-HPLC (220 nm) chromatogram of 2.75



RP-HPLC (220 nm) chromatogram of 2.76



RP-HPLC (220 nm) chromatogram of 2.78



RP-HPLC (480 nm) chromatogram of 2.78

8.1.5. Investigation of the chemical stability of compounds 2.56, 2.58-2.61, 2.63 and 2.68

8.1.5.1. Supplementary figure 8.2

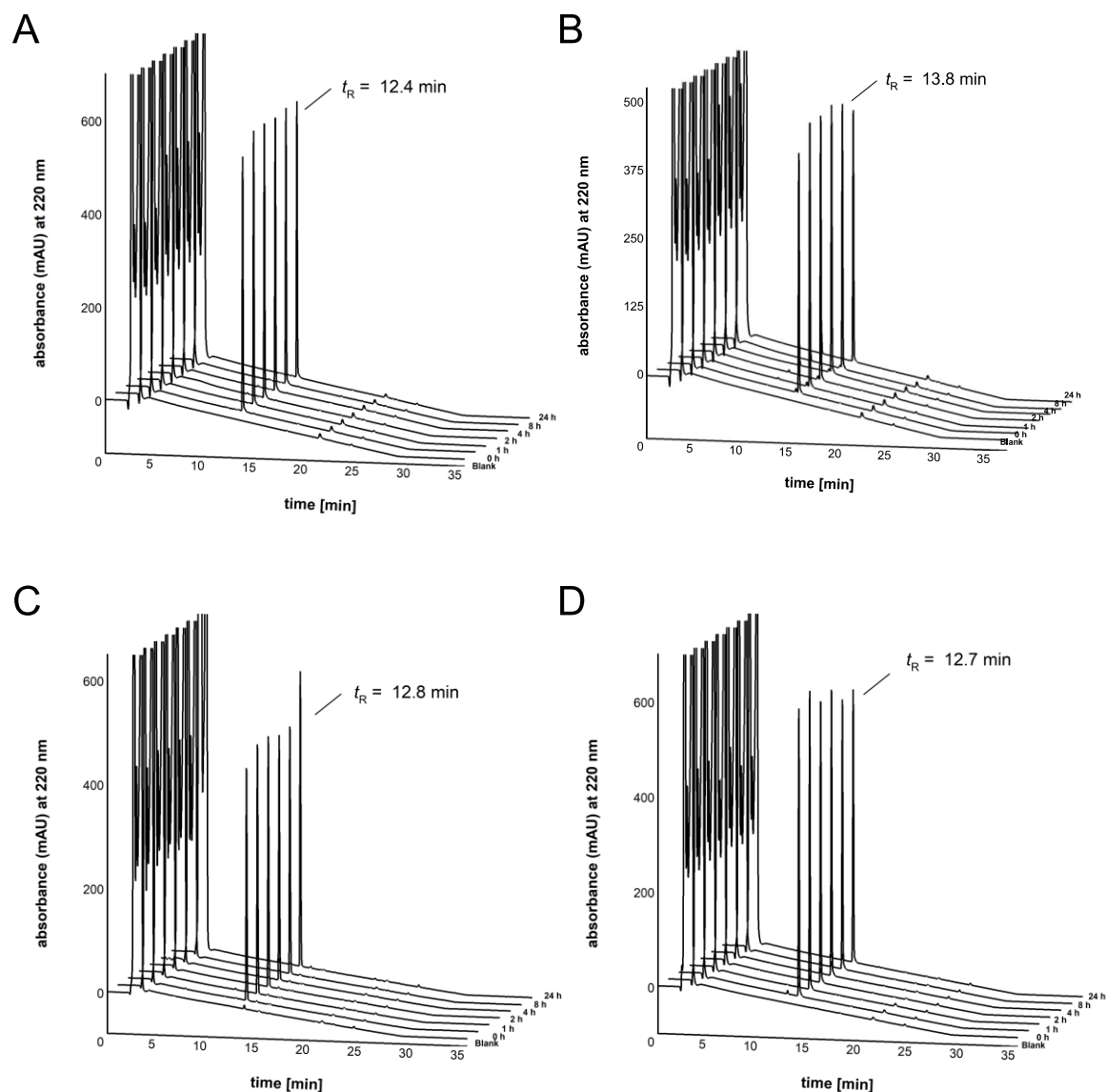


Figure 8.2. (A-D) Chromatograms of the reversed-phase HPLC analysis of (A) 2.56, (B) 2.58, (C) 2.59 and (D) 2.60 after incubation in a 10 mM HEPES buffer (pH 7.0) at rt for up to 24 h. 2.56, 2.58, 2.59 and 2.60 proved to be stable.

8.1.5.2. Supplementary Figure 8.3

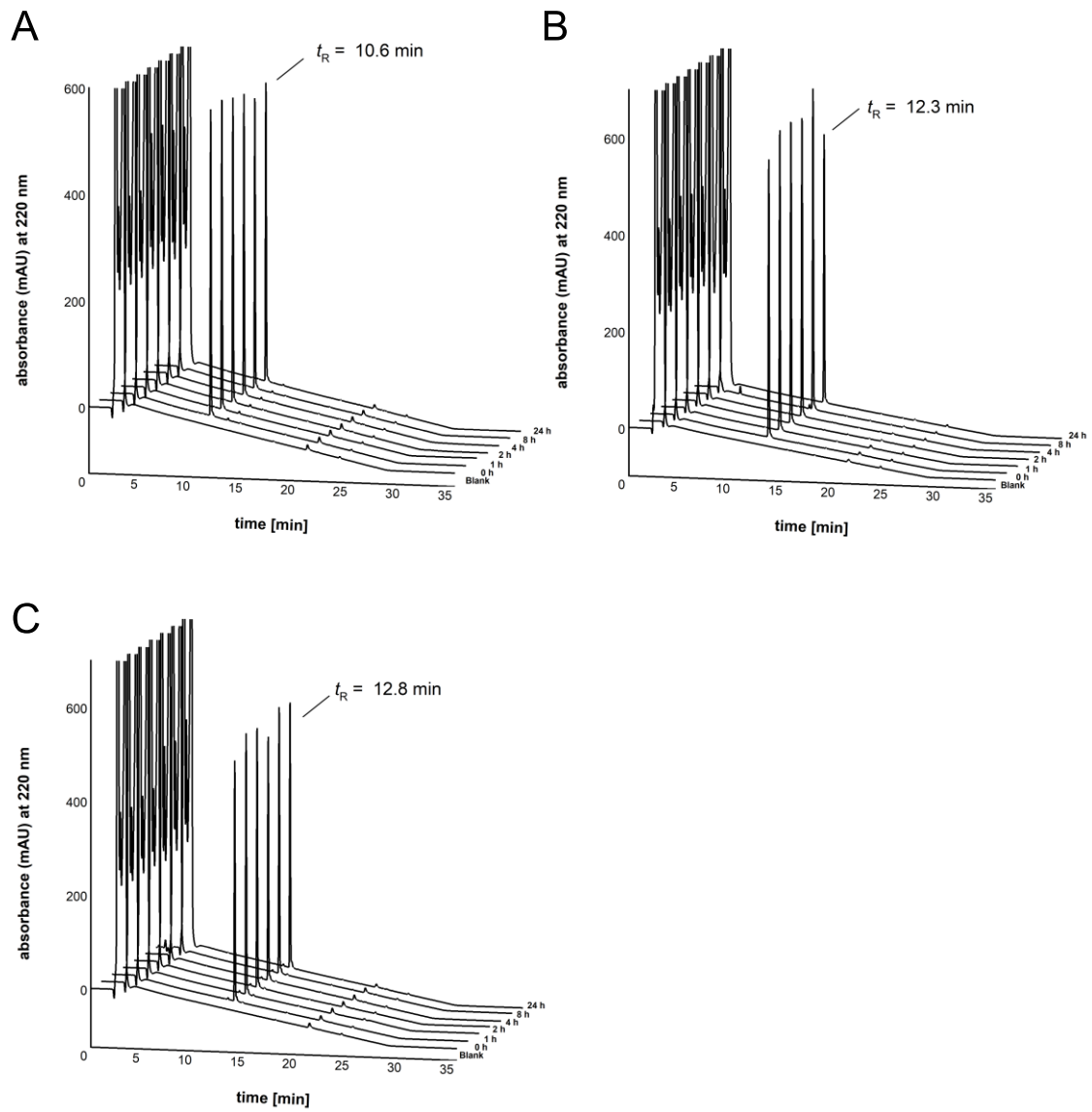


Figure 8.3. (A-C) Chromatograms of the reversed-phase HPLC analysis of (A) **2.61**, (B) **2.63** and (C) **2.68** after incubation in a 10 mM HEPES buffer (pH 7.0) at rt for up to 24 h. **2.61**, **2.63** and **2.68** proved to be stable.

8.2. Chapter 4

8.2.1. Supplementary figure 8.4

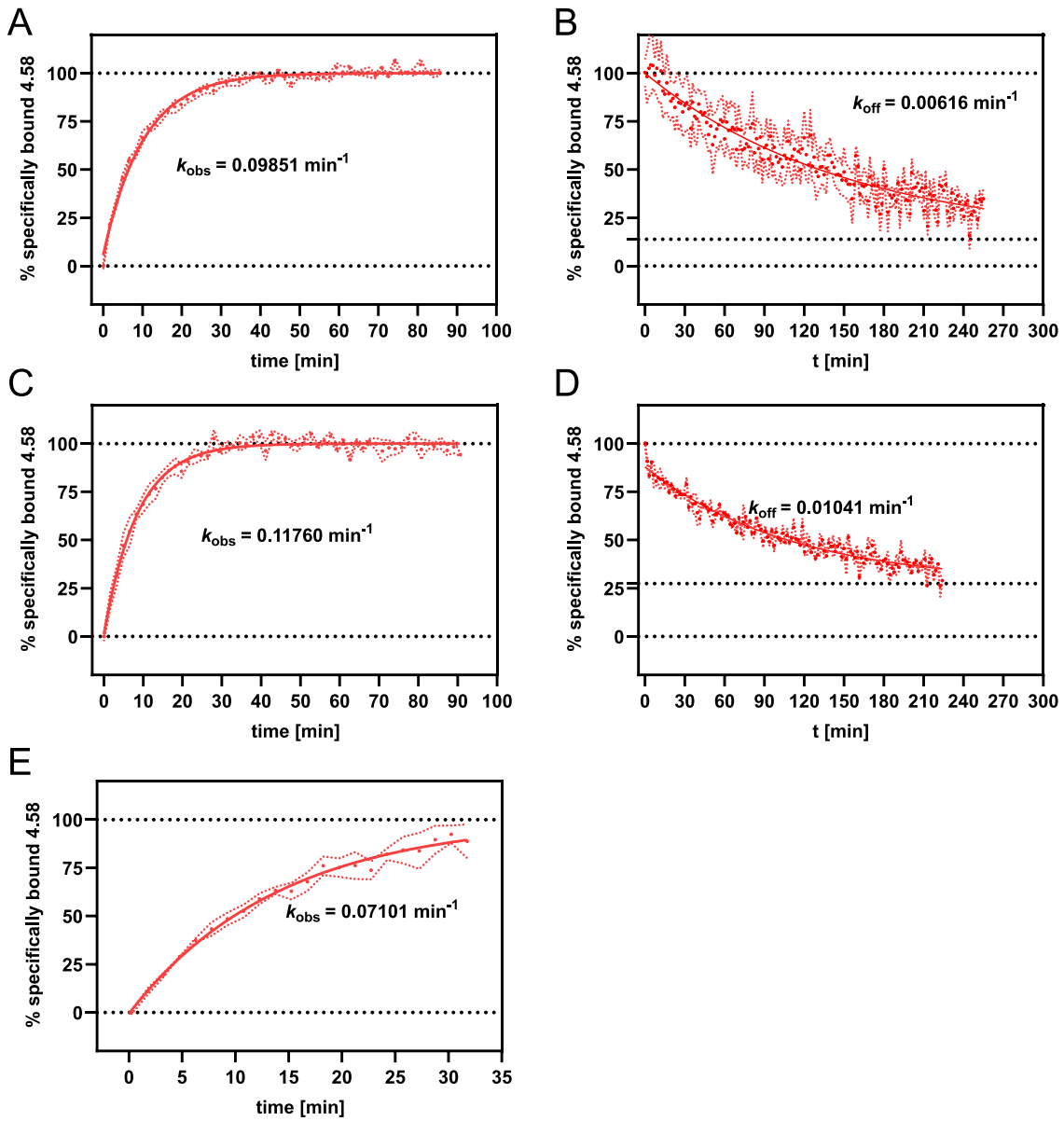
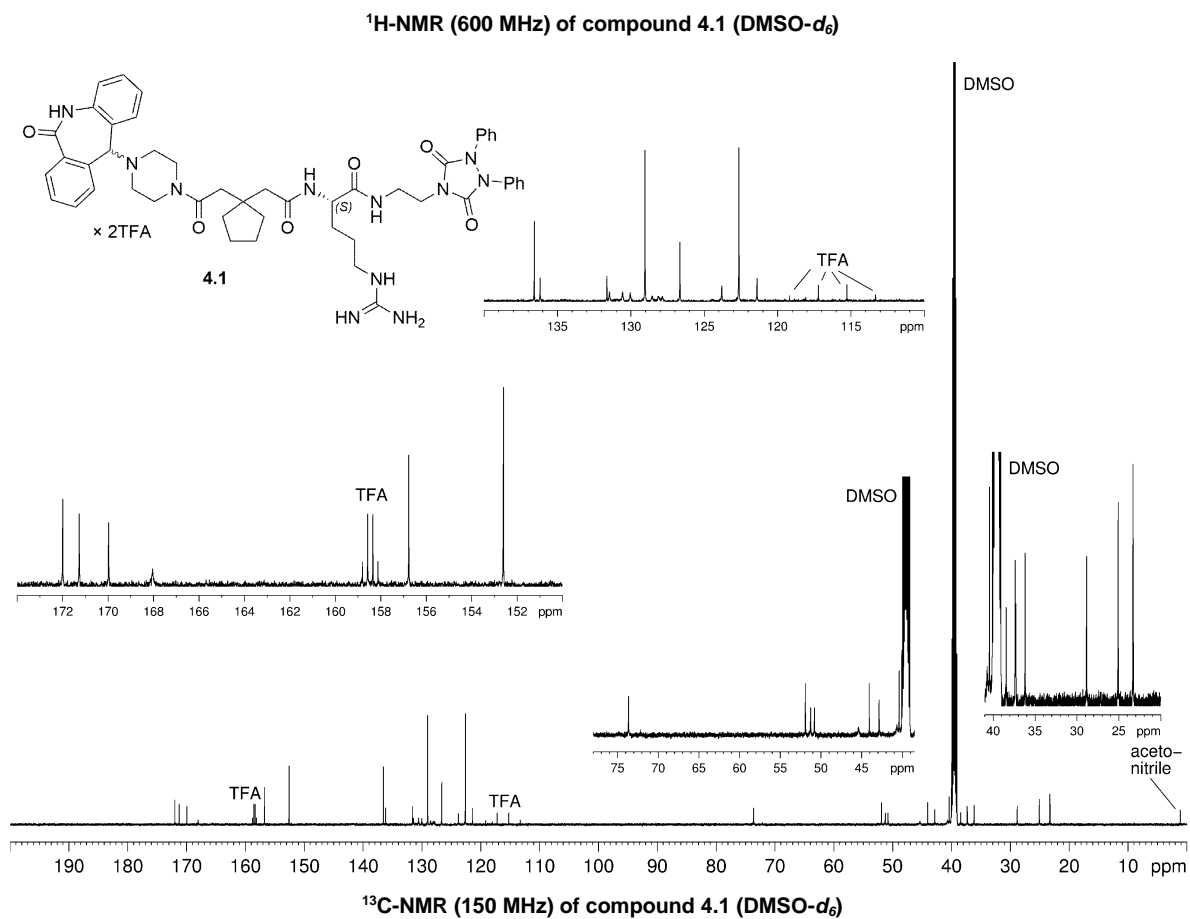
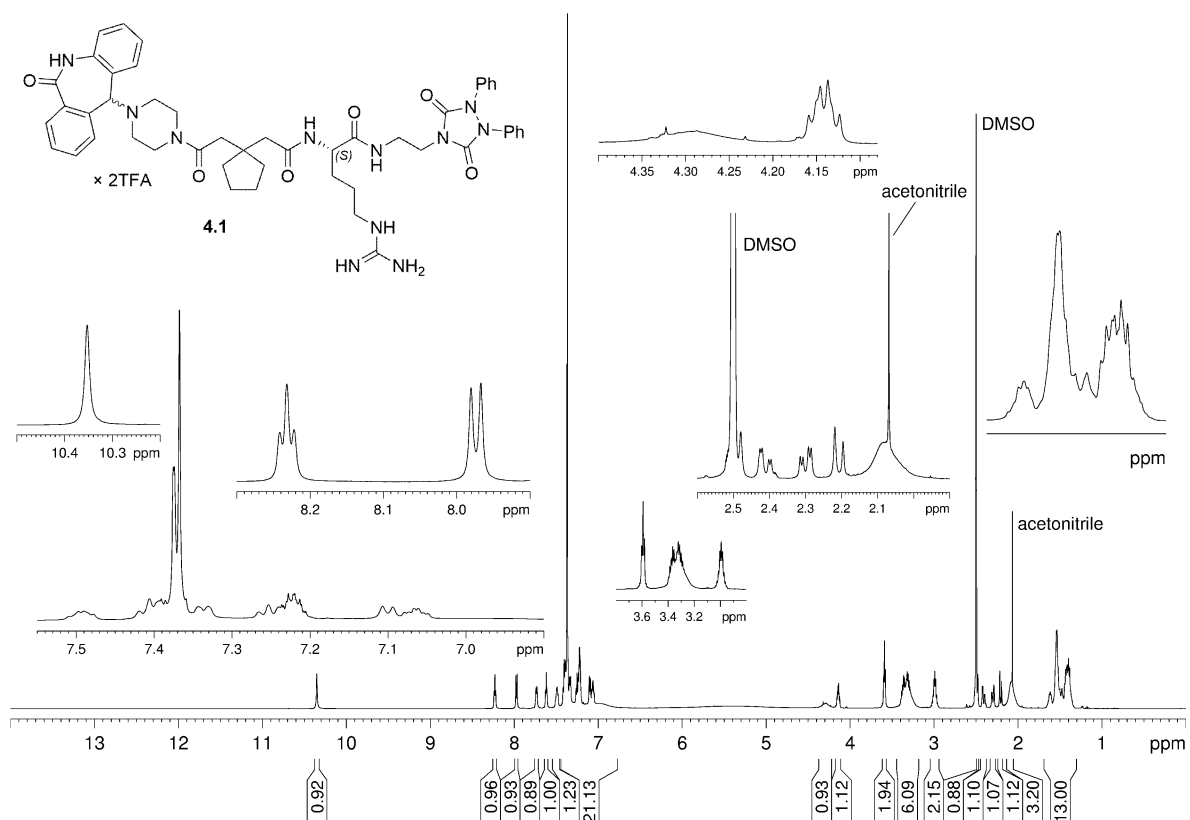
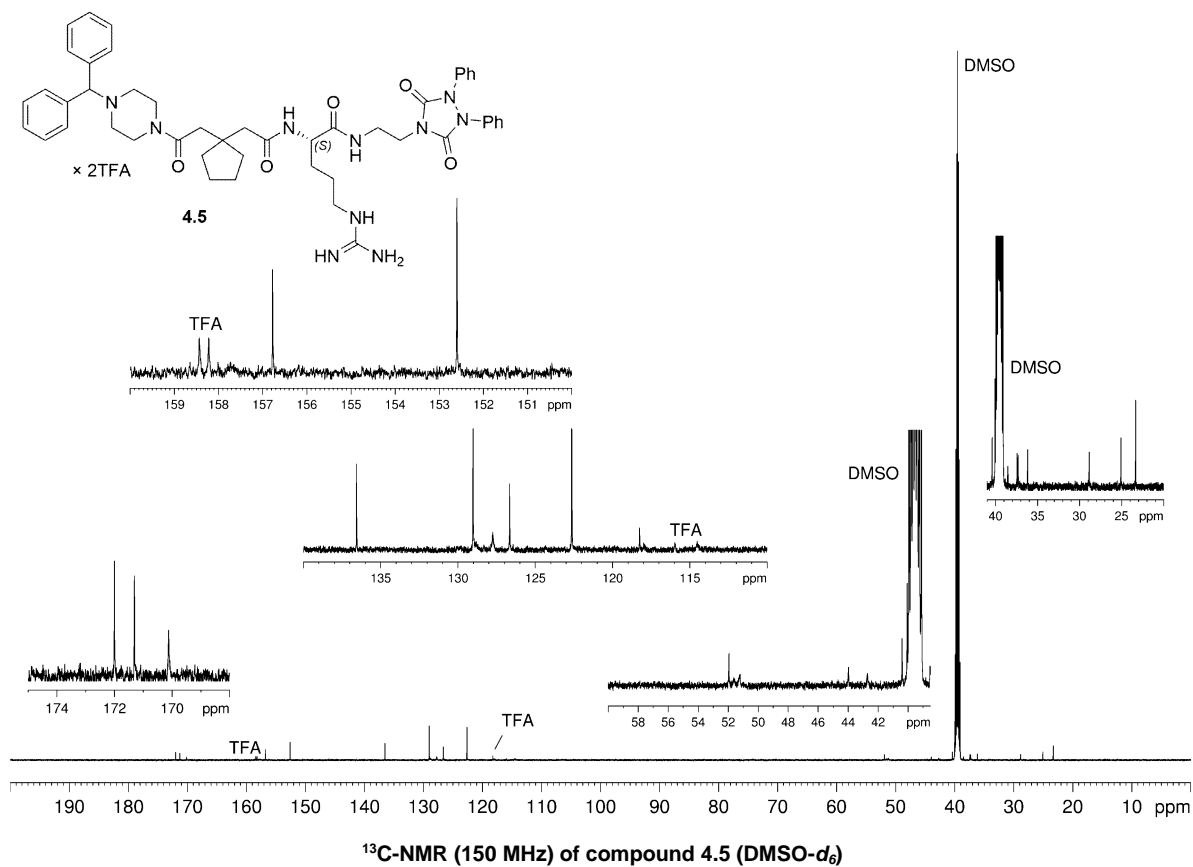
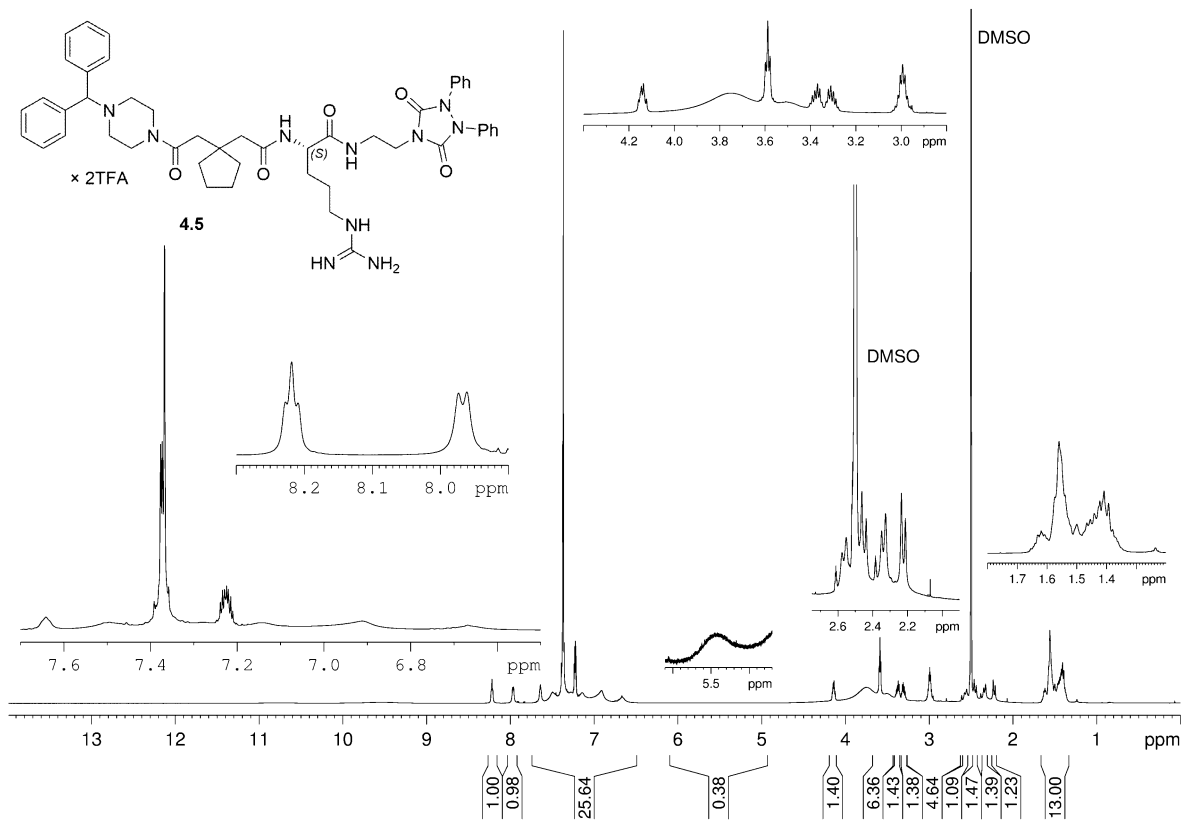
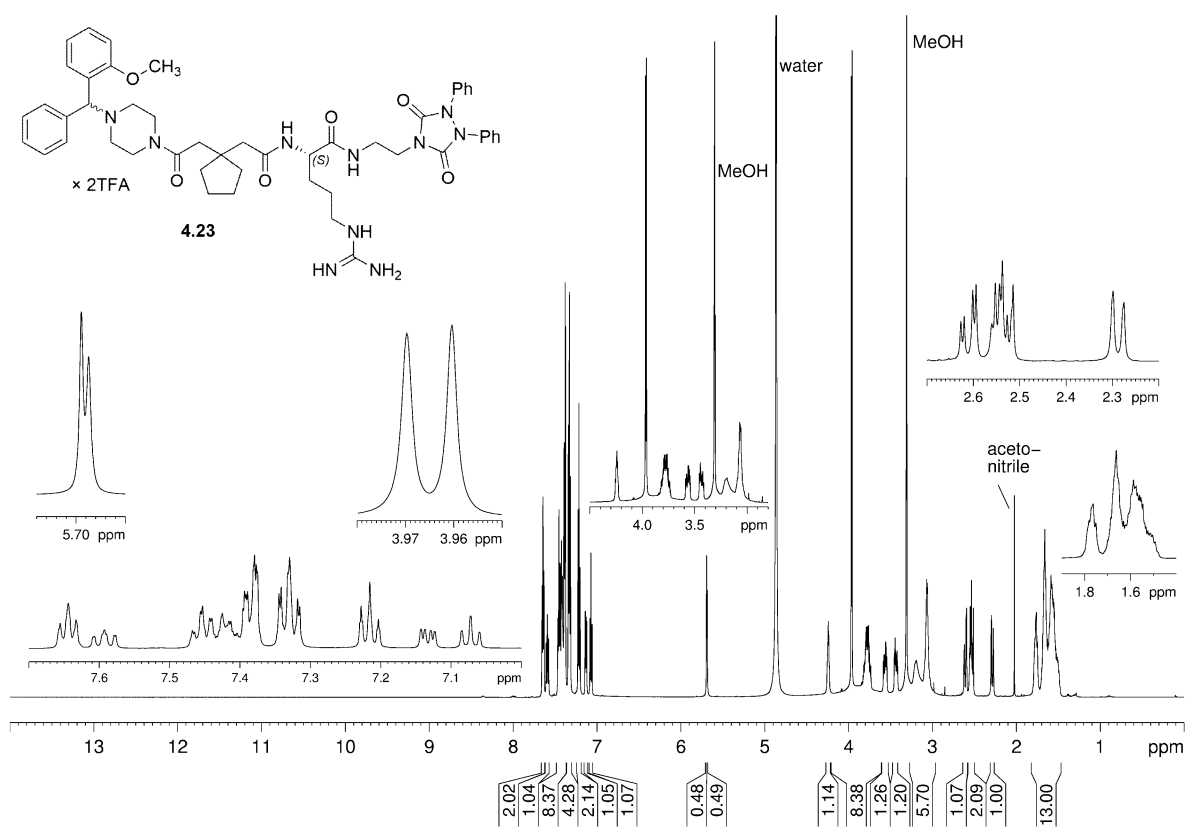
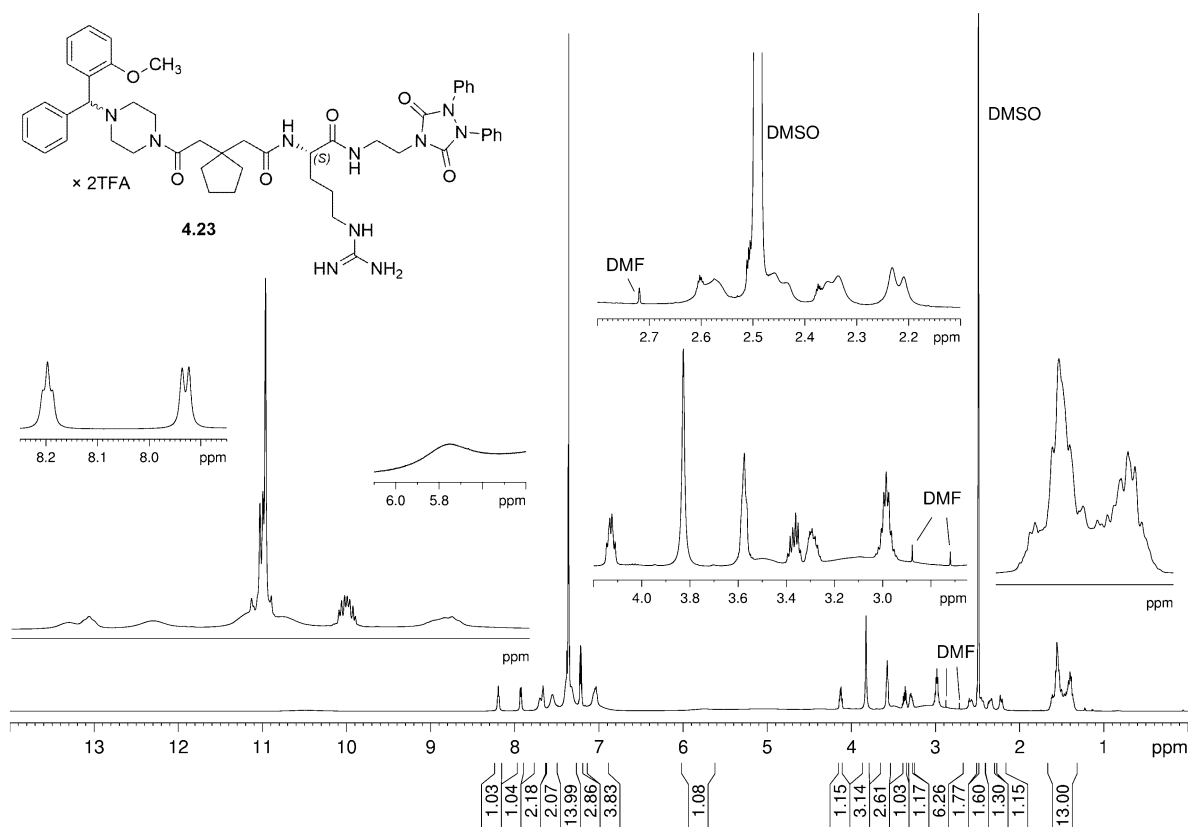
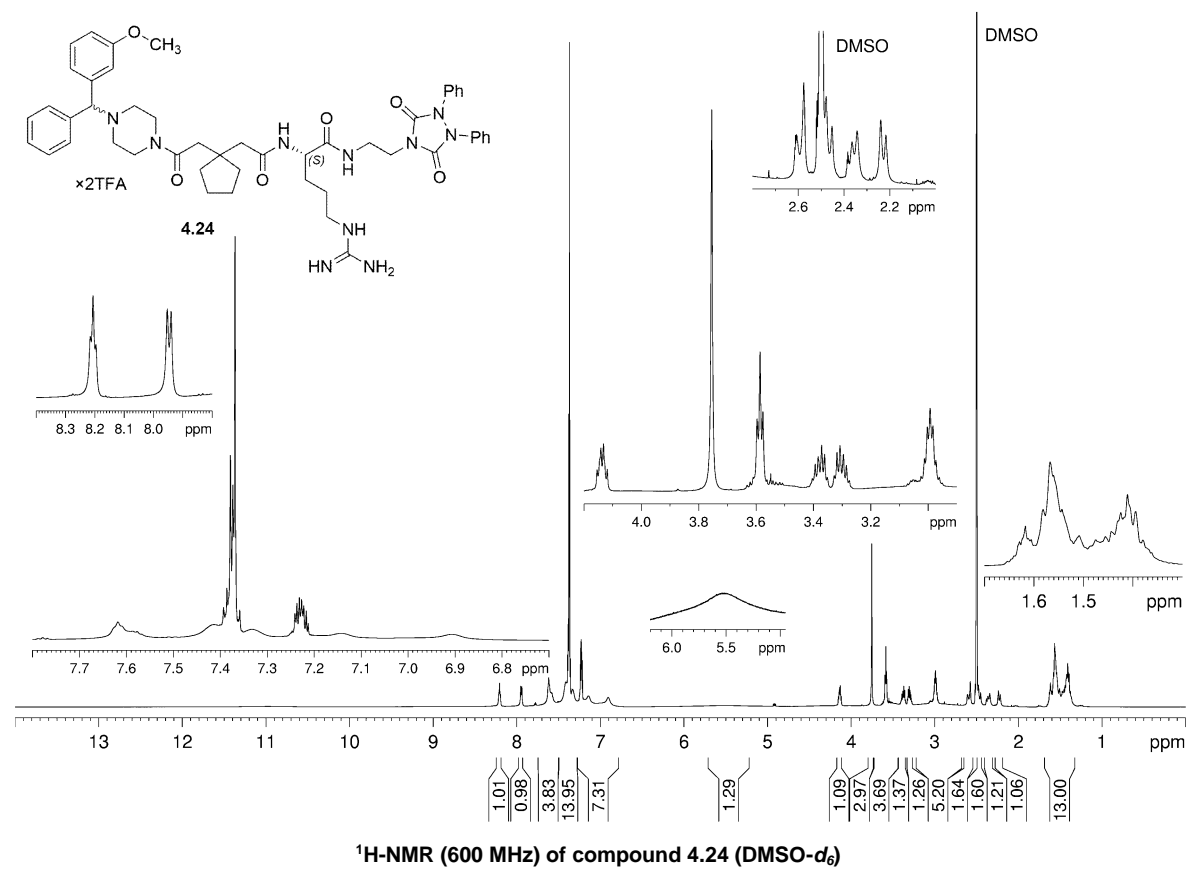
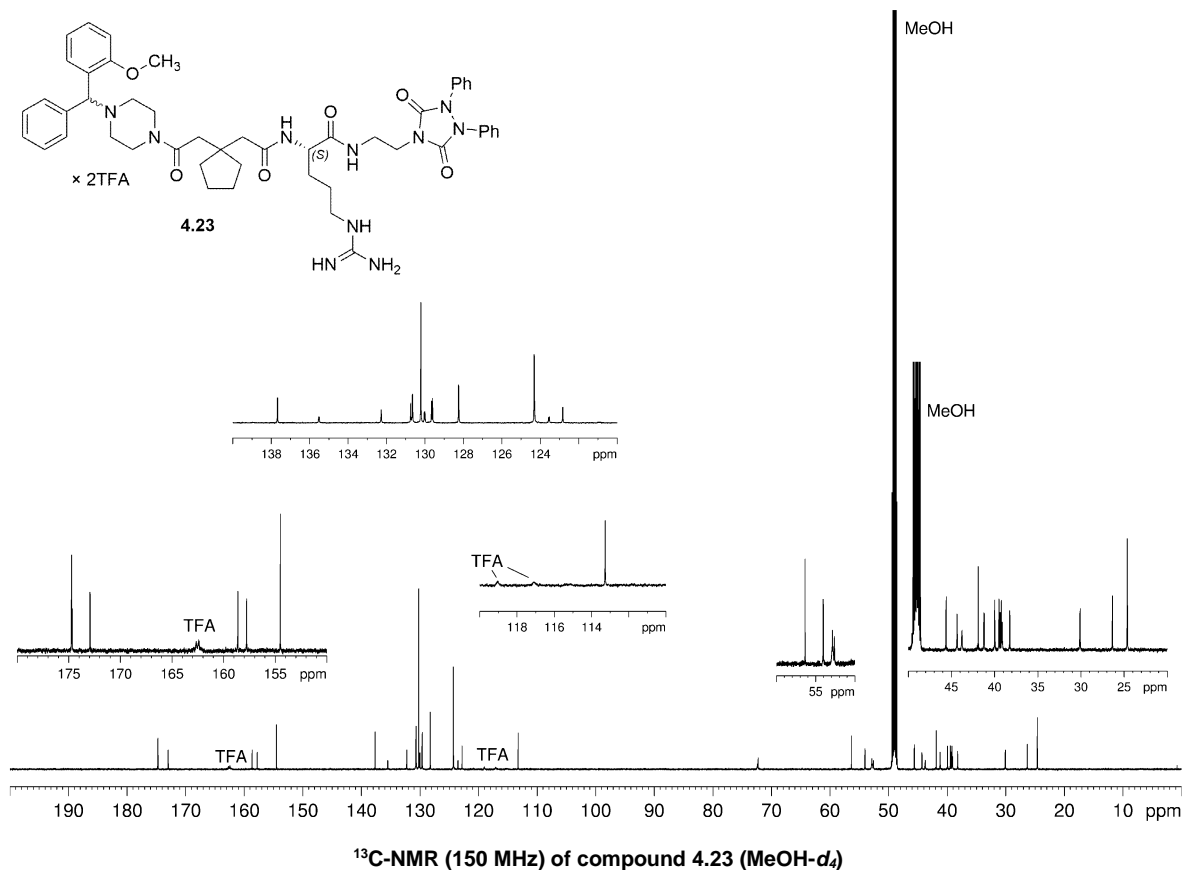


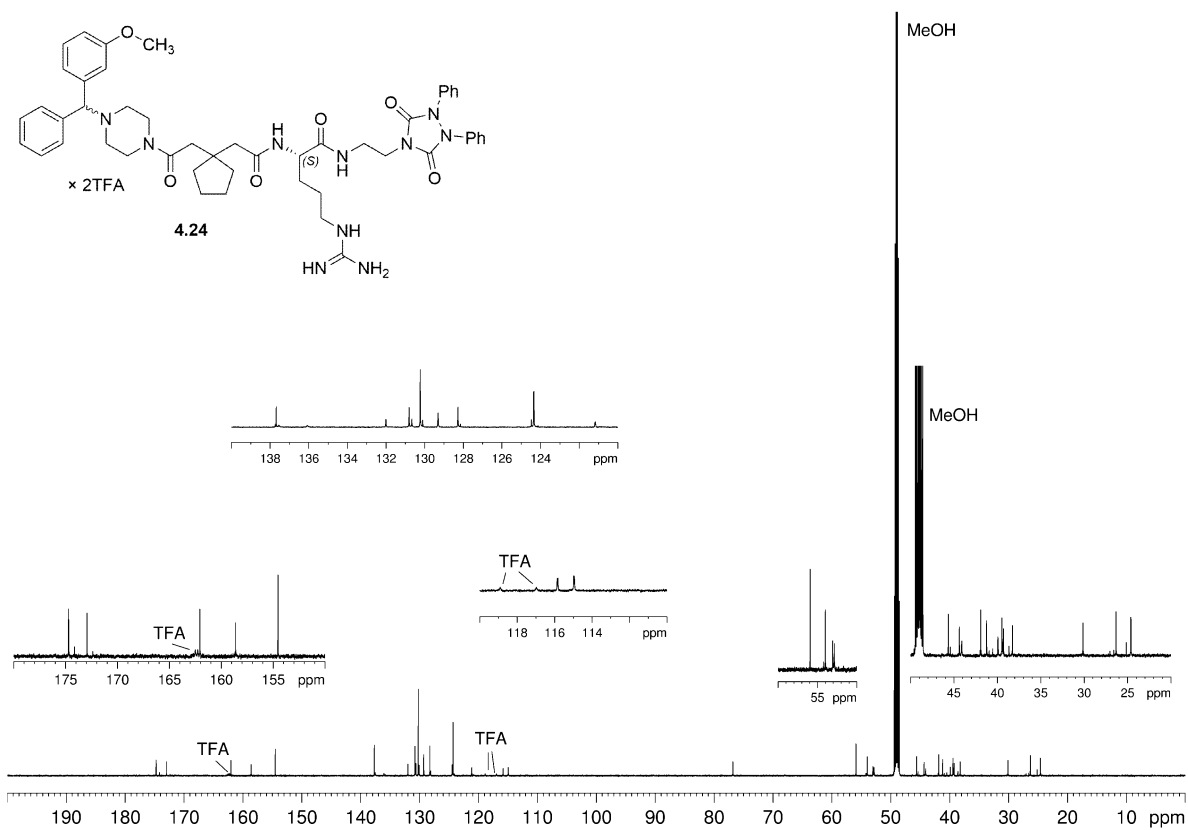
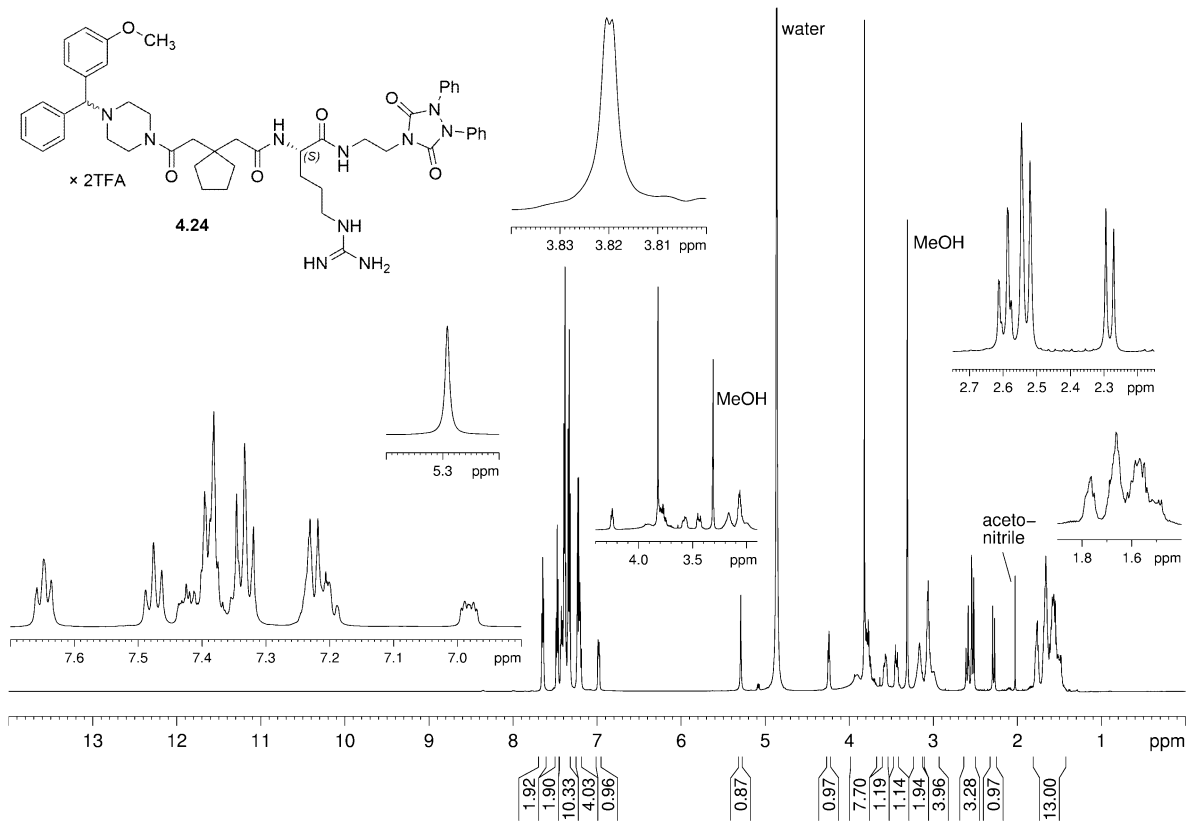
Figure 8.4. (A-E) Additional binding characteristics of **4.58** in BRET based binding assay in intact HEK293T Y₂(intraNLucD197) cells. Association for (A, C) 90 min and (E) 30 min of **4.58** (% specifically bound **4.58**) and dissociation for (B) 240 min ($B_{\text{plateau}} = 13.9\%$) and (D) 220 min ($B_{\text{plateau}} = 27.4\%$) as function of time (min) for determination of k_{obs} and k_{off} (nonlinear regression, one phase association or dissociation; Graphpad Prism 8). Data represents SEM of a single experiment performed in triplicate.

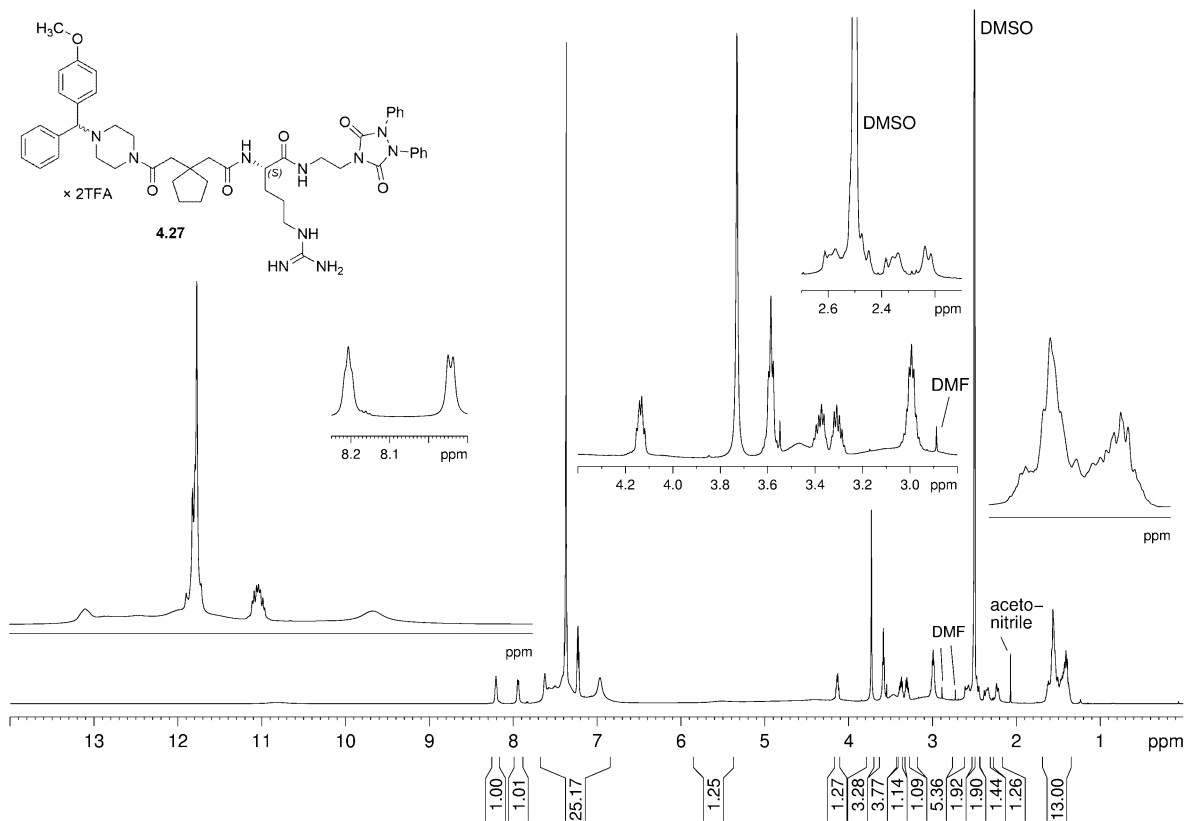
8.2.2. $^1\text{H-NMR}$ and $^{13}\text{C-NMR}$ spectra of compounds 4.1, 4.5, 4.23, 4.24, 4.27, 4.32, 4.50, 4.51 and 4.75



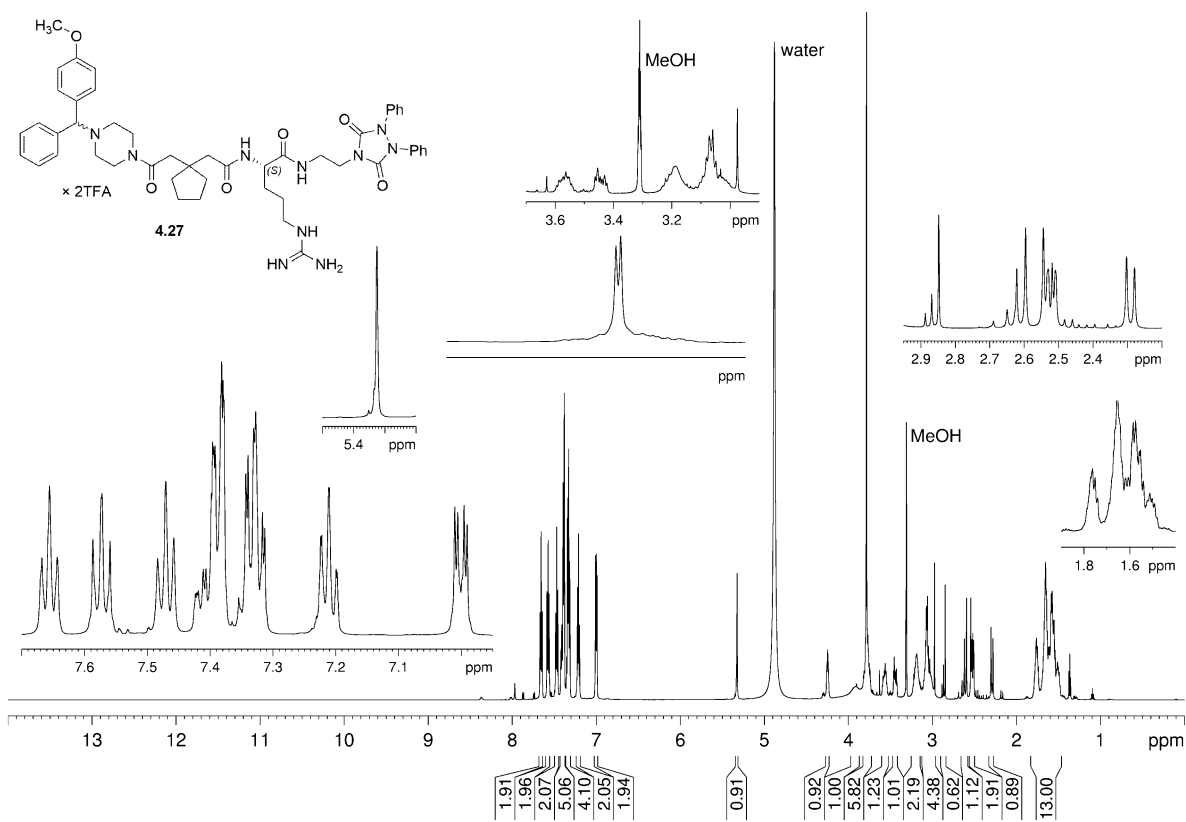




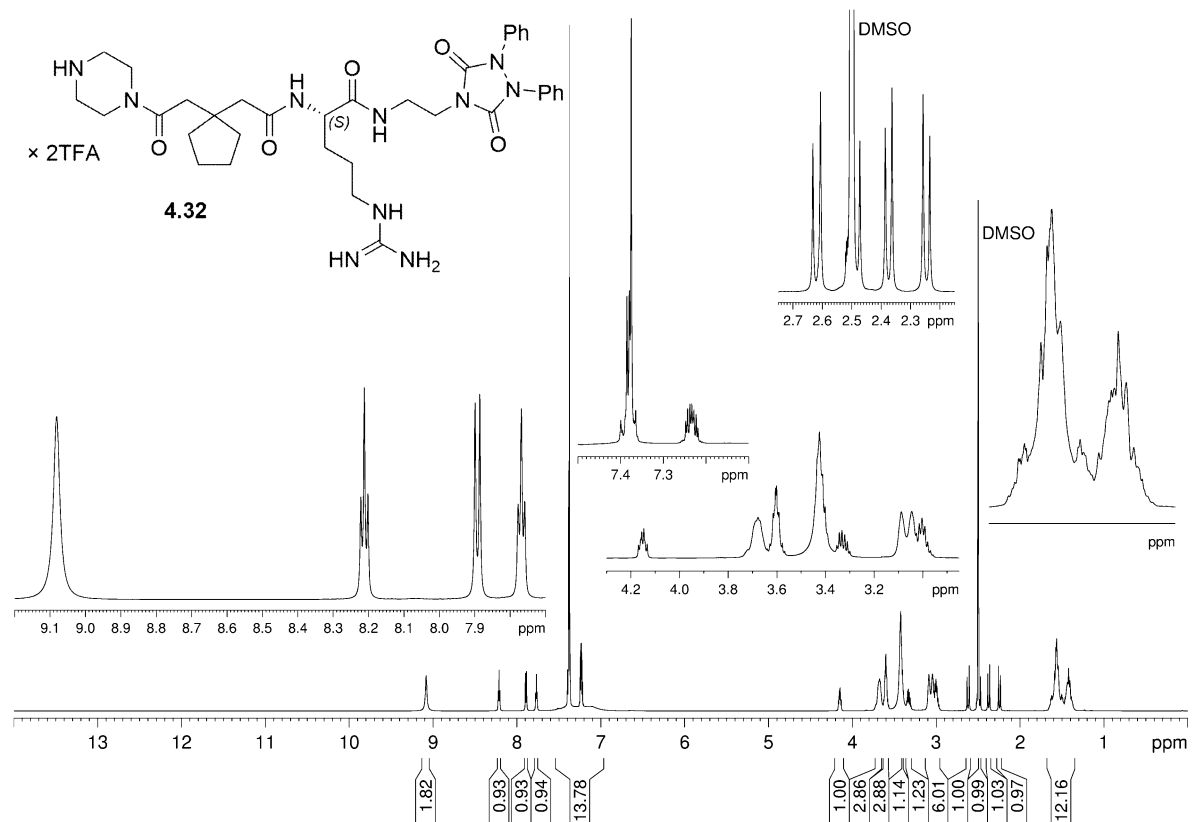
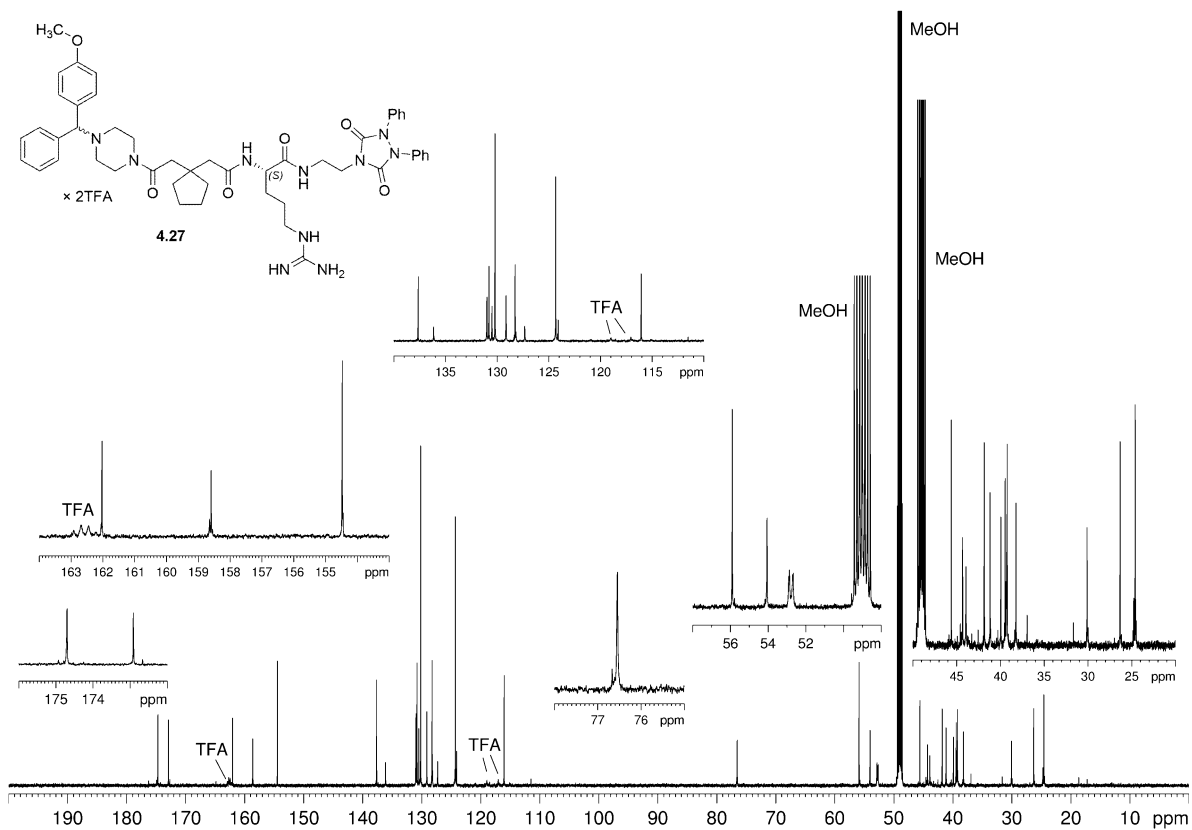


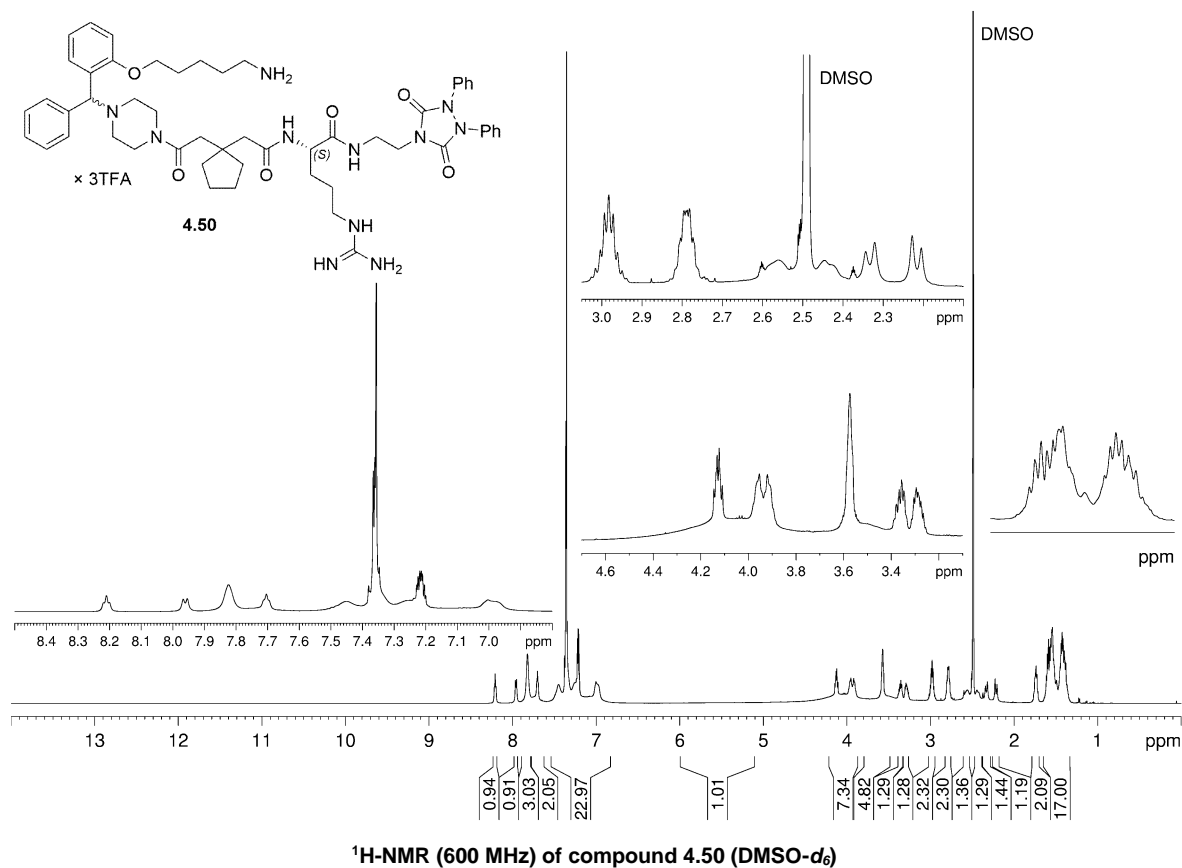
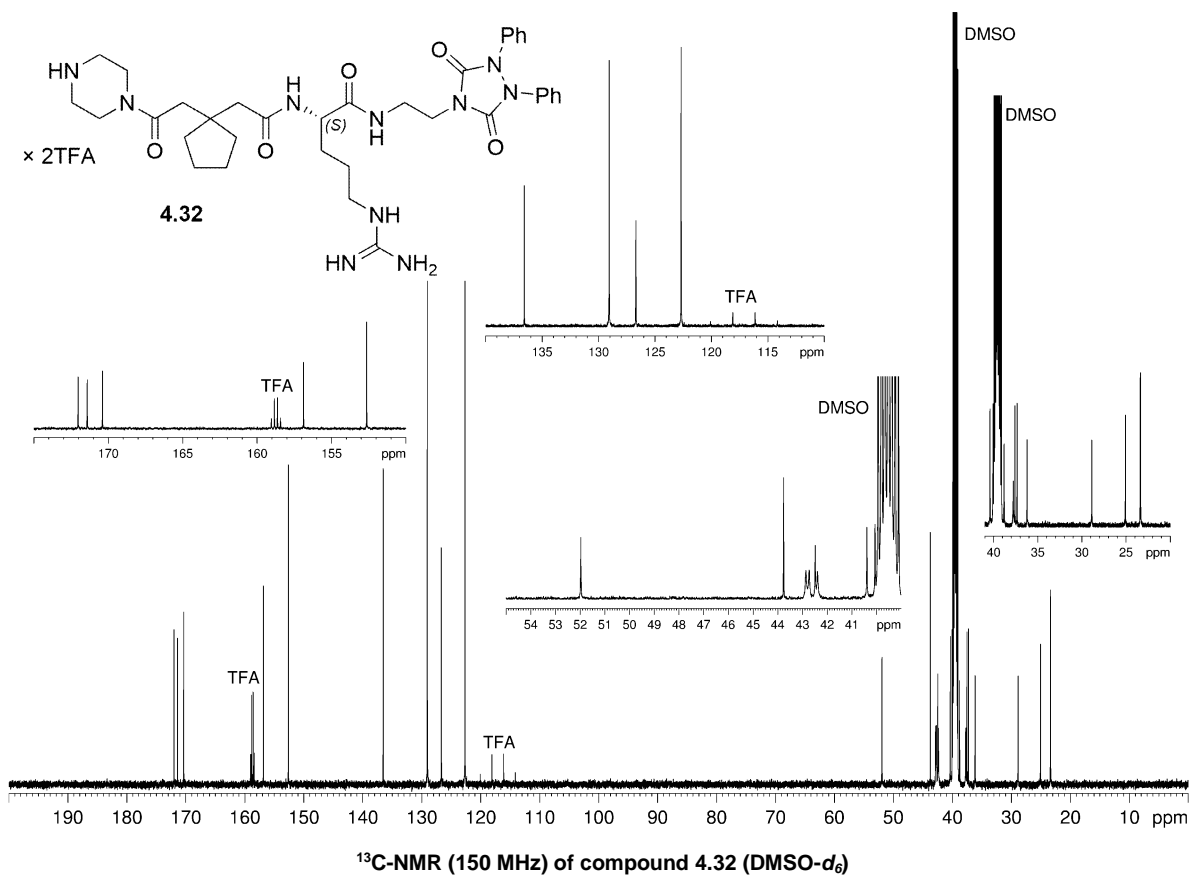


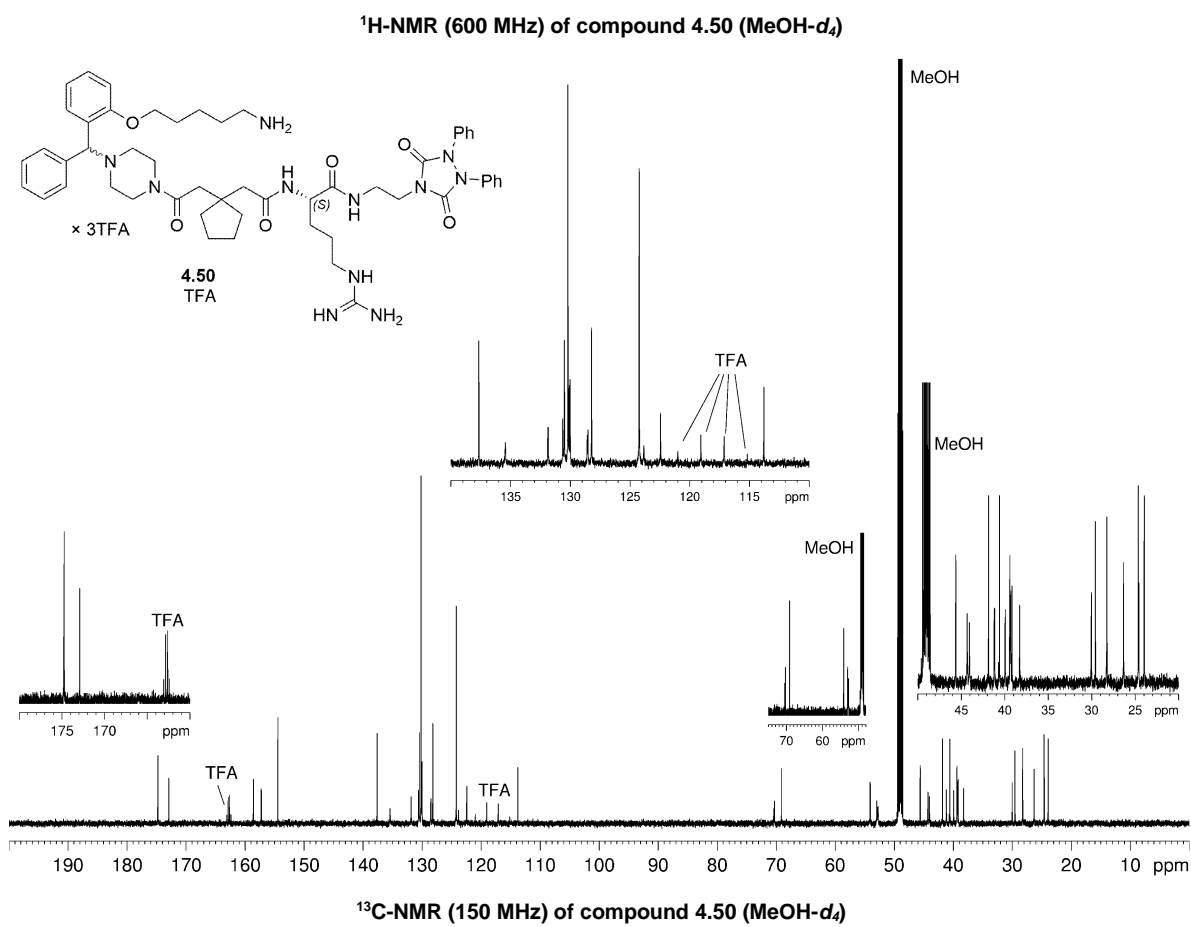
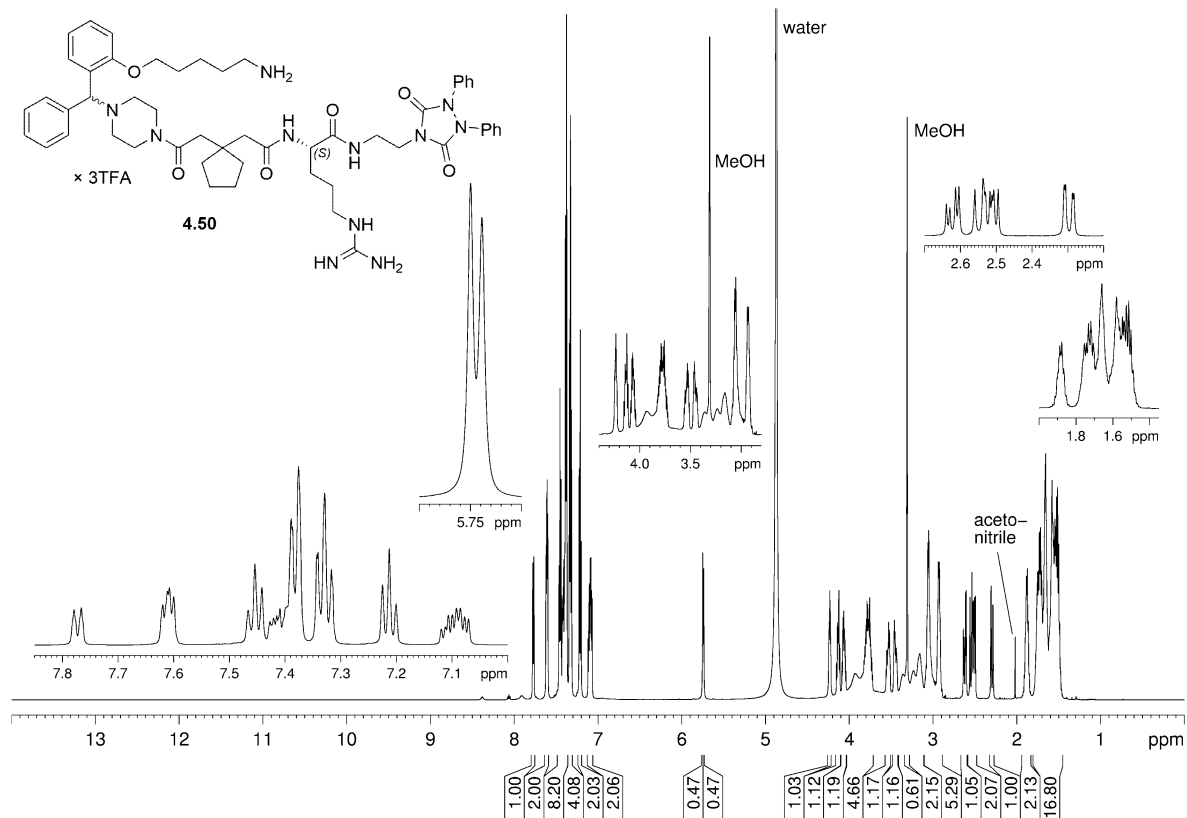
¹H-NMR (600 MHz) of compound 4.27 (DMSO-*d*₆)

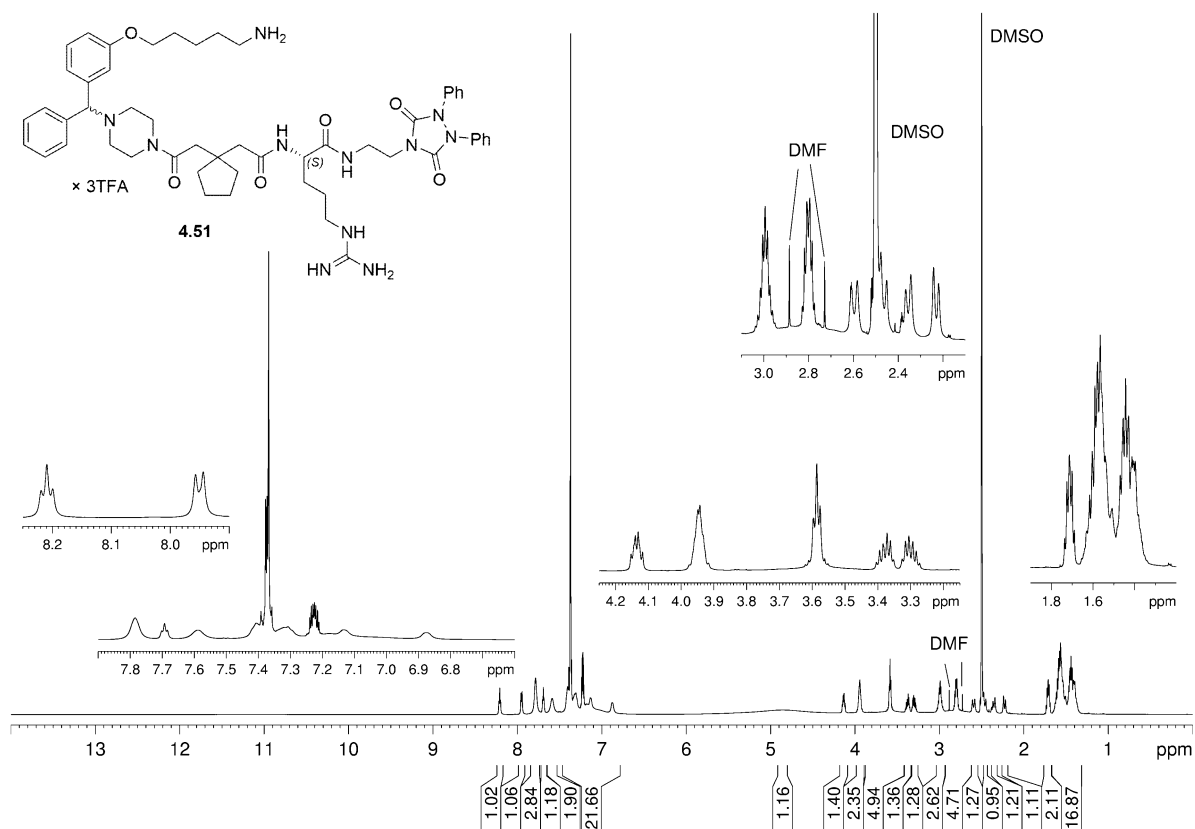


¹H-NMR (600 MHz) of compound 4.27 (MeOH-*d*₄)

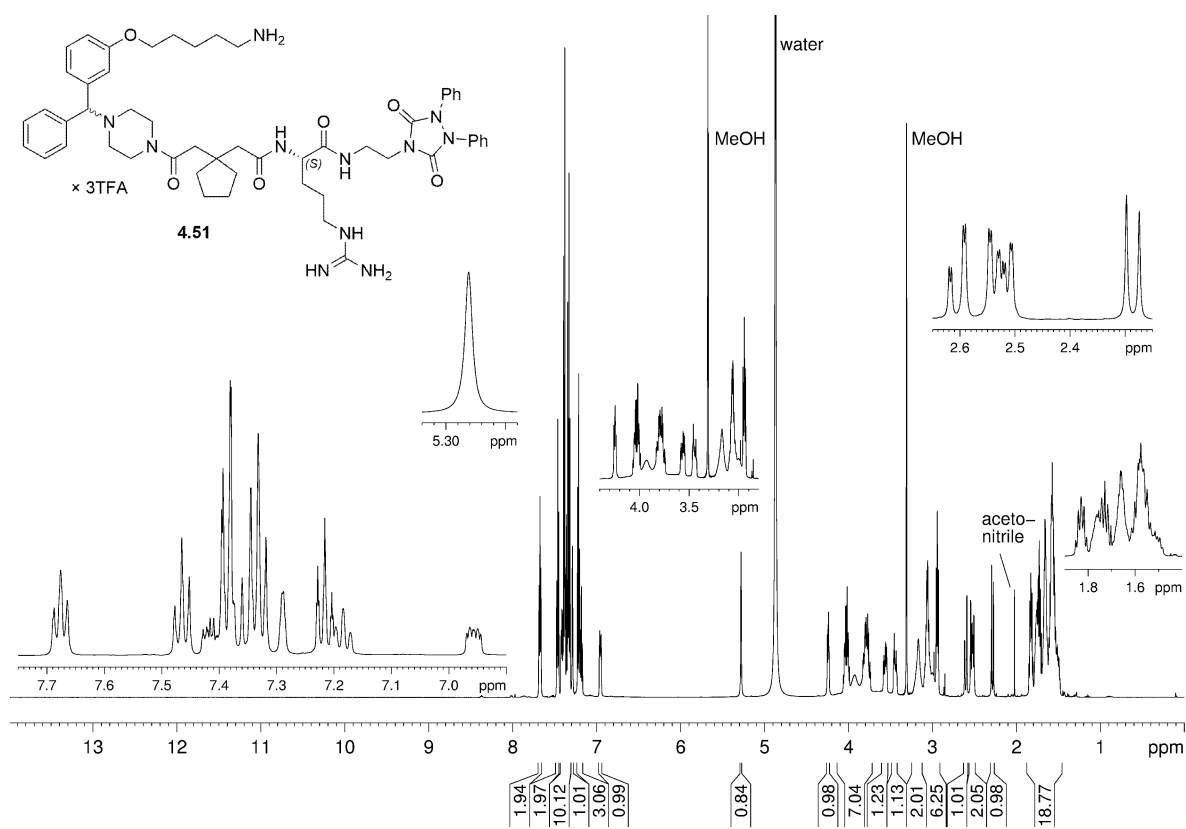




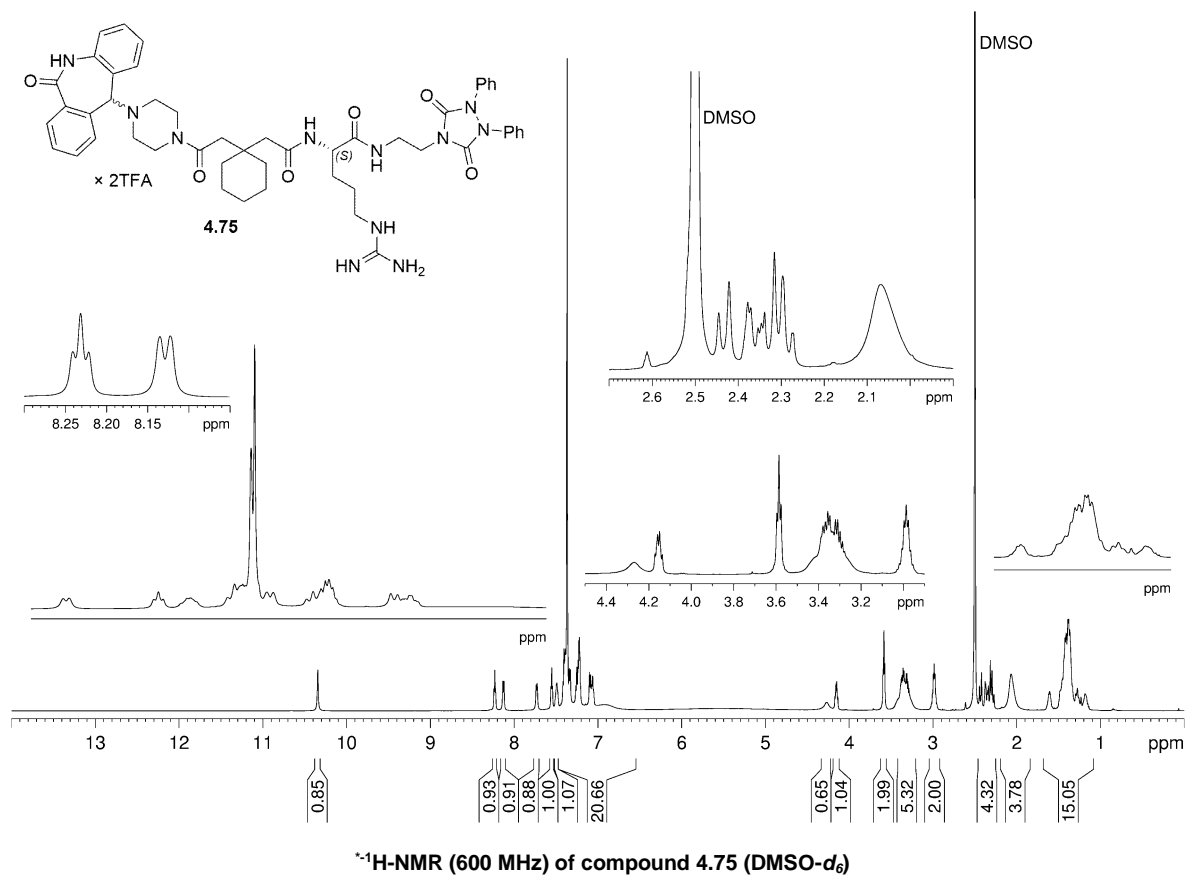
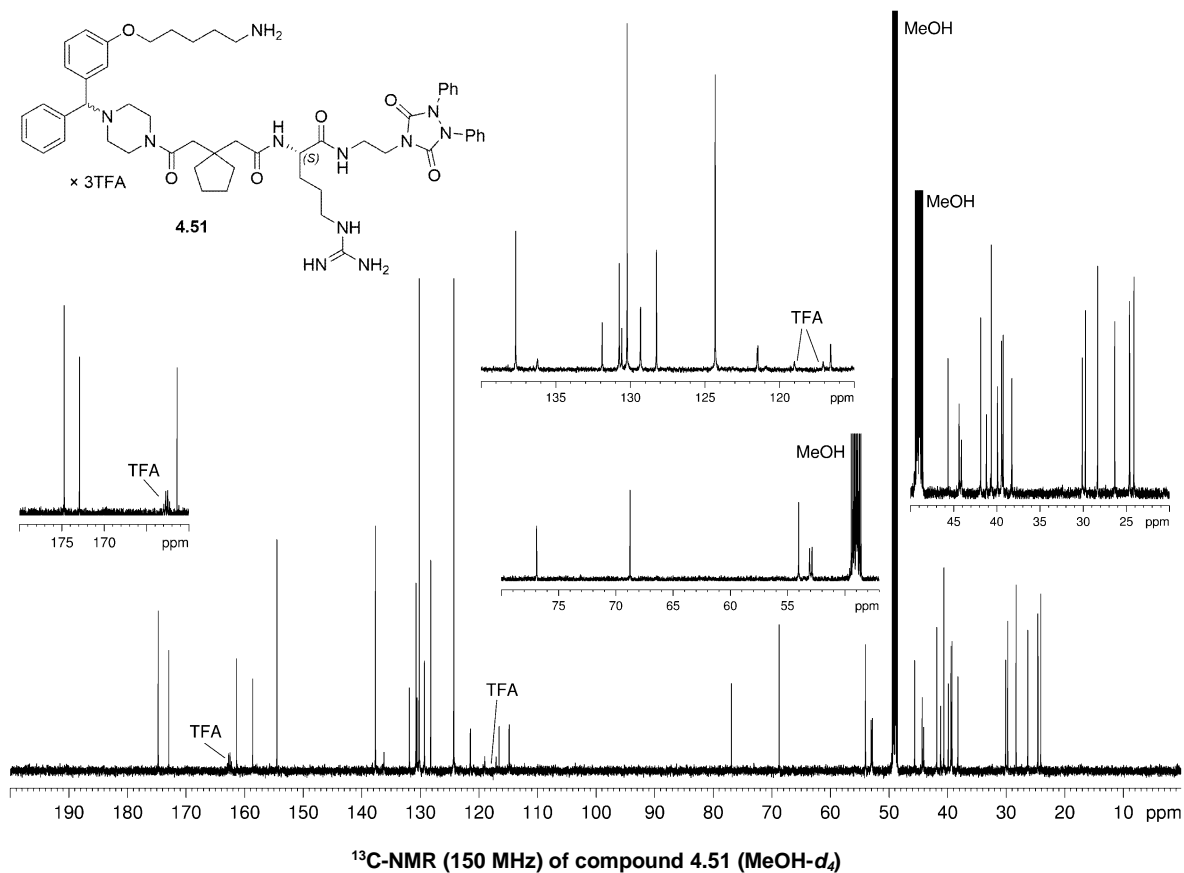


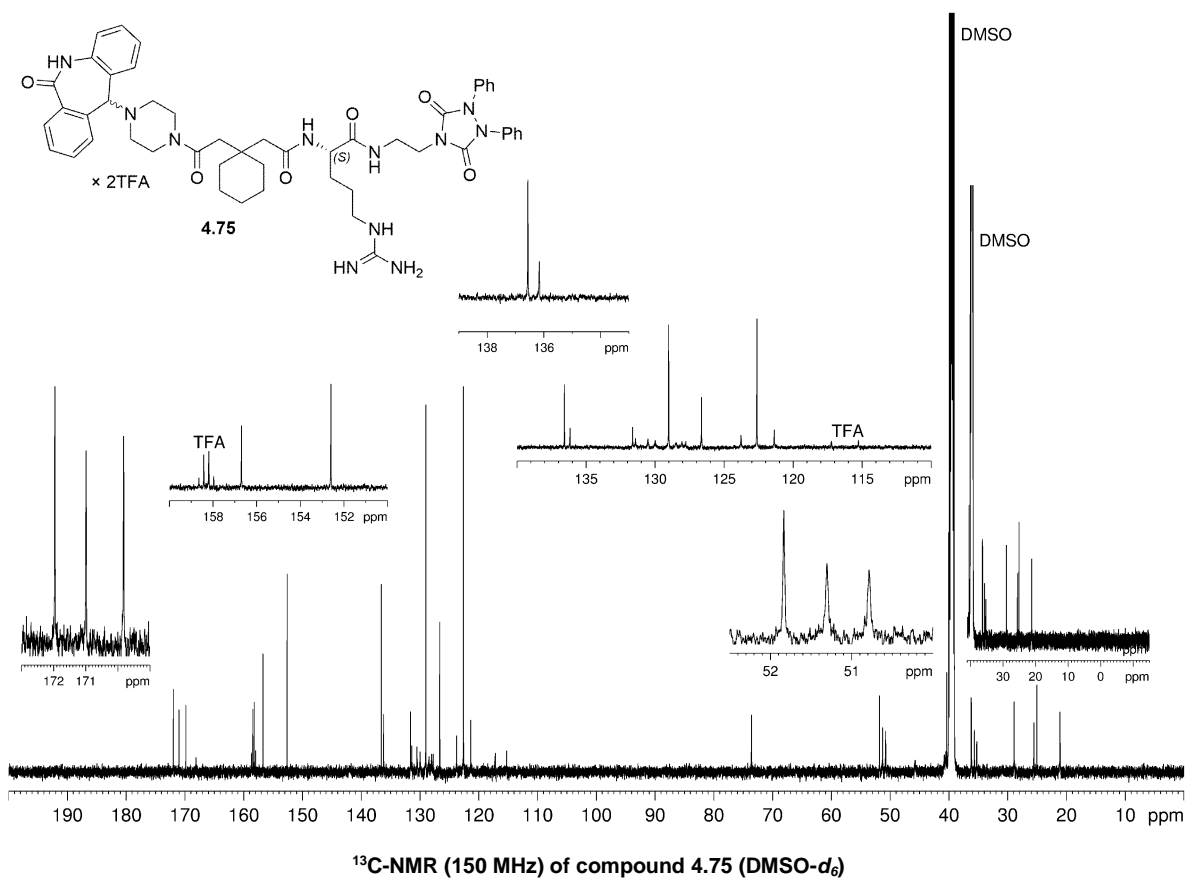


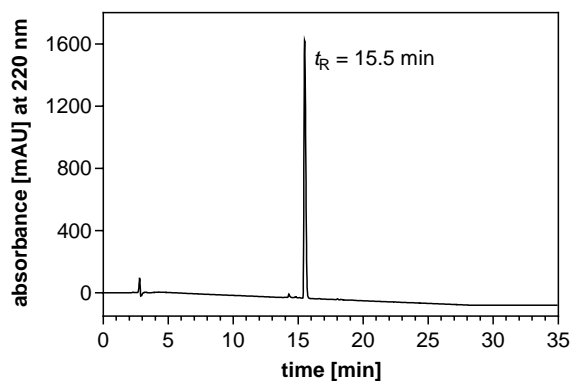
¹H-NMR (600 MHz) of compound 4.51 (DMSO-*d*₆)



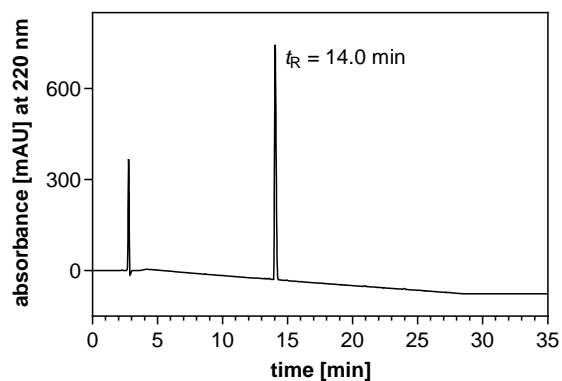
¹H-NMR (600 MHz) of compound 4.51 (MeOH-*d*₄)



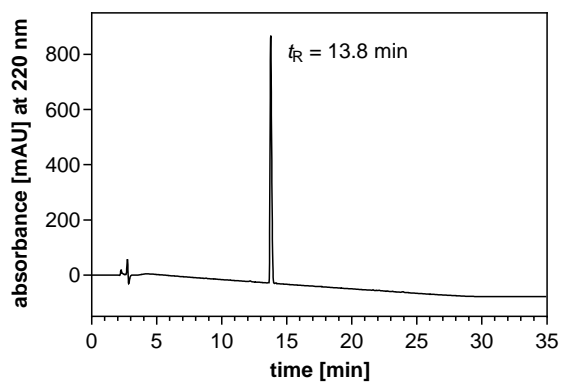


8.2.3. RP-HPLC purity chromatograms (220 nm) of compounds 4.1, 4.5, 4.23, 4.24, 4.27, 4.32, 4.50, 4.51, 4.58, 4.59, 4.61, 4.62 and 4.75

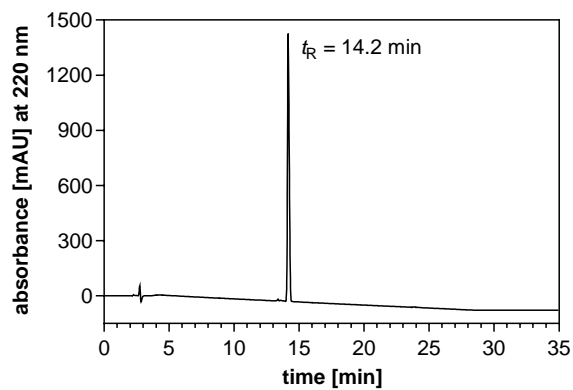
RP-HPLC (220 nm) chromatogram of 4.1



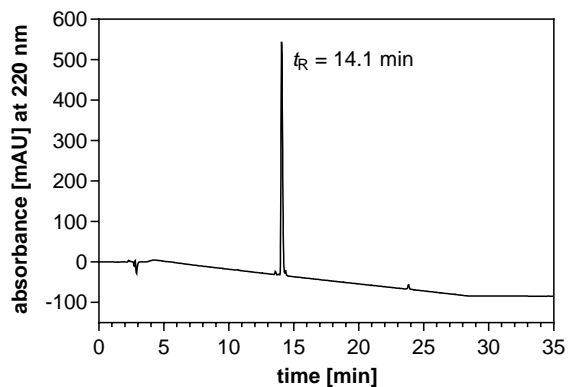
RP-HPLC (220 nm) chromatogram of 4.5



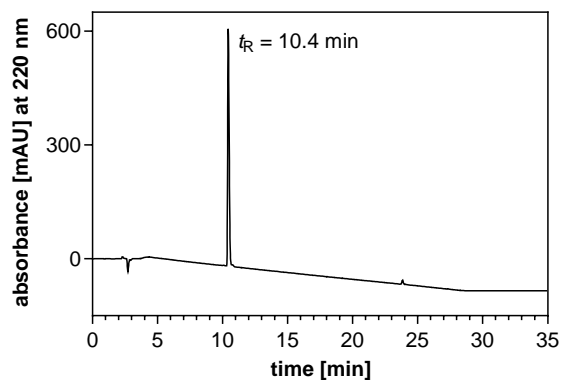
RP-HPLC (220 nm) chromatogram of 4.23



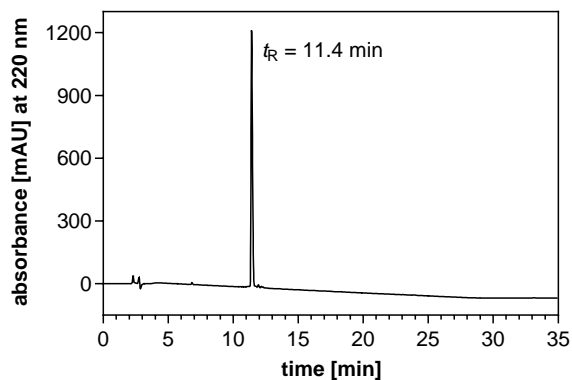
RP-HPLC (220 nm) chromatogram of 4.24



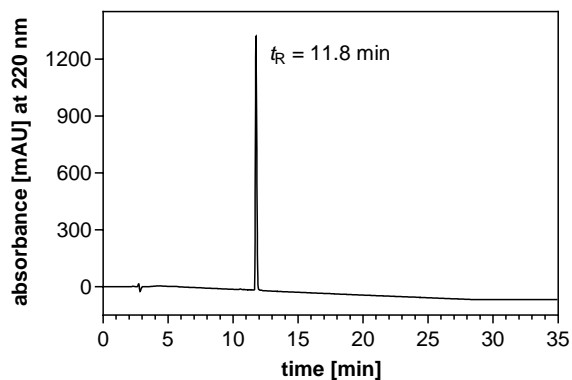
RP-HPLC (220 nm) chromatogram of 4.27



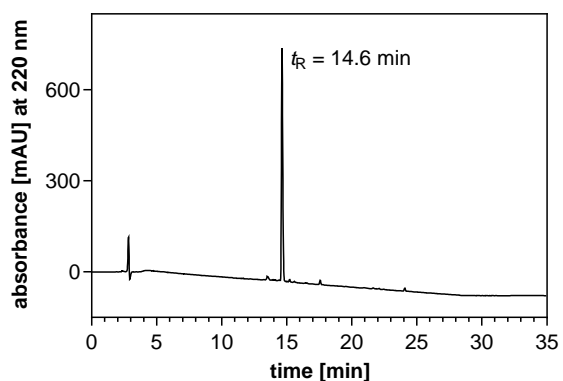
RP-HPLC (220 nm) chromatogram of 4.32



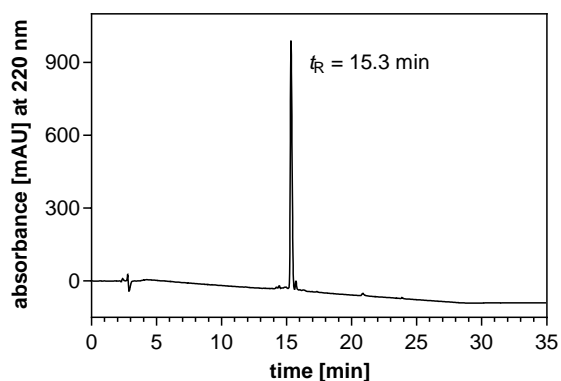
RP-HPLC (220 nm) chromatogram of 4.50



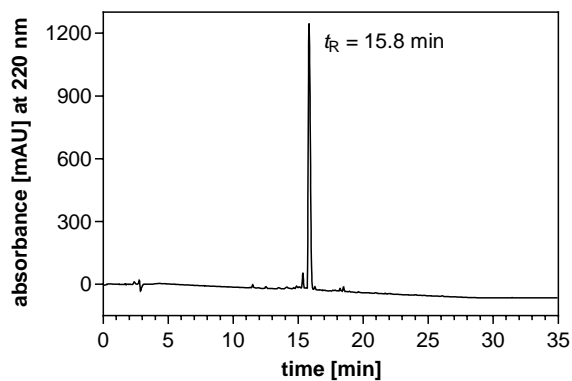
RP-HPLC (220 nm) chromatogram of 4.51



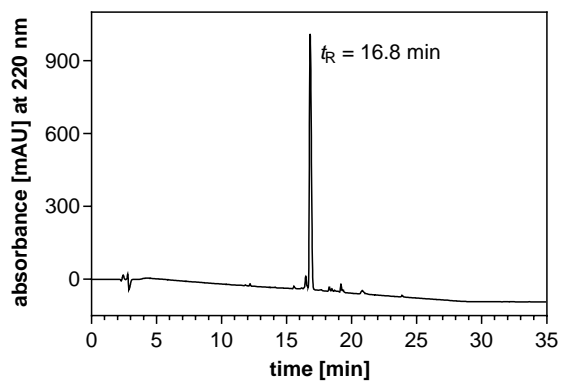
RP-HPLC (220 nm) chromatogram of 4.58



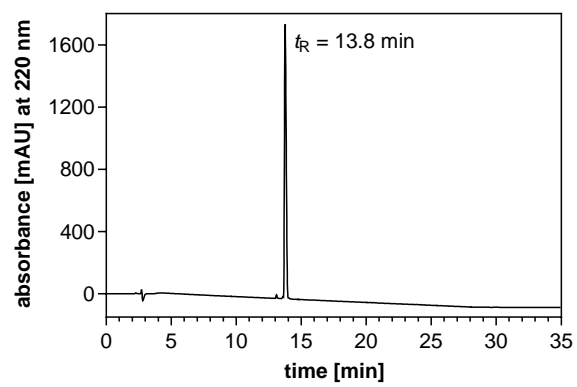
RP-HPLC (220 nm) chromatogram of 4.59



RP-HPLC (220 nm) chromatogram of 4.61



RP-HPLC (220 nm) chromatogram of 4.62



RP-HPLC (220 nm) chromatogram of 4.75

8.3. Chapter 5

8.3.1. Investigation of the chemical stability of compounds 5.9 and 5.30

8.3.1.1. Supplementary figure 8.5

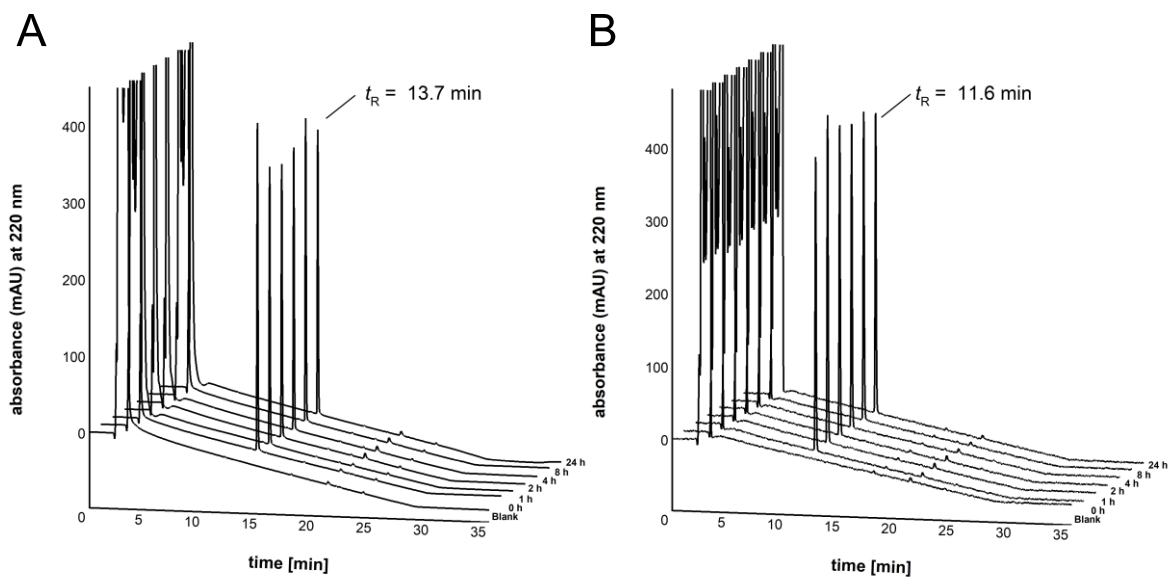
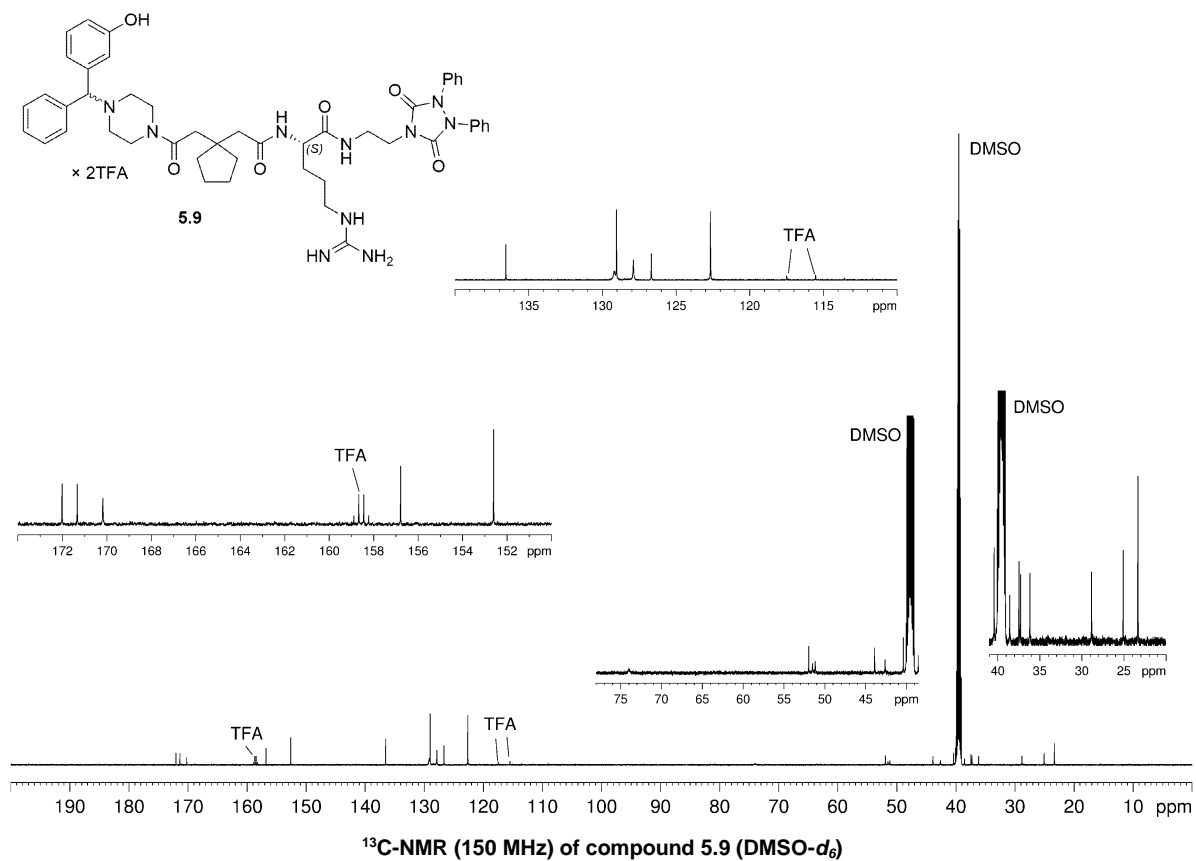
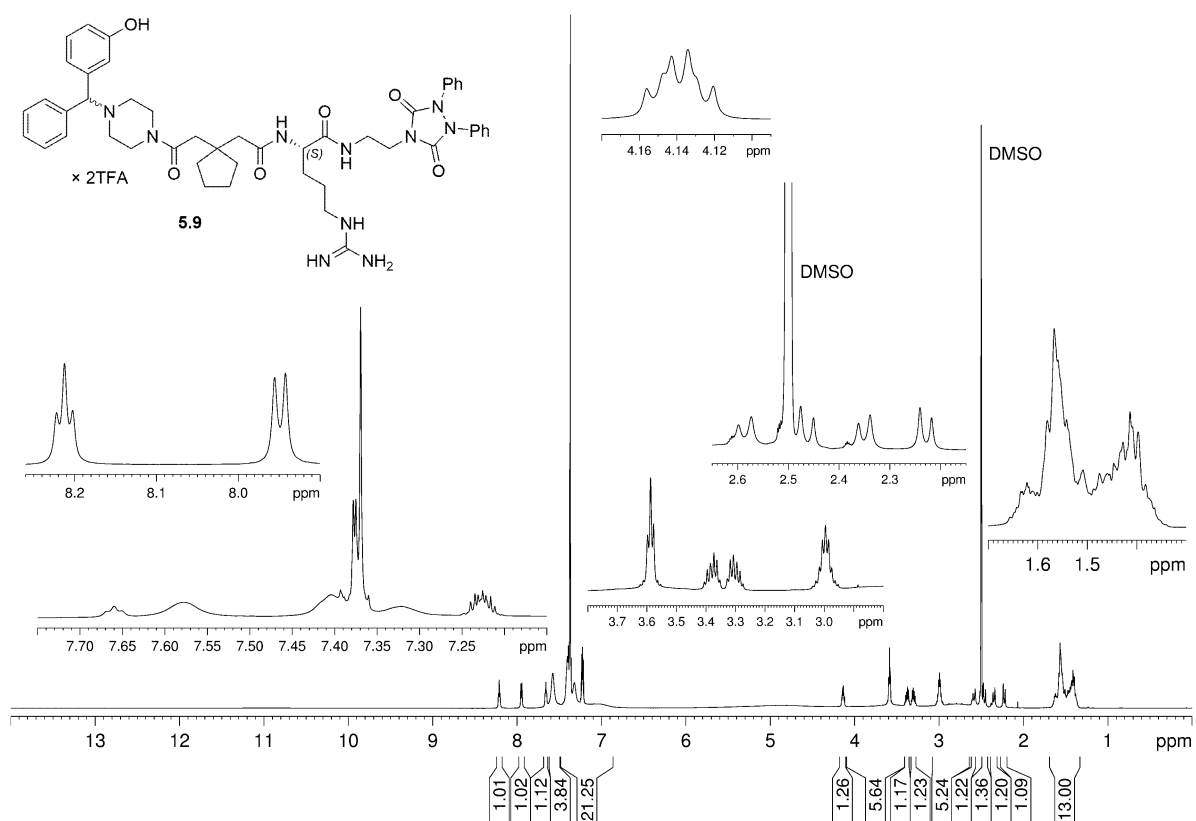
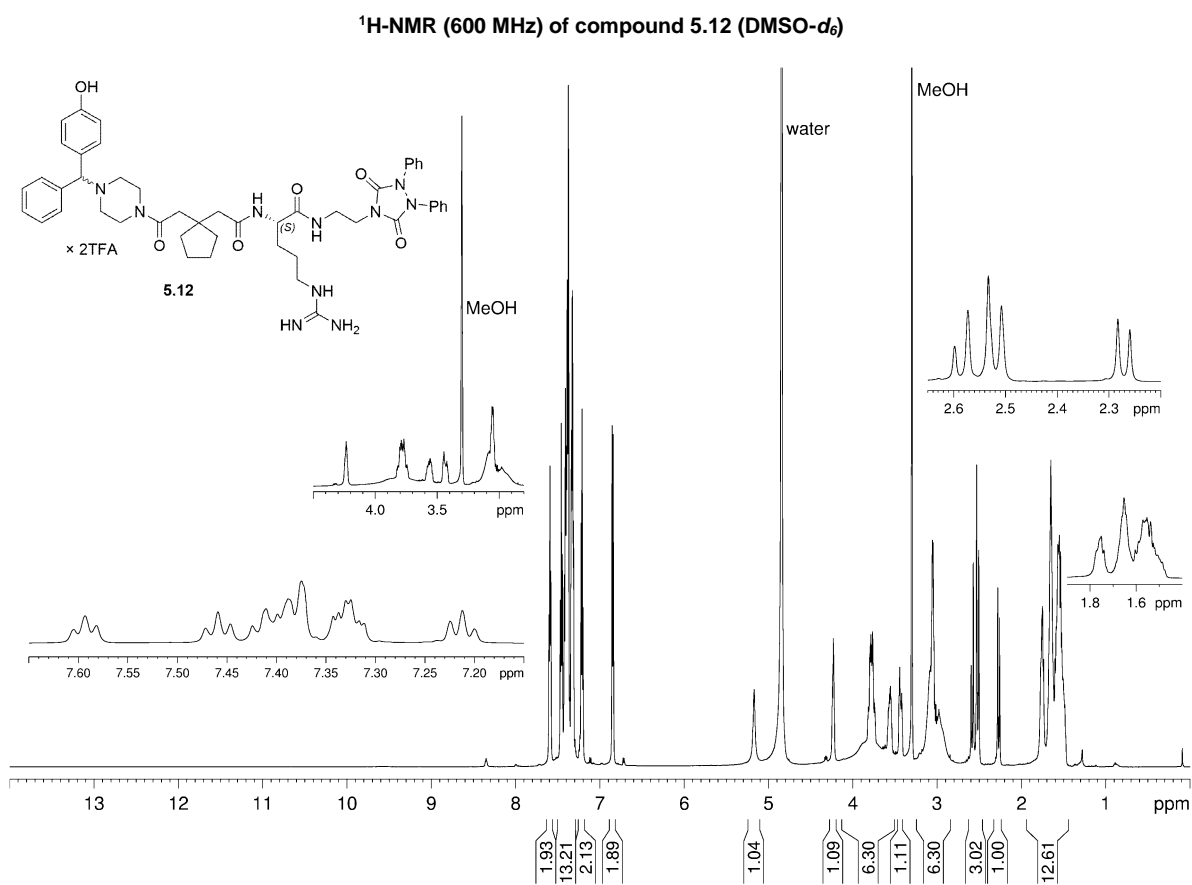
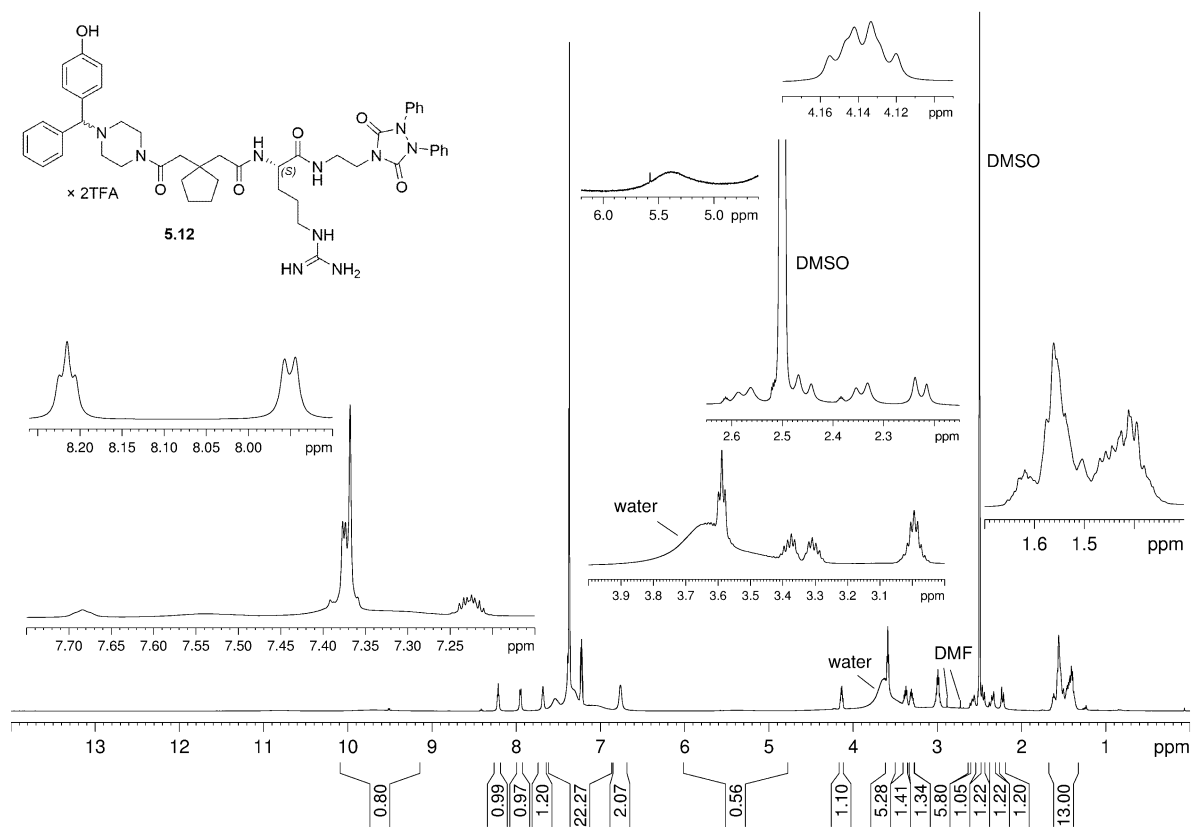
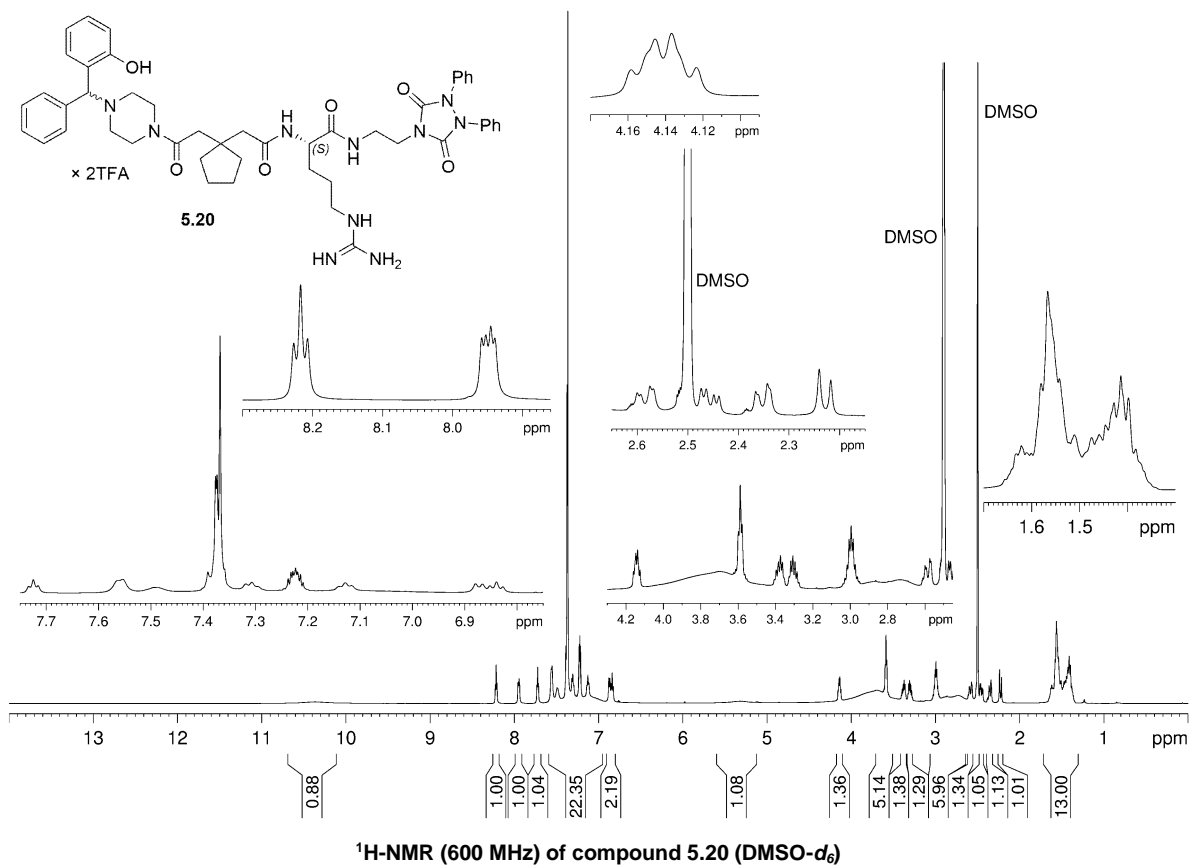
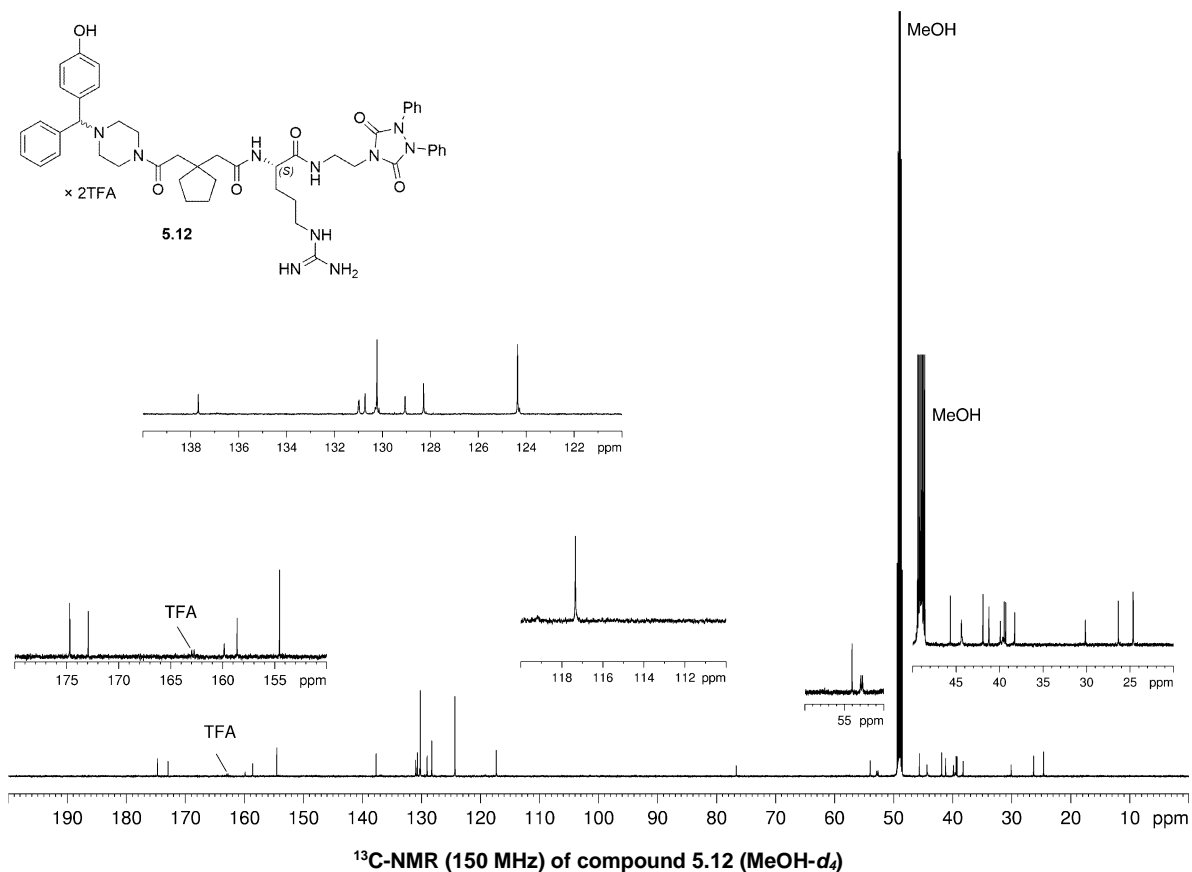
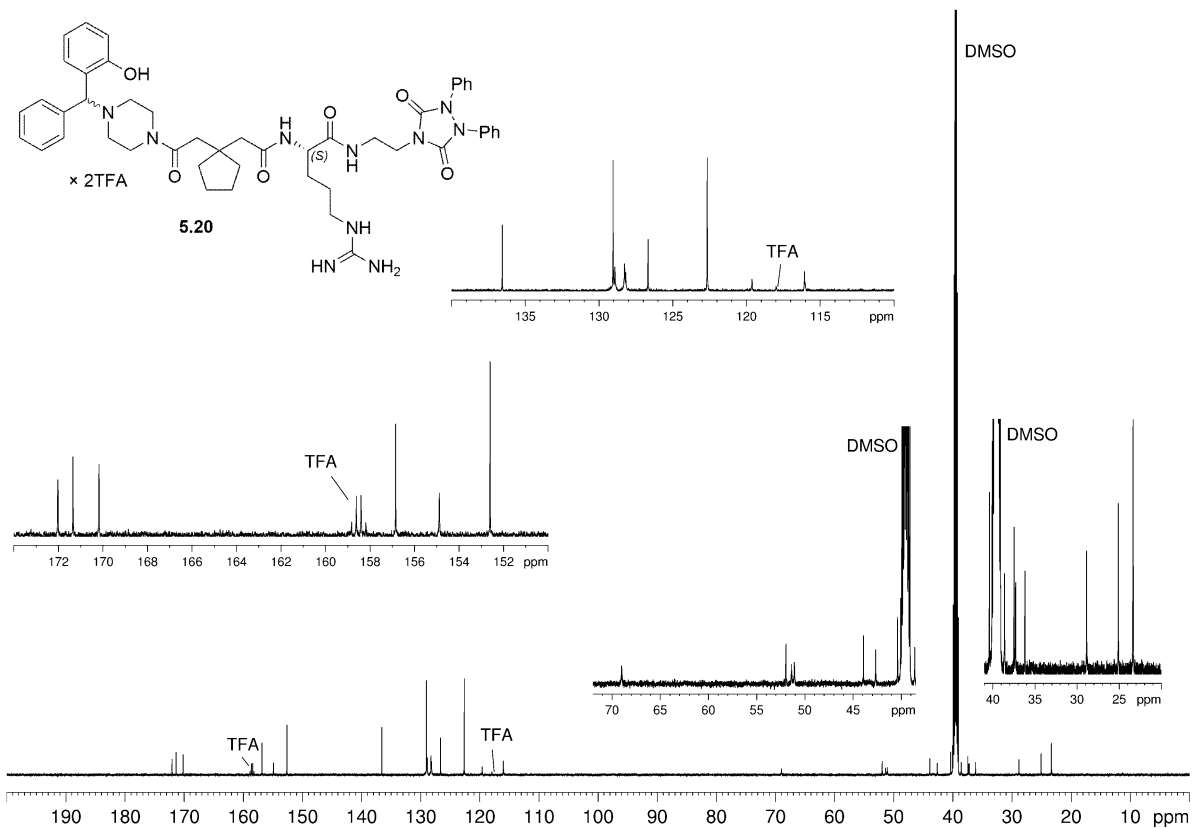
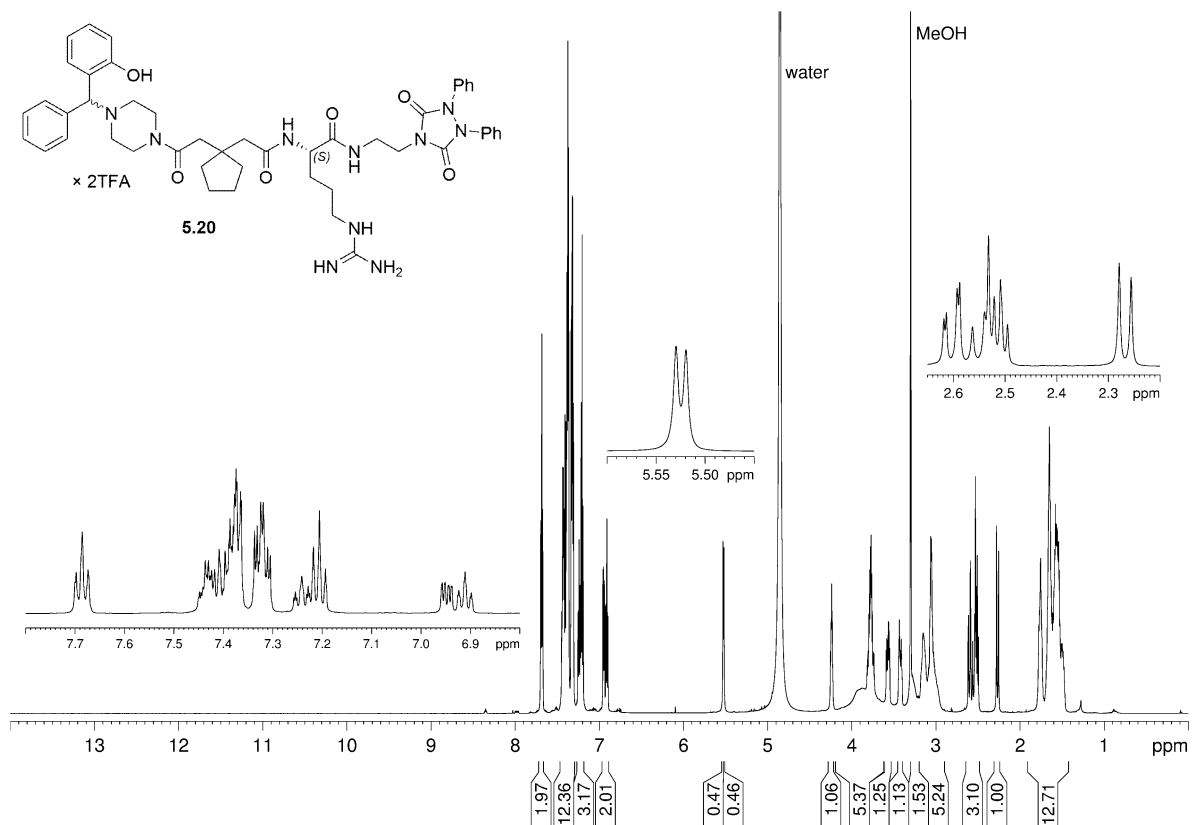


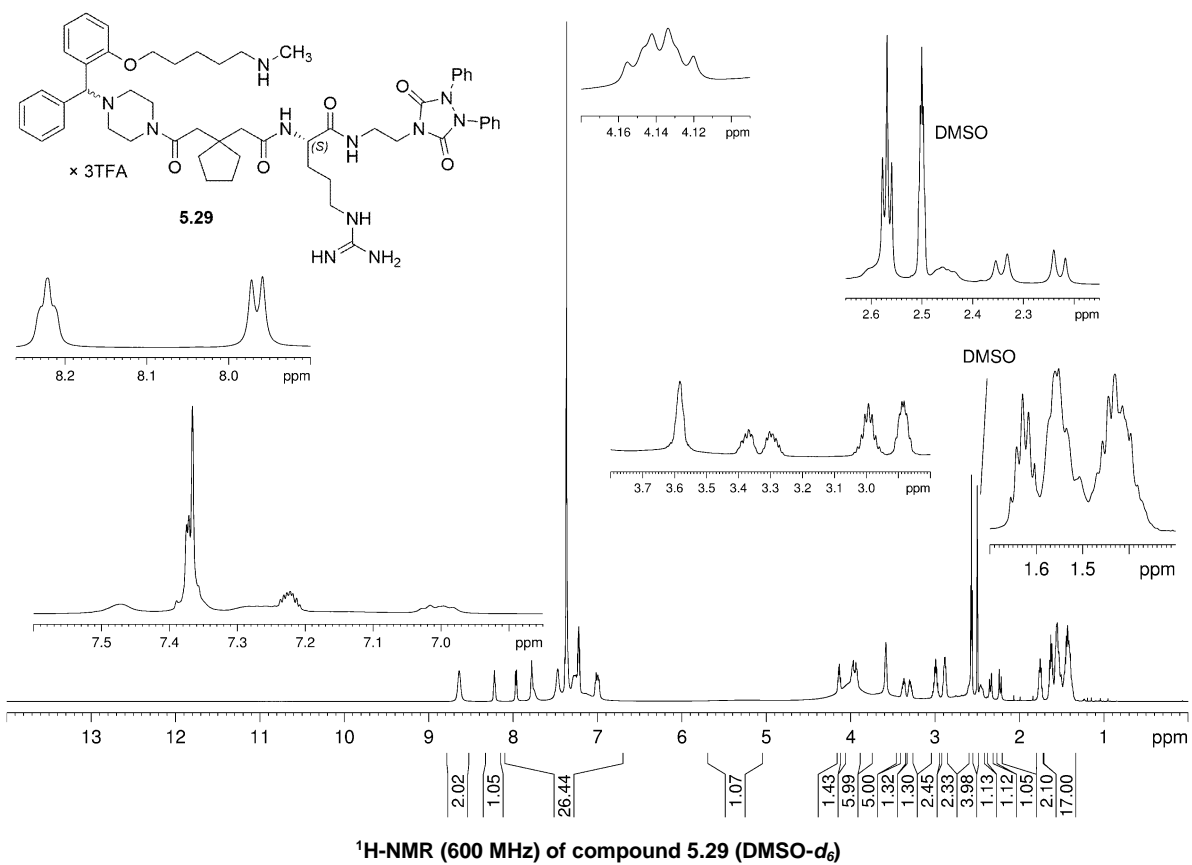
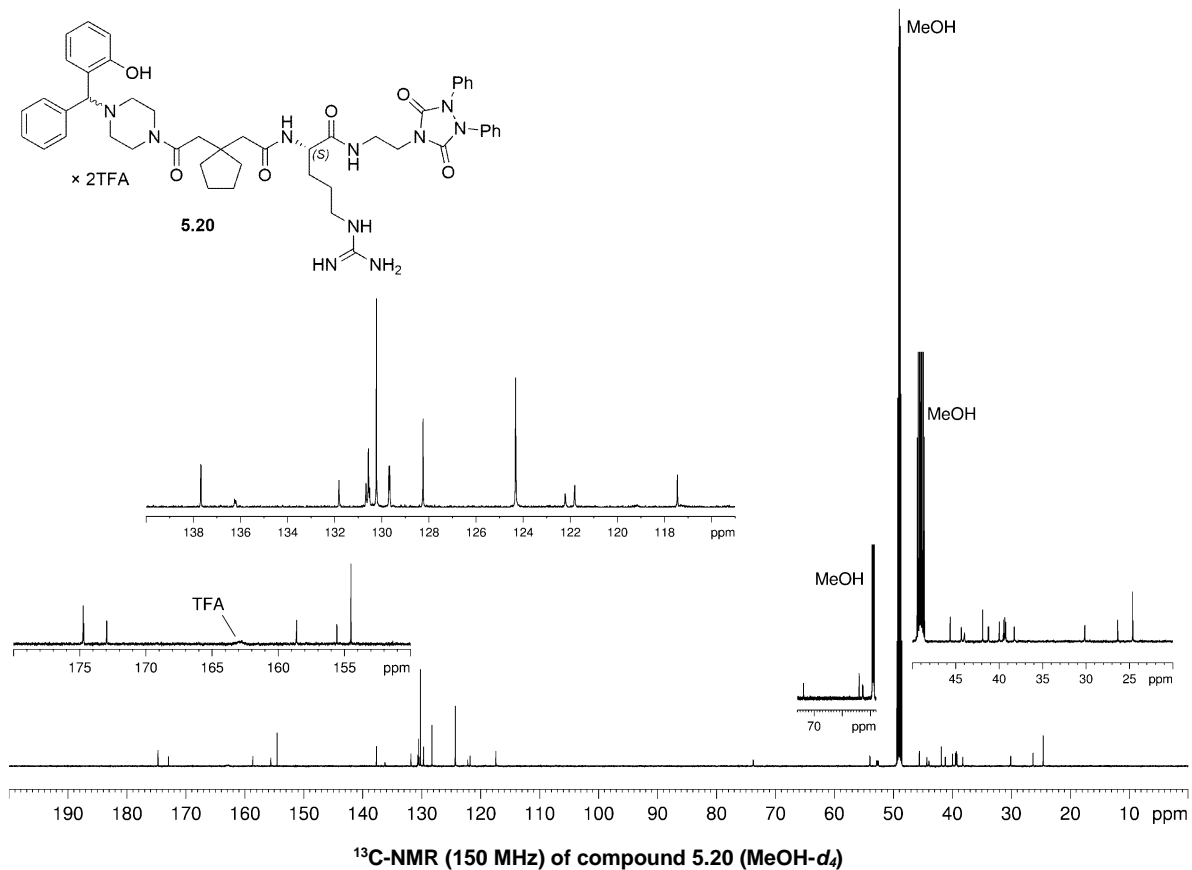
Figure 8.5. (A-B) Chromatograms of the reversed-phase HPLC analysis of (A) **5.9** and (B) **5.30** after incubation in a 25 mM HEPES buffer (pH 7.0) at rt for up to 24 h. **5.9** and **5.30** proved to be stable.

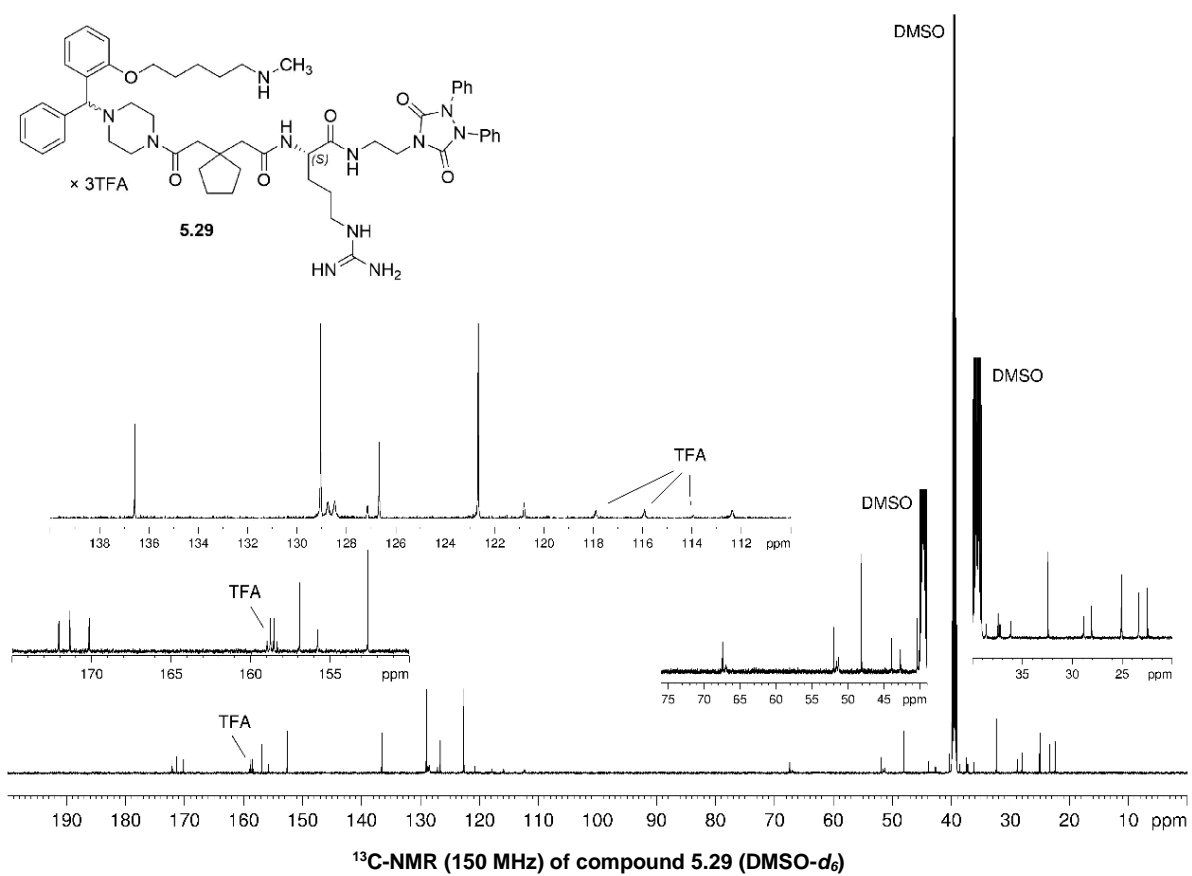
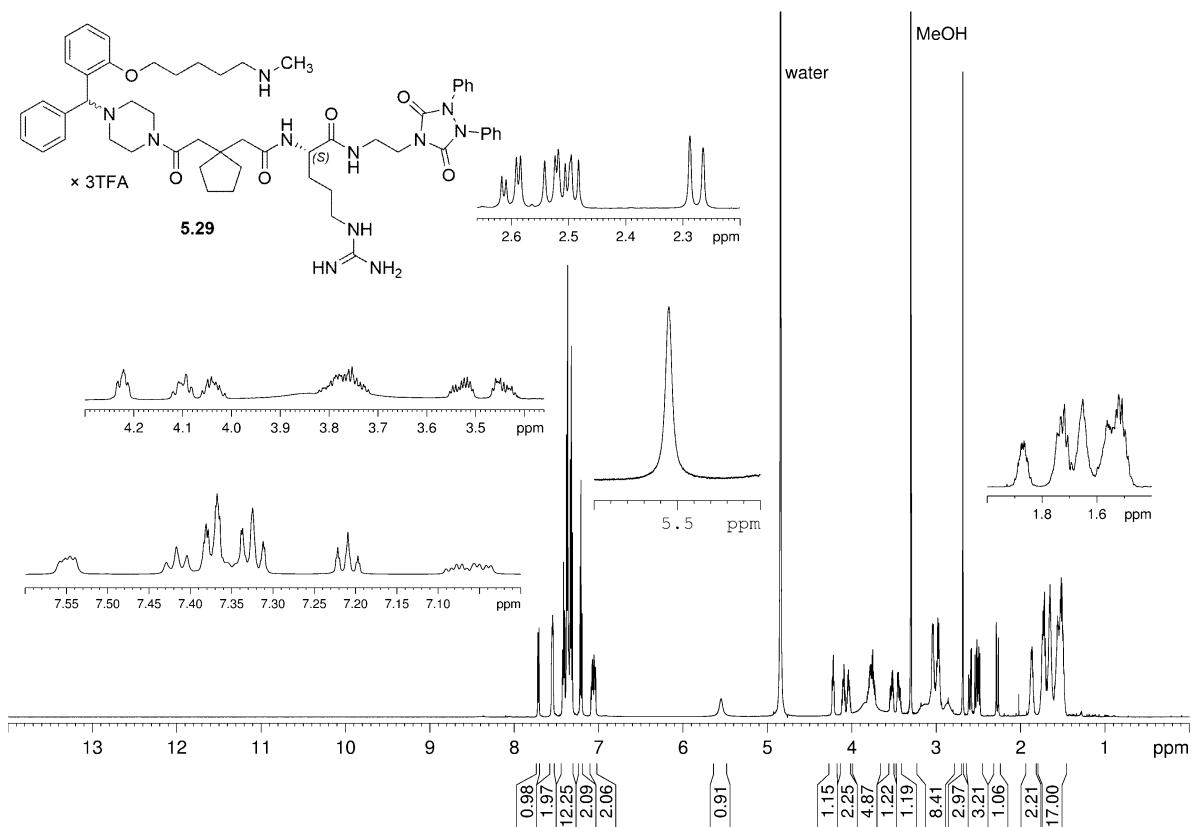
8.3.1. $^1\text{H-NMR}$ and $^{13}\text{C-NMR}$ spectra of compounds 5.9, 5.12, 5.20 and 5.29-5.32

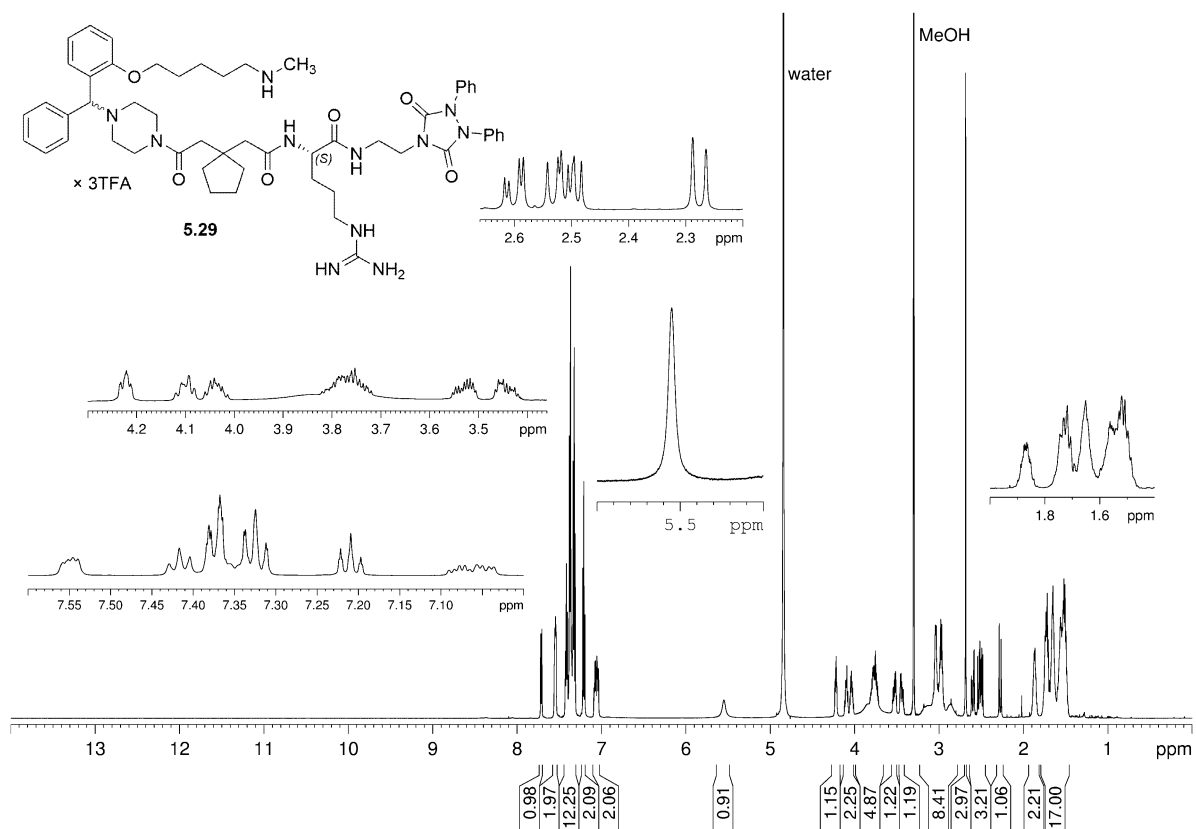
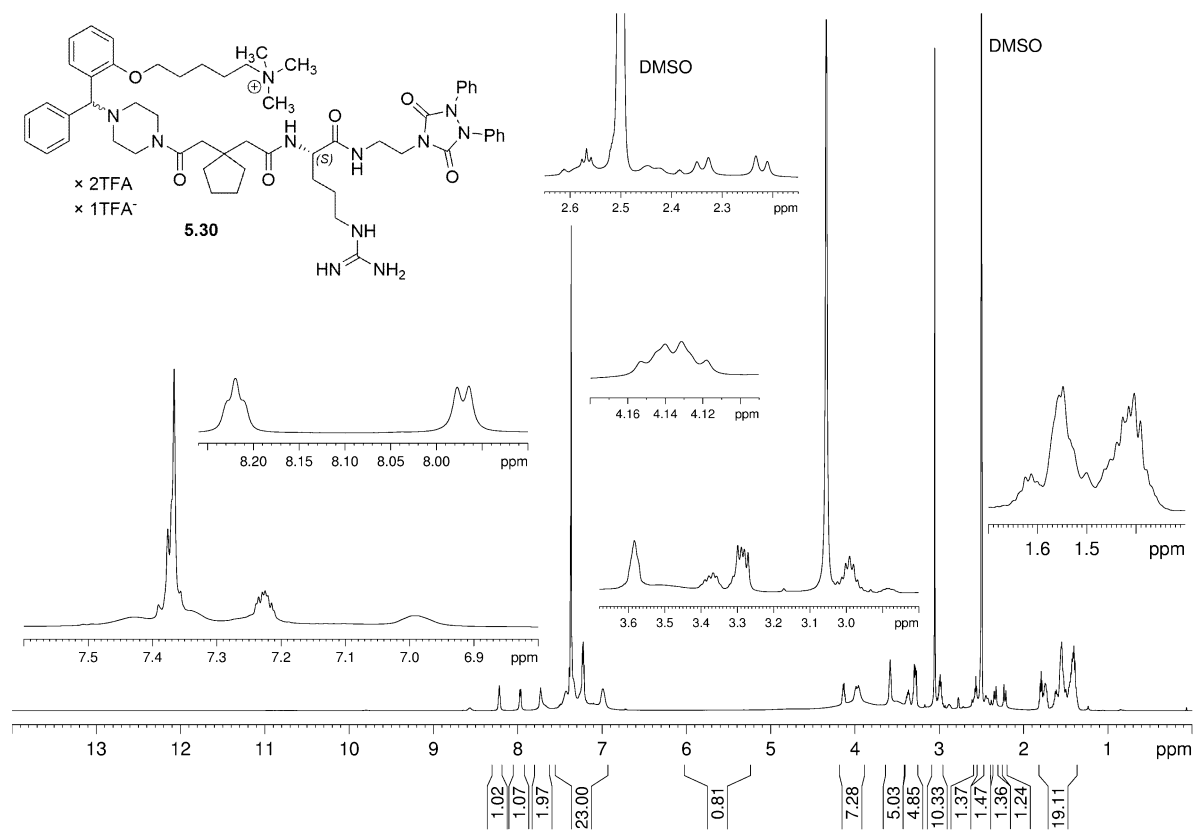


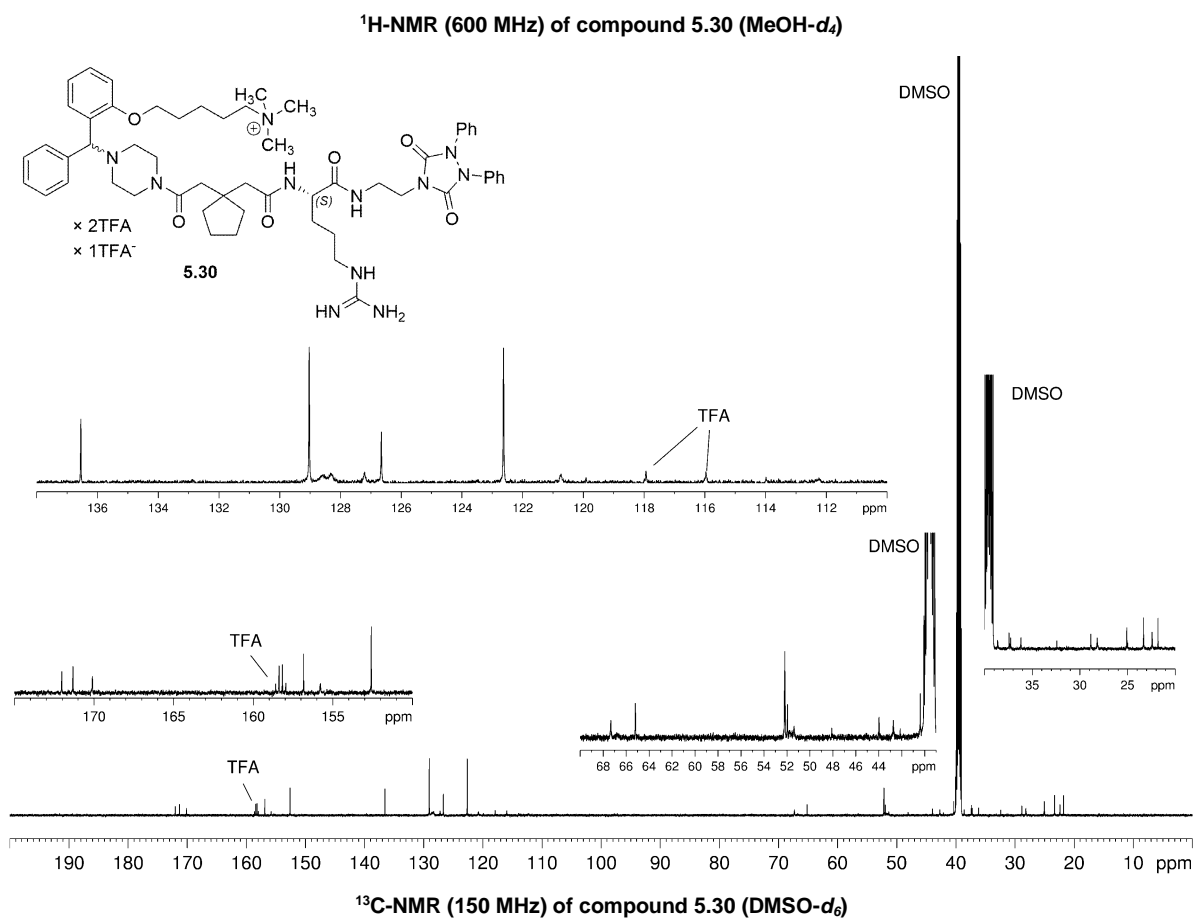
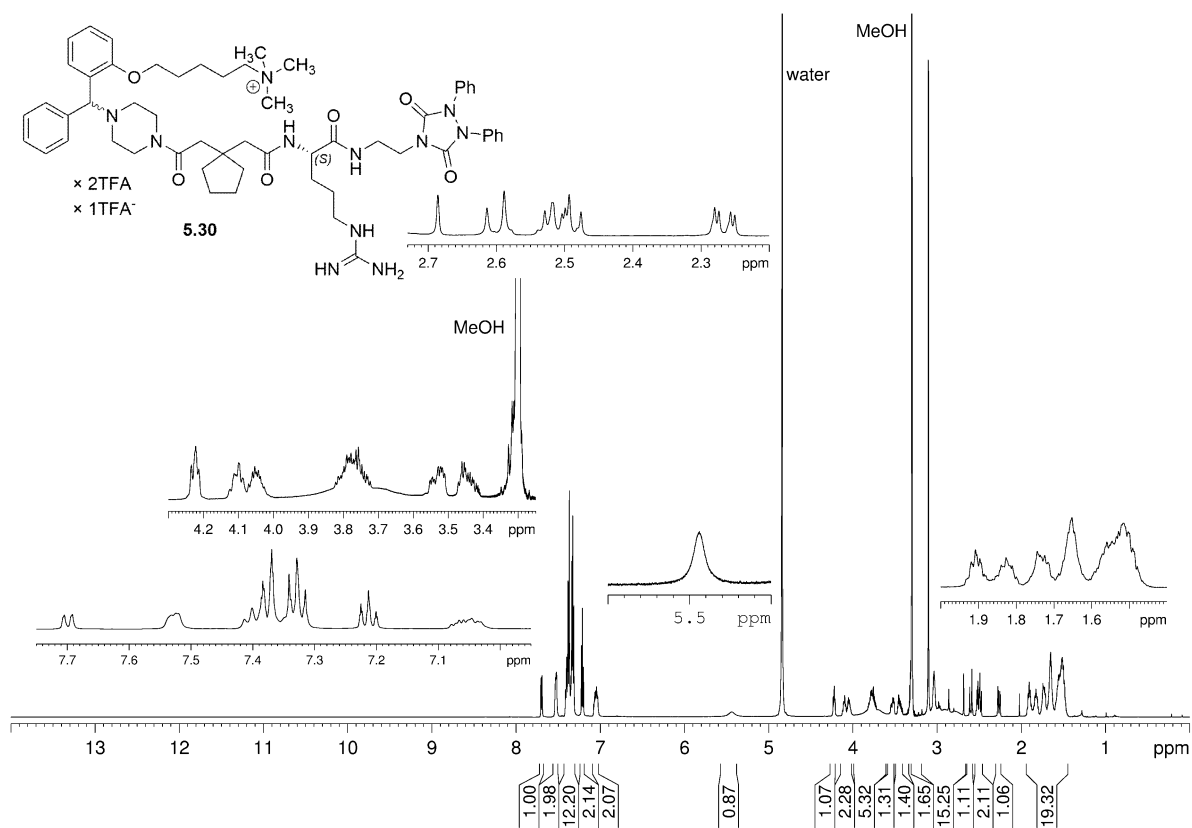


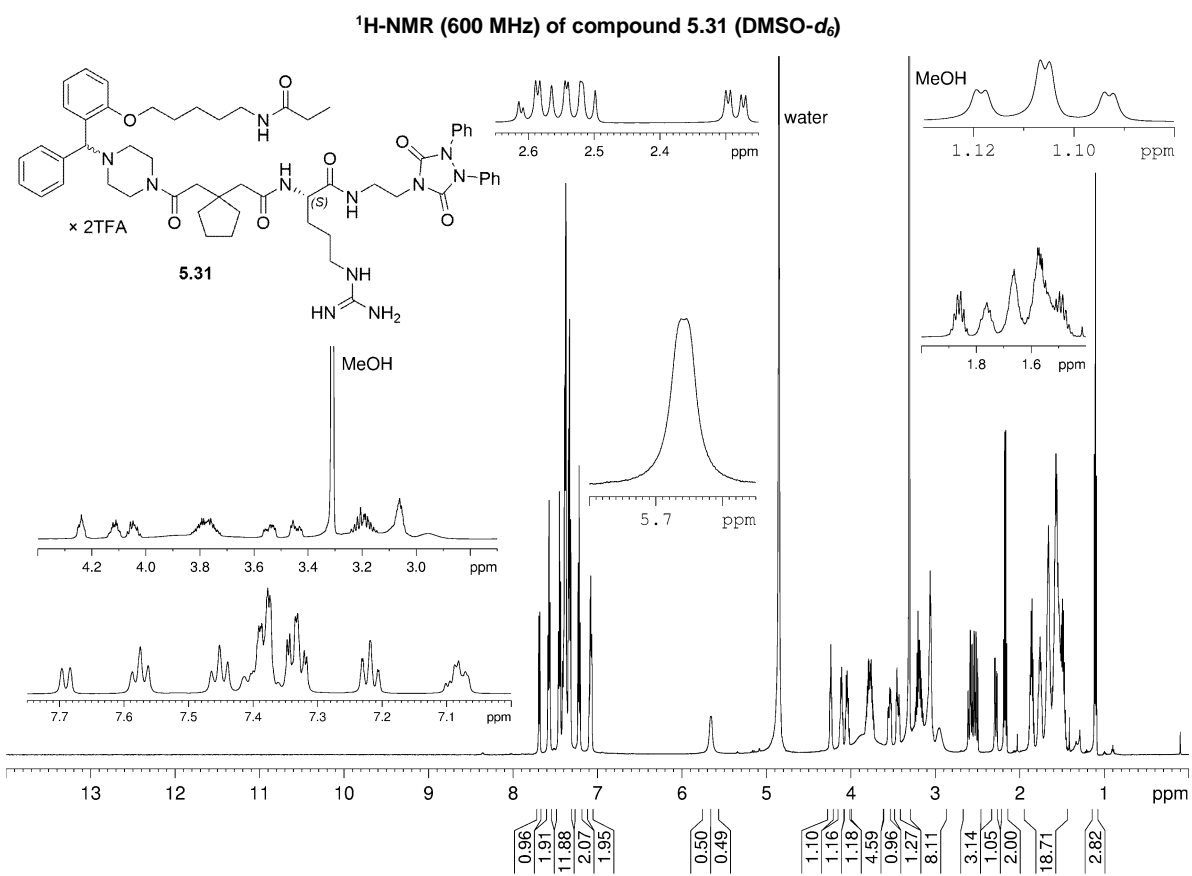
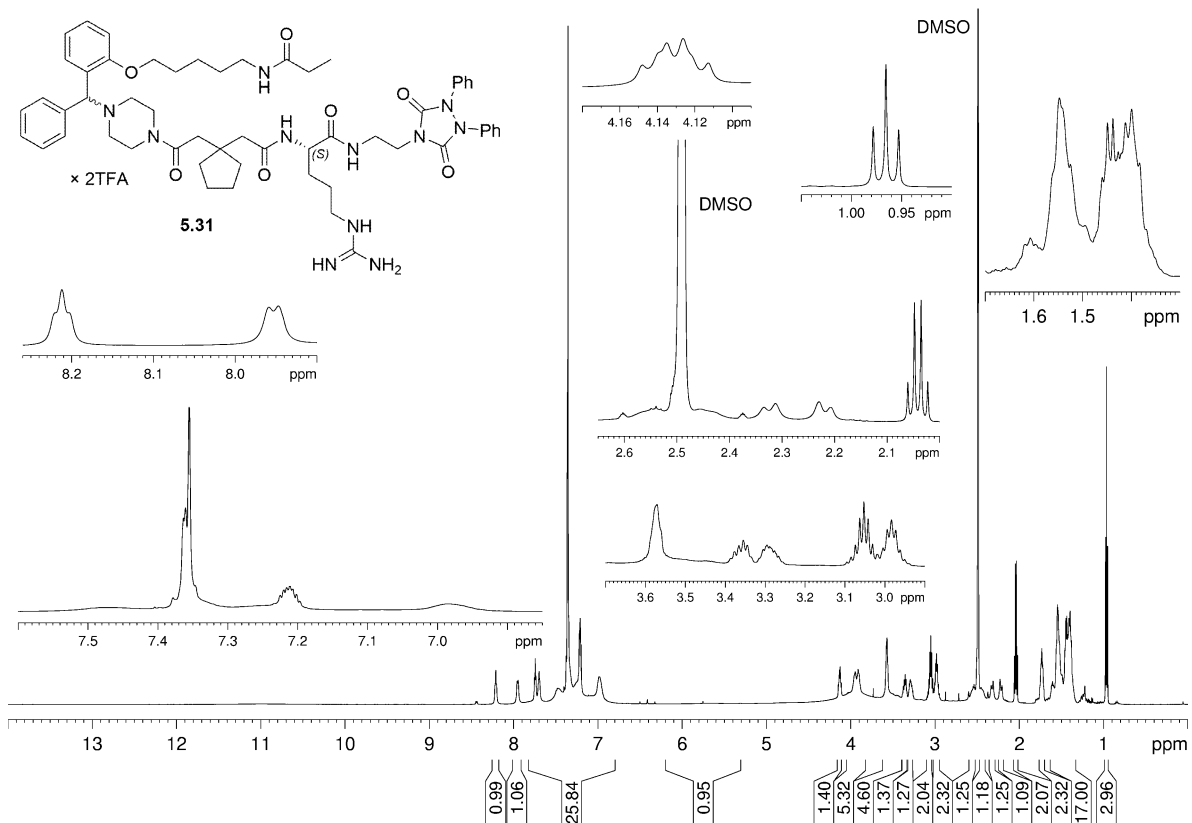


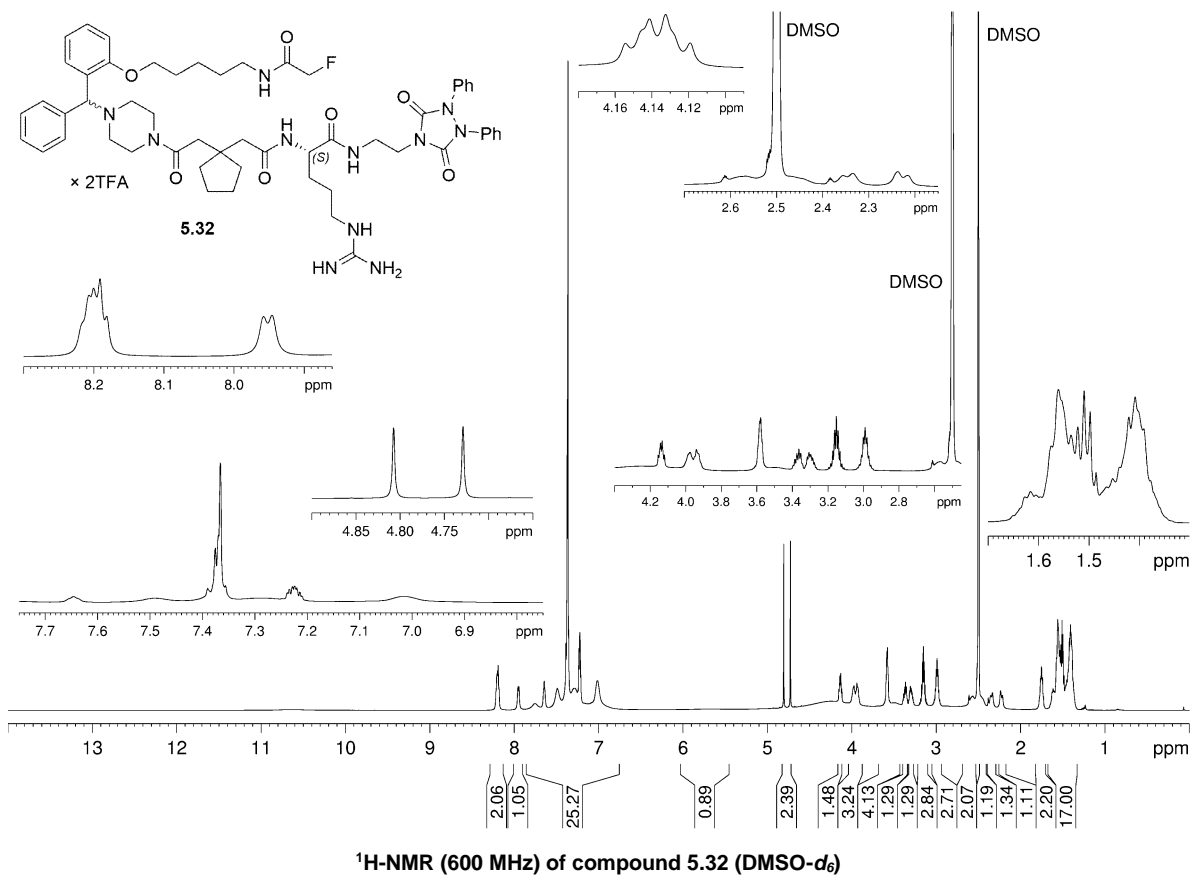
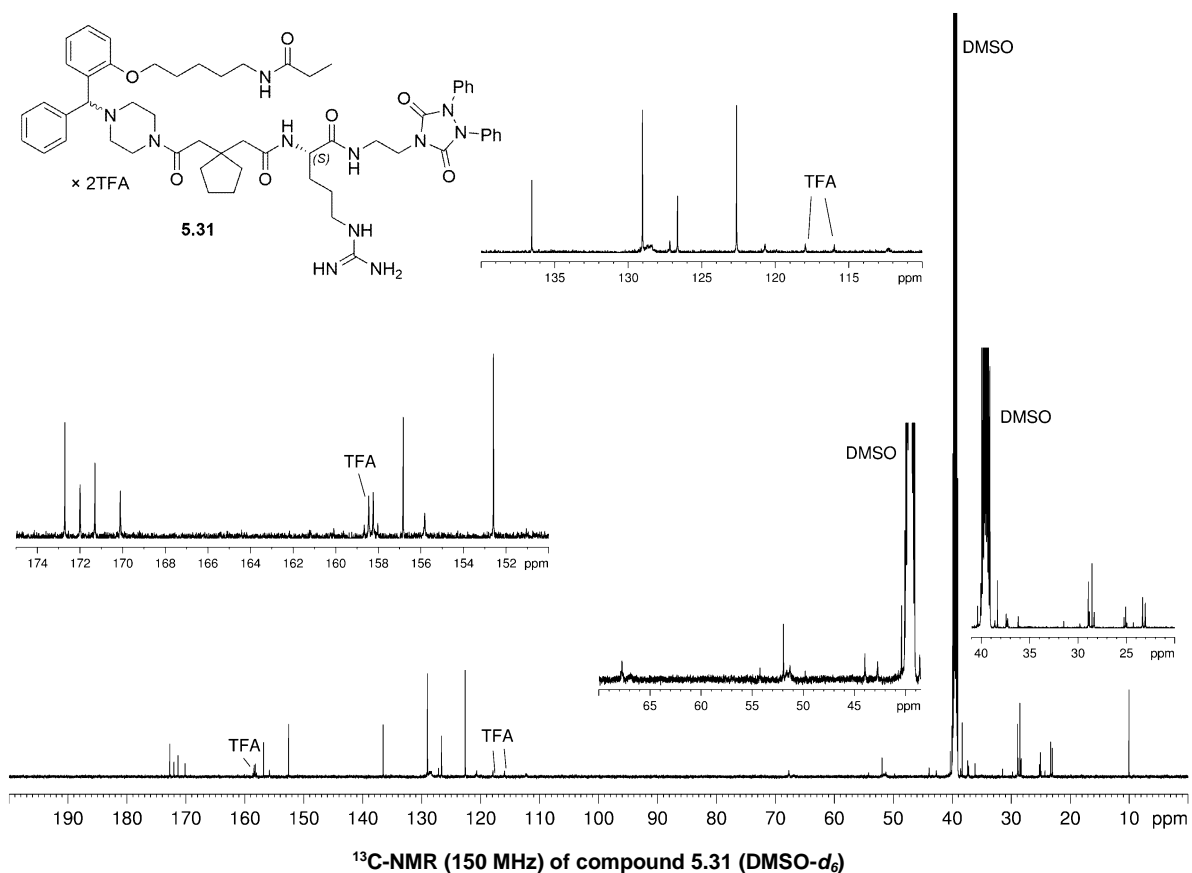


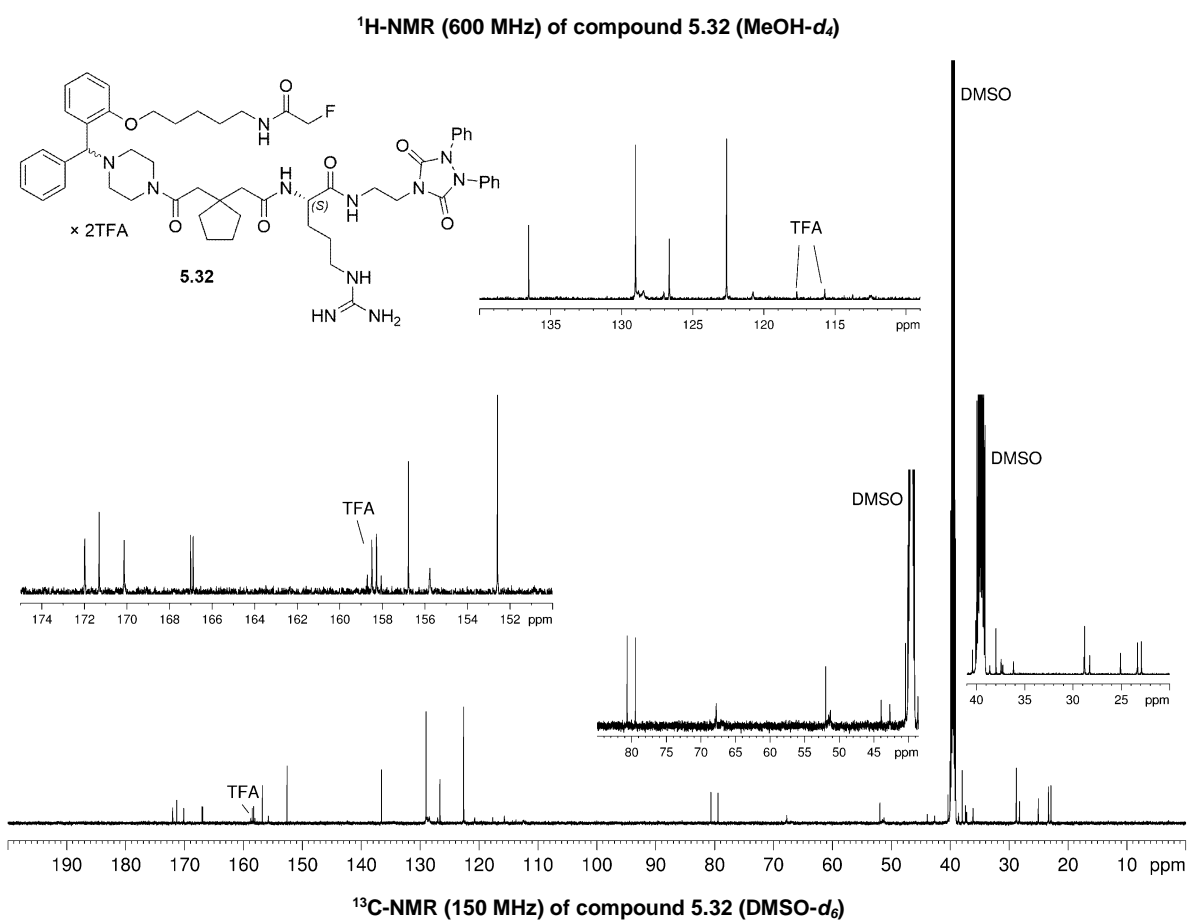
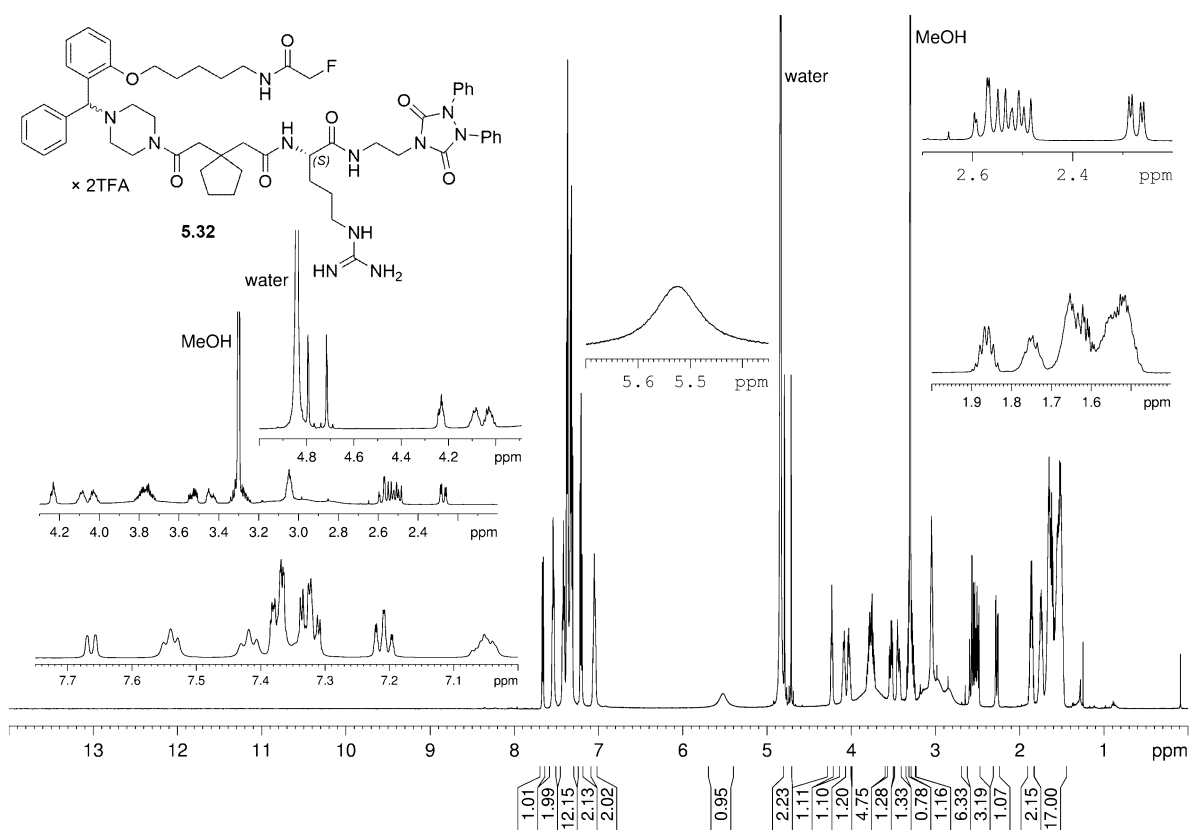


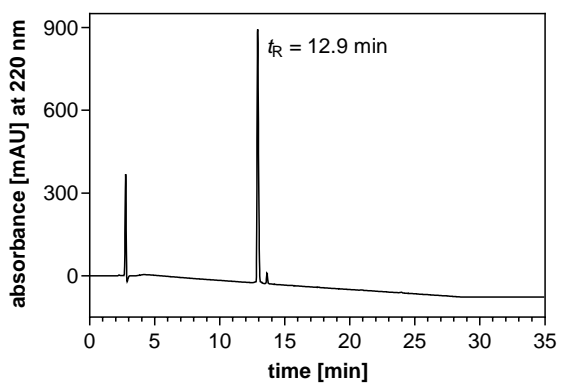
 ^{13}C -NMR (150 MHz) of compound 5.29 ($\text{MeOH-}d_4$) ^1H -NMR (600 MHz) of compound 5.30 ($\text{DMSO-}d_6$)



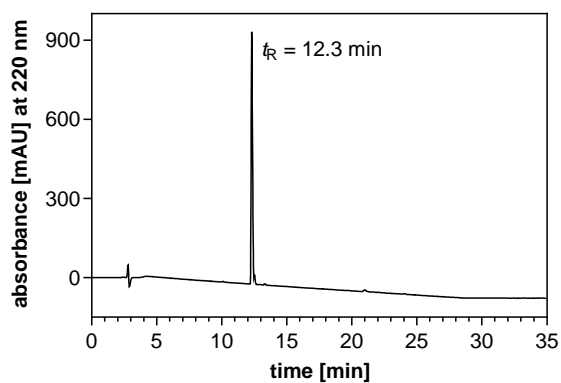




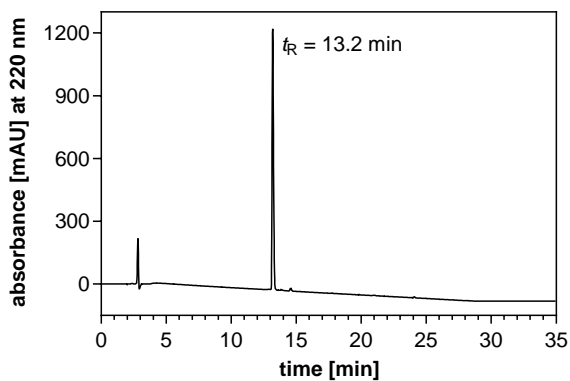


8.3.3. RP-HPLC purity chromatograms of (220 nm) compounds 5.9, 5.12, 5.20 and 5.29-5.32

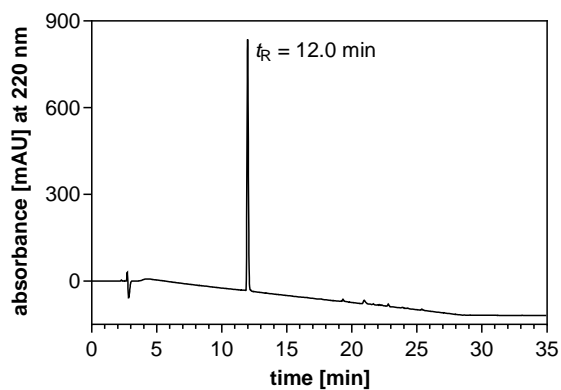
RP-HPLC (220 nm) chromatogram of 5.9



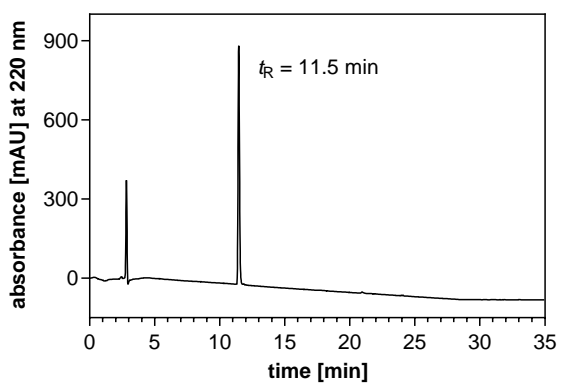
RP-HPLC (220 nm) chromatogram of 5.12



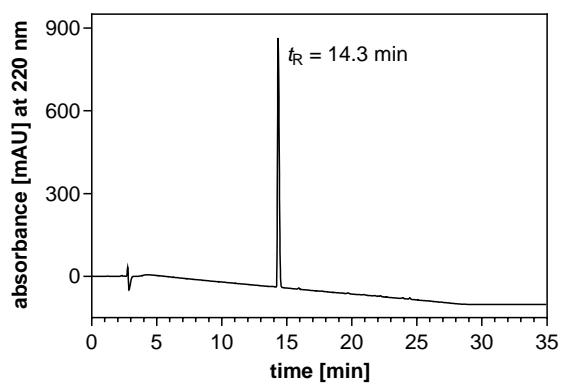
RP-HPLC (220 nm) chromatogram of 5.20



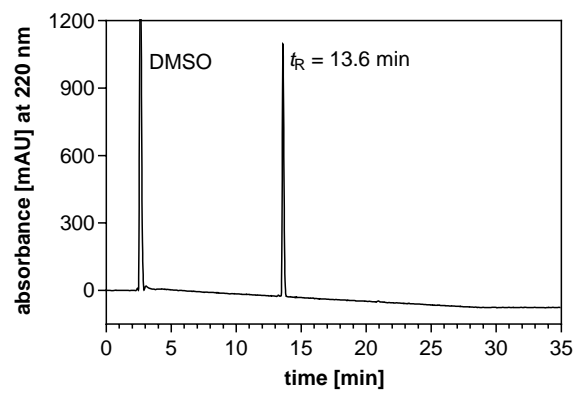
RP-HPLC (220 nm) chromatogram of 5.29



RP-HPLC (220 nm) chromatogram of 5.30

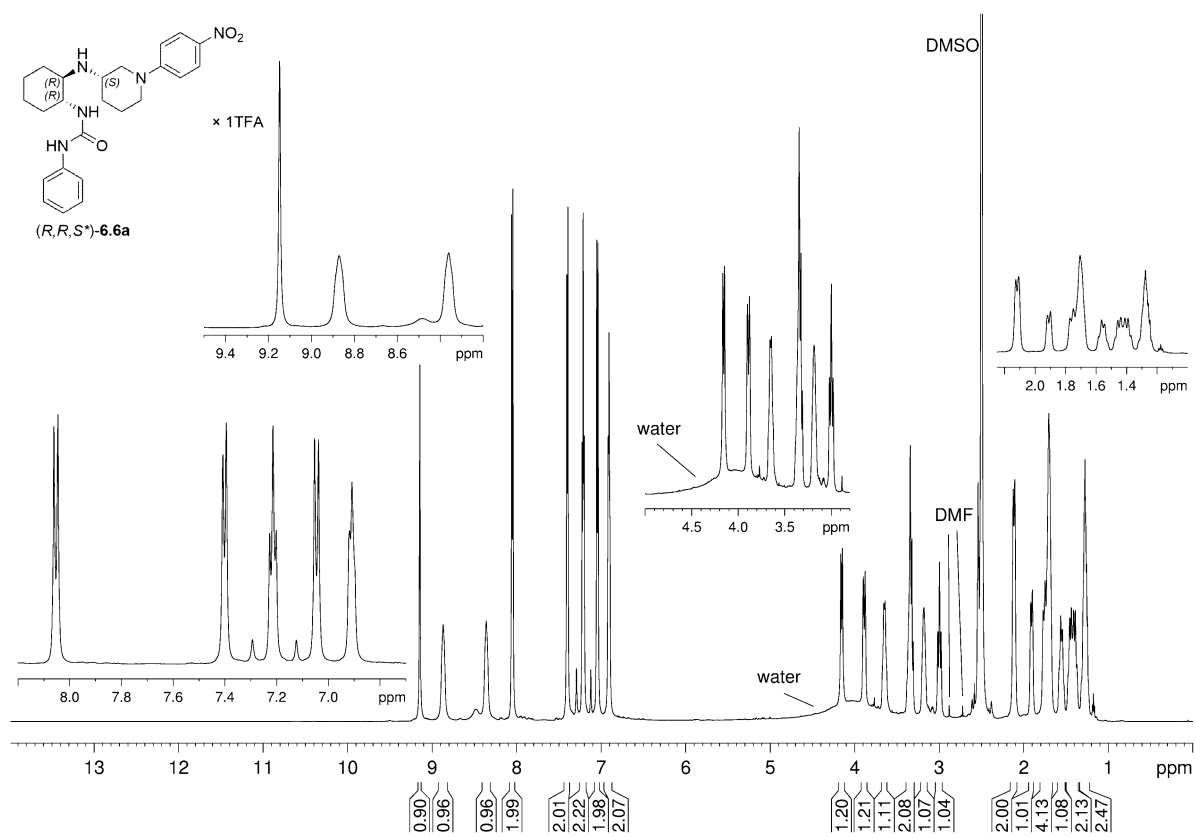


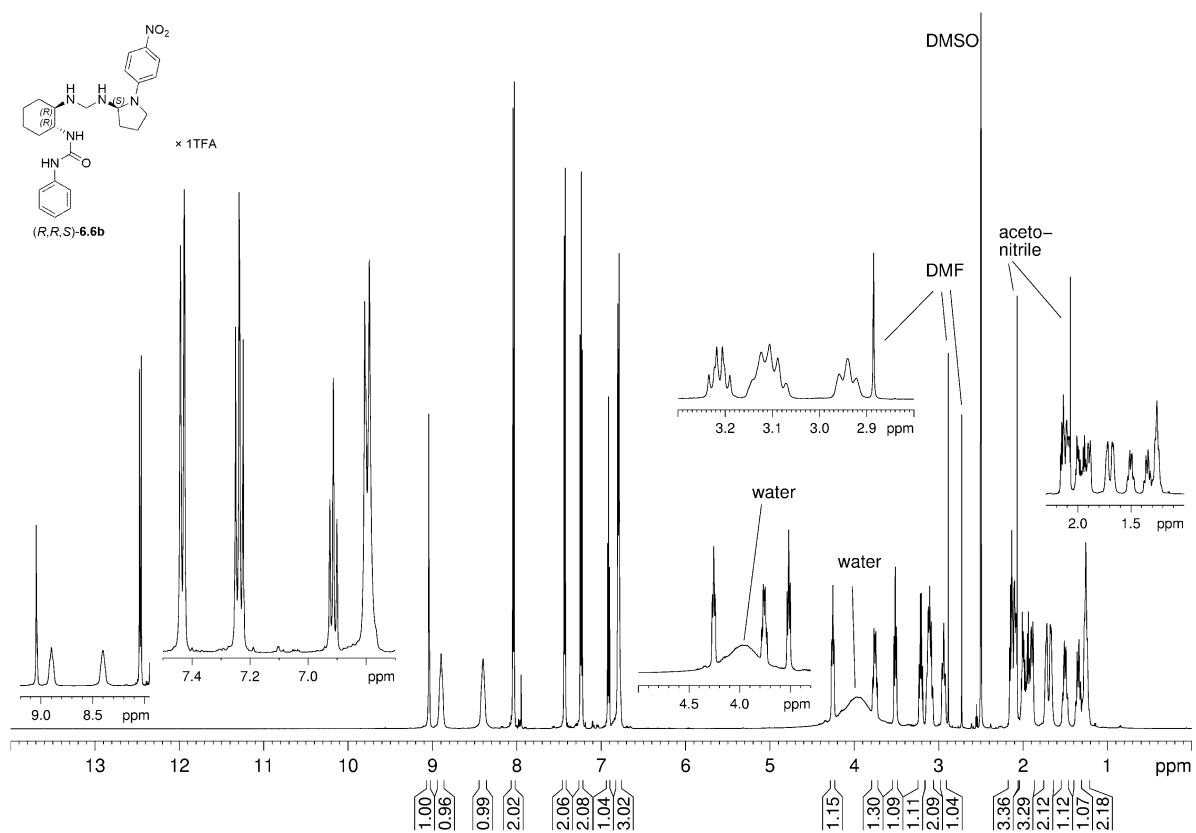
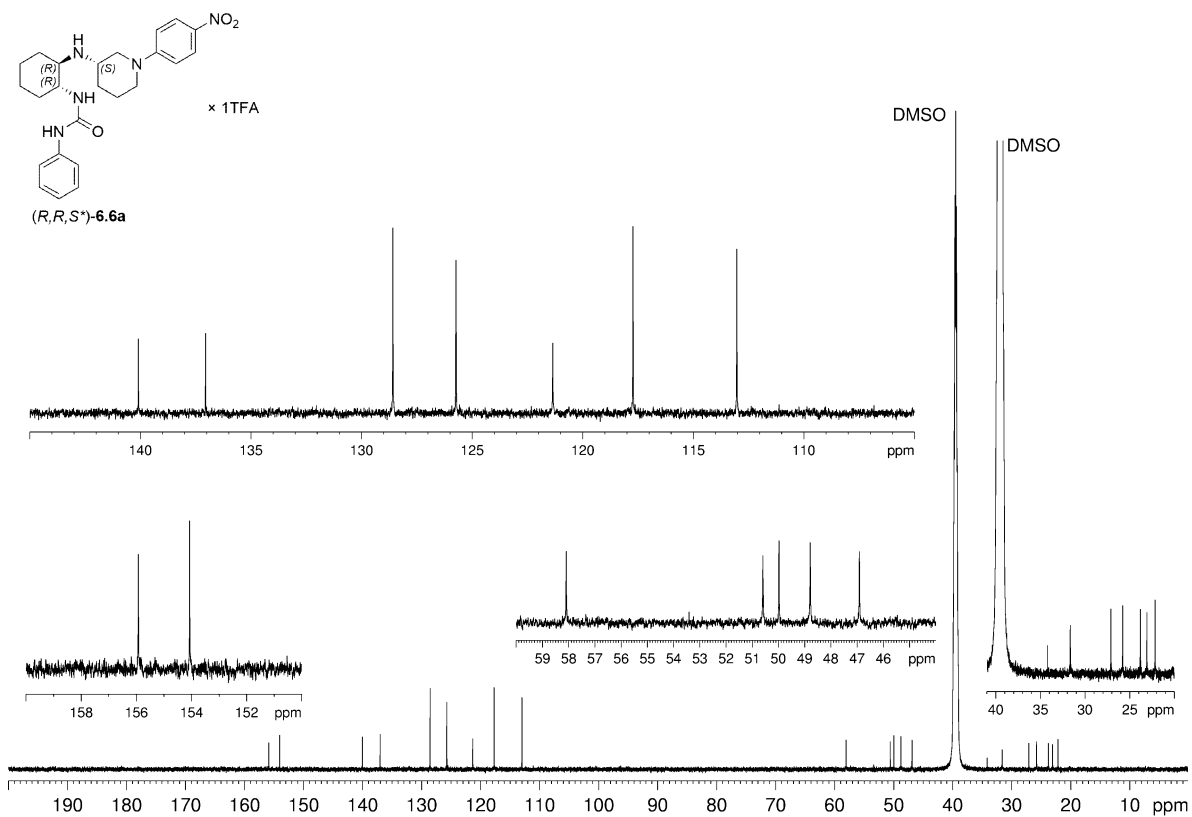
RP-HPLC (220 nm) chromatogram of 5.31

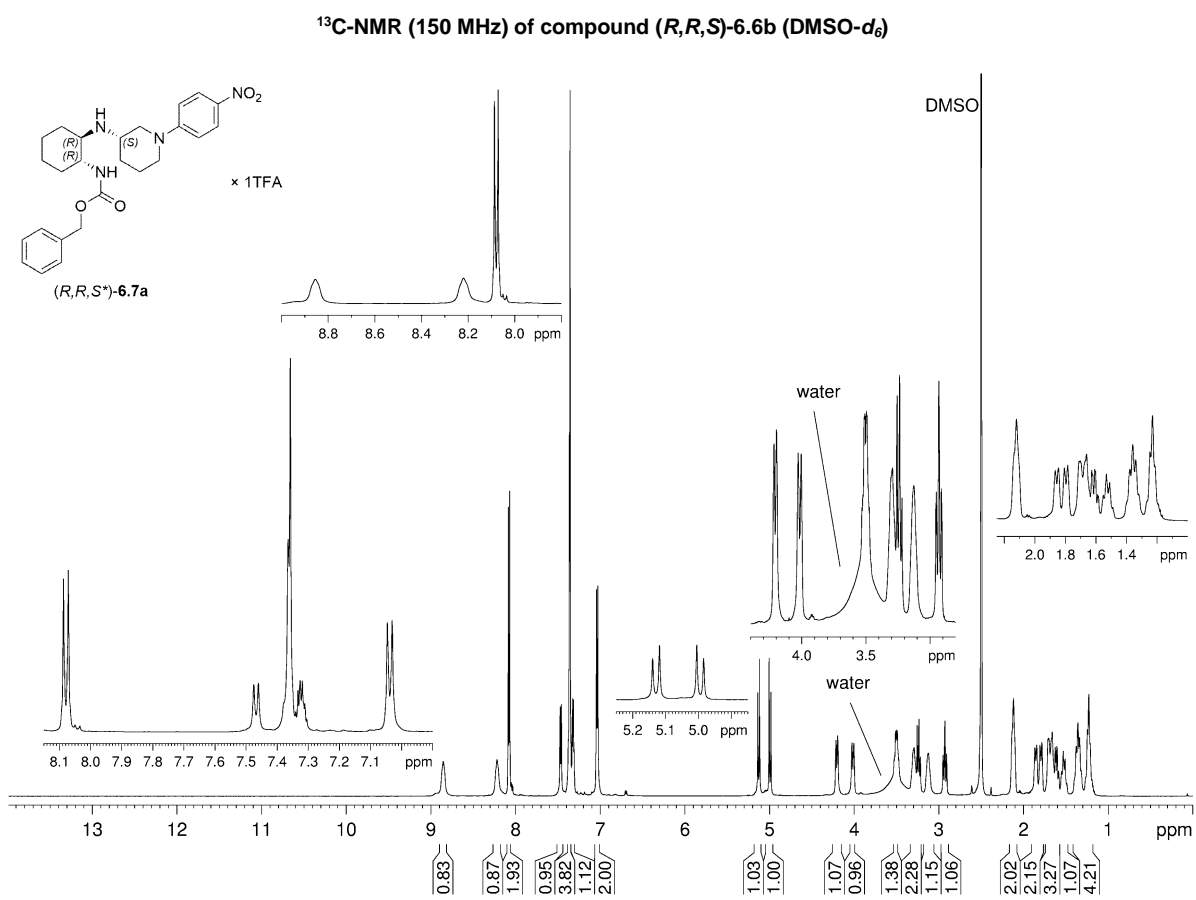
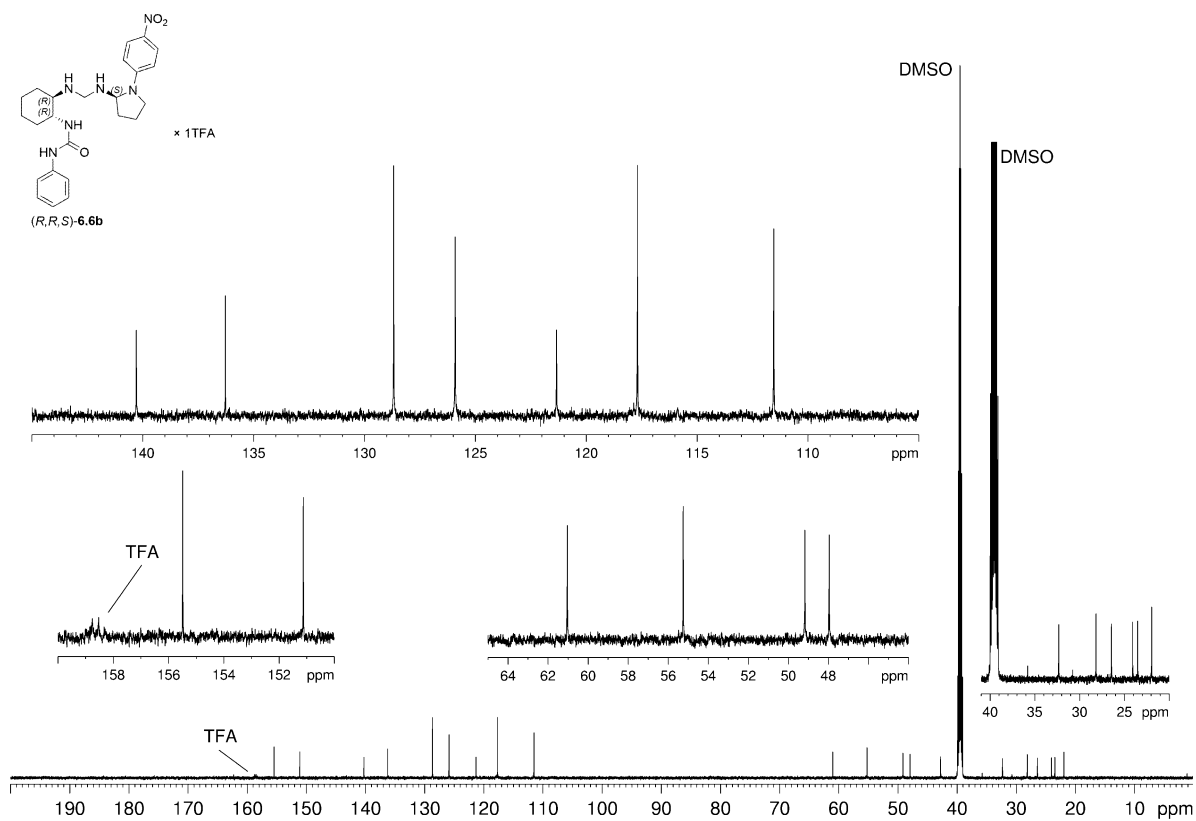


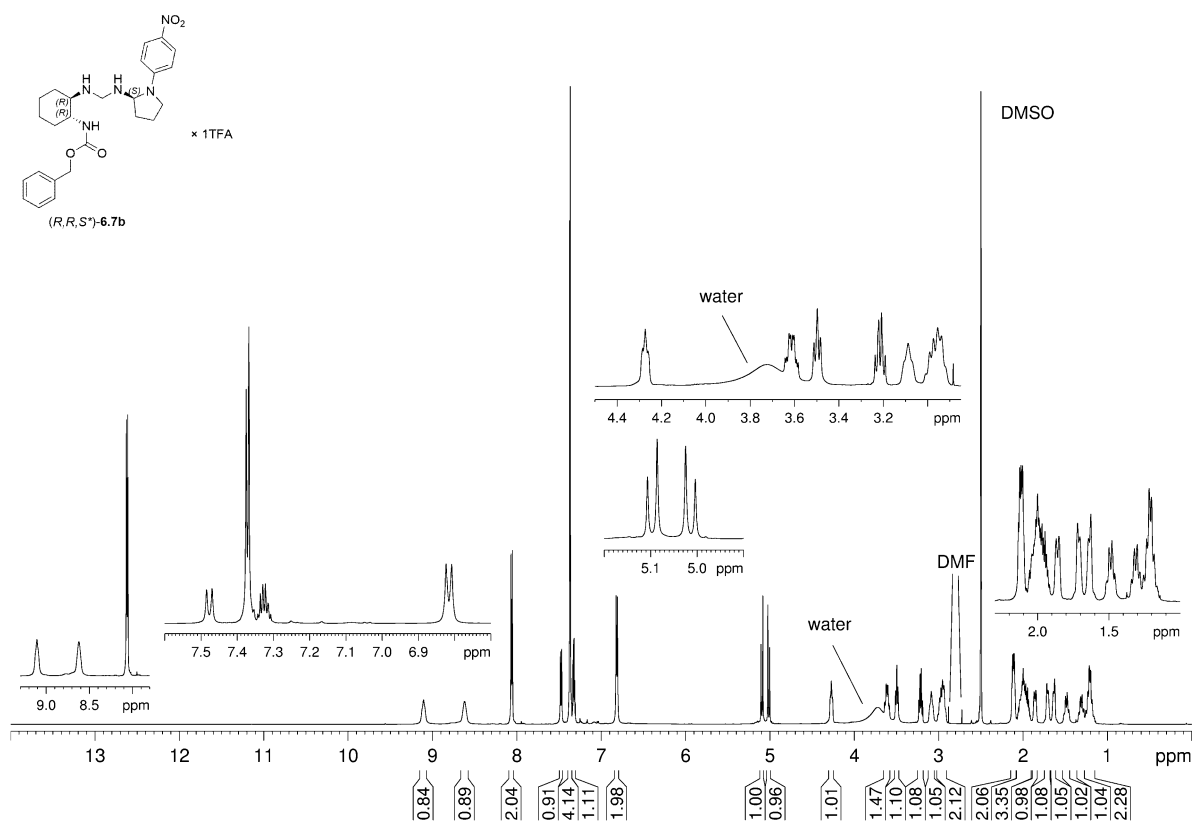
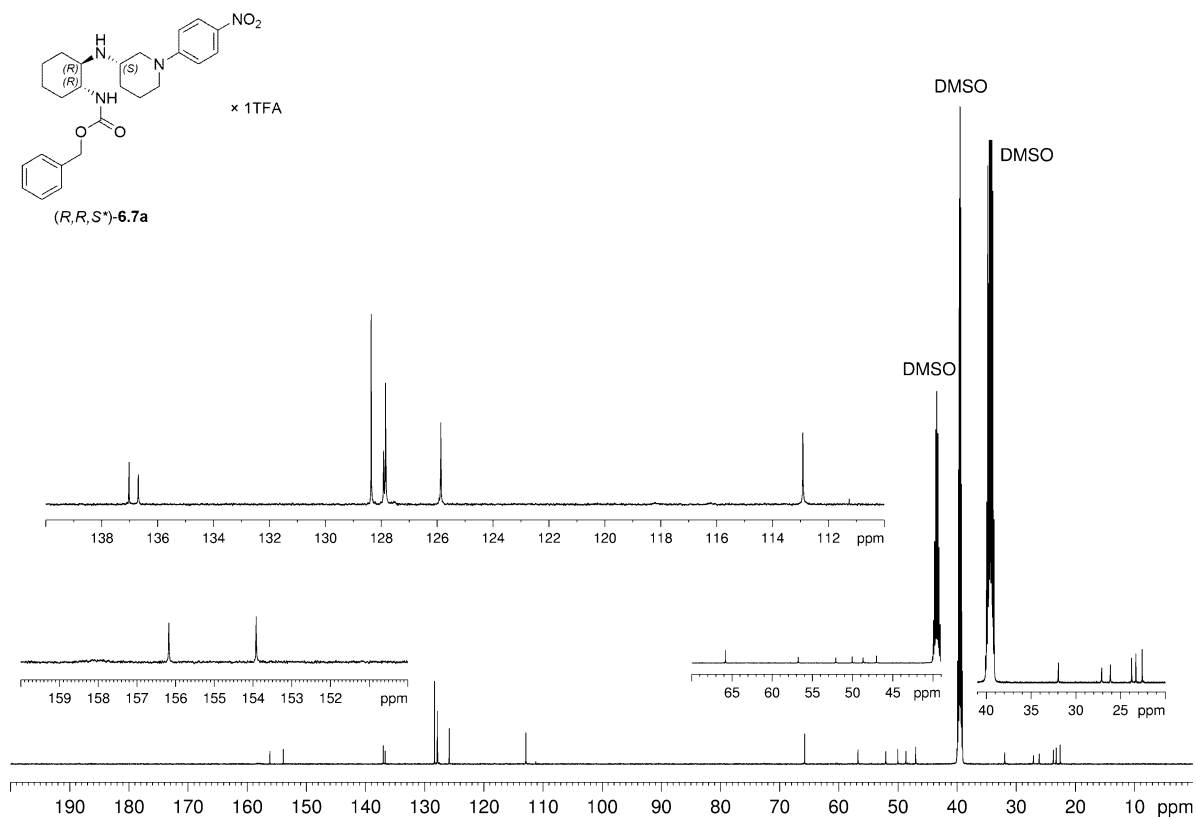
RP-HPLC (220 nm) chromatogram of 5.32

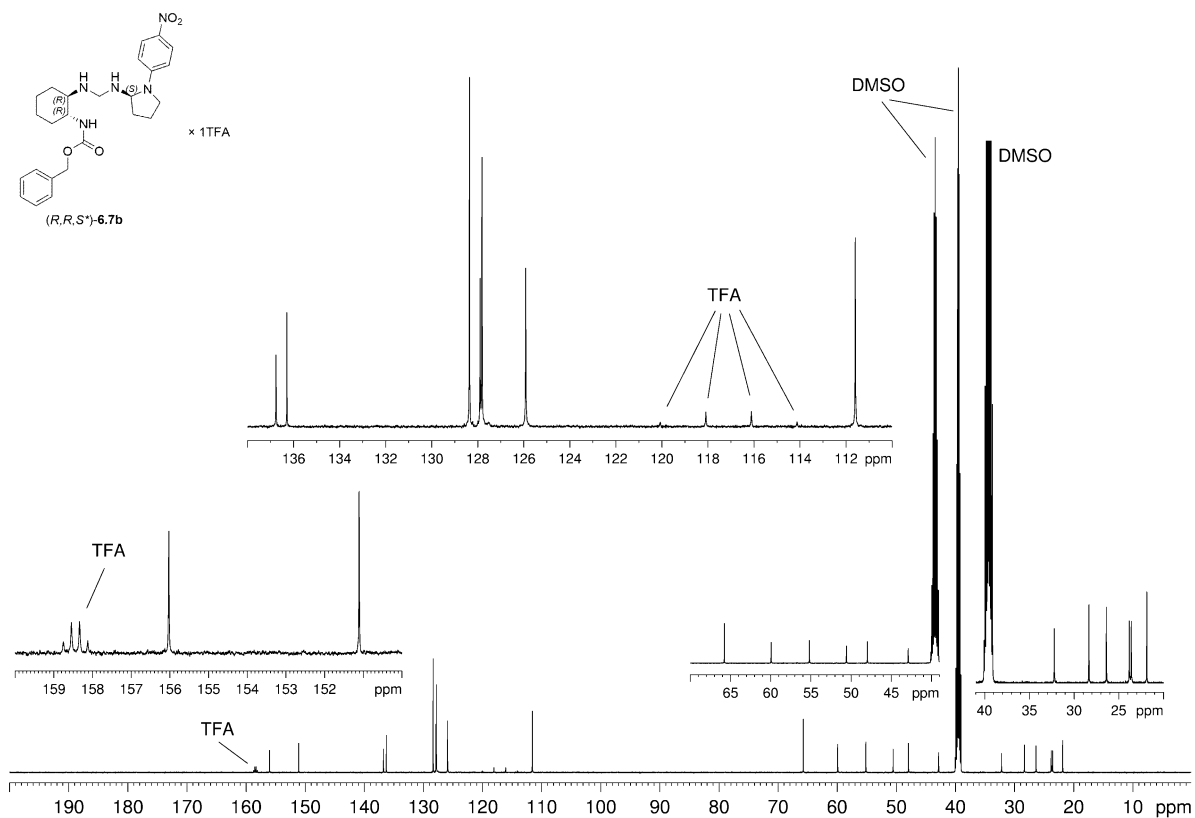
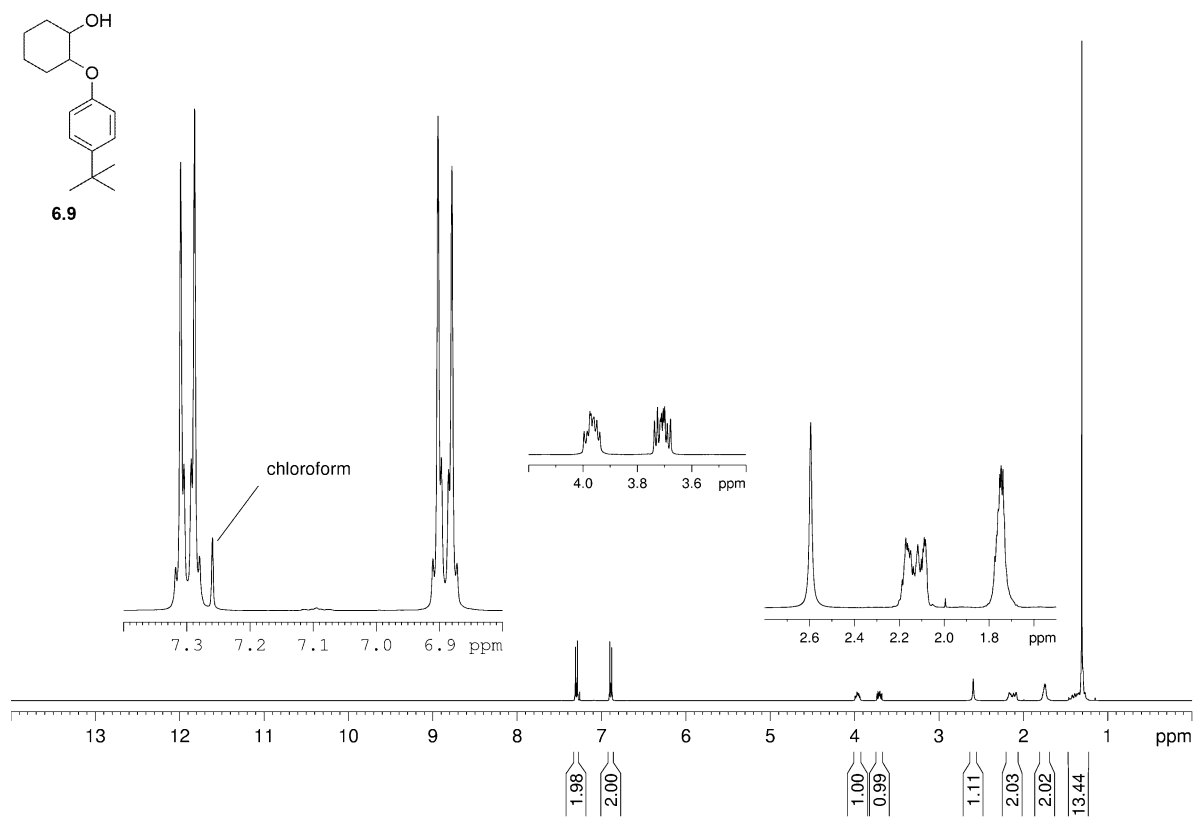
8.4. Chapter 6

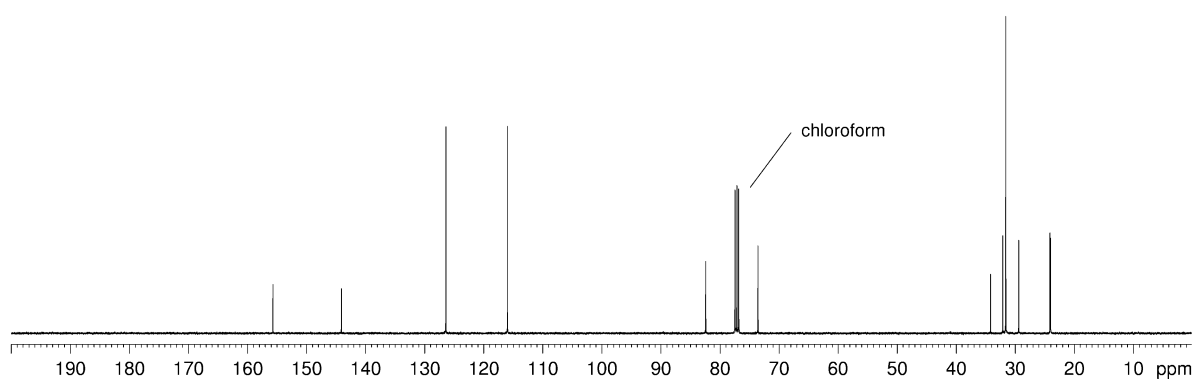
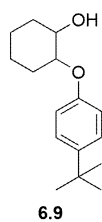
8.4.1. $^1\text{H-NMR}$ and $^{13}\text{C-NMR}$ spectra of compounds (R,R,S^*)-6.6a, (R,R,S)-6.6b, (R,R,S^*)-6.7a, (R,R,S^*)-6.6b, 6.7, 6.9, 6.12, 6.13, (S^*)-6.18a, (S^*)-6.18b, 6.34-6.44, 6.47 and 6.48 $^1\text{H-NMR}$ (600 MHz) of compound (R,R,S^*)-6.6a ($\text{DMSO-}d_6$)



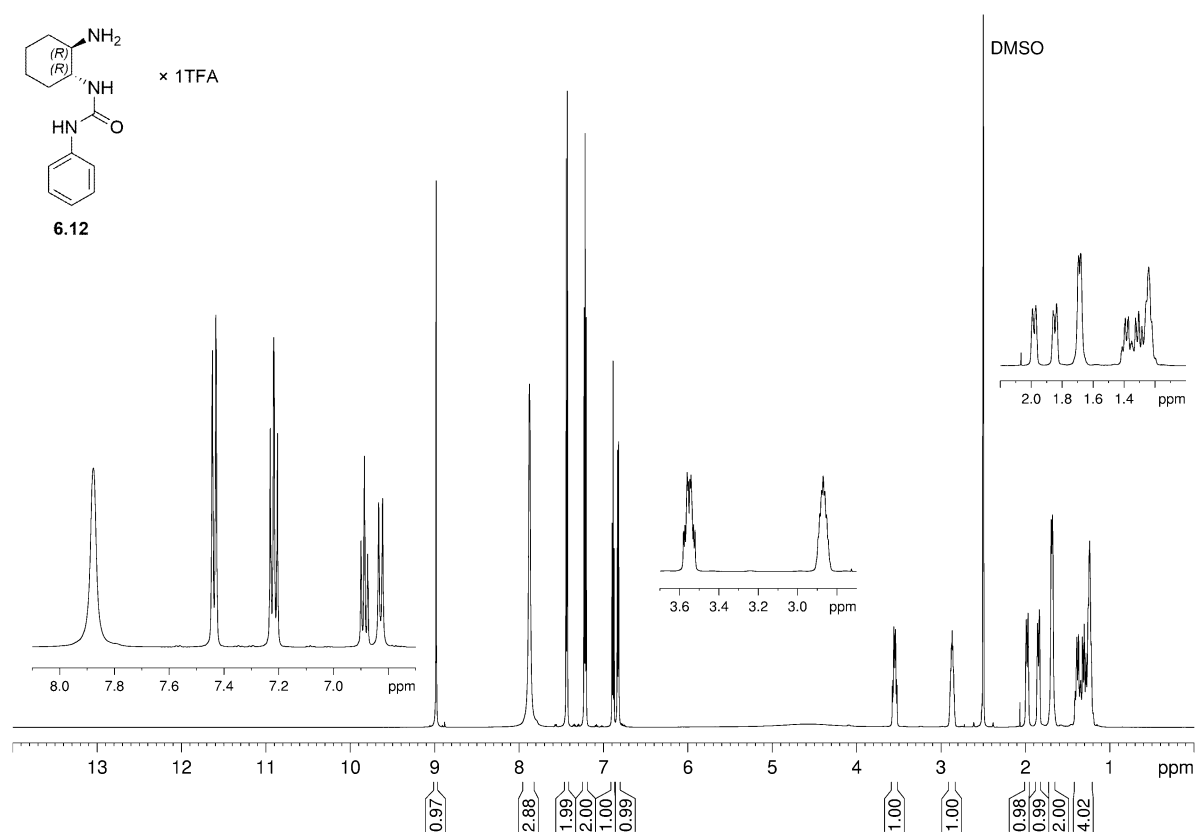
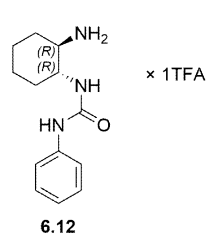




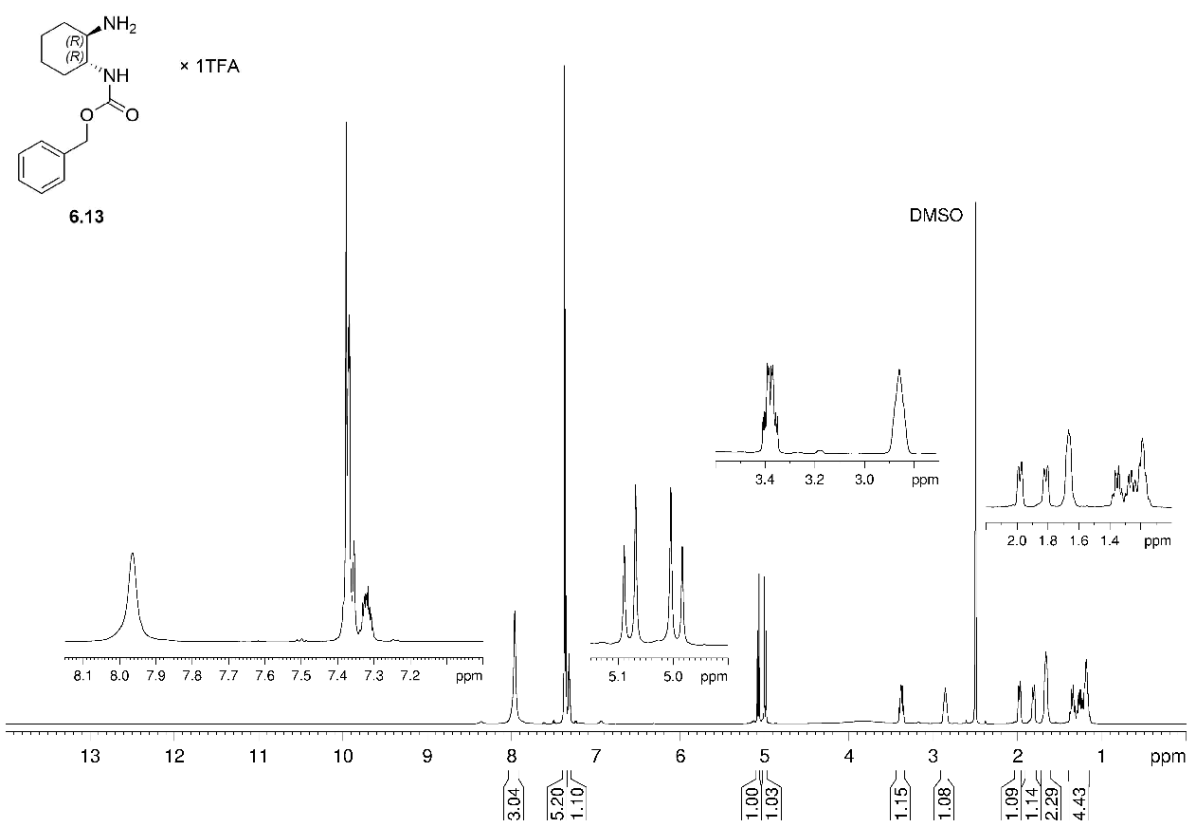
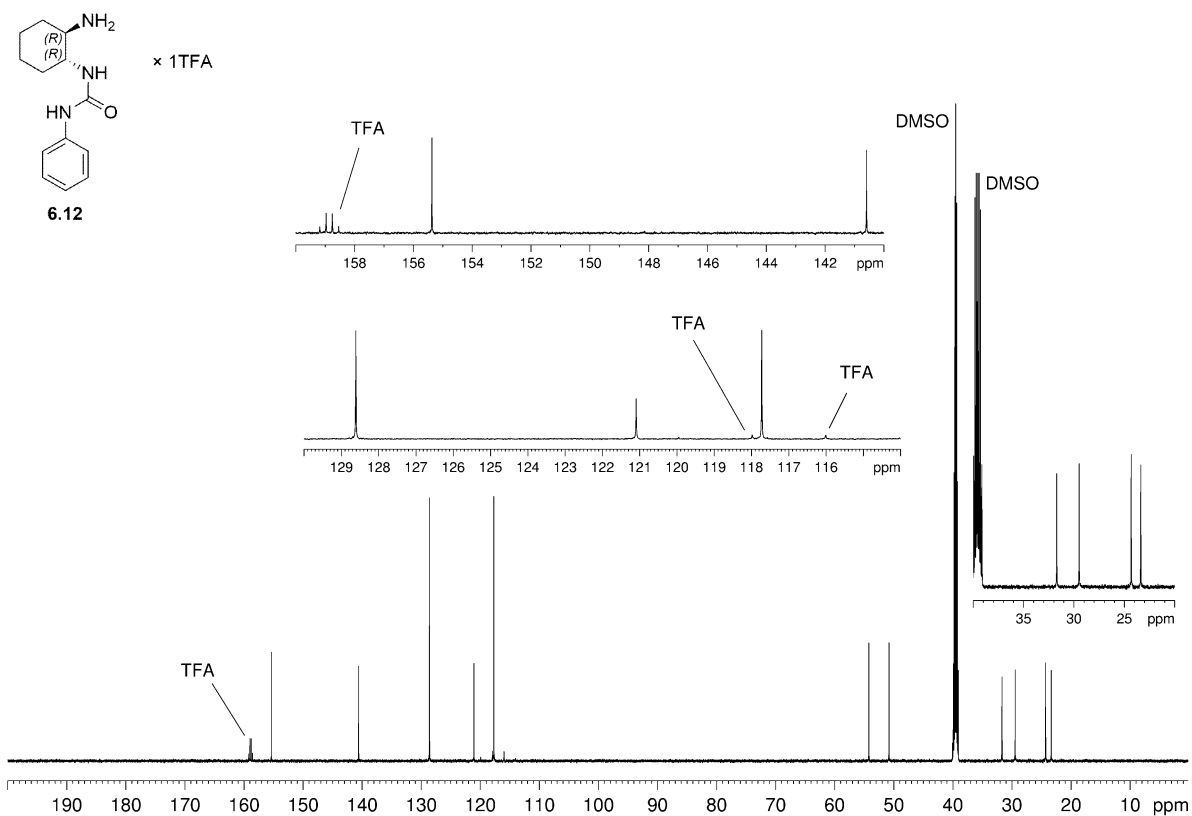
 $^{13}\text{C-NMR}$ (150 MHz) of compound (R,R,S^*) -6.7b ($\text{DMSO-}d_6$) $^1\text{H-NMR}$ (400 MHz) of compound 6.9 ($\text{DMSO-}d_6$)

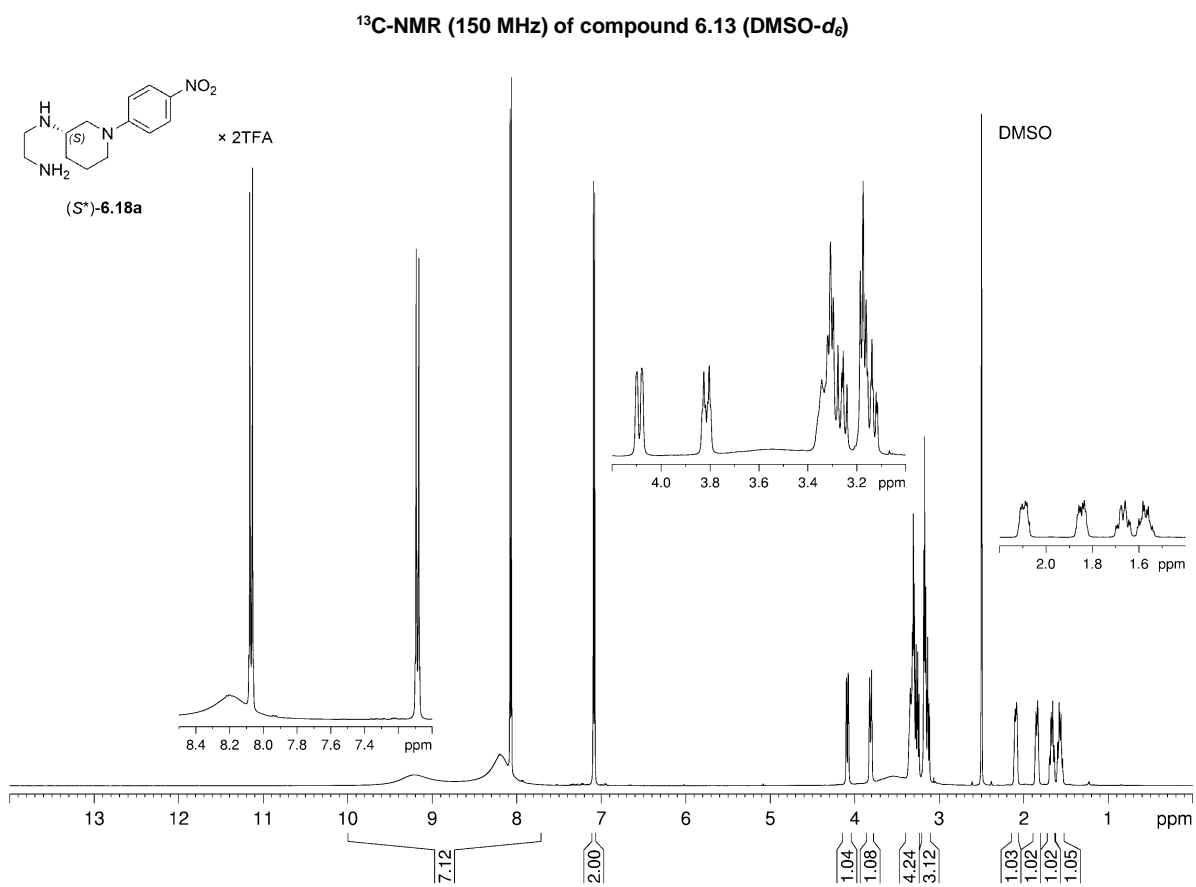
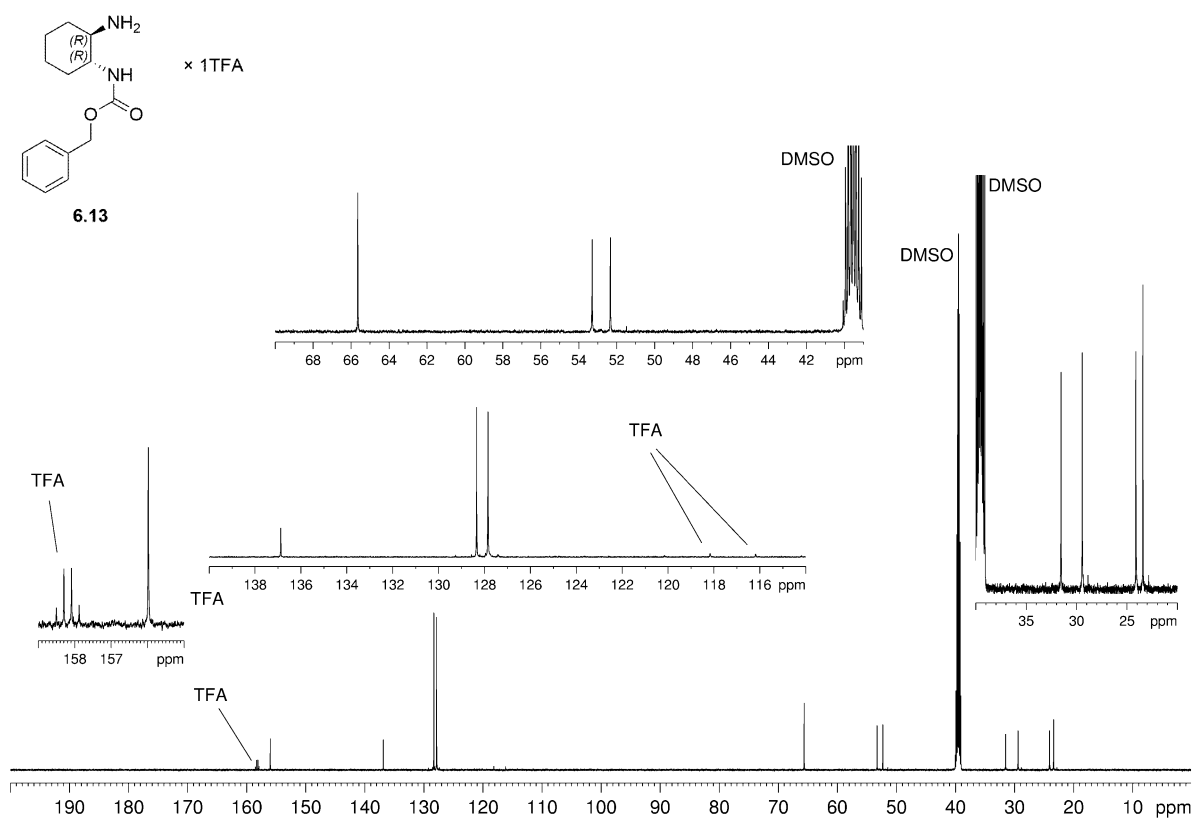


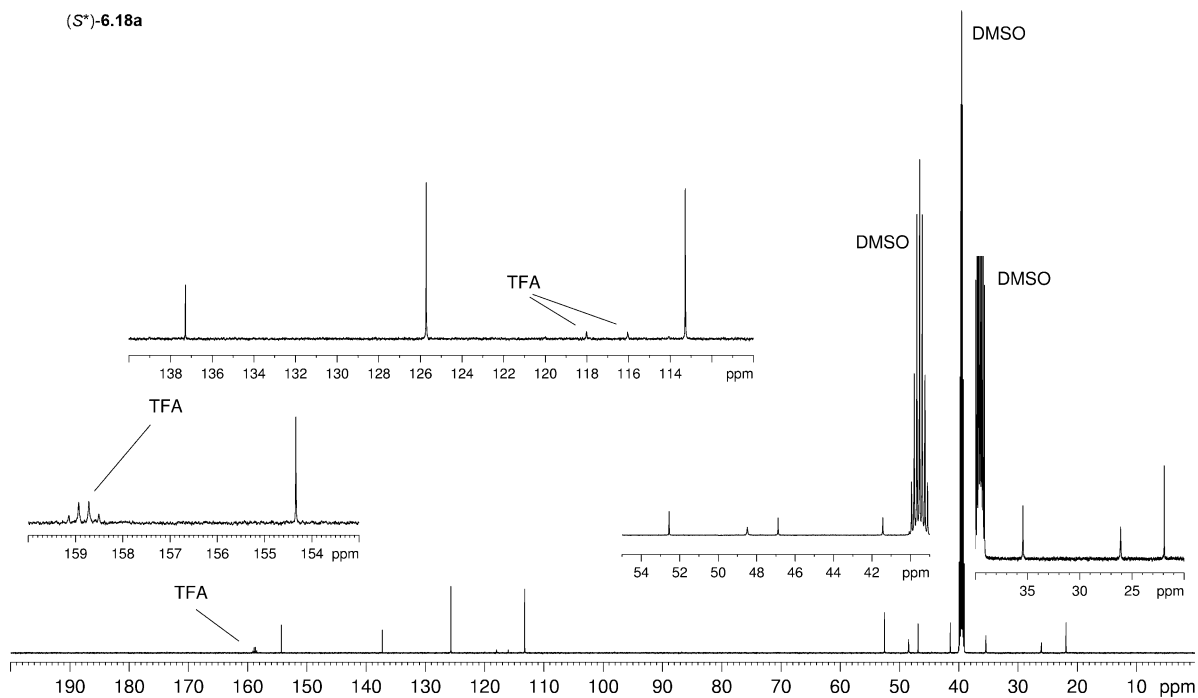
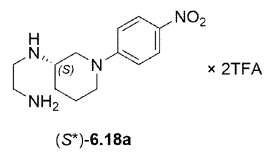
¹³C-NMR (101 MHz) of compound 6.9 (DMSO-*d*₆)



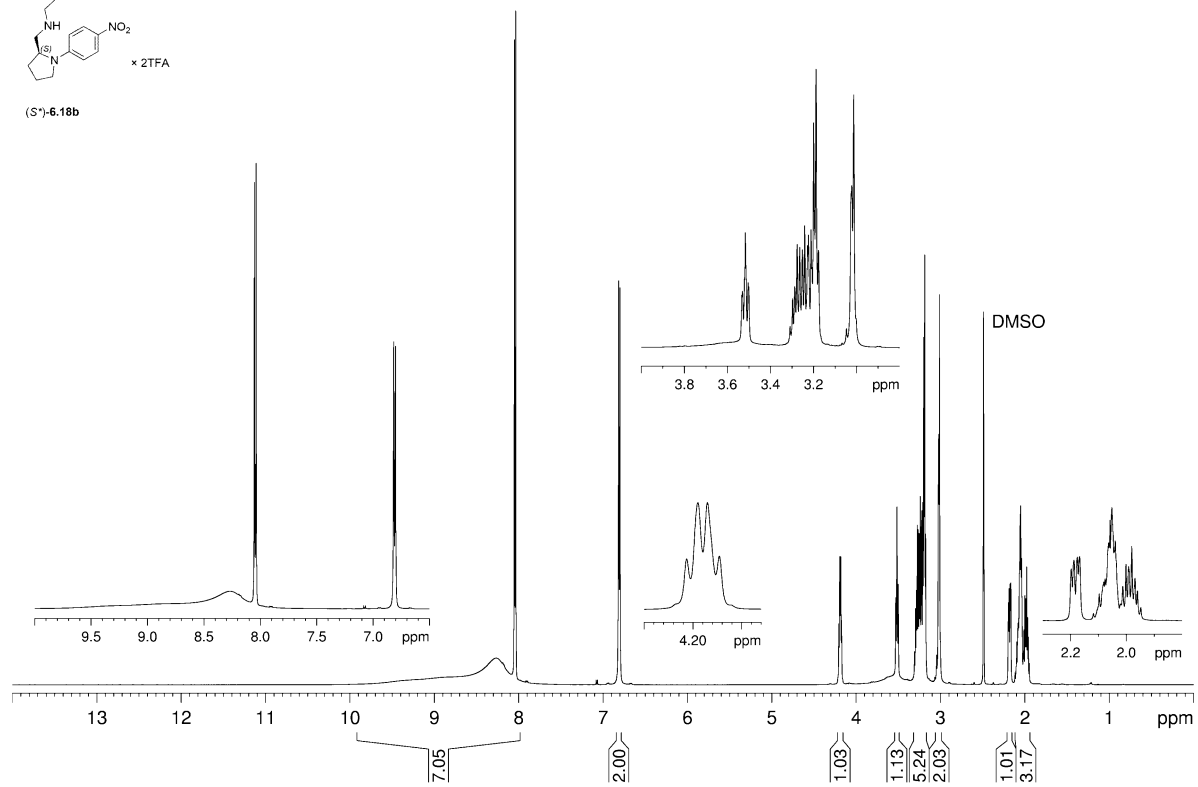
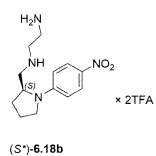
¹H-NMR (600 MHz) of compound 6.12 (DMSO-*d*₆)



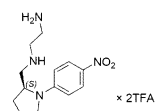




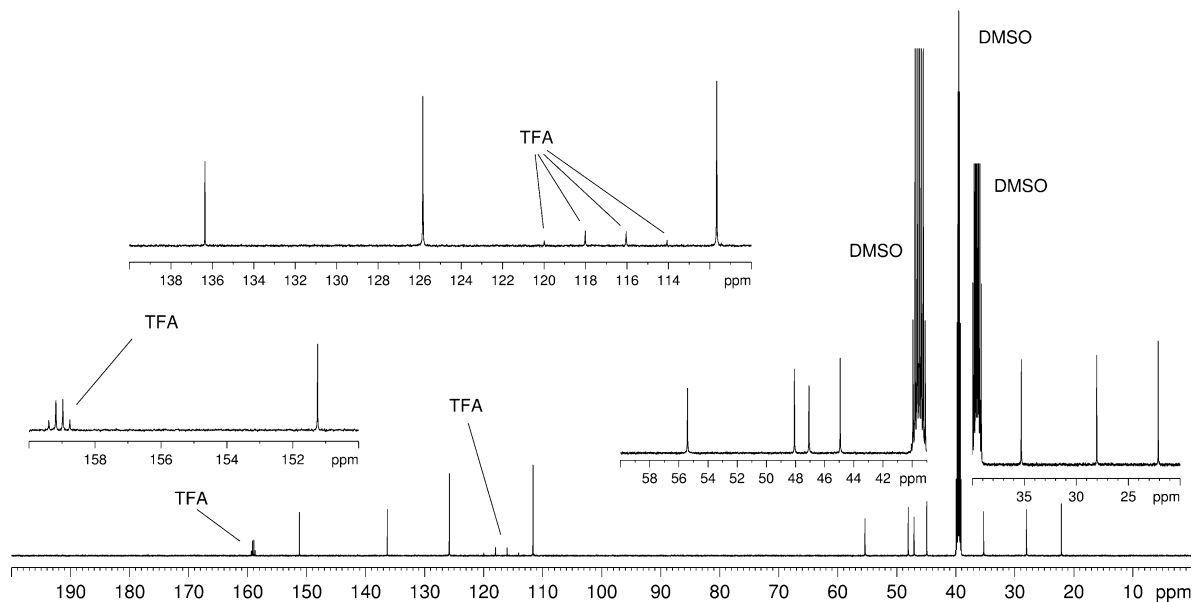
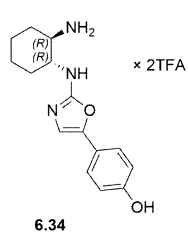
¹³C-NMR (150 MHz) of compound (S*)-6.18a (DMSO-d₆)



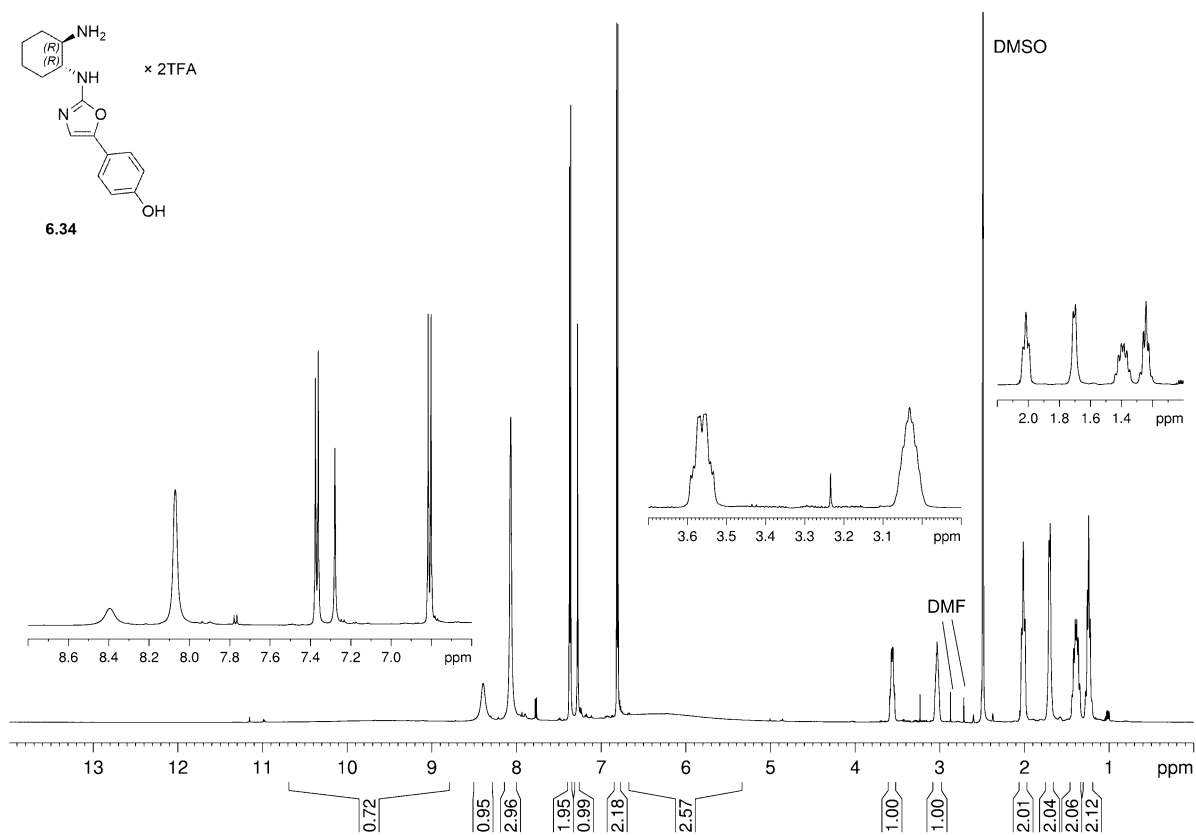
¹H-NMR (600 MHz) of compound (S*)-6.18b (DMSO-d₆)

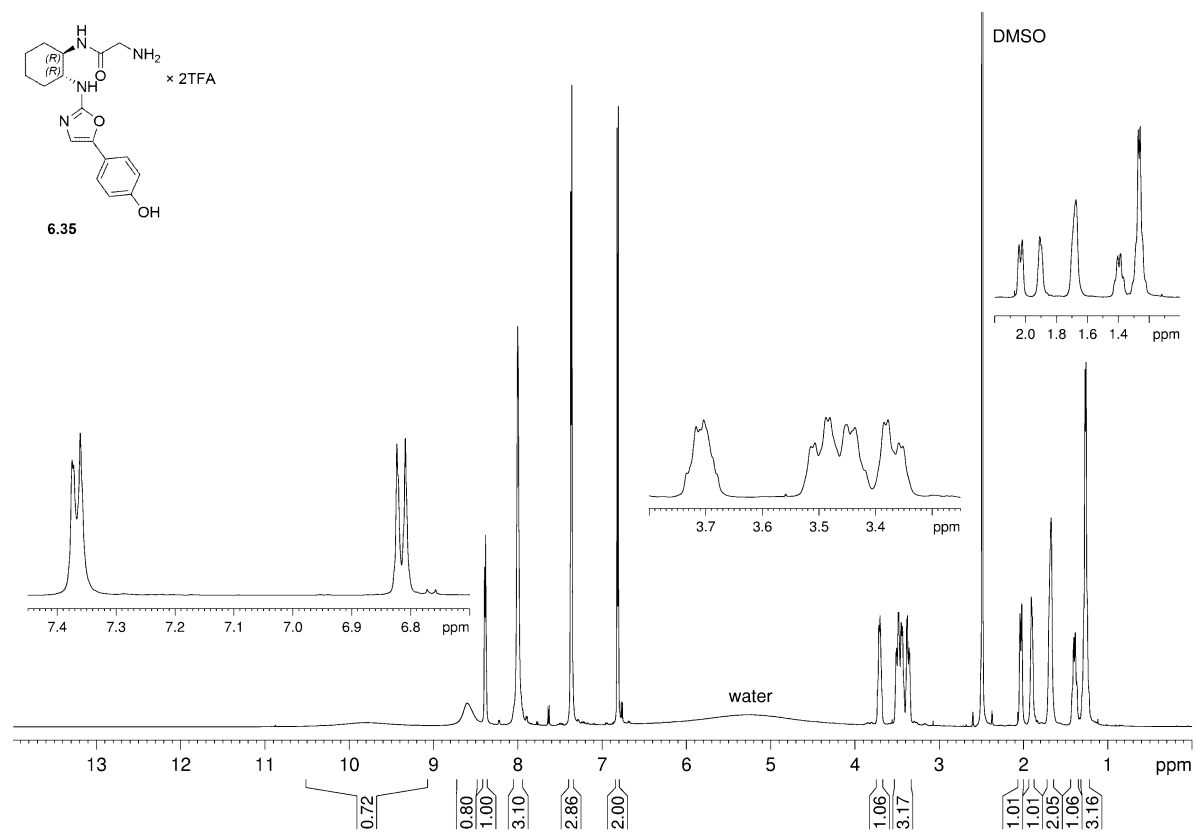
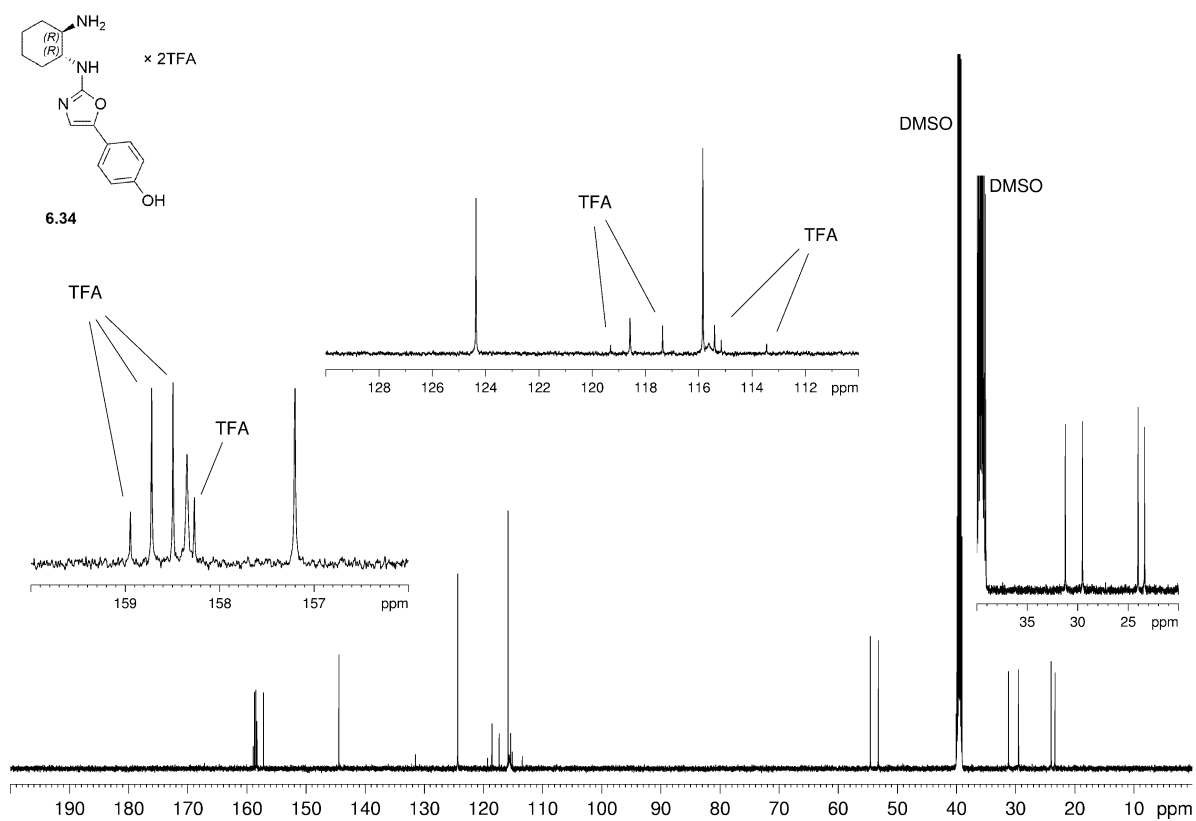


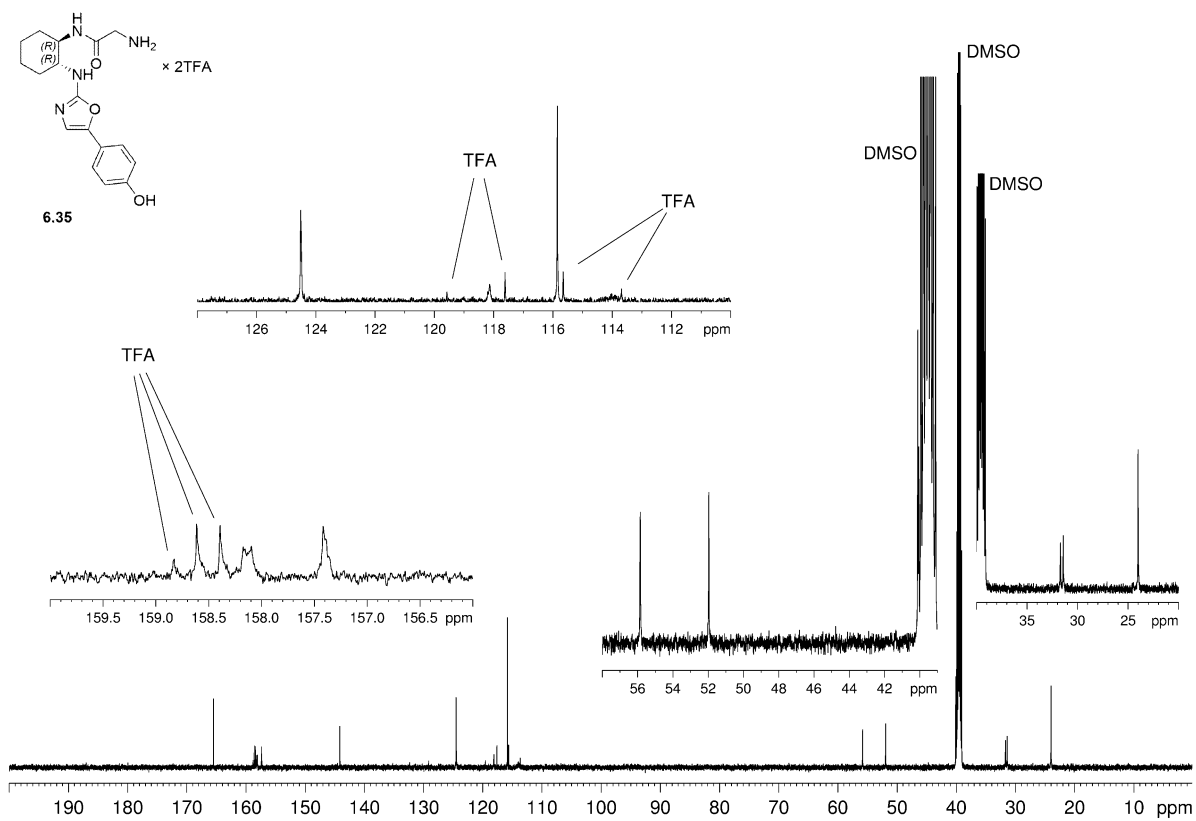
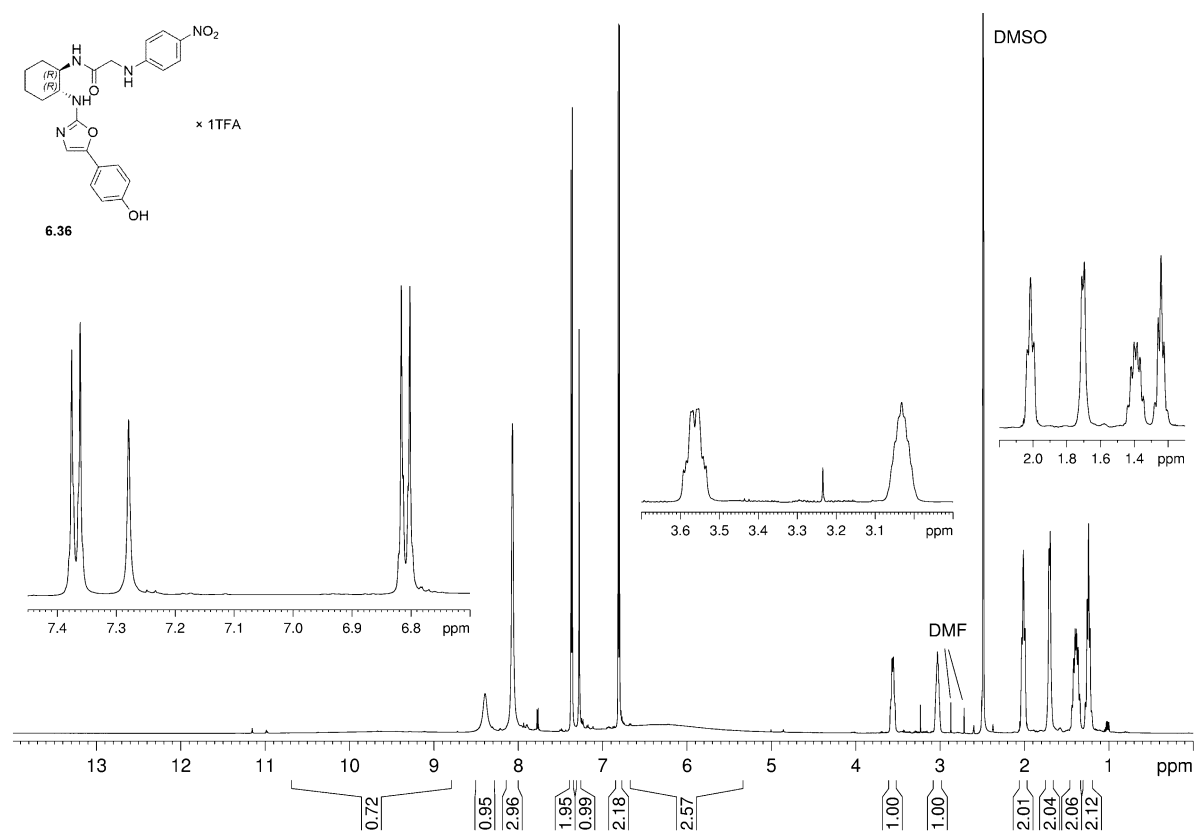
(S*)-6.18b

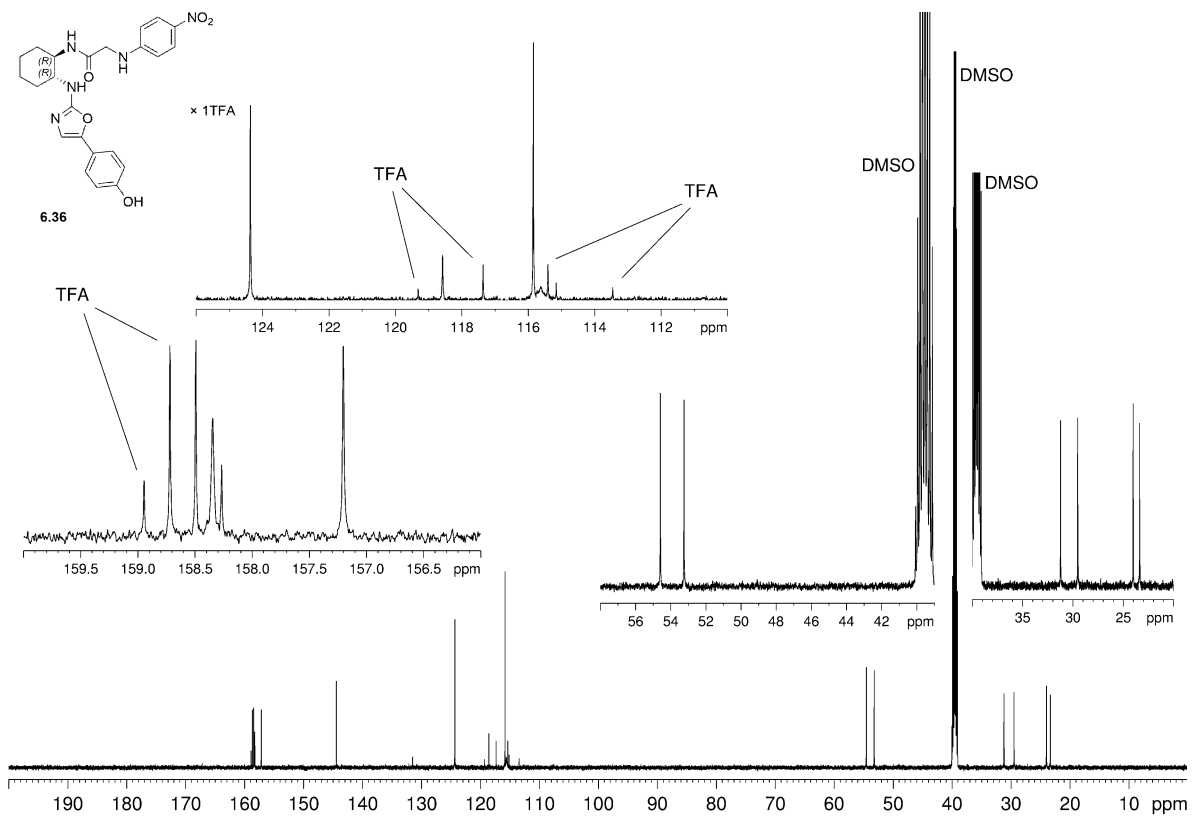
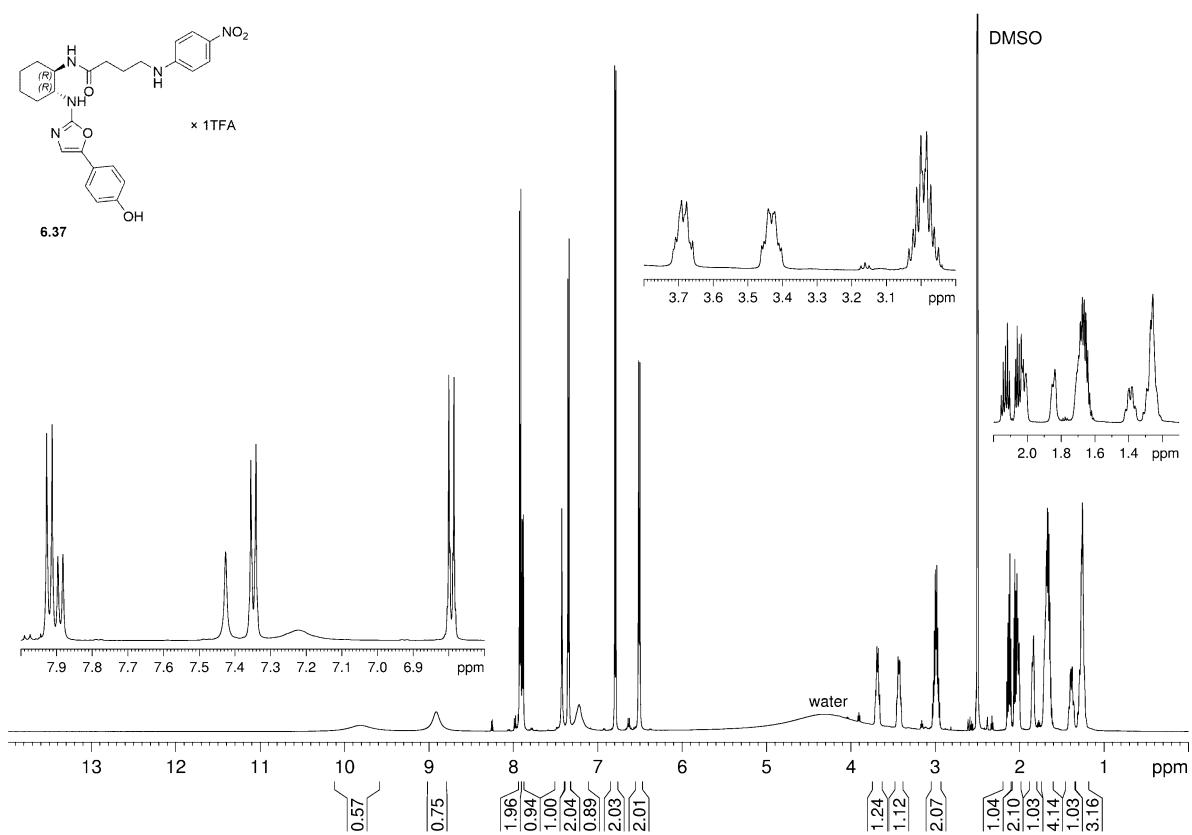
¹³C-NMR (150 MHz) of compound (S*)-6.18b (DMSO-d₆)

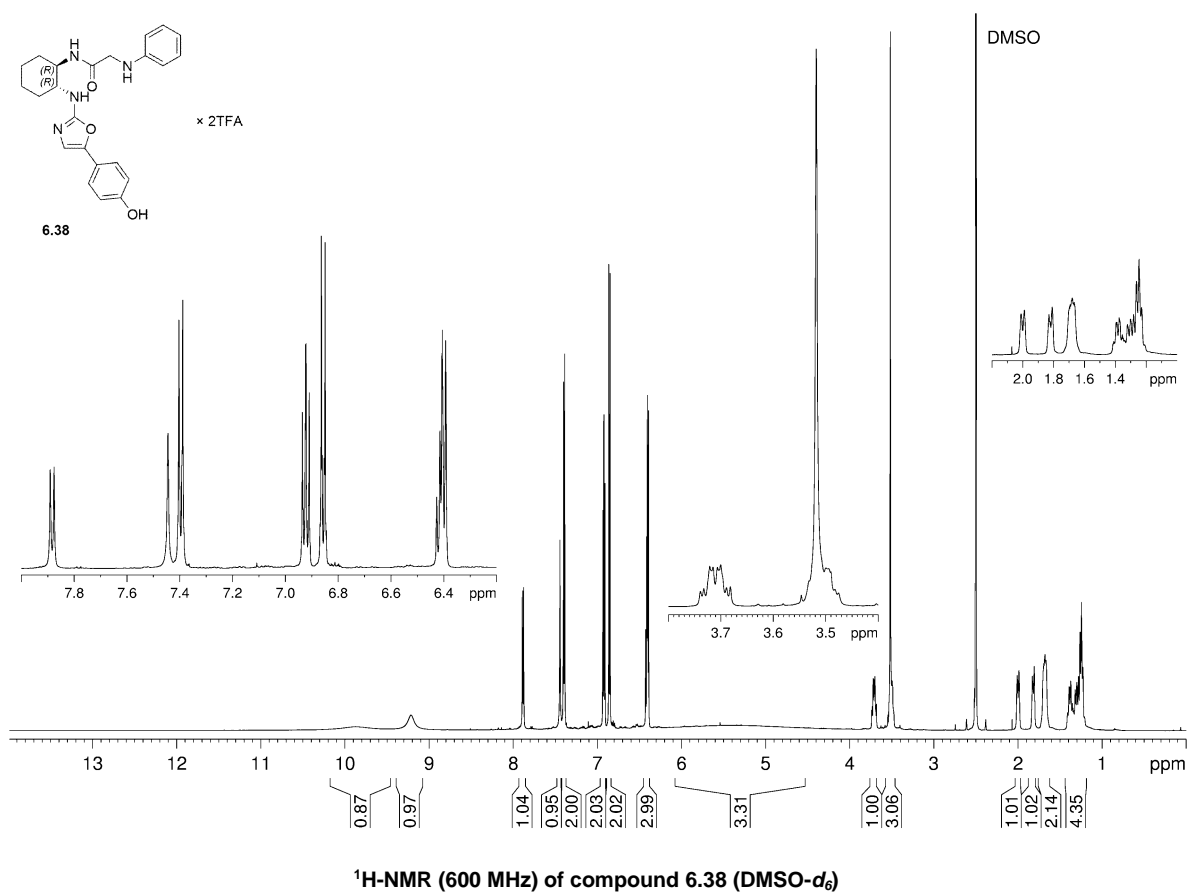
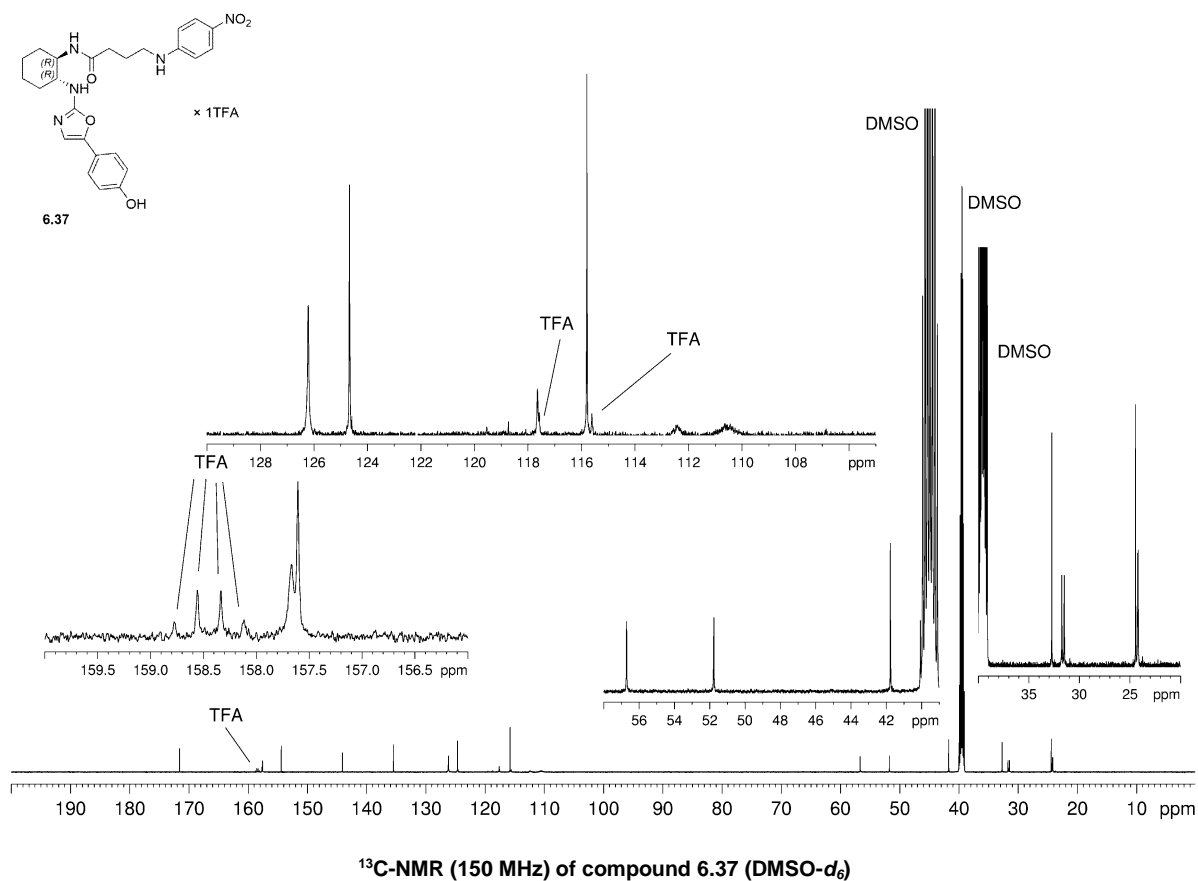
6.34

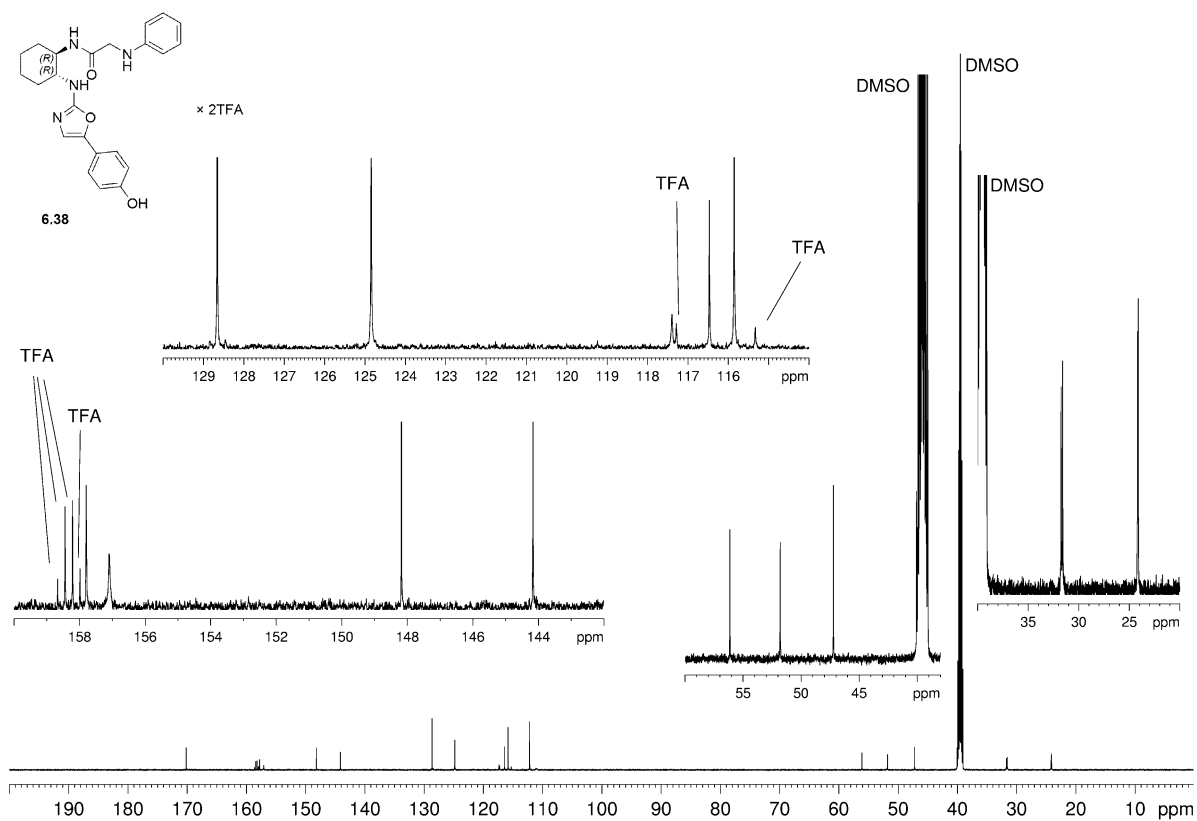
¹H-NMR (600 MHz) of compound 6.34 (DMSO-d₆)



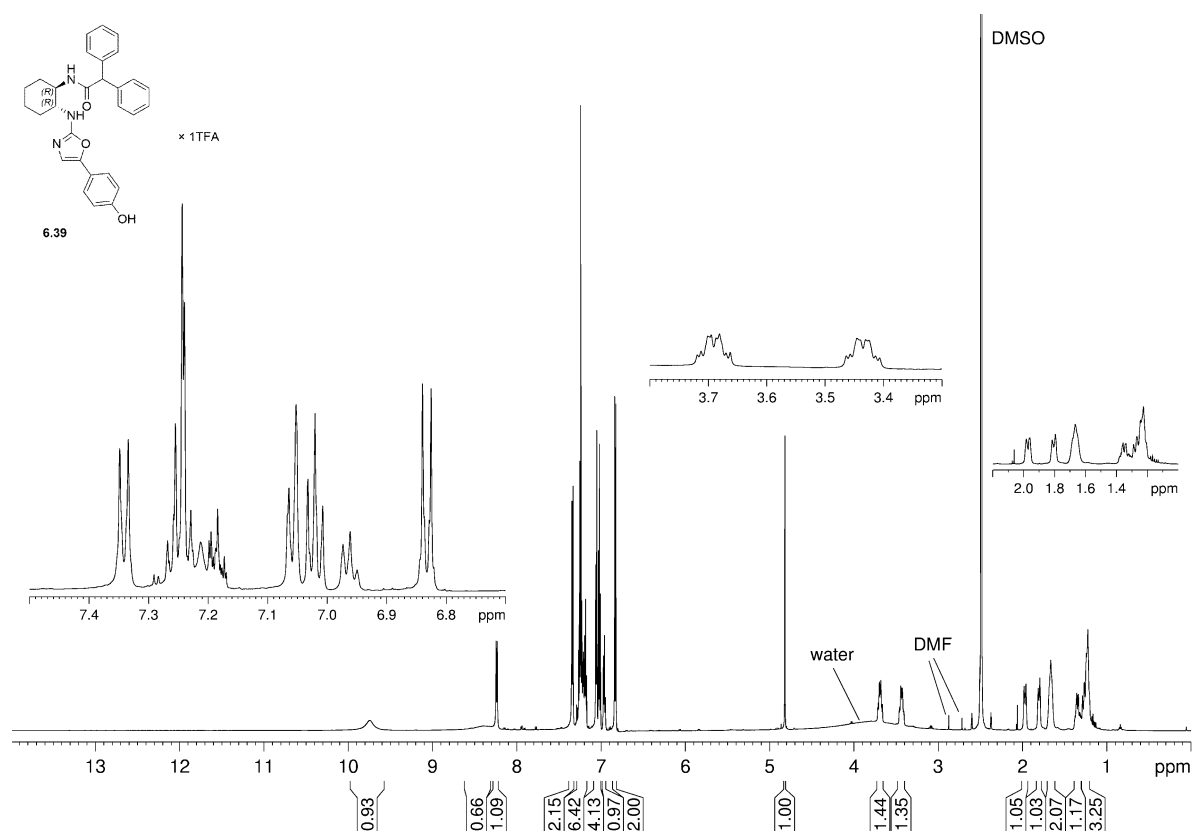
**¹³C-NMR (150 MHz) of compound 6.35 (DMSO-*d*₆)****¹H-NMR (600 MHz) of compound 6.36 (DMSO-*d*₆)**

**¹³C-NMR (150 MHz) of compound 6.36 (DMSO-*d*₆)****¹H-NMR (600 MHz) of compound 6.37 (DMSO-*d*₆)**

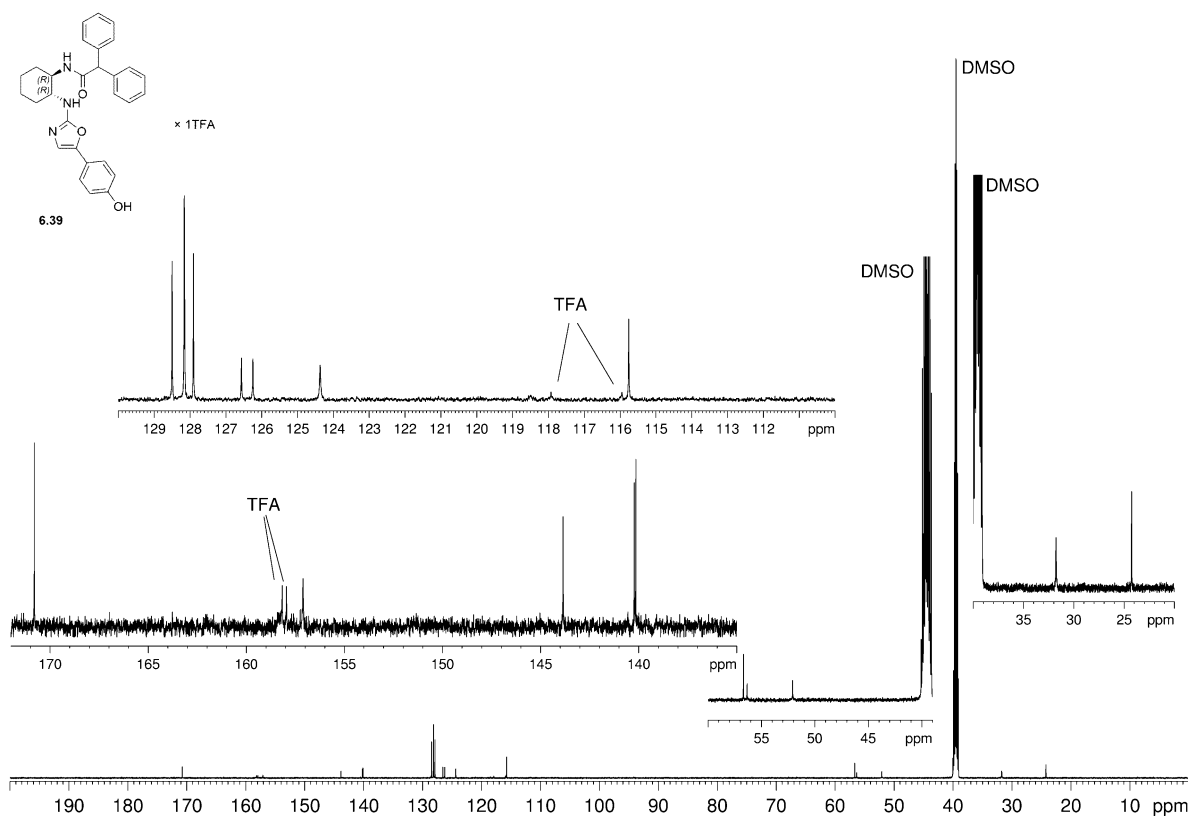




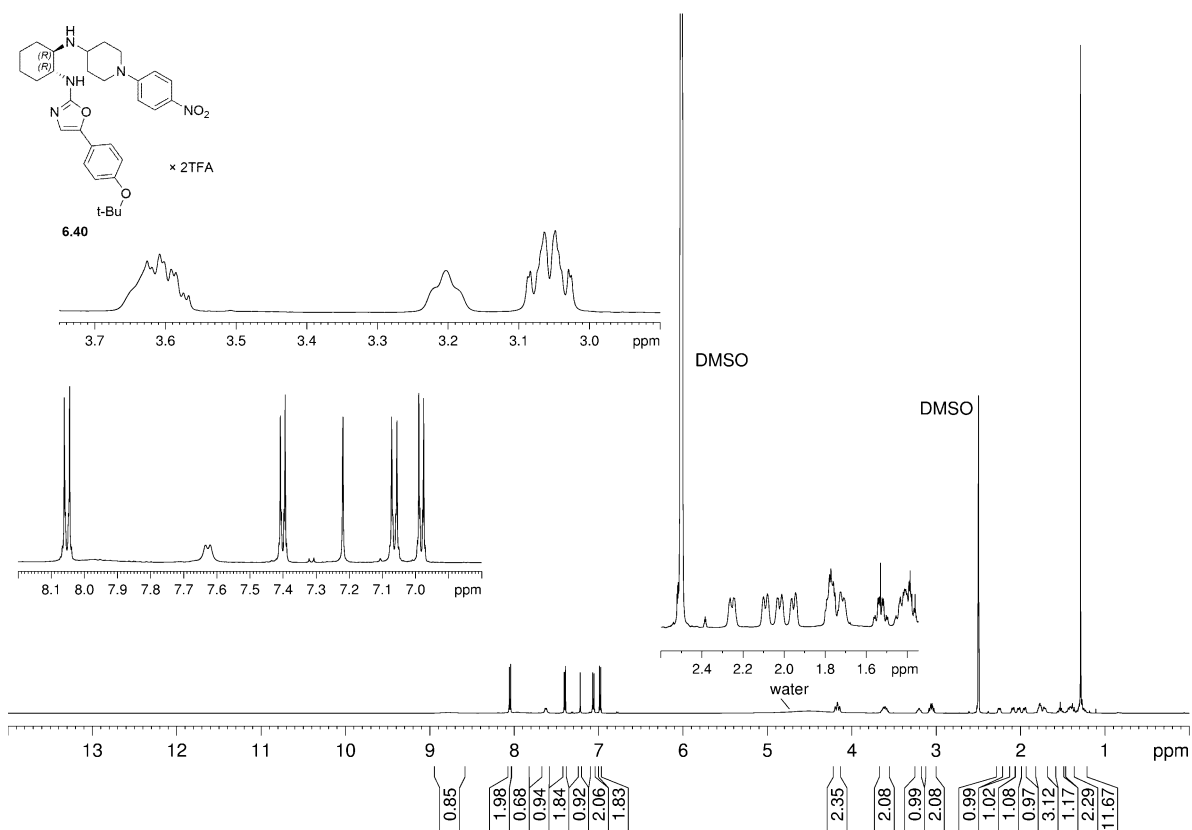
¹³C-NMR (150 MHz) of compound 6.38 (DMSO-*d*₆)



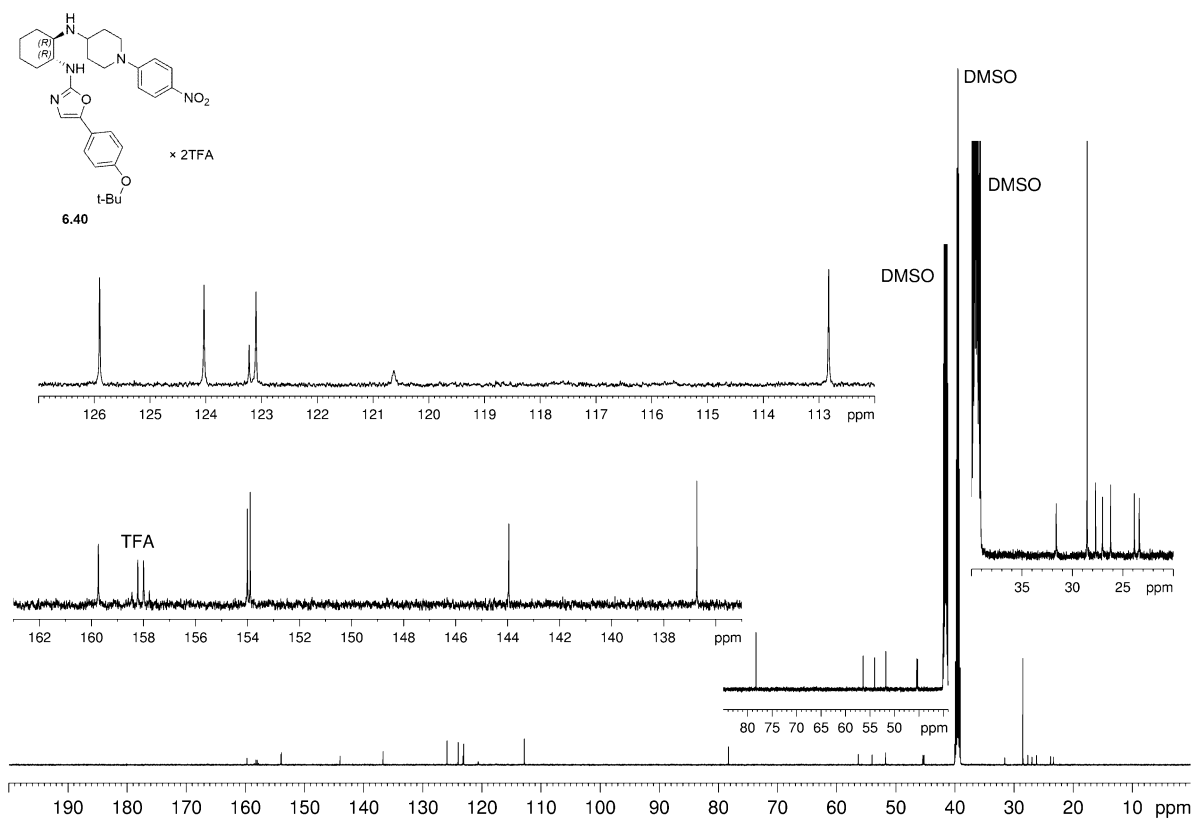
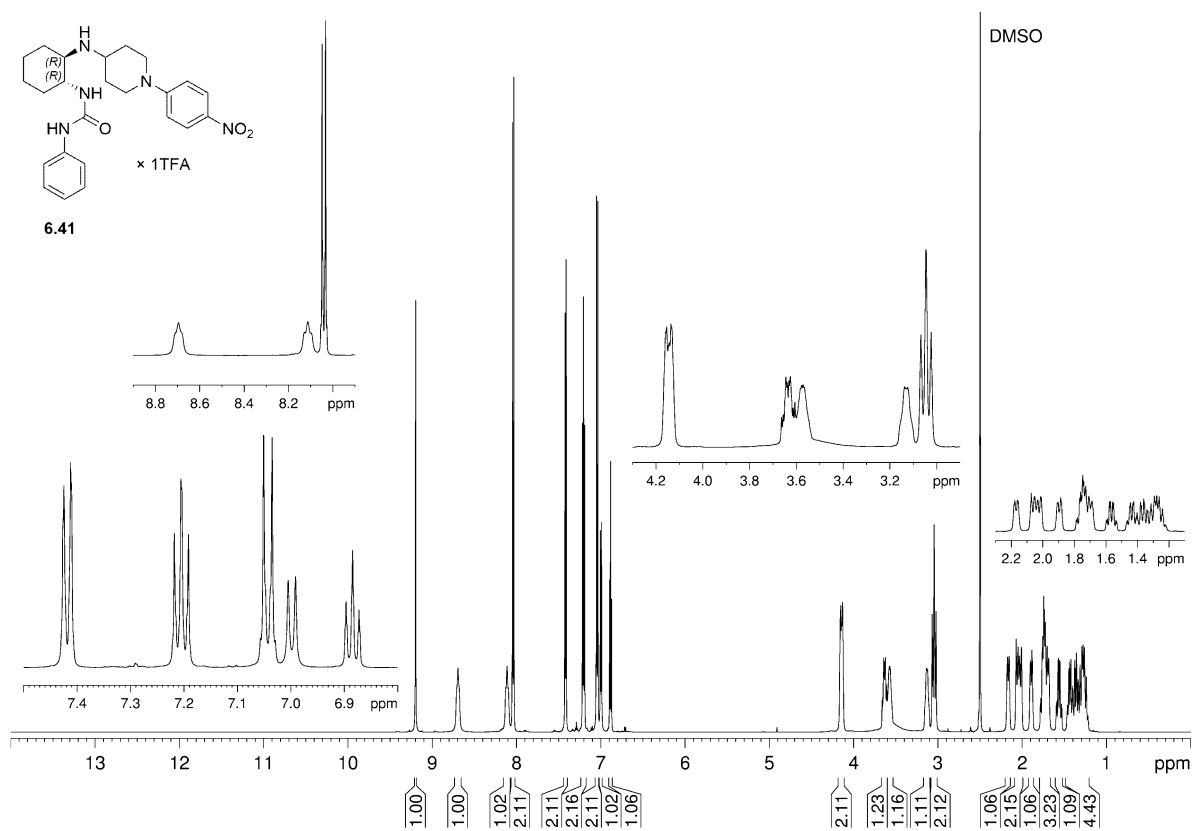
¹H-NMR (600 MHz) of compound 6.39 (DMSO-*d*₆)

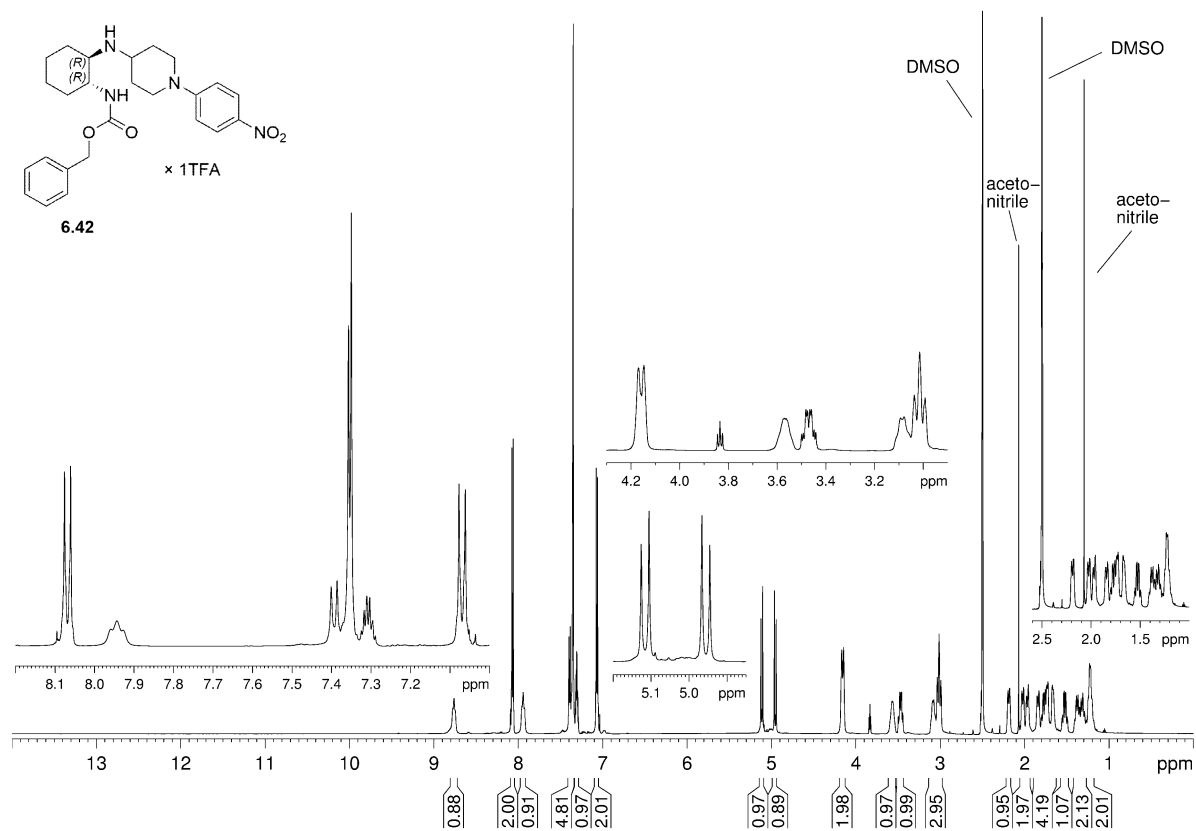
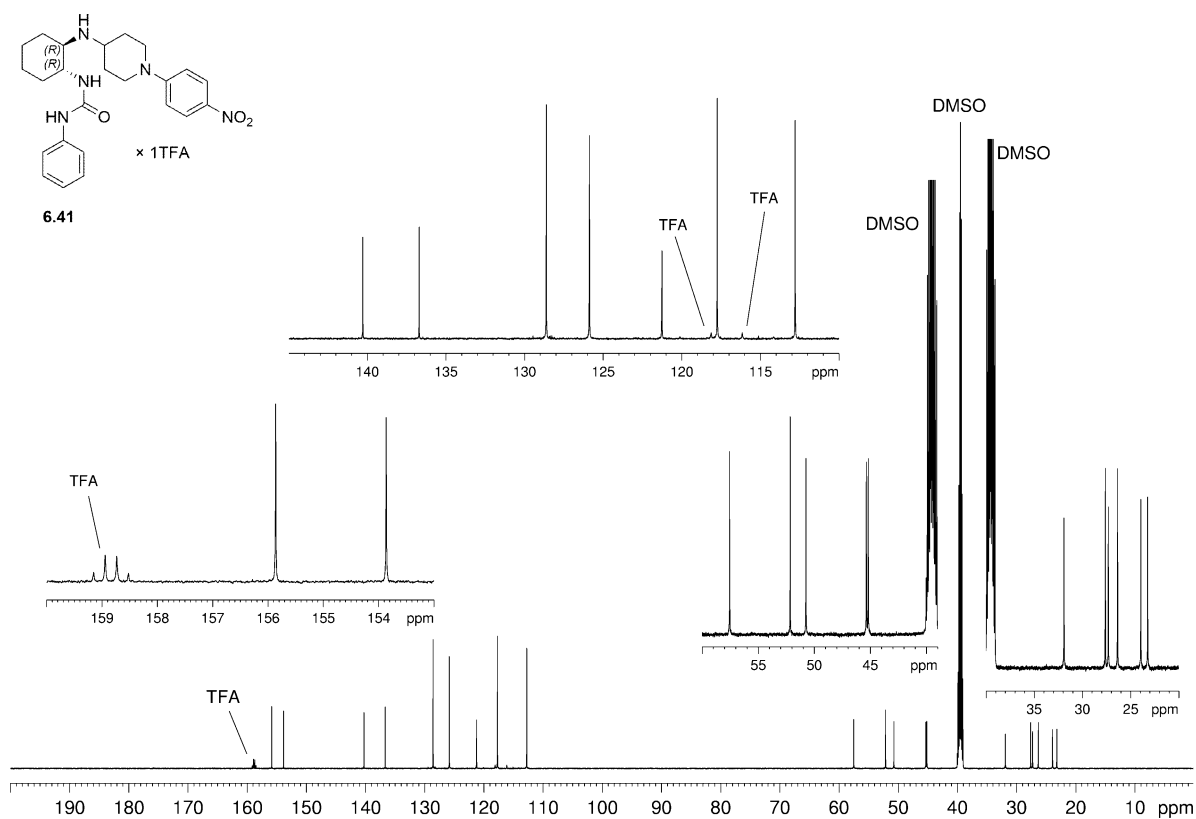


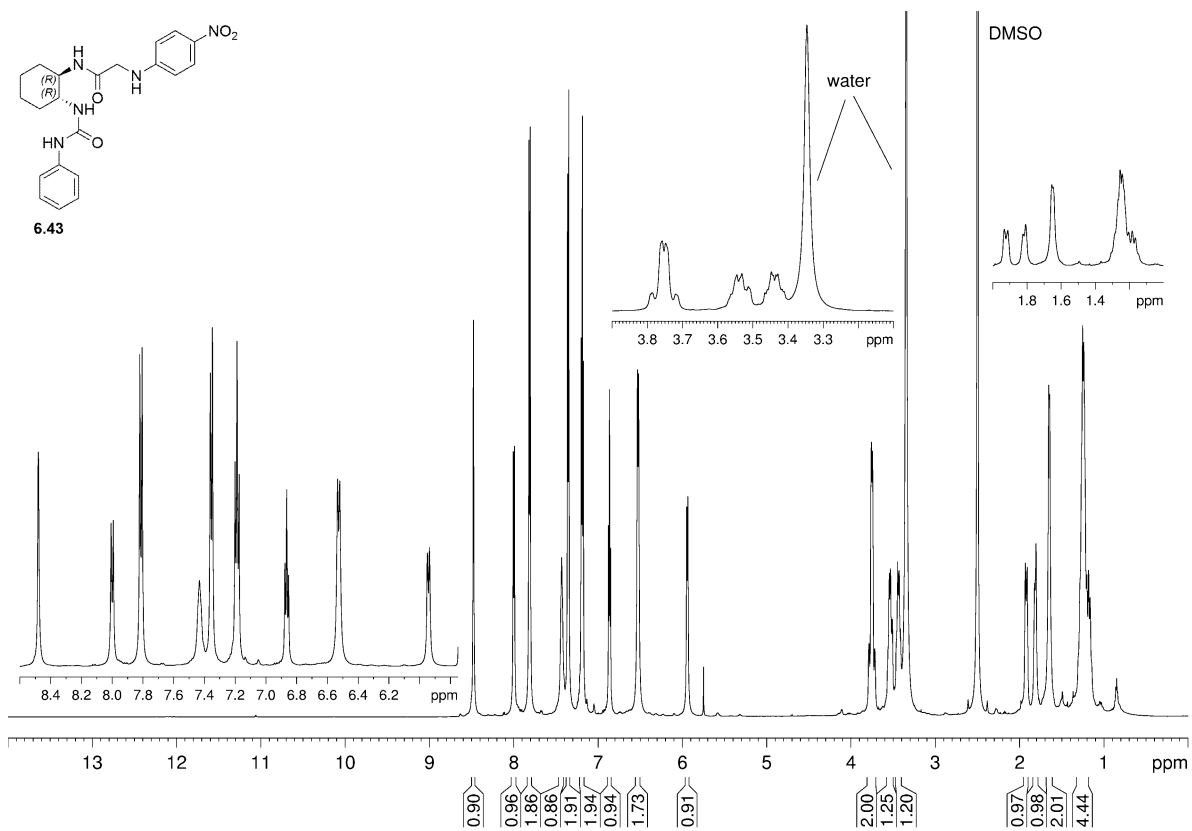
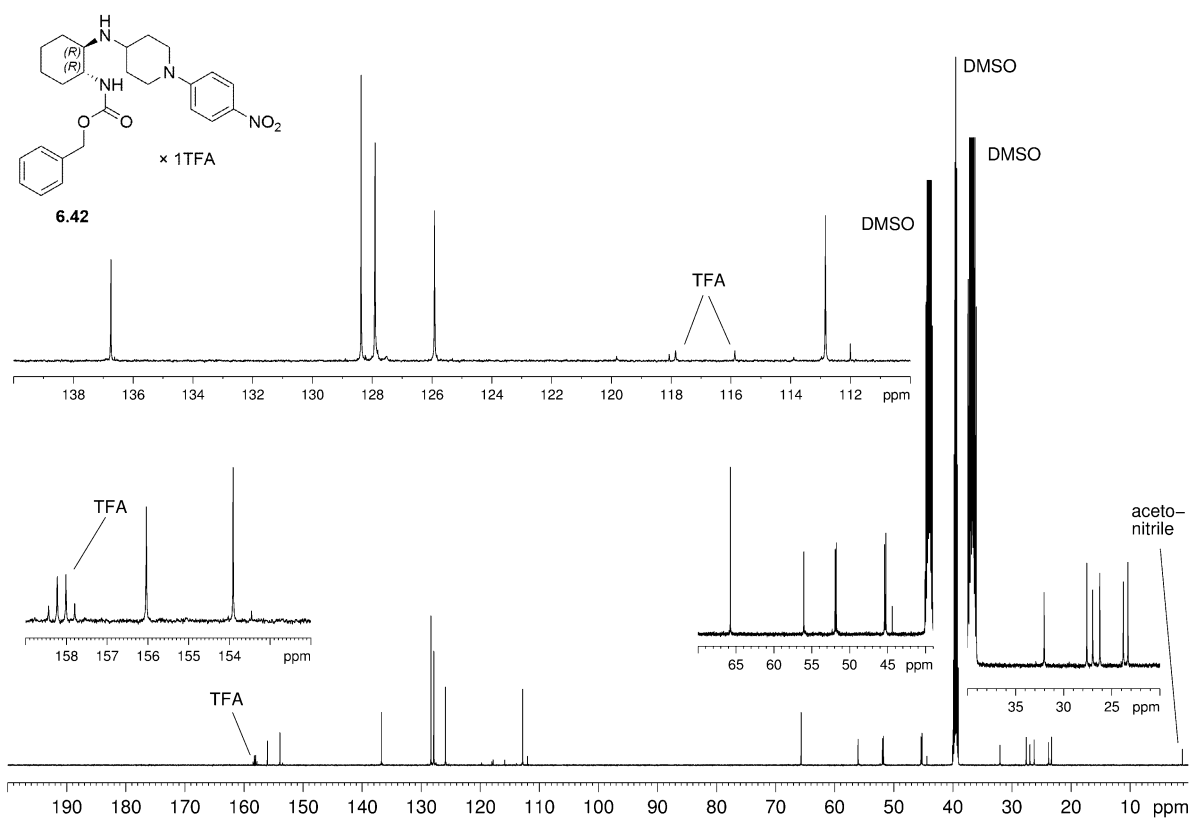
¹³C-NMR (150 MHz) of compound 6.39 (DMSO-*d*₆)

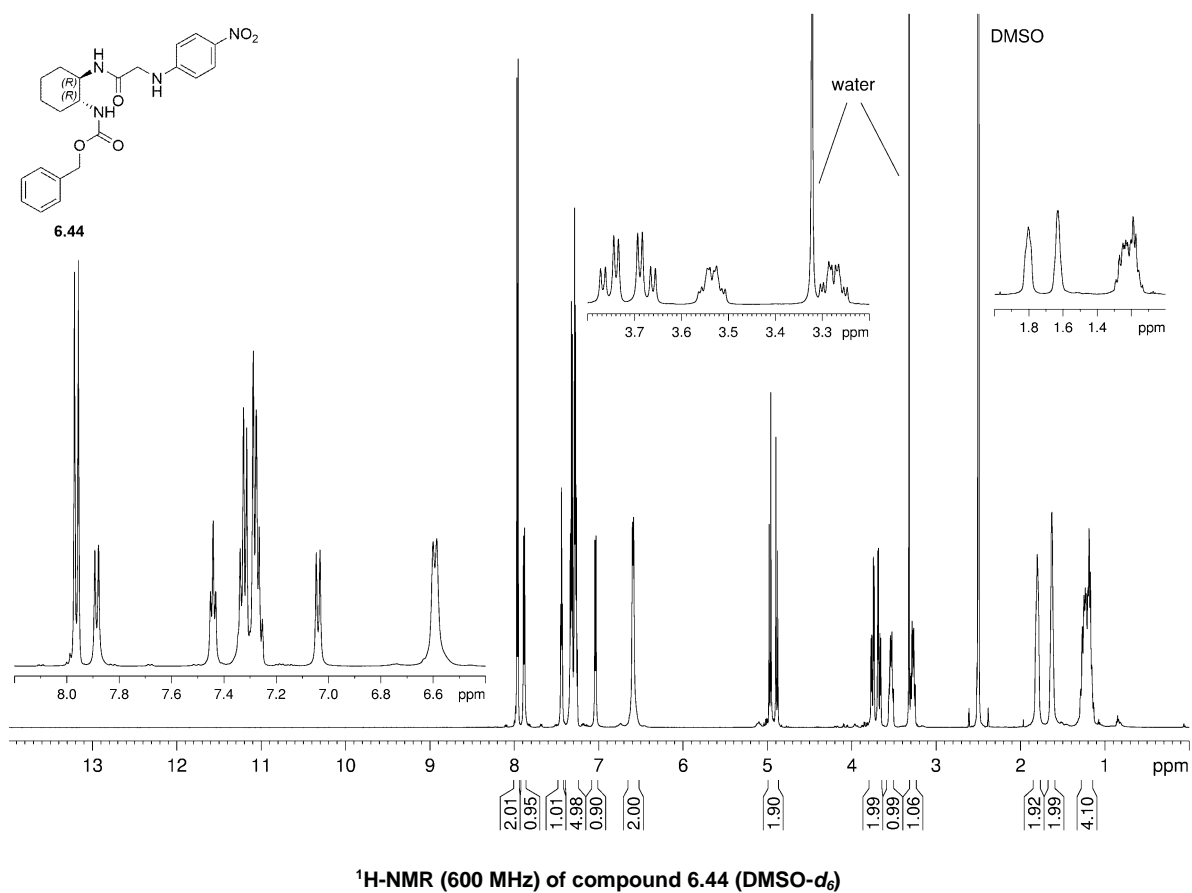
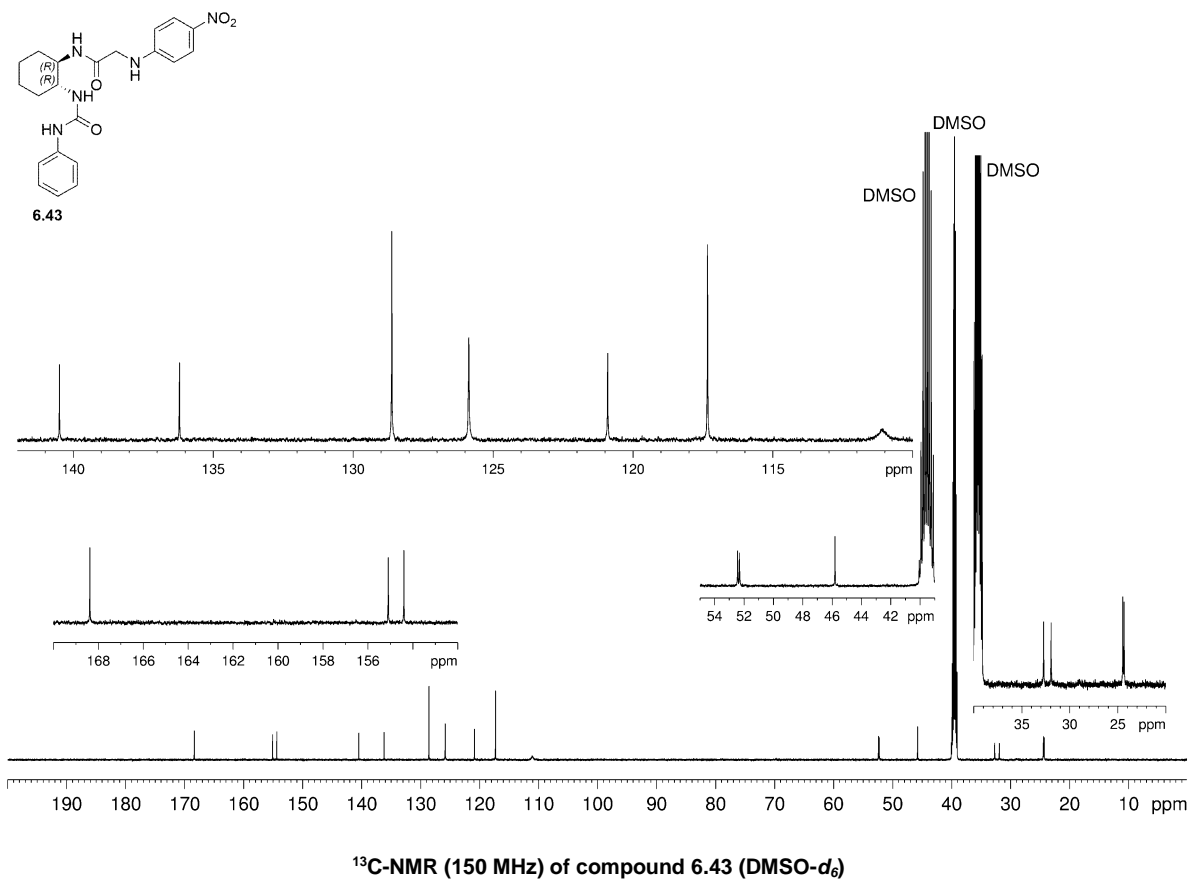


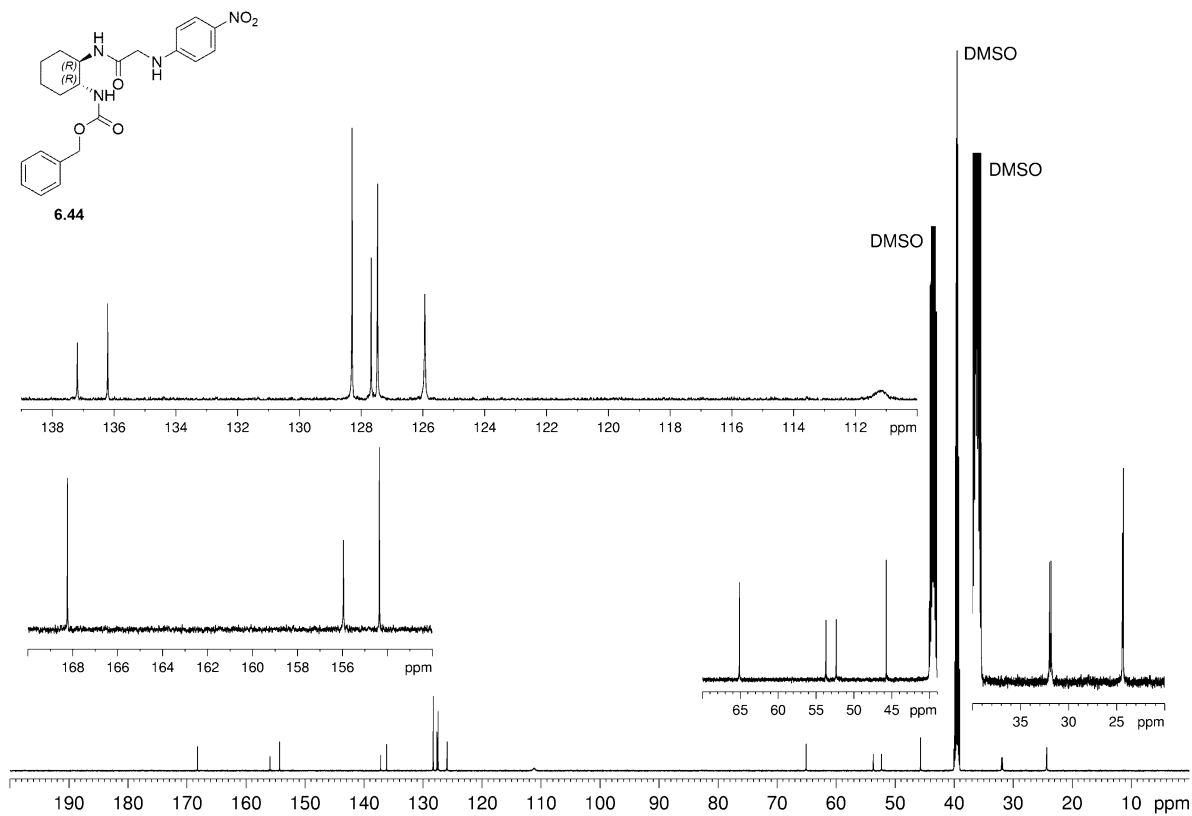
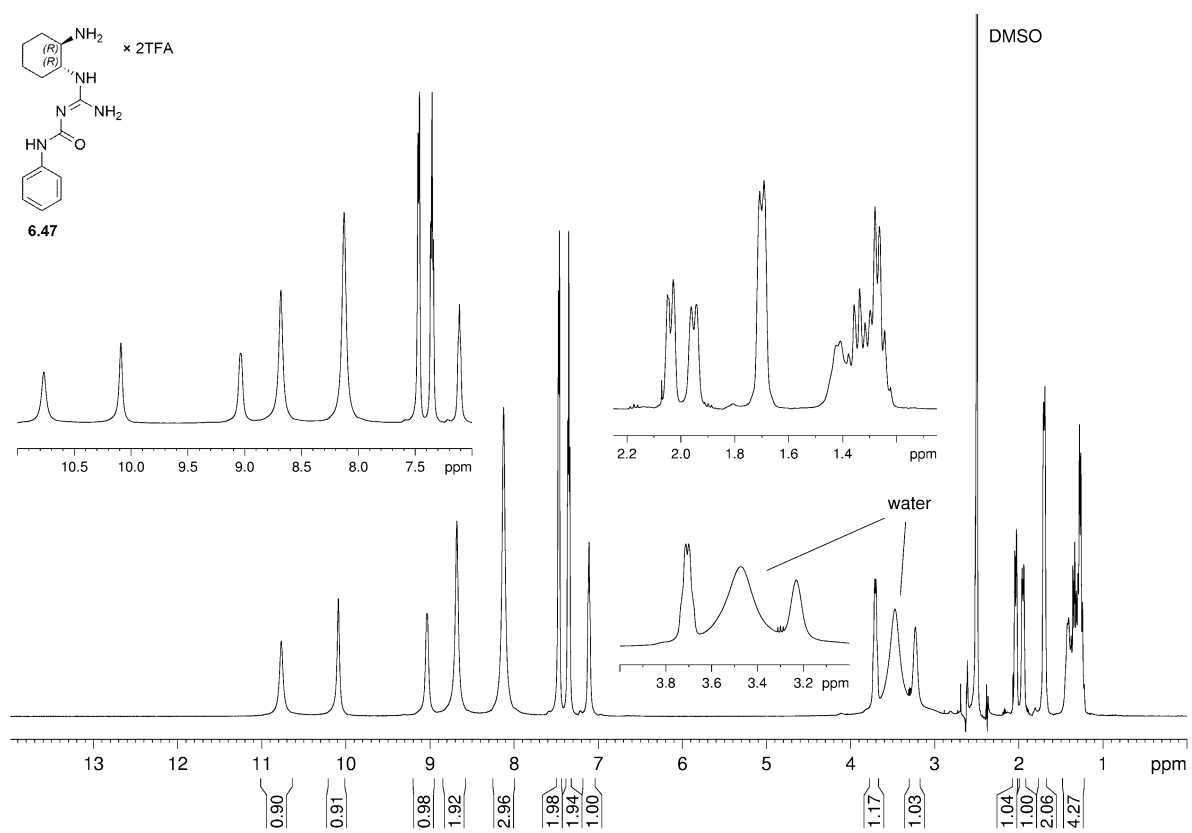
¹H-NMR (600 MHz) of compound 6.40 (DMSO-*d*₆)

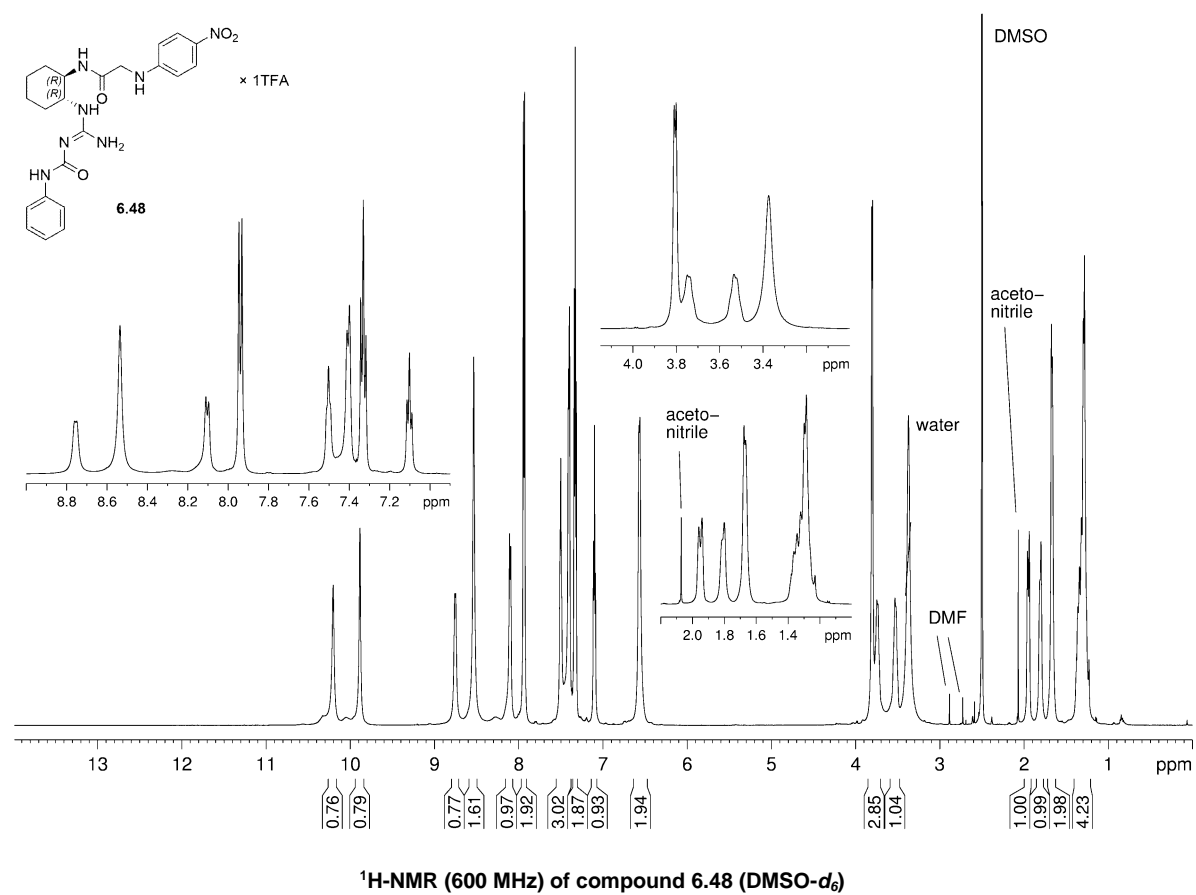
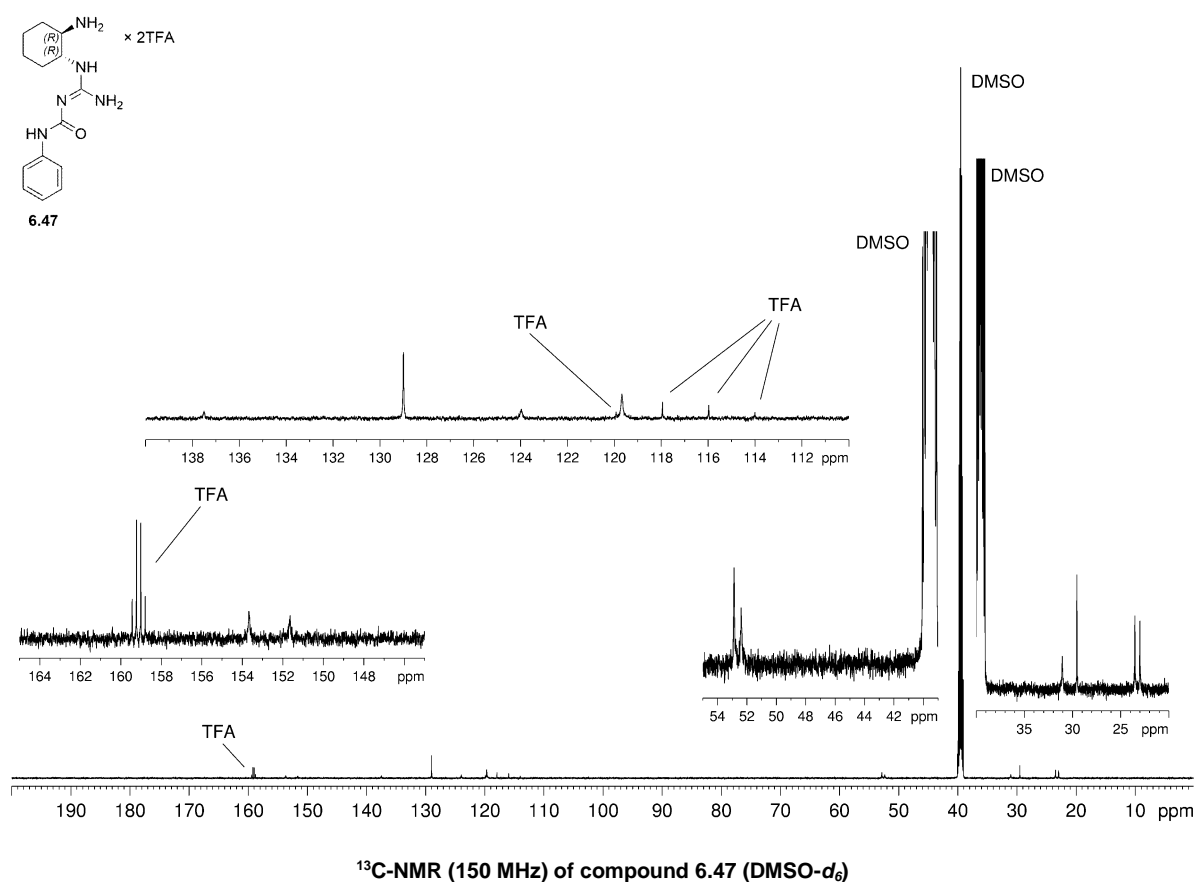
 $^{13}\text{C-NMR}$ (150 MHz) of compound 6.40 (DMSO-d_6) $^1\text{H-NMR}$ (600 MHz) of compound 6.41 (DMSO-d_6)

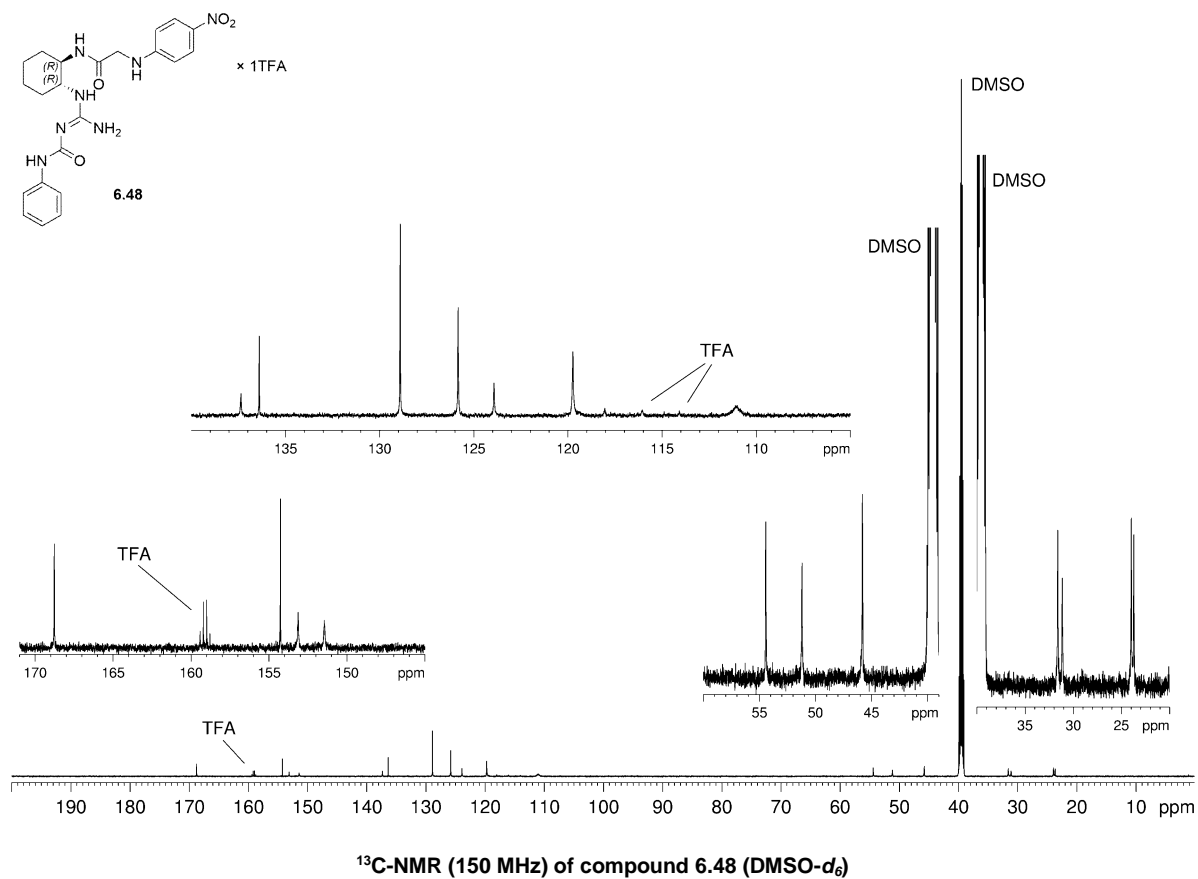




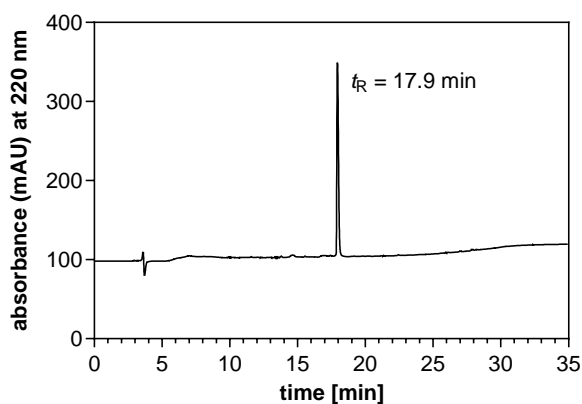


**¹³C-NMR (150 MHz) of compound 6.44 (DMSO-*d*₆)****¹H-NMR (600 MHz) of compound 6.47 (DMSO-*d*₆)**

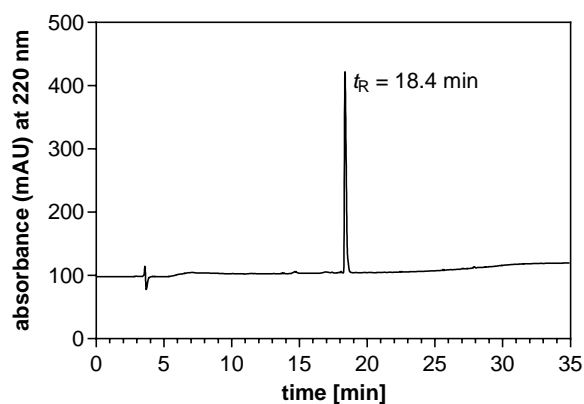




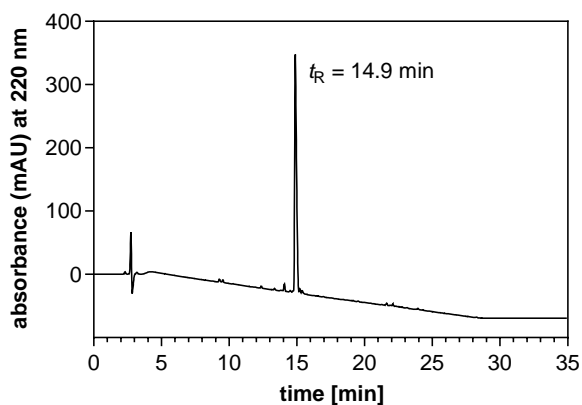
8.4.2. RP-HPLC purity chromatograms (220 nm) of compounds (*R,R,S**)-6.6a, (*R,R,S*)-6.6b, (*R,R,S**)-6.7a, (*R,R,S**)-6.6b, 6.7, 6.9, 6.12, 6.13, (*S**)-6.18a, (*S**)-6.18b, 6.34-6.44, 6.47 and 6.48



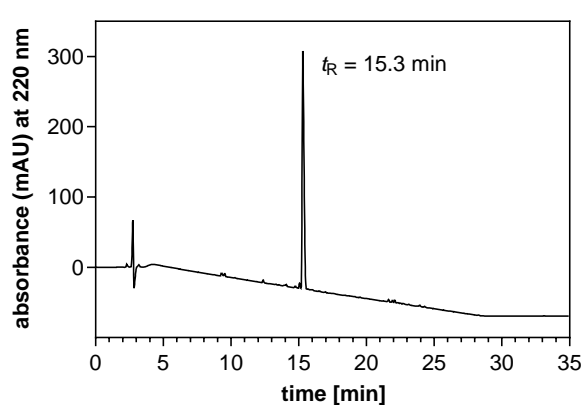
RP-HPLC (220 nm) chromatogram of (*R,R,S**)-6.6a



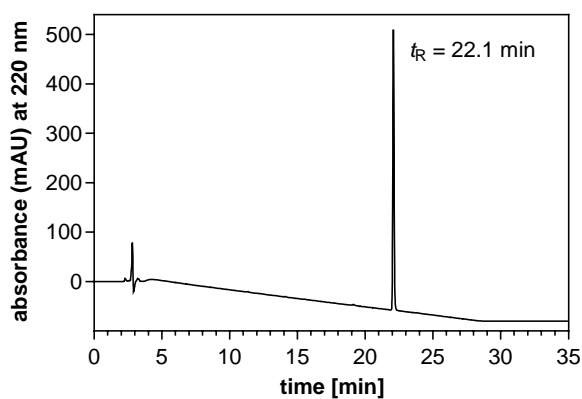
RP-HPLC (220 nm) chromatogram of (*R,R,S*)-6.6b



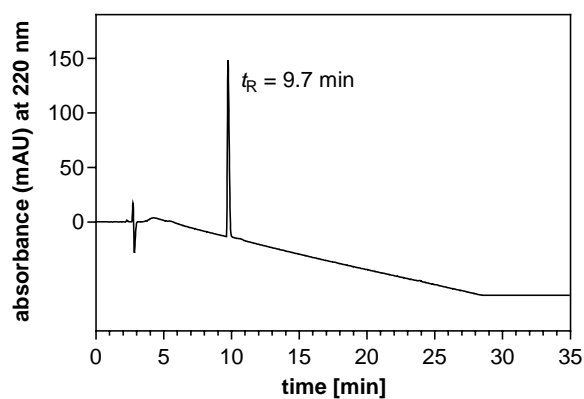
RP-HPLC (220 nm) chromatogram of (*R,R,S**)-6.7a



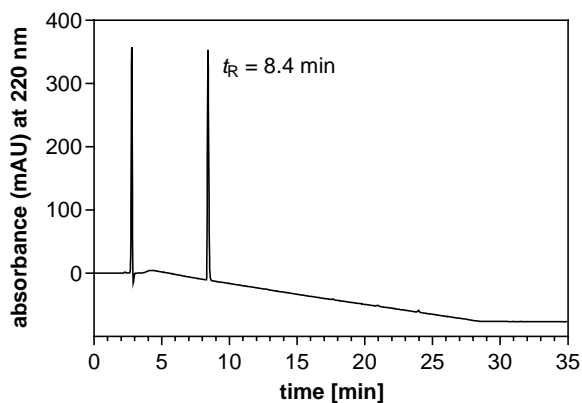
RP-HPLC (220 nm) chromatogram of (*R,R,S*)-6.7b



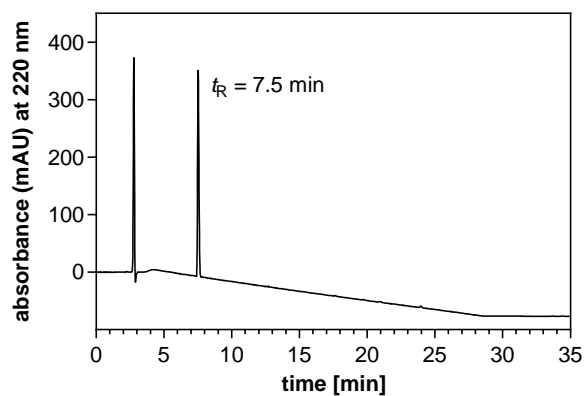
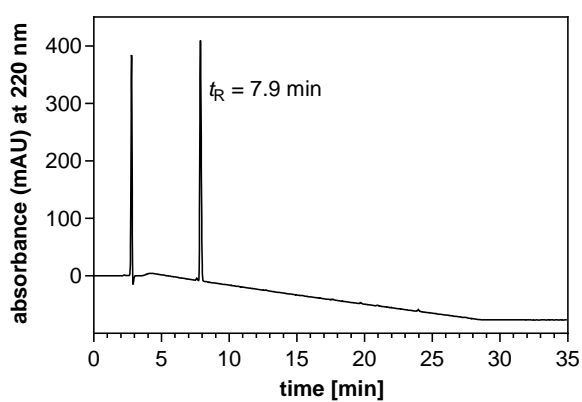
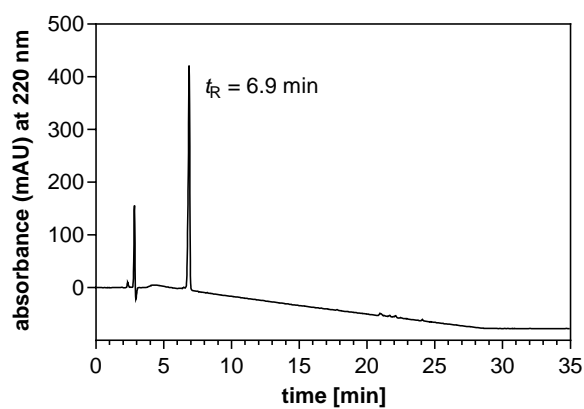
RP-HPLC (220 nm) chromatogram of 6.9



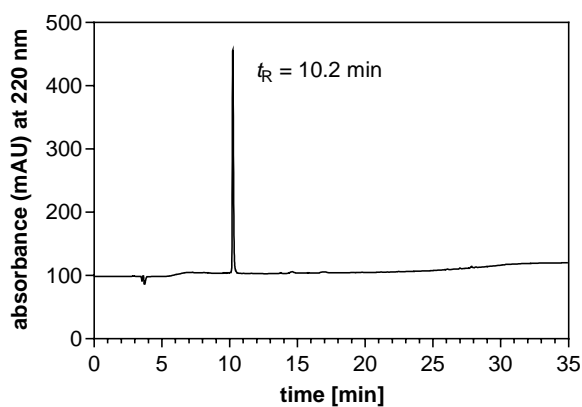
RP-HPLC (220 nm) chromatogram of 6.12



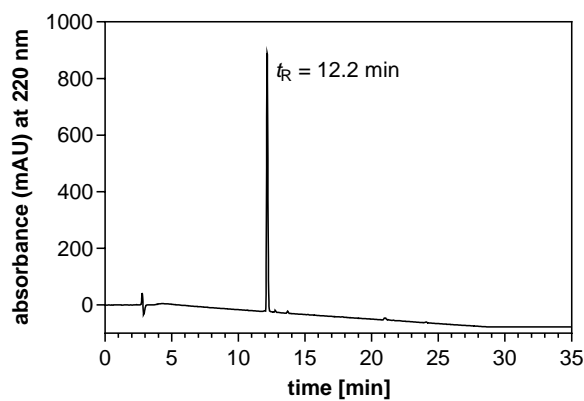
RP-HPLC (220 nm) chromatogram of 6.13

RP-HPLC (220 nm) chromatogram of (*S*^{*})-6.18aRP-HPLC (220 nm) chromatogram of (*S*^{*})-6.18b

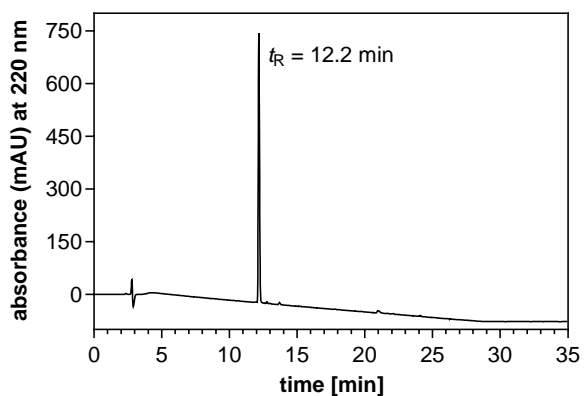
RP-HPLC (220 nm) chromatogram of 6.34



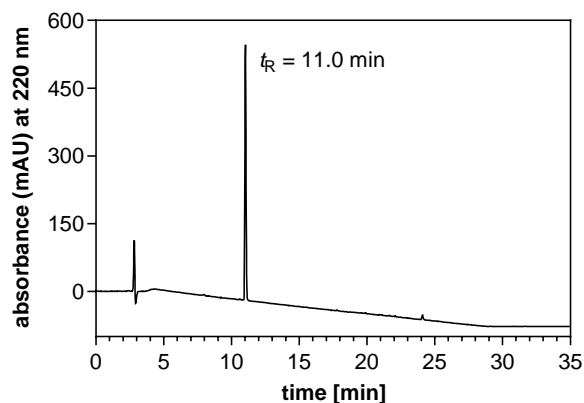
RP-HPLC (220 nm) chromatogram of 6.35



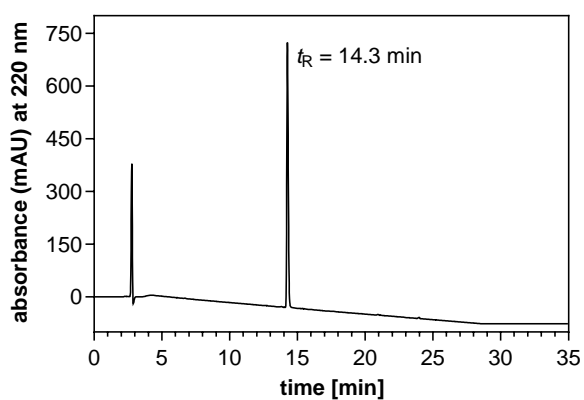
RP-HPLC (220 nm) chromatogram of 6.36



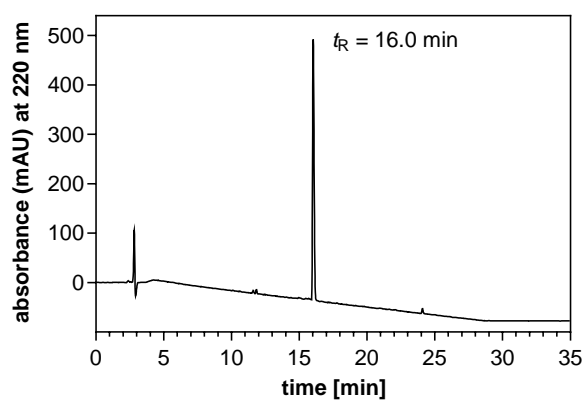
RP-HPLC (220 nm) chromatogram of 6.37



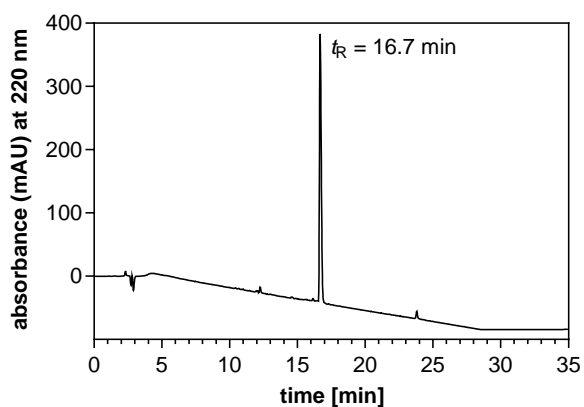
RP-HPLC (220 nm) chromatogram of 6.38



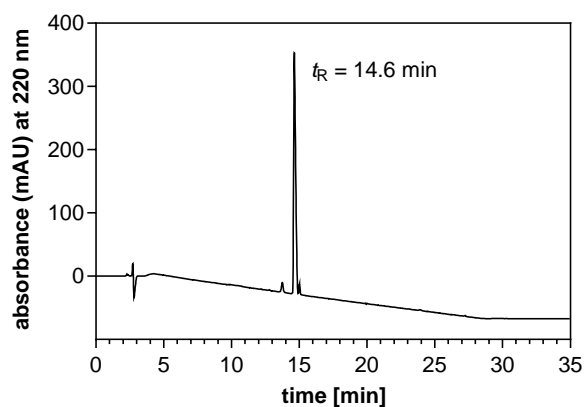
RP-HPLC (220 nm) chromatogram of 6.39



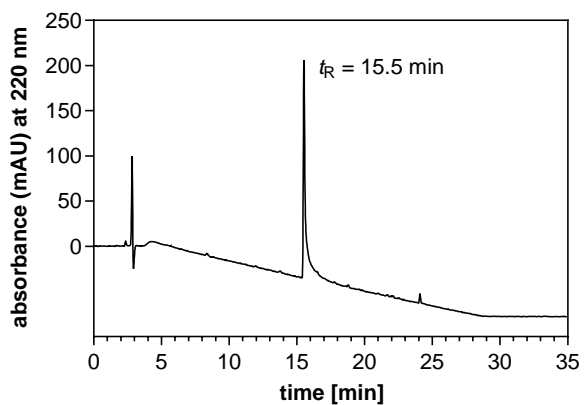
RP-HPLC (220 nm) chromatogram of 6.40



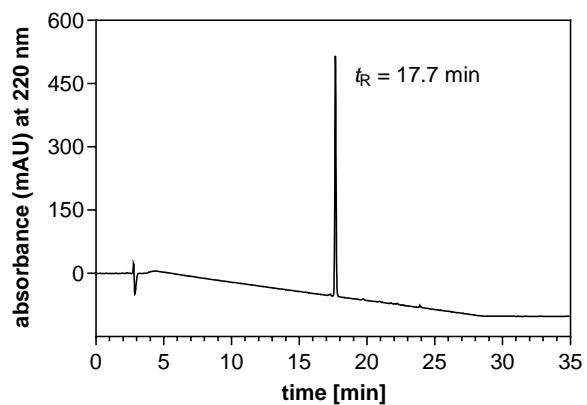
RP-HPLC (220 nm) chromatogram of 6.41



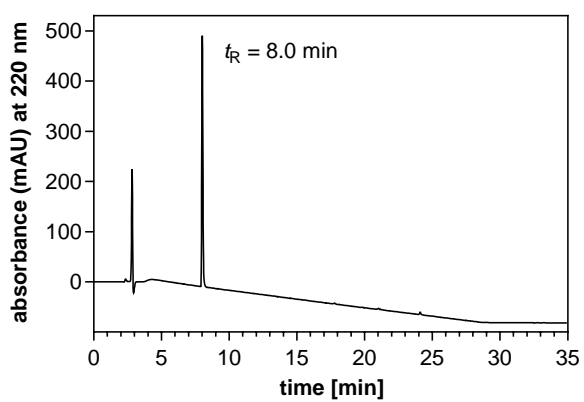
RP-HPLC (220 nm) chromatogram of 6.42



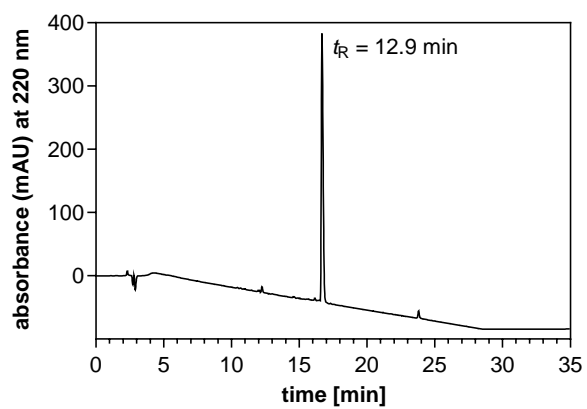
RP-HPLC (220 nm) chromatogram of 6.43



RP-HPLC (220 nm) chromatogram of 6.44



RP-HPLC (220 nm) chromatogram of 6.47



RP-HPLC (220 nm) chromatogram of 6.48

8.4.3. Crystal data of compounds (R,R,S)-6.6a and (R)-17

8.4.3.1. Crystal data of (R,R,S)-6.6a

C₂₄H₃₂ClN₅O₃, $M_r = 473.99$, monoclinic, P2₁ (No. 4), $a = 5.5823(2) \text{ \AA}$, $b = 15.1245(4) \text{ \AA}$, $c = 14.5029(4) \text{ \AA}$, $\beta = 94.173(2)^\circ$, $\alpha = \gamma = 90^\circ$, $V = 1221.23(6) \text{ \AA}^3$, $T = 122.96(11) \text{ K}$, $Z = 2$, $Z' = 1$, $\mu(\text{Cu K}\beta) = 1.222$, 30702 reflections measured, 4660 unique ($R_{int} = 0.0427$) which were used in all calculations. The final wR_2 was 0.0732 (all data) and R_1 was 0.0317 ($I > 2(I)$).

Table 8.3: Fractional atomic coordinates ($\times 10^4$) and equivalent isotropic displacement parameters ($\text{\AA}^2 \times 10^3$) for (R,R,S)-6.6a. U_{eq} is defined as 1/3 of the trace of the orthogonalised U_{ij} .

Atom	x	y	z	U_{eq}
Cl(1)	5693.9(12)	2828.7(4)	9551.4(5)	39.54(17)
O(3)	4422(3)	5381.4(12)	8181.1(11)	31.6(4)
N(5)	3125(4)	6769.0(14)	8525.9(14)	31.4(5)
O(1)	4763(4)	5393.0(16)	2826.3(12)	47.9(5)
N(2)	9360(4)	3483.1(15)	6375.2(14)	30.5(5)
N(3)	8225(4)	4399.9(14)	8674.1(13)	25.3(4)
N(4)	6116(4)	6115.6(14)	9442.8(14)	29.4(5)
O(2)	2609(5)	5942.4(18)	3858.9(16)	71.8(8)
N(1)	4233(5)	5458.7(18)	3630.0(16)	43.4(6)
C(18)	4565(4)	6047.7(17)	8687.0(17)	28.0(5)
C(4)	8100(5)	3968.1(18)	5710.6(16)	30.7(6)
C(19)	1347(5)	6887.7(17)	7791.0(18)	31.0(6)
C(3)	8632(5)	3902.0(19)	4774.8(17)	35.2(6)
C(10)	8668(5)	3438.3(16)	7329.5(16)	26.5(5)
C(20)	1428(5)	6466.9(19)	6939.6(18)	36.3(6)
C(7)	11050(5)	2780(2)	6168.2(17)	34.8(6)
C(13)	10885(5)	4343.3(19)	10087.2(17)	33.0(6)
C(2)	7381(5)	4387(2)	4102.3(17)	36.9(6)
C(17)	7285(4)	5381.7(17)	9955.6(16)	27.2(5)
C(11)	9764(5)	4209.2(17)	7900.6(16)	29.2(6)

Table 8.3 continued.

Atom	x	y	z	U_{eq}
C(1)	5558(5)	4943(2)	4337.4(17)	36.6(6)
C(9)	9617(5)	2538.3(17)	7667.1(18)	33.1(6)
C(8)	11808(5)	2397(2)	7116.6(19)	38.6(7)
C(12)	9320(4)	4948.5(17)	9465.2(16)	26.6(5)
C(5)	6241(5)	4547.5(19)	5925.9(18)	36.2(6)
C(14)	11773(5)	4779(2)	11000.3(18)	35.0(6)
C(24)	-529(5)	7459(2)	7928(2)	39.4(7)
C(15)	9633(5)	5101.4(19)	11494.8(17)	34.7(6)
C(16)	8223(5)	5764.1(18)	10894.8(17)	32.0(6)
C(22)	-2273(5)	7176(2)	6395(2)	44.2(7)
C(21)	-397(6)	6611(2)	6255(2)	42.4(7)
C(6)	4986(6)	5023(2)	5248.0(18)	40.0(7)
C(23)	-2309(5)	7606(2)	7233(2)	45.4(8)

Table 8.4. Anisotropic displacement parameters ($\times 10^4$) for (R,R,S)-**6.6a**. The anisotropic displacement factor exponent takes the form: $-2\pi^2 [h^2 a^{*2} \times U_{11} + \dots + 2hka^* \times b^* \times U_{12}]$

Atom	U_{11}	U_{22}	U_{33}	U_{23}	U_{13}	U_{12}
Cl(1)	43.3(4)	31.8(3)	43.8(4)	9.9(3)	5.3(3)	-5.4(3)
O(3)	36.2(10)	26.4(9)	31.6(9)	-5.1(8)	-1.2(7)	-2.2(8)
N(5)	35.6(12)	26.7(11)	31.6(11)	-4.0(9)	0.2(9)	2.7(10)
O(1)	53.1(13)	64.0(14)	25.6(10)	9.6(10)	-4.3(9)	-6.6(11)
N(2)	38.3(12)	30.1(12)	23(1)	-3.5(9)	2.5(9)	7.2(10)
N(3)	29.2(10)	22.9(10)	23.9(9)	-3.3(8)	2.9(8)	-3.4(9)
N(4)	35.6(12)	22.5(11)	29.7(11)	-4.2(9)	0.1(9)	0.0(9)
O(2)	95(2)	77.9(19)	42.3(13)	12.6(13)	-0.3(13)	44.6(17)
N(1)	51.8(15)	45.5(15)	31.6(12)	4.8(11)	-6.4(11)	1.5(13)

Table 8.4 continued.

Atom	U_{11}	U_{22}	U_{33}	U_{23}	U_{13}	U_{12}
C(18)	28.2(13)	29.4(14)	26.9(12)	0.4(11)	5.3(10)	-4.6(11)
C(4)	39.7(16)	28.3(14)	23.9(12)	-2(1)	1.5(11)	-0.5(12)
C(19)	32.9(14)	26.5(14)	33.4(14)	5.2(11)	1.6(11)	-2.8(11)
C(3)	43.5(16)	36.2(15)	26.5(13)	-2.7(11)	6.0(11)	3.7(13)
C(10)	33.0(14)	26.6(13)	19.9(11)	-2.7(10)	2.5(10)	0.1(11)
C(20)	42.8(16)	36.4(16)	29.8(13)	5.9(12)	2.9(12)	2.3(13)
C(7)	39.7(14)	33.4(14)	31.9(13)	-5.5(12)	6.1(11)	7.6(13)
C(13)	31.7(13)	34.7(16)	32.5(13)	-8.1(12)	0.5(11)	1.0(12)
C(2)	45.4(16)	42.9(17)	22.6(12)	-0.6(12)	4.3(11)	-2.2(14)
C(17)	28.7(13)	26.0(13)	27.2(12)	-2.5(11)	2.8(10)	-1.9(11)
C(11)	37.3(14)	25.8(14)	25.3(12)	-3.1(10)	8(1)	-3.3(11)
C(1)	47.6(17)	36.4(15)	24.9(12)	2.9(11)	-2.8(12)	1.5(13)
C(9)	45.5(16)	25.8(14)	27.9(13)	-1(1)	2.4(12)	0.2(12)
C(8)	45.4(16)	34.5(15)	35.8(15)	-0.1(12)	2.6(12)	13.1(13)
C(12)	27.3(13)	28.1(13)	24.7(11)	-7.6(10)	3.4(10)	-6.5(11)
C(5)	47.0(16)	38.5(16)	23.1(12)	-2.3(11)	2.0(11)	9.5(13)
C(14)	32.3(14)	39.6(16)	32.4(13)	-7.0(12)	-2.1(11)	0.5(12)
C(24)	35.5(15)	44.2(17)	38.7(15)	-0.9(13)	4.5(12)	1.9(13)
C(15)	32.9(14)	45.7(17)	25.3(12)	-5.7(11)	0.6(11)	-3.0(12)
C(16)	33.4(14)	32.9(15)	30.2(13)	-7.9(11)	5.0(11)	-4.0(12)
C(22)	38.8(16)	53.3(19)	39.7(16)	14.9(14)	-3.4(13)	-10.1(15)
C(21)	53.3(19)	42.7(18)	31.2(14)	7.3(12)	2.0(13)	-5.2(14)
C(6)	48.7(17)	41.7(17)	29.4(13)	-0.3(12)	0.8(12)	12.4(14)
C(23)	32.0(15)	54(2)	50.7(18)	10.6(14)	2.4(13)	4.1(13)

Table 8.5. Bond lengths in Å for (*R,R,S*)-**6.6a**.

Atom	Atom	Length/Å
O(3)	C(18)	1.246(3)
N(5)	C(18)	1.365(3)
N(5)	C(19)	1.414(3)
O(1)	N(1)	1.227(3)
N(2)	C(4)	1.365(3)
N(2)	C(10)	1.465(3)
N(2)	C(7)	1.466(3)
N(3)	C(11)	1.490(3)
N(3)	C(12)	1.509(3)
N(4)	C(18)	1.350(3)
N(4)	C(17)	1.463(3)
O(2)	N(1)	1.229(3)
N(1)	C(1)	1.449(4)
C(4)	C(3)	1.414(3)
C(4)	C(5)	1.411(4)
C(19)	C(20)	1.393(4)
C(19)	C(24)	1.383(4)
C(3)	C(2)	1.371(4)
C(10)	C(11)	1.532(3)
C(10)	C(9)	1.528(4)
C(20)	C(21)	1.387(4)
C(7)	C(8)	1.524(4)
C(13)	C(12)	1.517(4)
C(13)	C(14)	1.529(4)
C(2)	C(1)	1.382(4)

Table 8.5 continued.

Atom	Atom	Length/Å
C(17)	C(12)	1.531(3)
C(17)	C(16)	1.536(3)
C(1)	C(6)	1.386(4)
C(9)	C(8)	1.523(4)
C(5)	C(6)	1.369(4)
C(14)	C(15)	1.518(4)
C(24)	C(23)	1.381(4)
C(15)	C(16)	1.510(4)
C(22)	C(21)	1.378(4)
C(22)	C(23)	1.380(4)

Table 8.6. Bond angles in ° for (*R,R,S*)-**6.6a**.

Atom	Atom	Atom	Angle/°
C(18)	N(5)	C(19)	127.1(2)
C(4)	N(2)	C(10)	122.3(2)
C(4)	N(2)	C(7)	123.4(2)
C(10)	N(2)	C(7)	112.2(2)
C(11)	N(3)	C(12)	117.06(19)
C(18)	N(4)	C(17)	126.2(2)
O(1)	N(1)	O(2)	122.6(2)
O(1)	N(1)	C(1)	118.9(2)
O(2)	N(1)	C(1)	118.5(2)
O(3)	C(18)	N(5)	122.3(2)
O(3)	C(18)	N(4)	123.3(2)
N(4)	C(18)	N(5)	114.4(2)

Table 8.6 continued.

Atom	Atom	Atom	Angle ^o
N(2)	C(4)	C(3)	120.4(2)
N(2)	C(4)	C(5)	121.8(2)
C(5)	C(4)	C(3)	117.8(2)
C(20)	C(19)	N(5)	122.9(2)
C(24)	C(19)	N(5)	117.9(2)
C(24)	C(19)	C(20)	119.1(3)
C(2)	C(3)	C(4)	120.9(3)
N(2)	C(10)	C(11)	110.7(2)
N(2)	C(10)	C(9)	103.56(19)
C(9)	C(10)	C(11)	112.9(2)
C(21)	C(20)	C(19)	119.5(3)
N(2)	C(7)	C(8)	103.39(19)
C(12)	C(13)	C(14)	113.1(2)
C(3)	C(2)	C(1)	119.8(2)
N(4)	C(17)	C(12)	114.0(2)
N(4)	C(17)	C(16)	106.0(2)
C(12)	C(17)	C(16)	110.9(2)
N(3)	C(11)	C(10)	108.9(2)
C(2)	C(1)	N(1)	120.0(2)
C(2)	C(1)	C(6)	120.9(3)
C(6)	C(1)	N(1)	119.1(3)
C(8)	C(9)	C(10)	103.3(2)
C(9)	C(8)	C(7)	103.8(2)
N(3)	C(12)	C(13)	107.7(2)
N(3)	C(12)	C(17)	108.38(19)

Table 8.6 continued.

Atom	Atom	Atom	Angle ^o
C(13)	C(12)	C(17)	113.4(2)
C(6)	C(5)	C(4)	120.9(2)
C(15)	C(14)	C(13)	109.3(2)
C(23)	C(24)	C(19)	120.6(3)
C(16)	C(15)	C(14)	109.6(2)
C(15)	C(16)	C(17)	113.0(2)
C(21)	C(22)	C(23)	118.8(3)
C(22)	C(21)	C(20)	121.3(3)
C(5)	C(6)	C(1)	119.8(3)
C(22)	C(23)	C(24)	120.7(3)

Table 8.7. Hydrogen fractional atomic coordinates ($\times 10^4$) and equivalent isotropic displacement parameters ($\text{\AA}^2 \times 10^3$) for (*R,R,S*)-**6.6a**. U_{eq} is defined as 1/3 of the trace of the orthogonalised U_{ij} .

Atom	x	y	z	U_{eq}
H(5)	3321.08	7197.91	8913.38	38
H(3A)	7762.95	3886.18	8902.41	30
H(3B)	6908.29	4675.35	8440.6	30
H(4)	6448.15	6640.28	9641.72	35
H(3)	9847.41	3524.03	4613.31	42
H(10)	6913.65	3452.08	7335.34	32
H(20)	2697.29	6091.85	6830.81	44
H(7A)	12419.05	3018.18	5875.77	42
H(7B)	10274.41	2335.73	5767.24	42
H(13A)	12260.76	4160.7	9762.27	40
H(13B)	9976.46	3816.91	10218.09	40
H(2)	7758.09	4342.65	3489.89	44

Table 8.7 continued.

Atom	x	y	z	U_{eq}
H(17)	6072.1	4931.29	10060.52	33
H(11A)	11374.81	4056.7	8145.41	35
H(11B)	9864.08	4728.49	7512.74	35
H(9A)	10063.45	2548.28	8326	40
H(9B)	8429.74	2078.41	7536.33	40
H(8A)	12186.77	1773.07	7072.59	46
H(8B)	13196.22	2706.15	7398.88	46
H(12)	10324.66	5411.17	9219.42	32
H(5A)	5861.78	4607.1	6536.72	43
H(14A)	12686.91	4355.52	11385.8	42
H(14B)	12815.08	5272.61	10881.65	42
H(24)	-593.05	7745.51	8492.61	47
H(15A)	8611.54	4604.91	11626	42
H(15B)	10183.84	5374.57	12077.14	42
H(16A)	9240.87	6269.16	10791.57	38
H(16B)	6872.49	5971.26	11219.88	38
H(22)	-3492.28	7266.24	5932.36	53
H(21)	-353.19	6321.18	5691.44	51
H(6)	3754.98	5399.17	5397.94	48
H(23)	-3544.98	7999.81	7330.71	55

8.5.3.2. Crystal data of (R)-6.17

$C_{12}H_{16}N_2O_5S$, $M_r = 300.33$, monoclinic, $P2_1$ (No. 4), $a = 5.32850(10) \text{ \AA}$, $b = 10.3138(3) \text{ \AA}$, $c = 12.9123(4) \text{ \AA}$, $\beta = 98.477(3)^\circ$, $\alpha = \gamma = 90^\circ$, $V = 701.87(3) \text{ \AA}^3$, $T = 294(4) \text{ K}$, $Z = 2$, $Z' = 1$, $\mu(\text{Cu } K\alpha) = 2.258$, 8519 reflections measured, 2888 unique ($R_{int} = 0.0180$) which were used in all calculations. The final wR_2 was 0.0800 (all data) and R_1 was 0.0279 ($I > 2(I)$).

Table 8.8. Fractional atomic coordinates ($\times 10^4$) and equivalent isotropic displacement parameters ($\text{\AA}^2 \times 10^3$) for (*R*)-**6.17**. U_{eq} is defined as 1/3 of the trace of the orthogonalised U_{ij} .

Atom	x	y	z	U_{eq}
S1	6625.8(9)	2711.3(6)	5121.9(4)	57.21(17)
O3	7597(3)	2653(2)	6324.9(11)	56.3(3)
O1	7604(5)	1655(3)	4608(2)	89.0(7)
O2	3964(3)	2860(3)	5045.5(16)	82.9(6)
N1	10716(4)	3685(3)	8178.0(16)	63.5(5)
N2	4664(6)	8081(3)	8352(3)	91.0(9)
C7	9160(4)	4730(3)	8184.9(17)	55.0(5)
O4	4919(7)	8994(4)	7739(3)	123.1(11)
O5	3232(6)	8122(4)	9010(3)	124.3(12)
C10	6151(5)	6919(3)	8282(2)	67.0(6)
C9	5927(5)	5901(3)	8937(2)	70.1(7)
C8	7393(5)	4812(3)	8900.0(19)	63.3(6)
C12	9303(5)	5788(3)	7513(2)	63.4(6)
C11	7842(6)	6871(3)	7561(2)	70.1(7)
C2	10175(4)	2160(3)	6709(2)	61.0(6)
C6	10748(6)	2621(4)	8927(2)	78.0(7)
C3	11701(4)	3283(3)	7235(2)	65.3(6)
C4	9885(7)	1054(3)	7443(3)	82.8(9)
C5	9067(7)	1518(3)	8471(3)	80.8(8)
C1	7939(7)	4145(4)	4736(3)	83.1(9)

Table 8.9. Anisotropic displacement parameters ($\times 10^4$) for (R)-6.17. The anisotropic displacement factor exponent takes the form: $-2\pi^2[h^2a^{*2} \times U_{11} + \dots + 2hka^* \times b^* \times U_{12}]$

Atom	U_{11}	U_{22}	U_{33}	U_{23}	U_{13}	U_{12}
S1	49.0(3)	70.7(3)	53.4(3)	-3.8(3)	12.42(17)	-4.2(3)
O3	50.6(7)	67.3(8)	52.9(7)	1.5(8)	13.8(5)	11.4(8)
O1	94.2(15)	97.3(17)	76.7(14)	-28.6(13)	15.9(12)	4.5(13)
O2	47.5(8)	131.0(19)	70.4(11)	2.7(13)	8.8(7)	-2.8(13)
N1	64.0(11)	77.2(14)	49.1(10)	1.8(9)	7.3(9)	6.7(10)
N2	89.4(16)	98(2)	78.9(17)	-34.4(15)	-10.9(14)	23.8(15)
C7	51.0(10)	71.0(13)	41.5(10)	-5.3(9)	1.5(8)	-4.7(10)
O4	135(3)	96.8(19)	133(3)	6.4(19)	7(2)	45.5(19)
O5	125(2)	140(3)	109(2)	-48.4(19)	22.9(17)	43(2)
C10	67.0(14)	75.6(16)	54.4(13)	-18.4(11)	-4.6(11)	7.7(12)
C9	66.9(14)	92.4(18)	52.5(13)	-22.0(12)	13.5(11)	-1.3(13)
C8	69.4(14)	76.3(15)	45.8(11)	-4.0(10)	14.1(10)	-5.9(12)
C12	62.1(13)	77.3(16)	52.1(12)	0.0(11)	13.1(10)	0.1(11)
C11	76.6(15)	71.5(16)	59.8(15)	2.4(11)	2.2(12)	3.8(13)
C2	54.3(11)	65.5(13)	65.5(14)	1.0(11)	16.8(10)	20.5(10)
C6	78.5(14)	94.7(19)	58.3(13)	19.2(17)	1.6(11)	21.1(18)
C3	48.3(11)	86.7(16)	62.1(13)	0.6(12)	12.0(10)	11.7(11)
C4	98(2)	63.4(15)	89(2)	12.3(14)	20.0(17)	30.2(15)
C5	95(2)	74.4(17)	74.2(18)	30.3(15)	16.3(15)	21.0(16)
C1	79.8(18)	93(2)	74.9(19)	25.1(16)	6.2(15)	-14.0(16)

Table 8.10. Bond lengths in Å for (R)-6.17.

Atom	Atom	Length/Å
S1	O3	1.5644(15)
S1	O1	1.414(2)
S1	O2	1.4155(17)
S1	C1	1.739(3)
O3	C2	1.480(3)

Table 8.10 continued.

Atom	Atom	Length/Å
N1	C7	1.360(4)
N1	C6	1.461(4)
N1	C3	1.455(3)
N2	O4	1.250(5)
N2	O5	1.223(5)
N2	C10	1.447(4)
C7	C8	1.415(3)
C7	C12	1.403(4)
C10	C9	1.365(5)
C10	C11	1.388(4)
C9	C8	1.373(4)
C12	C11	1.368(4)
C2	C3	1.517(4)
C2	C4	1.505(4)
C6	C5	1.513(5)
C4	C5	1.533(5)

Table 8.11. Bond angles in ° for (*R*)-**6.17**

Atom	Atom	Atom	Angle/°
O3	S1	C1	103.22(15)
O1	S1	O3	110.18(15)
O1	S1	O2	119.04(17)
O1	S1	C1	109.20(18)
O2	S1	O3	104.77(10)
O2	S1	C1	109.21(19)

Table 8.11 continued.

Atom	Atom	Atom	Angle ^o
C2	O3	S1	120.06(14)
C7	N1	C6	122.6(2)
C7	N1	C3	121.8(2)
C3	N1	C6	111.6(3)
O4	N2	C10	118.2(3)
O5	N2	O4	123.4(3)
O5	N2	C10	118.4(4)
N1	C7	C8	121.1(2)
N1	C7	C12	121.6(2)
C12	C7	C8	117.3(2)
C9	C10	N2	119.9(3)
C9	C10	C11	120.9(3)
C11	C10	N2	119.2(3)
C10	C9	C8	120.3(2)
C9	C8	C7	120.6(3)
C11	C12	C7	121.6(2)
C12	C11	C10	119.3(3)
O3	C2	C3	107.3(2)
O3	C2	C4	107.1(2)
C4	C2	C3	113.2(3)
N1	C6	C5	111.0(2)
N1	C3	C2	110.9(2)
C2	C4	C5	112.2(2)
C6	C5	C4	110.1(3)

Table 8.12. Torsion angles in ° for (*R*)-**6.17**

Atom	Atom	Atom	Atom	Angle ^f
S1	O3	C2	C3	114.5(2)
S1	O3	C2	C4	-123.6(2)
O3	C2	C3	N1	66.5(3)
O3	C2	C4	C5	-70.4(4)
O1	S1	O3	C2	34.7(3)
O2	S1	O3	C2	163.8(2)
N1	C7	C8	C9	176.5(2)
N1	C7	C12	C11	-176.2(2)
N1	C6	C5	C4	56.4(3)
N2	C10	C9	C8	-177.8(2)
N2	C10	C11	C12	178.1(2)
C7	N1	C6	C5	95.7(3)
C7	N1	C3	C2	-99.6(3)
C7	C12	C11	C10	-0.9(4)
O4	N2	C10	C9	180.0(3)
O4	N2	C10	C11	1.6(4)
O5	N2	C10	C9	0.2(4)
O5	N2	C10	C11	-178.1(3)
C10	C9	C8	C7	0.2(4)
C9	C10	C11	C12	-0.2(4)
C8	C7	C12	C11	1.5(4)
C12	C7	C8	C9	-1.2(4)
C11	C10	C9	C8	0.5(4)
C2	C4	C5	C6	-49.5(4)
C6	N1	C7	C8	-2.7(4)

Table 8.12 continued.

Atom	Atom	Atom	Atom	Angle ^f
C6	N1	C7	C12	174.8(3)
C6	N1	C3	C2	58.3(3)
C3	N1	C7	C8	152.8(2)
C3	N1	C7	C12	-29.6(4)
C3	N1	C6	C5	-62.0(3)
C3	C2	C4	C5	47.7(4)
C4	C2	C3	N1	-51.5(3)
C1	S1	O3	C2	-81.9(3)

Table 8.13. Hydrogen fractional atomic coordinates ($\times 10^4$) and equivalent isotropic displacement parameters ($\text{\AA}^2 \times 10^3$) for (*R*)-**6.17**. U_{eq} is defined as 1/3 of the trace of the orthogonalised U_{ij} .

Atom	x	y	z	U_{eq}
H9	4775.66	5945.89	9411.99	84
H8	7222.74	4122.21	9348.45	76
H12	10418.74	5752.11	7023.9	76
H11	7980.16	7567.72	7115.56	84
H2	10966.99	1846.7	6117.63	73
H6A	10164.57	2933.73	9558.4	94
H6B	12472.73	2309.08	9114.44	94
H3A	13461.67	3024.58	7414.89	78
H3B	11630.51	4007.28	6752.51	78
H4A	11487.64	597.02	7597.04	99
H4B	8632.09	450.53	7102.27	99
H5A	7315.88	1805.45	8341.86	97
H5B	9184.23	805.51	8966.22	97
H1A	7432.99	4852.65	5142.1	125

Table 8.13 continued.

Atom	x	y	z	U_{eq}
H1B	7352.08	4297.22	4007.52	125
H1C	9755	4075.41	4847.04	125

8.5. Abbreviations

AcOH	acetic acid
aq	aqueous
a.u.	arbitrary unit
Anal.	Combustion elemental analysis
APCI	atmospheric pressure chemical ionization
Boc	<i>tert</i> -butoxycarbonyl
Bq	bequerel
br s	broad singlet
B _{max}	maximum number of binding sites
Bn	benzyl
BSA	Bovine serum albumin
BRET	bioluminescence energy transfer
c	concentration
Cbz	benzyloxycarbonyl
CHO cells	Chinese hamster ovary cells
CH ₂ Cl ₂	dichloromethane
COSY	correlated spectroscopy
°C	degrees Celsius
d	doublet
δ	chemical shift in parts per million
DCC	<i>N,N</i> -dicyclohexylcarbodiimide
DIPEA	<i>N,N</i> -diisopropylethylamine
DMEM	Dulbecco's modified eagle medium
DMF	<i>N,N</i> -dimethylformamide
DMSO	dimethylsulfoxide
dpm	disintegrations per minute
EC ₅₀	agonist concentration which induces 50% of the maximum response
EDC·HCl	1-ethyl-3-(3-dimethylaminopropyl)carbodiimid hydrochloride
ESI	Electrospray ionization

Et ₃ N	triethylamine
EtOAc	ethyl acetate
Et ₂ O	diethyl ether
EtOH	ethanol
FCS	fetal calf serum
Fmoc	9-fluorenylmethoxycarbonyl
FRET	Förster resonance energy transfer
h	hour(s)
GPCR	G-protein coupled receptor
G418	geneticin
HBSS	Hank's balanced salt solution
HEC-1b	human endometrial carcinoma cells
HEK293	human embryonic kidney cells
HEL cells	human erythroleukemia cells
HEPES	2-(4-(2-hydroxyethyl)-1-piperazinyl)ethanesulfonic acid
HMBC	heteronuclear multiple bond correlation
HPLC	high-performance liquid chromatography
hPP	human pancreatic polypeptide
HOBt	1-hydroxybenzotriazole
HR-MS	high resolution mass spectrometry
HSQC	heteronuclear single quantum coherence
IC ₅₀	inhibitor concentration which suppresses 50% of an agonist induced effect or displaces 50% of labelled ligand from the binding site
<i>J</i>	coupling constant in NMR spectroscopy (Hz)
<i>k</i>	retention factor
<i>K_b</i>	dissociation rate constant derived from a functional assay
<i>K_d</i>	dissociation rate constant derived from a saturation binding assay
<i>K_i</i>	dissociation constant derived from a competition binding assay
<i>k_{obs}</i>	observed association constant
<i>k_{off}</i>	dissociation rate constant

k_{on}	association rate constant
L-15	Leibovitz's L-15 medium
m	multiplet
M	molar ($\text{mol} \cdot \text{L}^{-1}$)
MeOH	methanol
min	minute
m/z	mass to charge ratio
M^+	parent molecular ion
NHS	N-hydroxysuccinimide
NMR	nuclear magnetic resonance
NOESY	nuclear Overhauser effect spectroscopy
NLuc	Nanoluc
(p)NPY	(porcine) neuropeptide Y
on	over night
Pbf	2,2,4,6,7-pentamethyldihydrobenzofuran-5-sulfonyl
PBS	phosphate buffered saline
PCC	pyridiniumchlorochromate
PET	positron emission tomography
Ph	phenyl
PYY	peptide YY
q	quartet
RP	reversed phase
rt	room temperature
SAR	Structure-activity relationship
s	singlet
SEM	standard error of the mean
t	time or triplet
<i>t</i> Bu	<i>tert</i> -butyl
TBS	<i>tert</i> -Butyldimethylsilyl
TLC	thin layer chromatography

TFA	trifluoroacetic acid
THF	tetrahydrofurane
t_R	retention time
$t_{1/2}$	half time
UV	ultraviolet
Y_xR	NPY receptor subtypes (X = 1, 2, 4, 5)

8.6. References

1. Yang, Z.; Han, S.; Keller, M.; Kaiser, A.; Bender, B. J.; Bosse, M.; Burkert, K.; Kogler, L. M.; Wifling, D.; Bernhardt, G.; Plank, N.; Littmann, T.; Schmidt, P.; Yi, C.; Li, B.; Ye, S.; Zhang, R.; Xu, B.; Larhammar, D.; Stevens, R. C.; Huster, D.; Meiler, J.; Zhao, Q.; Beck-Sickinger, A. G.; Buschauer, A.; Wu, B. Structural basis of ligand binding modes at the neuropeptide Y Y₁ receptor. *Nature* **2018**, 556, 520-524.

Eidesstattliche Erklärung

Ich erkläre hiermit an Eides statt, dass ich die vorliegende Arbeit ohne unzulässige Hilfe Dritter und ohne Benutzung anderer als der angegebenen Hilfsmittel angefertigt habe; die aus anderen Quellen direkt oder indirekt übernommenen Daten und Konzepte sind unter Angabe des Literaturzitats gekennzeichnet.

Einige der experimentellen Arbeiten wurden in Zusammenarbeit mit anderen Personen durchgeführt. Entsprechende Vermerke befinden sich in den entsprechenden Kapiteln (Chapter 2-6). Eine detaillierte Auflistung aller Kooperationen enthält zudem der Abschnitt "Acknowledgements and declaration of collaborations".

Weitere Personen waren an der inhaltlich-materiellen Herstellung der vorliegenden Arbeit nicht beteiligt. Insbesondere habe ich hierfür nicht die entgeltliche Hilfe eines Promotionsberaters oder anderer Personen in Anspruch genommen. Niemand hat von mir weder unmittelbar noch mittelbar geldwerte Leistungen für Arbeiten erhalten, die im Zusammenhang mit dem Inhalt der vorgelegten Dissertation stehen.

Die Arbeit wurde bisher weder im In- noch im Ausland in gleicher oder ähnlicher Form einer anderen Prüfungsbehörde vorgelegt.

Regensburg, den

Jonas Buschmann